The Quaternary geological evolution of the Belgian Continental Shelf, southern North Sea

Mieke Mathys

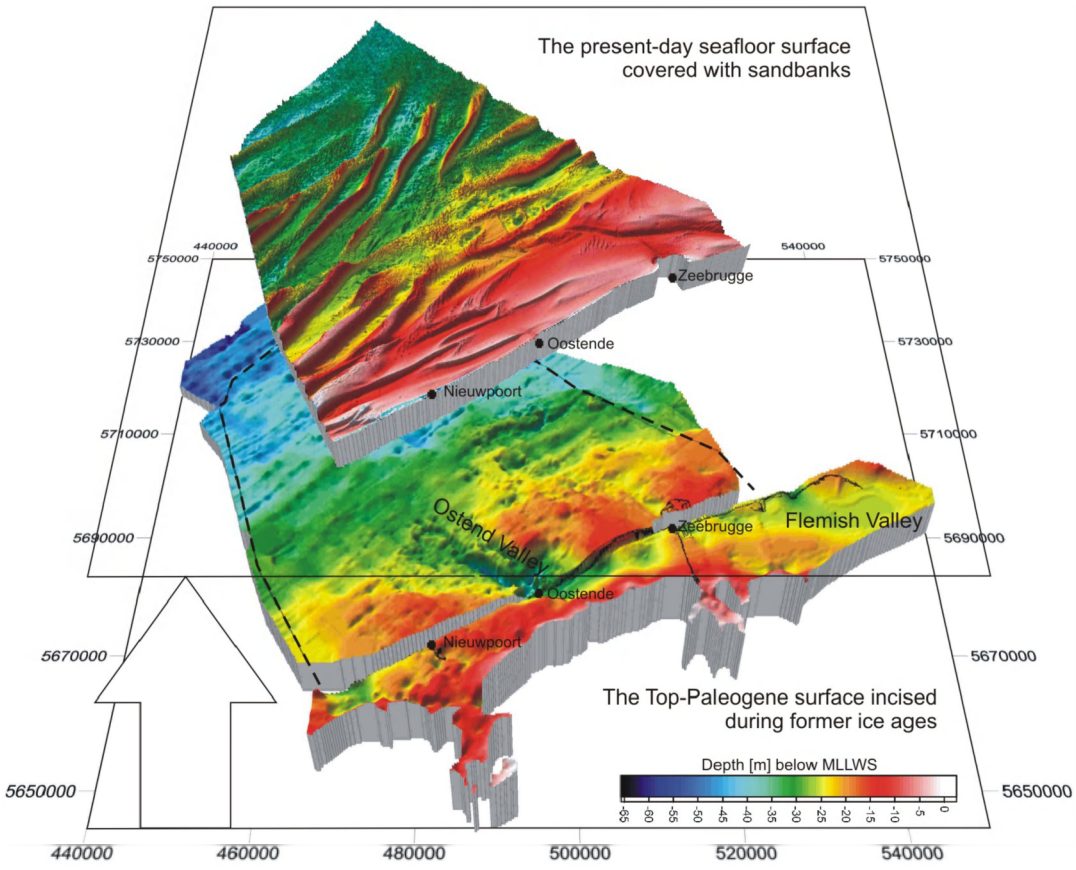

Academic year 2008-2009

Thesis submitted for the degree of Doctor of Science, Geology

Promoter: Prof. Dr. Marc De Batist
Co-promoter: Prof. Dr. Cecile Baeteman

UNIVERSITEIT GENT

The Quaternary geological evolution of the Belgian Continental Shelf, southern North Sea

This research was financially supported by FWO Flanders (*Fonds voor Wetenschappelijk Onderzoek - Vlaanderen*)

To refer to this thesis:
Mathys, M., 2009. The Quaternary geological evolution of the Belgian Continental Shelf, southern North Sea, PhD thesis, Ghent University, Belgium.

In Dutch: De Quartaire geologische evolutie van het Belgisch Continentaal Plat, zuidelijke Noordzee, Doctoraatsthesis, Universiteit Gent, België.

Front cover:
"From the Pleistocene incision of an incised valley, until the Holocene formation of sandbanks: the Quaternary evolution of the Belgian Continental Shelf, southern North Sea."
Top: the present-day seafloor surface in 3D. Digital terrain model on the basis of single-beam bathymetry from the Flemish Authorities (Department of Environment and Infrastructure, Waterways and Marine Affairs Administration, Division Coast, Hydrographic Office), completed with data from the Dutch and English Hydrographic Offices (compilation: Van Lancker et al. 2007).

Bottom: the Top-Paleogene surface in 3D, composed of an onshore grid covering the Coastal Plain (Meyus et al. 2000, Meyus et al. 2005) and an offshore grid covering the entire Belgian Continental Shelf based on the presented seismic data.
Depth is expressed in metres below MLLWS, projection and datum is UTM (31N), WGS84.

UNIVERSITEIT GENT

THE QUATERNARY GEOLOGICAL EVOLUTION OF THE BELGIAN CONTINENTAL SHELF, SOUTHERN NORTH SEA

De Quartaire geologische evolutie
van het Belgisch Continentaal Plat, zuidelijke Noordzee

Mieke Mathys

Academic year 2008-2009

Thesis submitted for the degree of Doctor of Science, Geology

Promoter: Prof. Dr. Marc De Batist
Co-promoter: Prof. Dr. Cecile Baeteman

Faculteit Wetenschappen

RCMG

Geological Survey of Belgium

FWO VLAANDEREN
Fonds Wetenschappelijk Onderzoek
Research Foundation – Flanders

Members of the reading committee:

Prof. Dr. M. De Batist (Ghent University, Belgium): promoter
Prof. Dr. C. Baeteman (BGD-KBIN, Belgium): co-promoter
Prof. Dr. A. Trentesaux (Université de Lille1, France)
Dr. S. Van Heteren (TNO Bouw en Ondergrond, The Netherlands)

Members of the examination committee:

Prof. Dr. J.P. Henriet (Ghent University, Belgium): chairman
Prof. Dr. M. De Batist (Ghent University, Belgium): secretary
Prof. Dr. C. Baeteman (BGD-KBIN, Belgium): co-promoter
Prof. Dr. A. Trentesaux (Université de Lille1, France)
Dr. S. Van Heteren (TNO Bouw en Ondergrond, The Netherlands)
Prof. Dr. F. Chiocci (Universitá di Roma 'La Sapienza', Italy)
Prof. Dr. P. Jacobs (Ghent University, Belgium)
Prof. Dr. F. Mostaert (guest professor Ghent University, Belgium)
Prof. Dr. V. Van Lancker (guest professor Ghent University, Belgium)

Voorwoord

Hierbij zou ik graag iedereen willen bedanken die me de afgelopen zes jaar geholpen heeft bij het realiseren van deze thesis. Enkele mensen verdienen extra vermeld te worden:

In de eerste plaats, mijn promotor Prof. Dr. Marc De Batist, die dit thesisonderwerp voorstelde. Tijdens mijn onderzoek heeft hij me vooral mijn eigen weg laten vinden, maar me ook steeds gestimuleerd om internationale contacten te onderhouden en deel te nemen aan buitenlandse conferenties. Tist, bedankt ook dat je zoveel uren vrije tijd besteed hebt aan het nalezen van mijn thesis (tot in het kleinste detail) en voor de constructieve opmerkingen.
Ik bedank eveneens mijn co-promotor, Prof. Dr. Cecile Baeteman, voor het beschikbaar stellen van de kernen en boorbeschrijvingen, en het kritisch nalezen van mijn thesis. Van haar heb ik de stiel geleerd van het beschrijven van kernen, en hoe wonderlijk een kustvlakte ineen steekt.
Een volgend dankwoord gaat uit naar Prof. Dr. Jean-Pierre Henriet, die mij als eerstejaars doctoraatsstudente engageerde voor een commerciële opdracht op de Thorntonbank. Zoiets geeft een boost aan je zelfvertrouwen.

Een aantal mensen hebben me enorm vooruit geholpen met mijn onderzoek door het ter beschikking stellen van data en apparatuur. I would like to thank Marc Schaming (Institut de Physique du Globe de Strasbourg), who gave a personal training on how to convert analogue seismic data into digital segy format. This was one the most essential keystones of my thesis. Hugo Vannieuwenhuyse en Prof. Dr. Eric Van Ranst (UGent) stelden een A0 scanner tot mijn beschikking voor het digitaliseren van oude, analoge seismische profielen. Ik wou ook graag Ellen De Clerck bedanken, zij voerde meer dan 7000 logboek posities handmatig in in een database. Op basis van deze gegevens berekenden José Ozer en Virginie Pison (MUMM-BMM) theoretische getijhoogtes voor de periode 1980-1994, noodzakelijk voor de getijdencorrectie van die oude seismische profielen. Koen Degrendele (Economische Zaken) voerde gelijkaardige berekeningen uit voor de recente, digitale data. Okke Batelaan (VUB) leverde de digitale Basis- en Top-Pleistoceen kaarten van de Kustvlakte en de Vlaamse Vallei. Alain Trentesaux (Université de Lille1) delivered the core descriptions and lithologs from the area of the Middelkerke Bank. Sue Dawson (University of Aberdeen) conducted diatom analyses for me. Een extra bedanking voor Karen Fontijn die alle beschikbare boorbeschrijvingen zeer nauwkeurig invoerde in access, een echt monnikenwerk. Verder wil ik ook Cees Laban, Freek Busschers en Kim Cohen bedanken voor de vruchtbare en interessante discussies over de Quartairgeologie van Nederland. Chantal Martens, bedankt voor die ene referentie waar ik nog wanhopig naar op zoek was.

De bemanning van de Bellini en het onderzoeksschip Belgica, en in het bijzonder commandant Peter Ramboer en commandant Lieven Goussaert, bedank ik voor de jarenlange professionele samenwerking. Ik waardeer oprecht hun inzet en de inspanningen om de vooropgestelde seismische profielen zo correct mogelijk te varen, zelfs in mistige omstandigheden doorheen de drukbevaren vaargeul en over zeer ondiepe zandbanken.

While attending conferences in Brussels, Rome and Ponza, St. Petersburg, Dunkerque and Cairns, I felt very welcomed by the IGCP scientific communities (IGCP 464, 526, 495). Thank you Vanessa Heyvaert, Peter Vos, Henk Weerts, Francesco Chiocci, Allan

Chivas, Michel de Mahiques and so many others to make each conference unforgettable!

Mijn collega's en vrienden van het RCMG bedank ik voor de taartmomenten en 'vergaderingen aan de overkant' (en dan vergeet ik nog de delhaize-uitstappen, kerstrecepties en kaas-en-wijn-nieuwjaarsetentjes), die zorgden voor de nodige ontspanning.
Een speciale bedanking nog voor de slachtoffers die zich vrijwillig opgaven voor de Belgica campagnes die ik organiseerde: Jasper, Katrien, Lieven, Dries, Annelies De Hauwere, Maud Nolmans, Vladimir Slodlodyan en Ivan Korolev. Koen, ik apprecieer het enorm dat jij steeds standby was voor de installatie en bediening van de apparatuur aan boord, het sleuren met kisten en het huren van de meest geschikte voer- en vaartuigen. Wim, bedankt voor de geofysische bijstand en raadgevingen aan boord, bedankt ook voor het oplossen van allerlei software problemen. Maar bovenal waardeer ik je advies en raad op persoonlijk vlak. Vera, bedankt om me wegwijs te maken in het organiseren van Belgica campagnes, voor de goeie samenwerking aan boord, en om me te betrekken in allerlei projecten. Tine, mijn eerste conferentie ooit, in Venetië, zal ik nooit vergeten, net als je advies en aanmoedigende commentaren bij mijn eerste artikel. Peter, merci om me te helpen met de getijdencorrecties en de swell en bandpass filtering van de seismische data; je Matlab scripts zijn super. Ook Arcview is net weer iets bevattelijker geworden dankzij Els, Kristien en Lies: bedankt! Als er iemand steeds enthousiast is en bereid om te helpen, dan is het David wel. Bedankt voor het uitlenen van literatuur, het beantwoorden van sedimentologische vragen en het rondsturen van toepasselijke cartoons ☺ . Marc, dankzij jou kwamen alle financiële beslommeringen in orde, en nog eens bedankt om de fax over te nemen ;-) . Katrien, bedankt voor je aanmoedigingen en om me af en toe vanachter mijn laptop te sleuren voor smoutebollen, een museumpje of een dansavond. Lieven, bedankt dat je me Global Mapper hebt leren kennen ☺ , en als goeie bureaugenoot steeds mijn gezaag hebt aangehoord. Ik apprecieer je uitgesproken mening over alles (ja, zelfs over mijn planten ☺), en hoe je ongegeneerd je gedacht durft zeggen.

Caro, Daan, Bart, Nele, Antoine, jullie wil ik bedanken voor de uitstapjes en etentjes (en om steeds gewillig al mijn frustraties aan te horen). Het deed echt deugd om mijn gedachten eens te verzetten. Wim en Ilse, Katrien en Koen, bedankt voor de gezellige familienamiddagen!

Mama en papa, bedankt dat jullie steeds in mij bleven geloven, probeerden te begrijpen waar ik nu eigenlijk mee bezig was, en de laatste jaren durfden blijven vragen hoe het er nu eigenlijk mee stond en hoe het vorderde met mijn 'tekeningen'.

Arvid, mijn doctoraat heeft de laatste jaren een beetje ons leven gedomineerd, het is nu eindelijk af. Ik wil je bedanken voor je niet-aflatende steun, voor het opofferen van je weekends en vakanties, de geanimeerde discussies aan de keukentafel, de editing van mijn tekst en je constructieve commentaren op de figuren. Bedankt dat je er altijd bent voor me.

Gent, april 2009

Mieke

Table of contents

List of figures

List of tables

1. Introduction

1.1 Background

With respect to the Quaternary deposits, the Belgian Continental Shelf (BCS) has remained one of the last unmapped and unknown areas of Belgium. Because of the absence of a distinct shelf break and the almost complete lack of subsidence (D'Olier 1981, Kiden et al. 2002, Vink et al. 2007), the BCS had very little accommodation space to accumulate and preserve Quaternary sediments. Moreover, sediment input by the major rivers (i.e. Scheldt, Rhine, Meuse) has been relatively limited during the Holocene (De Moor 1986, Beets and van der Spek 2000). Therefore the Quaternary cover on the BCS is very patchy and discontinuous, mostly shaped into sandbanks by past and modern tidal currents. The Quaternary cover has a maximum thickness of only 45 m, and is on average even less than 10 m thick. This thin, fragmented record is the main reason why it has been so difficult up to now to produce a coherent reconstruction of the Quaternary evolution of the BCS.
Nevertheless, a large amount of data is available from the BCS. Since the end of the '70's and beginning of the '80's, the BCS has been intensively surveyed in the framework of several national and international projects, resulting in one of the densest regional seismic grids of the world. More than 16,000 km of high-resolution reflection seismic profiles are available in the data files of the Renard Centre of Marine Geology (RCMG). In addition, an extensive series of cores and core descriptions have been acquired over the years and are stored in the repository of the Geological Survey of Belgium (GSB), amongst other things for investigating the subsurface in view of a potential exploitation of natural reserves. Previous analyses of these datasets, however, focused mostly on a single sandbank or a distinct sub-area of the BCS. E.g. De Moor (1985a, 1985b) presented a morphogenetic model for sandbanks, based on an extensive dataset from the Kwintebank. Van den Broeke (1984) focused on the Quaternary stratigraphy of the Hinder banks and De Maeyer et al. (1985) studied the Nieuwpoort Bank. In an attempt to extend the Quaternary interpretations of the Coastal Plain offshore, and to reconstruct a former, more seaward position of the coastline, Wartel and Vansieleghem (1985) chose the nearshore zone and Coastal Banks as their study area, while the Middelkerke Bank was the main point of interest of EC projects RESECUSED and STARFISH (Lanckneus et al. 1991, De Moor et al. 1993, Stolk and Trentesaux 1993, Trentesaux 1993, Berné et al. 1994, Heyse et al. 1995, Stolk 1996, Trentesaux et al. 1999).

For each of these sandbanks and sub-areas a new, local stratigraphy and interpretation was proposed in these studies. Even in the framework of two large-scale comprehensive projects on the geological structure and extension of potentially exploitable near-surface sediments of the entire BCS (Maréchal and Henriet 1983, 1986), every single sandbank was given its own stratigraphic interpretation, subdivision and nomenclature, as it was – at that time– not possible to correlate the complex Quaternary structure of the different sandbanks with one another.
So, notwithstanding the amount of information available, apart from the above-cited punctual detailed studies, the available data were never processed or interpreted in an integrated, coherent way. One of the reasons for this was that it would have been a truly immense endeavour at times when seismic records were only available on paper and when e.g. tidal corrections had to be performed manually. So in the present digital era, the main goal of the presented study is to archive, integrate and (re-)interpret all existing data-sets –seismics as well as cores– in order to develop a common stratigraphy for the Quaternary deposits on the BCS and a genetic model for the Quaternary geological evolution of the area.
As the BCS appears more often in the news nowadays, on issues such as the construction of offshore windmill parks or requests for extending sand and gravel extractions permits, reliable knowledge of the nature and composition of the shallow subsurface of the BCS, which is closely related to its geological evolution, is truly indispensable.

1.2 A digital approach

In order to be capable of integrating the immense available data-sets, and to be able to correlate the Quaternary internal structure of one sandbank to another, the old, paper seismic recordings had to be translated into a digital format. Almost 30 years after their acquisition, more than 4000 km of high-resolution seismic profiles were scanned, converted into digital 'SEG-Y' format, and integrated with 1300 km of modern, digitally acquired seismic data, and with more than 600 core descriptions.

Thanks to this digital approach all available data-sets could be easily integrated into one well-organised database. On the one hand, this enabled us to get a comprehensive overview of the internal structure of the patchy Quaternary cover and to understand the interrelationships between individual sandbanks. Instead of interpreting paper seismic records of several metres length, entire seismic profiles could now be conjured up on screen in an instant, and visualised in a pseudo-3D setting.
On the other hand, thanks to the more time efficient handling of the digital seismic profiles and produced maps, the interpretation of the seismic data could now be performed in more detail, so that this re-interpretation actually offered a surplus value to former studies. Instead of creating a model for the Quaternary evolution of the entire BCS by merely combining copied interpretations of the former fragmented investigations, the old data were re-evaluated and re-interpreted in more detail in order to find well-funded arguments for more precise interpretations. Vague terminology as 'valley infilling' was avoided and could now be narrowed down to e.g. 'a tidal-channel infilling in an outer-estuarine environment'.
Finally, this study offers one more additional value, as it incorporates new seismic data, creating a denser seismic network in certain key areas.

1.3 Development of a Quaternary evolutionary model

Notwithstanding the advantages of the digital approach, it was still a challenge to develop a genetic model for the Quaternary evolution of the BCS from the fragmented and thin Quaternary record.

The foundation for the work was already laid by De Batist (1989) and Jacobs and De Batist (1996), who thoroughly investigated the Paleogene (former Tertiary) deposits, and by Liu (1990) and Liu et al. (1992, 1993), who described in detail the morphology of the Top-Paleogene (former Top-Tertiary) surface, which also represents the base of the Quaternary deposits.
The seismic-stratigraphic interpretation of the Quaternary deposits started from the centrally located Middelkerke Bank, the internal structure of which had already been largely unravelled in previous studies (Lanckneus et al. 1991, De Moor et al. 1993, Stolk and Trentesaux 1993, Trentesaux 1993, Berné et al. 1994, Heyse et al. 1995, Stolk 1996, Trentesaux et al. 1999). Soon it became clear that the surrounding sandbanks were characterised by a similar internal structure as that of the Middelkerke Bank, and this opened new perspectives for extending the seismic stratigraphy of these sandbanks to the entire BCS.
Seven seismic units were identified in the Quaternary deposits on the BCS. They are bounded by erosional unconformities. After calibration of the seismic characteristics with the core data, these seismic units could also be assigned a lithological meaning. An incised valley offshore Oostende, i.e. the Ostend Valley (Maréchal and Henriet 1983), is filled with three of these seismic units, representing three successive phases in the transgressive estuarine infilling during a relative sea-level rise. The infill is truncated at the sea bed by a ravinement surface formed by shoreface erosion and marine planation during marine transgression. On top of this regional erosional surface lies a fourth seismic unit representing tidal-flat deposits, which developed behind a coastal barrier in a back-barrier environment. On top of this unit, separated by another erosional surface, lies a fifth seismic unit, which represents storm-generated sand ridges. A sixth seismic unit is interpreted as nearshore deposits consisting of reworked material of former tidal-flat deposits. The seventh, uppermost seismic unit represents the recent tidal sandbanks and inter-sandbank swale sediments.

As no unreworked datable material was recognised in the available cores, it has thus far not been possible to obtain reliable absolute ages for these seismic units. Instead, approximate ages were inferred from their depositional depth in comparison with a known relative sea-level curve for the area (Denys and Baeteman 1995, Siddall et al. 2006). So, the seismic-stratigraphic units represent certain depositional environments in a certain time frame, separated by erosional surfaces representing important phases in the Quaternary sea-level evolution or changes in the sedimentary dynamics in response to it. These seismic units are lithologically often highly heterogeneous, but the interpretation in terms of depositional setting gives end users a good indication of which lithology can be expected in the subsurface.

1.4 Study objectives

Apart from the main goal of reconstructing the Quaternary geological evolution of the BCS, some particular problems were tackled as well.

- Regarding the timing of incision of the Ostend Valley, most specialists agreed that this most likely did not happen before Saalian time and that the deepest scouring probably took place during the Eemian transgression (Mostaert et al. 1989, Mostaert and De Moor 1989, Liu 1990, Liu et al. 1993). However, concerning the valley's infilling history, opinions differed significantly. The basal units have been interpreted as Eemian marine and Weichselian fluvial sediments (Liu et al. 1993), as Holocene valley infill (Trentesaux 1993), as Late-Weichselian to Early-Holocene estuarine deposits (Berné et al. 1994), and as Weichselian estuarine deposits (Trentesaux et al. 1999). Thanks to the extended seismic grid and previously unexploited core data reaching into the deepest seismic units, we obtained new evidence to interpret and (relatively) date these lowermost Quaternary deposits and to close this debate.

- It has often been suggested that the Ostend Valley represents the seaward extension of the paleo-drainage systems of the onshore Flemish and Coastal Valley (Mostaert et al. 1989, Liu et al. 1992). However, merging the base-Quaternary surface from offshore with the newest base-Quaternary data from onshore (Meyus et al. 2005) yielded new insights concerning the course of the Coastal Valley. Not only the morphological continuation between the Flemish, Coastal and Ostend Valley incisions was examined, but –for the first time– also the sedimentological infilling and environmental setting of the different parts of this estuarine-fluvial system were compared.

- Wartel and Vansieleghem (1985) already recognised that the evolution of the Holocene Coastal Plain must –at certain stages– have involved a part of the area that is presently offshore. This was inferred amongst other things from the absence of a coastal barrier in the eastern Coastal Plain, and the presence of peat on the modern beach of Raversijde (Wartel and Vansieleghem 1985, Baeteman 2007a). So, for the reconstruction of the entire Quaternary evolution of the BCS we strived for an integrated approach, in which our model for the evolution of the (present-day) continental shelf was developed in coherence and in agreement with the history of the (present-day) onshore (western) Coastal Plain.

- Extra attention was paid as well to the origin of the sandbanks, because relatively little was still known about the mechanisms and timing of the formation of the tidal sandbanks (seventh seismic unit) on the BCS, and the 'banks' as a whole (i.e. as a morphological feature, composed not only of the tidal sandbank deposits at the top, but also containing older units at the base). Also, the reason for the differences in orientation of the four main sandbank fields (i.e. the Hinder Banks, the Flemish Banks, the Zeeland Ridges and the Coastal Banks) still remained unclear. We formulated a few suggestions regarding the formation mechanisms (e.g. the association with a retreating coastline or not) and the coherence and continuity between sandbank fields gave an indication of a simultaneous or related origin.

- Another point of interest was the origin of extensive gravel deposits found in between sandbanks at the present-day seafloor. As the gravel fragments are too large to have been transported under the prevailing tidal currents, other origins had already been suggested in previous studies, such as the presence of river terraces (Deleu and Van Lancker 2007). This hypothesis was kept in mind, and special attention was paid to the incorporation of the gravel lags when reconstructing the Quaternary evolution of the BCS.

1.5 Thesis outline

- In the first chapter (Chapter 2) following this introduction, the geographical setting of the study area within the southern North Sea is presented, followed by a review of what was known about the Quaternary deposits and history in the Belgian part of the North Sea prior to the redaction of this thesis.

- Chapter 3 (Methodology) gives an overview of the many surveys, during which the seismic and core data were acquired. The acoustic sources used for acquiring the data are introduced, as well as the different steps in converting the analogue seismic recordings into digital SEG-Y format. The integration of the core descriptions with the seismic profiles is discussed as well.

- Chapter 4 presents the main observations, i.e. the identification and characterisation of the seven seismic units. Genetically related units were grouped and are discussed together in more detail in Chapters 6, 7 and 8. These chapters successively treat a different depositional system: i.e. an incised valley (seismic units U1-U3), a straight coastline (seismic units U4-U6), and tidal sandbanks (seismic unit U7).

- Chapter 5 deals with the unconformity that marks the base of the Quaternary deposits on the BCS (also named Top-Paleogene surface). This unconformity has been linked with that on the onshore Coastal Plain and on part of the Dutch offshore region. The chapter discusses the observed river incisions, planation surfaces and the presence of the widespread gravel lag. Also, the Quaternary isopach map is presented in this chapter.

- The oldest Quaternary deposits on the BCS are found in the incised valley offshore Oostende: i.e. the Ostend Valley. The lower three seismic units (U1- U3) jointly make up the entire infilling of the Ostend Valley, and are therefore discussed together in Chapter 6. The chapter starts with a literature review of the processes involved in the evolution of an incised valley during a sea-level cycle. After a detailed description of the three seismic units, seismic and core data are integrated and the units are interpreted as transgressive estuarine deposits. Also, the erosional surfaces bounding these units are explained in the context of this interpretation, and paleo-reconstructions are presented. A chronostratigraphic framework is presented as well, and the formation and infilling of the Ostend Valley are linked with those of the Pleistocene Flemish Valley onshore.

- The following three seismic units (units U4-U6), all three of which extend outside the incised valley over large parts of the BCS, are discussed in detail in Chapter 7. This chapter discusses the evolution of a straight coastline during the Holocene sea-level rise. The seismic units are discussed in detail, and after integration with the core data, interpreted as tidal-flat deposits, storm-generated sand ridges and nearshore reworked tidal-flat deposits. The erosional surfaces separating the different units are discussed and paleo-reconstructions are presented. The chronostratigraphic framework and Holocene evolution of the BCS are presented and linked with the history of the development of the onshore Coastal Plain. In addition, numerical-model results presenting the evolution of large-scale tidal and wind-wave conditions during the course of the Holocene (van der Molen and van Dijck 2000, van der Molen and de Swart 2001a, 2001b, van der Molen 2002), and their changing contribution to the sand supplies to the Dutch and Belgian coasts, will be interwoven with the Holocene evolutionary history of the BCS.

- In Chapter 8, the uppermost seismic unit (U7) is discussed separately, as it makes up the bulk of the sandbanks (i.e. the morphological bank-shaped features on the seafloor). U7 is the only unit that is in accordance with the present-day hydrodynamic regime (i.e. as shown by the presence of sand dunes). After a literature review of the classification and origin of sandbanks, the seismic unit is discussed in detail for each sandbank in the four different sandbank fields, and correlated with the core data. The origin and evolution of the sandbanks on the BCS are discussed, and placed in a chronostratigraphic framework.

- Chapter 9 summarises the Quaternary evolution of the BCS and presents it in a larger framework of hydrodynamic changes in the Southern Bight of the North Sea. In addition, some general remarks and thoughts are proposed regarding the dissimilarities between the coastline migration during the Pleistocene and Holocene transgressions, and the availability and origin of sediments during the discussed Quaternary period.

- Chapter 10 formulates some general conclusions and highlights the most important innovations of the newly developed Quaternary evolutionary model.

2.
Geographical and general geological setting

Owing to its rather unique position in the southern North Sea basin just past the narrow passage of the Strait of Dover, the Belgian Continental Shelf (BCS) is characterised by strong tidal currents and the presence of prominent sandbank fields. This fact makes the BCS not an easy target for conducting seismic surveys or coring campaigns, as manoeuvring over and between shallow sandbanks against strong currents, or coring in thick packages of sand, is no small feat. Frequent storms and strong winds further complicate ship-based research in the area.

2.1 The North Sea

2.1.1 Geography

The North Sea is an epicontinental shelf sea located between the European continent, the Scandinavian peninsula and Great Britain (Fig. 2.1AB). It opens into the Atlantic Ocean via the narrow Strait of Dover (only 40 km wide) and the English Channel in the south, and into the Norwegian Sea in the North. It is commonly sub-divided into the relatively shallow southern North Sea (including e.g. the Southern Bight and the German Bight), the central North Sea, the northern North Sea, the Norwegian Trench and the Skagerrak. The North Sea continental shelf is more than 1000 km long, its surface area is 575,000 km², and the water volume is estimated at 54,000 km³ (De Moor 1986). The depth of the North Sea is 94 m on average, but increases towards the Atlantic Ocean to about 200 m at the edge of the continental shelf. The area south of the Texel Spur and Norfolk banks, i.e. the Southern Bight (Fig. 2.1C), consists of the Deep Water Channel (up to 50 m) in the west, which is connected to the Strait of Dover to the south, and of a shallow area (10-30 m) in the east (van der Molen and de Swart 2001a). The English Channel is relatively shallow as well: from a depth of about 30 m in the Strait of Dover it deepens gradually to about 100 m in the west. Seabed topography shows evidence of river-valley systems that were carved into the seabed during glacial periods when sea level was lower (OSPAR 2000), e.g. the Deep Water Channel (De Moor 1986). At present, some important rivers discharge into the North Sea. They provide a steady input of freshwater, but they supply relatively low amounts of sediment (Beets and van der Spek 2000).

2.1.2 Geology

The North Sea shelf area is underlain by a continental rift depression of Mesozoic age with a general north-south axis. This depression is covered with Mesozoic and Cenozoic post-rift deposits, several kilometres thick and originating from the surrounding land masses (e.g. Scandinavia, Black Forest and Vosges, the Alps). During the Quaternary, multiple invasions of Scandinavian and Scottish ice sheets spread over the northern and central parts of the North Sea (De Moor 1986, OSPAR 2000). This process was associated with large changes in sea level and in supply of additional sediment into the North Sea basin. It was also responsible for shaping the general style of the present-day underwater topography. During the last glacial maximum, sea level was ca. 120 m lower than today, and considerable parts of the North Sea were exposed.
During glacial stages, large rivers such as the Thames, Meuse and Rhine traversed the southern North Sea basin. They were blocked to the north by the ice sheet and forced to discharge through the Strait of Dover towards the English Channel (Smith 1985, Bridgeland and D'Olier 1995). These rivers carried large amounts of sediments into the southern North Sea Basin. On the Belgian Continental Shelf, most of the Pleistocene sediments originate from the discharge of the Rhine-Meuse system and the Flemish Valley (i.e. the paleo-Scheldt-Lys system) during these periods (Houbolt 1968).

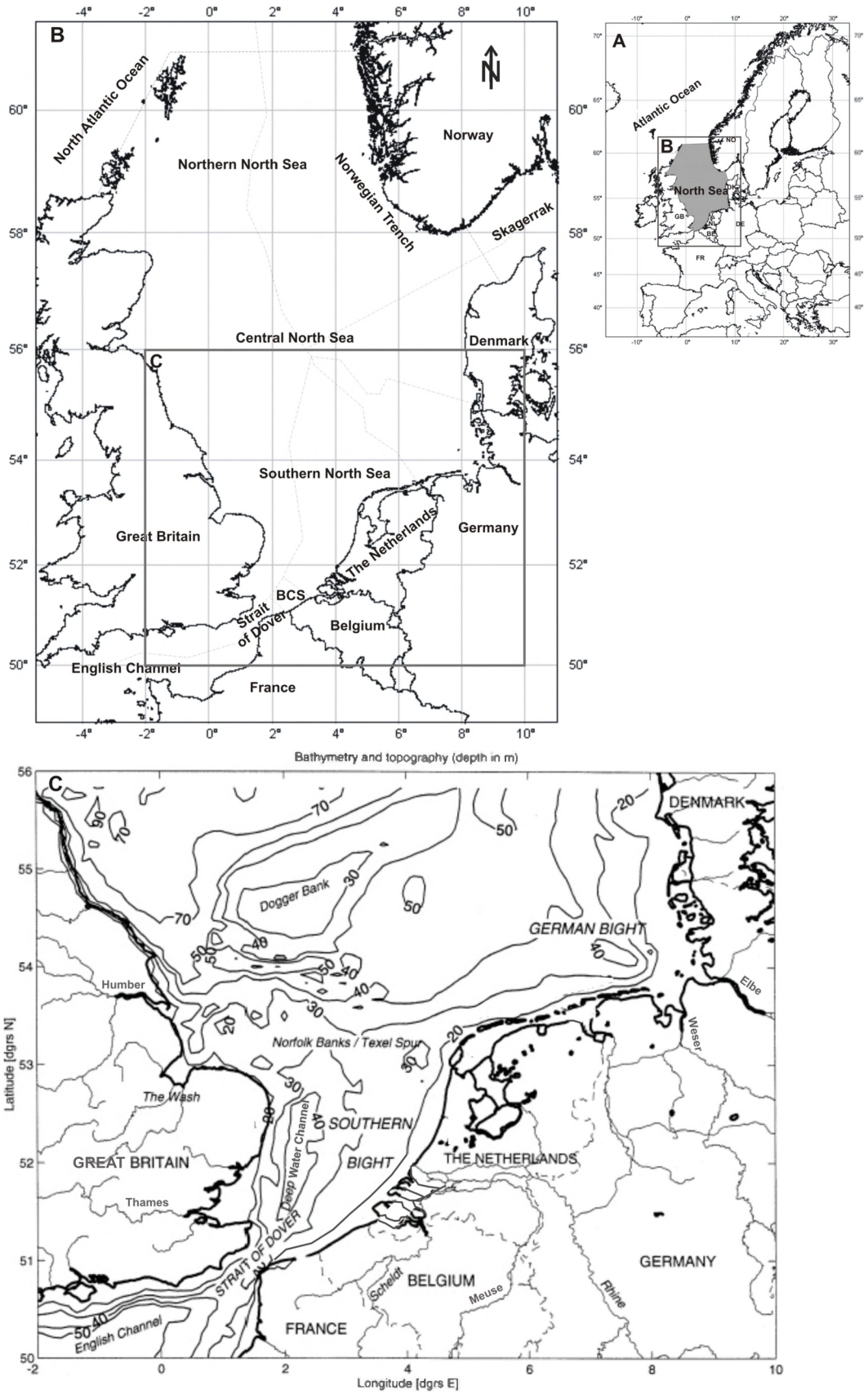

Fig. 2.1 (A) Geographical situation of the North Sea in north-western Europe as an inland sea of the Atlantic Ocean; (B) division of the North Sea continental shelf with indication of the Belgian Continental Shelf (BCS); (C) bathymetry (contour lines, m below mean sea level) of the southern North Sea (after van der Molen and van Dijck 2000). [Geographic Projection WGS84]

The blocking of the rivers in the north by ice sheets during the Elsterian and Saalian ice ages induced the formation of proglacial lakes (Gibbard 2007, Gupta et al. 2007, Busschers et al. 2008). It is believed that the torrential overflow of the proglacial lake formed during the Elsterian Glaciation (MIS12), some 425,000 years ago, eroded the Weald-Artois anticlinal ridge and formed the initial Strait of Dover (Gibbard 2007, Gupta et al. 2007). The level of the lake was about 30 m above today's sea level (Gibbard 2007). A second proglacial lake could develop during the Saalian Glaciation due to a coalescence of the Scandinavian and British ice in the central North Sea area, and the presence of a ridge north of the Dover Strait (possibly an outcrop of bedrock, or a moraine formed during the previous glaciation (Gibbard 2007). The Saalian proglacial lake reached heights similar to the present mean sea level (Busschers et al. 2008).

2.1.3 Sedimentology

The present-day distribution of seafloor sediments reflects the succession of depositional and erosional events during the Pleistocene and early post-Pleistocene periods. The northern North Sea is a classic example of an area of palimpsest deposits, consisting of reworked sediments supplied from within the shelf environment (Jacobs 2000). In addition, most of the Holocene sand in the southern North Sea is reworked from Pleistocene deposits (Beets and van der Spek 2000). At present, the rivers surrounding the Southern Bight only carry suspended matter to their mouths. And this was not much different during most of the Holocene, as bed load and part of the suspended load was being deposited in the alluvial plains to fill up the space created by the rapidly rising sea level (Beets and van der Spek 2000).

Relative sea level started to rise from the end of the last glaciation until about 6000 BP (7000 cal BP) (van der Molen and de Swart 2001a). Since then there have been only relatively minor changes. The resulting hydrographic circulation, as well as the wave and tidal regime, created the sedimentary dynamics and the sediment-distribution pattern seen today. Mainly sand and gravel deposits occur in the shallower areas and fine-grained muddy sediments accumulate in depressions (OSPAR 2000). In the Southern Bight, the sea-bed sediments consist mainly of fine to medium sands, with substantial gravel content along the British coast and in the Strait of Dover. The sands grade to silts and clays south of the Dogger Bank and toward the German Bight (van der Molen and de Swart 2001a, 2001b). The sea-bed sands show a general fining trend toward the northeast (van der Molen and de Swart 2001a). Tidal flats, such as those in the Wadden Sea, receive their sediments directly or indirectly from rivers and from adjacent North Sea areas. The suspended particulate matter settles to form either sandy or muddy sediments, according to its composition and the predominant local hydrodynamic conditions (OSPAR 2000).

2.1.4 Coastlines

The coastlines of the North Sea display a large variety of landscapes arising from differences in geology and vertical tectonic movements. In the OSPAR Commission 'Quality Status Report 2000' we read that the disappearance of the weight of the ice cover after the last glacial stage has led to the vertical uplift of the northern coastlines. The coastlines of Norway and northern Scotland are mountainous with many rocky islands, and are often dissected by deep fjords. The coasts of northern England and Scotland feature cliffs of various sizes, some with pebble beaches, but also intersected by river valleys. The eastern coast of England is characterised by estuaries such as those of the Humber and Thames, and by further expanses of sand and mud flats in areas such as the Wash. From the Strait of Dover to the western Danish coast, sandy

coastal barriers with extensive back-barrier basins prevail, with numerous estuaries (e.g. Scheldt, Rhine, Meuse, Weser and Elbe, Fig. 2.1C) and the tidal inlets and barrier islands of the Wadden Sea (OSPAR 2000).

2.1.5 Tides, waves, currents, wind

Tides in the North Sea result from the tidal waves in the Atlantic Ocean. The resulting oscillations propagate across the shelf edge, entering the North Sea both from the north and through the English Channel. Semidiurnal tides predominate. Fig. 2.2 shows the amplitude and phase of the tidal wave relative to the moon over Greenwich. Tidal currents represent the most energetic hydrologic process in the North Sea, stirring the entire water column in most of the southern North Sea and the English Channel (OSPAR 2000). Along the coasts, tidal currents are oriented parallel to the coastline and the exchanges between coastal (taken to be 20 km wide) and offshore waters are limited (OSPAR 2000). In the southern parts of the Southern Bight, maximum surface currents at spring tide are 1 m/s; they decrease to 0.7 m/s in the northern part and along the Dutch coast (van der Molen and de Swart 2001a, 2001b). More to the north and into the German Bight, the current velocities decrease even further (van der Molen and de Swart 2001a, 2001b).

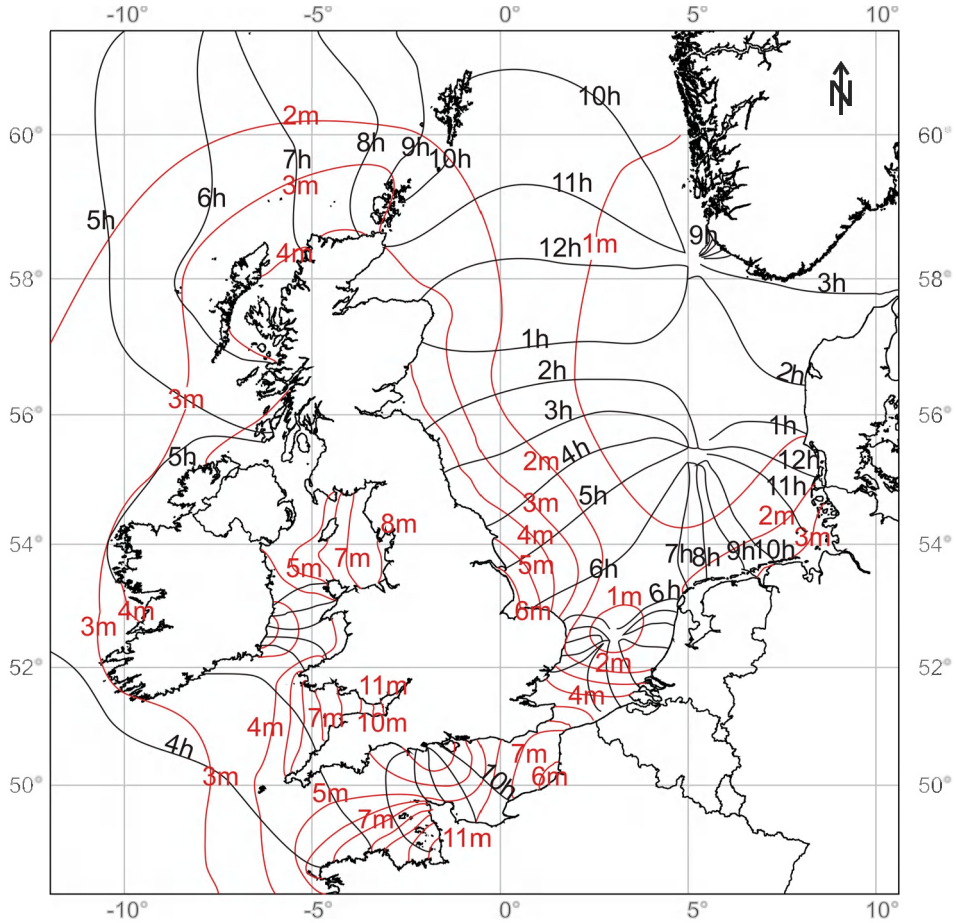

Fig. 2.2 Mean spring-tidal range (co-range lines in m) and co-tidal lines at time intervals referred to the time of the moon's meridian passage at Greenwich (OSPAR 2000). [Geographic Projection WGS84]

Apart from tides, the hydrodynamics and the sand-transport processes in the North Sea are also influenced by wind waves, wind-driven currents and density-driven currents. In the Southern Bight, wind waves can attain significant heights of up to 9 m. Significant wave heights are larger towards the north: up to 18 m in the central North Sea. Dominant wave directions are from the north and southwest, the largest waves coming from the north. General swell directions are from the north to northwest (van der Molen and de Swart 2001a).

2.2 The Belgian Continental Shelf

2.2.1 Geography

The BCS extends to about 65 km from the present-day coastline (65 km long), covering an area of about 3500 km². The sea-floor topography is characterised by the presence of sandbanks and swales (Fig. 2.3). In the swales, water depths can reach 30-40 m MLLWS (level of mean lowest low water at spring tide), whereas in the nearshore area minimal depths of less than 5 m can occur. The sandbanks can be tens of kilometres long, one to several kilometres wide, and up to 20 m high. They are mostly asymmetric in cross-section and their plan view commonly shows kinks. On the basis of their position and orientation they are grouped in the Coastal Banks, the Flemish Banks, the Zeeland Ridges and the Hinder Banks (Fig. 2.3). The Coastal Banks and the Zeeland Ridges are located quasi parallel to the coastline, whereas the Flemish and Hinder Banks are clearly oblique with respect to the coastline. The sandbanks display angles of 0-20° relative to the main axis of the tidal ellipse (Kenyon et al. 1981). In the offshore area, large dunes (2-8 m high) are also present, mostly superimposed on the sandbanks (Lanckneus et al. 2001). Closer to the coast, their occurrence is more restricted and the sandbanks are generally devoid of bedforms.

2.2.2 Quaternary geology of the BCS: a state of the art

The Top-Paleogene unconformity

The substratum of the BCS is composed of strata of various ages. The Paleozoic basement is formed by the relatively stable continental block of the Anglo-Brabant Massif, found at a depth of about -250 m (MLLWS) near the French border to -450 m near the Dutch border. It is overlain by a layer of chalk of Late-Cretaceous age, which is now found at a depth of about -150 to -350 m, dipping toward the NE (De Batist 1989). Paleogene deposits make up the upper part of the substratum, locally outcropping in between the discontinuous cover of Quaternary sediments. They were mainly deposited during the Thanetian to Rupelian, and they occur at a depth of -10 to -60 m (MLLWS), dipping in offshore direction (De Batist 1989).

The substratum is separated from the overlying Quaternary cover by a distinct angular unconformity. This erosion surface truncates the NE-dipping Paleogene strata and forms the base of the Quaternary deposits. This unconformity is diachronous and was probably formed in marine as well as fluvial circumstances over a long period of time and under the influence of a series of climatic changes (Mostaert et al. 1989). It is characterised by a distinct morphology (Liu et al. 1992, 1993). One of the most striking features is a major incised valley structure offshore Ostend, which was observed for the first time by Maréchal and Henriet (1983), who called it the 'Ostend Valley' (Fig. 2.4). Isolated sediment-filled depressions were observed in the centre of this incised valley,

comparable with depressions found in the present-day Western Scheldt estuary. They were interpreted as scour hollows, and the deepest were called the 'Sepia Pits' (Mostaert et al. 1989). It was believed up to now, that the Ostend Valley represents the seaward extension of the paleo-drainage systems of the onshore Flemish and Coastal Valley (Mostaert et al. 1989), and formed the link to the major Axial Channel in the Southern Bight in the North Sea (which corresponds to the present-day Deep Water Channel), via the Northern Valley (Liu et al. 1992) (Fig. 2.4). Apart from incised valleys, other morphological features can also be observed in the relief of the Base-Quaternary unconformity. The surface does not dip smoothly in offshore direction from below the Coastal Plain, but it rises first to form a kind of platform and then slopes down in basinward direction via a few well-defined planar elements. These planar elements are planation surfaces bounded by slope breaks, scarps, or ridges, defined and described by Mostaert et al. (1989), Liu (1990) and Liu et al. (1992, 1993) (Fig. 2.4).

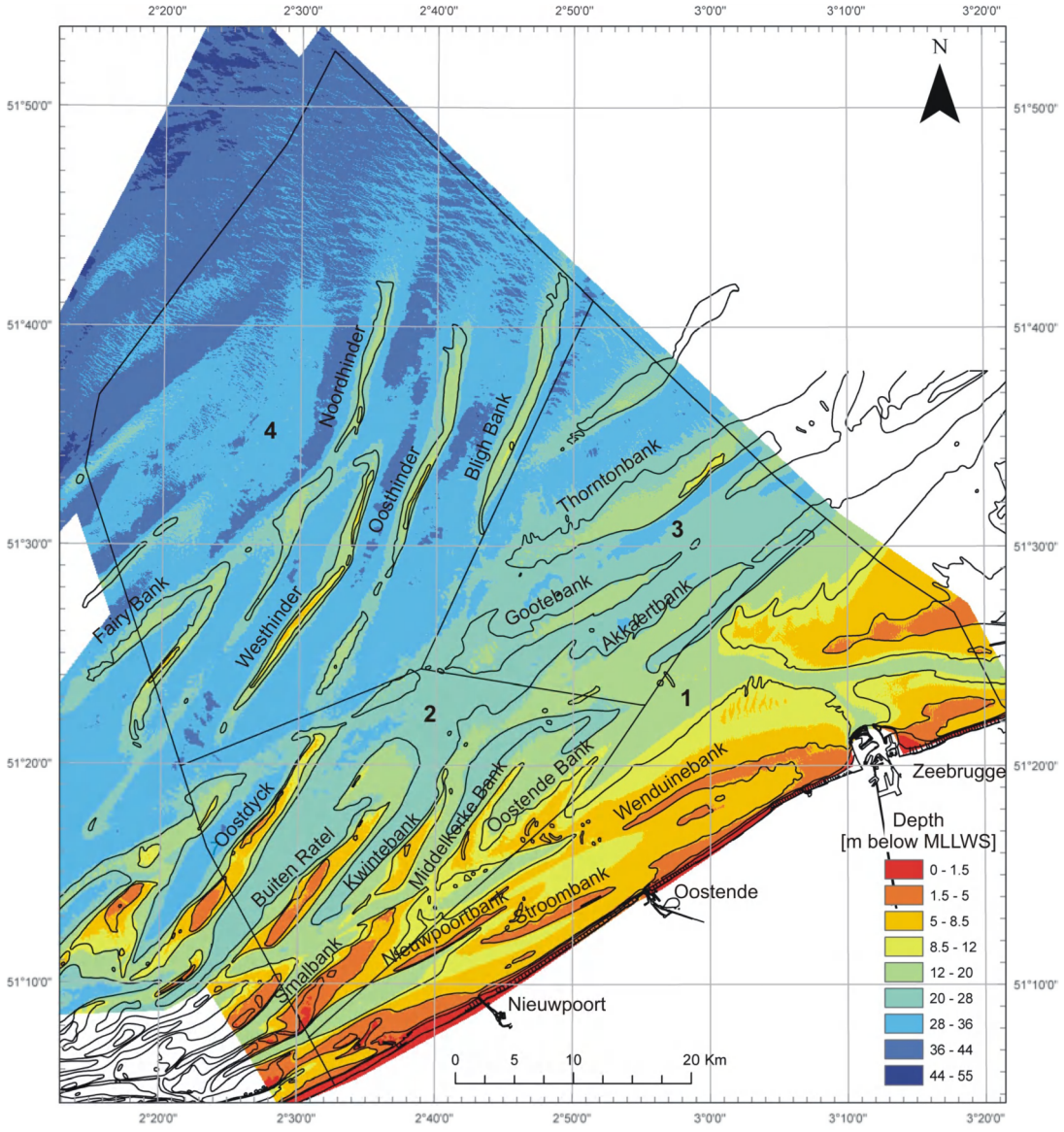

Fig. 2.3 Bathymetry of the Belgian Continental Shelf (m below MLLWS), based on single-beam echosounder data from the Ministry of the Flemish Community AWZ-WWK, completed with data from the Dutch and English Hydrographic Offices (compilation: Van Lancker et al. 2007). The sandbanks are grouped in: (1) Coastal Banks, (2) Flemish Banks, (3) Zeeland Ridges, and (4) Hinder Banks. [Geographic Projection ED50]

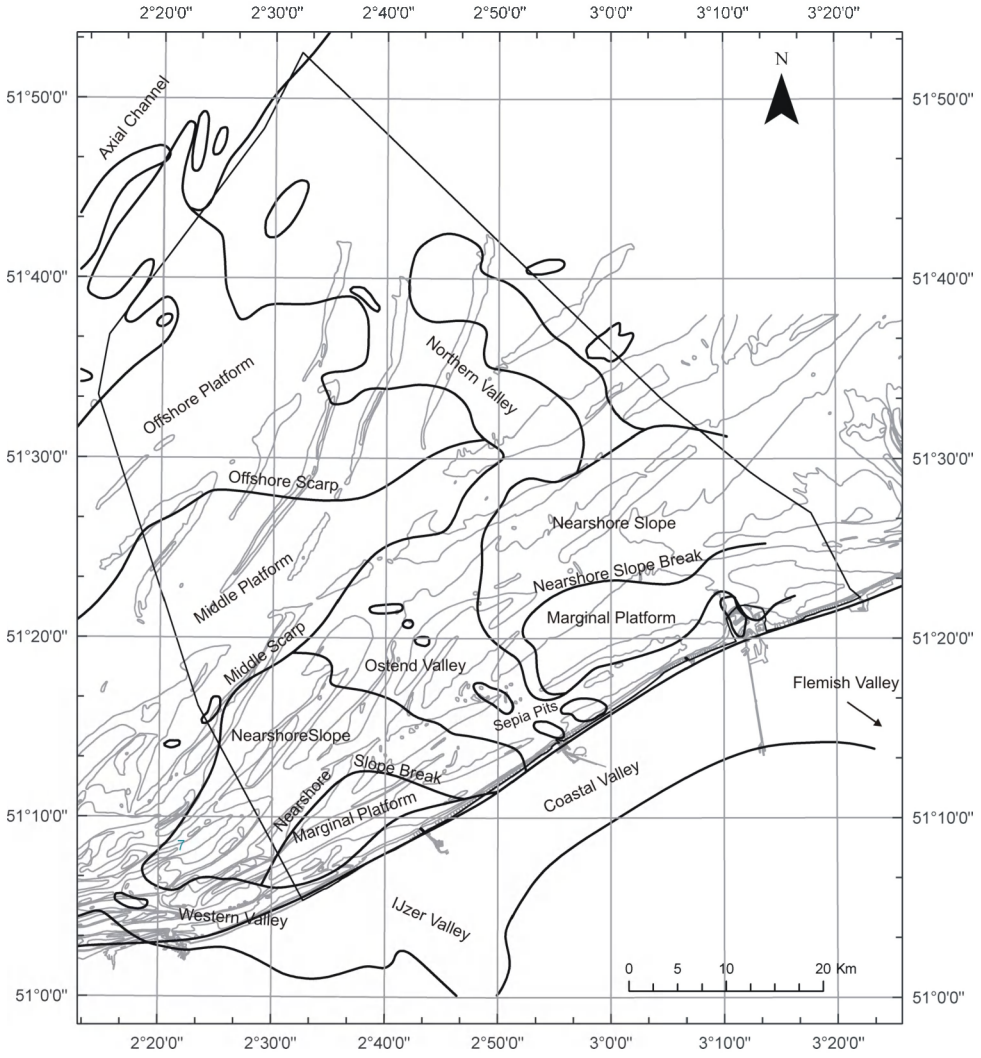

Fig. 2.4 Morphology of the Top-Tertiary surface (after Liu et al. 1992, 1993) on the Belgian Continental Shelf. For orientation purposes the present-day bathymetry is given in grey. [Geographic Projection ED50]

Owing to the depth of the incised valley, only a very limited number of drillings reached the valley floor, which made it impossible to date the infilling sediments. Consequently, it was still uncertain up to now when exactly the Ostend Valley was incised into the Paleogene substratum, and there was still considerable disagreement about the age and nature of the infilling sediments.

Maréchal and Henriet (1983) differentiated at least two incision phases, based on the presence of two distinct slope breaks in the steep wall of the incised valley; however, they were unable to date these stages. Based on the fact that fluvial incision in the Belgian Coastal Plain and Flemish Valley did not reach similar depths until Saalian times, an age older than Saalian was excluded (Mostaert et al. 1989, Mostaert and De Moor 1989). In the eastern Coastal Plain, the maximum deepening took place during the Eemian period, when the sea invaded the incised Coastal Valley. This may also be the age of the deepest scouring of the Ostend Valley and of the Sepia Pits. It has been suggested that the scour hollows were formed by tidal scouring during the early stages of the Eemian transgression when the sea invaded the area along the pre-existing fluvially incised valleys (Mostaert et al. 1989, Liu 1990, Liu et al. 1993). While Trentesaux (1993) proposed cautiously that the Ostend Valley could have been formed during the Weichselian, he did not rule out that it could have been shaped since the Saalian.

The planation surfaces observed in the base-Quaternary unconformity probably bear the stamp of marine abrasion processes, which must have played an active relief-forming role in periods of rising sea level during the Quaternary (Maréchal and Henriet 1983). Moreover, the several slope breaks separating these planation surfaces argue for a multi-phase erosional process. According to Mostaert et al. (1989), the age of the northward-dipping abrasion surface can be attributed to the Eemian, on the basis of paleo-geographic considerations. They stated that most of the area offshore Belgium has been dry land since Early-Pleistocene times. Some marine sedimentation took place in the southwest of the BCS during brief episodes during the Middle-Pleistocene interglacial stages (Paepe and Baeteman 1979, Sommé 1979), but it was only during the Eemian and the Holocene that the entire area became fully submerged (Kirby and Oele 1975, Mostaert et al. 1989). However, Liu et al.'s (1992) 'Offshore Scarp' and related 'Offshore Platform' (Fig. 2.4) had most likely already formed during Saalian time, as Kirby and Oele (1975) encountered Eemian and Weichselian deposits in a 'Quaternary Basin', which corresponds exactly to the region later identified as the Offshore Platform, located downslope of the Offshore Scarp (Liu et al. 1992). Also, Van den Broeke (1984) inferred the presence of open-marine Eemian deposits under the Hinder Banks in the area bounded by the Offshore Scarp.

The Quaternary evolution of the Belgian Continental Shelf

A possible age for the Ostend Valley infilling

Most specialist agree that the incision of the Ostend Valley and the formation of the scour hollows in the valley floor did probably not happen before Saalian time and that the deepest scouring could have occurred during the Eemian transgression. However, with regard to the infilling history of the Ostend Valley, opinions differ significantly.
Liu et al. (1993) observed two horizontal seismic reflectors at two different levels within the sedimentary infill of the Ostend Valley, and interpreted them as an expression of three different stages of infill. By analogy with findings in the Coastal Plain (Mostaert et al. 1989), they proposed an Eemian age for the sediments below the lower reflector (at the same level as the valley floor), a Holocene age for those above the upper reflector, and a Weichselian age for the intervening sediments, even though Mostaert et al. (1989) stated that in the Coastal Plain, Eemian deposits are commonly directly overlain by Holocene deposits.
Trentesaux (1993) and Berné et al. (1994) on the other hand, studied the internal structure of the Middelkerke Bank and proposed that the lower units, which make up the base of the Ostend Valley infill, are of Holocene age. They surmised, referring to Jelgersma et al. (1979) and Paepe and Baeteman (1979), that most of the Pleistocene deposits offshore the Belgian coast had been completely reworked during the last transgression and had become incorporated in the Holocene deposits. However, these two cited studies dealt specifically with the Dutch part of the North Sea and with the Belgian Coastal Plain, respectively, and not with the BCS. Paepe and Baeteman (1979) even state that marine deposits of Eemian age are present all over the eastern Belgian Coastal Plain.
Later, based on new ^{14}C ages obtained from juvenile marine shells, the age of the lower units in the Ostend Valley (underneath the Middelkerke Bank) was reconsidered. They were assigned a Middle-Weichselian age, and the overlying tidal-flat deposits were dated as Holocene (Stolk 1996, Trentesaux et al. 1999). These ^{14}C ages were, however, rather controversial. Stolk (1996) noted that the presence of non-reworked marine shells of Weichselian age in this area is rather remarkable, because at that time sea level was always more than 35 m below the present one (Streif 1990), whereas the dated samples were collected at depths of less than 27 m below present mean sea level.

Four phases in the Quaternary evolution of the Middelkerke Bank

Since the seismic-stratigraphic interpretation of the Quaternary deposits started from the centrally located Middelkerke Bank, as this sandbank is the best studied and best ground-truthed (Lanckneus et al. 1991, De Moor et al. 1993, Stolk and Trentesaux 1993, Trentesaux 1993, Berné et al. 1994, Heyse et al. 1995, Stolk 1996, Trentesaux et al. 1999), its internal structure (Fig. 2.5) and lithological characteristics are presented below. Regardless of the remaining uncertainties about their age, four main depositional phases following the last phase of valley incision were distinguished in the Middelkerke Bank, and might serve as a model for the infilling of the entire Ostend Valley: i.e. (1) valley infilling; (2) deposition of sub-tidal or tidal-flat deposits; (3) the construction of initial ridges or coastal banks; and (4) the development of tidal sandbanks.

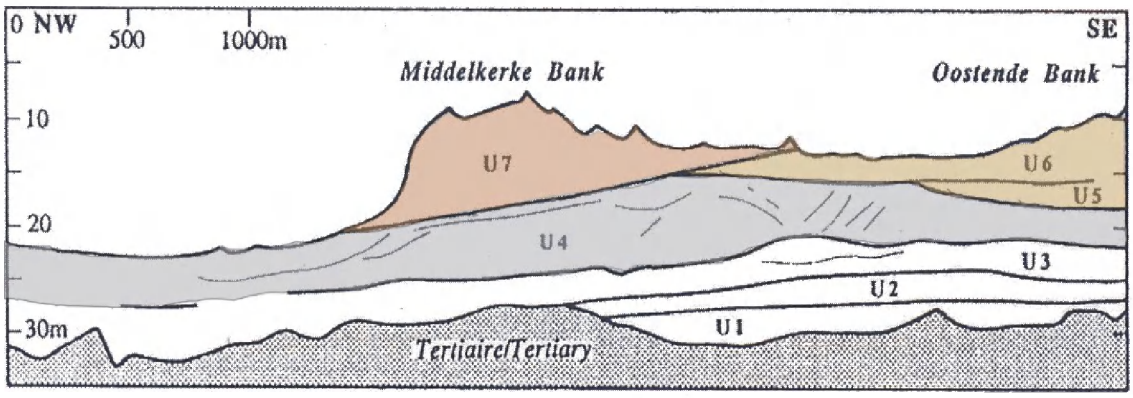

Fig. 2.5 Interpreted seismic profile of the Middelkerke and adjacent Oostende Bank showing the four depositional phases in the evolution of the Belgian Continental Shelf (adapted after Berné et al. 1994). U1, U2 and U3 represent the first phase after the stage of incision, the channel infilling; U4 represents deposition of subtidal or tidal-flat deposits; U5 and U6 are interpreted as nearshore storm-dominated sandbars; and U7 corresponds to the actual tidal sandbank.

During the first stage, an estuarine or tidally influenced environment developed inside the Ostend Valley, documented by the high humic content of the sediments filling in the scour hollows and incisions below the Middelkerke Bank (De Batist et al. 1993, De Moor et al. 1993, Liu et al. 1993, Trentesaux 1993, Trentesaux et al. 1993a, Trentesaux et al. 1993b, Trentesaux et al. 1999). Most common in the succession in the Middelkerke Bank (represented by Trentesaux's seismic units U1, U2 and U3) are beige to grey quartzitic sands, which show a gradual upward-increasing content of sea-urchin debris, and clay-silt-sand intercalations. Some shell layers and gravel lags occur also, especially along the base-Quaternary unconformity.

The available information from the Middelkerke Bank suggests that the second phase corresponds to a lagoonal or tidal-flat environment (seismic unit U4 in the Middelkerke Bank), possibly behind a coastal barrier (Trentesaux 1993, Trentesaux et al. 1993b, Berné et al. 1994, Heyse et al. 1995, Stolk 1996, Trentesaux et al. 1999). All authors agree on a Holocene age. The deposits are characterised by a very heterogeneous lithofacies, mainly consisting of clays, clay-silt-sand intercalations, and bioclastic sands. At the base, locally a gravel lag is present, which highlights the strong erosional processes that prevailed before or during the deposition of this unit.

On the basis of sedimentological and architectural features observed in the Middelkerke Bank, a third phase is thought to correspond to the formation of coastal sandbanks (seismic units U5 and U6 in: Trentesaux 1993, Trentesaux et al. 1993b, Berné et al. 1994, Heyse et al. 1995, Stolk 1996, Trentesaux et al. 1999). This phase is characterised by grey quartzitic sands and a high content of sea-urchin debris, which clearly marks the onset of fully marine conditions (Trentesaux et al. 1999).

With continuing rising sea level, these initial banks finally became isolated on the shelf and were subsequently capped by tidal sandbanks, i.e. the fourth phase (De Batist et al. 1993, De Moor et al. 1993, Liu et al. 1993, Trentesaux 1993, Trentesaux et al. 1993a, Trentesaux et al. 1993b, Trentesaux et al. 1999). This upper unit is shaped by modern processes and consists in the Middelkerke Bank of brown bioclastic sands (represented by seismic unit U7). Highly bioturbated, slightly bioclastic sand occupies the deepest zones and very shelly coarser sand occurs in the shallowest zones of the bank, which is in agreement with the present-day hydrodynamic conditions (Trentesaux et al. 1999). At the base, a lag deposit, containing shells and gravel, shows that these tidal sandbanks erosively overlap the underlying units (Stolk 1996).

At least some of these phases have been recognised in neighbouring sandbanks, but have never been correlated or (relatively) dated to create a common stratigraphy or a genetic model for the Quaternary geological evolution of the area.
In one of the first studies on the internal structure of the Kwintebank (De Moor 1985a, 1985b) it was already suggested that shallow river valleys on the exposed early Holocene continent gradually changed into an estuarine and peri-marine environment, which subsequently evolved into a tidal-flat area, also occupying the low interfluves. This series of events might correspond to phase 2 in the Middelkerke Bank.
Although not discerned in the Zeeland Ridges on the BCS (i.e. Thorntonbank, Akkaertbank and Goote Bank; Maréchal and Henriet 1986), 'initial ridges' similar to the ones from phase 3 in the Middelkerke Bank, were observed in the Zeeland Ridges on the Dutch continental shelf, where they consist of bluish-grey very fine sands (Laban and Schüttenhelm 1981).
As in the Middelkerke Bank, the Zeeland Ridges show brown medium sands as well (phase 4), erosively overlying the bluish-grey initial ridges (Laban and Schüttenhelm 1981). The presence of this erosive contact was already suggested by Houbolt (1968) since a colour transition between the two units is missing. The Nieuwpoort Bank also shows two stages in the development of the bank (De Maeyer et al. 1985), but no attempt was ever made to stratigraphically link these banks.
Nevertheless, several authors tried to deduce the origin and formation mechanisms of these sandbanks. E.g. Laban and Schüttenhelm (1981) suggested a Dover Strait origin for the sands making up the Zeeland Ridges, whereas Stride (1989), De Moor (1985a, 1985b) and Houbolt (1968) suggest a more local source for the Hinder and Flemish Banks. More details on this subject follow in the relevant Chapter 8.

2.2.3 Sedimentology

The North Sea is the best example of a tide-dominated autochthonous shelf (Davis 1992). It has a high tidal-current energy and displays great variety and complexity in its sediment patterns. 'Autochthonous shelves' are those on which sediment already present on the shelf is reworked and redistributed to equilibrate with existing conditions. This in contrast to allochthonous shelves, which derive their sediment from other adjacent environments, typically via rivers.
Apart from classification on the basis of process regime, shelves can also be classified according to stratigraphic architecture, which is determined by the balance between sediment supply (quantity and texture of sediment input) and creation of accommodation

space (i.e. the sum of subsidence, eustatic sea-level change, and degree of sediment bypassing to the slope) (Swift et al. 1991, Galloway and Hobday 1996). Autochthonous settings are typically characterised by an accommodation-dominated configuration. This means that the creation of accommodation space is larger than the sediment supply (Swift et al. 1991, Galloway and Hobday 1996). Even though the BCS is a relatively stable area, not affected by tectonic or (glacio)isostatic subsidence or uplift (D'Olier 1981, Kiden et al. 2002, Vink et al. 2007), and though no sediment bypassing is possible because of the absence of a distinct shelf break in the Southern Bight, the relatively small accommodation space created by the eustatic sea-level rise during the interglacials of the Quaternary was still larger than the available sediment, which induced a transgressive stratigraphic architecture. High accommodation/supply ratios induce a high reworking ratio which involves that the sediment is repeatedly resuspended before final burial (Galloway and Hobday 1996). This is what made the Quaternary sediments on the BCS to be so thin and spatially fragmented.
Also the Dutch shelf is an autochthonous shelf, but there the Quaternary cover is locally more than 600 m thick because of the tectonic setting. The Quaternary sediments accumulated in a linear through corresponding to the Central Graben of Mesozoic and Tertiary age (Caston 1977).

The Quaternary sediments of the BCS are characterised by a laterally as well as vertically complex and heterogeneous facies assemblage, which makes lateral correlation difficult. Nature and sorting of the surficial sediments are, however, related to the configuration of the sandbank-swale systems. The sand fraction (0.063-2 mm) preferentially takes part in the up-building process of sandbanks, while the coarser sands, gravels (> 2 mm) and the silt-clay fraction (< 0.063 mm) are mostly restricted to the swales. On the scale of the BCS, the surficial sediments generally coarsen in offshore direction (Lanckneus et al. 2001).

2.2.4 Tides, waves, currents, wind

A semi-diurnal macro-tidal regime prevails on the BCS, with a tidal amplitude of less than 4 m at neap tide and more than 5 m at spring tide. The SW-NE oriented flood current (> 1 m/s) is dominant and causes a residual flow in NE direction (Beets and van der Spek 2000). In the near-coastal zone, the tidal-current velocities reach their maximum value (0.6-1.2 m/s) during the flood (NE). The maximum current velocity offshore (0.8-1.4 m/s), along the Hinder Banks, is in the ebb direction (SW) (Lanckneus et al. 2001). The wind and wave climate is dominated by a SW to NW direction, and the main significant wave height at the shore is 0.5 to 1 m, with a 3.5-4.5 s wave period (Van Lancker 1999).
Evolutionary changes of large-scale tidal and wind-wave conditions during the Holocene, and their changing contribution to the sand transport have been modelled by van der Molen and van Dijck (2000), van der Molen and de Swart (2001a, 2001b) and van der Molen (2002), and results will be presented later (cf. Chapter 7 and 10).

3. Methodology

Since the end of the '70's and beginning of the '80's the BCS has been intensively surveyed in the framework of several national and international projects. This resulted in one of the densest regional seismic grids of the world. More than 16,000 km of high-resolution seismic profiles are available in the data files of the Renard Centre of Marine Geology (RCMG). But, notwithstanding the large amount of information available, apart from some detailed studies, the available data were never processed or interpreted in an integrated and coherent way. One of the reasons for this was that it would have been a truly immense endeavour at times when seismic records were available only on paper and when e.g. tidal corrections had to be performed manually. Thanks to currently available digital technologies, a large part of these paper seismic records could be digitised and imported in an interpretation workstation together with more recent, digitally recorded data. In addition, an extensive series of cores and core descriptions, which were acquired over the years and are stored in the repository of the Geological Survey of Belgium (GSB), could be added to this data base and could be used to ground-truth the seismic data.

3.1 Seismic data

3.1.1 Acquisition: seismic surveys

This study is based on an extensive geophysical data set that has been acquired during many cruises conducted between September 1980 and April 2007, on board of research vessels Belgica, Mechelen, Sepia II, Spa, and Bellini (overview list, Table 3.1). The seismic grid consists of 496 high-resolution single-channel reflection seismic profiles covering the entire BCS in an area of 3500 km² (overview map Fig. 3.1). Within 30 km from the coastline, the network is densest.
The seismic data were acquired with different types of seismic tools. Over the years, four types of sparker sources (i.e. the 'Xmas', 'Centipede', 12-electrode and SIG sparkers) and two types of boomer sources (i.e. the 'Seistec' and 'Uniboom') were used (Table 3.2, Fig. 3.2). The 'Xmas' and 'Centipede' sparkers produce a seismic signal with a peak frequency of 1100-1200 Hz, corresponding to a theoretical vertical resolution of about 35 cm (Rayleigh criterion). Operated at 300 J, these sparker signals can penetrate 50 m below seafloor (bsf) in sandy sediments (Fig. 3.3A, B, E). The two other sparker sources (12-electrode and SIG) are characterised by a lower peak frequency of 800-900 Hz, corresponding to a theoretical resolution of about 50 cm (Rayleigh criterion) and a penetration depth of 80 m bsf in sandy sediments (Fig. 3.3D). A single-channel streamer, composed of 8 hydrophones and with a length of 4.5 m was used as receiver.

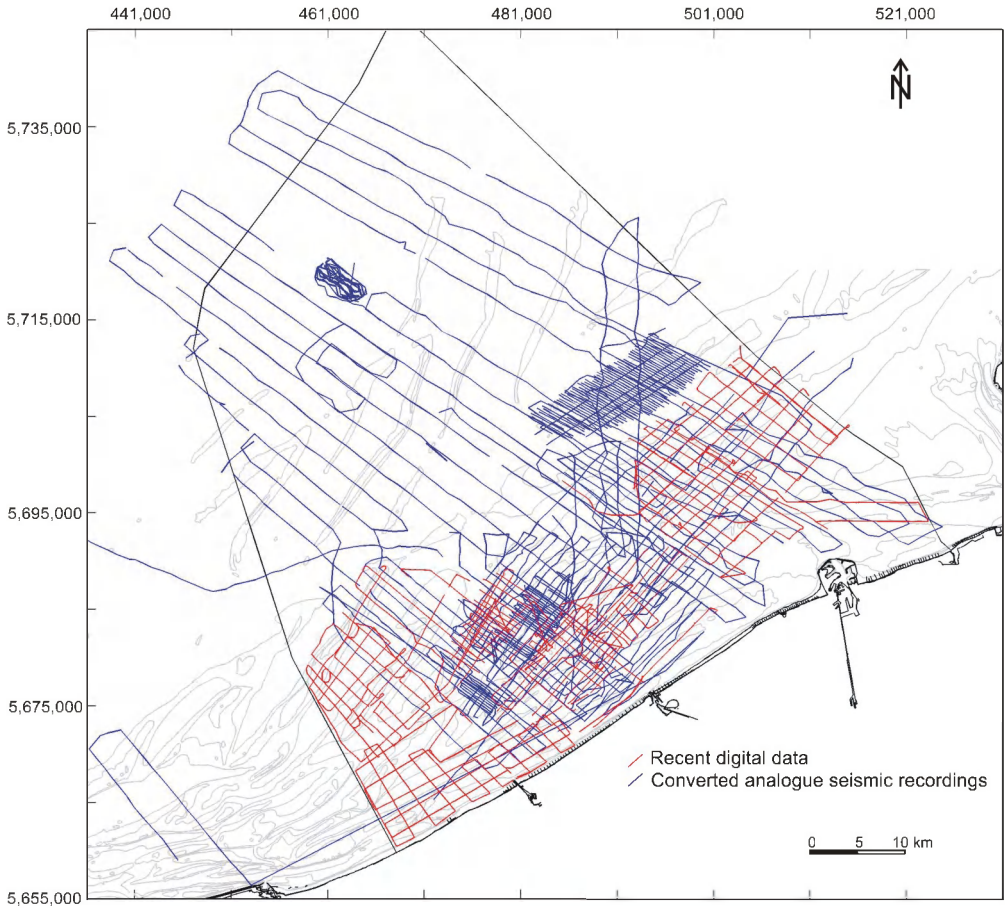

Fig. 3.1 Overview map of applied seismic network. More than 4,000 km of old high-resolution single-channel reflection seismic profiles (blue) were integrated in an interpretation workstation together with 1300 km of recent seismic data (red). [UTM WGS84]

Seismic survey	Period	Ship	Seismic profiles	Applied seismic equipment	Navigation	Total length used profiles (km)
SS	20/09/1980 - 22/09/1980	RV Mechelen, Spa.	SS01-SS08	X-mas sparker	DECCA Logbook	100,3
	26/10/1980 - 31/10/1981	Alkaid. John Murray.		X-mas sparker	DECCA Logbook	
	03/06/1981 - 07/06/1981	Sepia		X-mas sparker	DECCA Logbook	
Mijnwezen	28/04/1982 - 29/04/1982	RV Mechelen	MW01-MW26	X-Mas sparker	DECCA Logbook	451
	01/07/1982 - 08/07/1982	RV Sepia II		X-Mas sparker	DECCA Logbook	
	22/02/1983 - 25/02/1983	RV Spa		X-Mas sparker	DECCA Logbook	
BIMGO	15/05/1983 - 22/05/1983	RV Belgica	BI01-BI97	X-mas sparker and boomer (Uniboom?)	DECCA Logbook	2413,9
	01/07/1983 - 15/07/1983	RV Belgica		X-mas sparker and boomer (Uniboom?)	DECCA Logbook	
	20/09/1983 - 28/09/1983	RV Belgica		X-mas sparker and boomer (Uniboom?)	Lat Long Logbook (ED50)	
BGD 84-85	12/11/1984 - 16/11/1984	RV Belgica	BGD84_01	?	Lat Long Logbook	31,7
	23/09/1985 - 27/09/1985	RV Belgica		?	Lat Long Logbook	
	12/11/1985 - 15/11/1985	RV Belgica		?	Lat Long Logbook	
	29/06/1987 - 09/07/1987	?		?	Lat Long Logbook	
EEG	10/04/1989 - 20/04/1989	RV Belgica	EEG01-EEG14	boomer (Uniboom)	Lat Long Logbook	305,2
	19/06/1990 - 20/06/1990	?		boomer (Uniboom)	Lat Long Logbook	
Middelkerke 90	03/12/1990 - 07/12/1990	RV Belgica	MI01-MI10	Centipede sparker	Lat Long Logbook	111,9
Middelkerke 91	21/05/1991 - 22/05/1991	RV Belgica	MI91_01-MI91_19	Centipede sparker	Lat Long Logbook	140,7
Thomtonbank 94	11/10/1994 - 14/10/1994	?	P2-P61	?	Lat Long NAV files (WGS84)	451,8
B_Valérie	23/06/2003 - 25/06/2003	RV Belgica	KW030601-KW030615	Seistec boomer	Lat Long NAV files	
			Kwintebank1-Kwintebank2	Centipede sparker	Lat Long NAV files	99,3
B2004-15	05/07/2004 - 09/07/2004	RV Belgica	Ob040701-Ob040702	Seistec boomer	Lat Long NAV files	
			Ob040703-Ob040718	Centipede sparker	Lat Long NAV files	188
			Ob040719-Ob040723	SIG sparker	Lat Long NAV files	
B2005-04b	28/02/2005- 04/03/2005	RV Belgica	VLR030501-VLR030502	Centipede sparker	Lat Long NAV files	
			VLR030503	SIG sparker	Lat Long NAV files	28
B2005-17	04/07/2005 - 08/07/2005	RV Belgica	VLR070501-VLR070511	SIG sparker	Lat Long NAV files	
B2005-23	26/09/2005 - 06/10/2005	RV Belgica	VLR090501-VLR090513	Centipede sparker	Lat Long NAV files	84
			VLR100501-VLR100516	Centipede sparker	Lat Long NAV files	335
B2006-06	27/03/2006 - 30/03/2006	RV Belgica	Br030601-Br030608	Centipede sparker	Lat Long NAV files	
Bellini	10/07/2006 - 14/07/2006	Bellini	Np070601-Np070611	Centipede sparker	Lat Long NAV files	84
B2006-20a	26/09/2006 - 29/09/2006	RV Belgica	Br090601-Br090605	Centipede sparker	Lat Long NAV files	193
			Ob090601-Ob090607	Centipede sparker	Lat Long NAV files	132
B2007-09	16/04/2007 - 20/04/2007	RV Belgica	Br040701-Br040711	Centipede sparker	Lat Long NAV files	
			Ob04200701-Ob04200706	Centipede sparker	Lat Long NAV files	134

Table 3.1 Overview of performed seismic surveys

Seismic equipment	Frequency band (kHz)	Peak frequency (Hz)	Vertical Resolution (cm)	Penetration (m bsf)
Xmas sparker		1100-1200	35-50	50
Centipede sparker		1100-1200	35-50	50
12-electrode sparker		800-900	50-?	80
SIG sparker		800-900	50-?	80
Uniboom	1-3		10-40	12-20
Seistec	1-5		10-40	12-20

Table 3.2 Overview of applied seismic sources

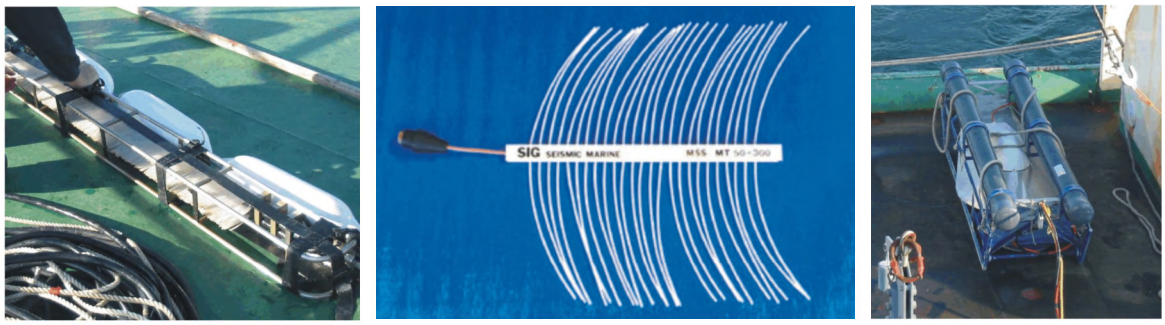

Centiped sparker (Design RCMG) | SIG sparker | Seistec boomer

Fig. 3.2 Overview of the seismic sources applied during the recent surveys (1990-2007). For technical specifications see Table 3.2.

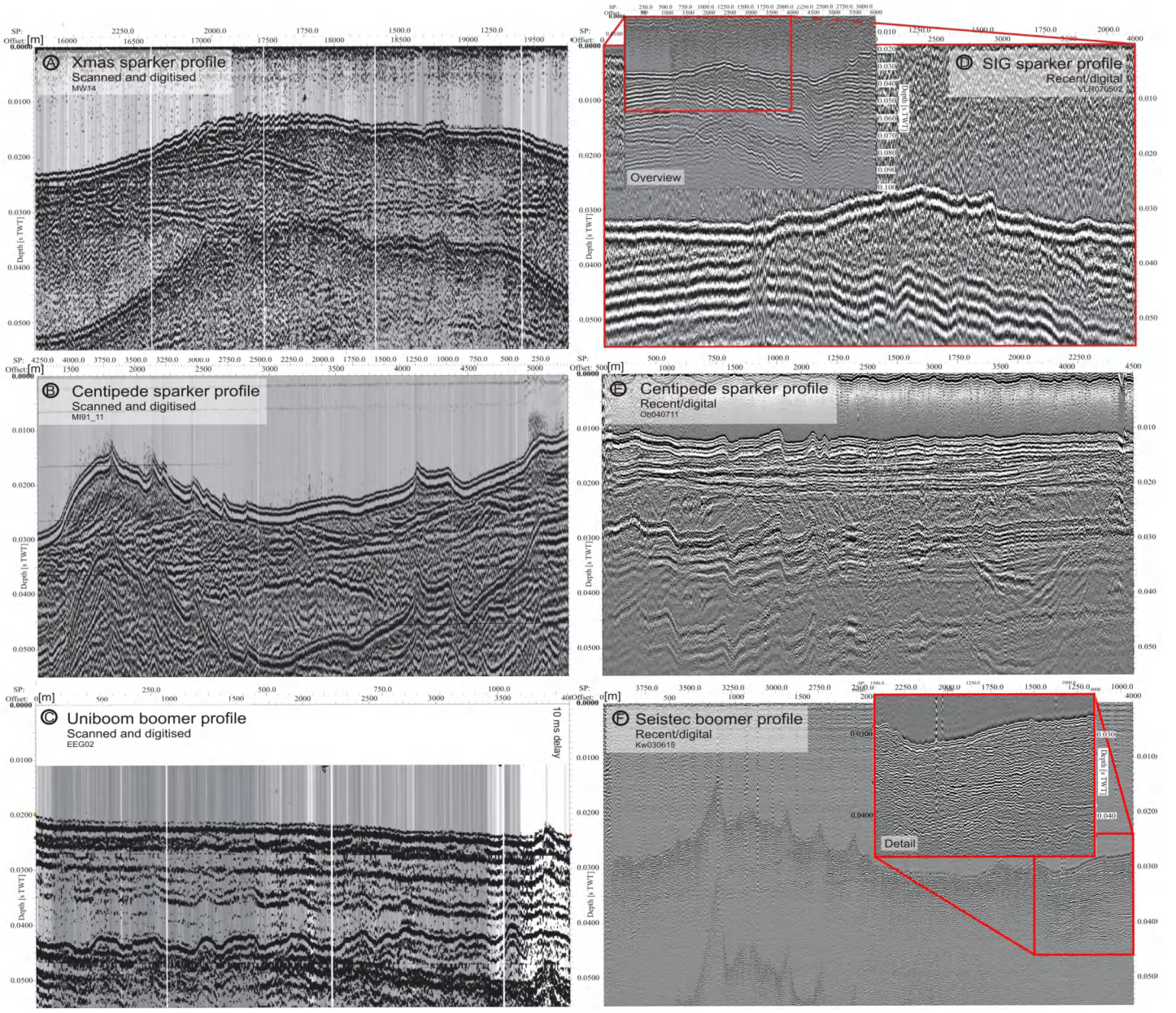

Fig. 3.3 Examples of high-resolution reflection seismic profiles. (A) digitised analogue Xmas sparker profile, (B) digitised analogue Centipede sparker profile, (C) digitised analogue Uniboom boomer profile, (D) recently acquired SIG sparker profile, (E) recently acquired Centipede sparker profile, (F) recently acquired Seistec boomer profile. The six large examples are all plotted with the same vertical (seconds TWT) and horizontal scale (m). Note how the SIG profile (D) has a lower resolution, showing less detail but a bigger penetration depth (see inset). Notice how the Seistec boomer profile (F) has a higher resolution, showing more detail when zoomed in (see inset), but a smaller penetration depth. The vertical white lines on the digitised analogue seismic records (A, B, C) represent former fixlines.

The 'Seistec' boomer source has a frequency range of 1-5 kHz and a theoretical (Rayleigh criterion) resolution of 10-40 cm. Its signal penetrated 12-20 m bsf ,depending on the sediment type in the subsurface (Fig. 3.3F). The 'Uniboom' has a frequency range of 1-3 kHz and similar resolution and penetration capacities. Owing to the plot parameters at the time of acquisition, digitised analogue Uniboom profiles show no detail (Fig. 3.3C).
The seismic profiles acquired before 1992, were analogue band-pass filtered on the field and, after a TVG (time-varied-gain) correction, graphically plotted on an EPC1600 variable-area greyscale plotter. From 1992 onwards, the seismic data were digitally recorded with Triton Elics International (Delph Seismic) software, following an initial analogue band-pass filtering and TVG correction.
From 1980 until 1983, a DECCA radio-positioning system with an accuracy of 50-200 m was used for navigation. After 1983, navigation was done successively with a Syledis and DGPS system. The accuracy of these systems is 2-3 m (relative position) and <1 m, respectively.

3.1.2 Conversion of analogue to digital data

More than 16,000 km of high-resolution seismic data were recorded on the BCS prior to 1991, but were only available in analogue paper format. So the seismic rolls and accompanying logbooks had to be digitised, in order to integrate them with the recent, digitally acquired seismic data. After a thorough evaluation of the quality of the paper seismic records, about 50% of the profiles were assigned a 'medium-bad' to 'good' quality label, and were considered of sufficient quality for further processing. These paper records were scanned on a roll-through A0 scanner, hereby generating 1-bit greyscale (black-and-white) 'tiff' images with 300dpi resolution (Fig. 3.4). About half of the obtained image files were translated to a digital seismic format (SEG-Y), using the specially developed software package 'SeisTrans' (EC project SEISCANEX) (Schaming et al. 2000, Miles et al. 2007). With the SeisTrans software (incorporated in Caldera Graphix) an initial coarse raster, consisting of vertical 'fix lines' (every 5-10 min) and horizontal timelines (every 10 ms), was drawn over the tiff image, (Fig. 3.4). This raster was then refined by choosing the sample step or sampling frequency, which is depending on the source frequency, and the trace width, which is depending on the shot rate. In each cell of the created mesh, a value is calculated from the ratio of black to white in the image. This value is written as an amplitude in a (digital) SEG-Y file. The SEG-Y conversion algorithm is explained in detail in Miles et al. (2007).

Navigation files corresponding to these data could be produced on the basis of the positions manually recorded in the logbooks for each 'fix line', i.e. navigation time lines as reference points every five or ten minutes along the sailed tracks recorded on the seismic paper plot. To be uniform with the more recently acquired seismic data sets, the projection and datum in which the fix points were given (i.e. geographic projection (latitude, longitude), European Datum 1950 (ED50)), were transformed to UTM WGS84 (Universal Transversal Mercator projection, World Geodetic System of 1984).

More than 4,000 km of seismic profiles were converted in this way from tiff image to SEG-Y file. In addition, eight modern seismic surveys were set up (between 2004 and 2007) in key areas where the analogue seismic network was not dense enough (Fig. 3.1). Together with the digitised analogue profiles, these digitally acquired seismic data were integrated in an interpretation workstation. This gives a total of nearly 5,300 km of high-resolution seismic profiles to reconstruct the Quaternary evolution of the BCS.

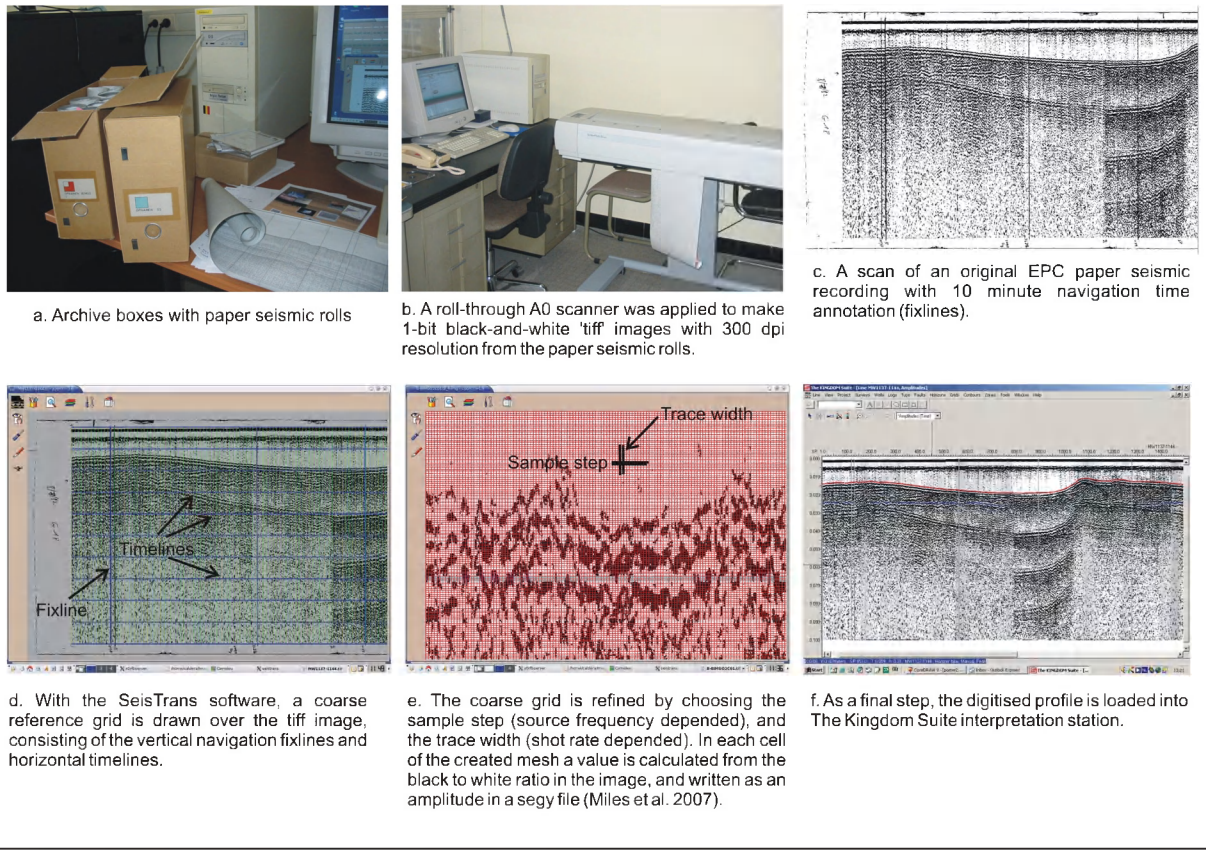

Fig. 3.4 The process of translating paper seismic recordings into digital SEG-Y format, using the software package 'SeisTrans' (Schaming et al. 2000, Miles et al. 2007).

3.1.3 Processing of seismic data

After conversion of the data to SEG-Y format a number of processing routines were tested with the aim to improve the data quality. Band-pass filtering, swell filtering or deconvolution filtering, however, did not appreciably improve data quality and this was therefore omitted.

However, before loading both the old and the new data into the interpretation workstation, the seismic profiles had to be corrected for the tide, i.e. converted to a common datum. This involved the application of a correction for differences in tidal amplitude during acquisition, which can generate discrepancies in water depth of more than 4 m for the same location. A mathematical tidal model delivered the theoretical water depth for every position along the sailed tracks, at the given time. For the old data, the correction was based on theoretical astronomical tides only (MUMM, Ozer pers. comm.); for the recent, digitally acquired seismic data the actual water depths of Nieuwpoort, Oostende and Zeebrugge were applied (Vlaamse Hydrografie - Afdeling Kust, former 'Administratie Waterwegen en Zeewezen (AWZ)' and FOD Kwaliteit en Veiligheid, Afdeling Kwaliteit en Innovatie, Continentaal Plat, Degrendele pers. comm.). Remaining discrepancies in water depth at the tie-points of two intersecting seismic lines were usually due to errors in positioning, especially on data from 1980-1983 when DECCA navigation was used. These positioning errors were in the order of 500-1000 m, but could be corrected using e.g. the contours of tidal sandbanks on bathymetric maps, as these features are considered stable (Veenstra 1964, Houbolt 1968, De Moor 1985b). The errors were at random, no constant shift was applied. Any other discrepancies were due to differences in towing depth of the seismic source or receiver, or caused by waves or swell.

The vertical scale of the seismic sections is given in seconds (Two Way Travel time). Corresponding interpreted sections are given in metres, unless noted otherwise. The time-to-depth conversion was done using an average sound velocity of 1500 m/s in the water column and 1650 m/s in the mainly sandy Quaternary deposits (Maréchal and Henriet 1983). This sound velocity gave excellent results for the correlation of core data with seismic profiles. Owing to the time-to-depth conversion, any occurrence of 'velocity-effects (i.e. pull-ups or pull-downs)' was avoided. All depths are referred to MLLWS (mean lowest low water at spring time), which is about 2.5 m below MSL (mean sea level) at Zeebrugge. Note that the MLLWS reference level is not a uniform datum as it connects the local MLLWS value of different locations.

3.1.4 Interpretation of seismic data

After applying the tidal corrections, the seismic data were loaded into 'The Kingdom Suite' interpretation workstation (Academic licensed SMT software). The interpretation of the seismic profiles started with tracing reflections, i.e. picking horizons on profiles crossing the Middelkerke Bank, which is centrally located on the BCS, about 13 km offshore. For this location a well-established seismic stratigraphy existed already, thanks to detailed studies carried out in the framework of the EC RESECUSED and STARFISH Projects (cf. Chapter 2.2.2). When tracing the Middelkerke Bank seismic stratigraphy to the surrounding sandbanks, it became clear that these had a similar internal structure. This opened the perspective to extend the seismic-stratigraphic interpretation of this central area on the BCS to the entire BCS. The labelling of the different seismic units previously defined in the Middelkerke Bank was therefore maintained where possible for the rest of the Belgian shelf (units U1 to U7). In total, seven seismic units were identified and correlated across the BCS. These units are bounded by erosional unconformities, which reflect important phases in the relative sea-level evolution or in the response of the sedimentary dynamics to the sea-level evolution. The seismic units were defined and described according to the sequence-stratigraphic approach (Mitchum and Vail 1977, Mitchum et al. 1977a, 1977b).

The upper bounding unconformities of each seismic unit and the underlying surfaces were gridded (inverse distance) to create the corresponding isobath maps, expressed in m below MLLWS. In order to preserve the details along the seismic profiles, a grid-cell size of 50 or 100 m was used. To overcome gridding artefacts caused by a grid cell size smaller than the average spacing between seismic profiles, the search radius for each grid node is kept 500-1500 m, depending on the local profile spacing. The inverse distance weighting power is 2. Afterwards, the boundaries of each grid were clipped to the real extent of the concerning seismic unit, as present on the seismic profiles.
By combining the isobath maps of the upper and lower bounding unconformities, isopach maps were produced as well (in metres). Projection and datum of the charts are UTM WGS84, unless noted otherwise. In order to be able to merge grids from both offshore and onshore data sets, the latter mostly expressed in UTM Lambert 72, they were conformed to the same coordinate system and spheroid (UTM WGS84). The reference levels (MLLWS for the offshore data and TAW for the onshore data) were considered to be equal, as the maximum difference between MLLWS and TAW (Tweede Algemene Waterpassing) is 0.508 m, which corresponds to the precision of the seismic data.

Thanks to this digital approach all available data sets were integrated in one well-organised database, and seismic profiles and maps could be conjured up on screen in an instant. This increased time efficiency made it possible to perform the seismic study in more detail, and to quickly get an overview of the internal structure of sandbanks, by e.g. opening one seismic profile after the other in a pseudo-3D presentation. The latter approach delivered important insights in the Quaternary evolution of the BCS.

We are aware that it is often difficult to recognise seismic reflections from interpreted seismic sections on the original, non-interpreted sections, presented here. Visualising seismic profiles on A4 scale strongly reduces the quality, as noise is enhanced and any detail is removed. We can assure, however, that the picking of the reflections was done meticulously, on a far more detailed scale than that can be shown here. Moreover, the interpretation of each single seismic profile is in fact realised, taking into account also the situations in every neighbouring parallel and intersecting profile, checking and double-checking until the final interpretations were consistent. When dealing with paleo-channels, adjacent seismic profiles were especially carefully compared to delineate the features and to define their continuity.

ID	Date	Type	# applied	Max. core length (m)	Extras
RGD	1936-1987	Vibrocore (Zenkovitz)	36	4	6 Pollen analyses
		Fushcore (Geodoff)	35	10.00	20 Macrofauna reports
		Straight drilling	3	20.6	1 Ostracods analysis
		Unknown	24	59.60	
BGD	1976	Vibrocore	134	5.18	
	1984 and 1986	Vibrocore (Zenkovitz)	219	5.05	215x Photos
Harbour expansion	1977	Vibrocore (Zenkovitz)	16	5.3	
Wartel and Vansieleghem	1983 and 1985	Vibrocore	1	0.80	
		Straight drilling	1	19.93	
		Unknown	2	3.50	
BGD	1986 and 1988	Straight drilling	10	80	10x Photos
Middelkerke Bank	1991	Vibrocore (Trilflip)	61	5.63	
	1993	Vibrocore	60	4.5	
Unknown	?	?	9	200.25	

Table 3.3 Overview of available core-data sets (detailed list in Appendix A)

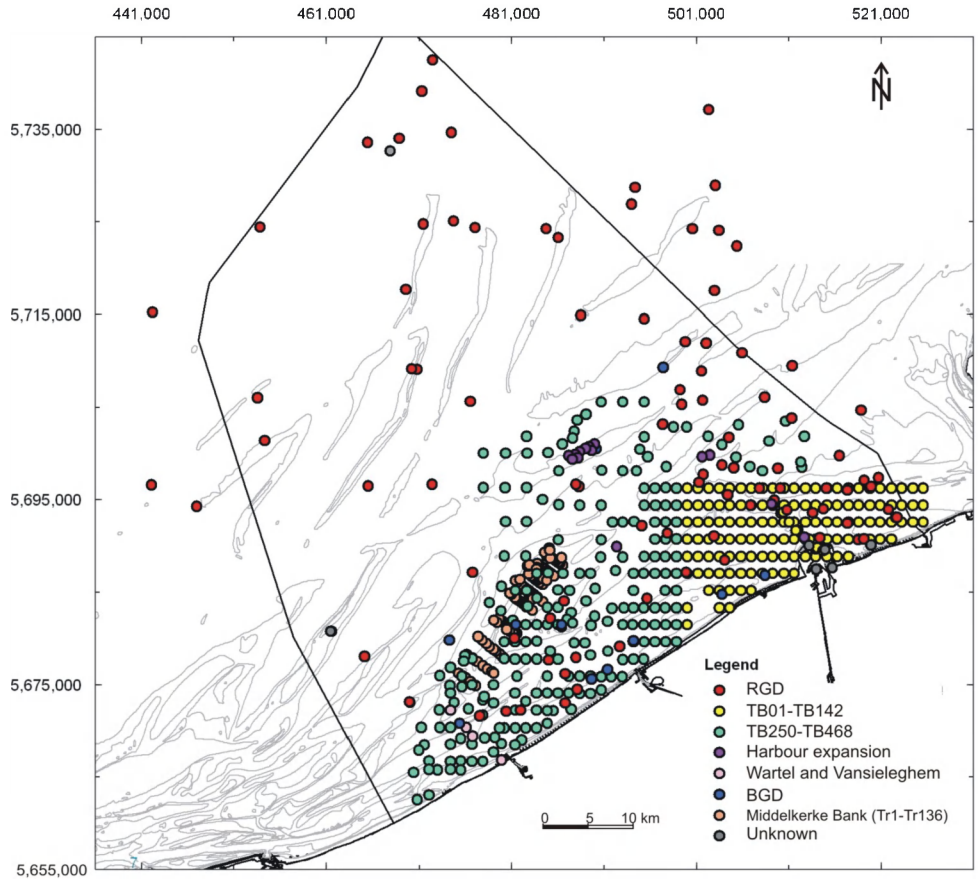

Fig. 3.5 Overview map of available core data. For technical details see Table 3.3 and Appendix A. [UTM ED50]

3.2 Core data

3.2.1 Acquisition: coring campaigns

Over 600 cores have been obtained in the study area since 1936, in the framework of several projects (Table 3.3, App. A, Fig. 3.5). Between 1936 and 1987, the Geological Survey of the Netherlands (formerly RGD, TNO-NITG, presently Bouw en Ondergrond) acquired 99 flush- and vibrocores, a lithological description of which is available in the archives of the GSB (Geological Survey of Belgium). For some of these cores, a paleontological report is available (molluscs, pollen, ostracods).
Meanwhile, in 1976, 1984 and 1986, the subsurface of the BCS was investigated for potential exploitation of natural reserves. Under the authority of the GSB, 353 vibrocores were acquired (TB01-TB142, TB250-TB468). Of 215 of these cores (TB250-TB464), photographs and detailed lithological descriptions are available.
In 1977, 16 vibrocores were collected as part of the harbour expansion of Zeebrugge, but only a summary description of the sediment is accessible. All above-mentioned vibrocores were obtained with a Zenkovitz corer (Fig. 3.6); they have a diameter of 7 cm and can be up to 5 m long.
With the aim of developing a paleo-geographical reconstruction of the former, more seaward position of the coastline, four cores were taken in the area offshore Nieuwpoort between 1983 and 1985 (Wartel and Vansieleghem 1985).

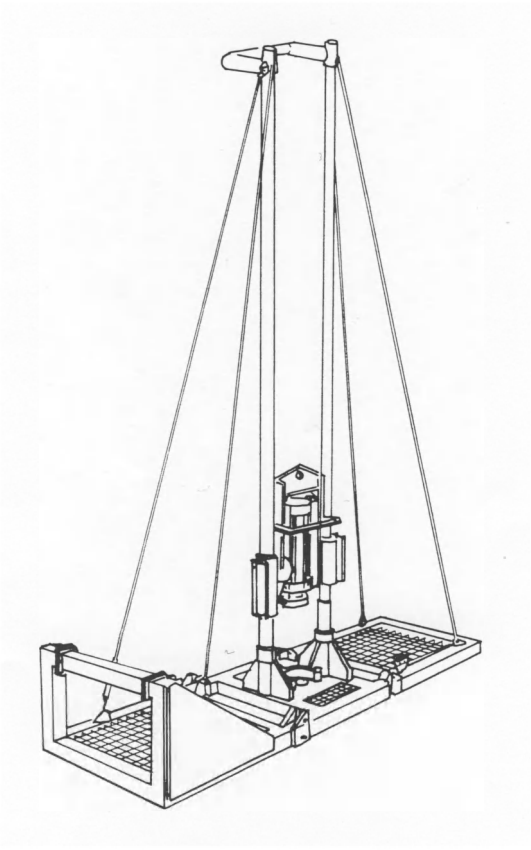

Fig. 3.6 A 'Zenkovitz' corer, applied for taking vibrocores until 1987 (HAECON 1986).

Core	Sample depth	Seismic unit
SEWB	2.40 m	U6
GR1	27.60 m	U3
	36.30 m	U3
	43.10 m	U1
SWB	1.43 m	U6
	3.50 m	U4
	5.40 m	U4
SB1	13.58 m	U4
SB2	18.84 m	U3
OSB	5.40 m	U5
	5.68 m	U5
	11.68 m	U4
	19.30 m	U2
UIT	2.40 m	U5
	5.50 m	U4
	9.50 m	U3
	12.80 m	U2
NWB	8.30 m	U5
	10.62 m	U3
	12.62 m	U2

Table 3.4 Diatom samples, sampling depth and corresponding seismic unit

In 1986 and 1988, the GSB conducted 10 straight drillings, acquiring 10 undisturbed cores (in Dutch: 'steekboring') in different locations in the near-coastal zone of the BCS (UIT, SB1, SB2, GR1, NWB, SEW, SEWB, GII, OSB, THB). The longest recovery is 80 m and the diameter is 10 cm. The 1 m core segments are kept at the GSB and, in contrast to the vibrocores, are still in a perfect state. Again, detailed core descriptions and photographs are available. Additionally, ^{14}C analyses were carried out on juvenile shells from some boreholes, but gave rather contradictory ages (cf. Chapter 2.2.2, Stolk 1996, Trentesaux pers. comm.).
In the framework of the EC RESECUSED and STARFISH projects (in 1991 and 1993), another 121 vibrocores (type 'Trilflip', Hoogendoorn and Kluwer 1990) were obtained in the Middelkerke Bank area, along selected seismic profiles (Tr01-Tr61, Tr90-Tr136, A-M). The cores have a diameter of 10 cm and a maximum length of 5.5 m. Detailed lithological descriptions (Trentesaux pers. comm.) and lacquer peels are still available. The latter are kept at TNO Bouw en Ondergrond (Utrecht, NL, Stolk pers. comm.).

3.2.2 Processing of cores and core descriptions

From all the cores ever acquired on the BCS, only the 10 long cores obtained by the GSB have been well preserved. Thus, for most of the cores, our study had to be based on the available borehole descriptions and photographs from the time of recovery. Parameters described are: mean grain size and admixture (mostly visually estimated by comparison with a graphic scale), colour, shell, peat and $CaCO_3$ content, as well as sedimentary structures. On some cores grain-size analyses were performed, and in some cases macrofauna was determined for dating purposes.
No other dating methods were used, although attempts have been made in the past to apply ^{14}C dating on juvenile shells. Note that ^{14}C ages in literature are sometimes given in ^{14}C years BP (Before Present, i.e. before 1950), and sometimes in cal BP (calibrated calendar years before present). In order to be able to compare certain ages and the time of important events, age indications in years BP found in literature were converted to calibrated years BP, using the software 'Oxcal 3.10' (Bronk Ramsey 1995, 2001). The atmospheric northern hemisphere curve (IntCal04.14c) was used as standard calibration curve (Bronk Ramsey 1995, Reimer et al. 2004).
From the preserved 10 long, undisturbed cores of the GSB, 20 samples were taken for diatom investigation, with the aim of determining depositional environments (by Sue Dawson, Aberdeen UK) (Table 3.4).
The level of detail of the core descriptions differed strongly between the several campaigns. For the flush cores, only sub-samples from regular intervals were described, but no continuous logs exist, making the descriptions unsuitable for identifying e.g. erosional contacts. One also has to be cautious with interpreting colour differences, as it is not always mentioned in what state the core was described (i.e. in wet/fresh conditions, or after drying and consequent oxidation).

3.2.3 Correlation of seismic and core data

The core data were used for calibrating the seismic data with the aim of obtaining a sedimentological ground-truthing for every seismic unit identified. As mentioned above, a sound velocity of 1650 m/s was applied for integrating the cores (depth in metres) with the seismic profiles (depth in seconds), and gave good results. However, of the 615 available cores, only about 70 had a length of more than 5 m (of which most were flush cores), which strongly limited the number of cores reaching the deepest seismic units.

4.
Observations

Seven seismic units, separated by erosional unconformities, have been identified within the Quaternary deposits on the BCS. A general description of the units is presented here, but more details follow in the next chapters, where genetically related units (i.e. belonging to the same depositional system) are discussed together. The angular unconformity separating the seven seismic units from the underlying substratum is considered the Top-Paleogene or Base-Quaternary surface, and will be discussed in detail in Chapters 5 and 6.

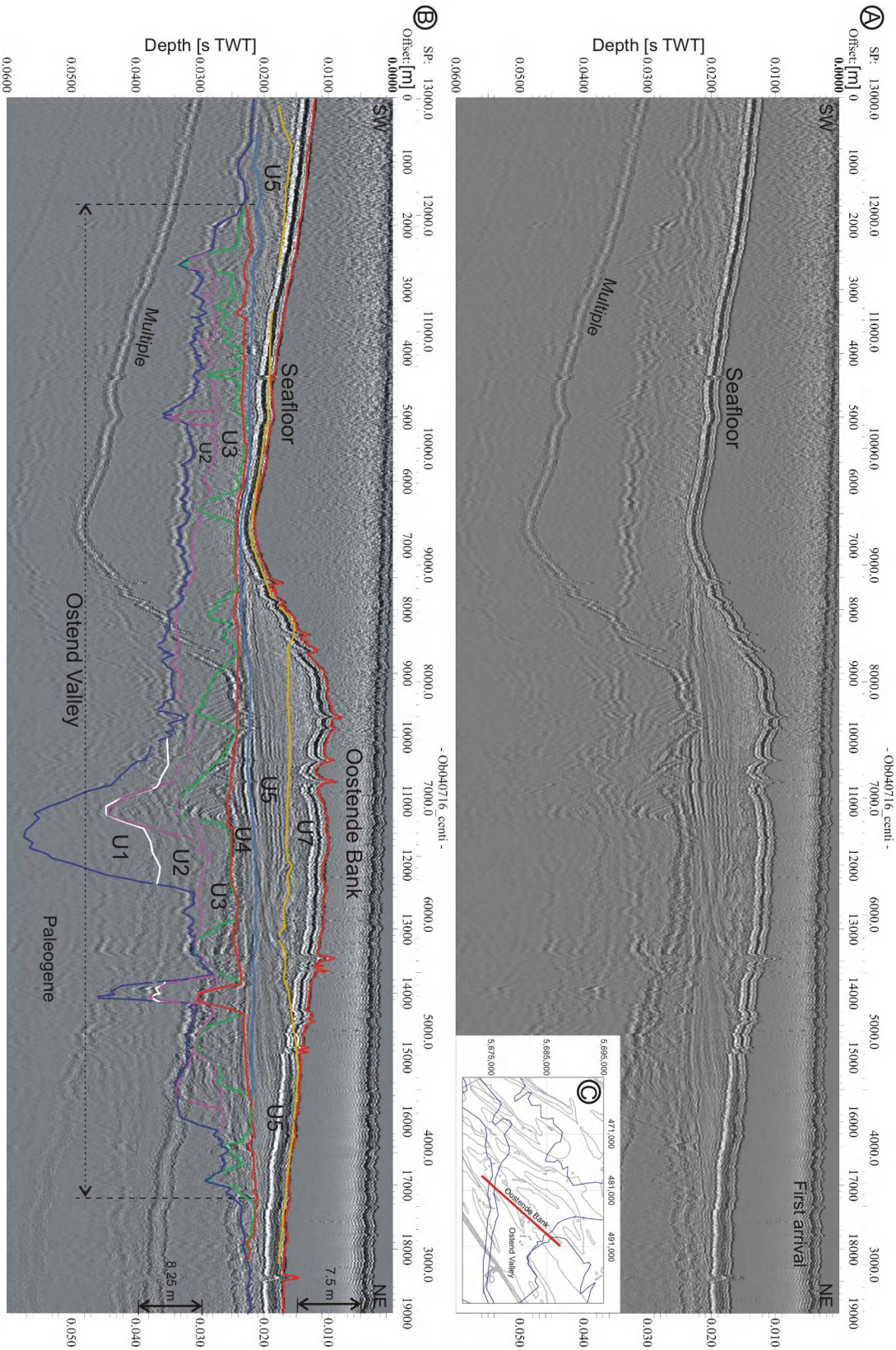
A
B
C
SP: 13000.0
Offset: [m] 0
0.0000
SW
NE
- Ob040716_cconti -
Depth [s TWT]
Seafloor
Multiple
First arrival
Oostende Bank
Ostend Valley
Paleogene
U1
U2
U3
U4
U5
U7
7.5 m
8.25 m

4.1 Seven seismic units

Per unit a short description of the seismic facies is given, as well as an isobath map, showing the extension and topography of the surface of each seismic unit, and an isopach map.

4.1.1 Seismic unit U1: the lowermost valley fill

Seismic unit U1 fills the deepest parts of a large valley incision in the Top-Paleogene surface offshore Oostende, i.e. the Ostend Valley (Fig. 4.1). It is bounded at its base by a strong reflector, named 'QT' (after the 'Quaternary-Tertiary' boundary), which marks the contact between the Quaternary deposits and the underlying Paleogene strata (in the past referred to as Tertiary). The top reflector of unit U1 is much weaker. It occurs near the limit of acoustic penetration and is commonly obscured by the presence of shallow gas or by the seafloor multiple. Where visible, the top reflector is in most cases quasi horizontal, laterally onlapping onto the QT surface, but locally interrupted by incisions of overlying units (Fig. 4.2A). The seismic unit shows a parallel-wavy internal reflector configuration, or a prograded fill, with tangential and parallel-oblique internal reflectors (Fig. 4.2B).
Fig. 4.3A displays the regional extent and topography of the surface of unit U1. The unit occurs in the central axis and along the north-eastern wall of the Ostend Valley, in distinct, deeply incised channels in the Top-Paleogene surface. The top bounding surface of U1 reaches its shallowest point at a depth of –25 m at the NE boundary of the Ostend Valley. In the central axis the main surface ranges from –28 m to –30 m in offshore direction. Locally, U1 is incised though by overlying units. The depth of these incisions can reach 5 to 8 m, but is generally less than 3 m.
Maximum thickness is reached in the central depression of the Ostend Valley, where the unit is about 25 m thick (Fig. 4.4A). Elsewhere, the unit is less than 5 m thick. The 0 m thickness contour is indicated to distinguish between white areas where U1 is not present (outside the contour) and white areas where the data quality is too poor to distinguish U1 but where U1 is expected (inside the contour).
Seismic unit U1 will be discussed in more detail in Chapter 6, together with units U2 and U3, because they jointly make up the total infill of the incised valley offshore Oostende.

Fig. 4.1 (page 30) Overview profile across the Ostend Valley showing the seismic-stratigraphic position of the seismic units in relation to each other and the valley incision. U1 is located in the deepest incised channel, U2 extends beyond this central incision, and U3 infills the entire Ostend Valley. Seismic units U4, U5 and U7 are no longer determined by the presence of the Ostend Valley, but extend over the entire width of the BCS (see also maps in Fig. 4.3). Seismic unit U6 is restricted to the nearshore area and not present on this profile. (A) Original seismic profile, depth in seconds TWT, reference level is MLLWS (0.0000 s); (B) interpreted seismic profile, on the right side indication of corresponding depth scales in metres, differently above and below the seafloor; (C) positioning of the seismic profile with reference to the present-day bathymetry (grey) and the location of the Ostend Valley (blue, cf. Fig. 2.4 and 5.1). From bottom to top: the dark blue line represents the top of the Paleogene or base of the Quaternary (QT reflector, discussed in Chapter 5); the top reflector of seismic unit U1 is indicated in white; the top of seismic unit U2 is indicated in purple, internal channels of U2 in bright purple. The top of seismic unit U3 is indicated in red, internal channels in green; the top of U4 is in blue, internal channels and prograding reflectors when present in U4 are in light blue; the top bounding reflector of U5 is indicated in orange and the seafloor in red, which defines the top of seismic unit U7 as well. When present, the top of U6 will be indicated in yellow. This colour code will be used throughout the thesis.

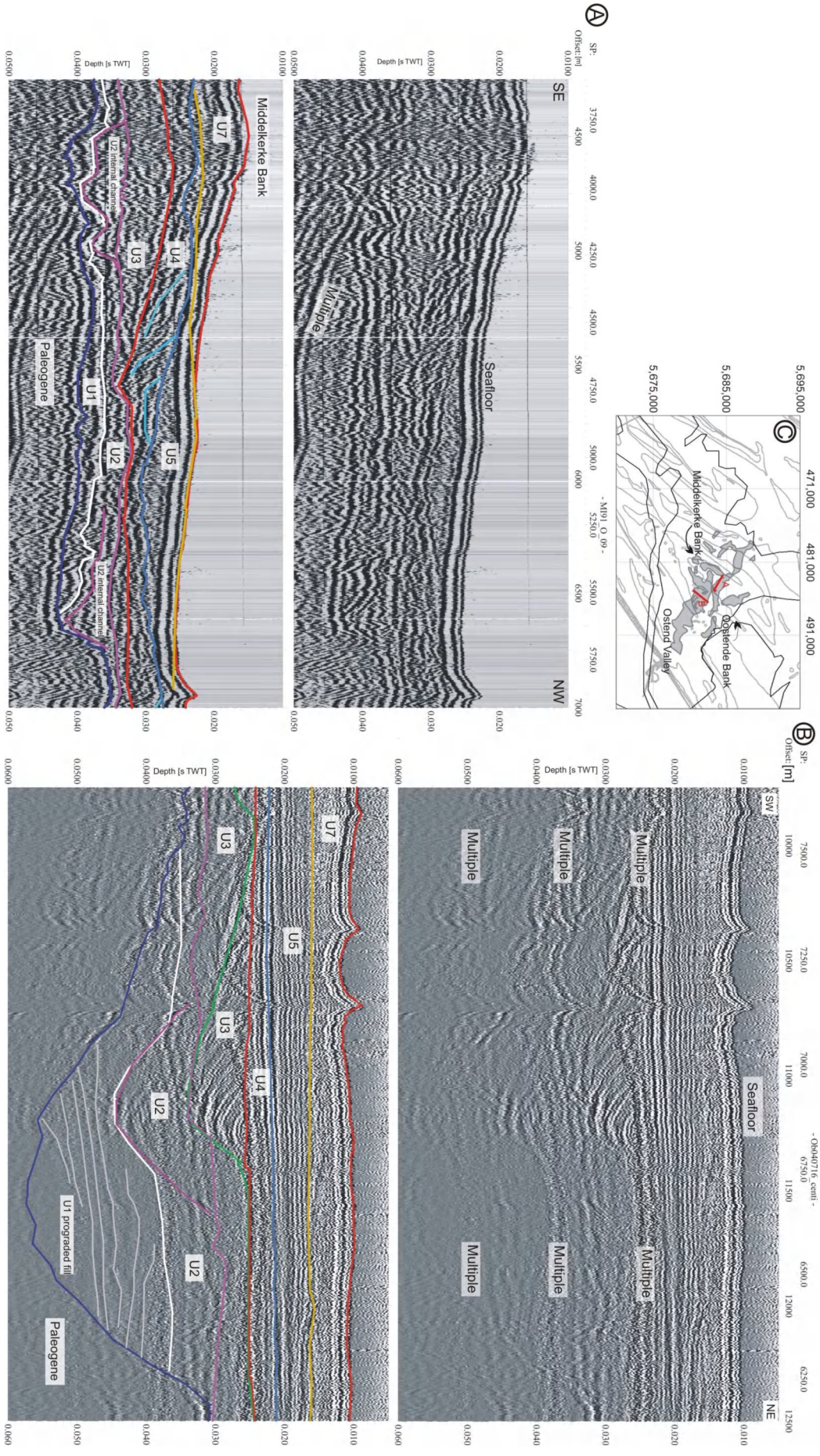
A
SE
NW
Seafloor
Multiple
Middelkerke Bank
Paleogene
U1
U2
U3
U4
U5
U7
U2 internal channels
Depth [s TWT]
C
5,695,000
5,685,000
5,675,000
471,000
481,000
491,000
Middelkerke Bank
Oostende Bank
Ostend Valley
B
SW
NE
Seafloor
Multiple
U1 prograded fill

Fig. 4.2 (page 32) Detailed seismic sections showing the internal reflection pattern and configuration of unit U1. (A) Incision of seismic unit U1 by overlying unit U2; (B) a prograded channel fill (detail of Fig. 4.1, note different scales); (C) positioning of the seismic profiles with reference to the present-day bathymetry (grey contours), the location of the Ostend Valley (black), and the extend of U1 (greyed area). Top sections are original seismic profiles, bottom sections are interpreted seismic profiles.

4.1.2 Seismic unit U2: the intermediate valley fill

The following seismic unit, U2, is no longer restricted to the deepest incisions of the Ostend Valley, but fills them up completely and even extends beyond them (Fig. 4.1). The unit is bounded at its base by the strong QT reflector, or by the upper bounding reflector of U1. At the top, U2 is better defined than U1, but again, because of its position at the limits of the seismic penetration and because of the presence of gas, especially in the southern part, the weaker top reflector can not always be observed. Where visible, it is in most cases quasi horizontal, occasionally slightly wavy, and locally incised by overlying units (Fig. 4.5). The reflector mainly onlaps onto the QT reflector, but occasionally it downlaps as well. Where the unit is thick enough, a wavy-parallel to sub-parallel reflector configuration is observed. The internal structure of the unit also reveals channels, mostly incised into the underlying unit U1 and even into the Top-Paleogene surface, and showing a prograded, complex or onlap fill (Fig. 4.5). The channels are clearly truncated at their top, making the upper boundary of U2 an erosional unconformity.
Fig. 4.3B displays the regional extent and topography of the surface of U2. In offshore direction, the unit only occurs in the distinct channels incised in the floor of the Ostend Valley. Further nearshore, the unit also extends beyond the boundaries of these channels, reaching the walls of the Ostend Valley. Here, the unit fills most of the Ostend Valley. In the SE part nearshore, the presence of gas obscures its occurrence. The surface of U2 slopes down in NW direction from about –21 m to –28 m, with an abrupt depth change of 3 m about halfway. Apart from this slope break, the surface also shows an axial depression with a width of 4 km and a depth between –25 and –27 m, as well as local incisions of up to 8 m below the average surface, caused by small channels in the overlying units.
Generally, U2 is less than 2 m thick. Maximum thickness is reached in the central depression of the Ostend Valley, where the unit is locally 14 m thick (Fig. 4.4B). The 0 m thickness contour is indicated to distinguish between white areas where U2 is not present (outside the contour) and white areas where the data quality is too poor to distinguish U2 but where U2 is expected (inside the contour).
Seismic unit U2 will be discussed in more detail in Chapter 6, together with units U1 and U3, because they jointly make up the total infill of the incised valley offshore Oostende.

Fig. 4.3 (page 34) Isobath maps of the top surfaces of seismic units: (A) U1; (B) U2; and (C) U3. The seismic units are shown with reference to the limit of the BCS and present-day coastline (light grey), and the main morphological features of the Top-Paleogene surface (in black the boundaries of the Ostend Valley and Nearshore Slope Break, adapted after Liu et al. (1992, 1993), discussed in detail in Chapter 5).

Fig. 4.4 (page 35) Isopach maps of seismic units: (A) U1; (B) U2; and (C) U3. The seismic units are shown with reference to the limit of the BCS and present-day coastline (light grey), and the main morphological features of the Top-Paleogene surface (in black the boundaries of the Ostend Valley and Nearshore Slope Break, adapted after Liu et al. (1992, 1993), discussed in detail in Chapter 5).

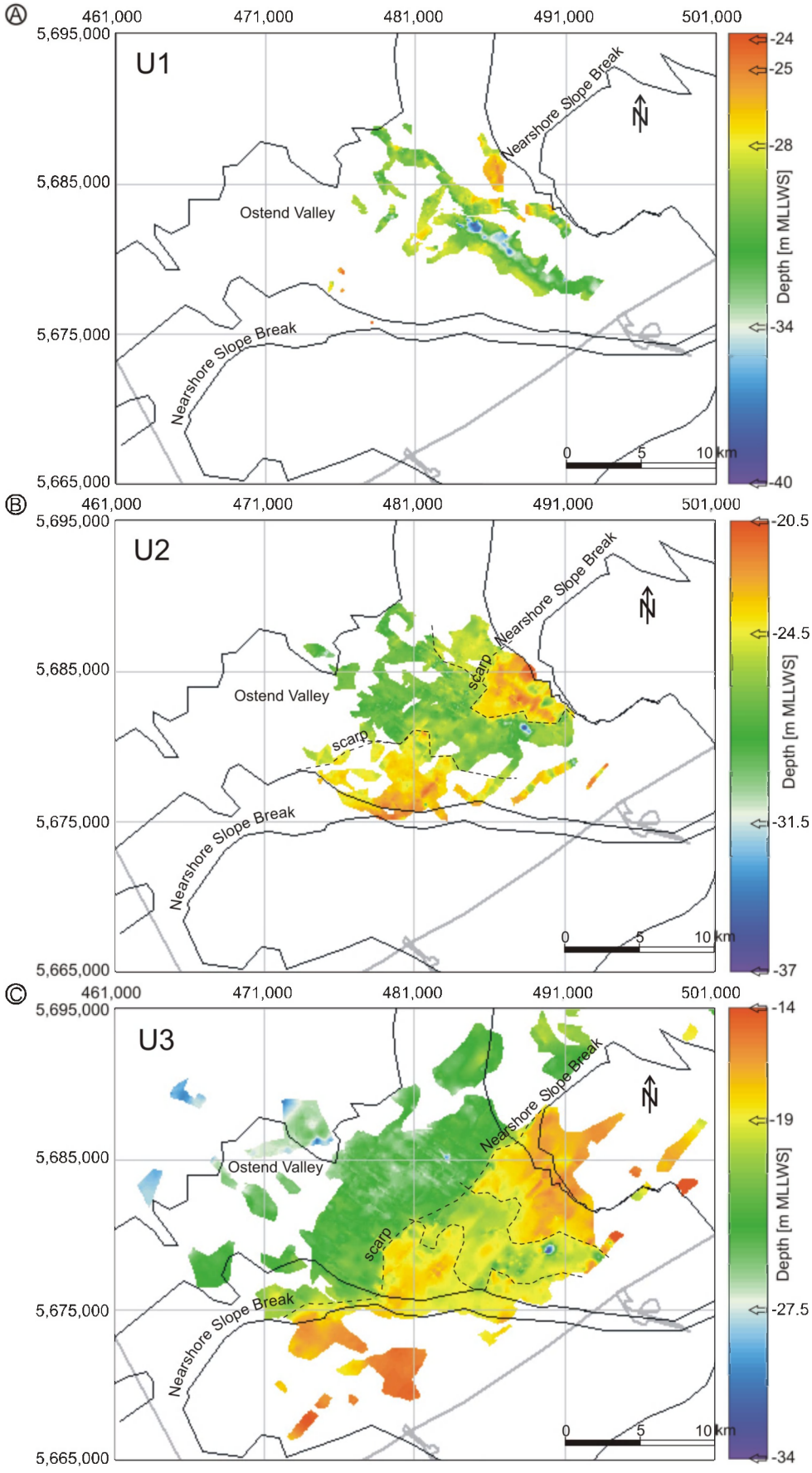
Ⓐ
U1
461,000
471,000
481,000
491,000
501,000
5,695,000
5,685,000
5,675,000
5,665,000
Ostend Valley
Nearshore Slope Break
Nearshore Slope Break
N
0
5
10 km
-24
-25
-28
-34
-40
Depth [m MLLWS]
Ⓑ
U2
461,000
471,000
481,000
491,000
501,000
5,695,000
5,685,000
5,675,000
5,665,000
Ostend Valley
scarp
scarp
Nearshore Slope Break
Nearshore Slope Break
N
0
5
10 km
-20.5
-24.5
-31.5
-37
Depth [m MLLWS]
Ⓒ
U3
461,000
471,000
481,000
491,000
501,000
5,695,000
5,685,000
5,675,000
5,665,000
Ostend Valley
scarp
Nearshore Slope Break
Nearshore Slope Break
N
0
5
10 km
-14
-19
-27.5
-34
Depth [m MLLWS]

Fig. 4.3

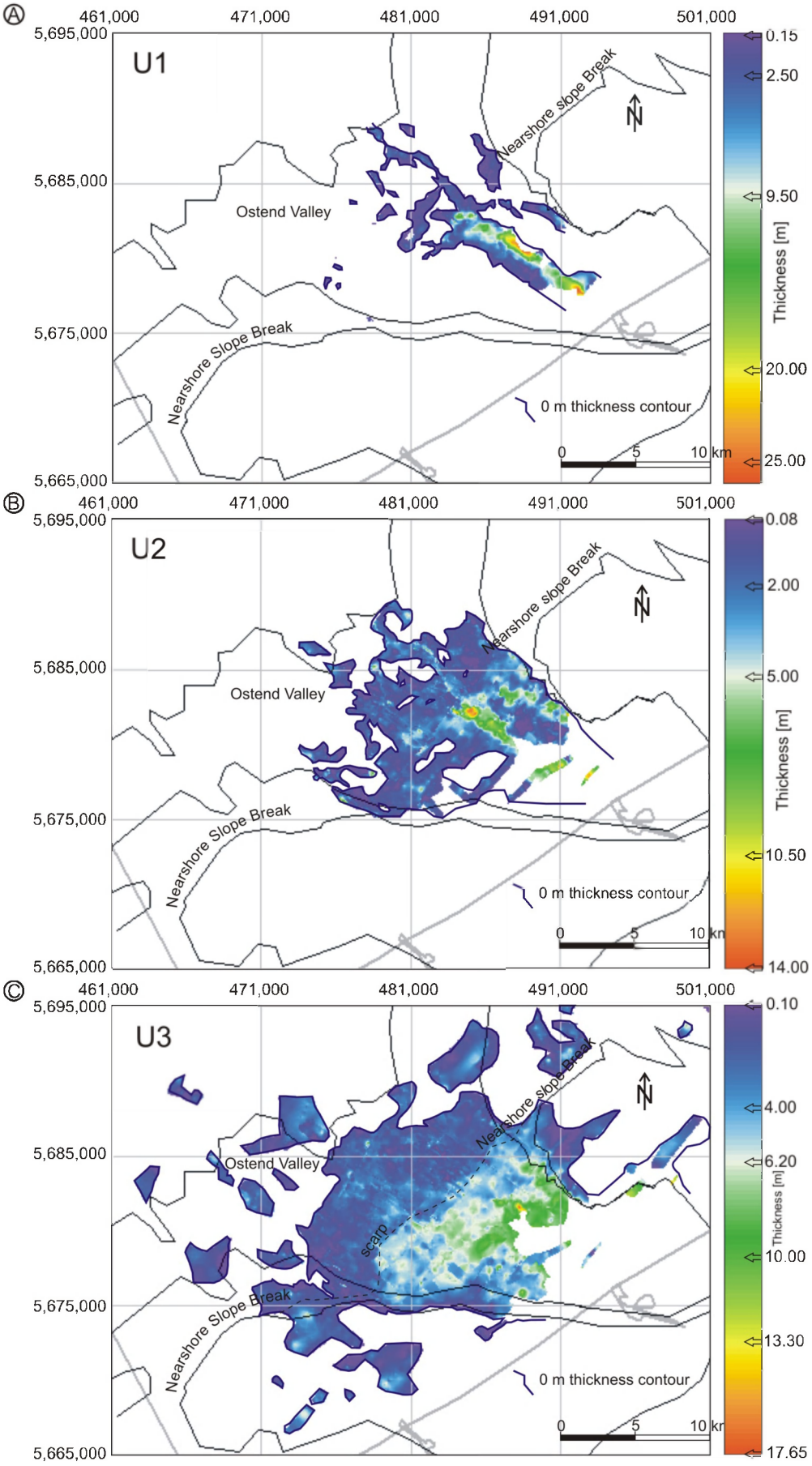
Ⓐ
461,000
471,000
481,000
491,000
501,000
5,695,000
5,685,000
5,675,000
5,665,000
U1
Nearshore slope Break
Ostend Valley
Nearshore Slope Break
0 m thickness contour
0
5
10 km
0.15
2.50
9.50
20.00
25.00
Thickness [m]
Ⓑ
U2
Nearshore slope Break
Ostend Valley
Nearshore Slope Break
0 m thickness contour
0.08
2.00
5.00
10.50
14.00
Thickness [m]
Ⓒ
U3
Nearshore slope Break
Ostend Valley
scarp
Nearshore Slope Break
0 m thickness contour
0.10
4.00
6.20
10.00
13.30
17.65
Thickness [m]

Fig. 4.4

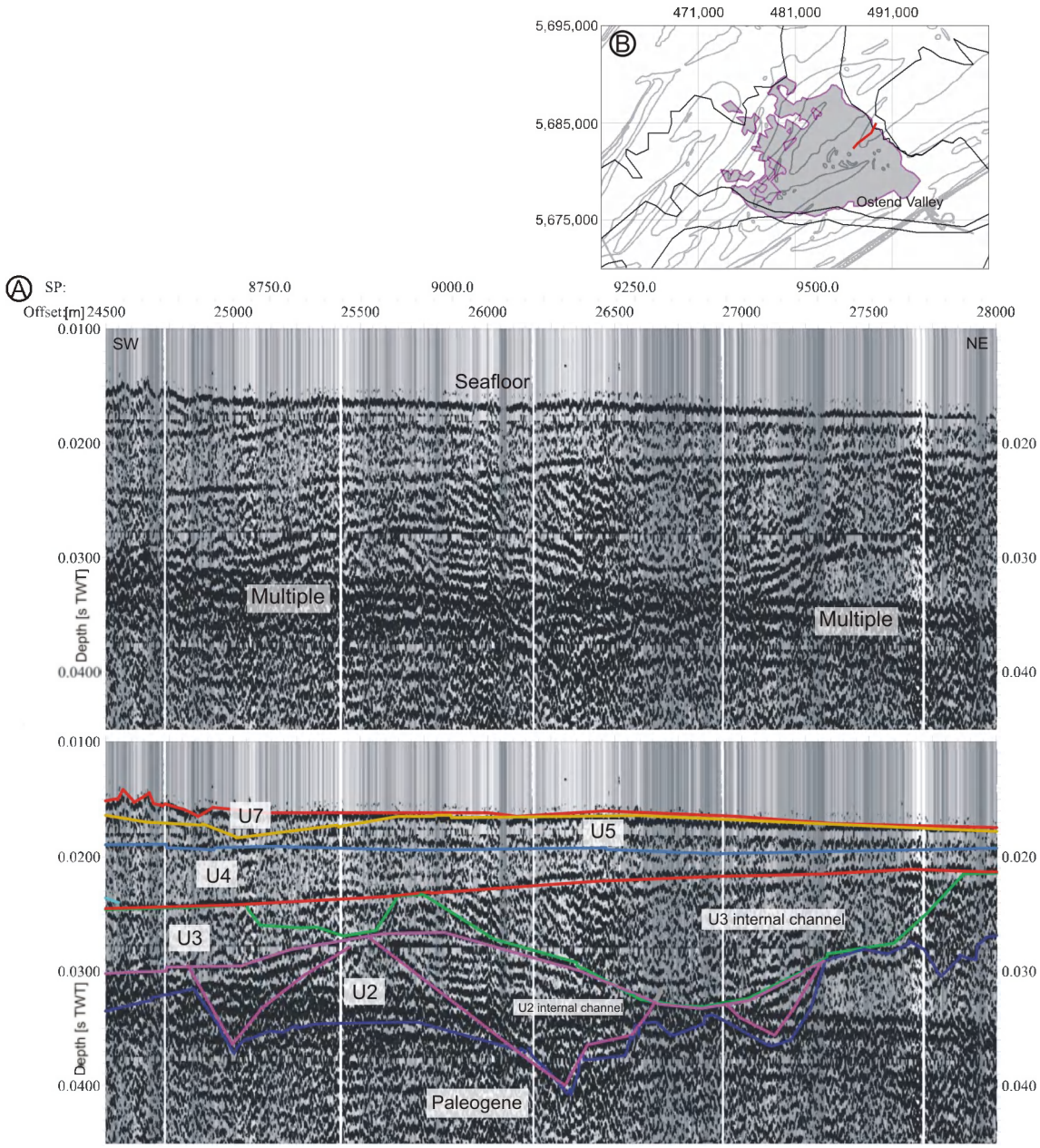

Fig. 4.5 (A) Detailed seismic section showing the internal reflection pattern and configuration of unit U2. The internal structure of the unit reveals channels, incising into the underlying Paleogene surface, showing prograded and onlap fill. The channels are clearly truncated at their top, making the upper boundary of U2 an erosional unconformity. The top section is the original seismic profile, the bottom section is the interpreted seismic profile. (B) Positioning of the seismic profile with reference to the present-day bathymetry (grey contours), the location of the Ostend Valley (black), and the extent of U2 (purple contour, grey area).

4.1.3 Seismic unit U3: the uppermost valley fill

Seismic unit U3 almost completely fills up the Ostend Valley, and even extends beyond it, infilling depressions in the Top-Paleogene surface (Fig.4.6B). The unit is bounded at its base by the strong QT reflector, or by the top bounding reflectors of U1 and U2. At the top, the unit is defined by a strong reflector, except in areas with high gas content, where the upper boundary is difficult to distinguish. The top reflector is slightly wavy, and locally incised by overlying units (Fig. 4.6A). The top reflector mainly downlaps onto the underlying surface, but it occasionally also onlaps against the Top-Paleogene surface. Where the seismic unit is not obliterated by the presence of the seafloor multiple, it

shows a transparent reflector configuration. The unit is also characterised by several channels which are often incising into the underlying units and which have a prograded fill. The internal channels are clearly truncated at their top, making the upper bounding reflector of U3 an erosional unconformity (Fig. 4.6B).
Fig. 4.3C displays the regional extent and topography of U3. It shows a large depocentre located in the Ostend Valley, and some isolated fragments beyond the valley borders in depressions in the Top-Paleogene surface. The surface of U3 slopes down in NW direction from –15 m to –30 m, with an abrupt depth change of 4 m (-20 to -24 m) (Fig. 4.6C), exactly at the Nearshore Slope Break of the Paleogene surface (Liu et al. 1992). Apart from this scarp, the surface also shows an axial, meandering depression with a width ranging from 600 m nearshore to 4 km offshore and a depth between –19.5 and –21 m, as well as some local incisions of up to 6 m below the average surface, caused by channels of overlying units.
Unit U3 is mostly less than 4 m thick in the area North of the scarp and outside the Ostend Valley (Fig. 4.4C). South-east of the scarp, the thickness ranges between 4 and 10 m, with a maximum of 18 m in the deepest internal channel. The 0 m thickness contour is indicated to distinguish between white areas where U3 is not present (outside the contour) and white areas where the data quality is too poor to distinguish U3 but where U3 is expected (inside the contour).
Seismic unit U3 will be discussed in more detail in Chapter 6, together with units U1 and U2, because they jointly make up the total infill of the incised valley offshore Oostende.

4.1.4 Seismic unit U4: extensive sheet-like deposit

Seismic unit U4 occurs over the entire width of the BCS and up to the present-day coastline (Fig. 4.8A). Its distribution is no longer restricted to the area of the Ostend Valley (Fig. 4.7A). The unit is bounded at its base by the top bounding reflector of U3, and by the QT reflector (Fig. 4.7). At the top, the unit is bounded by a strong reflector, except in areas with high gas content, where the upper boundary is difficult to distinguish. The top reflector is continuous and mostly straight. In the area offshore Zeebrugge it is strikingly horizontal, but elsewhere, it may also be wavy or undulating. The top reflector mainly downlaps onto the underlying surface, but it occasionally also onlaps against the Top-Paleogene surface. Where U4 is thick enough, the unit shows a complex combination of tangential or parallel-oblique prograding seismic reflector patterns, slightly wavy parallel internal reflectors, and many channel structures (Fig. 4.2A, 4.6C). Locally, a transparent reflector configuration occurs as well (not due to gas masking). The channel structures are characterised by a prograding or complex fill pattern (Fig. 4.7B), and sporadically by an onlapping fill pattern. In some places, the channels are deeply incised into the underlying units. The channels and internal reflections of U4 are clearly truncated at their top, making the top boundary of U4 an erosional unconformity.
Fig. 4.8A displays the topography and regional extent of U4, which is no longer governed by the presence of the Ostend Valley (which is nearly entirely filled up by the three underlying units), but rather by the imprint of the overlying units and by the effect of present-day hydrodynamic processes (Fig. 4.6C). The surface of U4 slopes down in NW direction, from –7 m to –28 m MLLWS, with an abrupt drop of 3-4 m (from about –12 m to –16 m), at a distance of 5-13 km offshore from the present-day coastline (13 km in the most north-eastern part of U4). Apart from this scarp, the surface also shows a clear imprint of the present-day seafloor topography.
Expressed as a surface percentage, only 47% (435 km²) of unit U4 is more than 3 m thick (ca. 3.5 ms TWT) (Fig. 4.9A). The thickest parts are found landward of the scarp in the surface of U4, where locally thicknesses up to 13 m are observed. Offshore this scarp, U4 has a thickness of 8 m below the Kwintebank and in the vicinity of the Middelkerke Bank.

Seismic unit U4 will be discussed in detail in Chapter 7, together with units U5 and U6, because all three are located in the nearshore area (<30 km offshore) and extend outside the incised valley over large parts of the BCS.

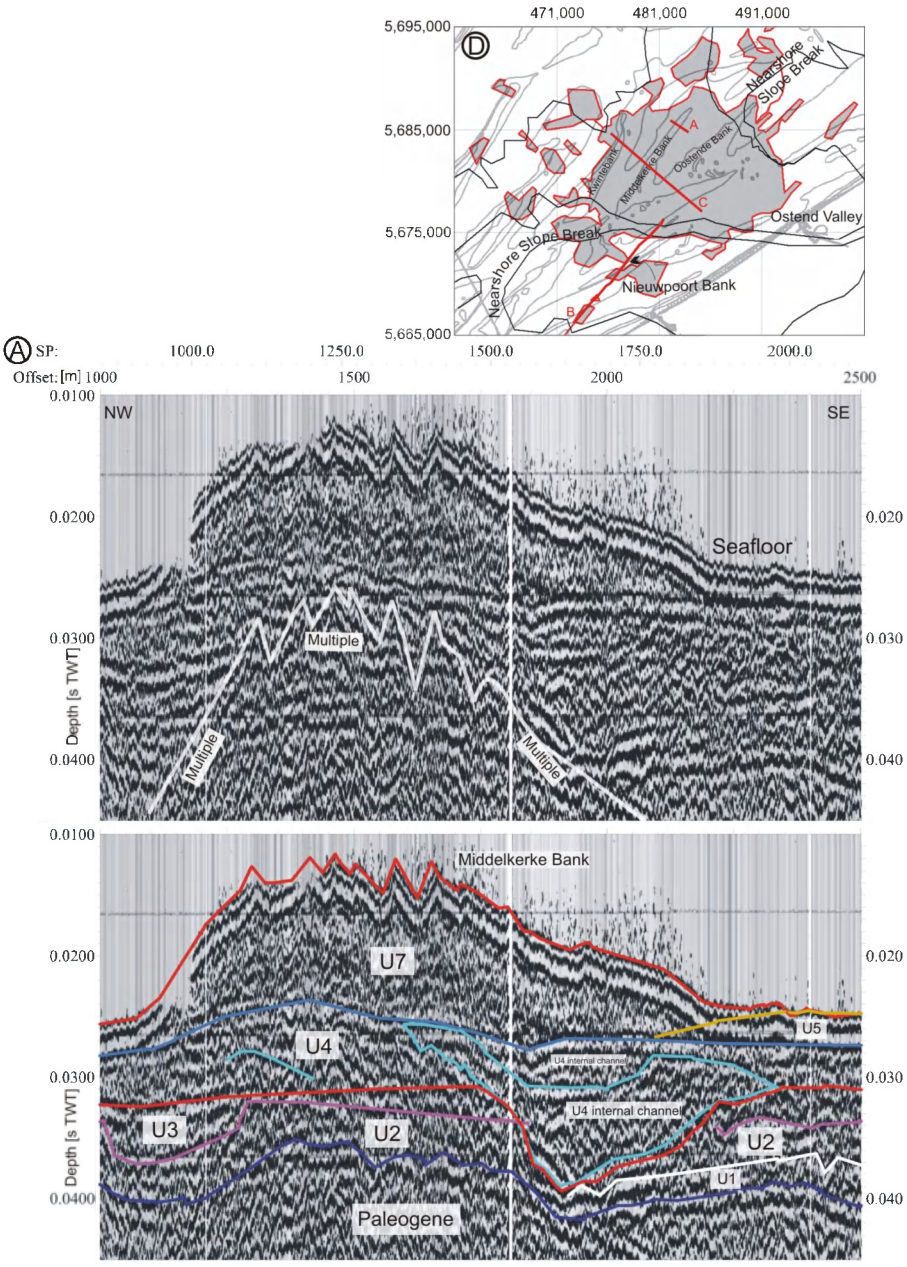

Fig. 4.6 (this and following page) Detailed seismic sections showing the internal reflection pattern and configuration of unit U3. (A) Incision of seismic unit U3 by a channel of overlying unit U4; (B) unit U3 extends beyond the Ostend Valley, infilling depressions in the Top-Paleogene surface; (C) the surface of U3 shows an abrupt depth change or 'scarp' of 4 m (-20 to -24 m MLLWS) exactly at the 'Nearshore Slope Break' of the Paleogene surface (Liu et al. 1992) (cf. (D)). Also note how the top of seismic unit U4 is determined by the imprint of the overlying units (U5 and U7) and by present-day hydrodynamic processes (erosion in the swales between the U7 banks). Top sections are original seismic profiles, bottom sections are interpreted seismic profiles. (D) Positioning of the seismic profiles with reference to the present-day bathymetry (grey contours), the location of the Ostend Valley (black), and the extent of U3 (red contour, grey area).

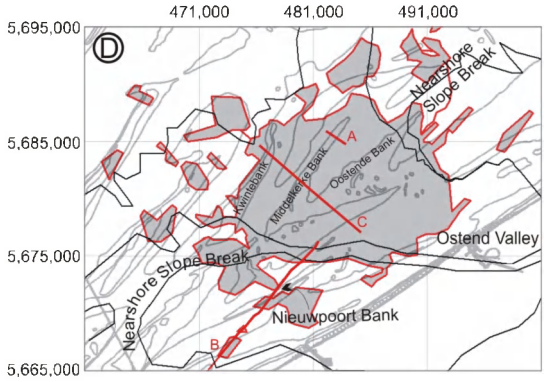
471,000
481,000
491,000
5,695,000
5,685,000
5,675,000
5,665,000
D
Nearshore Slope Break
A
Kwintebank
Middelkerke Bank
Oostende Bank
C
Ostend Valley
Nearshore Slope Break
Nieuwpoort Bank
B

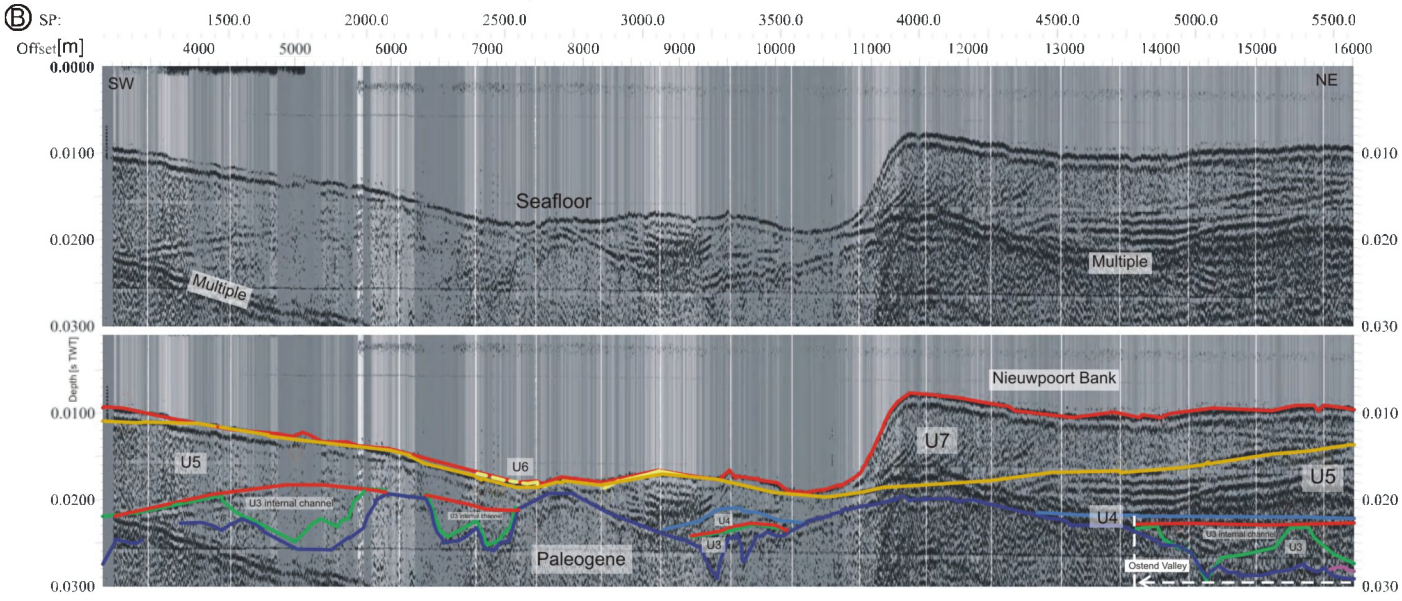
B
SP:
Offset:[m]
SW
NE
Seafloor
Multiple
Multiple
Nieuwpoort Bank
U7
U5
U6
U5
U4
U3 internal channel
Paleogene
Ostend Valley
Depth [s TWT]

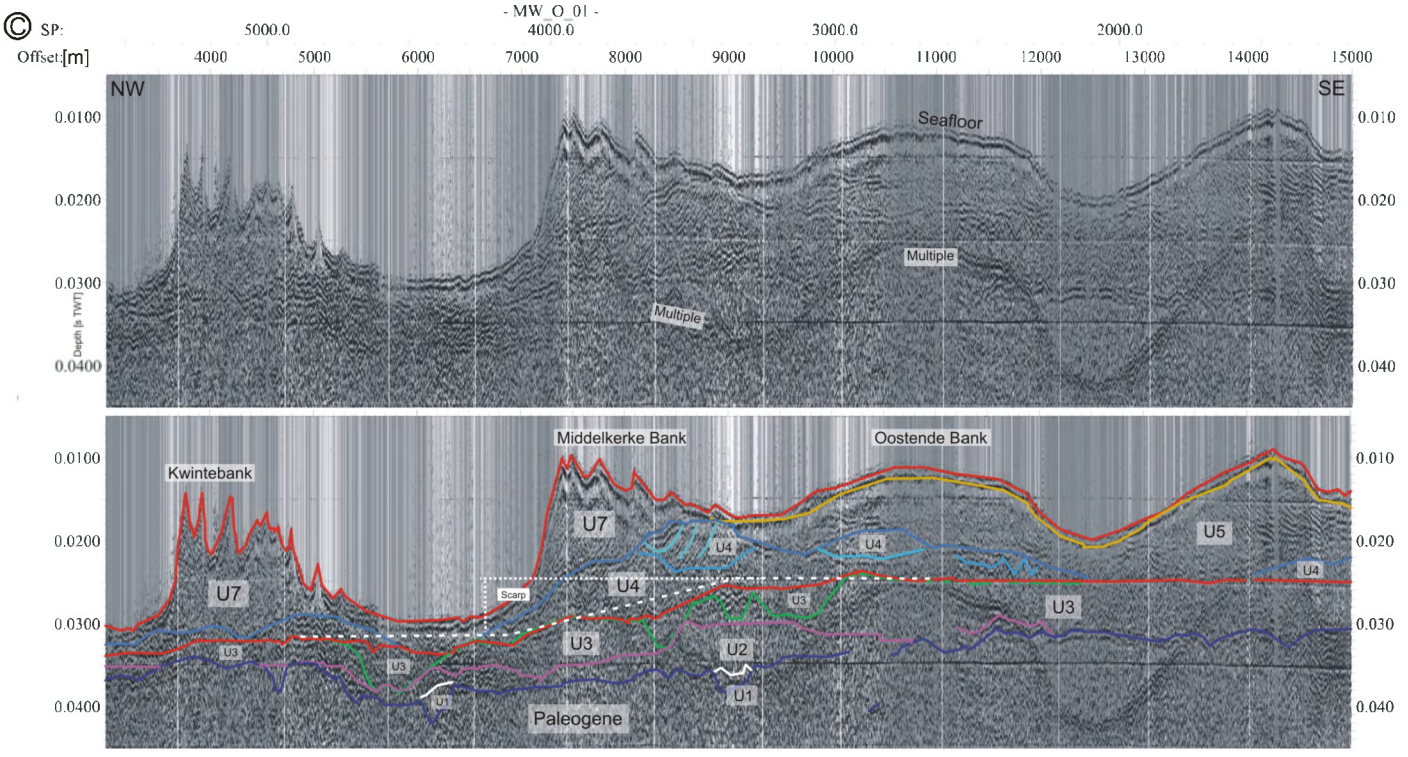
- MW_O_01 -
C
SP:
Offset:[m]
NW
SE
Seafloor
Multiple
Multiple
Middelkerke Bank
Oostende Bank
Kwintebank
U7
U7
U4
U4
U4
U5
U4
Scarp
U3
U3
U3
U3
U2
U1
U1
Paleogene
Depth [s TWT]

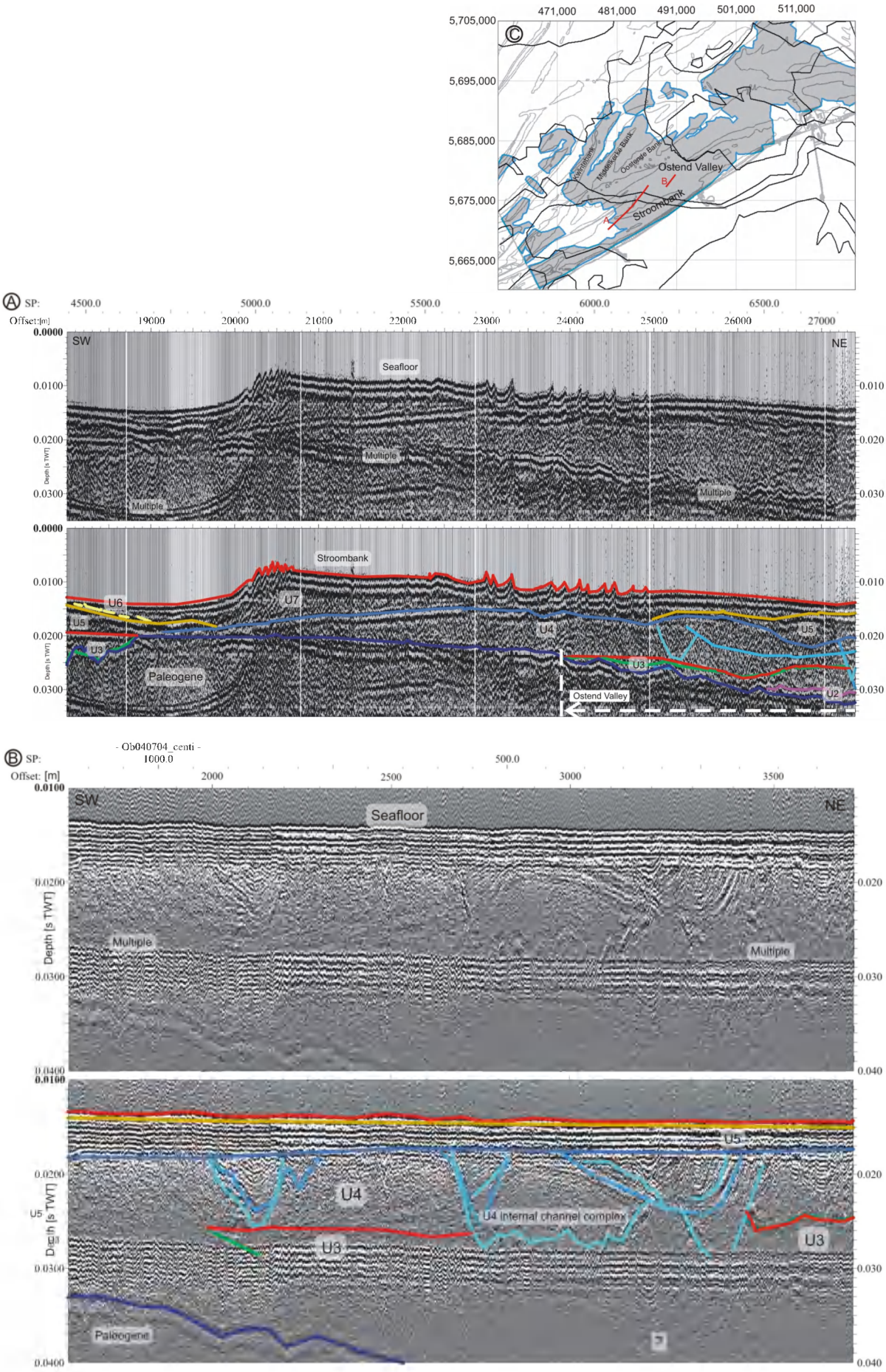
471,000
481,000
491,000
501,000
511,000
5,705,000
5,695,000
5,685,000
5,675,000
5,665,000
Ostend Valley
Stroombank
A
B
SW
NE
Seafloor
Multiple
Stroombank
U6
U7
U5
U4
U3
U2
Paleogene
Ostend Valley
Depth [s TWT]
Offset: [m]
- Ob040704_centi -
U4 internal channel complex

Fig. 4.7 (page 40) Detailed seismic sections showing the internal reflection pattern and configuration of unit U4. (A) Unit U4 is no longer restricted to the area of the Ostend Valley and extends beyond it (over the entire width of the BCS and up to the present-day coastline, Fig. 4.8A); (B) here U4 is a complex entity of channel structures with a prograded or complex fill. Top sections are original seismic profiles, bottom sections are interpreted seismic profiles. (C) Positioning of the seismic profiles with reference to the present-day bathymetry (grey contours), the location of the Ostend Valley (black), and the extent of U4 (blue contour, grey area).

Fig. 4.8 (page 42) Isobath maps of the top surfaces of seismic units: (A) U4; (B) U5; and (C) U6. The seismic units are shown with reference to the limits of the BCS, the present-day coastline, and the present-day bathymetry (light grey). In (B) and (C) the fine black contours represent the areas of the respective seismic unit emerging at the present seafloor.

Fig. 4.9 (page 43) Isopach maps of seismic units: (A) U4; (B) U5; and (C) U6. The seismic units are shown with reference to the limits of the BCS, the present-day coastline, and the present-day bathymetry (light grey). The 0 m thickness contour is indicated to distinguish between white areas where the unit is not present (outside the contour) and white areas where the data quality is too poor to distinguish the unit but where it is expected (inside the contour).

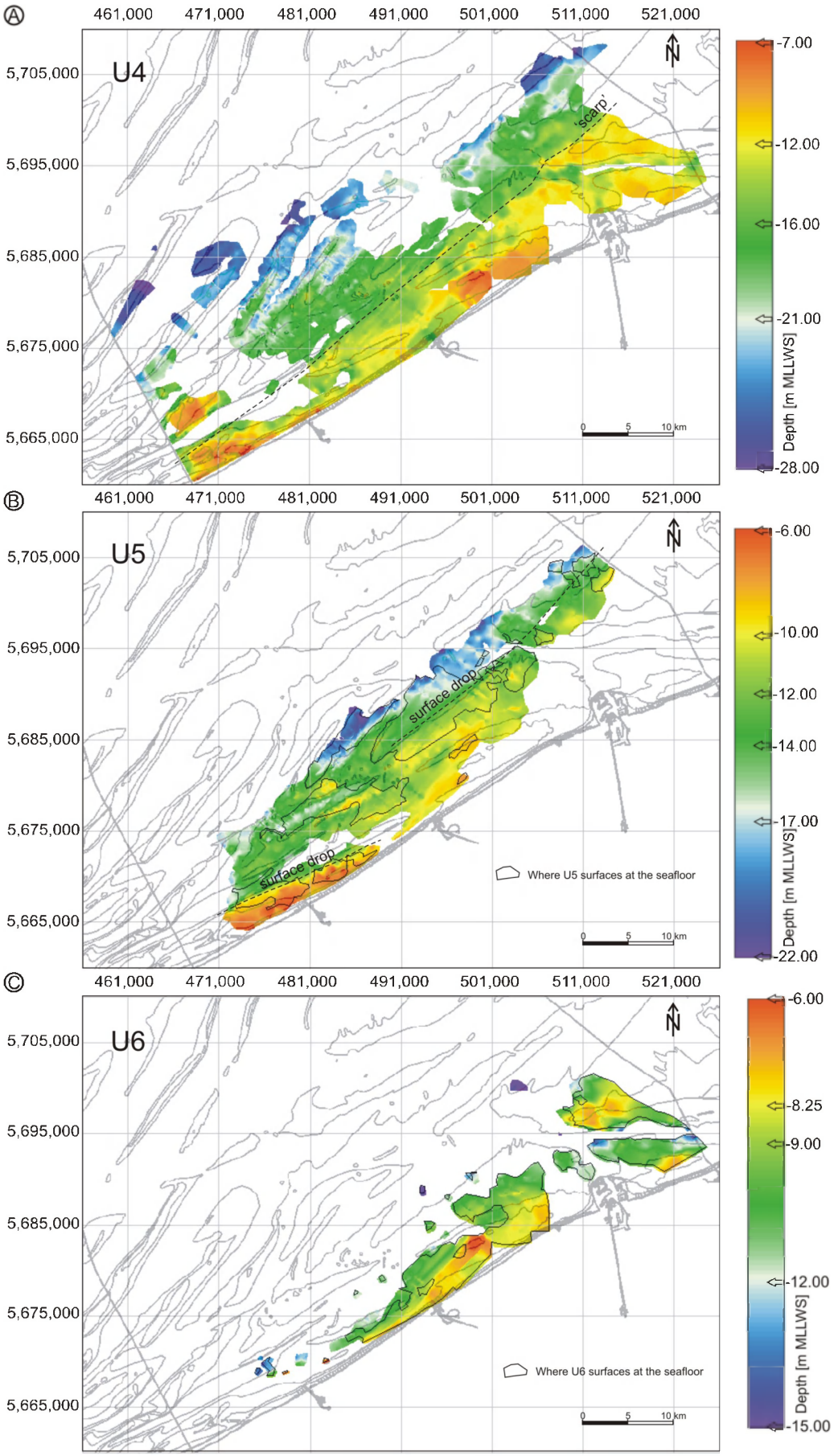
Ⓐ
461,000
471,000
481,000
491,000
501,000
511,000
521,000
5,705,000
5,695,000
5,685,000
5,675,000
5,665,000
U4
'scarp'
0 5 10 km
-7.00
-12.00
-16.00
-21.00
-28.00
Depth [m MLLWS]
Ⓑ
U5
surface drop
surface drop
Where U5 surfaces at the seafloor
-6.00
-10.00
-12.00
-14.00
-17.00
-22.00
Ⓒ
U6
Where U6 surfaces at the seafloor
-6.00
-8.25
-9.00
-12.00
-15.00

Fig. 4.8

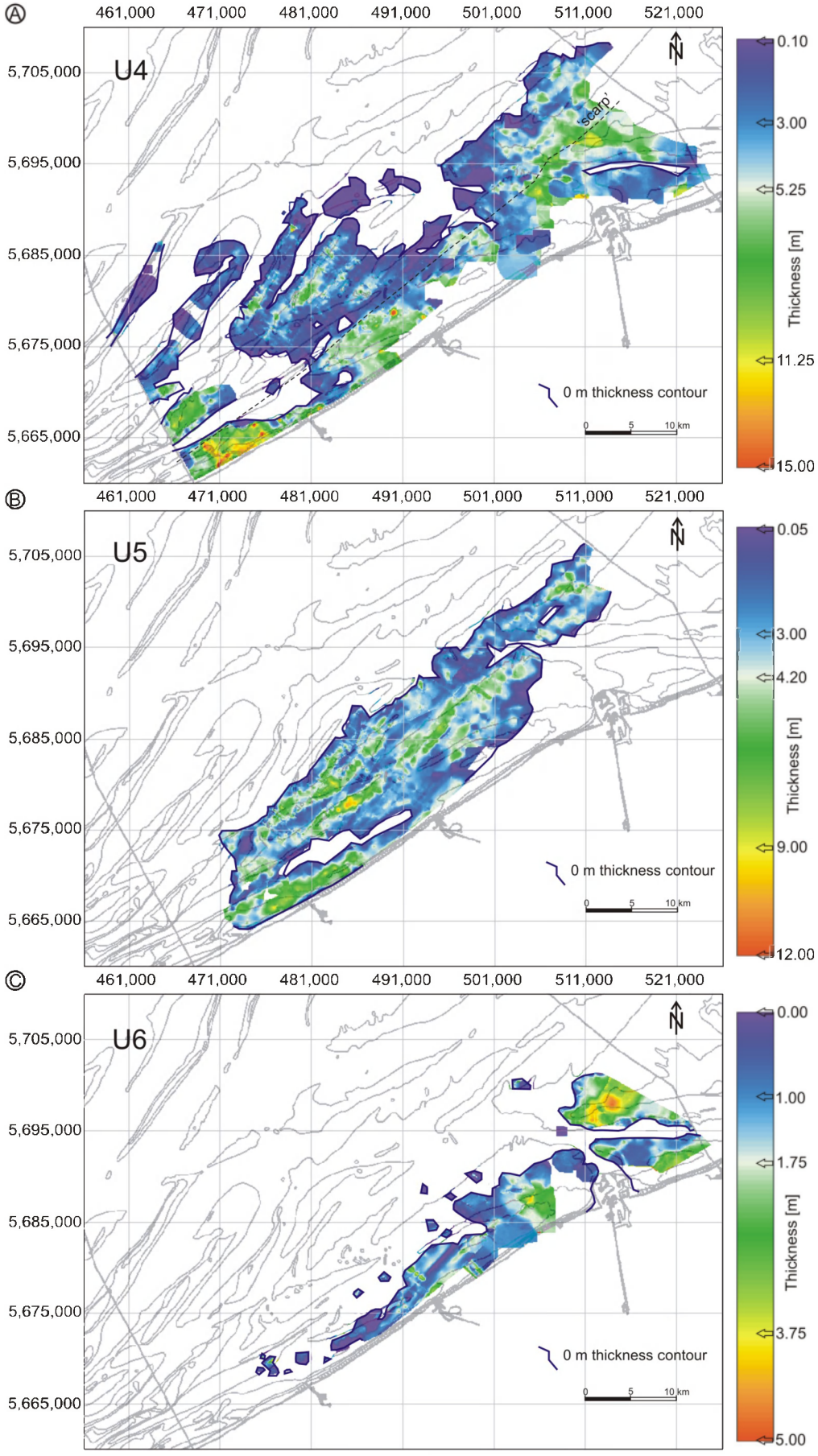
Ⓐ
461,000
471,000
481,000
491,000
501,000
511,000
521,000
5,705,000
5,695,000
5,685,000
5,675,000
5,665,000
U4
'scarp'
0 m thickness contour
0 5 10 km
0.10
3.00
5.25
11.25
15.00
Thickness [m]
Ⓑ
U5
0 m thickness contour
0 5 10 km
0.05
3.00
4.20
9.00
12.00
Thickness [m]
Ⓒ
U6
0 m thickness contour
0 5 10 km
0.00
1.00
1.75
3.75
5.00
Thickness [m]

Fig. 4.9

4.1.5 Seismic unit U5: local sequence of bank-shaped deposits

Seismic unit U5 occurs along almost the entire present-day coastline of the BCS (57 km). It is the first seismic unit that is exposed at the present-day seafloor over a large area, i.e. over 39% (220 km²) of its surface. At its base, the unit is bounded by the top bounding reflectors of U4 and U3, and by the QT reflector. In areas with high gas content the lower boundary is difficult to distinguish. At the top, the unit is defined by a strong reflector, which forms the seafloor reflector in large areas. The top reflector is continuous and downlaps onto the underlying surface at the seaward boundary of the seismic unit. At the landward side, between Nieuwpoort and Oostende, the seismic profiles did not reach close enough to the shore to allow determining the landward extent of seismic unit U5. Between Oostende and the Dutch border, the top bounding reflector onlaps the top bounding reflector of U4, or laterally merges with it. In those areas, both units are truncated and both top bounding reflectors (of U4 and U5) form part of the same erosional surface (Fig. 4.10A). Unit U5 mainly exhibits a lens- (Fig. 4.10A) or bank-like external form (Fig. 4.10B), with a prograding (tangential- and parallel-oblique) or channel-like internal seismic reflector pattern. In the nearshore zone, the unit is more sheet-like or very thin (Fig. 4.10B) and a transparent reflector configuration dominates. In some areas gas obliterates the seismic signature. Some of the internal structures are clearly truncated (Fig. 4.10A), making at least part of the upper boundary of U5 an erosional unconformity.

Fig. 4.8B displays the distribution of U5 and the topography of its upper bounding surface. Although the unit extends over almost the entire width of the BCS, its distribution is restricted to a NE-SW oriented, 12-km-wide strip along the present-day coastline in the SW, narrowing to a width of 6 km at 12 km off the present-day coastline in the NE.

The surface of U5 slopes down in NW direction from –6 m to –22 m, with a sudden drop (scarp) of 8 m (from about –6 to –14 m) at a distance of 2-4 km offshore the present-day coastline in the SW, and a smaller drop of 5 m (from about –12 to –17 m) at a distance of 10 km offshore in the NE. In the more offshore part, the surface exhibits a sequence of nearly coast-parallel highs (up to -8 m) and depressions (down to –16 m). A large part of this relief forms the present-day seafloor topography.

The major part of U5 is less than 3 m thick, but beneath the coast-parallel highs, the unit can reach a thickness of 6 to even 12 m (Fig. 4.9B).

Seismic unit U5 will be discussed in detail in Chapter 7, together with units U4 and U6, because all three are located in the nearshore area (<30 km offshore) and extend outside the incised valley over large parts of the BCS.

Fig. 4.10 (page 45) Detailed seismic sections showing the internal reflection pattern and configuration of unit U5. (A) U5 consists of a lens form, note how the top reflector onlaps on the top bounding reflector of U4, or laterally merges with it in those areas where both units are truncated; (B) U5 displays a bank form with a prograding (tangential and parallel oblique) seismic-reflection pattern; however, in the nearshore zone the unit is more sheet-like with a transparent reflection configuration. Top sections are original seismic profiles, bottom sections are interpreted seismic profiles. (C) Positioning of the seismic profiles with reference to the present-day bathymetry (grey contours), and the extent of U5 (orange contour, grey area).

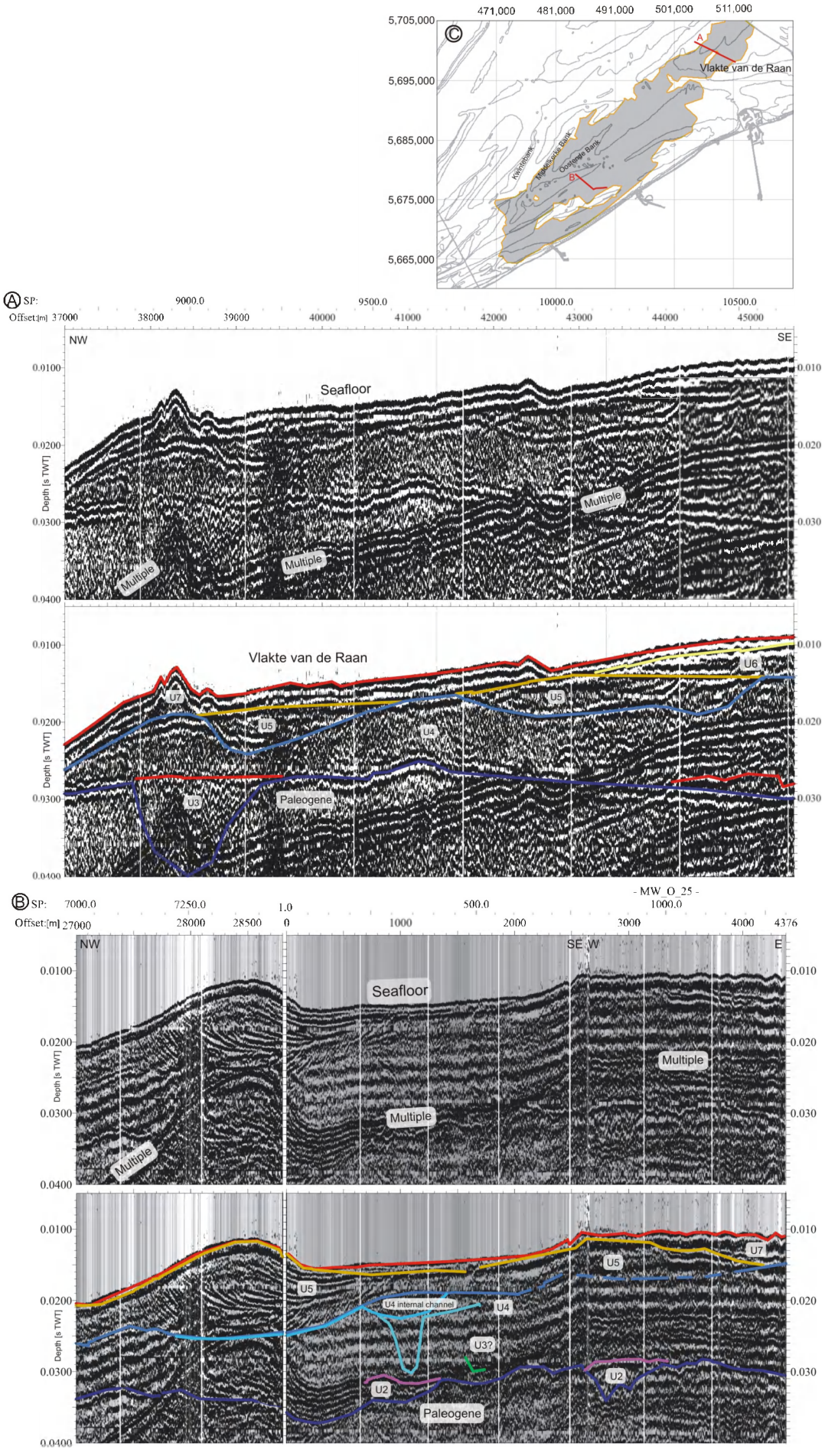
471,000
481,000
491,000
501,000
511,000
5,705,000
5,695,000
5,685,000
5,675,000
5,665,000
C
A
B
Vlakte van de Raan
Kwintebank
Middelkerke Bank
Oostende Bank
A SP:
Offset:[m]
9000.0
9500.0
10000.0
10500.0
37000
38000
39000
40000
41000
42000
43000
44000
45000
NW
SE
Seafloor
Multiple
Depth [s TWT]
0.0100
0.0200
0.0300
0.0400
0.010
0.020
0.030
Vlakte van de Raan
U7
U6
U5
U4
U3
Paleogene
B SP:
Offset:[m]
7000.0
7250.0
1.0
500.0
1000.0
27000
28000
28500
0
1000
2000
3000
4000
4376
- MW_O_25 -
NW
SE
W
E
Seafloor
Multiple
U5
U4 internal channel
U4
U3?
U2
Paleogene
U7

4.1.6 Seismic unit U6: the uppermost, nearshore sheet-like structure

Seismic unit U6 is a thin unit that is present as a sediment drape over the nearshore parts of units U4 and U5 (Fig. 4.11). The lower boundary of the unit is thus formed by the top bounding reflectors of U4 and U5. It is formed by a strong, straight, more or less horizontal reflector, which truncates the underlying units (Fig. 4.11). This boundary is difficult to distinguish in areas with high gas content. Most of the unit is defined at the top by the high-amplitude reflector that represents the seafloor. The top reflector is continuous and always downlaps onto the underlying surface. U6 is generally too thin to allow its seismic facies to be imaged, but occasionally some wavy-parallel or prograding reflectors occur.
Fig. 4.8C displays the topography and regional occurrence of U6. The unit is restricted to a 14-km-wide strip along the present-day coastline near the Dutch border, which narrows to a width of 2.5 km near Middelkerke and eventually disappears farther along the coastline to the SW. Some isolated outliers of this unit occur farther offshore, but these have been deduced from lithological evidence rather than from the seismic data.
The upper bounding surface of U6 is rather flat and ranges from about -6 to -9 m MLLWS at the top, to -12 m in offshore direction and towards the present-day incisions of the Scheur and the harbour entrance of Zeebrugge (Fig. 4.11). In the isolated patches offshore, the surface of U6 occurs down to -15 m (Fig. 4.8). Most of this relief actually corresponds to the present-day seafloor topography, and is probably influenced by present-day hydrodynamic conditions, as 87% of the surface of U6 is exposed at the seafloor.
Unit U6 is up to 5 m thick, and this is on the highest point of the Vlakte van de Raan. Elsewhere, U6 is on average < 1 m thick (Fig. 4.9C).
Seismic unit U6 will be discussed in detail in Chapter 7, together with units U4 and U5, because all three are located in the nearshore area (<30 km offshore) and extend outside the incised valley over large parts of the BCS.

4.1.7 Seismic unit U7: widespread bank-like and interbank sheet-like deposits

Seismic unit U7 is the upper most seismic unit and occupies almost the entire BCS (ca. 70% of 3560 km²). Where present, it is exposed at the present-day seafloor. In the nearshore area units U5 and U6 crop out at the seafloor (Fig. 4.6C, 4.10AB, 4.11 and 4.12A), and in the swales between the sandbanks the Paleogene is often exposed (Fig. 4.12B). At its base, the unit is bounded by the top bounding reflectors of U4, U3 and by the QT reflector. At the top, the unit is defined by the strong seafloor reflector, which downlaps onto the underlying surface. Unit U7 consists mainly of bank-shaped deposits with a prograding (tangential and parallel-oblique) internal seismic reflector pattern (in case of high-quality seismic data) (Fig. 4.12A). In the swales between the banks, and at the extremities of some banks, the unit is more sheet-like and mostly characterised by a transparent reflector configuration, although a parallel even, quasi-horizontal reflection pattern can be present as well (Fig. 4.12B).
Fig.4.13A displays the topography and regional occurrence of U7, which characterises most of the present-day seafloor topography. The contour of U7 is defined as the area where the distance between the seafloor reflector and the underlying surface (composed of U4, U3 (and IVDB), and QT) is more than 1.5 m. The surface of U7 slopes down in NW direction ranging from –2 m in the nearshore part to –50 m farthest offshore, showing a series of parallel banks and swales.
Unit U7 varies in thickness from 2 to 24 m under the sandbanks, to less than 1.5 m in the swales. The thickness of the U7 bank deposits generally increases in offshore direction (Fig. 4.13B).

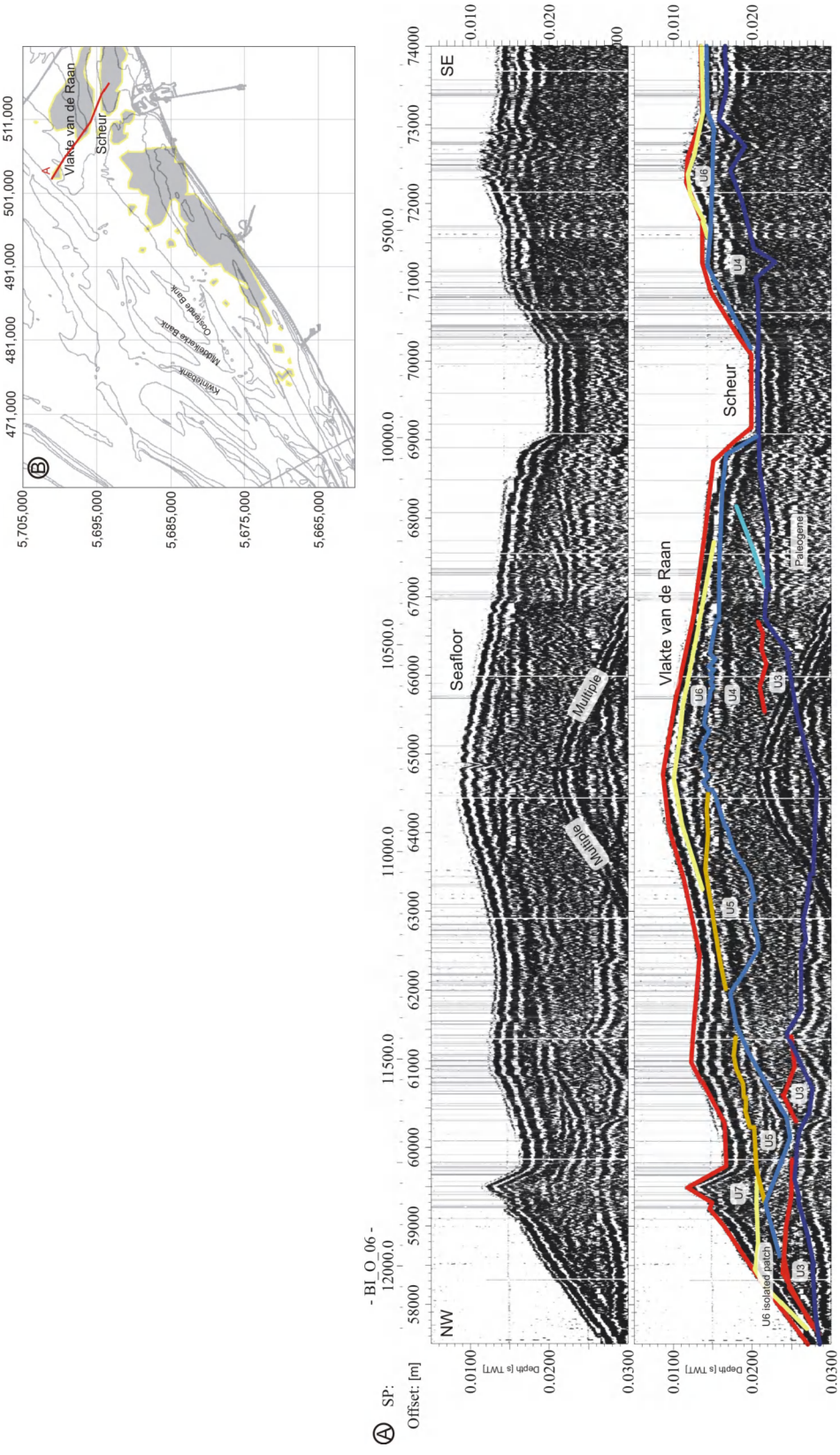

Fig. 4.11 (A) Detailed seismic section showing the internal reflection pattern and configuration of unit U6. U6 is a thin unit draped over the nearshore parts of units U4 and U5. Note the basal boundary which is a quasi-horizontal reflector, truncating the underlying units, and a deeper isolated patch of U6 farther offshore. The top section is the original seismic profile, the bottom section is the interpreted seismic profile. (B) Positioning of the seismic profiles with reference to the present-day bathymetry (grey contours), and the extent of U6 (yellow contour, grey area).

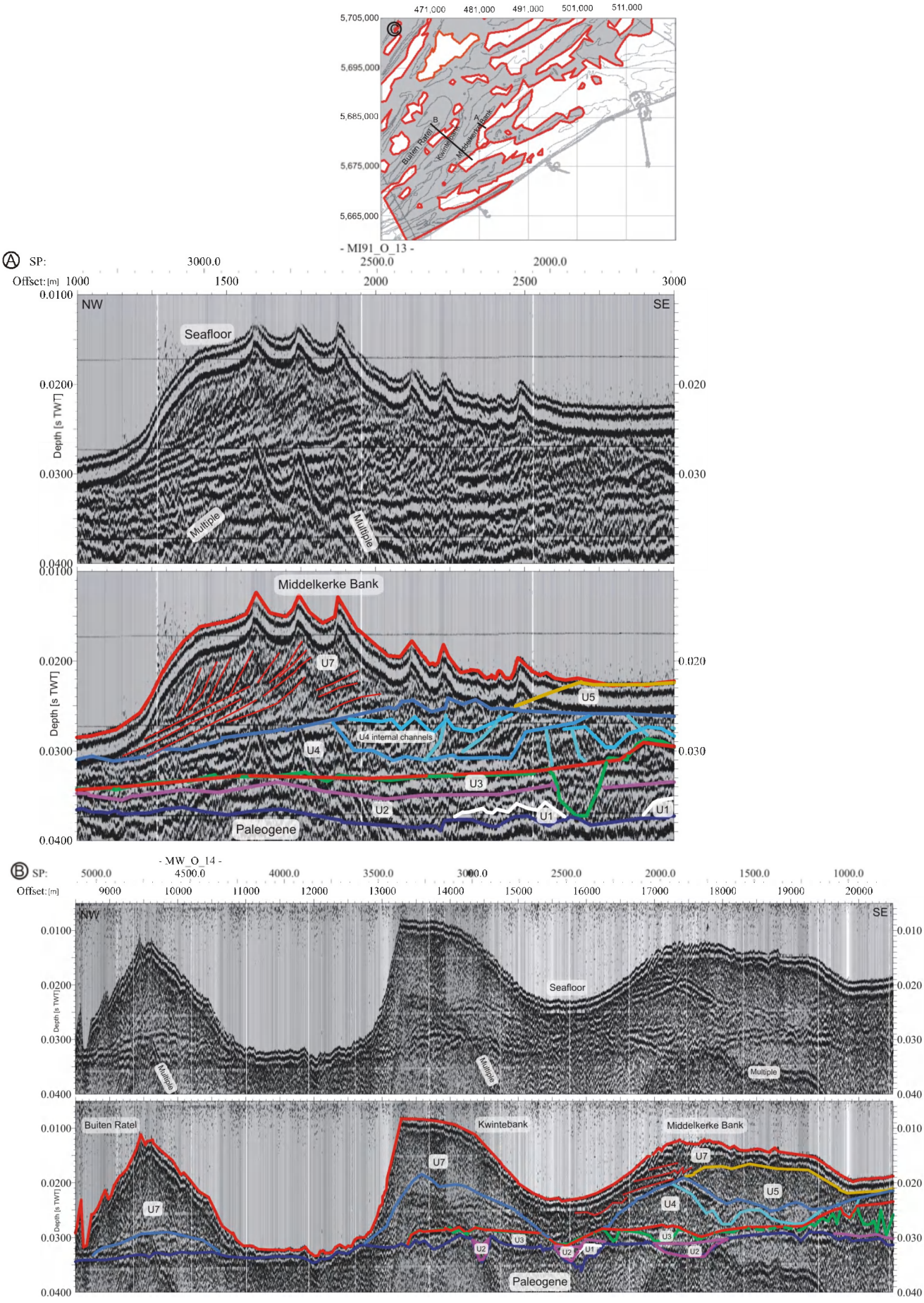
471,000
481,000
491,000
501,000
511,000
5,705,000
5,695,000
5,685,000
5,675,000
5,665,000
C
Buiten Ratel
Kwintebank
Middelkerke Bank
A
B
- MI91_O_13 -
Ⓐ SP:
3000.0
2500.0
2000.0
Offset: [m] 1000
1500
2000
2500
3000
NW
SE
Seafloor
Multiple
Multiple
Depth [s TWT]
0.0100
0.0200
0.0300
0.0400
0.020
0.030
Middelkerke Bank
U7
U5
U4
U4 internal channels
U3
U2
U1
U1
Paleogene
- MW_O_14 -
Ⓑ SP:
5000.0
4500.0
4000.0
3500.0
3000.0
2500.0
2000.0
1500.0
1000.0
Offset: [m]
9000
10000
11000
12000
13000
14000
15000
16000
17000
18000
19000
20000
NW
SE
Seafloor
Multiple
Multiple
Multiple
0.010
0.040
Buiten Ratel
Kwintebank
Middelkerke Bank
U7
U7
U7
U5
U4
U3
U3
U2
U2
U1
U1
U2
Paleogene

Seismic unit U7 is discussed separately in Chapter 8, because it forms the bulk of the sandbanks, and makes up most of the present-day bathymetry. It is the only unit that is in accordance with the present-day hydrodynamic regime (i.e. as shown by the presence of dunes).

Fig. 4.12 (page 48) Detailed seismic sections showing the internal reflection pattern and configuration of unit U7. U7 is the upper most seismic unit and covers almost the entire BCS, making up the present-day bathymetry, except for: (A) the nearshore area where units U5 emerges at the seafloor, and (B) in the swales where the Paleogene is exposed. Unit U7 consists mainly of: (A) bank forms with a prograding (tangential and parallel-oblique) internal seismic reflector pattern, whereas (B) in the swales and at the extremities of some banks, the unit is more sheet-like and sometimes characterised by a parallel even, nearly horizontal reflector pattern. Top sections are original seismic profiles, bottom sections are interpreted seismic profiles. (C) Positioning of the seismic profiles with reference to the present-day bathymetry (grey contours), and the extent of U7 (red contour, grey area).

Fig. 4.13 (page 50) (A) Isobath map of the top surface of seismic unit U7. Seismic unit U7 is the upper most seismic unit and covers almost the entire BCS, making up the present-day bathymetry, except for the nearshore area where units U5 and U6 emerge at the seafloor (fine black and red contours, respectively), and in the swales where the Paleogene is exposed. The red shaded areas were not covered by seismic profiles, but core data revealed that U6 emerges at the seafloor in these zones as well. (B) Isopach map of seismic unit U7. The seismic unit is shown with reference to the limits of the BCS, the present-day coastline, and the present-day bathymetry (light grey).

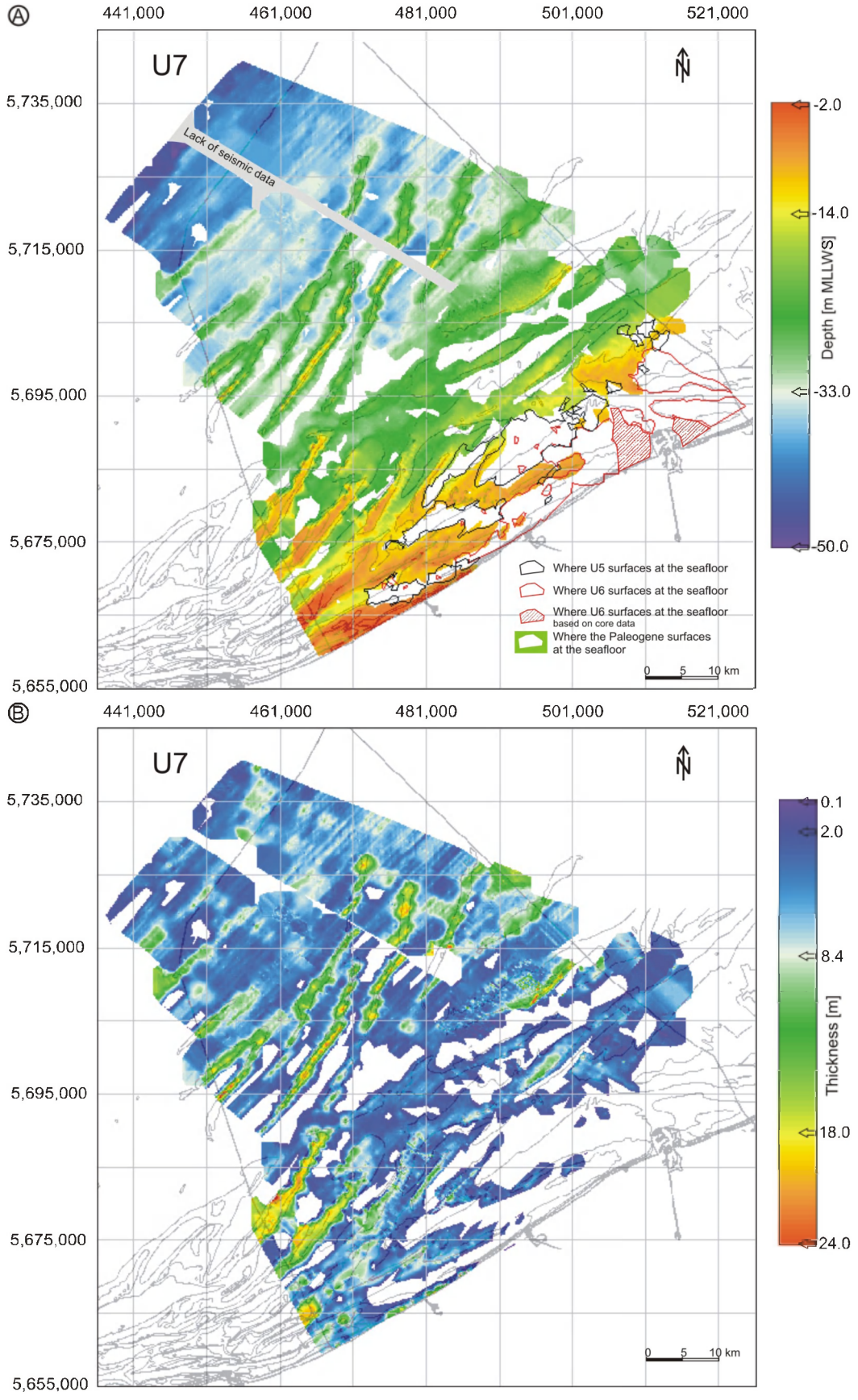
Ⓐ
441,000
461,000
481,000
501,000
521,000
U7
N
5,735,000
5,715,000
5,695,000
5,675,000
5,655,000
Lack of seismic data
-2.0
-14.0
-33.0
-50.0
Depth [m MLLWS]
Where U5 surfaces at the seafloor
Where U6 surfaces at the seafloor
Where U6 surfaces at the seafloor based on core data
Where the Paleogene surfaces at the seafloor
0 5 10 km
Ⓑ
441,000
461,000
481,000
501,000
521,000
U7
N
5,735,000
5,715,000
5,695,000
5,675,000
5,655,000
0.1
2.0
8.4
18.0
24.0
Thickness [m]
0 5 10 km

Fig 4.13

5.
The Top-Paleogene unconformity

The Top-Paleogene unconformity, in previous studies usually referred to as the 'Top-Tertiary surface', is an unconformity separating older strata of Paleogene (and possibly some of Neogene) age from the overlying Quaternary deposits. As such, it represents, in fact, also the base of the Quaternary deposits in the study area. The presented seven seismic units all occur in the sedimentary sequence above the unconformity. The Top-Paleogene unconformity has been moulded by different processes during several phases in time. It carries even an imprint of the modern bank-trough topography, and locally emerges at the present-day seafloor, where it is still being remodelled by the present-day hydrodynamic processes. Some of the geomorphological elements of the Top-Paleogene unconformity that have been moulded during earlier phases can still be observed in the present-day bathymetry. The Offshore Scarp e.g. is still visible between the Hinder Banks, while others are completely hidden and covered by overlying deposits. The low relief of the present-day seabed belies the complexity and irregularity of the underlying, buried relief. It is hard to imagine that below the sea bed covered with sandbanks a major incised valley system is present.

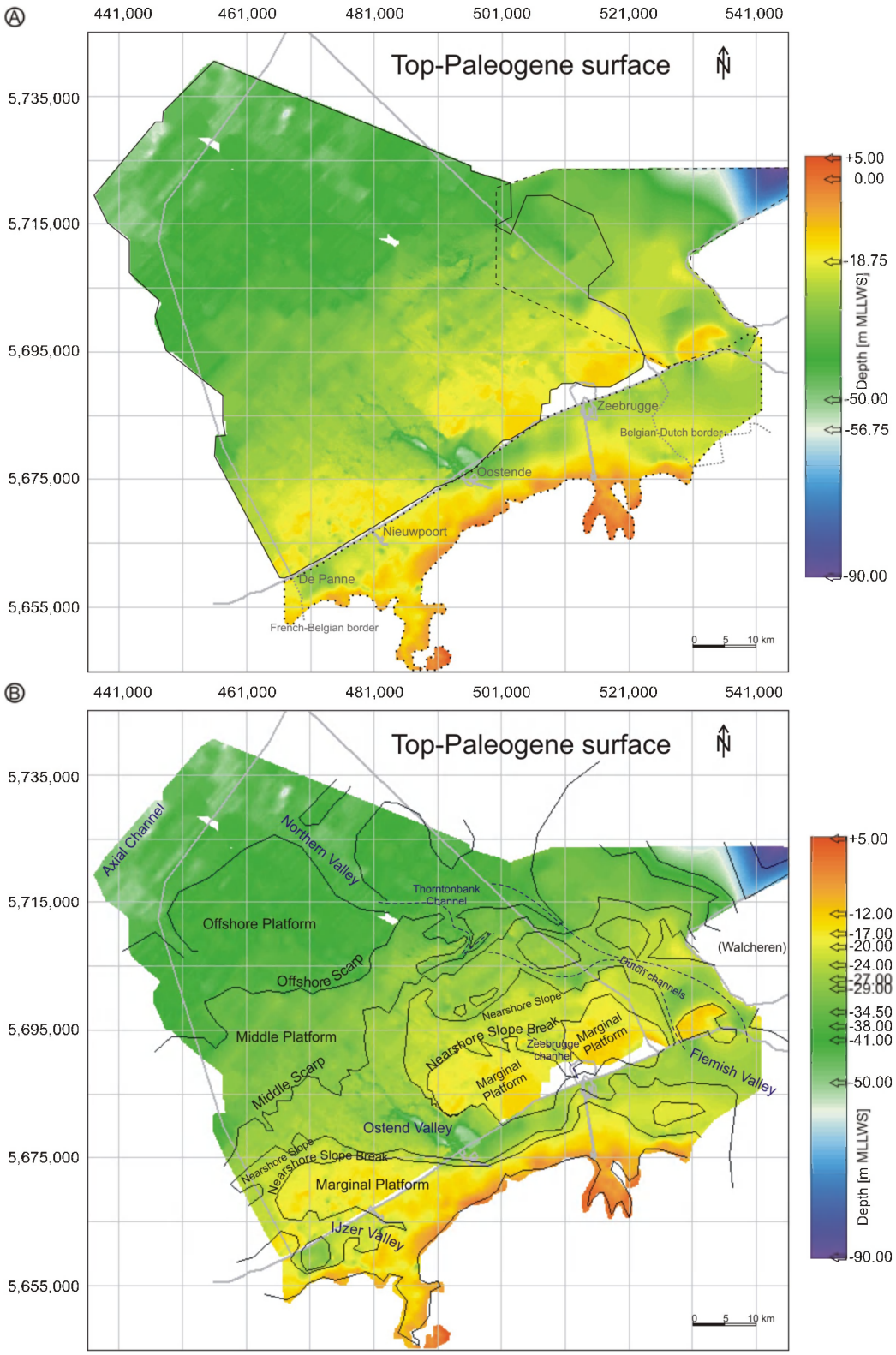

Fig. 5.1 (A) The presented Top-Paleogene surface is a composite surface consisting of an onshore grid covering the coastal plain (dotted contour, Meyus et al. 2000, 2005), an offshore grid covering part of the Dutch sector (dashed contour, Ebbing et al. 1992), and an offshore grid covering the entire BCS based on the presented seismic data (full contour). (B) Interpreted Top-Paleogene surface, showing planation surfaces bounded by slope breaks and scarps, and incised valleys and channels. Most of these morphological features were described for the first time by Mostaert et al. (1989) and later in more detail by Liu (1990), and Liu et al. (1992). The same nomenclature is used here, although some slopes or platform boundaries have been drawn slightly differently because of new evidence from the denser seismic network (cf. Fig. 5.3).

5.1 Introduction: a surface composed of several grids

The morphology and relief of the Top-Paleogene unconformity is illustrated in Fig. 5.1A. The surface shown on this figure is a composite surface constructed from three separate surface grids: an onshore grid covering the Coastal Plain (Meyus et al. 2000, Meyus et al. 2005), an offshore grid covering part of the Dutch sector (Ebbing et al. 1992), and an offshore grid covering the entire BCS based on the presented seismic data.
The onshore grid represents, in fact, the base of the Pleistocene deposits in the Coastal Plain, so it only provides information on the Top-Paleogene unconformity where Pleistocene deposits occur. The grid is drawn up (in m TAW) from a selection of core data, in the framework of developing a Flemish groundwater model (VGM, Meyus et al. 2005). The offshore grid in the Dutch sector was created on the basis of an isobath map, constructed from seismic data (in m LLWS) for a geological map in the area of the Rabsbank (oil and gas concession blocks S7, S8, S10 and S11). The grid on the BCS was created from all available seismic data presented here, with reference level MLLWS. Owing to the fact that the seismic network is not very dense in the northern part of the BCS, subtle gridding artefacts reveal the orientation of the seismic profiles in the gridded surface.
In order to merge these three separately created grids, they were conformed to the same coordinate system and spheroid (UTM WGS84). The reference levels (MLLWS, LLWS and TAW) were considered to be equal, as the maximal difference between MLLWS and TAW in Nieuwpoort is 0.508 m and therefore within the precision limits of the seismic data. The different grids do not match seamlessly (data gaps exist in the nearshore area because of shallow water depths), but the whole provides a good overview. The apparently discrepancy between the offshore and onshore grid near Oostende is due to a difference in applied data and grid detail. The offshore grid is created from seismic data and provides thus more detail on the continuity of channels, whereas the onshore grid is created from punctual core data, of which the coverage is not as dense, and borings did not always reach deep enough to distinguish the deeply incised channels.

5.2 Description of the Top-Paleogene unconformity and new observations compared to former interpretations

5.2.1 Seismic-stratigraphic characteristics of the Top-Paleogene unconformity

The unconformity at the top of the Paleogene deposits is strongly apparent on most seismic profiles (indicated as QT reflector) (Fig. 5.2). The term 'QT' refers to the contact between the Quaternary deposits and the underlying Paleogene strata (in the past referred to as Tertiary). Apart from the seafloor reflector, QT is the most prominent reflector in the entire seismic dataset. In the nearshore area, where a lot of gas is present, the QT reflector was frequently the only one visible. So the Top-Paleogene surface could be created from all the digital seismic data available on the BCS.
In the study area, the Top-Paleogene unconformity represents the erosion surface and significant stratigraphic hiatus between the underlying, gently NE-ward dipping Lower and Middle-Eocene formations (Thanetian to Rupelian, De Batist 1989) and the overlying Quaternary deposits (Jacobs and De Batist 1996). The erosion surface is an angular unconformity, dipping slightly (0.05%) towards the NNW and characterised by incisions and depressions. Its average depth ranges between –50 m (MLLWS) at the most seaward boundary of the study area and 0 to -5 m in the most landward section (Fig. 5.1A). The deepest point, however, is located north of the island Walcheren where the Top-Paleogene unconformity reaches -90 m MLLWS (Ebbing et al. 1992) (Fig. 5.1A).

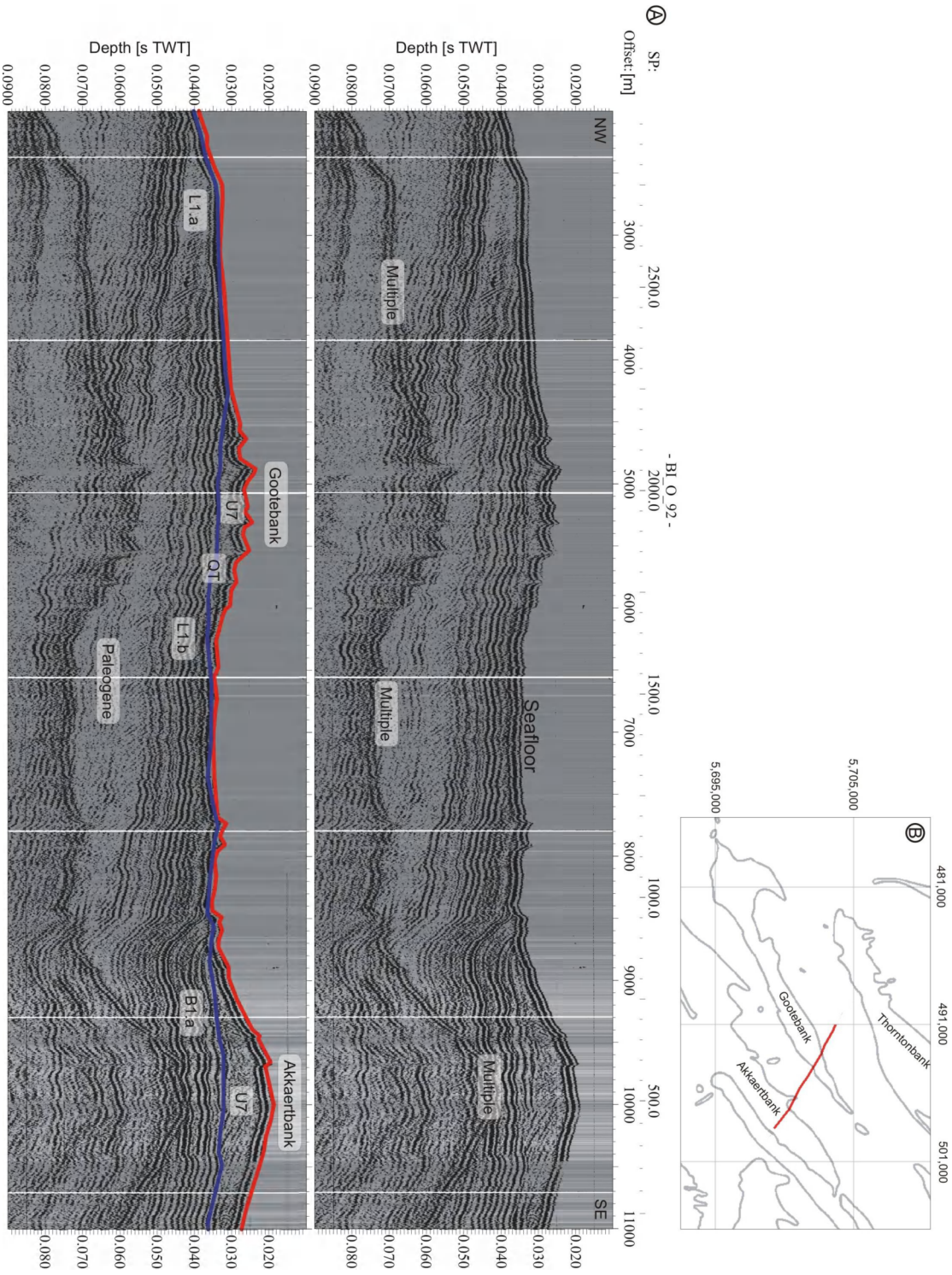

Fig. 5.2 (A) The angular unconformity at the top of the Paleogene deposits is strongly apparent on most seismic profiles (indicated as QT reflector in blue). It represents the erosional boundary and significant stratigraphic hiatus between the Middle-Eocene formations and the overlying Quaternary deposits. L1.a represents the Beernem Member of the Aalter Formation, L1.b represents the Oedelem Member of the Aalter Formation, and B1.a represents the Wemmel Member of the Maldegem Formation. These formations all belong to the Lutetian (Middle-Eocene) (Jacobs and De Batist 1996). The top section is the original seismic profile, the bottom section is the interpreted seismic profile. (B) Positioning of the seismic profile with reference to the present-day bathymetry (grey contours).

5.2.2 Geomorphological description of the Top-Paleogene unconformity

Planation surfaces bounded by scarps or slope breaks

The Top-Paleogene unconformity can geomorphologically be characterised by a series of planation surfaces bounded by slope breaks and scarps. These morphological features were described for the first time by Mostaert et al. (1989) and later in more detail by Liu (1990) and Liu et al. (1992) (Fig. 2.4). The nomenclature introduced by Liu (1990) and Liu et al. (1992) will be used here, although some slopes or platform boundaries have been defined slightly differently because of new evidence from the denser seismic network (Fig. 5.1B and Fig. 5.3). The 'Marginal Platform' steps down in offshore direction via a 'Nearshore Slope Break' to the 'Nearshore Slope', which itself gently slopes farther down in seaward direction, until it reaches, across the boundary of a paleo-valley, via the 'Middle Scarp', the relatively flat region of the 'Middle Platform'. Farther offshore the Middle Platform changes across the 'Offshore Scarp' into the 'Offshore Platform'. Even farther offshore, the 'Axial Channel' is present (Balson and D'Olier 1988).

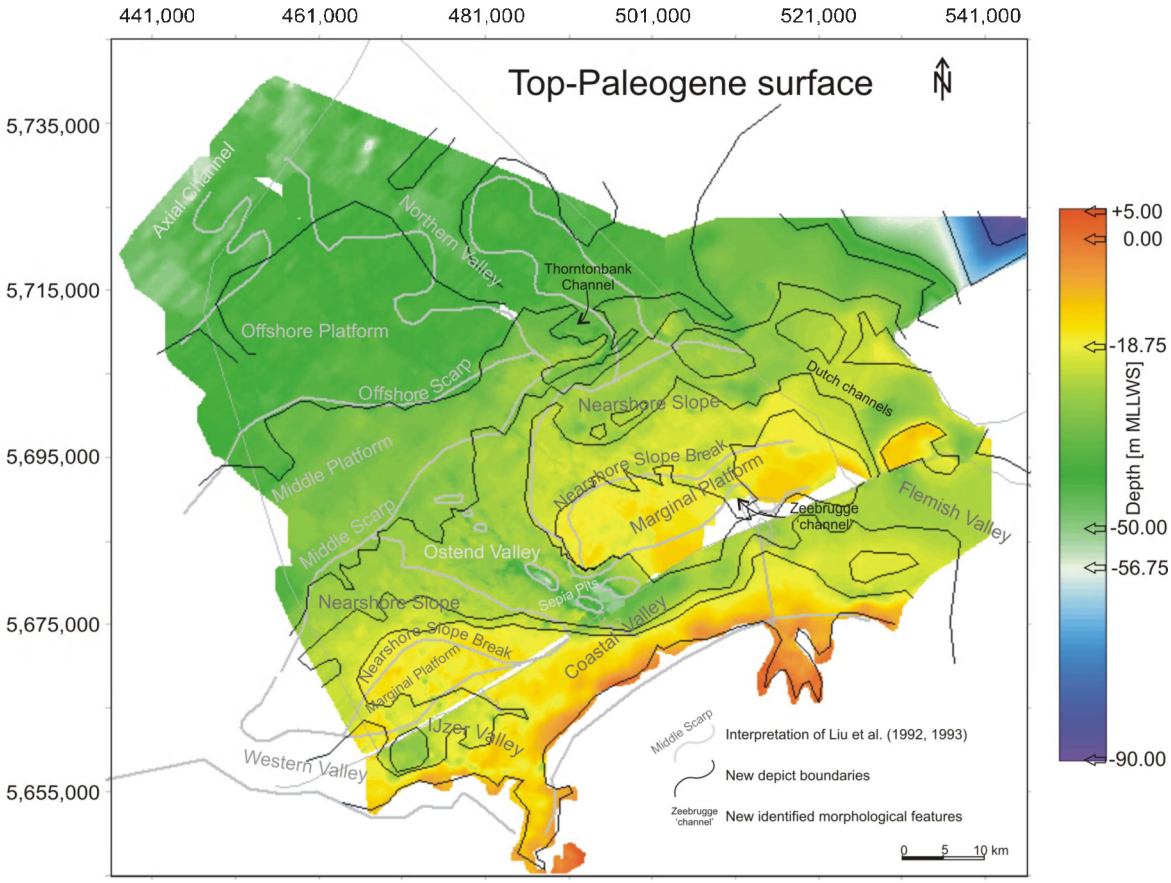

Fig. 5.3 The original interpretation of the Top-Paleogene surface of Liu et al. (1992, 1993) (light-dark grey), compared with the new interpretation (in black). Some slopes or platform boundaries have been drawn differently because of new evidence from the denser seismic network, but the same nomenclature is used (cf. Fig. 5.1B). Note how the denser seismic network created as part of this study shows that the Sepia Pits are in fact connected to elongated incisions. The IJzer Valley is no longer connected to the Coastal Valley. It occupies a drainage basin completely separated from the Ostend Valley drainage system by the western Marginal Platform that continues onshore. Also the Northern and Ostend Valley are now considered as two separate drainage systems.

The offshore section of the Marginal Platform has a main depth of about -17 m, with a minimum depth of -12 m (Fig. 5.1B). The Nearshore Slope Break separates the Marginal Platform from the Nearshore Slope by a drop of about 4 m, from -20 to -24 m MLLWS. The Nearshore Slope forms a gently sloping surface, ranging in depth between -24 to -27 m. The Middle Platform has a depth ranging between -29 m and -34.5 m; its southern boundary, the Middle Scarp, is generally marked by a gentle drop of some 2 m. Its northern boundary, however, is characterised by a drop of 6 to 8 m at the Offshore Scarp, to a level of -41 m MLLWS. Farther offshore the Offshore Platform shallows to -36 m and then gently slopes down to -38 m at the boundary with the Axial Channel, in which depths of -50 m are encountered.

Valley and channel incisions

Apart from the planation surfaces, Liu et al. (1992) also recognised several paleo-channels incised in the Top-Paleogene unconformity. The most prominent one is the 'Ostend Valley', introduced for the first time by Maréchal and Henriet (1983).
Offshore Oostende, a large NW-SE oriented funnel-shaped depression is incised into the Paleogene substratum, with a tail end stretching parallel with the coastline below the Coastal Plain, towards the NE (Fig. 5.1B). This paleo-valley has a strong asymmetrical profile with a gentle south-western slope and a steeper north-eastern flank. Taking into account the infilling pattern of the incised valley, the -24 m (MLLWS) isobath of the Top-Paleogene unconformity is used as the outer boundary of the valley instead of the -25 m isobath used by Liu et al. (1992). The valley is 6 km wide at its narrowest point and about 21 km at its offshore end. At the nearshore part, the valley floor is incised about 7 m into the Paleogene deposits, to -26 m, whereas at the offshore end, the base is situated 2.5 m below the overall top of the Paleogene substratum, at a depth of -27.5 m (MLLWS).

The tail end of the Ostend Valley, located along the present-day coastline, is part of what was formerly called the 'Coastal Valley', which was believed to extend beneath the entire Belgian Coastal Plain (Mostaert et al. 1989, Liu et al. 1992, Figs. 2.4 and 5.3). It was assumed that the Coastal Valley was joined by the 'Flemish Valley' near the Dutch-Belgian border, and that it joined the 'IJzer Valley' near the Belgian-French border (De Moor and Tavernier 1978, Mostaert et al. 1989, Liu et al. 1992), turning NW offshore France to form the Western Valley (Liu et al. 1992). However, the most recent data of the Top-Paleogene surface onshore (Meyus et al. 2005), and a denser nearshore seismic grid, clearly show that the IJzer Valley in the SW occupies a drainage basin completely separated from that of the Ostend Valley by the western Marginal Platform and its onshore continuation. Nevertheless, the Ostend Valley most likely still forms the seaward extension of the Flemish Valley in the NE (cf. discussion 5.3.1). The meandering connection has a width of 4-5 km, over a distance of at least 35 km (birds' flight distance), and is incised down to -25 to -36 m TAW (~MLLWS).

According to Liu et al. (1992) the Ostend Valley extends farther offshore into the 'Northern Valley' (Fig. 2.4). In the northern part of the BCS, however, limited data are available, which makes the contours of the Northern Valley less distinct. A very dense seismic grid is present though, over the Thorntonbank, at the assumed transition between the Northern and Ostend Valley (Fig. 5.1B). It shows a narrow channel with a width of only 1-4 km, incised to a depth of -50 m, 16 m below the surrounding Paleogene surface, which can hardly be the link between the 21-km-wide Ostend Valley and the Northern Valley, even if the Ostend Valley would have become that wide not until later. Most likely the Northern and Ostend Valleys represent two separate drainage systems. The Northern Valley and the deeply incised channel below the Thorntonbank are aligned with and most likely belong to a small drainage system that is present in the Dutch sector. This drainage system consists of two small channels linked with the Ostend Valley-Flemish Valley connection; they are incised to a depth of -30 m, and are 1-2.5 km

wide. Finally, a funnel-shaped depression is present offshore Zeebrugge. It is linked with the connection between the Ostend and Flemish Valley. This incision to a depth of -24 m is 1.5 km wide near Zeebrugge and becomes 5 km wide farther offshore.

5.2.3 Description of the Quaternary isopach map

Fig. 5.4 represents the isopach map of the Quaternary deposits. The thickest sequence of Quaternary sediments is present in the central depression of the Ostend Valley, where the Quaternary cover is 45 m thick. However, on 40% of the Belgian Continental Shelf surface, the Quaternary cover is less than 5 m thick. In a large part of this area, between the Offshore Scarp and the Nearshore Slope, the Paleogene substrate simply emerges at the present-day seafloor in the troughs between the sandbanks. Disregarding the extreme value in the Ostend Valley, the Quaternary cover is generally 10-25 m thick below the sandbanks. This isopach map clearly illustrates how thin and fragmented the Quaternary cover on the BCS actually is.

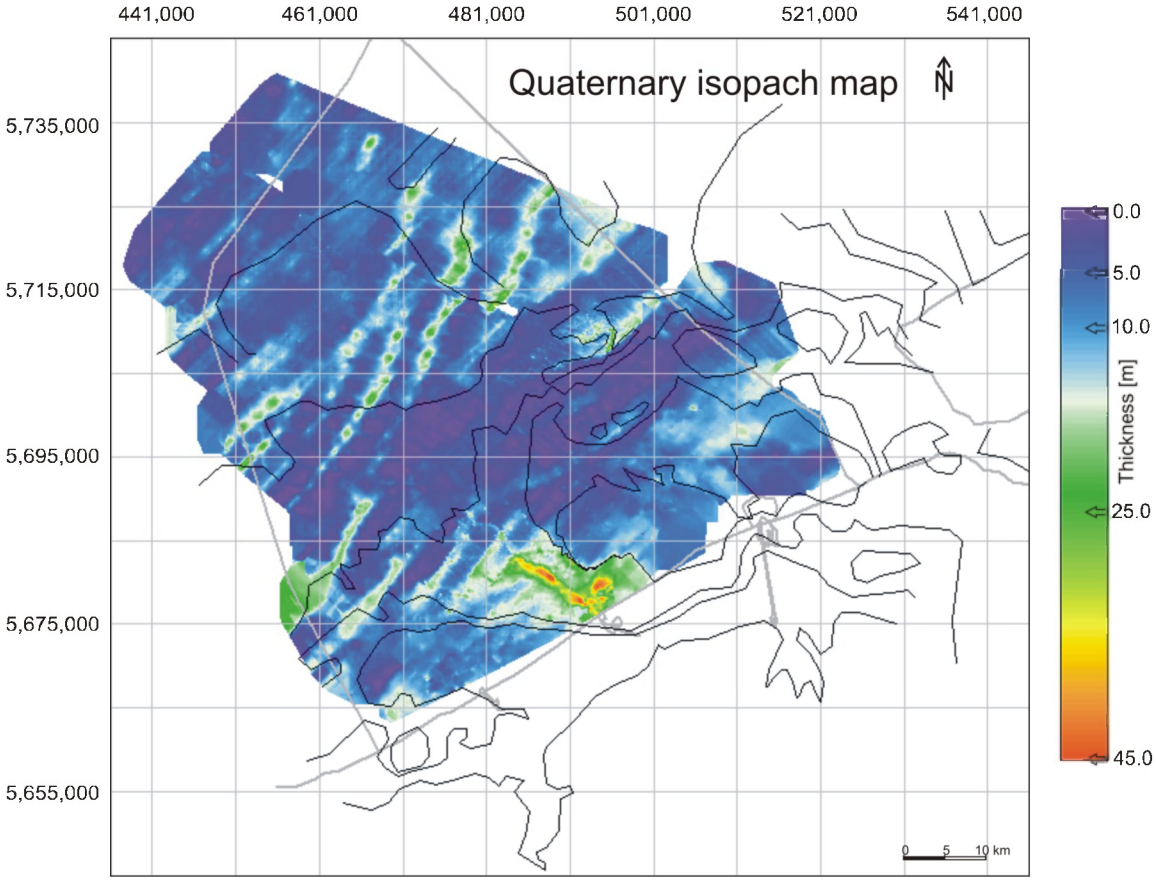

Fig. 5.4 The Quaternary isopach map with reference to the limit of the BCS and present-day coastline (grey), and the main morphological features of the Top-Paleogene surface (black).

Ⓑ

Zone I.: Hinder Banken area, swale east of the Oosthinder
Acoustic technique: video - Inspector color camera
Description: video frames, with their locations indicated on the multibeam image
Campaign name: St0424

Lat: 51° 27' 44" **Long:** 2° 40' 32"

Lat: 51° 27' 50" **Long:** 2° 38' 48"

Zone II.: Hinder Banken area, swale east of the Westhinder
Acoustic technique: video - Inspector color camera
Description: video frames, with their locations indicated on the multibeam image
Campaign name: St0502
Date: 8-9 February 2005

Lat: 51° 26' 26" **Long:** 2° 39' 46"

Lat: 51° 25' 45" **Long:** 2° 31' 8"

Lat: 51° 24' 54" **Long:** 2° 29' 36"

Fig. 5.5 (page 58) (A) Thematic map showing the gravel and coarse-sand distribution at the seafloor on the BCS (adapted after Van Lancker et al. 2007). (B) Examples of video images, showing the presence of gravel in the swales between the Hinder Banks (Zone I. east of the Oosthinder, Zone II. east of the Westhinder) (adapted after Van Lancker et al. 2007). The locations are indicated on multibeam images. The zones where the video and multibeam data are recorded are indicated with red circles on (A).

5.2.4 Lithological description of the Top-Paleogene unconformity

Few cores reached the Top-Paleogene surface in the nearshore area, but farther offshore, the surface emerges at the seafloor between the sandbanks and could be penetrated.
Directly above the Top-Paleogene unconformity, at the base of the overlying units, a gravelly lag deposit is commonly present. It consists of a heterogeneous mixture of silex and sandstone boulders and pebbles, and abundant shell fragments, mostly in a sandy matrix. More detailed descriptions of this lag deposit will follow in the next chapters when the base of the overlying units will be described. Where the Paleogene substratum emerges at the seafloor, in the troughs between the sandbanks, gravel has been visualised by multibeam, side-scan-sonar, and video data (Van Lancker et al. 2007, Fig. 5.5).

5.3 Discussion

5.3.1 Chronostratigraphic framework

Interpretation and dating of planation surfaces: the Offshore Platform

The Top-Paleogene unconformity is probably a polygenetic surface diachronously formed in marine as well as fluvial circumstances over a long period of time and under the influence of a series of different climatic conditions (Maréchal and Henriet 1983, Mostaert et al. 1989). The planation surfaces probably bear the stamp of marine abrasion processes, which must have played an active relief-forming role in periods of higher sea levels during the Quaternary (Maréchal and Henriet 1983). Moreover, the several slope breaks separating these planation surfaces argue for a multi-phase erosional process. According to Mostaert et al. (1989), the formation of the northward-dipping planation surfaces started at the earliest in Eemian times, based on paleo-geographic considerations. Some marine sedimentation took place in the southwest of the BCS during brief episodes in the Middle-Pleistocene interglacial stages (Paepe and Baeteman 1979, Sommé 1979), but it was only during the Eemian and Holocene interglacials that the entire area fully submerged and experienced a period of marine conditions (Kirby and Oele 1975, Mostaert et al. 1989). However, the 'Offshore Scarp' as determined by Liu et al. (1992), and the related 'Offshore Platform' were most likely already formed during Saalian time, as Van den Broeke (1984) determined the presence of Eemian deposits under the Hinder Banks in the area bounded by the Offshore Scarp (later these Eemian deposits will be referred to as 'IVDB Eemian' deposits) on the basis of marine fauna. Also, Kirby and Oele (1975) encountered Eemian deposits –overlain by Weichselian deposits – in a 'Quaternary Basin' incised in the Paleogene substratum below the Fairy and Sandettie Bank. This Quaternary Basin forms the SW extension of the Offshore Platform incised in the Paleogene substratum below the Hinder Banks (Fig. 5.6).

On the basis of a comparison of the location of the Offshore Platform, the Offshore Scarp and the Quaternary Basin with a paleo-geographic reconstruction of the Rhine-Meuse drainage system during a final phase in the MIS6 stage (i.e. Drente Glaciation at the end of the Saalian Ice age, when the ice-sheet margin reached as far south as the central part of the Netherlands) (Busschers et al. 2008), we can infer that the Offshore Scarp and Offshore Platform were most likely formed by the incising Meuse river (Fig. 5.7C). During the maximum ice-sheet extent of the Saalian glaciation ("Amersfoorter Stadium" during the Drente glaciation MIS6), the Rhine-Meuse system entered a proglacial lake with a lake level that was similar to the present mean sea level (Fig. 5.7A). The Rhine-Meuse system most likely formed a delta close to the present Dutch coastline. However, during the subsequent deglaciation, the Meuse deeply incised into the former proglacial Rhine-Meuse braidplain in response to the lowering of the lake level and final drainage of the proglacial lake (Fig. 5.7B). The emptying of this Saalian proglacial lake probably represented the second of two megafloods identified by Gupta et al. (2007), which created the Strait of Dover in the south (Gibbard 2007). Therefore, it is most likely that the incising Meuse valley diverted SW-ward toward the Dover Strait, forming the Offshore Platform, Scarp and Quaternary Basin. A Saalian proglacial lake could develop because of a coalescence of the Scandinavian and British ice sheets in the central North Sea area, and a ridge north of the Dover Strait (possibly an outcrop of bedrock, or a barrier formed by moraine deposited during the previous glaciation (Gibbard 2007). According to Cohen (pers. comm. 2007) the proglacial lake could have left coarse-grained material. A previous, similar event, which deepened the Weald-Artois anticlinal ridge, formed the initial Strait of Dover, originated from a proglacial lake present during part of the Elsterian Glaciation (MIS12), some 425,000 years ago (Gibbard 2007, Gupta et al. 2007).

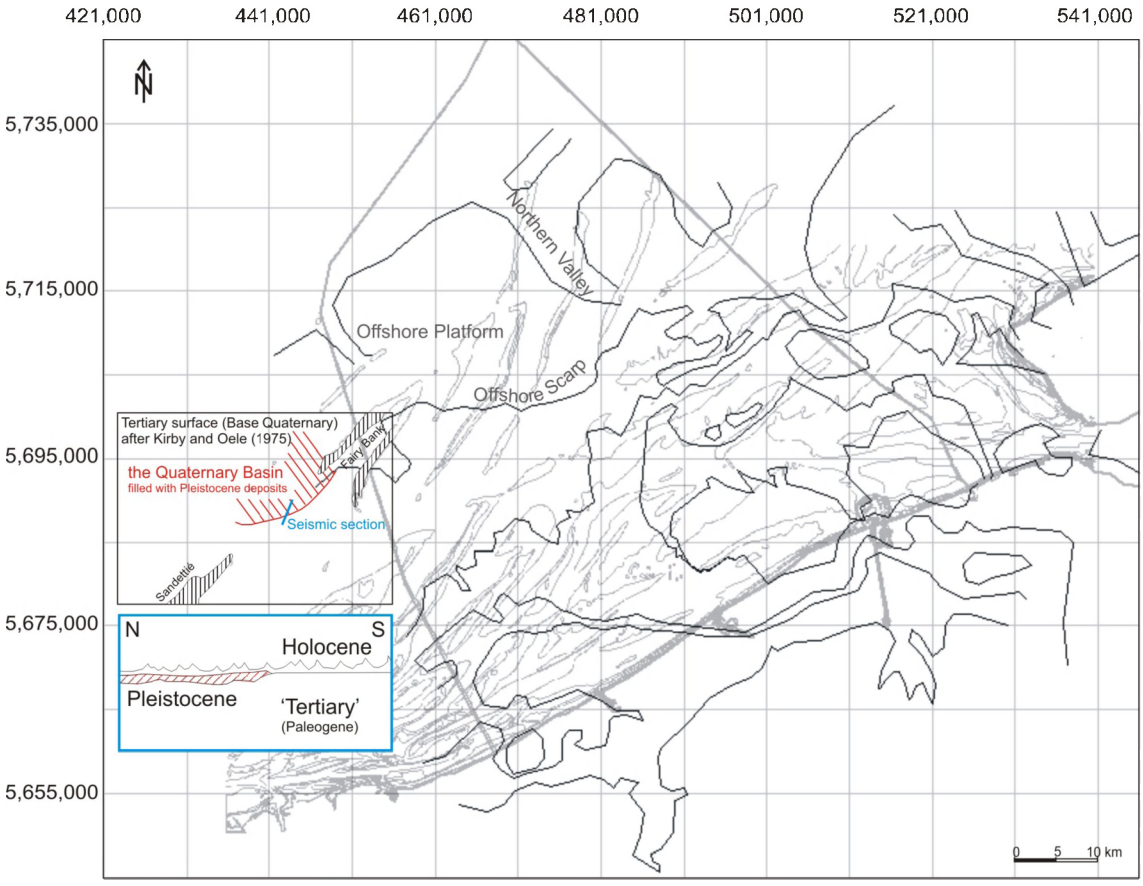

Fig. 5.6 A 'Quaternary Basin' incised in the Tertiary (Paleogene) substratum below the Fairy and Sandettie Bank (Kirby and Oele 1975), forms the SW extension of the Offshore Platform incised in the Paleogene substratum below the Hinder Banks.

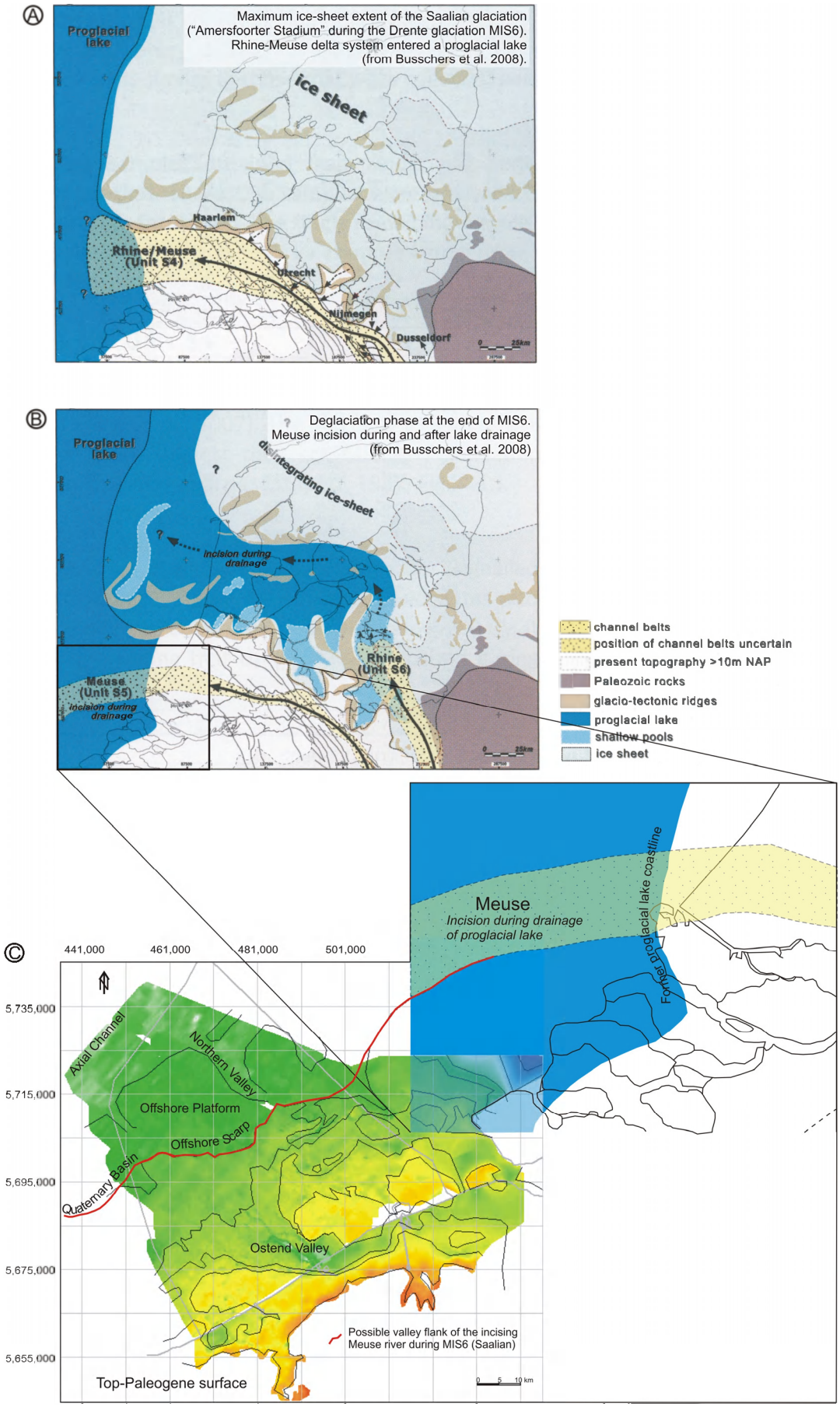
A
Proglacial lake
Maximum ice-sheet extent of the Saalian glaciation
("Amersfoorter Stadium" during the Drente glaciation MIS6).
Rhine-Meuse delta system entered a proglacial lake
(from Busschers et al. 2008).
ice sheet
Haarlem
Rhine/Meuse
(Unit S4)
Utrecht
Nijmegen
Dusseldorf
B
Proglacial lake
Deglaciation phase at the end of MIS6.
Meuse incision during and after lake drainage
(from Busschers et al. 2008)
disintegrating ice-sheet
incision during drainage
Meuse
(Unit S5)
incision during drainage
Rhine
(Unit S6)
channel belts
position of channel belts uncertain
present topography >10m NAP
Paleozoic rocks
glacio-tectonic ridges
proglacial lake
shallow pools
ice sheet
C
441,000
461,000
481,000
501,000
5,735,000
5,715,000
5,695,000
5,675,000
5,655,000
Meuse
Incision during drainage
of proglacial lake
Former proglacial lake coastline
Axial Channel
Northern Valley
Offshore Platform
Offshore Scarp
Quaternary Basin
Ostend Valley
Possible valley flank of the incising
Meuse river during MIS6 (Saalian)
Top-Paleogene surface
0 5 10 km

Fig. 5.7

Fig. 5.7 (page 61) (A) During the maximum ice-sheet extent of the Saalian glaciation ("Amersfoorter Stadium" during the Drente glaciation MIS6), the Rhine-Meuse system entered a proglacial lake that reached heights similar to the present mean sea-level, and most likely formed a delta close to the present Dutch coastline (Busschers et al. 2008). (B) During the following deglaciation, i.e. the final phase in the MIS6 stage, the Meuse incised deeply into the former Rhine-Meuse braidplain during and after the proglacial-lake drainage (Busschers et al. 2008). Note how the maximum proglacial-lake extent and Meuse incision after lake drainage are drawn in the same reconstruction. (C) The Offshore Scarp, Offshore Platform and Quaternary Basin lie perfectly in line with the incising Meuse, and were most likely formed by this incising river during and after lake drainage.

In view of the above-described succession of events, the 'Offshore Platform' planation surface most likely represents the floor of an incised river valley of Saalian age, and not an Eemian marine abrasion surface. In the next chapter, it will become clear though that at least the 'Nearshore Slope Break', separating the 'Nearshore Slope' and 'Marginal Platforms' was formed during the Eemian transgression, as postulated by Mostaert et al. (1989).

Interpretation and dating of incised valleys: the Axial Channel, Northern and Ostend Valleys

The Axial Channel

The major Axial Channel incised into the Paleogene substratum (Liu et al. 1992), corresponds to the 'Deep Water Channel' still present in the present-day seafloor (van der Molen and van Dijck 2000, van der Molen and de Swart 2001a, 2001b, Schüttenhelm and Laban 2005). It originated, according to Balson and D'Olier (1988), already during the Mid-Miocene, and was further eroded during the Pliocene. The fact that Quaternary infilling sediments are missing suggests that during the Late-Pleistocene and Holocene, further scouring of the channel took place. It is highly likely that after the first, Elsterian proglacial lake drainage, the Thames and Scheldt, which were realigned through the newly formed Dover Strait (Gibbard 2007), passed through this Axial Channel, which lies in line with the Lobourg Channel to the south (Balson and D'Olier 1988, Bridgeland and D'Olier 1995, Antoine et al. 2003, Gupta et al. 2007). It is only after the second, Saalian lake drainage that the Meuse and Rhine were also diverged southward (Gibbard 2007), the latter only since the Weichselian as during the Saalian lake drainage the Rhine was still directed northwards (Busschers et al. 2008).

The Northern Valley and associated drainage systems

The Northern Valley and the deeply incised channel below the Thorntonbank cut through the Offshore Platform and Scarp, respectively. This implies that they are younger than these features, which were formed during emptying of the Late-Saalian lake (Fig. 5.1B). Then again, the Northern Valley and Thorntonbank Channel are filled with IVDB Eemian deposits (as far as the limited seismic grid in the northern area can allow establishing the continuation of the unit from farther offshore), which implies an older age for the formation of these structures. The Dutch channels in line with them are filled with mostly Eemian deposits and with Weichselian (Kreftenheye Formation) sediments in the northernmost part of the Dutch grid, near the Thorntonbank (Ebbing et al. 1992, Ebbing and Laban 1996). The infilling of the Zeebrugge depression might also of be of Eemian age, judging from the depositional depth of the infilling unit compared to that in the nearby Dutch sector.

The Ostend Valley

Extending the above-presented surface grid representing the morphology of the Top-Paleogene unconformity on the BCS, Dutch shelf and Coastal Plain towards the east (Flemish Valley grid supplied by Meyus et al. 2005), it becomes evident that the Ostend Valley lies in line with the Flemish Valley (Fig. 5.8A). The Flemish Valley is defined by De Moor (1996) as a deep valley system that extended the axis Demer-Rupel-Scheldt to the NW during the Late-Pleistocene, containing tributaries in the valleys of the Dender, Upper-Scheldt and Lys (Leie), and which later became entirely filled (Bogemans and Baeteman 2003) (Fig. 5.8B). According to an earlier definition of Tavernier and De Moor (1974), the Flemish Valley is more extended and comprises also the northerly basins, i.e. a low-lying plain situated to the north of Gent (Bogemans and Baeteman 2003). On most illustrations and maps available in literature, the IJzer Valley and the so-called Coastal Valley were always drawn as part of the Flemish Valley drainage system (De Moor and Tavernier 1978, Mostaert et al. 1989, Liu et al. 1992) (e.g. Fig. 2.4 and Fig. 5.3). The most recent data of the top of the Paleogene substratum onshore (Meyus et al. 2005), and a denser nearshore seismic network, however, show that the IJzer Valley occupies a drainage basin separated from the Ostend Valley-Flemish Valley drainage system (Fig. 5.1 and Fig. 5.3).

Prior to the discovery of the Ostend Valley in the offshore area, it was generally believed that the Flemish Valley discharged into the North Sea to the north between the present-day Cadzand and Vlissingen, in the Netherlands (De Moor and Heyse 1974, Ebbing and Laban 1996, Gullentops and Wouters 1996, Wintein 2004). However, Fig. 5.8A shows no convincing continuation to the North of a river valley as large as the Flemish Valley. On the contrary, the morphology of the Top-Paleogene unconformity shows a local high in the centre of the assumed northward path of the Flemish Valley. The Ostend Valley, on the other hand, forms a continuous extension of the Flemish Valley, curved in the same way to the NW as the IJzer Valley. Ebbing and Laban (1996) assumed that the channel system observed off Walcheren ('Dutch channels') was the main continuation of the deepest incised branch of the Flemish Valley (the Lys) and the Waardamme (Fig. 5.8C). Judging from this figure, it seems that they were not aware of the presence of a major incised valley on the BCS. Presumably, several thalwegs discharged in different directions in the North Sea, but the Ostend Valley most likely formed the more important, or even the main seaward branch of the Flemish Valley.

Owing to the depth of the Ostend valley, only a very limited number of drillings reached the valley floor. Because of this, it is almost impossible to date the time of incision and the infilling sediments. As already mentioned above (Chapter 2), Maréchal and Henriet (1983) differentiated at least two incision phases, on the basis of the presence of two distinct slope breaks in the steep flank of the incised valley, however, without dating these stages. Trentesaux (1993) proposed cautiously that the Ostend Valley could have been formed during the Weichselian, but he did not rule out that it could also have been shaped since the Saalian. As the fluvial incision in the Flemish Valley and the Belgian Coastal Plain did not reach depths similar to the Ostend Valley (-27.5m MLLWS) until Saalian times (Mostaert et al. 1989, Mostaert and De Moor 1989, De Moor 1963 in: De Moor and Van De Velde 1995, Tavernier and De Moor 1974), an older age for the incision of the Ostend Valley, which lies in line with the Flemish Valley, can be excluded. During the Saalian glacial period the thalwegs in the Flemish Valley and in the paleo-IJzer were incised to depths of -25 m TAW (~MLLWS) (De Moor and Van De Velde 1995, Bogemans and Baeteman 2003), whereas the valleys incised during former glacial periods in the Early and Middle Pleistocene (De Moor et al. 1996, De Moor 1963, Tavernier and De Moor 1974), presently stand out as gravel terraces at heights of +30 m and +60 m TAW (De Moor and Van De Velde 1995, De Moor et al. 1996).

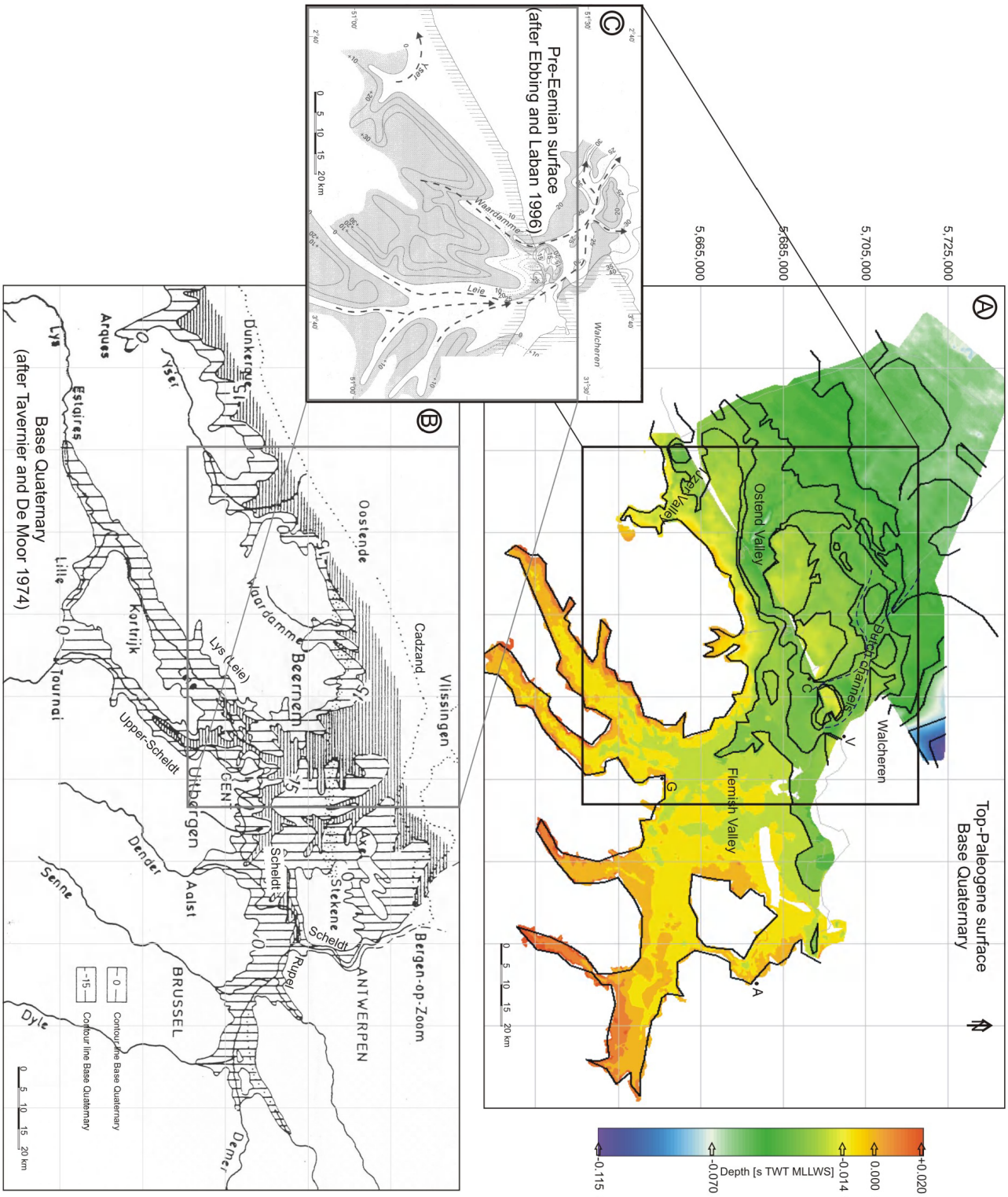
A
Top-Paleogene surface
Base Quaternary
N
451,000
471,000
491,000
511,000
531,000
551,000
571,000
591,000
611,000
5,725,000
5,705,000
5,685,000
5,665,000
Walcheren
Ostend Valley
Flemish Valley
Zeebrugge Valley
Burst channels
V
C
G
A
0 5 10 15 20 km
Depth [s TWT MLLWS]
+0.020 (+16.5 m)
0.000 (0.00 m)
-0.014 (-12.0 m)
-0.070 (-55.0 m)
-0.115 (-90.0 m)
C
Pre-Eemian surface
(after Ebbing and Laban 1996)
Walcheren
Leie
Waardamme
Ysel
0 5 10 15 20 km
B
Base Quaternary
(after Tavernier and De Moor 1974)
Oostende
Vlissingen
Cadzand
Waardamme
Beernem
Lys (Leie)
Kortrijk
Upper-Scheldt
Tournai
Lille
Arques
Estaires
Lys
Yser
Dunkerque
Uitbergen
Aalst
Dender
Senne
Dyle
Dender
Scheldt
Stekene
Rupel
ANTWERPEN
Bergen-op-Zoom
BRUSSEL
Contour line Base Quaternary
0
-15
Contour line Base Quaternary
0 5 10 15 20 km

Fig. 5.8 (A) (page 64) The offshore and onland (Meyus et al. 2005) Top-Paleogene or Base-Quaternary surfaces combined in a single grid (expressed in s TWT below MLLWS), which shows how the Ostend Valley lies in line with the Flemish Valley. (B) The Flemish Valley and its tributaries. The Flemish Valley is a deep valley system that extended the axis Demer-Rupel-Scheldt to the NW during the Late-Pleistocene, containing extensions in the valleys of the Dender, Upper-Scheldt and Lys (Leie), and which later became buried (De Moor 1996). According to an earlier definition the Flemish Valley also comprises the northerly basins (Tavernier and De Moor 1974). (C) Ebbing and Laban (1996) assumed that the channel system observed off Walcheren ('Dutch channels') was the main continuation of the deepest incised branch of the Flemish Valley (the Lys) and the Waardamme, in agreement with the general believe that the Flemish Valley discharged in the North Sea to the North between the present-day Cadzand and Vlissingen. However, the presented Top-Paleogene surface (A) shows a local high in the centre of the assumed northward path of the Flemish Valley. The Ostend Valley, on the other hand, forms a continuous extension of the Flemish Valley, curved in the same way to the NW as the IJzer Valley.

The age of the higher terraces is indirectly derived from macro- and micro-paleontological evidence (marine fauna and flora, terrestrial plant fragments, bone fragments) found in the lowest deposits (Tavernier and De Moor 1974).

In the next chapter, several arguments will be put forward, indicating that the Ostend Valley was most likely incised during the Saalian glaciation (MIS6).

Chronological synthesis of available elements

During the maximum ice-sheet extent of the Saalian glaciation a proglacial lake formed, with a lake level similar to the present-day mean sea level (0 m NAP, +2.3 m TAW) (Busschers et al. 2008). In the Netherlands, dated deltaic deposits of the Rhine-Meuse system are found at this high level (Busschers et al. 2008). In the Belgian sector, apart from some coarse-grained material on the presumed lake floor, little or no evidence of a former lake shoreline is expected to be found, as this shoreline was most likely destroyed by the subsequent Eemian relative sea-level rise, which reached similar heights (Cohen, pers. comm. 2007, Fig. 6.27). A deltaic setting in the Flemish Valley might, however, be expected.

During the ensuing deglaciation, the proglacial lake overtopped the ridge north of the Dover Strait, causing a break-through, and subsequently drained. With dropping base level, the Meuse deeply incised into the former proglacial Rhine-Meuse braidplain and sought its way south, towards the Dover Strait, forming the Offshore Platform, Offshore Scarp and 'Quaternary Basin' on its way. Most likely, the Ostend and IJzer Valleys started incising at the same time, with dropping lake level, in a final phase of Drente glaciation MIS6.

The Northern Valley and Thornton Channel cut through the former Meuse valley, but are infilled with Eemian deposits. This suggests that these structures formed when the melt water outflow diminished, and only the deeper Axial Channel was still occupied as main drainage path. These smaller flows sought their way farther to the north towards the Axial Channel. It is possible that the Dutch channels and Zeebrugge channel were already formed before, immediately after the start of the lake drainage, contemporaneous with the incision of the Ostend Valley. Alternatively, they could also have formed later, when the discharge diminished and slowed down, the water finding a short-cut towards the Axial Channel. This might explain why there is no clear, wide continuation of the Ostend Valley towards the Axial Channel. Nevertheless, some small outlets are visible in the Offshore and Middle Scarp in line with the Ostend Valley. These could indicate a northerly extension, but with smaller discharge, towards the central depression in the North Sea (Fig. 5.1B).

During the subsequent sea-level rise (Eemian, MIS5e), the Ostend Valley and smaller channels got infilled. This, as well as the genetic origin of the Nearshore Slope Break will be discussed in detail in the next chapter. In the 'Quaternary Basin' a renewed incision and infilling with fluvial Weichselian deposits are observed (Kirby and Oele 1975, Ebbing et al. 1992). Indeed, during the Weichselian lowstand, the Meuse occupied –together with the Rhine this time– the same position as during the Saalian lowstand during and after the lake drainage, in the western Netherlands (Busschers et al. 2007). Offshore, the Meuse most likely also occupied, the same southward-directed drainage channels as during the Saalian. According to Gibbard (2007), also the Rhine also diverged southward after the Saalian proglacial-lake drainage. Knowing that during and shortly after the Saalian lake drainage the Rhine was still draining northward (Busschers et al. 2008), this implies that this southward diversion occurred during the Weichselian lowstand, and that the joint southward drainage of the Rhine and Meuse started at that time. Earlier, Bridgeland (2002) stated that the drainage direction of the Thames-Rhine river system during the last lowstand (Weichselian) was still questionable.

5.3.2 Origin of gravel lag

The gravel lag, covering the Top-Paleogene unconformity, is present below overlying units or sometimes emerging at the seafloor in the troughs between the sandbanks, and may have multiple origins. Most authors agree that gravels cannot be transported under the present-day tidal hydrodynamic conditions (Veenstra 1964, Houbolt 1968, Veenstra 1969, Maréchal and Henriet 1983). This implies that gravel in the troughs between the sandbanks must have been supplied before the present-day hydrodynamic conditions got established, or that their origin must be local.
According to Cohen (pers. comm. 2007) the Saalian proglacial lake that covered the entire BCS may have deposited a coarse-grained basal layer. According to Maréchal and Henriet (1983), the Ostend Valley could have been one of the supply routes for gravel to the BCS during sea-level lowstands. Older publications attribute the gravel found in the Hinder Banks area to ancient courses of the rivers Rhine and Meuse (Tesch and Reinhold 1946), but although the *sands* in the Hinder Banks area are typically Rhine-derived, brought there by river action during periods of lower sea level (Baak 1936 in: Houbolt 1968, Veenstra 1964, Schüttenhelm and Laban 2005), the sediment (gravel) samples obtained in the Hinder Banks area by Veenstra (1969) and Kirby and Oele (1975) did not contain any Rhine or Meuse gravel. Veenstra (1969) suggests that the gravel he encountered was transported by Paleogene rivers, which took up material from a weathering residue on the Ardennes. This could explain the high percentage of resistant rocks (flint, chert, quartz, quartzite) in the gravel between Belgium and England.
A general mechanism for the redistribution of river-derived gravel is proposed by Swift et al. (1991). Quaternary lowstands rejuvenate rivers as they cross the exposed shelf, and in many cases, the lowstand shelf valleys contain gravel. With rising sea level, the retreating shoreface cuts into these gravelly valley fills and redistributes them as a marine basal transgressive gravel. Mostly the gravel is overlain by several metres of sand, but in areas of strong storm or tidal currents the sand sheet may be discontinuous or lacking altogether, so that the basal gravels are exposed in windows through the sand sheet, which is the case in some areas of the BCS.
What should be considered as well, is the presence of gravel in the Paleogene substrate itself (e.g. sandstone banks, large concretions (Veenstra 1969)), from which the finer material could have been winnowed out by tidal or wave processes, leaving a gravel lag. According to Veenstra (1969), flint cobbles and large Paleogene concretions in the deeper part of the Southern Bight probably originate from rather local Cretaceous and Paleogene outcrops at the seafloor. Kirby and Oele (1975), however, propose a southern (French) origin for the gravel fraction they encountered in the Hinder Banks area, though without proposing a transport mechanism. According to Bridgeland (2002), there is still

no consensus about the drainage direction of the Thames-Rhine river system during the last lowstand (Weichselian), which could have been directed southward or northward. However, even if it would have been directed northward, based on its position this system could not have supplied flint originating from Cretaceous deposits in northern France (Fig. 5.9). The Thames, on the other hand, could have supplied flint from the Cretaceous deposits in SE England. Alternatively, it is not completely unlikely that the Ostend Valley may have delivered gravel originating from France, via the ancient Scheldt river, which is part of the Flemish Valley and cuts through Cretaceous deposits in northern France (Fig. 5.9).

Whatever the source of the gravel is, the relief of the Top-Paleogene unconformity has been strongly modified during later marine transgressions and regressions. Consequently, the gravel lag must have been strongly reworked, to such an extent that in situ Elsterian or Saalian lake deposits are not expected to be present.

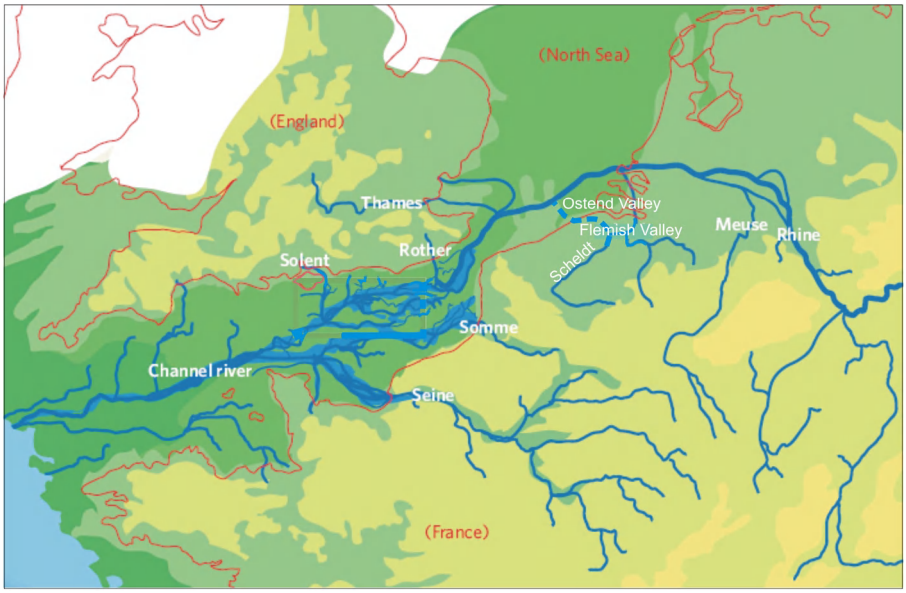

Fig. 5.9 River systems during the last glacial maximum (Weichselian). Adapted after Gibbard (2007).

5.4 Conclusion

The Top-Paleogene unconformity on the BCS represents the erosional boundary and significant stratigraphic hiatus between Lower and Middle Eocene formations and the overlying Quaternary deposits. This boundary is an angular unconformity, characterised by a number of planation surfaces, bounded by slope breaks and scarps, and several incised valley structures. These morphological features have been described in literature before, but some slopes or platform boundaries have now been defined slightly differently because of new evidence from a denser seismic network.
In order to link the offshore and onland situations, a composite Top-Paleogene surface was created. The surface consists of an onshore grid covering the Coastal Plain, an offshore grid covering part of the Dutch sector, and an offshore grid covering the entire BCS created from the presented seismic data. This composition shows how the Ostend Valley occupies a drainage basin completely separated from that of the IJzer Valley by a high between Nieuwpoort and Oostende and its offshore continuation. So, the Coastal Valley does not extend beneath the entire Belgian Coastal Plain, but its eastern section does connect the Flemish Valley with the Ostend Valley. This is in contrast to the earlier

hypothesis that the Flemish Valley discharged into the North Sea to the north, proposed before the Ostend Valley was discovered offshore. The Top-Paleogene surface also shows that the Ostend and the Northern Valley, located farther offshore, represent two separate drainage systems, in contrast to what was alleged before. More likely, the Northern Valley and a deeply incised channel below the Thorntonbank belong to an aligned smaller drainage system present in the Dutch sector.

A chronological framework was proposed for the formation of the planation surfaces and incised valleys. During the maximum ice-sheet extent of the Saalian glaciation, a proglacial lake formed. In the course of the following deglaciation, the proglacial lake overtopped a ridge north of the Dover Strait, causing a break through and subsequent drainage. With dropping base level, the Meuse incised deeply into the former proglacial Rhine-Meuse braidplain and sought its way south, towards the Dover Strait, forming the planation surface 'Offshore Platform', the 'Offshore Scarp' and the 'Quaternary Basin' on its way. Most likely the Ostend and IJzer Valleys started incising at the same time, with dropping lake level. When the melt water outflow diminished, and only the deeper Axial Channel was still occupied as main drainage path, smaller flows sought their way farther to the north, cutting through the former Meuse valley towards the Axial Channel, forming the Northern Valley and Thornton Channel. Some small outlets in the Offshore and Middle Scarp aligned with the Ostend Valley might indicate a northerly extension of the Ostend Valley as well, but with a smaller discharge. During the following sea-level rise, the Offshore Platform, the Ostend Valley, and the smaller channels got infilled and the planation surface 'Nearshore Slope Break' was formed (discussed in next chapter). And in the course of the following sea-level lowering, the Meuse occupied the same position as during the Saalian lowstand, now joined by the Rhine, and renewed incisions occurred in e.g. the Quaternary Basin.

Most likely, those rivers supplied part of the gravel found in the present offshore area which covers the Top-Paleogene unconformity in the form of a gravel lag. However, Paleogene rivers have also been suggested as gravel suppliers. Possibly, with rising sea level, the retreating shoreface breached these gravelly valley fills and redistributed them as a marine basal transgressive gravel. Another origin for the gravel to consider is the substrate itself. The finer material could have been winnowed out from the substrate by tidal or wave processes, leaving a gravel lag, consisting of sandstone and large concretions. Generally the gravel is overlain by several metres of sand, but in areas of strong storm or tidal currents the sand sheet may be discontinuous or lacking altogether, so that the basal gravels are exposed in windows through the sand sheet, which is the case in some areas of the BCS.

The Quaternary cover overlying the Top-Paleogene unconformity of the BCS, is thin and fragmented. Forty percent of the BCS surface is covered with less than 5 m of Quaternary sediments. In large parts of this area, the Paleogene substrate simply emerges at the present-day seafloor in the troughs between the sandbanks. Thickest sequences are found in the deeply incised central depression of the Ostend Valley.

6.
Pleistocene incision and infilling of the Ostend Valley

The most prominent structure in the Top-Paleogene surface is the funnel-shaped incision of the Ostend Valley. Such valleys are mostly incised during relative sea-level fall, and subsequently infilled during lowstand, and the following sea-level rise and highstand phase. One speaks of an incised-valley system (incision plus infilling, Dalrymple et al. 1994). A valley fill can be simple, representing a single sea-level cycle, or compound, representing multiple sea-level cycles with associated incision and deposition (Zaitlin et al. 1994).
This chapter focuses on the evolution of the incised valley, and especially its transgressive infilling. It sketches the changing configuration of an embayed coastline. While in the next chapter the development of a linear coastline will be discussed, which has a completely different evolutionary history.

6.1 Introduction: the Ostend Valley, an incised-valley system

The Ostend Valley on the BCS is clearly an incised valley (Fig. 5.1B), most likely incised in the Top-Paleogene surface during a period of significant relative sea-level fall. Together with its sedimentary fill, it forms an incised-valley system (Dalrymple et al. 1994). Incised-valley systems generally evolve from river valleys, deepened during relative sea-level fall, into estuaries as valleys drowned during subsequent sea-level rise (Dalrymple et al. 1994, Zaitlin et al. 1994).
Conform the definition of Dalrymple et al. (1992) an estuary is regarded here as the "*seaward portion of a drowned valley system which receives sediment from both fluvial and marine sources and which contains facies influenced by tide, wave and fluvial processes. The estuary is considered to extend from the landward limit of tidal facies at its head to the seaward limit of coastal facies at its mouth.*". So the terms "estuary" and "estuarine" refer only to transgressive coastal areas and not to areas with brackish-water as included in the definition of Pritchard (1967), who defined estuaries as "*semi-enclosed coastal water bodies having a free connection with the open sea and within which sea water is measurably diluted by fresh water derived from land drainage*".
An estuary is a typical transgressive feature (Dalrymple et al. 1992) and forms in a formerly incised river valley when relative sea-level rise exceeds sediment supply, creating an embayed coast (Fig. 6.1). Depending on the wave and tidal power, an estuary can be tide-dominated, wave-dominated or mixed. If the rate of sediment supply is sufficient (relative to the size of the valley), estuaries become filled and cease to exist when the rate of sea-level rise slows and less accommodation space is created. Embayed coastlines then are transformed into deltas with a lobate coastline -if the sediment is supplied directly by the river- or linear prograding coasts (strandplains or open-coast tidal flats) if the sediment is delivered or redistributed by marine processes (waves or tides, respectively) (Dalrymple et al. 1992) (Fig. 6.1).

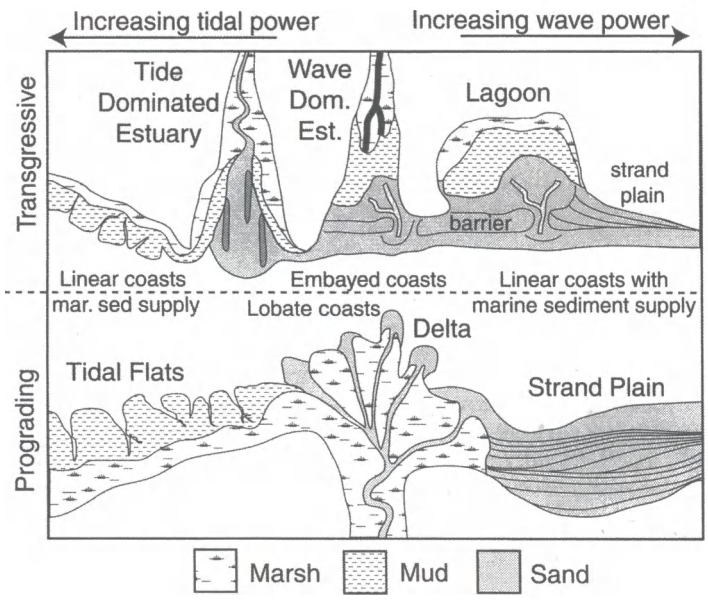

Fig. 6.1 Maps of idealised coastal depositional environments, showing the relationship between wave and tidal power, prograding and transgressive environments, and different geomorphic types (after Boyd et al. 1992 in: Harris et al. 2002)

6.1.1 An incised valley during a relative sea-level cycle

An incised-valley system can be described according to the generalised sequence-stratigraphic model of Zaitlin et al. (1994). An incised valley system can be divided into three segments, each of which experiences a different depositional history and has a distinct stratigraphic organisation, which results from transgression followed by highstand deposition. Fig. 6.2A shows the sequence-stratigraphic model of Zaitlin et al. (1994), which is valid for a wave-dominated estuary. Fig. 6.2B shows an adaptation of this model, applicable to a tide-dominated estuary in an incised valley. The most seaward portion of a valley system (segment 1) initially experiences (lowstand to transgressive) fluvial and estuarine deposition, but is transgressed by the shoreline so that the estuarine deposits are overlain by marine sands and shelf muds. The middle portion (segment 2) of the system is the zone occupied by the estuary at the time of maximum transgression. The lower part of the valley fill consists of a transgressive, fluvial to estuarine succession like in segment 1, but is overlain by a progradational fluvial succession that accumulates during the sea-level high-stand. This progradational succession is a bayhead delta in case of a wave-dominated estuary according to the model of Zaitlin et al. (1994) (Fig. 6.2A). In case of a tide-dominated estuary the transgressive succession is overlain by progradational sand bars or tidal flats (Dalrymple et al. 1992) (Fig. 6.2B). The most landward portion of the valley (segment 3) lies beyond the limit of marine influence. It remains fluvial throughout its history, and is overlain by terrestrial deposits.

The stratigraphic organisation of an incised-valley system is characterised by a number of stratigraphically significant surfaces (Fig. 6.2). The surface that defines the valley form is the *sequence boundary*. Filling of the valley begins during the lowstand, but typically continues through the succeeding transgression. Hence, the *transgressive surface* is the flooding surface separating the Lowstand Systems Tract and the Transgressive Systems Tract. The *initial flooding surface* is the estuarine-fluvial contact. If little fluvial deposits accumulated during the transgression, this surface corresponds to the transgressive surface. Erosion by tidal currents in tidal inlets or tidal channels creates a *tidal ravinement surface*, which is confined to segment 1 and the seaward part of segment 2 of the incised valley. More regional erosion by waves at the retreating shoreface in a wave-dominated environment, produces a *wave ravinement surface* that separates estuarine sediments from overlying marine deposits in segment 1. In a tide-dominated environment the surface separating the estuarine sediments from overlying marine deposits is also called a *tidal ravinement surface*. Dalrymple and Choi (2007) speak of a *transgressive ravinement surface*. A more general term which is in the future text used for both wave and (shelf) tidal ravinement surfaces is *marine transgressive surface*. The *maximum flooding surface* corresponds to the time of maximum transgression.

An incised valley that is filled during one relative sea-level cycle, i.e. sea-level fall to subsequent highstand, is termed a simple fill, whereas a compound fill represents multiple cycles of incision and deposition. In the most complete succession, a simple incised-valley fill consists of lowstand and/or transgressive fluvial deposits, overlain by estuarine sediments. As an estuary continues to migrate landward, the upper portion of the transgressive succession is generally removed by shoreface or tidal-channel erosion. At the point of maximum transgression, the shoreline will stabilise and the estuary will fill in situ, if the highstand is of sufficient duration and enough sediment is supplied. At this location, the transgressive succession will be overlain by a progradational deposit. Progradation beyond the seaward end of the estuary will occur either as a delta or as a beach-ridge plain or open-coast tidal flats depending on the river supply. If sea level falls before the valley is filled, the transgressive to highstand estuarine deposits will be dissected during the following lowstand and overlain by a second valley-fill succession (Dalrymple et al. 1992).

6.1.2 Wave- versus tide-dominated estuaries during relative sea-level rise

The nature and organisation of the incised-valley estuary is controlled by the interplay between marine processes (waves and tides) and fluvial processes. Depending on the dominant marine process, estuaries can be wave-dominated, tide-dominated, or mixed-energy systems (Dalrymple et al. 1992, Dalrymple and Choi 2007) (Fig. 6.1). Wave-dominated estuaries occur on exposed coastlines with a relatively small tidal influence (Roy et al. 2001), while tide-dominated estuaries are generally found on low-gradient coasts characterised by meso- to macrotidal ranges (Dalrymple 1992). Tidal dominance occurs if tidal currents are responsible for more sediment transport than river currents or waves, and thus determine the larger geomorphology. Mixed-energy environments can be strongly tide-influenced settings, that have near-equal influence of waves and tidal currents (Dalrymple and Choi 2007).
On the inner BCS any modern estuary would be tide-dominated. The typical funnel shape of the Ostend Valley shows that this former estuary was also tide-dominated. Incised-valley systems that have a regular, funnel-shaped geometry are likely to be tide-dominated environments (Dalrymple et al. 1992). The tidal prism of an estuary (area within an estuary landward of the cross-section of interest, multiplied by the average tidal range in that area) increases seaward as a result of the progressive increase in the area flooded and drained during each tide. Consequently, channels show a seaward increase in cross-sectional area, accomplished by a seaward increase in the width of the channel (as water depth does not increase significantly). This seaward widening is exponential and is responsible for the classical funnel-shaped geometry of tide-dominated systems (Dalrymple and Choi 2007).
Geomorphologically, the tidal dominance is shown by the predominance of tidal-channel networks observed in the seismic units, and by the absence of wave-generated coast-parallel barriers with one or more tidal inlets (Fig. 6.2B) and flood-tidal deltas (Dalrymple et al. 1992), although they could have been eroded during transgression (Dalrymple and Choi 2007).

Fig. 6.2 (page 73) (A) Idealised longitudinal section of a simple incised-valley system (IVS) with a wave-dominated regime, showing the different depositional environments, system tracts, and stratigraphic surfaces (modified after Zaitlin et al. 1994). (B) Schematic section along the axis of a tide-dominated estuary in an incised valley, showing the distribution of facies resulting from transgression of the estuary, followed by estuary filling and progradation of sand bars or tidal flats (modified after Dalrymple et al. 1992). (C) Schematic vertical cross-section of a tide-dominated estuary located within an incised valley, showing the different depositional environments, systems tracts, and stratigraphic surfaces (modified after Dalrymple and Choi 2007). Note that the erosive surface between the estuarine and open-marine sediments is called a (marine) transgressive ravinement or tidal ravinement surface in case of a tide-dominated estuary, as equivalent of the wave ravinement surface in a wave-dominated estuary (A). LST = Lowstand Systems Tract, TST = Transgressive Systems Tract, HST = Highstand Systems Tract. Marine deposits are indicated in yellow, estuarine deposits in blue, and fluvial sediments in brown.

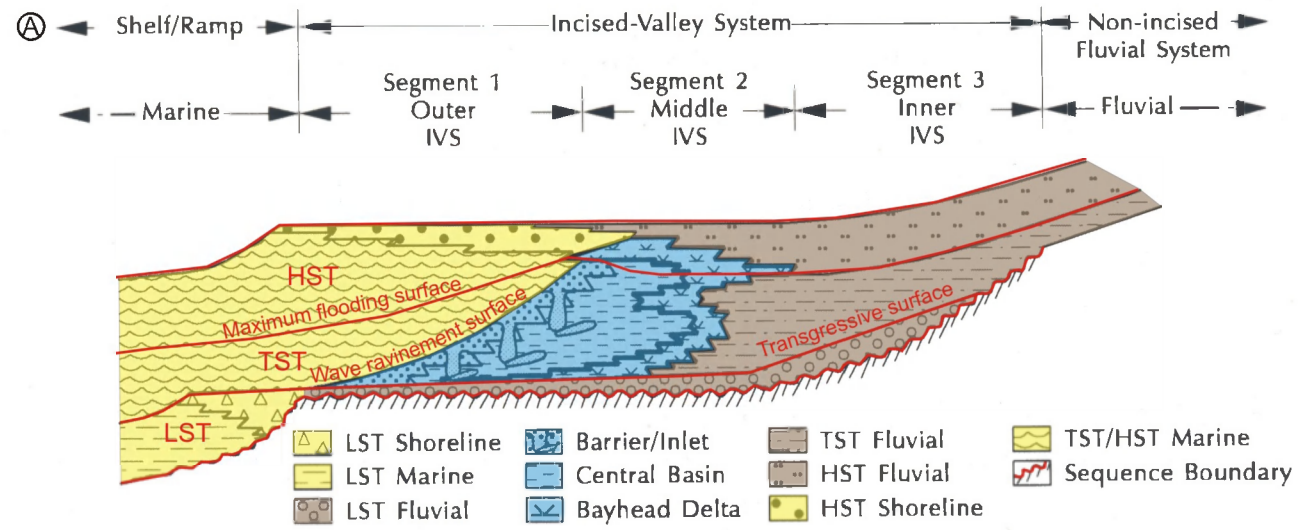
Ⓐ
Shelf/Ramp
Incised-Valley System
Non-incised Fluvial System
Marine
Segment 1 Outer IVS
Segment 2 Middle IVS
Segment 3 Inner IVS
Fluvial
HST
Maximum flooding surface
TST
Wave ravinement surface
Transgressive surface
LST
LST Shoreline
LST Marine
LST Fluvial
Barrier/Inlet
Central Basin
Bayhead Delta
TST Fluvial
HST Fluvial
HST Shoreline
TST/HST Marine
Sequence Boundary

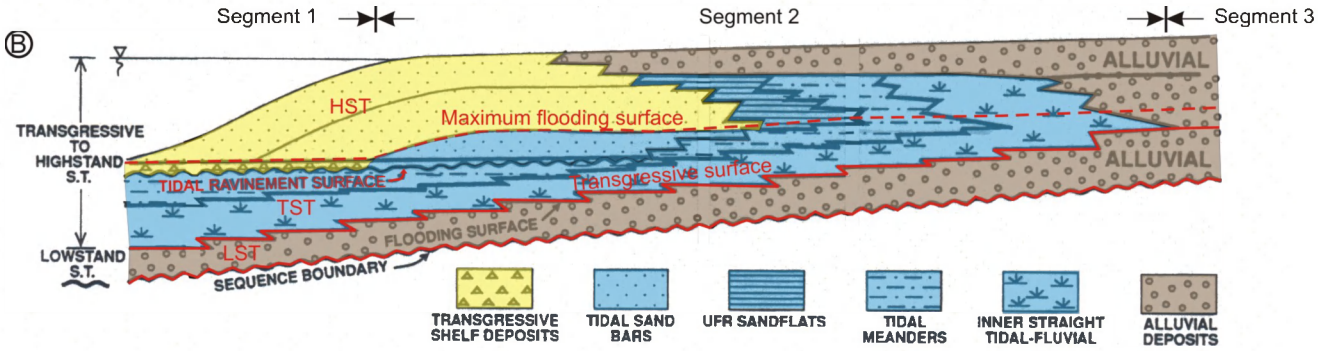
Ⓑ
Segment 1
Segment 2
Segment 3
TRANSGRESSIVE TO HIGHSTAND S.T.
LOWSTAND S.T.
HST
Maximum flooding surface
ALLUVIAL
ALLUVIAL
TIDAL RAVINEMENT SURFACE
Transgressive surface
TST
FLOODING SURFACE
LST
SEQUENCE BOUNDARY
TRANSGRESSIVE SHELF DEPOSITS
TIDAL SAND BARS
UFR SANDFLATS
TIDAL MEANDERS
INNER STRAIGHT TIDAL-FLUVIAL
ALLUVIAL DEPOSITS

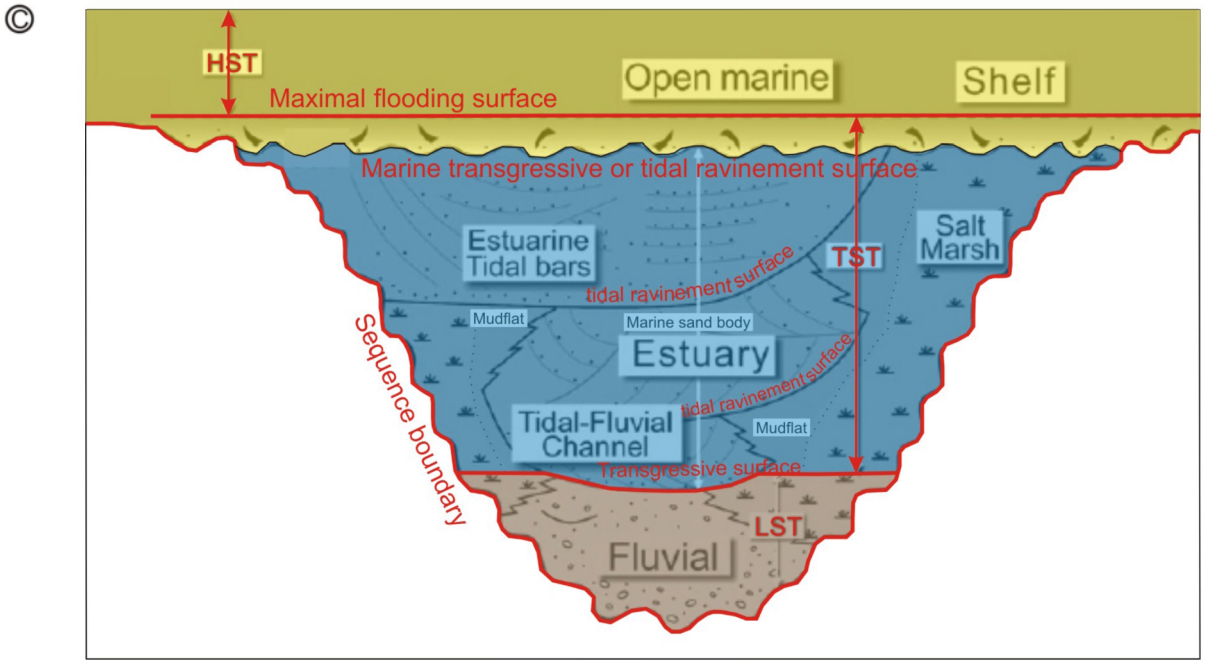
Ⓒ
HST
Maximal flooding surface
Open marine
Shelf
Marine transgressive or tidal ravinement surface
Estuarine Tidal bars
Salt Marsh
TST
tidal ravinement surface
Mudflat
Marine sand body
Estuary
Sequence boundary
tidal ravinement surface
Tidal-Fluvial Channel
Mudflat
Transgressive surface
LST
Fluvial

6.1.3 A tide-dominated estuary

Tide-dominated estuaries have been described in detail by Dalrymple and Choi (2007) and Dalrymple et al. (1992). Fig. 6.3 gives the schematic division of a tide-dominated estuary, an overview of the prevailing processes, and the sedimentological characteristics (after Dalrymple and Choi 2007). Tide-dominated estuaries receive sediment from both the river at the head of the estuary and from the adjacent shelf by tidal currents. As a result, grain sizes are coarsest at the mouth and head of the estuary, with a bedload convergence (BLC) in between. Unlike wave-dominated estuaries, however, no fine-grained lagoonal facies are present, because tidal currents penetrate into the estuary much more easily than waves do. Consequently, the distinct tripartite facies distribution (sandy barrier - muddy lagoon - sandy bay-head delta) of wave-dominated estuaries (Roy 1984, Reinson 1992, Dalrymple et al. 1992, Zaitlin et al. 1994) does not occur in tide-dominated systems. Instead, in tide-dominated estuaries muddy sediments accumulate primarily in tidal flats and marshes along the sides of the estuary where tidal currents are weakest. Tidal currents are strongest in the sandy channels that run along the entire length of the estuary axis (Dalrymple et al. 1992). The relatively coarse axial sands are finest and contain the largest number of mud drapes in the vicinity of the BLC, where the "turbidity maximum" of suspended sediment is situated (Dalrymple et al. 1992, Dalrymple and Choi 2007).

Dalrymple and Choi (2007) distinguished a *fluvial-tidal transition* zone, or river-dominated (but marine-influenced) section where the net transport is seaward, extending from the "tidal limit", where tidal action is just sufficient to leave a recognizable record, to the BLC; a *middle estuary* where the net transport is landward, extending from the BLC to an ill-defined location near the mouth of the estuary and including at least the "tidal maximum" (see below); and an *outer-estuarine*, marine-dominated section at the mouth, where the bedload transport is landward as well (Fig. 6.3).

In the outer estuary, tidal-current energy exceeds wave energy, and elongated shore-normal sand bars are typically developed. These bars dissipate the wave energy that does exist. The incoming flood tide is compressed into a progressively smaller cross-sectional area because of the funnel-shaped geometry, and the tidal range and tidal currents increase landward. Beyond a certain distance, frictional dissipation exceeds the effects of amplification caused by convergence, and from that point, the tidal energy decreases landward, reaching zero at the tidal limit. As a result, the maximum tidal-current velocities occur within the middle estuary, near the place where the distributary channels bifurcate. This area is referred to as the "tidal maximum". The total-energy minimum is located landward of the tidal maximum; it is the area of the BLC and the "turbidity maximum", i.e. a zone of significantly elevated suspended-sediment concentrations. This region typically contains tight meanders, and is located between two "straight" sections (Dalrymple et al. 1992). The outer straight section comprises the elongated tidal sand-bar zone (outer estuary), which passes into broad, upper-flow-regime sand flats (UFR) in the area of the tidal maximum (middle estuary), where the estuary is broad but becomes confined to a single channel farther headward (Dalrymple et al. 1992) (Fig. 6.2B). The inner straight reach comprises the fluvial-tidal transition and passes directly into the river channel upstream from the tidal limit.

Together, the elongated tidal sand bars of the outer estuary and the broad, upper-flow-regime sand flats of the middle estuary form the 'marine sand body' (Dalrymple et al. 1992).

The deposits of a tide-dominated shelf seaward of the estuary typically consist of a thin layer of relatively coarse sand and/or gravel that may be built up locally into elongate tidal bars (or shelf-sand ridges) and/or large compound dunes, all overlying the (marine) transgressive ravinement surface (Dalrymple and Choi 2007).

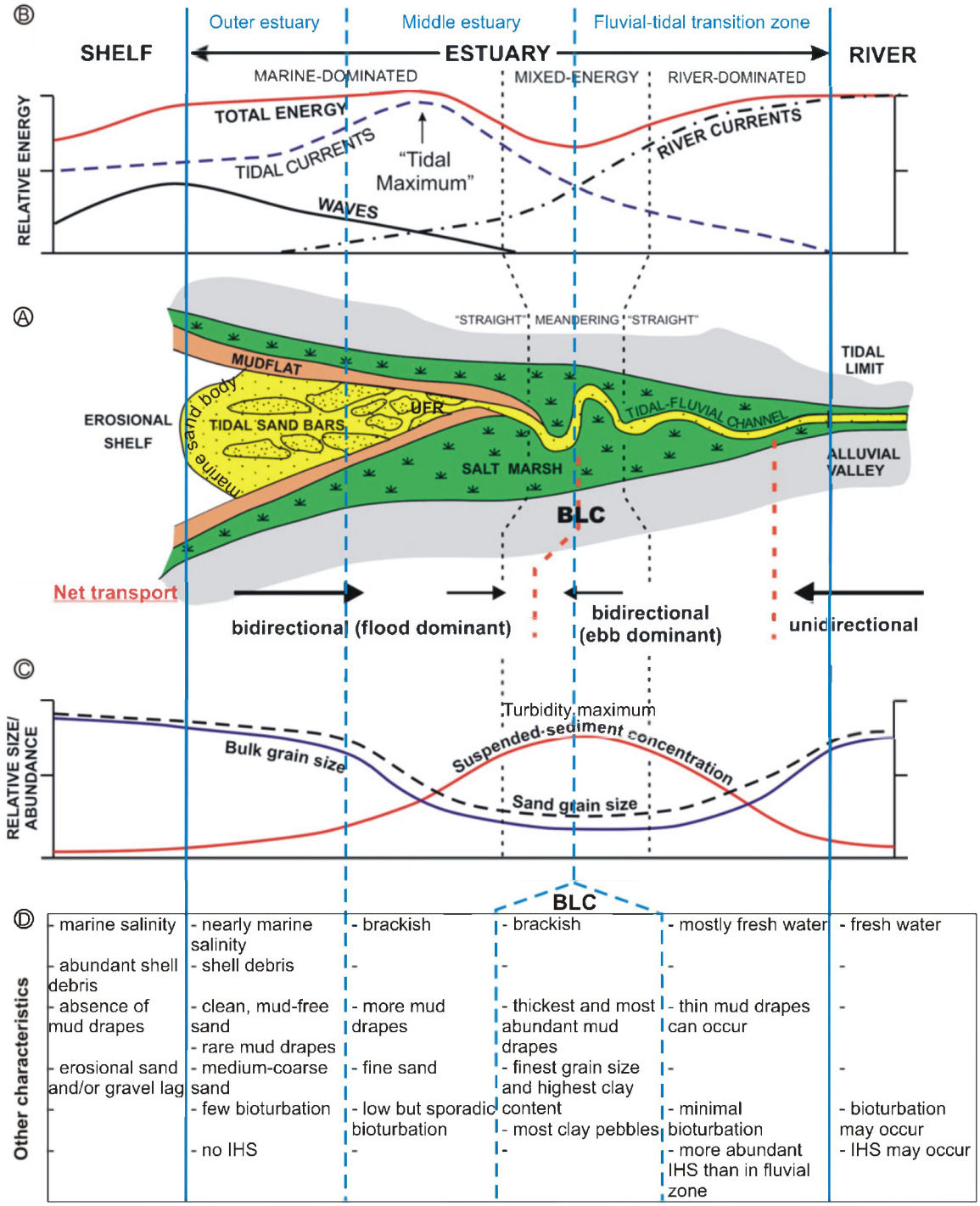

Fig. 6.3 (A) Schematic map of a tide-dominated estuary. Note the funnel shape, the systematic changes in channel geometry ("straight-meandering-straight"), the presence of elongate tidal bars and upper-flow-regime (UFR) tidal flats in the seaward and middle part respectively (jointly the marine sand body), and the fringing muddy tidal flats and salt marshes (modified after Dalrymple and Choi 2007). (B) Longitudinal variation of the intensity of the three main physical processes, and the resulting directions of net sediment transport. Note the development of a bedload convergence (BLC) at the location of the tightly meandering portion of the channel (Dalrymple and Choi 2007). (C) Longitudinal variation of the grain size of the sand fraction, the suspended-sediment concentration, and bulk grain size (Dalrymple and Choi 2007). (D) Main characteristics of the different parts of a tide-dominated estuary, the adjacent shelf and river (derived from text Dalrymple and Choi 2007). IHS = inclined heterolithic stratifications.

6.1.4 The Ostend Valley

The cross-section of an incised-valley system with a tide-dominated regime is shown in Fig. 6.2C. Cross-sections of the Ostend Valley show several seismic units separated by erosional surfaces (Fig. 4.1), but from the seismic data only it cannot be deduced whether the infilling is a compound fill, in which the erosional surfaces separate different sea-level cycles and represent successive incisions (sequence boundaries) as was assumed by Maréchal and Henriet (1983) and Liu et al. (1993). Or whether the incised-valley system is a simple fill, in which the erosional surfaces represent internal, local surfaces like a transgressive surface or tidal ravinement surfaces of a single sea-level cycle, i.e. erosional surfaces formed by a stacked system of small channels. It is not known either if the infillings of the Ostend Valley represent a complete succession or not, as the preservation potential of an incised valley and its infillings depends on the intensity of subsequent marine and fluvial erosion, fluvial sediment supply, and rate of relative sea-level rise.

6.2 Observations

6.2.1 Seismic-stratigraphic interpretation

After the general description of the basal three seismic units in chapter 4, and of the Top-Paleogene surface in chapter 5, a small section of the latter surface (i.e. the incised valley offshore Oostende), and the three infilling units are described in this chapter in more detail. The lowermost units are discussed together, as they jointly make up the total infill of the incised valley offshore Oostende. The seismic grid used to analyse this restricted area consists of 1700 km of profiles covering a total area of about 1100 km².

QT reflector: the Top-Paleogene surface

In the previous chapter the Top-Paleogene surface has been described, more specifically the planation surfaces and the presence of incised valleys and channel structures. In this chapter the Ostend Valley will be described in more detail.
The Ostend Valley shows a number of narrow, elongated, winding incisions, of which the most prominent is located along its central axis. A second one meanders along the north-eastern valley flank, with a (main) branch continuing in the central depression (Fig. 6.4). Like the Ostend Valley, also the incisions show an asymmetrical cross-section with a steep and a gentle channel wall, which is especially clear in the most offshore part (Figs. 6.6 and 6.7A, C, E). There, the steepest side is alternately located at the NE and SW side of the winding incision. At the nearshore part, the average valley floor of the Ostend Valley is ca. 7 m incised into the Paleogene deposits to –26 m; at the offshore end the bed is situated 2.5 m below the overall Paleogene surface at a depth of -27.5 m (MLLWS). Some of the incisions deviate from this general pattern and show landward deepening or an undulating channel floor. The depth of the central incision ranges from -34 m (MLLWS) at the mouth, to -56 m at the nearshore end, where it is scoured 30 m below the bed of the main valley floor. The incision along the NE valley margin ranges from -37 m (MLLWS) at the nearshore end, where it is scoured 11 m below the bed of the main depression, to -28 m farther offshore. Where it continues with an undulating but overall seaward-deepening course between -30 m and -36 m.

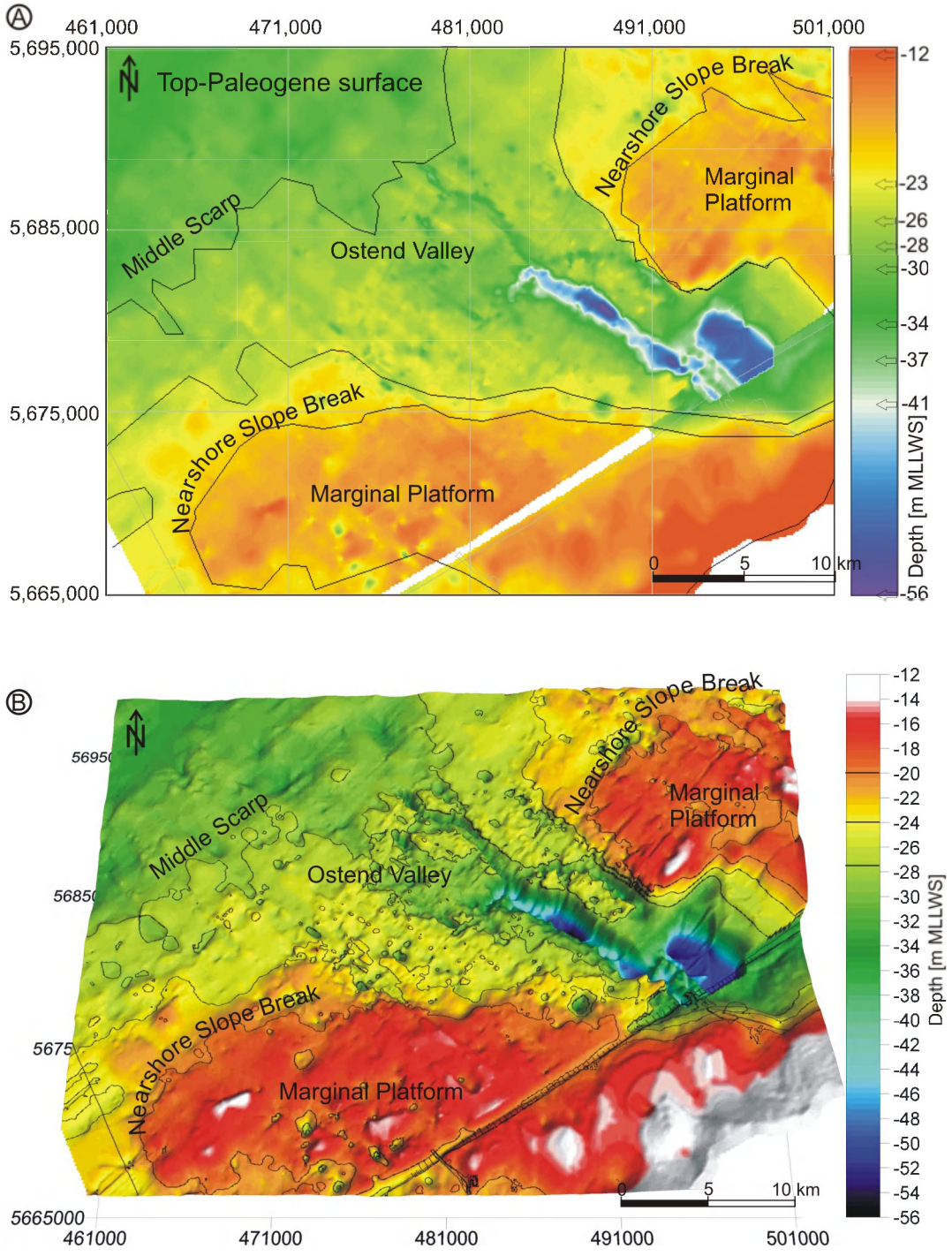

Fig. 6.4 (A) Detail of the isobath map of the Paleogene surface (QT reflector), focussing on the Ostend Valley. The Ostend Valley shows a number of narrow, elongated, winding incisions in its valley floor, of which the most prominent is located along its central axis. A second one meanders along the north-eastern valley margin, with a (main) branch continuing in the central depression. (B) A 3D presentation of the same detailed section. The -20 m, -24 m, and -27.5 m contours approximate the Nearshore Slope Break, Ostend Valley boundary, and Middle Scarp, respectively.

At the time when the Ostend Valley was described for the first time (Maréchal and Henriet 1983), isolated pits comparable with those found in the present-day Western Scheldt estuary were recognised in the centre of the paleo-valley. They were identified as scour hollows, and the deepest were named the 'Sepia Pits' (Mostaert et al. 1989, Liu et al. 1993) (Fig. 5.3). The current denser seismic network made it possible to establish that these pits are in fact connected to elongated incisions, described above.

Unit 1: the lowermost valley infill

Seismic unit U1 infills the deepest parts (i.e. scour hollows) of the incisions in the central axis and along the north-eastern margin of the Ostend Valley (Fig. 6.5A). The top reflector is mostly quasi horizontal, laterally onlapping on the QT surface, and locally incised by overlying units. In the most offshore part of the unit though, the top reflector is inclined subparallel to the gentle flanks of the channel incisions (Fig. 6.6), alternately located at the NE and SW side (Figs. 6.7ACE). There, it downlaps onto the channel floor, forming a prograded fill, with tangential- and parallel-oblique internal reflectors in the direction of the steepest side of the asymmetrical channels. Most likely the inclined channel infill is not limited to the offshore area, but here, U1 is located close to the seafloor, where data quality is best. In the more nearshore area, U1 is located deeper below the seafloor and in areas where the presence of shallow gas can obliterate the seismic signal.
The top bounding surface of U1 reaches its shallowest point at a depth of –25 m at the NE boundary of the Ostend paleo-valley. In the central axis the surface ranges from –28 m to –30 m in offshore direction, showing an additional deepening of about 3 m where a prograded fill is present. The deepest part of the bounding surface is always located near the steep side of the channel (Fig. 6.5A).
The thickness of unit U1 is determined by the asymmetrical form and depth of the channels which U1 is infilling, and the incision depth of the overlying units.

Unit 2: the intermediate valley infill

Seismic unit U2 fills up the space left in the deeply incised channels above U1 (Figs. 6.6 and 6.7), but is not restricted to these incisions and extends beyond them, in the more nearshore zone reaching to the margins of the Ostend Valley (Fig. 6.5B). The unit infills most of the entire Ostend Valley, except for the SE nearshore zone were the presence of gas obscures its existence. The surface of U2 slopes down in NW direction from –21 m to –28 m, with an abrupt depth change of 3 m about halfway. Apart from this scarp, the surface also shows an axial depression with a width of 4 km and a depth between –25 and –27 m, as well as local incisions by small channels of overlying units extending up to 8 m below the intact U1 surface, as already described in Chapter 4.
The pattern of internal channels of U2 is presented in Fig. 6.8A. It seems that the erosive internal channels are mostly restricted to the area south-east of the scarp in the U2 surface. North-west of the scarp, it seems as if U2 merely infills (not erosively) the space left above U1 in the deeply incised channels in QT (Figs. 6.7ACD).
Along the NE side of the Ostend Valley, the straight section of the channel network is 1 km wide. After the first bifurcation the second-order channels are about 600 m wide, narrowing farther offshore to 400 m, and to 250 m in the third-order channels. The central channel narrows in offshore direction from 900 m to 300 m. The channels in the SW area are between 300 and 600 m wide.

Fig. 6.5 (page 79) Isobath maps of the top surfaces of seismic units: (A) U1; (B) U2; and (C) U3. The surfaces of the seismic units are shown in 3D on top of the underlying Top-Paleogene surface (QT reflector, grey depth scale), combined with the surfaces of U1 and U2 (blue depth scales) in (B) and (C) respectively. The -20 m, -24 m, and -27.5 m contours approximate the Nearshore Slope Break, Ostend Valley boundary, and Middle Scarp respectively.

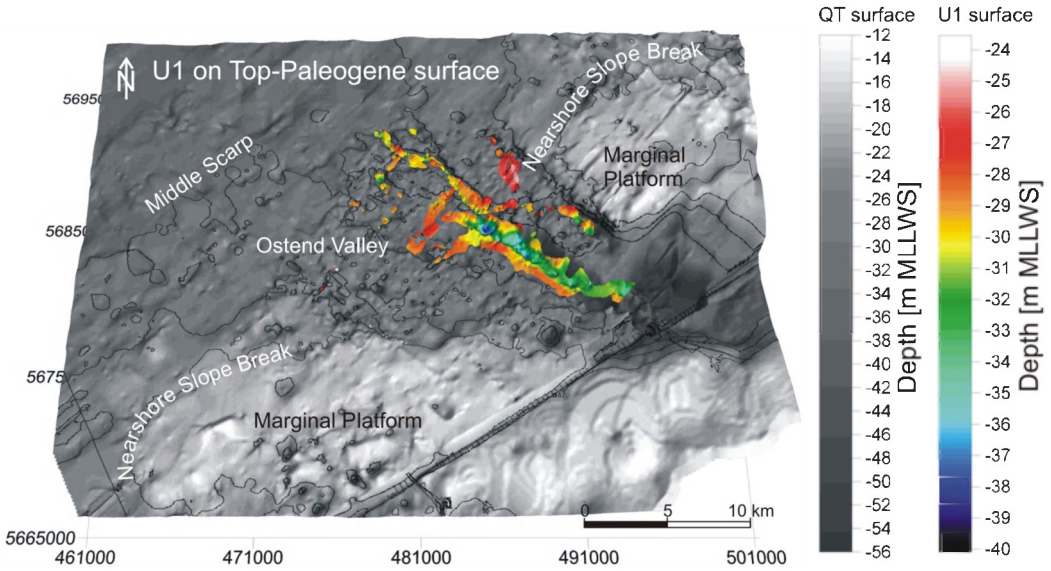
U1 on Top-Paleogene surface
Middle Scarp
Nearshore Slope Break
Marginal Platform
Ostend Valley
Nearshore Slope Break
Marginal Platform
0 5 10 km
5665000
461000
471000
481000
491000
501000
QT surface
U1 surface
Depth [m MLLWS]
Depth [m MLLWS]

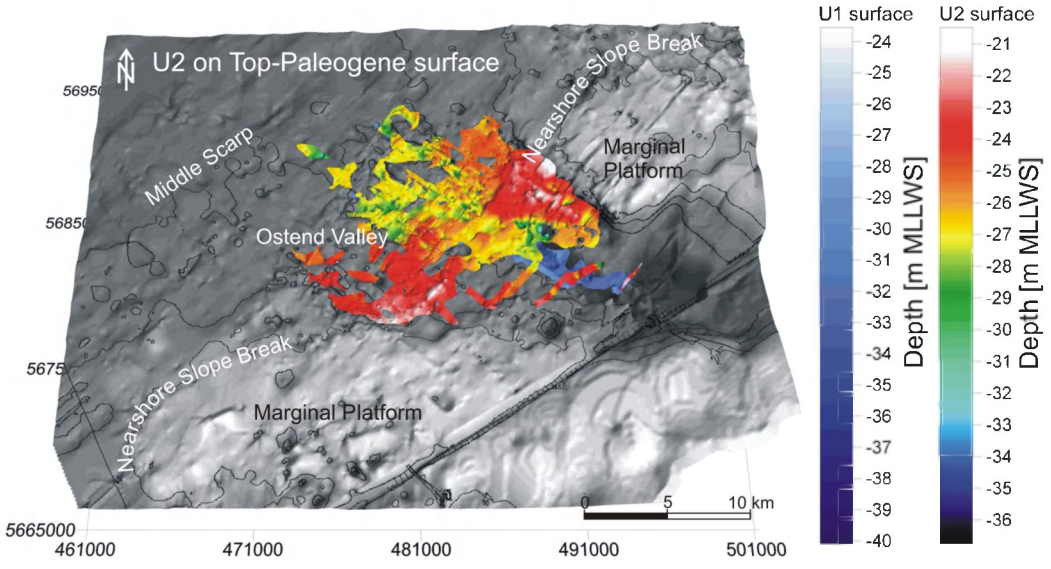
U2 on Top-Paleogene surface
Middle Scarp
Nearshore Slope Break
Marginal Platform
Ostend Valley
Nearshore Slope Break
Marginal Platform
0 5 10 km
5665000
461000
471000
481000
491000
501000
U1 surface
U2 surface
Depth [m MLLWS]
Depth [m MLLWS]

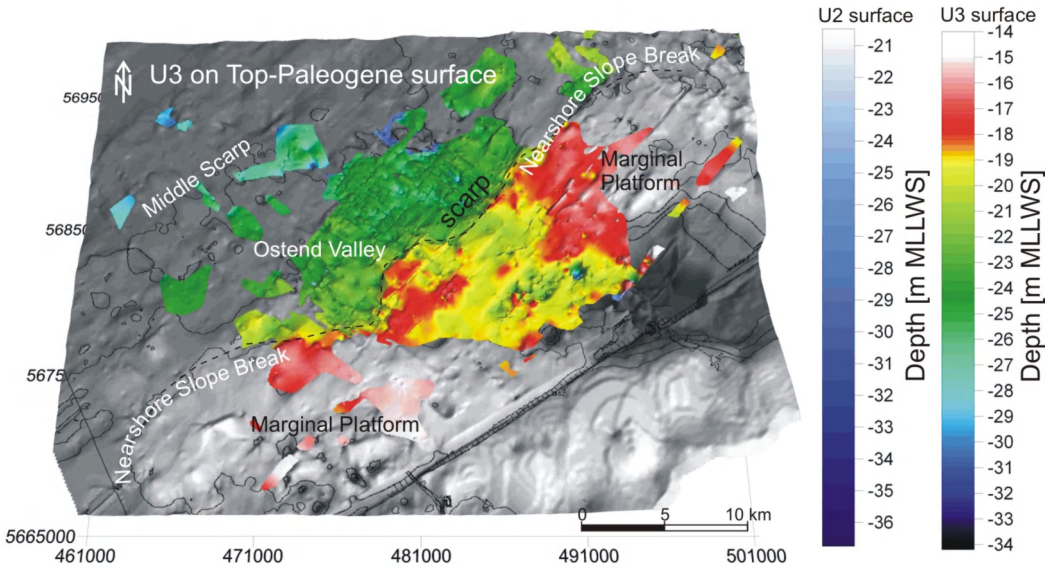
U3 on Top-Paleogene surface
Middle Scarp
Nearshore Slope Break
Marginal Platform
Scarp
Ostend Valley
Nearshore Slope Break
Marginal Platform
0 5 10 km
5665000
461000
471000
481000
491000
501000
U2 surface
U3 surface
Depth [m MLLWS]
Depth [m MLLWS]

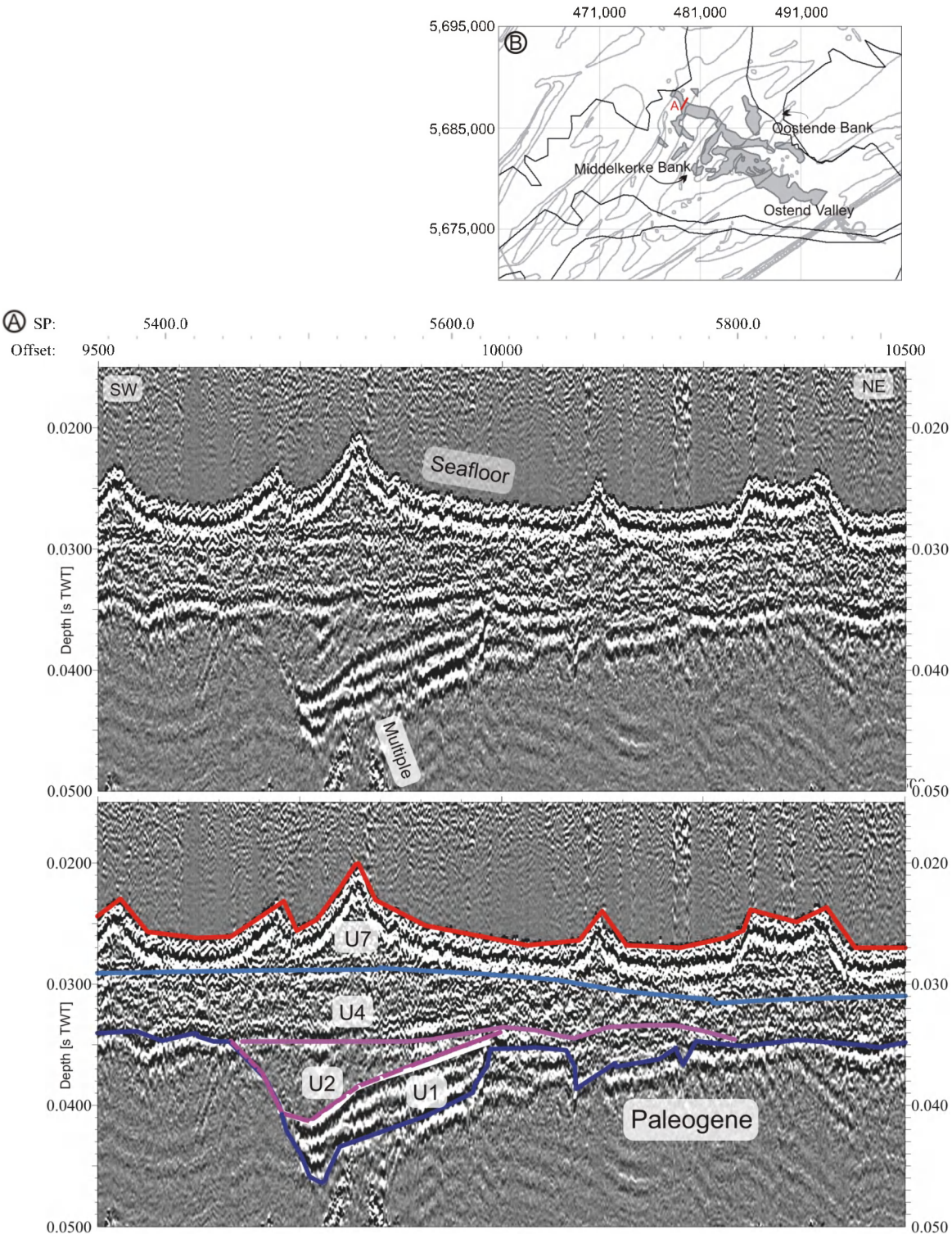

Fig. 6.6 Detailed seismic section showing the internal reflection pattern and configuration of unit U1. (A) Farthest offshore, the top reflector of U1 is inclined subparallel to the gentle wall of the asymmetrical channel incision. Here, the unit shows a prograded fill, with tangential-oblique internal reflectors in the direction of the steepest side of the channel; (B) positioning of the seismic profile with reference to the present-day bathymetry (grey contours), the confines of the Ostend Valley (black), and the extent of U1 (grey area). The top section is the original seismic profile, the bottom section is the interpreted seismic profile.

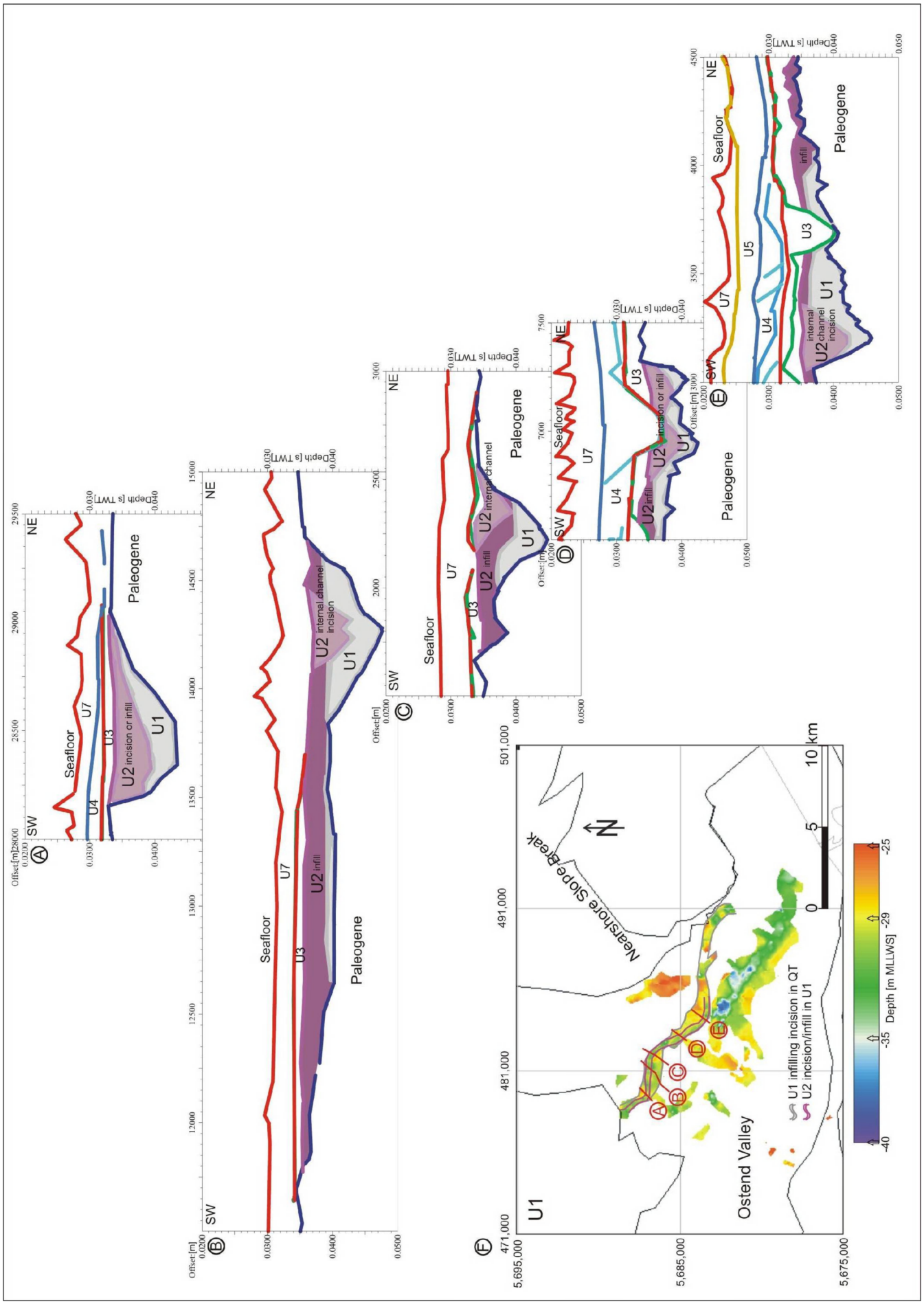
A
B
C
D
E
F
SW
NE
Seafloor
U7
U5
U4
U3
U2
U1
incision or infill
internal channel incision
infill
Paleogene
Offset [m]
Depth [s TWT]
Nearshore Slope Break
Ostend Valley
U1 infilling incision in QT
U2 incision/infill in U1
Depth [m MLLWS]
10 km
5
0
N
471,000
481,000
491,000
501,000
5,695,000
5,685,000
5,675,000

Fig. 6.7

Fig. 6.7 (page 81) (A) to (E): Five successive seismic profiles across a sinuous channel, incised in the Top-Paleogene (QT) surface. Note how the U1 fill is located alternately at the NE and SW side of the channel (A-C-E), at the inside of the channel bends, whereas seismic unit U2 fills up the space left in the deeply incised channel above U1, at the outside of the bends. In between the channel bends (B and D), the channel is more symmetrical, and U2 is limited to the middle part of the channel. Note how on the one hand U1 is clearly incised by individual channels of U2 in (B) and (E). On the other hand, in (A), (C) and (D) the surface of U1 can represent a non-erosional surface as well, U2 gradually infilling the open area adjacent to U1, as no clear U2 internal channel could be distinguished. (F) Positioning of the seismic profiles with reference to the isobath map of U1.

The thalwegs have an undulating course, and rang in depth between –30 m and –40 m in the central channel, between –25 and –34 m in the NE area, and between –25 and –30 m in the SW area. The overall deepening is in nearshore direction.
Generally U2 is less than 2 m thick, except in the bigger channels, where its thickness ranges between 5 and 9 m, and in the smaller channels, where its thickness ranges between 2 and 5 m (Fig. 6.9A). The U2 infill adjacent and on top of U1 in the deeply incised channels in QT clearly shows a meandering pattern. Maximum thickness is reached in the central depression of the Ostend Valley, where the unit is locally 14 m thick.

Unit 3: the uppermost valley infill

As already mentioned in Chapter 4, seismic unit U3 fills up the Ostend Valley almost completely, and extends beyond it, filling other depressions in the Top-Paleogene surface as well (Fig. 4.6B). The surface of U3 slopes down in NW direction ranging between –15 m and –30 m, with an abrupt depth change of 4 m (-20 to -24 m) exactly at the Nearshore Slope Break of the Paleogene surface (Fig. 6.5C). Apart from this scarp, the surface also shows an axial, meandering depression with a width ranging from 600 m nearshore to 4 km offshore and a depth between –19.5 and –21 m, as well as some local incisions by channels of overlying units that extend up to 6 m below the intact surface.
The internal structure of the unit reveals many channels with a prograded fill, mostly eroding the underlying units. The internal channels are clearly truncated at their top, making the upper boundary of U3 an erosional unconformity.
The pattern of internal channels of U3 is presented in Fig. 6.8B. It is a dense network of waterways mainly located within the Ostend Valley and south-east of the scarp in the U3 surface. Their width ranges between 200 m and 1000 m, and they can be incised 1 to 10 m deep, with one extreme value of 28 m, below the U3 surface. Depth of the strongly undulating channel floors ranges between –32 m MLLWS (one extreme value of –46 m) and –20 m.
Mostly U3 is less than 4 m thick in the area north of the scarp and outside the Ostend Valley (Fig. 6.9B). South-east of the scarp, thickness ranges between 4 and 10 m, with a maximum of 18 m in the deepest internal channel.

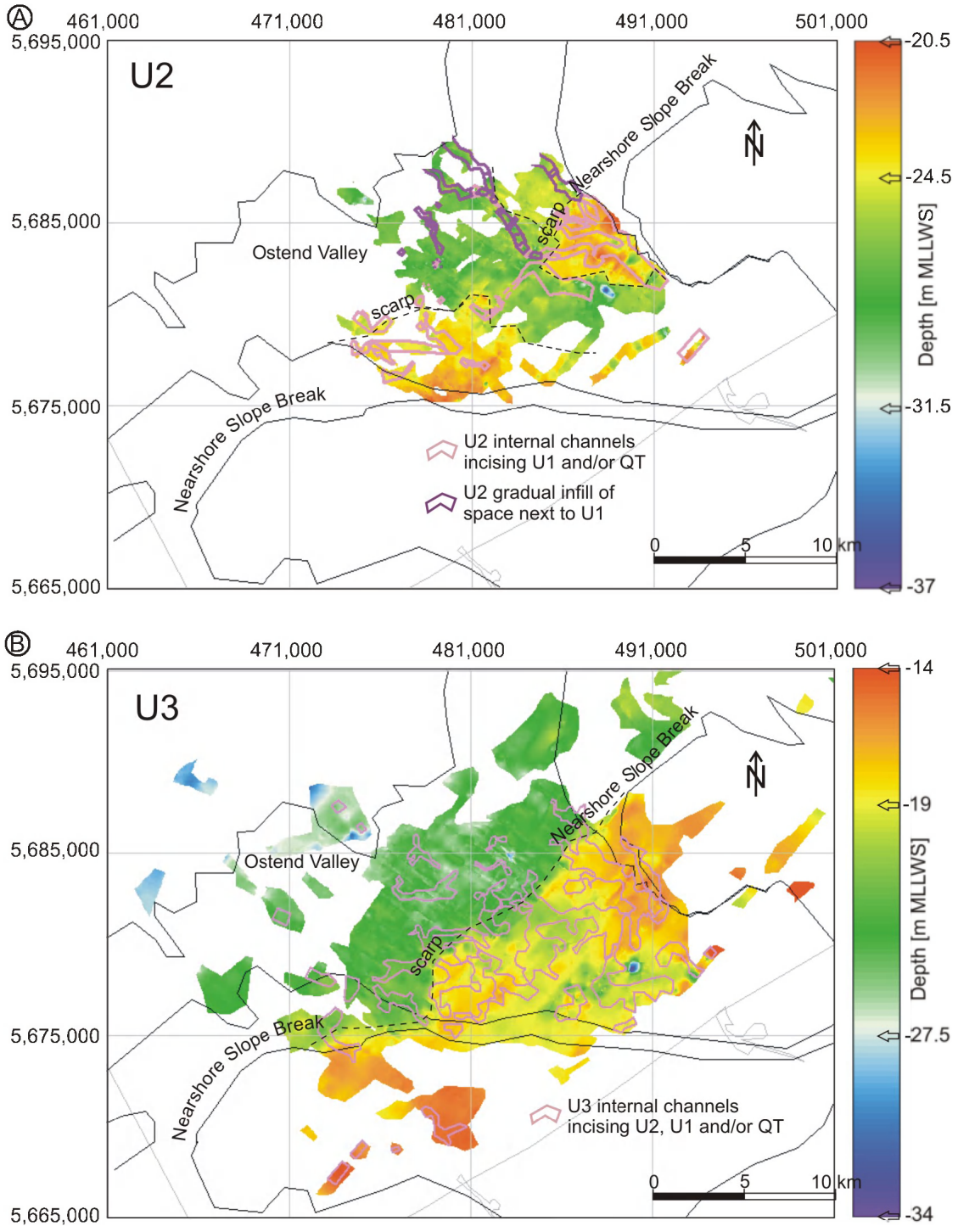

Fig. 6.8 (A) Pattern of internal channels of seismic unit U2, visualised with reference to the isobath map of the top surface of U2. The erosive internal channels are mostly restricted to the area south-east of the scarp in the U2 surface. North-west of the scarp, U2 merely infills (not erosively) the space left above U1 in the deeply incised channels in QT (cf. Figs. 6.7ACD). (B) Pattern of internal channels of seismic unit U3, visualised with reference to the isobath map of the top surface of U3. It is a dense network of waterways mainly located within the Ostend Valley and south-east of the scarp in the U3 surface.

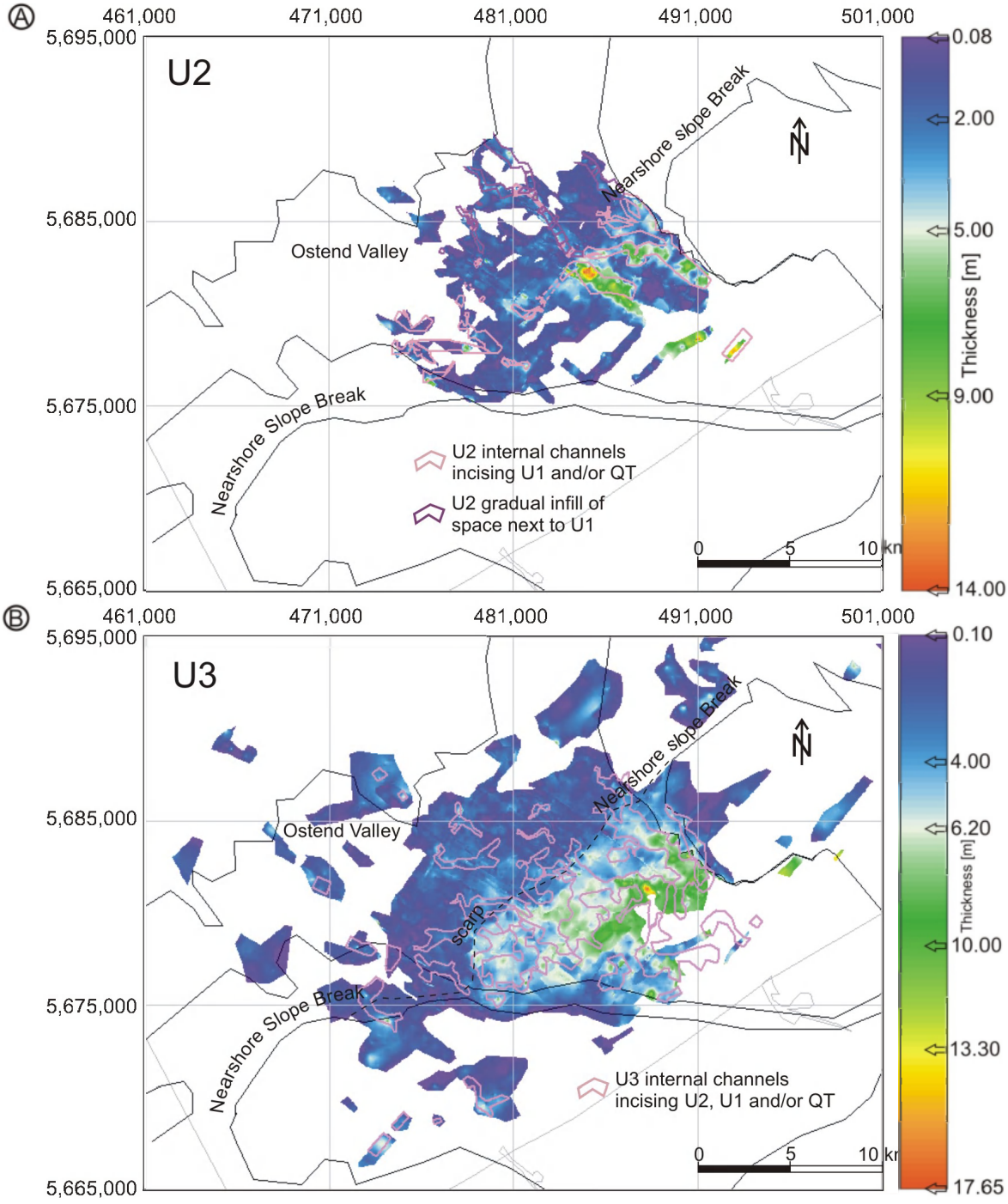

Fig. 6.9 (A) Pattern of internal channels of seismic unit U2, visualised with reference to the isopach of U2. Generally U2 is less than 2 m thick, except for the channels, where thickness ranges between 5 and 9 m in the bigger channels and between 2 and 5 m in the smaller ones. The U2 infill adjacent to and on top of U1, clearly shows a meandering pattern. Maximum thickness is reached in the central depression of the Ostend Valley, where the unit is locally 14 m thick. (B) Pattern of internal channels of seismic unit U3, visualised with reference to the isopach of U3. A maximum thickness of 18 m is reached in the deepest internal channel.

6.2.2 Lithological description

Only a limited number of boreholes reached the lowermost three units. U1 was encountered in only two long boreholes of the GSB (OSB, GR1), the same applies to U2 (UIT, OSB), and unit U3 was present in 9 cores (Tr08, Tr95, Tr96, 6 long GSB boreholes). Fig. 6.10 shows the positions of the cores. Detailed lithologs are shown in App. B, and the corresponding photographs are provided in App. C. the number of boreholes remains limited but the merger of various core-data sets allowed the lithological analysis of the most complete database to date.

No distinct lithofacies could be defined, because too few cores were available to deduce some general, lithological similar packages. Moreover, the cores display a large variety of sedimentary characteristics, including mud layers, shells, organic debris, echinoderm debris, bioturbation, and strongly varying colours. Therefore was opted to discuss the lithology in function of characterising the three seismic units. As a result a comprehensive description of the lithology follows in the discussion (6.3.1), where the cores are correlated with the seismic units. In advance though, some typical lithological phenomena are shown: an alternation of sloping, wavy clay and sand layers with some shell content, which occurs at the base of both OSB (Fig. 6.11) and GR1; a typical heterogeneous mixture of shells, shell fragments, clay balls, and gravel erosionally overlying underlying sediments (Fig. 6.11); an alternation of blue-grey clay and brown-grey silt laminations with a high humic and low carbonate content, containing root penetrations in NWB (Fig. 6.12); and a gravel lag on top of the Paleogene occurs in UIT (Fig. 6. 13), SB1, SB2, and SWB. Discussion follows in the next section (6.3.1).

6.3 Discussion

6.3.1 Integration of seismic data and lithology: genetic interpretation of the seismic units

We observed that the Ostend Valley is infilled with three seismic units separated by erosional surfaces. But from the seismic data alone, it cannot be deduced whether the infilling is a compound fill, in which the erosional surfaces represent successive incisions by river action during different sea-level lowerings, and separate units representing each time a cycle of fluvial, estuarine and marine infillings, or a simple fill, in which the erosional surfaces represent internal, local surfaces like tidal ravinements or a transgressive surface of a single sea-level cycle, the units representing different depositional environments.
In order to interpret the infillings of the Ostend Valley, the seismic data were integrated with the core data. Fig. 6.14A shows a fence diagram of seismic profiles along the longitudinal axis of the Ostend Valley. The five cores projected on the seismic lines present the transition from a more seaward to a more landward environment (UIT, OSB , SB1, SB2 , GR1) (Fig. 6.14B). Fig. 6.15 presents a transverse cross-section through the Ostend Valley, showing two cores on the interfluves along the incised valley (NWB, SWB), and three within the valley (SB1, SB2, GR1). The core data were correlated with the seismic profiles using an average sound-wave velocity of 1650m/s. This appears to be a good approximation of reality as the erosional contacts within the cores correspond almost perfectly with the seismically determined unit boundaries (Fig. 6.16AB).

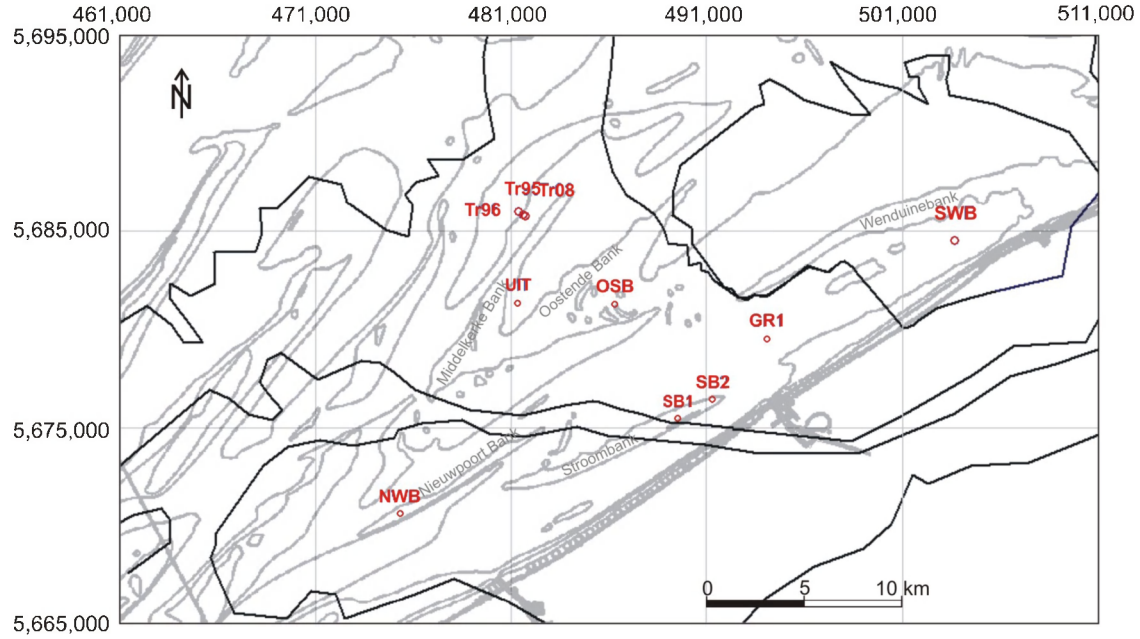

Fig. 6.10 Location map of the cores reaching the lowermost units (U1, U2, U3), with reference to the limits of the Ostend Valley. Coordinates in UTM, WGS84.

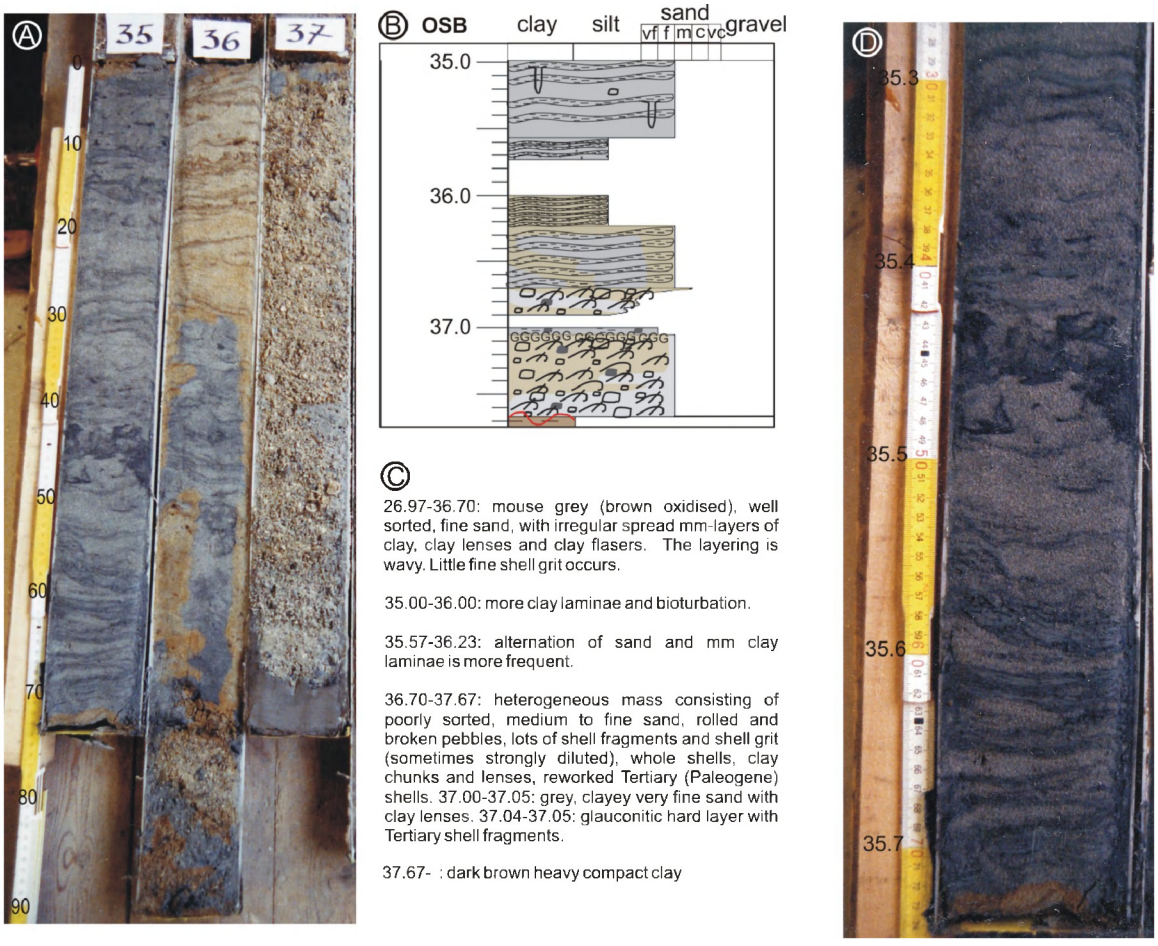

Fig. 6.11 A detail of the lithology of core OSB: (35.00-36.70 m bsf) an alternation of inclined, wavy clay and sand layers with some shell content, later interpreted as IHS (inclined heterolithic stratification); and at the base (36.70-37.67 m bsf) a heterogeneous mixture of shells, shell fragments, clay balls, and gravel with an erosive base, interpreted as a channel-floor deposit. (A) photograph, (B) corresponding litholog, (C) lithological description, (D) detailed photograph.

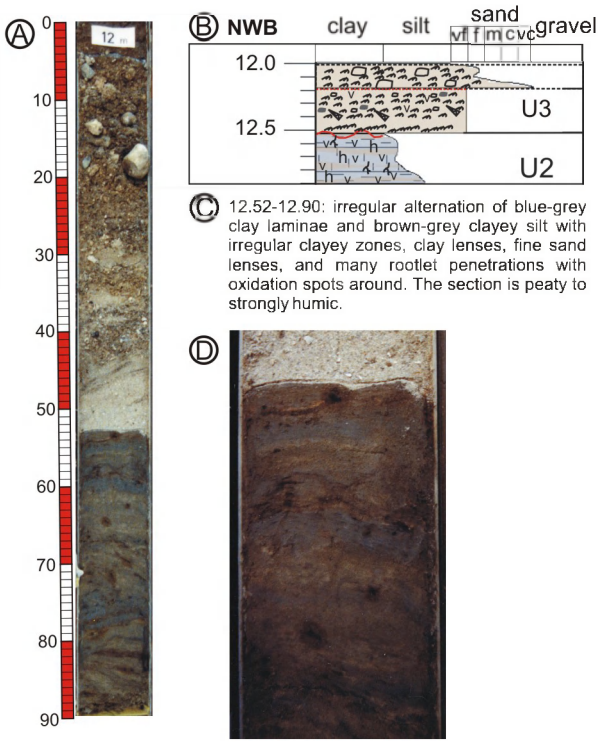

Fig. 6.12 Detail of the lithology of core NWB (12.52-12.90 m bsf): an alternation of blue-grey clay and brown-grey silt laminations with a high humic and low carbonate content, containing root penetrations, later interpreted as a salt-marsh deposit. (A) photograph, (B) corresponding litholog, (C) lithological description, (D) detailed photograph.

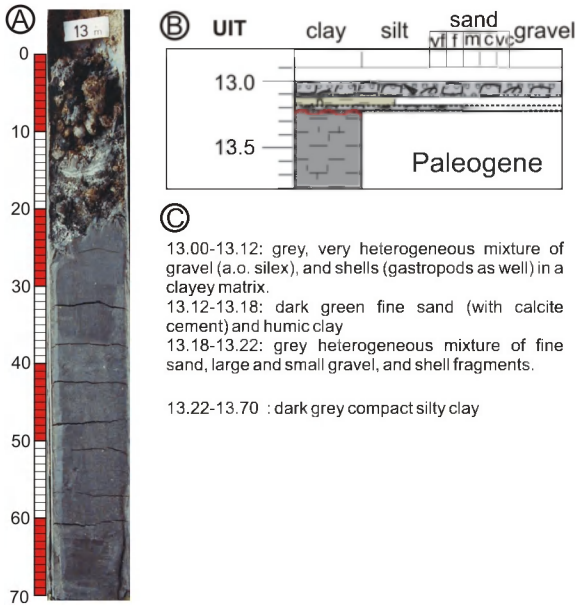

Fig. 6.13 Detail of the lithology of core UIT: a gravel lag (13.00-13.22 m bsf) on top of the Paleogene compact clay (13.22-13.70 m bsf). (A) photograph, (B) corresponding litholog, (C) lithological description.

Unit U1

The deepest seismic unit, U1, was only revealed in two cores (OSB, GR1) in the central part of the Ostend Valley. In OSB, U1 corresponds to about 10 m of grey well-sorted fine sand with frequent irregularly formed clay laminae and flasers (Fig. 6.11). Occasionally some concentrations of grit and shell fragments occur, as well as bioturbations. The base of the unit is characterised by 1 m of heterogenic coarse shell sand, containing lots of shell grit, fragments (some strongly dissolved), whole shells, gravel and flat rolled clay chunks, also some glauconite is present. A similar well-sorted sand of about 4 m thick with irregular clay laminae is present in the most nearshore core GR1. The lower boundary of U1 is sharp in both cores and forms the erosional contact with the underlying Paleogene clay.

The interpretation of sediments observed in only a few cores has to be treated with caution. Nevertheless, in light of the seismic evidence, the sedimentary facies of U1 is interpreted as being indicative of a tide-dominated estuarine environment.

Fig. 6.14 (pages 88 and 89) Composed lateral cross-section through the Ostend Valley. (A) Fence diagram of seismic profiles correlated with cores UIT, OSB, SB1, SB2 and GR1. (B) Schematic overview of the cores along the axis of the Ostend Valley (from offshore to nearshore) showing the lithologs of the cores in more detail.

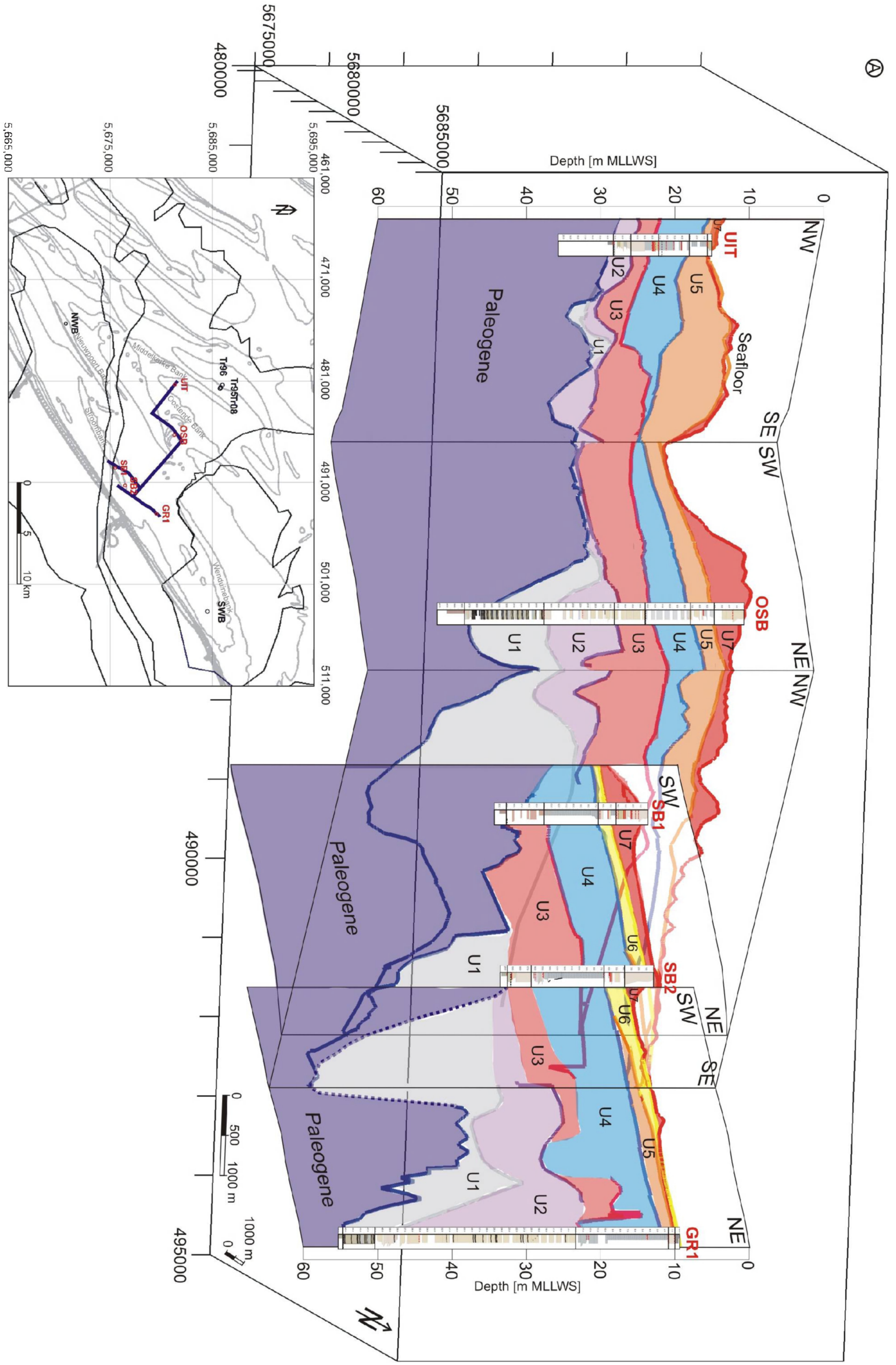
A
Depth [m MLLWS]
0
10
20
30
40
50
60
NW
SE
SW
NE
NW
SW
NE
SW
SE
NE
UIT
OSB
SB1
SB2
GR1
Seafloor
Paleogene
U1
U2
U3
U4
U5
U6
U7
5675000
5680000
5685000
480000
490000
495000
0 500 1000 m
1000 m
N
461,000
471,000
481,000
491,000
501,000
511,000
5,665,000
5,675,000
5,685,000
5,695,000
NWB
SWB
Middelkerke Bank
Oostende Bank
Nieuwpoort Bank
Stroombank
Wenduinebank
Tr96
Tr95Tr08
0 5 10 km

Fig. 6.14 (A)

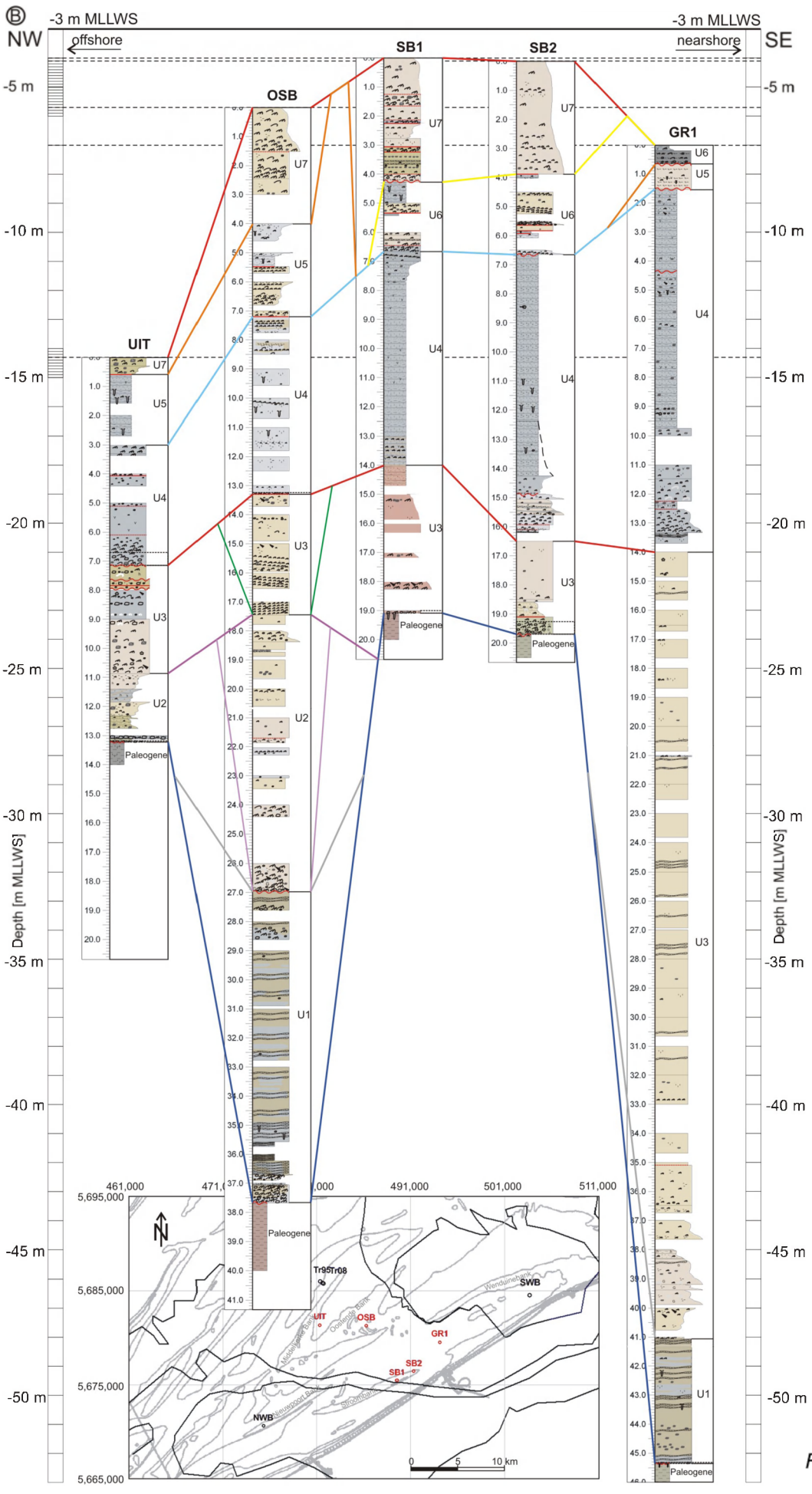
B
NW
SE
-3 m MLLWS
offshore
-3 m MLLWS
nearshore
UIT
OSB
SB1
SB2
GR1
U1
U2
U3
U4
U5
U6
U7
Paleogene
Depth [m MLLWS]
-5 m
-10 m
-15 m
-20 m
-25 m
-30 m
-35 m
-40 m
-45 m
-50 m
461,000
471,000
491,000
501,000
511,000
5,695,000
5,685,000
5,675,000
5,665,000
Tr95Tr08
SWB
NWB
0
5
10 km

Fig. 6.14 (B)

The seismic data show that U1 is infilling sinuous channels cut into the Paleogene subsurface, these can however be both fluvial or estuarine in origin. In light of the concept of the incised-valley system (Zaitlin et al. 1994), both environments can be expected at the base of the Ostend Valley.
The prograding inclined internal reflectors of seismic unit U1 (Fig. 6.6) are interpreted as the lateral-accretion bedding of point-bars, formed at the inside of channel meanders (Fig. 6.7). Point-bars consist of erosionally based, fining-upward successions (Dalrymple and Choi 2007), which is consistent with the lithofacies of U1. Point-bars are a common feature of migrating channels of both fluvial and estuarine origin.
But the fact that the facies consist of sand with clay laminations, especially at the base of U1 in OSB (Fig. 6.11), argues for an interpretation as 'inclined heterolithic stratification' (IHS) (Thomas et al. 1987). Inclined heterolithic stratification is a term used to characterise "modern and ancient large-scale, waterlain, lithologically heterogeneous siliciclastic sedimentary sequences, whose constituent strata are inclined at an original ("depositional") angle to the horizontal or paleo-horizontal" (Thomas et al. 1987). The lithologically heterogeneous composition is an alternation of coarser- and finer-grained units, which can show a large variety of thicknesses ranging from decimetre-thick beds to millimetre- or submillimetre-thick laminae. The majority of IHS deposits are products of point-bar lateral accretion within meandering channels (Thomas et al. 1987). In inclined heterolithic stratification, each inclined bed consists of an alternation of sands and muds, which is thought to be more common in estuarine than in fluvial channels (Thomas et al. 1987 in: Beets et al. 2003).
The presence of mud pebbles could be an additional indication for an estuarine depositional environment. Mud pebbles are a common constituent of channel-lag deposits in many tide-dominated and tide-influenced sedimentary environments, because of the abundance of slack-water drapes and muddy tidal-flat and salt-marsh deposits (Dalrymple and Choi 2007).
The presence of abundant shells in the coarse-grained lag at the base of U1 in OSB, argues for an estuarine environment as well; in riverine channel lags, shells are naturally uncommon (Thomas et al. 1987).
A final factor indicative of an estuarine environment is bioturbation. On the one hand, the original stratification and structure of U1 is easily visible trough the bioturbation, which is one of the more immediately obvious distinctions between estuarine deposits and those formed in an open-marine environment, where bioturbation is generally much more pervasive (Dalrymple and Choi 2007). And on the other hand, is the relative abundance of the bioturbation structures in U1 also a reason to interpret this unit as remnants of tidal channel point-bars, in stead of those of fluvial origin, which show low diversity and very low abundance of bioturbation structures (Thomas et al. 1987).
In light of this evidence, U1 is interpreted as the lateral-accretion unit of a migrating estuarine channel. Why apparently no fluvial lowstand deposits are present at the base of the Ostend Valley, which would be expected according to the stratigraphic model of an incised valley (Zaitlin et al. 1994), is explained later in section '6.3.5 Saalian glaciation'.

The number and thickness of clay-laminations or mud drapes, the abundance of bioturbation, the presence of mud pebbles, and the sand-size distribution are only a few characteristics which give indications of the possible depositional location within an estuary (Dalrymple and Choi 2007). In U1, mud drapes are regularly present, but they are only really abundant at the base of U1 in OSB. Bioturbation is sporadic and only a few mud pebbles or flat rolled clay pieces occur. It is likely that at the location of the cores, U1 was deposited at a certain distance away from the turbidity maximum and bedload convergence in the middle portion of the tide-dominated estuary (Fig. 6.3 and 6.17A) where the highest concentrations of mud pebbles and mud drapes occur. Moreover, U1 is not deposited in tight meandering channels (merely sinuous), which is characteristic for the bedload convergence zone. At both ends of the estuary, in the area of the 'outer estuarine bars' and the 'fluvial zone', mud drapes and bioturbation are rare.

Shell debris, on the other hand, is generally abundant in the outer estuarine zone and increasingly rare toward the fluvial-tidal transition zone. For U1, accumulation either in the 'middle estuary' or in the 'fluvial-tidal transition' zone is therefore the most likely (Fig. 6.3). In the fluvial-tidal transition zone, water flow in a tide-dominated estuary is dominated by the river and the suspended-sediment concentration is relatively low. Mud drapes are only abundant during phases of low discharges of the river. According to Dalrymple and Choi (2007), the fluvial-tidal transition zone belongs to the straight part of the 'straight-meandering-straight' succession of the tide-dominated estuary. This would suggest that seaward of the location of seismic unit U1, sinuosity of the estuary channel(s) should increase, passing into tight meanders, which is not evident from the seismic data. So U1 is probably deposited in the middle estuary, at some seaward distance from the bedload convergence and turbidity maximum (Fig. 6.17A). In general, the amount of mud should increase upward through the channel succession. But in GR1 mud drapes are more abundant in the lower part of U1, which could be an indication of a more marine influence in the upper part.
In the middle estuary, water flow is dominated by the tidal currents, and the net transport direction is landward. Because of a stressed environment, due to strong tidal currents near the tidal maximum, the level of bioturbation is generally low, but still sporadic due to higher salinity conditions in contrast to the fluvial-tidal transition zone (Dalrymple and Choi 2007).

Along the longitudinal axis of the Ostend Valley (Fig. 6.14B), the lithofacies of GR1 and OSB, although 8 km apart, show no systematic sedimentological differences. Possibly because the tidal channels, in which both cores are taken, are directly connected and constitute a whole.
Looking at the transverse profile (Fig. 6.15), only the deepest core GR1, in the axial part of the Ostend Valley, contains U1. In this initial phase, the water level did not reach the higher flanks of the valley. In GR1, a major part of the unit is most likely eroded by the overlying deposits, since the top of U1 is located here at –48 m MLLWS, while the shallowest occurrence of U1 on the seismic data is –25 m. The top of U1 in OSB is -33 m. One would also expect the presence of U1 in UIT, since the Paleogene surface at that location is -27.5 m, but no remnants were found.

Unit U2

Seismic unit U2 is present in only two (possibly three) cores. In UIT this unit corresponds to a grey-brown to green-brown fine sand with clay-sand laminations, containing humic clay lenses, clay pebbles and peat fragments, some zones with shell-fragment concentrations, and zones with high calcium precipitation. At the base a 20-cm-thick grey heterogenic layer of gravel (a.o. silex) and shells (a.o. *Corbicula*) is present in a clayey and fine-sandy matrix, which is very calcareous. In OSB U2 consists of about 6.5 m of light grey-brown fine to very fine sand with sporadic fine shell grit, locally some clay lenses and a single reworked peaty layer. Downward, the lithology becomes coarser with relatively coarse shell fragments located in horizontal layers (some zones dissolved), clay chunks, sporadic gravel and peat fragments, and zones enriched in calcium. At the base of U2, this facies changes into a 2-m-thick poorly-sorted grey-brown gravely sand with plenty of grit and shell fragments (a.o. oyster), lots of flat rolled clay chunks (clay pebbles), gravel (some pebbles), and some slightly glauconitic lumps.

Fig. 6.15 (pages 92 and 93) Composed transverse cross-section through the Ostend Valley. (A) Fence diagram of seismic profiles correlated with two cores on the interfluves along the incised valley (NWB, SWB), and three within the valley (SB1, SB2, GR1). (B) Schematic overview of the cores across the Ostend Valley (from SW to NE) showing the lithologs of the cores in more detail.

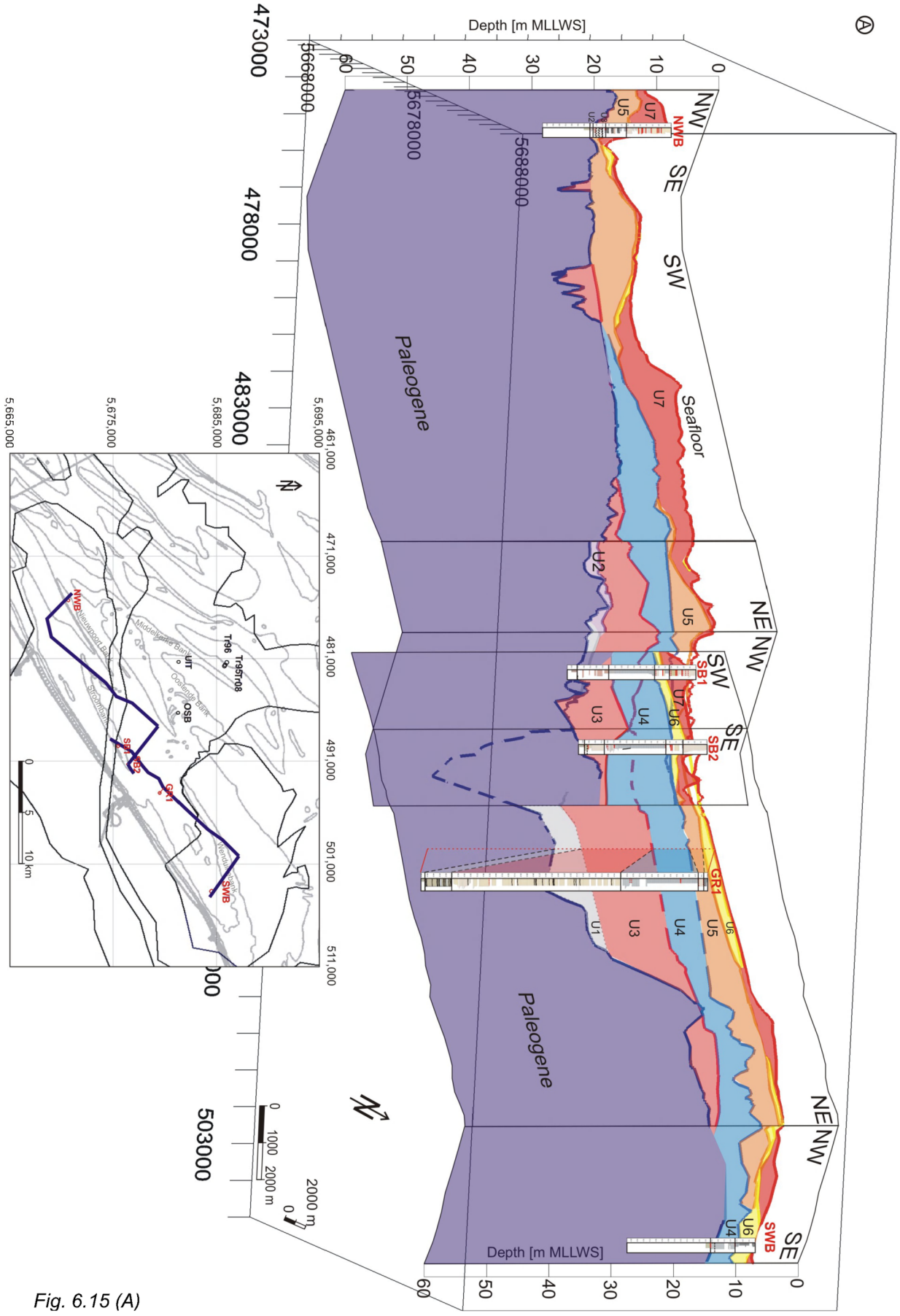
Depth [m MLLWS]
NW
SE
SW
NE
NWB
SWB
SB1
SB2
GR1
U1
U2
U3
U4
U5
U6
U7
Paleogene
Seafloor
473000
478000
483000
503000
5668000
5678000
5688000
5,665,000
5,675,000
5,685,000
5,695,000
461,000
471,000
481,000
491,000
501,000
511,000
Middelkerke Bank
Oostende Bank
Nieuwpoort Bank
Tr96
Tr95Tr08
UT
OSB
0
5
10 km
0
1000
2000 m
2000 m
0

Fig. 6.15 (A)

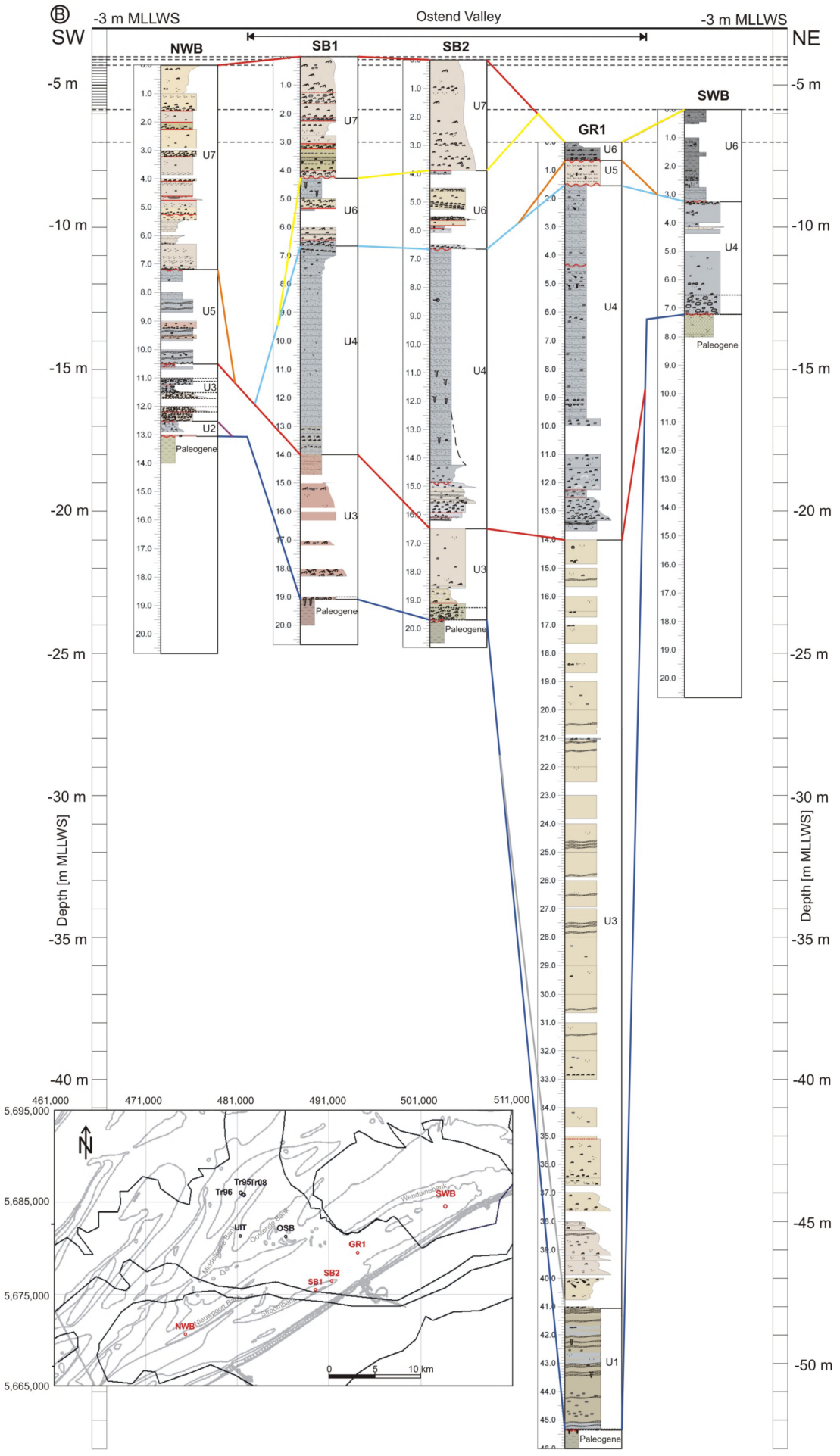
Ⓑ
SW
NE
-3 m MLLWS
Ostend Valley
-3 m MLLWS
NWB
SB1
SB2
GR1
SWB
U7
U6
U5
U4
U3
U2
U1
Paleogene
-5 m
-10 m
-15 m
-20 m
-25 m
-30 m
-35 m
-40 m
-45 m
-50 m
Depth [m MLLWS]
461,000
471,000
481,000
491,000
501,000
511,000
5,695,000
5,685,000
5,675,000
5,665,000
Tr95Tr08
Tr96
UIT
OSB
Oostende Bank
Middelkerke Bank
Nieuwpoort Bank
Stroombank
Wenduinebank
0
5
10 km

Fig. 6.15 (B)

The lower limit of U2 is sharp and erosional in OSB, where the unit base is visible as a channel on the seismic data. In UIT the lower boundary of U2 is sharp and forms the erosional contact with the underlying Paleogene clay.

Again, the interpretation of a unit observed in only two cores (but on a large number of seismic profiles) has to be treated with caution. Nevertheless, the seismic and sedimentary facies of U2 provide ample indications of deposition in an estuarine environment.
On the seismic data one can see that U2 fills in the space in the channels in which the point-bars of U1 are located. And then spreads out to an area covering almost the entire Ostend Valley, showing a network of internal channels itself. Unit U2 is therefore interpreted as a subsequent phase in the infilling of the Ostend Valley in a tide-dominated estuarine environment. An estuarine setting is supported by the presence of humic particles and peat fragments, which suggests the proximity of salt and freshwater marshes, which is typical for an estuarine setting. In a tide-dominated estuary (Fig. 6.3) tidal channels and flats are fringed by salt marshes and after sufficient silting up also freshwater marshes develop.
The lithofacies of U2 shows a clear difference between core UIT and core OSB. In OSB, the unit is more sandy, almost no clay laminations occur, shell grit occurs in thin layers, and a coarse gravel- and shell-lag is present at the base. Whereas in UIT frequent clay laminae occur, and shell fragments are present only as concentrations. These differences can be explained by the fact that core OSB is taken within a tidal channel (Fig. 6.16B), where high-energy conditions prevailed and coarse material was transported. The coarse lag at the base of U2 in OSB represents the coarse and erosional channel floor (Fig. 6.11). Whereas U2 in UIT represents a lower-energy setting (possibly a tidal flat) with deposition of clay laminae/mud drapes, and only occasionally of coarser material. The 20-cm-thick gravel lag at the base of U2 in UIT probably represents material eroded from the Quaternary-Paleogene surface, and corresponds to the lower seismic boundary of U2. The gravel lag most probably contains remnants of the possibly completely eroded unit U1.

Judging from the characteristics of U2 in UIT, the unit is probably deposited farther seaward in the tide-dominated middle estuary than U1 (Fig. 6.17A). Here, clay laminae are present but not abundant because of the distal position with respect to the bedload convergence. Mud pebbles and bioturbations are less frequent as well, but the shell-debris content is higher than in U1 because of the stronger marine influence. Also the presence of oyster fragments in OSB indicates a more seaward position or a more direct marine influence. Oysters, which are tolerant of brackish water, moderate suspended sediment concentrations, and moderate- to high-energy conditions because of their reef-building ability, are particularly common in marginal-marine settings, although they are not restricted to these environments (Dalrymple and Choi 2007).

The transverse cross-section through the Ostend Valley (Fig. 6.15), shows that unit U2 is encountered in neither of the cores. Although, one would expect to find U2 in SB1, SB2 and GR1 on the basis of the depositional depth of seismic unit U2 (-28 to –21 m MLLWS). In GR1, U2 is completely eroded by a channel of the overlying unit U3. Although not visible on the seismic data (due to the presence of gas), the lithofacies of U3 in GR1 shows a clear channel infilling with channel-floor deposits (see next paragraph ‘Unit U3’). In SB1 or SB2 no such evidence exists, but probably any present U2 deposits were completely eroded by the overlying unit U3. The seismic data from the corresponding locations show that the upper boundary of U2 is an erosional contact.
Although not corresponding to the overall depositional depth of seismic unit U2, it is possible that U2 is present in NWB, a core located west of the Ostend Valley. The layer concerned is located between -17.3 and -16.8 m and consists of a 0.5-m-thick alternation of blue-grey clay and brown-grey silt laminations with a high humic and peat content, a

low carbonate content, and root penetrations (Fig. 6.12). It represents a typical supratidal salt marsh environment, the peat remnants probably originating from an eroding freshwater marsh nearby. From the paleo-reconstruction in the following chapter it will become clear that this layer probably corresponds to salt marsh deposits at the margin of the middle estuary of U2.
Here, U2 directly overlies the Paleogene green-grey compact clay, with a sharp and erosional contact, but no gravel lag is present.

Unit U3

Seismic unit U3 is present in nine cores. Three vibrocores (Tr08, Tr95, Tr96) along the NW side of the Middelkerke Bank were long enough to reach seismic unit U3. In this area U3 consists of a yellow-green to green-grey fine to medium sand, zones with very few shells alternate with zones containing many gastropods, white shell fragments, some gravel and clay chunks. In UIT, the most seaward long core, U3 is a 4-m-thick brown-green to brown-grey fine to medium-fine sand with occasional clay laminae. The facies contains concentrations of gravel (pebbles, silex) and shell fragments (a.o. oysters), some humic particles and sea-urchin debris. The unit becomes more heterogeneous and coarser grained toward the base. In OSB, U3 is characterised by a 4-m-thick layer of light-brown (beige) poorly-sorted clayey fine sand, containing fine black shell grit. The grit content strongly increases downward and is concentrated in horizontal and inclined laminae. Locally some clay lenses and little pebbles occur. In the shell sand, a zone of increased dissolved-calcium content is present. In SB1, more landward, U3 is a 5-m-thick brown well-sorted fine sand, with clay laminations in the upper part. The facies contains some fine shell grit and fragments (a.o. *Hydrobia*). Near the base, the unit contains more shell fragments, and ends in a heterogeneous mixture of gravel, glauconitic sand, Paleogene shell fragments, and (beach-rock) cementations. In SB2, U3 is a light grey-brown to grey-brown well-sorted fine sand, containing sporadic fine clay laminations, very little shell grit and few shell fragments. Towards the base, more clay laminae, shell grit and shell fragments (a.o. oysters) are present. The basal part is a brown to grey-green heterogeneous, poorly-sorted mixture of shell grit, fragments (some strongly dissolved), whole shells, gravel, glauconitic sand, with a high carbonate content. In the most landward core GR1, U3 is a 21-m thick grey-brown (beige) silty very fine sand with irregular clay flasers, very few (white) shell fragments, and some diffuse layers formed by a concentration of shell grit and sea-urchin needles. The base of U3 consists of a 6-m-thick brown-grey clayey glauconite containing fine to medium sand, containing lots of shell grit, numerous shell fragments (a.o. oysters), clay chunks, and a few humic particles. On the basis of the depositional depth of seismic unit U3 (shallowest occurrence -16 m), NWB outside the Ostend Valley could also contain facies U3. The sediments between -14.8 and -16.8 m MLLWS consist in that area of 1-m-thick dark grey sandy clay, with lots of shell fragments, gravel and amorphous peat particles, underlain by a 1-m-thick grey-brown heterogenic layer, containing shell fragments and silex boulders (up to 5 cm), fining downward into a fine sand with fine shell fragments and few clay and peat chunks. It makes a sharp and erosional contact with the underlying layer (possibly U2) of blue-grey and brown-grey, humic and peaty clay-silt laminations, with root penetrations, that indicate in situ vegetation growth.

In SB1 and SB2, U3 directly overlies the Paleogene deposits, and the base of the unit corresponds to a gravel lag with a sharp erosional contact with the underlying Paleogene clay. In OSB and GR1 the transition from U3 to the underlying units is also sharp and erosional. Here, U3 corresponds to locally incised channels as can also be observed from the seismic profiles (OSB). The transition from U3 to U2 in UIT is more gradual.
In the cores were the top of unit U3 was encountered, this boundary is marked by a sharp erosional contact overlain with a gravel lag or other coarse material. On seismic records, it is visible as a strong reflection.

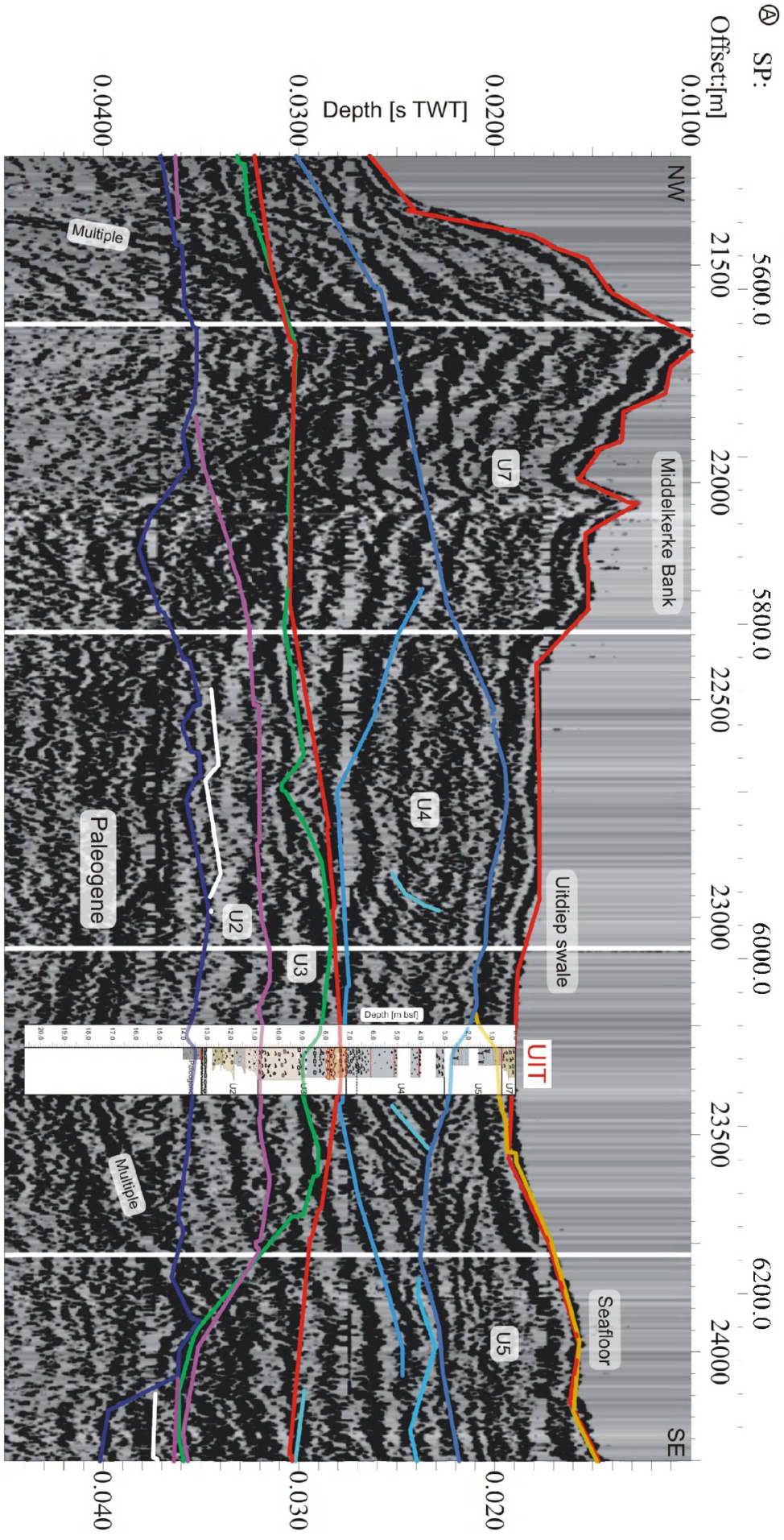
SP:
Offset:[m]
Depth [s TWT]
NW
SE
Multiple
Middelkerke Bank
Uitdiep swale
Seafloor
Paleogene
U7
U4
U2
U3
U5
UIT
Depth [m bsf]

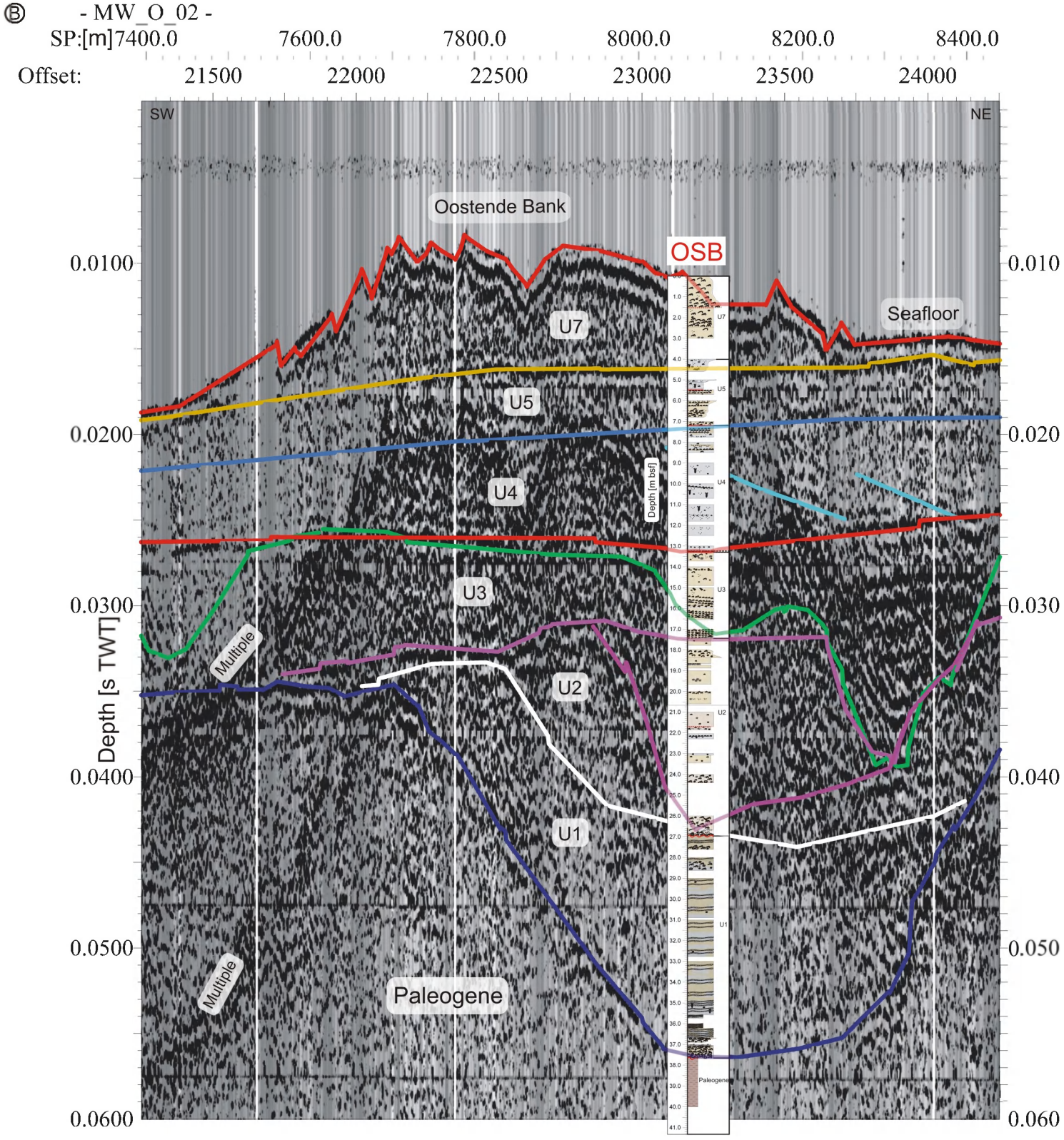

Fig. 6.16 (A) (page 96) Integration of seismic profile MW24 and core UIT in detail; (B) (above) Integration of seismic profile MW02 and core OSB in detail. The core data were correlated with the seismic profiles using an average sound velocity of 1650m/s. The erosional contacts within the cores coincide almost perfectly with the seismic unit boundaries

Unit U3 is interpreted as the last phase in the infilling of the Ostend Valley in a tide-dominated estuarine environment. On the seismic data one can see that unit U3 covers the entire Ostend Valley and extends even beyond it, filling up depressions around it. Seismic unit U3 shows a dense, chaotic network of tidal channels. The core data reveal a typical tidal-flat mollusc fauna (a.o. *Hydrobia*), and the presence of occasionally humic mud pebbles and sporadic clay flasers or laminae.

Along the longitudinal transect through the Ostend Valley, from the most nearshore cores (SB1, SB2, GR1) to the most offshore cores (Trentesaux vibrocores), the lithofacies of U3 shows a tendency of decreasing clay content, and an increasing shell-fragment content (Fig. 6.14B). Judging from the characteristics of U3 in SB1, SB2 and GR1, that part of the unit is probably deposited in a more seaward section of the middle estuary (Fig. 6.17A). The lithofacies features of OSB, UIT and the vibrocores, suggest sedimentation in the outer estuarine-bar section of the tide-dominated estuary, even farther seaward (Fig. 6.17A).
In the seaward part of the middle estuary, mud drapes and clay laminae are present but not abundant because of the distance to the bedload convergence. Also mud pebbles and bioturbations are less frequent or even absent compared to the more landward middle estuary. The shell debris content is higher than farther landward, but only sporadic compared to the outer estuarine-bar section, where shell debris can be an important constituent (Dalrymple and Choi 2007). Also the presence of oyster fragments and sea-urchin debris in GR1 indicate a more seaward position or a more directly marine influence (probably via the channel in which GR1 was cored).
The outer estuarine-bar section is characterised by high concentrations of shell debris, low levels of bioturbation because of the nearly constant movement of sand, the presence of oyster fragments, a coarser (bulk, bedload) grain size, and the absence (or nearly absence) of mud drapes and clay content because of its great distance to the bedload convergence and turbidity maximum. In the outer estuarine-bar section, U3 in the three vibrocores and UIT core are coarser grained than in the more landward OSB core. They contain heterogeneous layers of coarse shell fragments, gravel and mud pebbles, whereas OSB contains abundant fine shell debris sorted in thin layers. It is uncertain if this is due to the fact that OSB is located more landward, i.e. closer to the bedload convergence.

Along the transverse cross-section (Fig. 6.15), SB1, located closest to the flank of the Ostend Valley, contains more clayey material than SB2 and GR1, which are located closer to the valley axis. This could be due to the proximity of mud flats. The farther away from the tidal channels in the axial part, the finer the grain size becomes.
In NWB, the 2 m of gravely sands overlying the U2 salt marsh deposits, could represent a migrating tidal channel corresponding to outer-estuarine sediments as in U3. Specifically, the grey-brown heterolithic lower metre looks very similar to the U3 facies in UIT. However, the sandy unit shows a coarsening upward, and no typical coarse-grained channel floor. Another option is that the coarse, erosional overlying layer testifies to initial marine input. The thickly walled shells indicate a high-energy environment, possibly a beach. Also the colonies of *Bryozoa* on the shells point to marine influence.
To the east of the Ostend Valley, the Paleogene surface in core SWB is located at a depth of –13.2 m MLLWS, which is well above the shallowest occurrence of seismic unit U3 (-16 m MLLWS). Later will be determined that salt marsh deposits could theoretically have developed during estuarine phase U3 up to a height of -13.5 m, and fresh water deposits even to a higher level (paragraph 6.3.3). But fresh water deposits have not been encountered in SWB.

Summary

To summarise (Fig. 6.17AB), seismic unit U1 consists of tidal-channel infillings (OSB, GR1), probably deposited in a middle estuary, not too far from the bedload convergence or turbidity maximum. The overlying unit U2, near UIT and OSB, was also deposited in the middle estuary, but farther seaward, as it contains more shell debris and fewer clayey layers than U1. The nearshore part of the upper unit U3 (SB1, SB2, GR1) is probably deposited in the same environment, since it has the same lithological characteristics. The channel deposits in this part of U3 (GR1) are similar to the channel deposits of U2 (OSB), and the tidal-flat deposits in this part of U3 (SB2) are very alike the ones in U2 (UIT), except for the fact that U2, unlike U3, contains peat fragments.
The outer part of U3 (UIT, OSB) was most likely deposited in an outer estuary, as it contains almost no clay pebbles or laminae, but lots of shell debris and coarser material. However, it must be noted that the channel sediments in the outer estuary in OSB (U3) show great similarities with the sediments of the middle estuary in OSB (U2). This can be explained by the fact that the channel of U3 is incised into the underlying channel fill of U2, reworking much of its sediment. This is not an uncommon phenomenon. It was also reported by Baeteman (2005b) that tidal channels in the Coastal Plain tend to incise existing, older channels. Since sandy channel fills are more easily erodible than adjacent cohesive mud flats deposits (Baeteman 2005b).

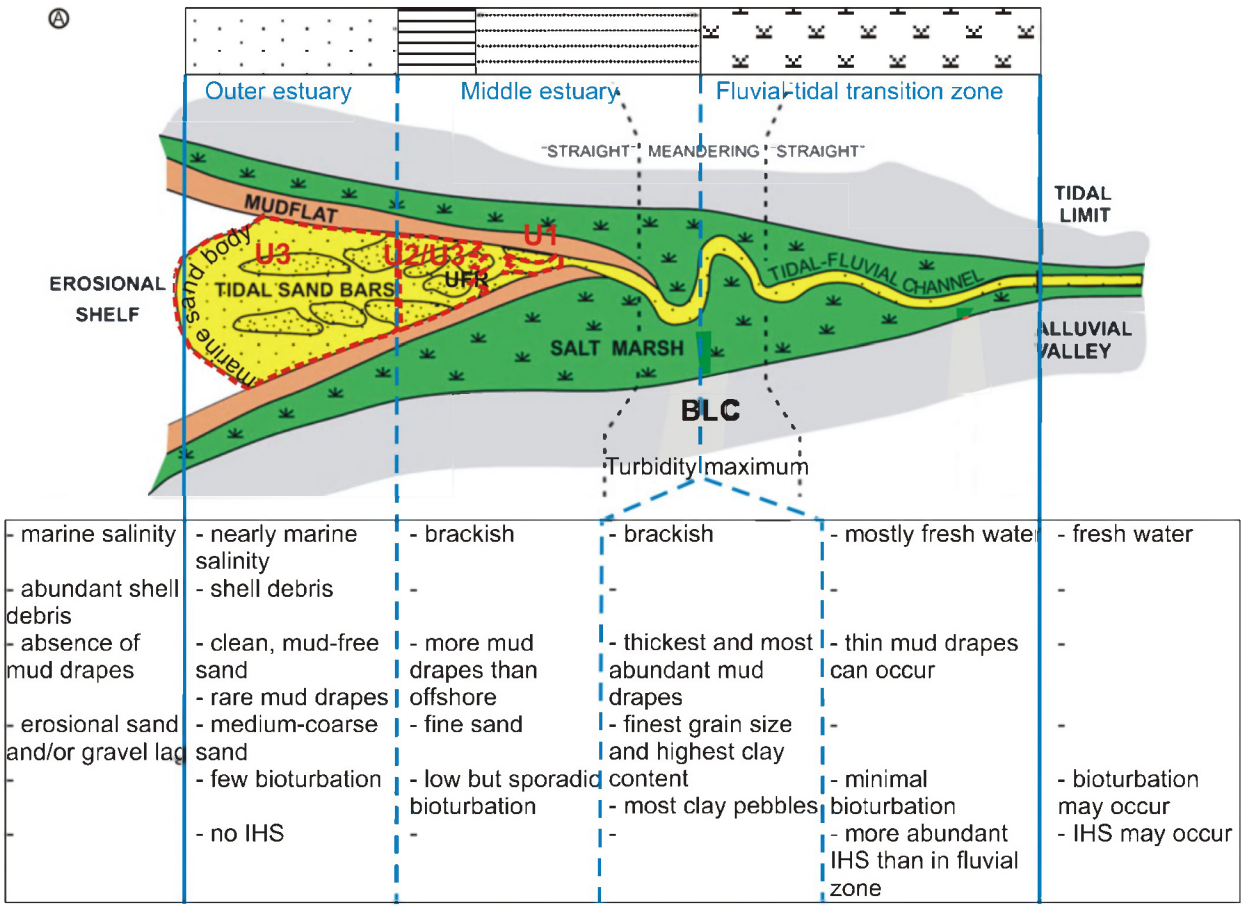

Fig. 6.17 (A) Map view of a tide-dominated estuary with its different depositional environments and characteristics, with indication of the interpretations of the seismic units.

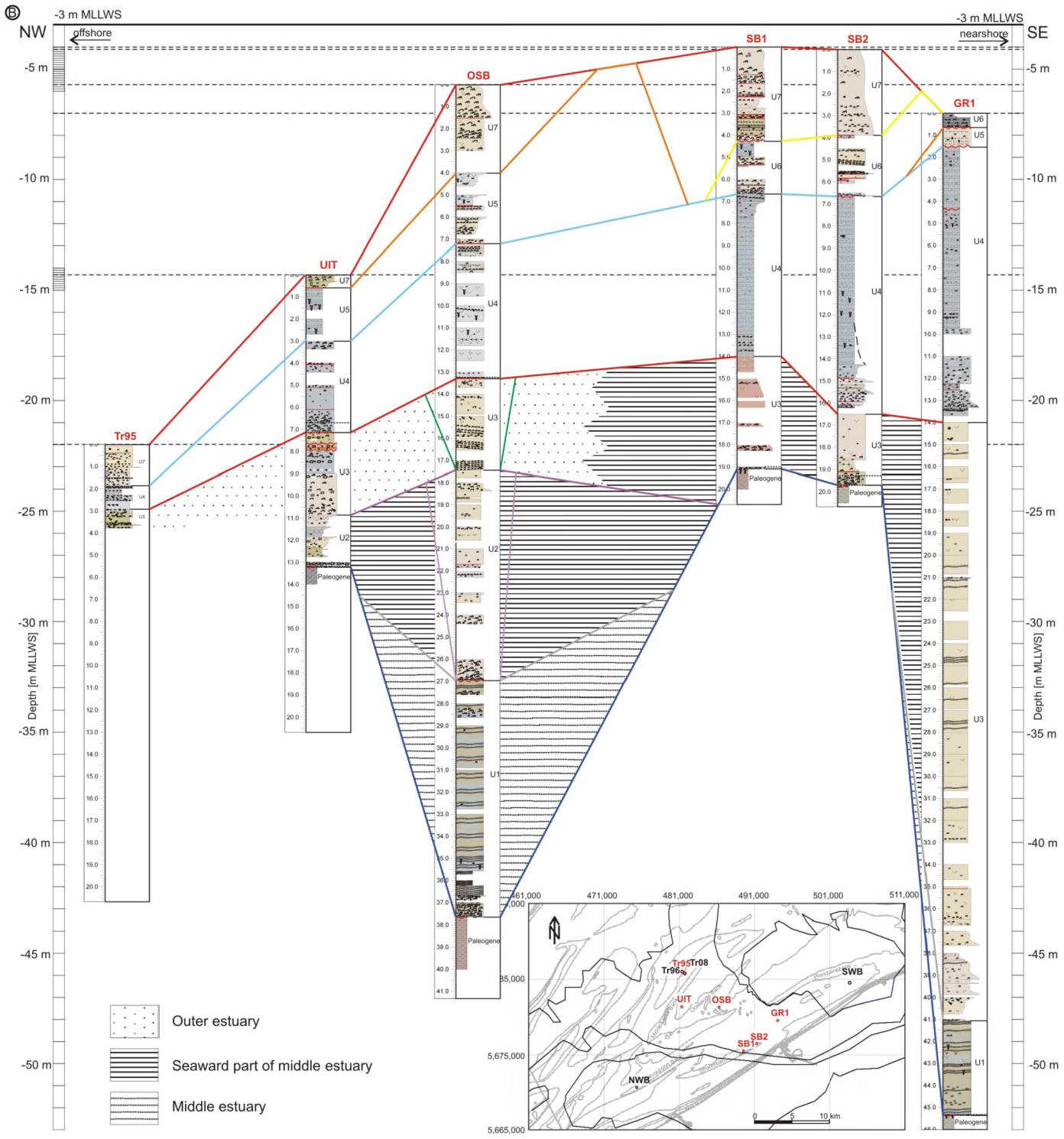

Fig. 6.17 (B) Schematic axial cross-section through the Ostend Valley, showing the lithological changes of a seismic unit from offshore to nearshore and the differences in lithology between the seismic units, in the context of a tide-dominated estuary consisting of an outer, middle and transition zone.

So in the nearshore cores (SB1, SB2, GR1), the sedimentary environment evolved upward from a middle estuary (U1 in GR1), to a more seaward middle estuary (U3 in SB1, SB2, GR1) (Fig. 6.17B). In OSB, in the middle of the Ostend Valley, the environment changes from a middle estuary (U1), over a more seaward estuarine environment (U2), to an outer estuarine setting (U3). In the outer region of the Ostend Valley (UIT, Tr08, Tr95, Tr96), the sediment characteristics change upward from a seaward middle estuarine setting (U2) into an outer estuarine environment (U3). So within each core, the lithofacies shows an increasing marine influence from the lower unit to the upper unit. Within a seismic unit, although only clearly observed in U3, the lithofacies shows laterally a decreasing marine influence from the outer cores to the nearshore cores (Fig. 6.17B). Going from offshore to nearshore, each depositional environment (e.g. middle estuary) occurs in a higher position. This overall trend implies that the estuary migrated landward through time.

6.3.2 Interpretation of the seismic erosional surfaces and internal channels in function of the genetic interpretation

The base of the Ostend Valley

On the basis of the above interpretation we know that the basal deposits in the Ostend Valley have an estuarine origin, and that little or no fluvial deposits are present underneath. So the base of seismic unit U1 represents the *transgressive surface*, which in this case corresponds to the surface that defines the valley form, i.e. the *sequence boundary* represented by the Top-Paleogene surface (Fig. 6.18).
The gravels found on top of the Paleogene clays in UIT, SB1 and SB2 were not considered a separate unit, as the layer was too thin to be distinguished on seismic profiles. This gravelly deposit could be reworked coarse fluvial material brought into the estuary by tidal currents, or it could represent coarse remnants of the underlying Paleogene, when fines were washed out by tidal currents during the estuarine phases. Alternately, the gravel could represent a fluvial deposit after all. A detailed study of the inclusions could not give however a definite answer. If the gravels found in UIT, SB1 and SB2 would represent remnants of fluvial deposits, this would imply that the Ostend Valley was at least that wide before the estuarine infilling set in. The transgressive surface would be situated above these gravels. In that case, it would correspond to the *initial flooding surface*, i.e. the estuarine-fluvial contact, and the gravel deposit would represent a Lowstand Systems Tract.

Most likely the sequence boundary or base of the Ostend Valley has a multi-genetic origin. The wide part of the Ostend Valley with a maximum depth of -27.5 m was incised by fluvial action during a former sea-level lowering and lowstand, while during the estuarine infilling phase U1, tidal channels scoured into the Paleogene substratum to depths of -56 m (Fig. 6.18B). At the base of the channels in U1 only coarse, shelly channel floor deposits are found (OSB, GR1), no gravel lag as described above. It might be suggested that the deep incisions in the Ostend Valley were formed by fluvial action during the sea-level lowering as well, after which they were infilled with U1 during the following sea-level rise. But, seismic unit U1 shows meandering channels, infilled with typical point-bar (lateral-accretion) structures, which indicates that U1 was deposited while this channel was developing and channel bends were migrating, so during the sea-level rise. Another argument for the multi-genetic origin of the Ostend Valley base, is the fact that the large incised channel in the centre becomes shallower in seaward direction, which is impossible for a river channel.

Ⓐ

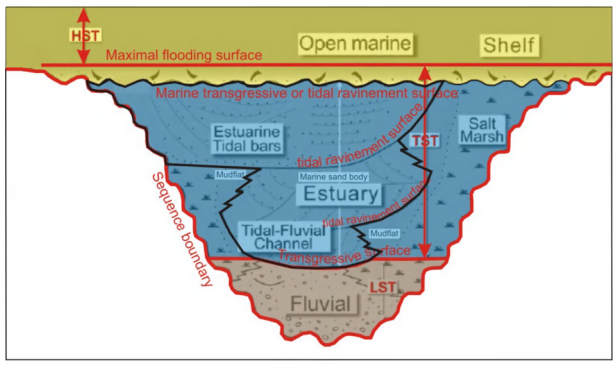
HST
Maximal flooding surface
Open marine
Shelf
Marine transgressive or tidal ravinement surface
Estuarine Tidal bars
Salt Marsh
tidal ravinement surface
TST
Mudflat
Marine sand body
Estuary
Tidal-Fluvial Channel
Sequence boundary
Transgressive surface
LST
Fluvial

Ⓑ

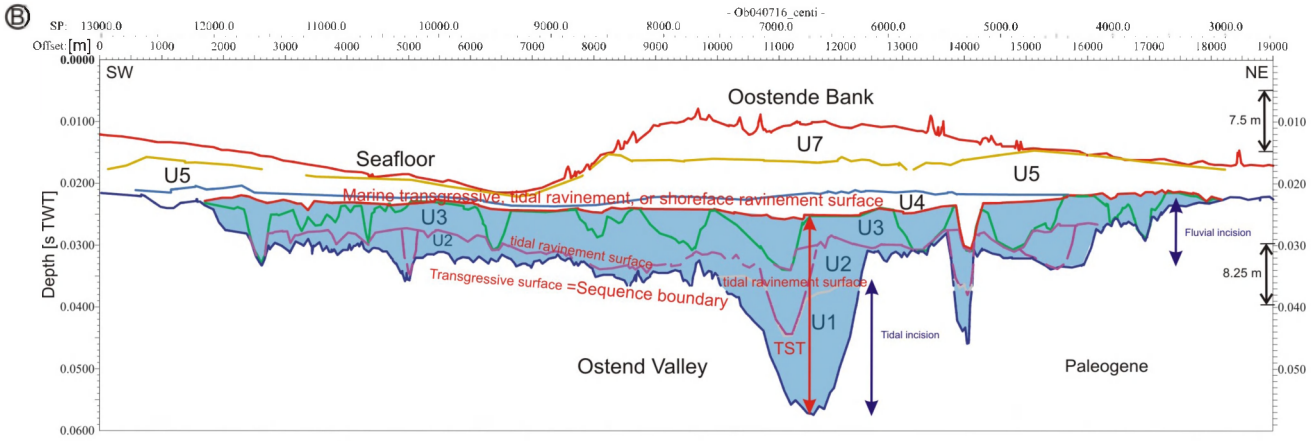
- Ob040716_centi -
SW
NE
Oostende Bank
Seafloor
U7
U5
U4
U3
U2
U1
Marine transgressive, tidal ravinement, or shoreface ravinement surface
tidal ravinement surface
Transgressive surface =Sequence boundary
TST
Tidal incision
Fluvial incision
7.5 m
8.25 m
Ostend Valley
Paleogene
Depth [s TWT]

Ⓔ

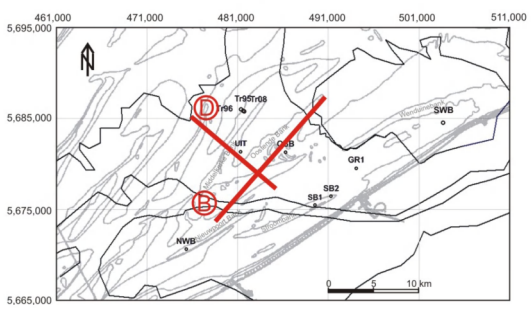
461,000
471,000
481,000
491,000
501,000
511,000
5,695,000
5,685,000
5,675,000
5,665,000
SWB
NWB
GR1
SB1
SB2
0
5
10 km

Ⓒ

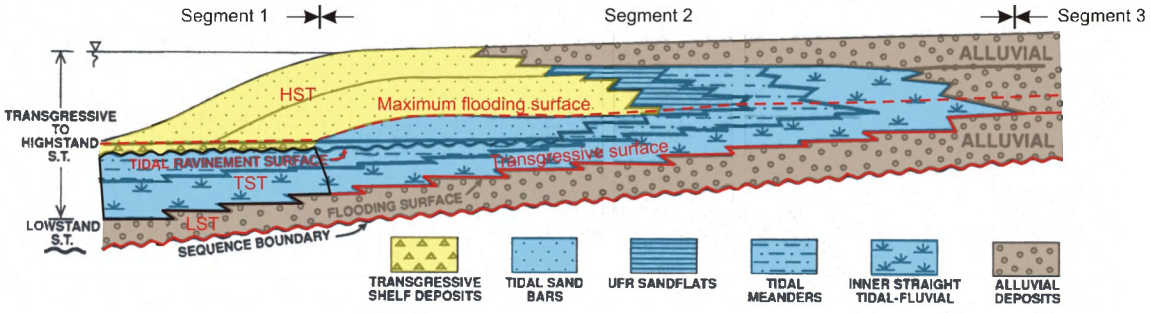
Segment 1
Segment 2
Segment 3
TRANSGRESSIVE TO HIGHSTAND S.T.
LOWSTAND S.T.
HST
Maximum flooding surface
TIDAL RAVINEMENT SURFACE
TST
Transgressive surface
FLOODING SURFACE
LST
SEQUENCE BOUNDARY
ALLUVIAL
ALLUVIAL
TRANSGRESSIVE SHELF DEPOSITS
TIDAL SAND BARS
UFR SANDFLATS
TIDAL MEANDERS
INNER STRAIGHT TIDAL-FLUVIAL
ALLUVIAL DEPOSITS

Ⓓ

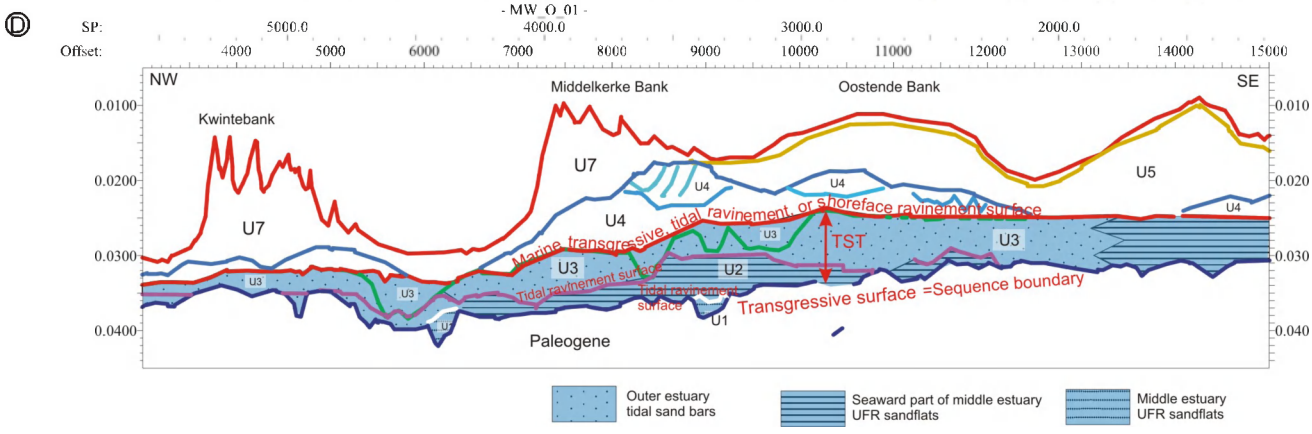
- MW_O_01 -
SP:
Offset:
NW
SE
Kwintebank
Middelkerke Bank
Oostende Bank
U7
U5
U4
U3
U2
U1
Marine transgressive, tidal ravinement, or shoreface ravinement surface
Tidal ravinement surface
TST
Transgressive surface =Sequence boundary
Paleogene
Outer estuary tidal sand bars
Seaward part of middle estuary UFR sandflats
Middle estuary UFR sandflats

Fig. 6.18 (page 102) Examples of seismic profiles (across and along the Ostend Valley) with indication of the stratigraphical erosional surfaces following the models of an incised-valley system (IVS) with tide-dominated estuary regime. (A) Schematic transverse cross-section through an IVS, modified after Dalrymple and Choi (2007). (B) Transverse cross-section through the Ostend Valley showing the different stratigraphic surfaces. The infilling of the Ostend Valley consists of a simple fill. Note however that a LST and HST are not present. In model (A) the equivalent part of what is preserved within the Ostend Valley is outlined in black. It concerns only the marine sand body of the TST, no mud-flat sediments or salt-marsh deposits have been preserved (cf. 6.3.3). (C) Schematic section along the axis of a tide-dominated estuary in an IVS, modified after Dalrymple et al. (1992). (D) Lateral cross-section through the Ostend Valley showing the different stratigraphic surfaces. A LST and HST are not present, although the gravel lag found on top of the QT surface could represent fluvial deposits, i.e. part of a LST. As U3 is completely transgressed by the shoreline, the entire infilling of the Ostend Valley belongs to segment 1. The facies distribution within the Ostend Valley is indicated. In model (C) the equivalent part of what is preserved within the Ostend Valley is outlined in black. Note however that no tidal-fluvial or tidal meander, but only UFR and outer-estuary tidal sand-bar deposits are preserved. (E) Positioning of the seismic profiles with reference to the contours of the Ostend Valley and the position of the cores.

Internal erosional surfaces (U1-U2, U2-U3)

From the integration of the seismic and lithological data it is clear that the Ostend Valley fill is a simple fill, the product of a landward-migrating (transgressive) estuary, with internal erosional surfaces separating three estuarine phases. No fluvial lowstand, or deltaic or tidal-flat highstand deposits are present in between the estuarine phases, so a compound fill is excluded. The erosional surfaces, bounding seismic units U1 and U2 represent *tidal ravinement surfaces* (Fig. 6.18). During transgression, the facies within a tide-dominated estuary shift headward. In the process, migrating tidal channels coupled with wave action erode all or part of the more headward facies, leaving an incomplete record of the estuarine deposits in shallow marine areas that lie seaward of the final shoreline (Dalrymple 1992). There are numerous local discontinuities (tidal ravinement surfaces) produced by tidal-channel erosion. The units bounded by these erosional surfaces were deposited by progradation of broad sand flats (in the middle estuary) or by migration of elongated sand bars (in the outer estuary).

Apart from local incisions by individual channels of the overlying unit U3, the erosional surface of seismic unit U2 also shows a large axial depression and an abrupt depth change (Fig. 6.19), which most likely are formed by the erosive action of the tidal channels in between the elongated sand bars of the outer estuary in U3. The amalgamation of these channel scours produced the equivalent of a ravinement surface, i.e. one of the tidal ravinement surfaces.
The contact between the seaward middle-estuarine part of U3 (in cores SB1, SB2, GR1), and the seaward middle-estuarine deposits of U2 (Fig. 6.17B) is not visible on the seismic data, in part because the presence of gas obliterates seismic unit U2 in the area of SB1, SB2 en GR1. Since we expect that the contact is gradual, as it concerns similar depositional environments (although deposited in a different time phase/step), recognition of this feature on seismic profiles would be difficult even in the absence of shallow gas.

The surface of U1 (U1-U2 boundary) is much more difficult to interpret. On the one hand there are sections where U1 is clearly incised by individual tidal channels of U2 (Fig. 4.2B, 6.7B,E), or where an erosional depression, not directly linked to clear-cut incising channels, is visible in the surface of U1 (Fig. 6.7C). On the other hand there is also the farther offshore section where the surface of U1 often seems to correspond to a

depositional (lateral-accretion) surface of a point bar in a migrating sinuous channel (Figs. 6.6, 6.7A). There, it seems as if U2 is just gradually infilling the open area adjacent to the point-bars, without eroding part of them. The boundary line between the two different U1 surface types coincides with the abrupt depth change in U2, which is the transition between the lower offshore area where U2 occurs only in the incised valleys, and the higher, landward area where U2 is more extensive (Fig. 6.8A). So it is most likely only because U2 is much more eroded offshore, which is why only remnants of U2 are found in the deepest incised channels, that makes it appear as if U2 is merely (not erosively) infilling the channels. Due to the erosion we cannot see that this infilling probably represents an incised channel in an existing sinuous channel of U1, and that the U1 infilling represents remnants of point-bars (Fig. 6.20). The reason why the point-bar features in U1 are so distinct on the seismic profile in the more offshore meandering channel, is probably due to their shallow position below the seafloor reflector there, which is well within the limits of seismic penetration. In the more nearshore area, the U1 infilling lies sometimes too deep to distinguish clear internal reflectors.
In conclusion, U2, representing the seaward middle estuary, is probably as erosive as the outer estuary of U3. Thus, the surface of U1 represents a tidal ravinement surface such as U2-U3.

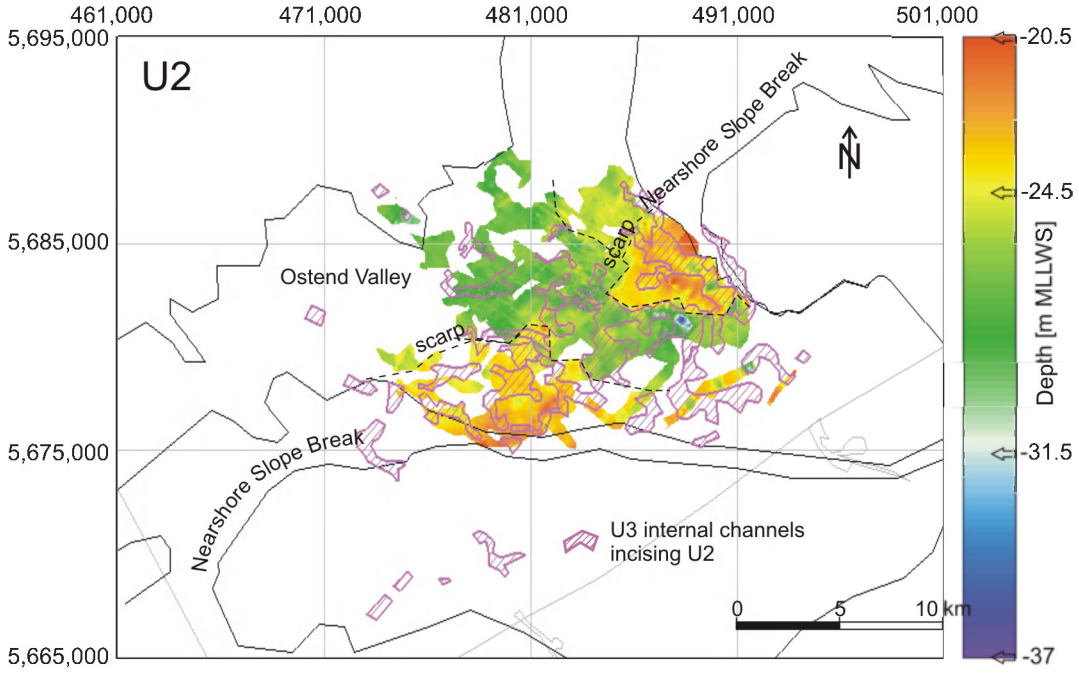

Fig. 6.19 Pattern of internal channels of seismic unit U3, visualised on top of the isobath map of the top surface of U2. Depressions in the erosional surface of U2 can be partly explained by local incisions of individual internal channels of the overlying unit U3, but there are also a large axial depression and an abrupt depth change (scarp). The latter are most likely formed by the erosive action of the tidal channels in between the elongated sand bars of the outer estuary in U3. The amalgamation of these channel scours produced the equivalent of a ravinement surface, i.e. a tidal ravinement surface.

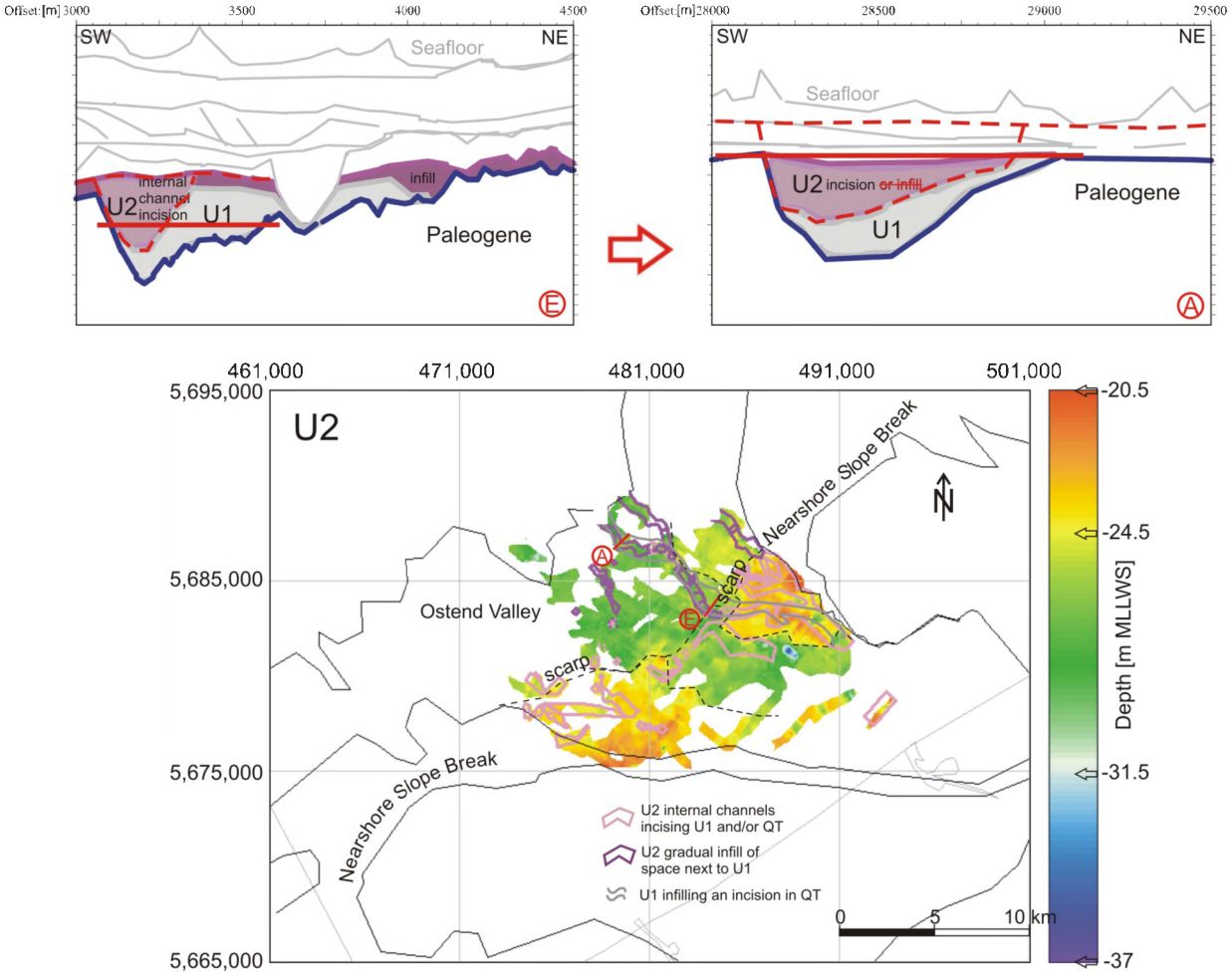

Fig. 6.20 Panels (E) and (A) of Fig. 6.7, located north and south of the sudden depth change (scarp) in the surface of U2, respectively. The left panel shows how U1 is clearly incised by an individual channel of U2, whereas on the right panel the surface of U1 seems to represent a depositional (non-erosional) surface, U2 gradually infilling the accommodation space adjacent to U1, as no clear U2 internal channel can be distinguished. The figure illustrates how erosion (full red line in panel (E)) can lead to a situation in panel (A). U2 is much more eroded offshore (leaving only remnants of U2 in the deepest incised channels), which makes it appear as if U2 is merely infilling the space next to U1. Most likely this fill does *represent an internal channel of U2 that incised in U1, the surface of U1 not being a depositional surface of point-bars.*

Erosional surface U3

The scarp

The erosion after the estuarine infilling of the Ostend Valley, was that severe that seismic unit U3 was completely levelled with the QT-boundary/Top-Paleogene surface. Remnants of U3 are only left in depressions in the Top-Paleogene substratum. The erosional surface of seismic unit U3 shows a scarp or slope break of about 4 m high (from -24 m to -20 m MLLWS), at about 11 km from the present-day coastline. As shown on the map in Figs. 4.3C and 6.8B, the scarp in U3 is located on the same line as the Nearshore Slope Break in the Top-Paleogene surface. A comparison of a seismic profile along the central axis of the Ostend Valley (Fig. 6.21B), with a parallel seismic profile outside the valley (Fig. 6.21A) shows that the scarp in U3 coincides in height and outline with the Nearshore Slope break cut in the Top-Paleogene clays of the interfluve. This has several implications: it is an indication that the Nearshore Slope Break in the Top-Paleogene surface was formed *after* the infilling of the Ostend Valley, but more importantly, it indicates that the scarp in U3 is not a depositional structure, but an

erosional feature, which was created by a regional erosive process active over the entire width of the Belgian Continental Shelf. The surface of U3 most likely corresponds to the ravinement surface formed when the estuary continued to translate landward, and the upper portion of the transgressive succession was removed by shoreface or tidal-channel erosion in open-marine conditions (Dalrymple 1992, Dalrymple et al. 1992, Dalrymple et al. 1994, Zaitlin et al. 1994). In general, one speaks of a wave ravinement surface in case of shoreface erosion in wave-dominated or mixed-energy conditions, the equivalent in a tide-dominated system is a tidal erosion surface formed on the shelf, i.e. again a tidal ravinement surface (Dalrymple 1992, Dalrymple et al. 1992, Zaitlin et al. 1994) (Fig. 6.18). So tidal ravinement may also occur on the shelf (Dalrymple 1992), but tidal currents are usually channelized parallel to the axis of the incised valley, in contrast to being spread uniformly along the shoreline as wave action is. Unlike a tidal ravinement surface, which has a channelized morphology and is generally localised within the incised valley, the wave ravinement surface is relatively planar and of regional extent, extending over both the incised valley and the interfluves. So although the Ostend Valley is interpreted as a tide-dominated estuary, the erosional surface of U3 clearly resembles a wave ravinement surface. Also the profile of the scarp of U3 and the laterally joined Nearshore Slope Break look very alike a drowned shoreface, displaying similar slopes: 0.27° for the scarp, and 0.042° and 0.0118° for the adjacent shelves. Typically, a shoreface has a concave-upward profile, which is in equilibrium with the waves that shape it and has a gradient of about 1/200 (about 0.3°), which decreases seaward into the offshore zone to 1/2000 (about 0.03°) (Walker and Plint 1992).

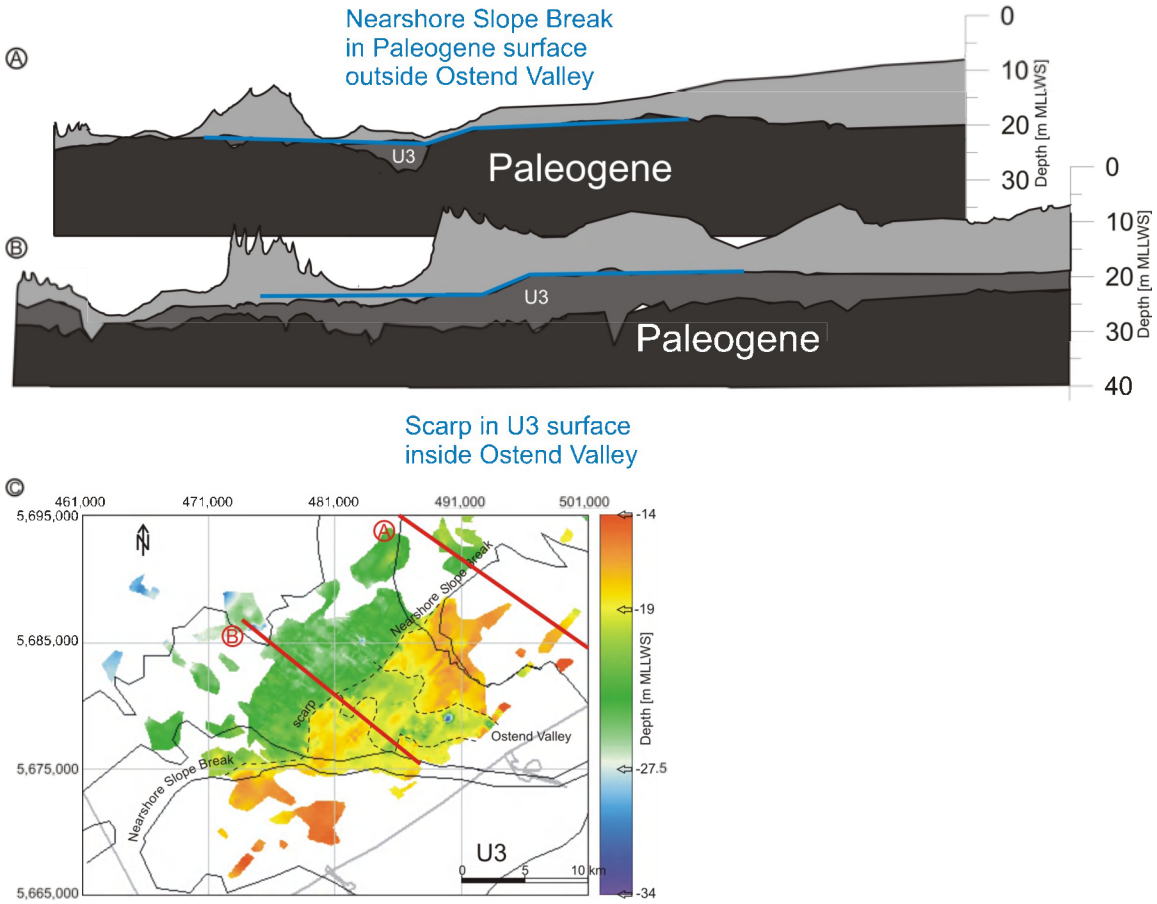

Fig. 6.21 Comparison of (A): a seismic profile outside the Ostend Valley, with (B): a parallel seismic profile along the central axis of the valley, shows that the scarp in U3 coincides in height and outline with the Nearshore Slope Break cut in the Paleogene clays of the interfluve. (C) Position of the seismic profiles with reference to the isobath map of the top of U3.

Although it concerns here a tide-dominated estuary (as the typical funnel-shape shows), wave action cannot be ignored at the seaward end of the estuary, because of the large, open-water fetch that characterises the marine basin (Dalrymple and Choi 2007). Wave energy at the bed will increase landward from the shelf toward the shallower water at the coastline (Fig. 6.3), reaching a maximum at the mouth of the estuary. Because of the open-mouth character of tide-dominated systems, wave energy will penetrate some distance into the estuary, but frictional dissipation in shallow water will cause the waves to decrease in importance in a landward direction. The mouth of tide-dominated estuaries will experience more wave action than areas either seaward or landward. Whether or not wave action dominates locally over tidal currents in this area depends e.g. on the intensity of the tidal currents that vary as a function of the tidal prism (Dalrymple and Choi 2007). The erosional surface at the top of U3 is most likely formed by a combination of wave and tidal action. So, it is better to talk about shoreface erosion, and a shoreface ravinement surface, but not in a sense that it was formed by wave action only. A more general term is 'marine transgressive surface'. We believe that a combination of tides and waves can create the scarp-like feature. Why this scarp, a fossil shoreface, was preserved, will be explained in paragraph "6.3.4 Chronostratigraphic framework", where a possible age for the erosional surface of U3 and the formation of the Nearshore Slope Break is proposed.

River imprint

Apart from the scarp, there is also the imprint of a sinuous river in the surface of seismic unit U3 (Fig. 4.3C). The incision is formed after the formation of the scarp, because a valley cut off by a scarp would show a narrowing in the deeper truncated part, which is not the case. The valley most likely represents a renewed incision during the following lowstand, and would form the base (sequence boundary) of a new infilling sequence. But by that time the Ostend Valley was already completely infilled, and levelled with the adjacent Paleogene surface, so we do not speak of a compound fill.

The gravels found in NWB and SWB are probably linked with this multi-genetic erosional surface, but will be discussed in more detail in the next section (6.3.3) and the next chapter, where the Top-Pleistocene surface is discussed (7.3.2, Top-Pleistocene).

On top of the marine transgressive surface, no HST deposits have been preserved. Therefore, the *maximum flooding surface*, which represents the surface at the moment of maximum flooding (base of HST), could not be determined (Fig. 6.18). If the gravels encountered in NWB and SWB were deposited during marine transgression, the maximum flooding surface would at least be located above that level. If the gravels were, however, deposited during renewed fluvial action during the following sea-level fall and lowstand, the maximum flooding surface would be located below it.
Note that the entire fill of the Ostend Valley has been transgressed by the shoreline, so its preserved remnants belong exclusively to the most seaward portion of the incised-valley system, i.e. segment 1 (Fig. 6.18C).

6.3.3 Depositional depth of the different estuarine facies during the infilling of the Ostend Valley and paleo-landscape reconstructions

From the integration of the seismic and core data, the position of the main sections of an estuary (middle estuary, outer estuary, fluvial-tidal transition) could be determined along the axis of the Ostend Valley, i.e. a more landward or seaward location of the seismic units was deduced. Because the few cores were all located in the marine sand body, or axial sands of the estuary, except for NWB and SWB, they did not contain any evidence on the lateral position of mud flats, salt or fresh water marshes within each section.

Nevertheless, analysis of transverse seismic cross-sections through the Ostend Valley allowed the inference of the depositional depth of mud flats and salt marshes. The resulting depth constraints were used to reconstruct the lateral position of the different estuarine environments (mud flats, sand flats, salt or fresh water marshes) on a map for each estuarine phase (U1, U2, U3), i.e. paleo-landscape reconstructions (Fig. 6.24A, B, C), keeping in mind that U1, U2 and U3 are diachronous and that any link to estuarine phases with a particular sea level is a (necessary) simplification.

If we compare a schematic cross-section of a tide-dominated estuary in an incised valley (Dalrymple and Choi 2007), with a cross-section of the Ostend Valley, some differences are clear (Fig. 6.18AB and 6.22AB). On the schematic cross-section, the sandy channels or axial sands (marine sand body) are erosively flanked by muddy tidal-flat and salt-marsh sediments. During transgression the estuarine funnel deepened and widened, and migrated up the valley. This process was accompanied by erosion of adjacent and underlying sediments by tidal currents in the channels (Zaitlin et al. 1994). This erosion caused the sand bars and sand-flat deposits, to overlie or abut erosionally against mud flat and salt marsh sediments along the margins of the estuary (Dalrymple et al. 1992), i.e. the transgressive estuarine funnel is bounded on its sides and base by a tidal ravinement surface. On the Ostend Valley cross-section, however, the tidal ravinement surfaces separating the seismic units are not erosively flanked by tidal flats or salt marshes, but abut directly on the Paleogene substratum. The seismic units represent in fact just the axial sands or marine sand body (tidal channels and sand flats); any mud-flat and salt-marsh deposits were probably completely eroded (Fig. 6.18B). They formed narrow fringes along the margins of estuaries and were easy prey for migrating tidal channels. Fig. 6.22B shows a reconstruction of the estuarine at the end of the valley fill, when the mud flats and salt marshes were still intact. These uppermost fine-grained sediments were truncated by later shoreface erosion.

The position of sand flats, mud flats, and salt marshes can be constrained taking into account their typical relationship to high- and low-water levels, and their height above water level of the tidal channels at low tide whose fills are easily recognisable on the seismic data.
A mean tidal range of 4 m was proposed, with a 4.5 m-tidal range during spring tide, and a 3 m-tidal range during neap tide (Fig. 6.23). These are arbitrary values chosen in accordance with the present-day mean tidal ranges in Oostende, not taking into account variations within the estuary due to valley convergence and friction. Tidal channels always stay in subtidal position, below mean low water, even during spring tide. Mud and sand flats are intertidal environments typically occurring between high water at neap tide, and mean low water level (Fig. 4.1 in: Baeteman 2008). For convenience it is assumed that sand flats occur to a level in the middle of the intertidal realm, exactly in between high water at neap tide and mean low water (1.75 m above the tidal channel level in Fig. 6.23). Salt marshes develop in supratidal conditions, above high water at neap tide (3.5 m above the tidal-channel level), and freshwater marshes can develop above the high-water level at spring tide (4.25 m above tidal-channel level).

Fig. 6.22 (page 109) Comparison of: (A) a schematic transverse cross-section through an IVS, modified after Dalrymple and Choi (2007), and (B) a transverse cross-section through the Ostend Valley. The infilling of the Ostend Valley consists only of a marine sand body of the estuarine infilling (outlined in black for U3); no mud flats or salt marshes have been preserved. (B) A reconstruction of a typical cross-section of U3 before shoreface erosion truncated the mud-flat and salt-marshes deposits, showing how much of the unit probably was removed (light blue).

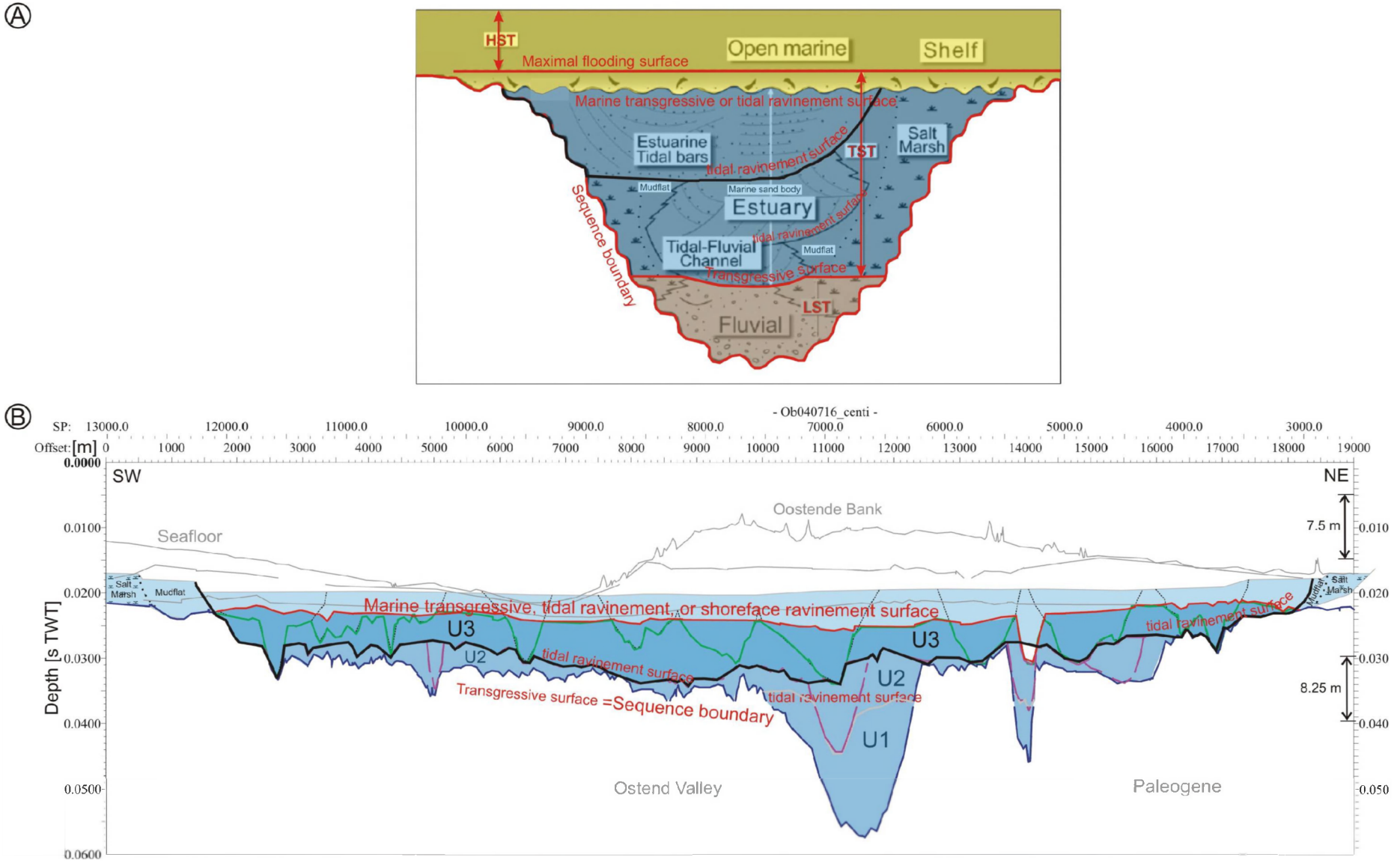
Ⓐ
HST
Maximal flooding surface
Open marine
Shelf
Marine transgressive or tidal ravinement surface
Estuarine Tidal bars
tidal ravinement surface
TST
Salt Marsh
Mudflat
Marine sand body
Estuary
Sequence boundary
tidal ravinement surface
Tidal-Fluvial Channel
Mudflat
Transgressive surface
LST
Fluvial
Ⓑ
- Ob040716_centi -
SP: 13000.0 12000.0 11000.0 10000.0 9000.0 8000.0 7000.0 6000.0 5000.0 4000.0 3000.0
Offset: [m] 0 1000 2000 3000 4000 5000 6000 7000 8000 9000 10000 11000 12000 13000 14000 15000 16000 17000 18000 19000
Depth [s TWT]
0.0000
0.0100
0.0200
0.0300
0.0400
0.0500
0.0600
SW
NE
Seafloor
Oostende Bank
7.5 m
8.25 m
Salt Marsh
Mudflat
Marine transgressive, tidal ravinement, or shoreface ravinement surface
U3
U2
U1
tidal ravinement surface
Transgressive surface =Sequence boundary
Ostend Valley
Paleogene

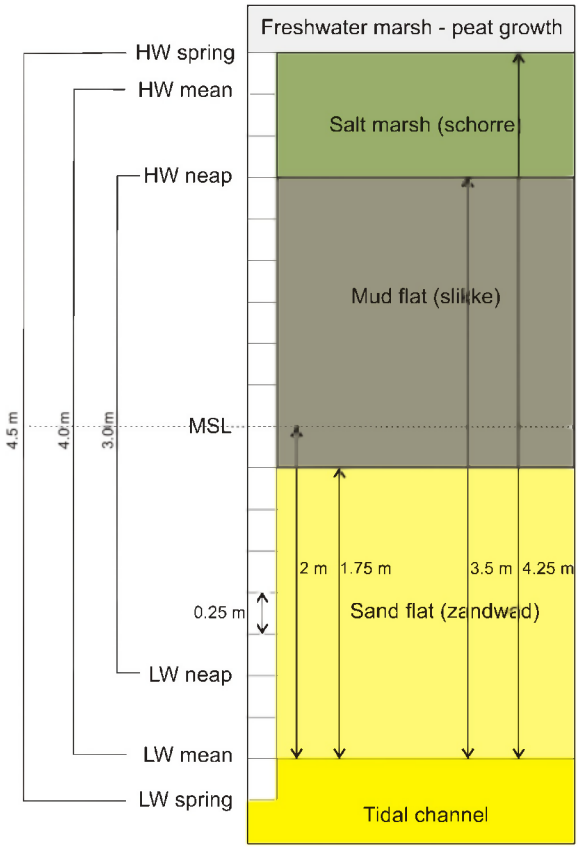

Fig. 6.23 Position of the different environments of a tidal-flat system in relation to the tidal levels. HW = high water, LW = low water, spring = at spring tide, neap = at neap tide. Relationships are deduced from Fig. 4.1 in: Baeteman (2008).

Depositional depths during estuarine phase U1

During the initial phase of estuarine infilling of the Ostend Valley probably also mud flats and salt marshes developed outside the tidal channels, to which U1 is restricted. The depositional depth of possible mud flats and salt marshes is inferred from the depth of the tidal channels, which is related to the mean low water level. It is assumed that the upper limit of the tidal-channel deposits corresponds to the level where U1 is entirely located within the incised channels, which corresponds to a depth of –29 m MLLWS. So tidal flats were drawn, up to the presumed high-water line at neap tide, which was located 3.5 m above the mean low-water level, at –25.5 m. Salt marshes extend to a depth of about –25 m, which is the assumed *spring*-tide high-water level for that moment, 1 m above the high-water level at *neap* tide.

Depositional depths during estuarine phase U2

As was documented above, the entire seismic unit U2 represents remnants of only the axial sands of the middle estuary, containing tidal channels and sand flats, as the unit shows an erosional base and many internal channels, which is not the case for mud flats or salt marshes (Fig. 6.22A). U2 embodies the upper-flow-regime sand flats of the marine sand body in the middle estuary, as defined by Dalrymple et al. (1992), with intervening tidal channels. It is assumed that the tidal-channel infillings formed below mean low water level. And as these infillings make part of the shallowest occurrence of seismic unit U2 at -21 m, the mean low-water line was once located at –21 m. This implies a neap high water line at –17.5 m in this second estuarine phase. Sand flats occurred up to a depth of about -19.5 m, mud flats developed to a depth of -17.5 m and salt marshes could have reached -17 m.

Depositional depths during estuarine phase U3

For the final phase of the estuarine infilling of the Ostend Valley, it is assumed that the part of seismic unit U3 located within the Ostend Valley represents only the marine sand body of the estuary, composed of the upper-flow-regime sand flats in the middle estuary and the tidal-bar deposits in the outer estuary (Dalrymple et al. 1992). Mud flats or salt marshes have not been recognised within U3. The unit shows an erosional base (sharply truncating U2), a typical product of migrating tidal channels and tidal bars; mud flats and salt marshes would not show an erosional lower boundary (Fig. 6.22A).
The reconstruction in Fig. 6.24C shows the time when the shallowest preserved sand flats of seismic unit U3, at -16 m, were deposited. At that time, tidal channels were probably still open below –17.75 m (below the mean-low-water line), mud flats developed to a height of about -14 m and salt marshes grew to a height of -13.5 m.

Paleo-landscape reconstructions

Three phases in the estuarine infilling of the Ostend Valley are visualised in schematic paleo-landscape reconstructions. Each reconstruction takes into account the position of the cores within the estuary, the internal tidal channels, the inferred depositional depths of mud flats and salt marshes, the shallowest depth of deposition of the associated seismic unit, the funnel shape of the estuary, and the general principles of Dalrymple and Choi (2007) concerning tide-dominated estuaries.

The tidal channels for each unit were truthfully drawn on the basis of the seismic data, and freely connected to a speculated meandering part of the estuary. The position of the meandering section of the estuary is based mainly on the abstracted, schematic map of a tide-dominated estuary after Dalrymple and Choi (2007) (Fig. 6.3), and is drawn directly landward of the funnel-shaped, outer ‘straight’ section. According to these authors the meandering section is located landward of the tidal maximum, where the tidal currents decrease again to shelf values, owing to friction. Comparing this spatial pattern to the present-day Western Scheldt estuary, the meandering section would be located around Dendermonde, 120 km from the estuary mouth, the tidal maximum being located between Antwerpen and Temse (Fig. 5 in Dalrymple and Choi 2007). The funnel-shaped section of the Western Scheldt is about 80 km long, so twice as long as that of the Ostend Valley. From the estuary mouth, a distance of about 60 km is therefore chosen for the position of the meandering section in the Ostend Valley, measured on the map of phase U3 on which the estuary mouth is detectable. This choice is in good agreement with meander-like depressions seen in the Top-Paleogene map. For the two older units/phases, the meandering section or bedload convergence is drawn progressively farther seaward, taking into account the interpretation of the cores (their position within the estuary with respect to the bedload convergence). The length of the middle estuary was kept constant on the assumption that the coastal-zone gradient and tidal range stayed the same, as these jointly determine the length of the estuary (Dalrymple et al. 1992).
Note that the present-day Western Scheldt is not entirely natural. The tidal influence of the Scheldt reaches much more landinward, because of human impact like dredging (de Kraker 2002). Proportionally comparison with the Ostend Valley is acceptable, however.

present MSL

2.3 m

reference level is present MLLWS ~TAW

	U1	U2	U3
Freshwater marsh			
HW spring	-24.75 m MLLWS	-16.75 m MLLWS	-13.50 m MLLWS
Salt marsh			
HW neap	-25.50 m MLLWS	-17.50 m MLLWS	-14.25 m MLLWS
Mud flat			
MSL	-27.00 m MLLWS	-19.00 m MLLWS	-15.75 m MLLWS
	-27.25 m MLLWS	-19.25 m MLLWS	-16.00 m MLLWS
Sand flat			
LW mean	-29.00 m MLLWS	-21.00 m MLLWS	-17.75 m MLLWS
Tidal channel			

Table 6.1 Overview of assumed depositional depths of the different tidal environments during each estuarine phase, with reference to the present-day MLLWS.

Basically, the assumed water levels (determined above for each unit (Table 6.1)) are drawn as isobaths of the Paleogene surface, but are in some areas corrected for the fact that the initial shape of the Ostend Valley changed due to erosion in a later stage. It is assumed that the eroded part of the valley flank continued in a smooth curve from the remaining valley margin.
It is important to realise that the reconstructed coastlines are based merely on the present-day topography of the Top-Paleogene surface, and not on the landscape of the Paleogene surface at that time. The Top-Paleogene surface has been modified until the present day, and former coastlines were probably located farther offshore than shown here. Some parts of the coastlines were reconstructed on the basis of the position of the estuary (at the seaward end of the outer estuary); these are indicated with dashed lines.

Estuarine phase U1

The initial phase of the estuarine infilling of the Ostend Valley is visualised in Fig. 6.24A. It represents a moment in time when mean sea level was -27 m MLLWS and the middle estuary was located in the vicinity of cores GR1 and OSB. Tidal-channel deposits were limited at depths greater than –29 m MLLWS, tidal flats formed up to –25.5 m, and salt marshes grew to a height of –25 m.
These levels are drawn as isobaths of the underlying Paleogene surface, and not projected on the drowned landscape of that time, because that landscape cannot be reconstructed accurately because of subsequent erosion. Thus the map represents in fact the maximum possible lateral extent of each environment. The shallowest occurrence of seismic unit U1 is -25 m, which is in line with the inferred depositional depths based on the position of tidal channels.
The figure shows how most of seismic unit U1 is limited to the sub-tidal area, consisting of lateral-accretion deposits (point-bar remnants) left by migrating tidal channels incised in the Paleogene subsurface, and in some adjacent tidal flats. The width of the mud flats relative to the sand flats is speculative here, simply drawn proportionally to the schematic map of Dalrymple and Choi (2007) (Fig. 6.3). The reconstruction suggests that originally, U1 was present at the location of UIT. The associated deposits were probably eroded by migrating tidal channels at the onset of the following estuarine stage, when the more seaward part of the middle estuary reached the area. During formation of U1, the estuary was still very narrow with steep valley flanks. Little place was available for the development of salt or freshwater marshes, which could explain the absence of humic or

organic material in U1. The seaward extent of the estuary is uncertain. The abrupt widening visible on the map is due to later erosion of an initially narrow estuary (by migrating tidal channels or by the increased marine influence).

On the basis of the lithology of U1, which represents middle-estuarine deposits at a distance seaward from the turbidity maximum, the position of the bedload convergence or meandering section, where the turbidity maximum occurs, was drawn a certain distance from the cores. The meandering section starts landward of the tidal maximum, which in turn is located where the distributary channels bifurcate, at the landward end of the funnel-shaped section (Dalrymple and Choi 2007).
In the reconstruction, the tidal maximum corresponds to the position of the deepest tidal channels of U1. Most likely the so-called 'scour hollows' were formed by extremely rapid tidal-currents around the tidal maximum, which were intensified in the narrow valley. During later phases, the tidal channels were narrower and shallower (max. 14 m depth in U2 compared to 30 m depth in U1, assuming that erosion does not account for the 16-m difference), probably because the Ostend Valley became wider, which reduced the amplification of the tidal range due to the decreased convergence, and because the tidal maximum was located farther inland. There are no observations of scour hollows in the present-day Coastal Plain, where the inland extension of the estuary should be located.

A large contrast exists between the straight, wide and deep central channel, and the thin, meandering channel at the NE side of the Ostend Channel. might reflect a difference in discharge characteristics. The difference in discharge could be linked to a difference in use of the channels. It is known that ebb and flood are mutual evasive and use different channels (van Veen et al. 2005). During flood the tidal wave comes in over a large area, separating the water over several smaller channels, while during ebb, the drained water is forced into a few deep channels which feed the main ebb channel. Possibly the smaller channels represent flood channels, whereas the central channel represents the main ebb channel. An ebb channel is primarily open to the ebb current, and gets shallower at the seaward end (Rieu et al. 2005, van Veen et al. 2005), which is exactly what is observed in the central channel in the Ostend Valley. A flood channel is open to the flood current and shallows only at its landward end. The configuration resembles the schematic sketch of ebb and flood channels in the Thames estuary by van Veen et al. (Fig. 14 in: van Veen et al. 2005). From the sea, a number of flood channels try to penetrate the inlet, while a central rather straight ebb channel drains away the water again. Initially the flood carries little sand and only starts entraining sand as it propagates shoreward. Meandering action may bring the ebb channel in connection with any of the flood channels, which possibly has happened at the NE side of the valley where the meandering flood and central ebb channel intersect.

Estuarine phase U2

Fig. 6.24B presents the following phase of the estuarine evolution of the Ostend Valley, when mean sea level was -19 m MLLWS. Seismic unit U2 represents the seaward part of the middle estuary (around cores UIT and OSB), and has eroded most of the underlying sediments of the middle estuary represented by U1, forming a tidal ravinement surface and incising U1 channels. Tidal channels occurred up to -21 m, sand flats up to -19 m, mud flats up to -17.5 m and salt marshes up to -17 m.
During this phase, the estuary was much wider than before and had migrated farther landward. The middle estuary, the tidal maximum, and the BLC were now located farther landward than during the earlier phase, and mud flats and salt marshes could develop more extensively. By the second estuarine phase, probably enough time had passed for the silting up of the estuary sides to allow for the development of freshwater marshes, which explains the presence of peat fragments in the U2 lithofacies. Within the Ostend Valley, where seismic unit U2 is located, few mud-flat or salt-marsh sediments have

been found, likely because most were eroded later by migrating tidal channels of the following estuarine phase. Salt marsh sediments do occur in U2 in an area flanking the Ostend Valley, as shown by core NWB. In NWB salt-marsh deposits are present between -17.3 and -16.8 m, which corresponds to the supposed depositional depth of salt marshes during phase U2. The fact that salt-marsh deposits were found in one of just a few cores penetrating unit U2 implies that more high-intertidal and supratidal sediments have been preserved but that they are so fragmented that they are difficult to recognize on seismic profiles.
The expected sand-flat deposits at the locations of cores SB1 and SB2 were probably eroded as well during the following estuarine phase. The outer-estuarine deposits were completely eroded as well. Farthest offshore, only the deepest fills of seismic unit U2 (middle estuary) have been preserved (Fig. 6.20). The eroded surface of U2 is shown in Fig. 6.19.
The infilling of the neighbouring incised valley, a precursor of the IJzer valley, is inferred, based only on the present-day Paleogene topography, not taking into account possible fills present at that time.

The bedload convergence in the meandering section was drawn as discussed in the introductory remarks. The meanders start landward of the tidal maximum, which is located where the distributary channels bifurcate, at the landward end of the funnel-shaped section (Dalrymple and Choi 2007). It is unclear if the tidal maximum corresponds to intensive erosional bedforms, as no seismic or core data are available in that zone close to shore.

It was not possible to determine if the distributary channels were flood or ebb oriented. Possibly the central tidal channel in U2 was an ebb channel shallowing at its seaward end. Whereas the channel along the NE side of the Ostend Valley shallowed only at its landward end, and is probably a flood channel. Other, even smaller channels were probably all flood-dominated channels during this phase.

Fig. 6.24 (page 115) Paleo-reconstructions showing the transgressive estuarine infilling of the Ostend Valley. (A) Estuarine phase U1, (B) estuarine phase U2, (C) estuarine phase U3, and (D) schematic map of a tide-dominated estuary with its different depositional environments, serving as legend for (A), (B) and (C) (modified after Dalrymple and Choi 2007). Orange transparent overlays represent presumed Paleogene surfaces located higher than presently preserved. BLC = bedload convergence, UFR = upper-flow-regime tidal flats. Zeebrugge harbour and BCP limit in light grey. Contours of the Ostend Valley and neighbouring platforms in (fine) black.

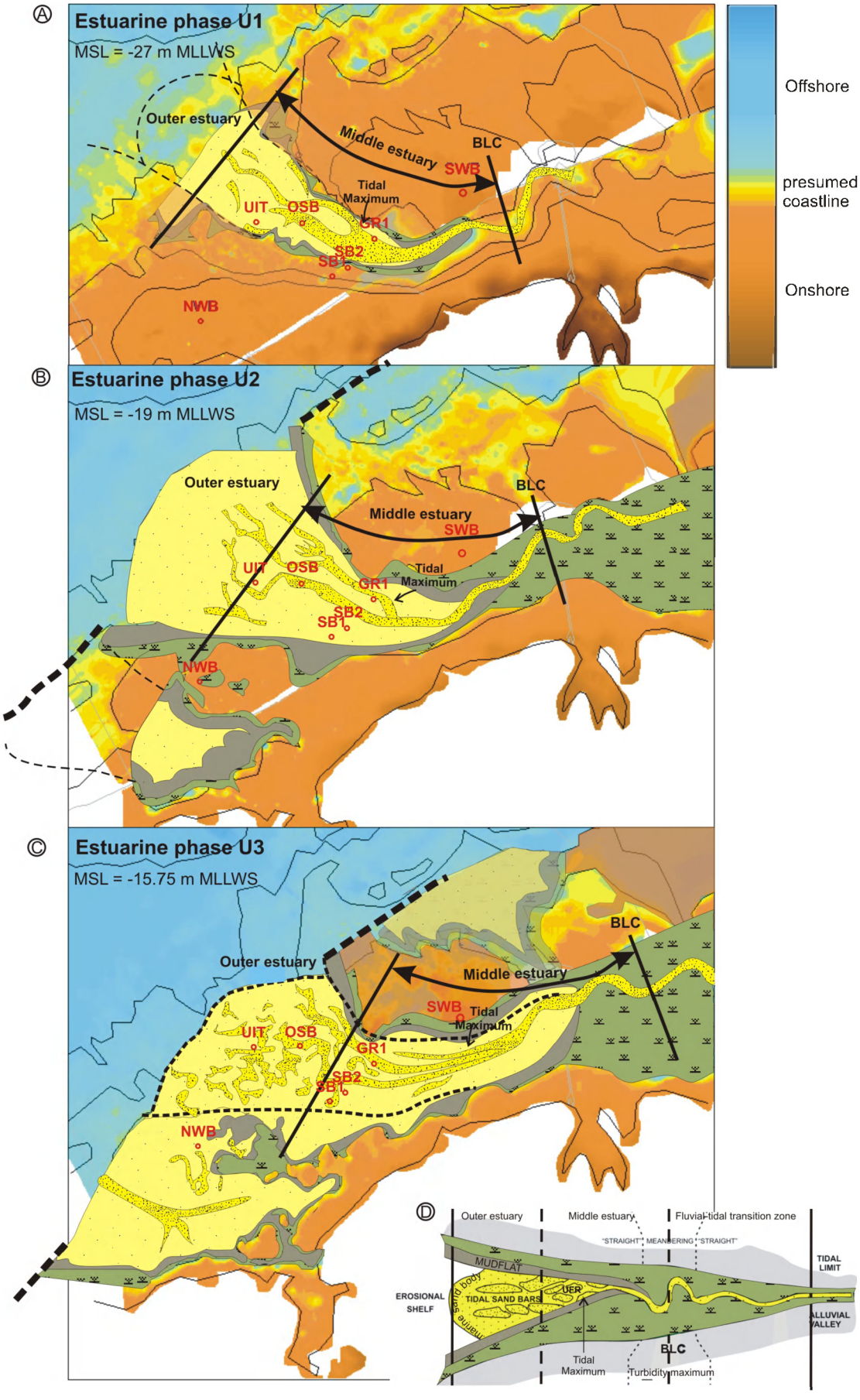
Ⓐ
Estuarine phase U1
MSL = -27 m MLLWS
Outer estuary
Middle estuary
BLC
SWB
Tidal Maximum
UIT
OSB
GR1
SB2
SB1
NWB
Offshore
presumed coastline
Onshore
Ⓑ
Estuarine phase U2
MSL = -19 m MLLWS
Outer estuary
Middle estuary
BLC
SWB
UIT
OSB
Tidal Maximum
GR1
SB2
SB1
NWB
Ⓒ
Estuarine phase U3
MSL = -15.75 m MLLWS
Outer estuary
Middle estuary
BLC
SWB
Tidal Maximum
UIT
OSB
GR1
SB2
SB1
NWB
Ⓓ
Outer estuary
Middle estuary
Fluvial-tidal transition zone
"STRAIGHT"
MEANDERING
"STRAIGHT"
MUDFLAT
TIDAL LIMIT
EROSIONAL SHELF
TIDAL SAND BARS
UER
ALLUVIAL VALLEY
Tidal Maximum
BLC
Turbidity maximum

Estuarine phase U3

Fig. 6.24C visualises the final phase of the estuarine infilling of the Ostend Valley and adjacent areas, when mean sea level was -15.75 m MSL. In the area of SB1, SB2 and GR1 the seaward part of the middle estuary was located. The outer estuary lies around UIT and OSB, where the underlying middle-estuarine sediments of U2 were severely eroded during formation of U3.
The shallowest occurrence of seismic unit U3 at -16 m concerns sand-flat deposits adjacent to tidal channel fills. Given this fact, tidal channels occurred probably below -17.75 m (below mean low water), mud flats developed to a height of -14.25 m and salt marshes could grow to a height of -13.5 m. All these values are projected on the Paleogene surface, which is corrected as accurately as possible for any later erosion of the Ostend Valley flanks. Dashed lines indicate the supposed original valley contours. Note that it is uncertain if the widening near SB1, SB2, and GR1 existed at that time, as it does not fit the expected streamlined funnel shape. It is possible that this is just due to local scouring processes at that time, or that this widening was formed during a later stage, when the outer estuary shifted even farther landward or when the sea transgressed the area.
During the third phase, the estuarine environment migrated more and more inland. The outer estuary, the middle estuary, the tidal maximum, and the BLC were located more landward than during the earlier phases, and the mud-flat and salt-marsh zones shifted inland as well.
Where cored, U3 contains almost no organic material, only some isolated humic particles. This fact may reflect an overall increase of marine influence (increased sand-flat area), but it should be noted that all cores except NWB are located in an area far from any salt-marsh zones present during the third phase. Not surprisingly, core NWB is the only one with significant organic matter.

The bedload convergence in the meandering section was drawn as discussed in the introductory remarks. No data are available from the present-day Coastal Plain to check if the tidal maximum coincides with the presence of deep scour hollows, as observed in U1.
The chaotic channel-like structures in the outer estuary are presumably tidal channels in between elongated tidal bars (or tidal sand ridges). In the course of time, the tidal sand bars between the tidal channels probably expanded and merged (Harris 1988, Dalrymple et al. 1992, Heap et al. 2004). But as a result of later open-marine erosion the internal channels of U3 in the outer estuary were strongly truncated, especially north of the scarp, which is presumably why only isolated remnants of the channels in between broadened sand bars have been preserved, and no continuous channels can be traced. Also, the architecture of tidal sequences is complex because of the migration and stacking of successive channels and the presence of erosional surfaces of several different orders (Dalrymple and Choi 2007).
The seaward limit of the outer estuary in phase three was located where the outermost internal channel of U3 is observed. The distributary channels drawn in the landward part of the middle estuary are inferred.
The mud-flat and salt-marsh deposits adjacent to the marine sand body were eroded, along with the (flanks of the) Ostend Valley, by the incoming sea. The abrupt narrowing of U3, especially at the NE margin of the unit, is a reflection of that process. The sudden decrease in the lateral extension of U3 coincides with the scarp in the erosional surface (Fig. 4.3C). North of the scarp (i.e. in the lower located part) only the deeper infillings of U3, where the valley is more narrow, are preserved. But the U3 infilling was at least as wide as in the upper part, south of the scarp, which is how it is drawn in the reconstruction. Assuming that the original walls of the Ostend Valley continuously extended offshore.

The reconstruction shows that outer-estuary deposits are to be expected in NWB, and could be represented by the 2-m-thick coarse-grained deposits erosionally overlying the U2 salt-marsh deposits. In that case, the marine transgressive surface would be located at -14.8 m or higher, which is very shallow so far offshore. Alternatively, these sediments could in fact be open-marine deposits as suggested in paragraph 6.3.1 (Unit U3) on the basis of lithological evidence. Under this scenario, the open-marine transgression completely eroded any outer-estuarine sediments in NWB to a depth of -16.8 m. A third possibility is that the lower metre of the coarse-grained sands was deposited by outer-estuarine tidal channels, as they are very similar to the U3 deposits in UIT, while the upper metre was deposited in open-marine conditions. In this case the marine transgressive surface (shoreface-ravinement surface) occurs in NWB at -15.8 m, which corresponds well with the shallowest occurrence of the erosional surface of U3, above the scarp, at -16 m MLLWS. More landward the open-marine erosion is probably represented by the gravelly sand lag overlying the Paleogene clay in SWB, at a depth of -13.2 m MLLWS. Owing to this shallow position of the Paleogene surface no salt marshes could have been present in this area at that time, which is visualised in the reconstruction.

The reconstruction also shows the infilling of a neighbouring depression offshore Zeebrugge. By the time MSL was about -16 m, the rising sea reached that area. This latter hypothesis was developed on the assumption that the depression in the Paleogene topography was not filled during an earlier phase of deposition.

6.3.4 Chronostratigraphic framework

Our re-analysis has shown that the infillings of the Ostend Valley are estuarine. It is also clear hat they were deposited during a single sea-level cycle, and not during several sea-level cycles as was previously proposed (Maréchal and Henriet 1983, Liu et al. 1993). However, there is still the question of when (during which sea-level rise) this estuarine environment was established.

Former concepts in literature

Regarding the incision of the Ostend Valley and the formation of the central incised channels (formerly called 'scour hollows') in the valley floor, opinions were more or less consistent that this happened not before Saalian time (Mostaert et al. 1989, Mostaert and De Moor 1989) and that the deepest scouring probably occurred during the Eemian transgression (Mostaert et al. 1989, Liu 1990, Liu et al. 1993). But concerning the infilling history of the Ostend Valley, opinions have differed significantly. Liu et al. (1993) proposed three stages of infill by analogy with findings in the Coastal Plain: an Eemian age for the sediments in the scour hollows, and a Weichselian and Holocene age for the subsequent overlying infillings of the Ostend Valley. Trentesaux (1993) and Berné et al. (1994) proposed that the lower units of the Middelkerke Bank (corresponding to U1-U2-U3), which are part of the Ostend Valley infill, are of Holocene age. They surmised, referring to Jelgersma et al. (1979) and Paepe and Baeteman (1979), that most of the Pleistocene deposits off the Belgian coast had been completely reworked during the last transgression and had become incorporated in the Holocene deposits.
So the attempts to put the incision and infilling of the Ostend Valley in an absolute time frame, have mainly been based on relative datings, and on comparison with the onland situation. Indeed, very little datable material is present in the few cores that reach the lowermost infillings of the valley. On only one occasion, in an attempt to get an absolute age for the infilling of the Ostend Valley, juvenile marine shells obtained from the UIT core were picked for ^{14}C dating. Based on these results the lower units of the Middelkerke Bank were assigned a Middle-Weichselian age (Stolk 1996, Trentesaux et

al. 1999). These ^{14}C ages are however controversial. It is very implausible to find non-reworked marine shells with an age of 40 ka-50 ka BP in this area, because in that period mean sea level was always more than 42 m below the present one (Shackleton 2000 in Fig. 6.27), whereas the dated samples were collected at depths of less than 29 m below present mean sea level (-27 m MLLWS). The most probable reason for the obtained contradictory ages was that the shells were not radiogenic enough to give a precise age (pers. comm. Alain Trentesaux 2005), and that the radiocarbon-dating technique was used at its upper limit. Given this fact, it is likely that the fill was formed before the Middle Weichselian, at a time when sea level was higher than -27 m MLLWS. Radiocarbon dating on peat fragments was no option either, moreover because the fragments present in the cores are detrital.

New evidence for a chronostratigraphic framework

The new seismic-stratigraphic information and lithological indications provide three clues to construct a more detailed and well-founded relative chronologic framework.

Mean sea level during the estuarine infilling (U1-U2-U3)

From the above reconstructions it is clear that depositional environments like tidal channels, mud and sand flats, salt marshes, etc., which are typically linked to a certain sea level, occurred at a higher position in each unit. This implies that seismic units U1, U2 and U3 represent estuarine infillings during a relative sea-level rise, which caused a transgression or landward migration of the shoreline and all other sedimentary environments (Catuneanu 2002). Indeed estuaries, as defined by Dalrymple et al. (1992), form only under transgressive conditions (Boyd et al. 1992, Dalrymple et al. 1992, Dalrymple and Choi 2007). During this infilling of the Ostend Valley, the mean sea level at that time rose from -27 m to about -16 m (reference level present-day MLLWS). Expressed with reference to the present-day Mean Sea Level (which lies 2.3 m above TAW ~MLLWS) this becomes about -29.5 m to -18.5 m MSL (Table 6.1). This in order to allow comparison with the later introduced sea-level curves (Fig. 6.27).

Mean sea level during the formation of the scarp in U3

After the estuarine transgressive infilling a large scale erosional phase occurred, which was able to erode not only a scarp of 4 m in the sandy surface of unit U3, but at the same time the slope break in the clays of the Top-Paleogene surface of the adjacent interfluves. Most likely the erosional surface corresponds to the ravinement surface formed by shoreface and tidal-channel erosion with continuing rising sea level (Dalrymple et al. 1992, Zaitlin et al. 1994). As the coast moved landward across the continental shelf, the inner estuary expanded into the drowning upland while part of the outer estuary was removed.
It is highly unlikely that the erosional surface was formed during a relative sea-level lowering, as one would expect in such a case a renewed, more or less shore-normal incision of the river, and not a planation surface with a shore-parallel slope break (scarp). A 4-m-deep imprint (to a depth of -21 m) of a sinuous (river) valley is observed, but *across* the scarp, which implies that it formed *after* the intensive erosional phase that formed the scarp. The river-valley imprint probably corresponds to the renewed incision of the Ostend valley during a regression/sea-level drop, following the shoreface erosion and marine planation.

The 4 m scarp could either represent a stillstand or slow down in the sea-level rise (Swift et al. 1991), or contrarily an acceleration, leaving the previous erosional surface (lower shoreface) about 4 m below the new maximum depth of wave and tidal erosion (King 1963), or a combination of both (Thieler et al. 1999).

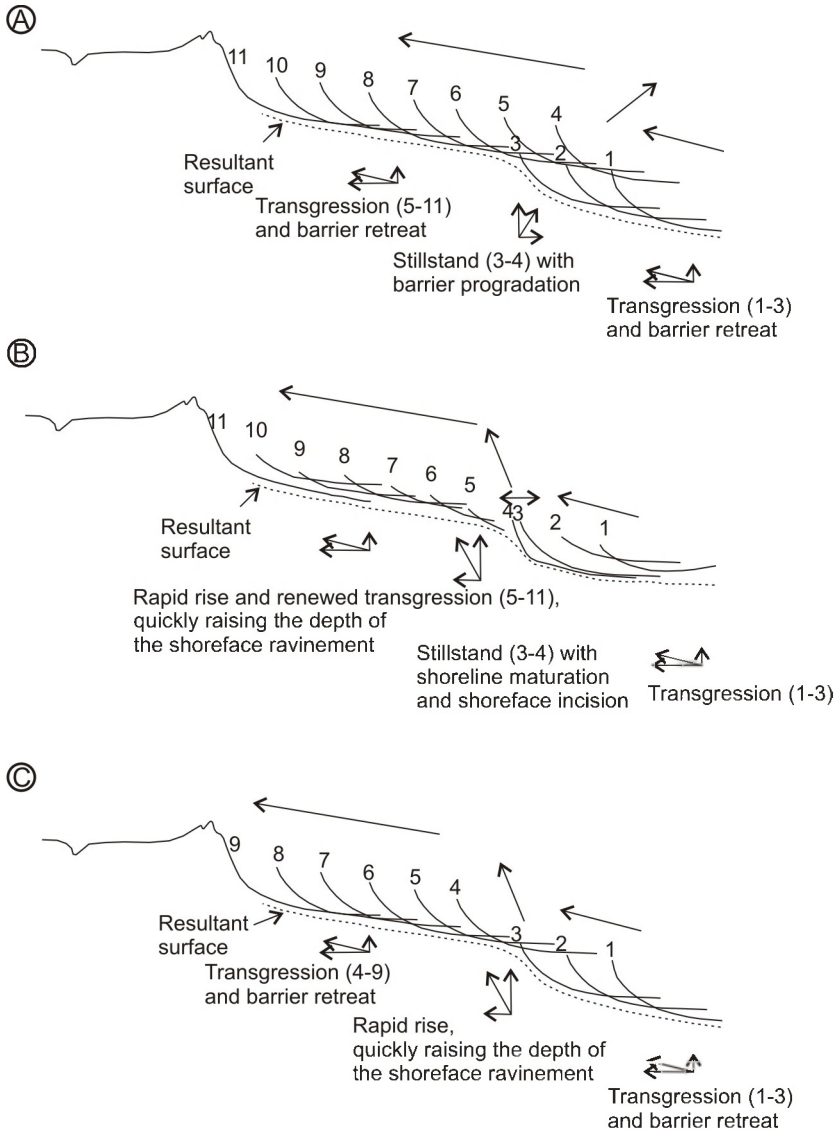

Fig. 6.25 Three possible schemes for the formation of a scarp. (A) A scarp is formed due to a stillstand or slow down in the sea-level rise, which caused, after a period of transgression and barrier retreat, a short phase of shoreline progradation. When the erosional shoreface retreat resumed, the regressive, prograding deposits were only partly destroyed and now form the scarp, that represents a relict lower shoreface. Modified after Swift et al. (1991). (B) Here the scarp is formed by a combination of slow down and acceleration in the relative sea-level rise. The scarp indicates a pause in the transgression during periods of relative stillstand or slow sea-level rise that permitted shoreline incision (Thieler et al. 1999). But the preservation of this shoreline is here explained by a rapid sea-level rise, terminating the stillstand, during which the depth of shoreface ravinement was quickly raised above the previous shoreline level. (C) The third scheme is proposed for the Belgian shelf situation, in which the large, continuous sloping planation surface at the foot of the scarp is most likely formed by a combination of wave and tidal action under a steadily rising sea-level (after the idea of King (1963)), forcing the shoreface to continuously migrate landward. Rather than that the whole planation surface and shoreface matured during a single sea-level slow down or stillstand. At a certain moment, an acceleration took place, steepening the shoreface ravinement surface. After that, sea level continued rising at the same pace as before the acceleration.

E.g. on the New Jersey shelf (Fig. 6.25A), a scarp is present, which is believed to have formed due to a stillstand or slow down in the sea-level rise (Swift et al. 1991). After a period of transgression and barrier retreat, a short phase of shoreline progradation occurred. When the erosional shoreface retreat resumed, the regressive, prograding deposits were only partly destroyed and now make up the scarp, which thus represents a relict lower shoreface. In our case though, the scarp or slope break is moulded in the Top-Paleogene surface and no prograding deposits are present. Still, it is possible that the slow down did not last long enough to form prograding deposits, or that the discontinuous shoreline retreat did initially leave an imprint in the Paleogene substrate, and that possible remnants of this regressional phase were later further eroded.
On the U.S. Atlantic shelf and the Gulf of Mexico many examples are known of paleo-shorelines that indicate pauses in transgression during periods of relative stillstand or slow sea-level rise hat permitted shoreline development and maturation (e.g. shoreface incision) (Thieler et al. 1999). The preservation of these shorelines is here explained by a rapid sea-level rise, terminating each stillstand, during which the depth of shoreface ravinement was quickly raised above the previous shoreline level (Fig. 6.25B). So here a combination of slow down and acceleration in the relative sea-level rise is proposed.
In our situation, the large, continuous sloping planation surface at the foot of the 'scarp' is most likely formed by a combination of wave and tidal action under a steadily rising sea-level (after the idea of King (1963)), forcing the shoreface to continuously migrate landward (Fig. 6.25C), rather than that the whole planation surface and shoreface matured during a single sea-level slow down or stillstand. Thus, the planation surface more likely represents a diachronous than isochronous surface. At a certain moment, an acceleration took place, which created the steeper part in the shoreface ravinement surface. After a while, when MSL was about 4 m higher, sea level probably continued rising at the same pace as before the acceleration, which is inferred from the similar slope angles.

Whether the scarp is formed by a relative sea-level slow down or acceleration, it represents in both cases a fossil lower shoreface. The lower shoreface is defined as the portion of the seafloor that lies below everyday (fair-weather) wave base, which is the depth at which sediments are not stirred by wave action (= half wave length). The depth of fair-weather wave base typically varies between 5 to 15 m MSL (Walker and Plint 1992).
This implies that if the former wave base is known, the mean sea level can be reconstructed on the basis of the position of this lower shoreface. Based on present-day wave periods (3.5-4.5 s in fair-weather conditions, Van Lancker 1999), a theoretical (deep-water) wave length of 19 to 32 m can be calculated, which would give a wave base of 9.5-16 m. However, the foot of the shoreface (lower shoreface) along the Belgian present-day coastline is located at an average depth of only -5 m MLLWS (-7.3 m MSL) (IMDC 2007), which demonstrates that the depth of a lower shoreface can not so straightforwardly be linked to the mean sea level through the wave base. Not only the impact depth of waves (wave base) determines the depth of the lower shoreface, also the influence of sediment availability and tidal action should be taken into account, especially in case of broad planation surfaces as in our situation, which cannot be formed by wave action only, unless under very slowly rising sea level (King, 1963). The impact of tidal action is, however, much more difficult to assess. Therefore the present-day depth of the foot of the shoreface is used as the definition for the position of the fossil lower shoreface.

Using the position of the foot of the present-day shoreface as a reference (i.e. 5 m below the lowest low water line at spring tide, or 7.3 m below mean sea level), the fossil lower shoreface (base of the scarp) could have been formed at a former mean sea level of -19 m $MSL_{present}$ (Fig. 6.26), which practically corresponds to the proposed mean sea level at the time when the shallowest occurrence of U3 was deposited (-18.5 m MSL). This means that the outer estuarine part of U3 was already being eroded by marine transgression, while at higher levels U3 still developed. Immediately afterwards, the relative sea-level rise accelerated over 4 m (to -15 m MSL), eroding the upper parts of U3 together with the adjacent headlands.

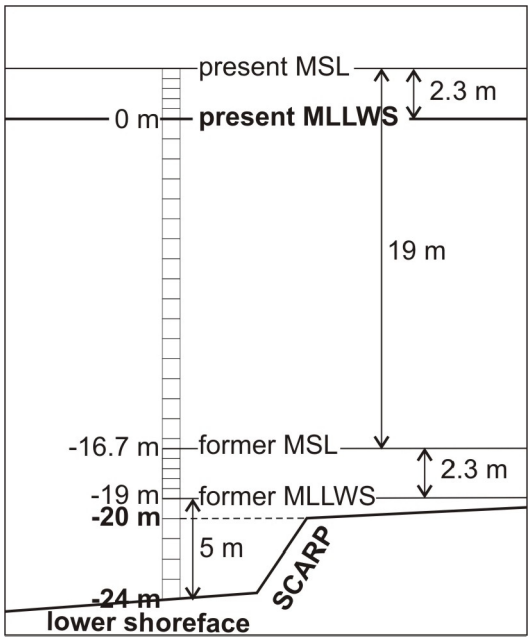

Fig. 6.26 The base of the scarp represents a fossil lower shoreface, which was probably located 5 m below the lowest low water line at spring tide (MLLWS) of that time, in analogy to the Belgian present-day situation. So, the lower shoreface located at -24 m $MLLWS_{present}$ was probably formed at a time when the lowest low water line at spring tide was -19 m $MLLWS_{present}$. In order to compare with the global relative sea-level curves, i.e. former mean sea level with reference to the present mean sea level: the lower shoreface was formed when MSL was -19 m $MSL_{present}$.

Deposits overlying the scarp and renewed river incision in U3

A final point to take into account in the relative dating of the incision and infilling of the Ostend Valley is the fact that in the Middelkerke Bank, on top of the erosional surface, tidal-flat (or lagoonal, subtidal) deposits were encountered (Trentesaux 1993, Berné et al. 1994, Stolk 1996), which are part of the here presented more extended seismic unit U4, which will be described in detail in the next chapter. Based on the depth of rootlets and comparison with similar deposits in the Netherlands (former Elbow Formation), an early Holocene age was proposed for the deposits in the Middelkerke Bank (Heyse et al. 1995, Trentesaux et al. 1999). The fact that shallow-water deposits are located on top of a marine-ravinement surface, is evidence of a sea-level lowering in between. The fact that these tidal flats are located above the renewed river valley incision, implies a new period of relative sea-level rise following the sea-level lowering. As tidal flats are rarely encountered in an incised valley during a sea-level lowering.

Overview of new evidence and critical reflections on former concepts

In assigning an age to the incision and subsequent infilling of the Ostend Valley, we are looking for a time span containing: (1) a relative sea-level drop to at least -30 m MSL during which the Ostend Valley was incised, (2) followed by a relative sea-level rise from at least -29.5 to -18.5 m MSL, when the infilling of the Ostend Valley occurred, (3) a subsequent sudden rise in the sea level of about 4 m, (4) followed by a renewed incision of the Ostend Valley, to a depth of -21 m MLLWS, during a relative sea-level drop, and (5) once again a sea-level rise during which a tidal-flat environment could develop. The data record gives no evidence of relative sea-level highstands or lowstands, apparently only the most prominent erosional features and transgressive deposits were preserved in the sedimentary record.
So, based on this interpreted succession of events, the interpretation of Trentesaux (1993) and Berné et al. (1994), that the infillings of the Ostend Valley are entirely of Holocene age, must be rejected. Berné et al. (1994) interpreted the erosional surface at the base of the tidal-flat deposits as a first (higher) order ravinement surface during the Holocene transgression, and the erosional surface at the top of the tidal-flat deposits as a second ravinement surface due to shoreface retreat. Following their interpretation, the second ravinement surface would represent a regional wave ravinement surface, created by wave erosion at the retreating shoreface, while the first ravinement surface would then represent a local tidal ravinement surface, produced by tidal channels associated with the sand bars extending along a tide-dominated estuary, as described by Zaitlin et al. (1994), formed during the initial Holocene transgression. It is however evident now, thanks to the more extensive seismic network, that the first erosional surface is not local, but that it represents a large planation surface, extending beyond the Ostend Valley, covering a large part of the BCS, and that it also represents a ravinement surface formed due to shoreface erosion during a transgression. So the underlying units cannot be of Holocene age too.

Fitting the new evidence with the Quaternary relative sea-level curve

As already mentioned, the fluvial incision in the Flemish Valley and the Belgian eastern Coastal Plain (to which the Ostend Valley is connected, cf. previous chapter) did not reach depths similar to the Ostend Valley (-27.5m MLLWS) until Saalian times (De Moor 1963 in: De Moor and Van De Velde 1995, Tavernier and De Moor 1974, Mostaert et al. 1989, Mostaert and De Moor 1989). So, an age older than Saalian for the incised Valley is excluded. During the Saalian glacial period the thalwegs in the Flemish Valley and the paleo-IJzer were incised to depths of -25 m TAW (~MLLWS) (De Moor and Van De Velde 1995, Bogemans and Baeteman 2003), whereas the valleys incised during previous glacial periods in the Early and Middle Pleistocene (Mindel and Pre-Mindel age, De Moor 1963, Tavernier and De Moor 1974, De Moor et al. 1996), presently stand out as gravel terraces at heights of +30 m and +60 m TAW (De Moor and Van De Velde 1995, De Moor et al. 1996). Note that during the Pleistocene no significant subsidence or uplift took place.
However, three sea-level lowerings occurred during the Saalian glacial period during which the Ostend Valley could have been incised (MIS10-8-6), and three successive rises during which the incision could have been infilled (MIS 9-7-5e) (Fig. 6.27). It is, however, unlikely that the Ostend Valley was incised to its final depth during the oldest Saalian lowstands (MIS10, MIS8). In that scenario, the estuarine infilling and following marine transgression during the next interstadial (MIS9, MIS7, respectively), would have been followed by renewed incision during the next Saalian lowstands (MIS8, MIS6), and by tidal-flat development during the next transgressions (MIS7, MIS5e), while there are no indications at all of the subsequent Weichselian glaciation and the most recent Holocene transgression. Most likely the Ostend Valley was not incised before the MIS6 glacial stadium of the Saalian period.

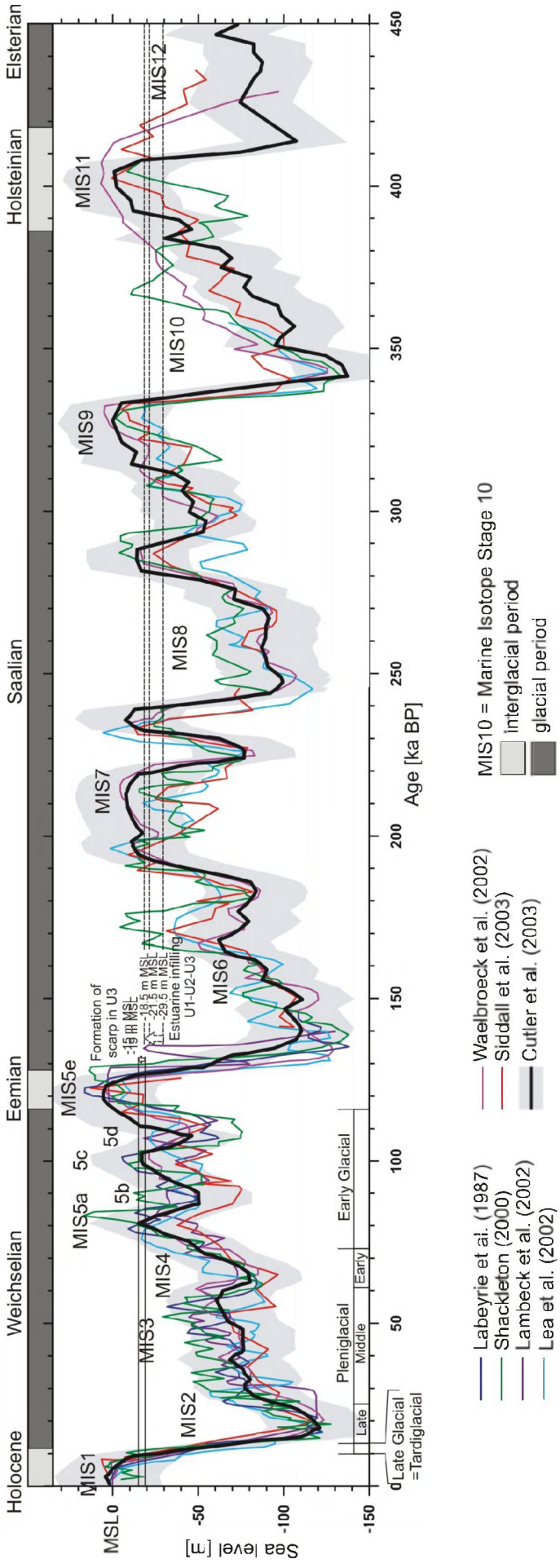

Fig. 6.27 Different global sea-level curves for the past 450 ka (modified after Siddall et al. 2006, adding the sea-level curve of Lambeck et al. 2002), with indication of glacial and interglacial periods, the Weichselian classification (Blaser 2007, Verbruggen et al. 1991, De Moor and Van De Velde 1995), and the different Marine Isotope Stages (McMillan 2005, table 1 on http://nl.wikipedia.org/wiki/Eemien). The figure shows also the proposed MSL values during the estuarine infilling of the Ostend Valley (during phases U1, U2, U3, i.e. -29.5 m, -21.5 m, and -18.5 m MSL resp.), and the supposed MSL when the scarp was formed

So, if the estuarine transgressive infilling of the Ostend Valley cannot have been of Holocene age, and most likely not of Saalian age, then looking at the global sea-level curves presented in Fig. 6.27, there are three periods during which the transgressive infilling could have taken place: during the Eemian interglacial (MIS5e) (Labeyrie et al. 1987, Shackleton 2000, Lambeck et al. 2002, Lea et al. 2002, Waelbroeck et al. 2002, Cutler et al. 2003, Siddall et al. 2003), and during the interstadials of the Weichselian glacial period (MIS5c and 5a) according to the two older sea-level reconstructions (Labeyrie et al. 1987, Shackleton 2000). Taking into account that after the presumed 4 m jump in the relative sea-level rise, the sea level must have at least continued rising for a while, to be able to create the upper planation surface of the 'scarp'. This assumption excludes MIS5a of Cutler et al. (2003) and Waelbroeck et al. (2002).

Note that neither a 4 m deceleration, nor acceleration is observed in either of the relative sea-level curves. Most likely because the resolution of these global sea-level curves is not sufficient for the semi-enclosed North Sea basin.

If the simple estuarine transgressive infilling of the deeply incised Ostend Valley would have happened during the Weichselian interstadials (MIS5c or MIS5a), then the question would arise why older (Eemian) deposits were not preserved. There are two options: (1) Eemian sediments were never deposited in the valley because the valley was only incised afterwards during the initial Weichselian sea-level lowerings (MIS5d and MIS5b), or (2) during MIS5d and MIS5b Eemian deposits were completely eroded from a Saalian (MIS6) incised valley. In the first case, the expected offshore continuation of the Saalian incision and Eemian infilling of the Flemish Valley is absent from the BCS, which is highly unlikely. It is equally unlikely that Weichselian incisions would have eroded all previous Eemian deposits.

Proposed timeframe

Taking into account all these arguments, the most plausible timeframe is that the Ostend Valley was incised during the Saalian (MIS6) glacial, during the same period that the Flemish Valley and eastern Coastal Valley were incised to similar depths (De Moor 1963 in: De Moor and Van De Velde 1995, Tavernier and De Moor 1974, Mostaert et al. 1989, Mostaert and De Moor 1989). The maximum deepening there took place during the Eemian period, when the sea flooded the incised coastal valley. The deeply incised channels infilled by units U1 and U2 were formed by tidal scouring of the valley floor during the early stages of the Eemian transgression, as suggested before by Mostaert et al. (1989), Liu (1990) and Liu et al. (1993). After the estuarine infilling, planation took place as the Eemian marine transgression continued, governed by continuing sea-level rise. With the next sea-level lowering(s) during the Weichselian, renewed, limited incision of the Ostend Valley took place. any Weichselian fills were possibly eroded by incising rivers during the following sea-level drop, or removed by wind erosion during the cold and dry Pleniglacial, when the Flemish Valley was blocked from the Ostend Valley by a cover-sand ridge. During the Holocene transgression a tidal-flat environment developed on top of the Eemian erosional surface with Weichselian valley imprint.

Additional evidence in support of the thesis that the estuarine infilling of the Ostend Valley is of Eemian age, comes from a depositional sequence in the Netherlands. Ebbing and Laban (1996) described in the nearshore area adjacent to the BCS an Eemian sequence (dated using pollen and diatom analyses) consisting of fine- to medium-grained sand, gravelly and shelly at the base, with some clay layers, and containing a mollusc association indicating a fresh to brackish estuarine environment. This sequence was deposited in terraces. The upper terrace ranges in elevation from -27 m to -23 m NAP (= -24.7 to 20.7 m TAW), which corresponds exactly to the elevation of the 'scarp' found in U3 (-24 to -20 m MLLWS). Also the base of the Eemian sediments, the

supposed Late Saalian morphology, is located at a depth of -31 m NAP (= -29m MLLWS), very similar to the incised Saalian Ostend Valley (-27.5 m MLLWS).

6.3.5 Linking the Flemish and Ostend Valley

As already shown in the previous chapter, the Ostend Valley most likely formed the seaward extension of the Flemish Valley. In the following text the intertwined evolution of both valleys will be sketched, taking into account the above proposed timeframe for the incision and infilling of the Ostend Valley.

Saalian glaciation

During the Saalian glaciation (probably MIS6 as discussed above), the Ostend Valley was incised to a depth of -27.5 m MLLWS (offshore) and -26 m MLLWS (more nearshore), which is comparable to the erosional depths of the Flemish Valley in the same period. During the Saalian, the thalwegs in the Flemish Valley were locally incised to depths of -15 and -25 m TAW (~MLLWS) (Tavernier and De Moor 1974, De Moor and Van De Velde 1995, Fig. 2 in: Verbruggen et al. 1991).
Saalian deposits in the Flemish Valley (formation of Zoetendale, formation of Adegem) consist of grey-green, glauconite-containing medium to coarse sand, with many silex boulders, broken silex fragments, and reworked Paleogene shells as inclusions. The sands are interpreted as energy-rich fluvial sediments, deposited under fluvioperiglacial circumstances during sea-level lowstands by rivers with large capacities. The gravel could be originating from the wash out of Paleogene deposits due to the quick erosion of the interfluves (De Moor and Heyse 1974).
The Saalian sediments in the Flemish Valley rarely exceed a thickness of 5 m (De Moor and Van De Velde 1995) because of important erosion after their deposition (De Moor and Heyse 1974, De Moor and Van De Velde 1995, De Moor et al. 1996). De Moor (1996) talks of a gravel lag at the base of the Quaternary, that is hardly ever more than 0.5 to 1 m thick, due to later incisions. This erosion took place at the transition of the full glacial stage to the following warmer period (Eemian) (De Moor and Heyse 1974), in agreement with the model of Vandenberghe (1995). The climate improvement and the disappearance of the permafrost at the beginning of the Eemian interglacial caused, before the actual sea-level rise, a new incision during which lots of material was eroded from the Flemish Valley.
This renewed fluvial incision is probably also the reason why in the Ostend Valley no fluvial sediments were recognised beneath the estuarine infillings. And not only because tidal scouring took place at the start of the estuarine transgression (Dalrymple 1992, Zaitlin et al. 1994). Still, the gravely layers at the top of the Paleogene surface with a maximum thickness of 0.5 m resemble the Saalian infillings of the Flemish Valley, and could correspond to similar fluvio-periglacial Saalian remnants. This would mean that where this gravel is present (cores UIT, SB1, SB2), the Ostend Valley was already at least that wide (and deep) incised before the tidal scouring and estuarine infilling took place.

Eemian interglacial

During the Eemian sea-level rise, the Ostend Valley developed into a landward-migrating tide-dominated estuary. Since the Ostend Valley forms the seaward continuation of the Flemish Valley, one would expect to find the landward section of the estuary system of phases U1, U2, U3 (the fluvial-tidal transition zone) in the Flemish Valley. With continuing sea-level rise, the estuary would have kept on migrating landward through the eastern Coastal Plain, into the Flemish Valley, which would leave middle- and outer-estuarine deposits.

Link Flemish Valley-Ostend Valley

Initially, it seemed as if this had been the case. The lithology of the middle and outer estuarine deposits of the Ostend Valley (described in section 6.3.1) is very similar to the facies of the Flemish Valley (De Moor and Heyse 1974, De Moor and Van De Velde 1995, De Moor et al. 1996), interpreted by the authors as marine or estuarine. The marine or estuarine sandy facies is characterised by grey medium fine sands with clayey lenses, containing marine shells, plant remnants and humic layers (sometimes holding glauconite, De Moor et al. 1996). At the base reworked Paleogene shells occur, as well as silex and quartz gravel and wood fragments (De Moor and Van De Velde 1995). The unit was deposited in a energy-rich marine or estuarine environment, both sub- and intertidal. The lack of fine fraction is attributed to the intense currents in estuarine environments (Heyse 1979). The coarser grained sands could be beach or offshore sediments, or deposited near river mouths in coastal zones (De Moor and Heyse 1978 in: De Moor and Van De Velde 1995).

But taking into account the deduced former relative sea-levels and the topography of the Paleogene surface, one must conclude that the estuarine infillings of the Flemish Valley form no direct continuation of the Ostend Valley infillings. When the Ostend valley gradually became completely infilled and the marine influence came closer and closer, the upper estuarine sediments were eroded by open marine action. A (4 m) stepped marine planation surface formed in a period when mean sea-level changed, possibly rapidly, from -16.7 m MLLWS (-19 m MSL) to -12.7 m MLLWS (-15 m MSL). At these sea-levels the interfluves in the present-day offshore area and Coastal Plain were soon completely drowned, and the low located Flemish Valley and its tributaries became inundated (Fig. 6.28). An area up to the Flemish Valley was completely exposed to open marine erosion, so it is unlikely that the estuarine marine sand body of the Ostend Valley had time to migrate all the way landinward up the Flemish Valley, with rising sea level. Moreover because by that time, the Eemian transgression slowly reached its end, and the highstand set in, making the landward migration of an estuary impossible. Because, if the rate of sediment supply is sufficient, then estuaries become filled and cease to exist when the rate of sea-level slows (Dalrymple et al. 1992).

So the marine or estuarine infillings of the Flemish Valley most likely belong to a newly formed estuary in the drowned bay, when the area of the Ostend Valley and Coastal Plain were already fully marine (Figs. 6.29A and C). De Moor and Heyse (1974) distinguished in the Flemish Valley tidal channel deposits, formed by intense tidal currents in the wide estuarine or offshore area (form. of Kaprijke), overlain by intertidal and coastal barrier deposits (form. of Moerkerke), and tidal-flat (wadden) deposits (form. of Meetkerke), partly formed behind sand barriers of the Moerkerke formation.

Most likely, the marine and estuarine sediments in the Ostend Valley look the same as the facies of the formations of Kaprijke, Moerkerke and Meetkerke in the Flemish Valley, because similar tidal processes were active in the embayment of the Flemish Valley, and comparable material is available (underlying Paleogene substratum, Saalian deposits, the same river input). And not, as was initially thought, because the marine sand body of the Ostend Valley estuary migrated all the way up to the Flemish Valley.

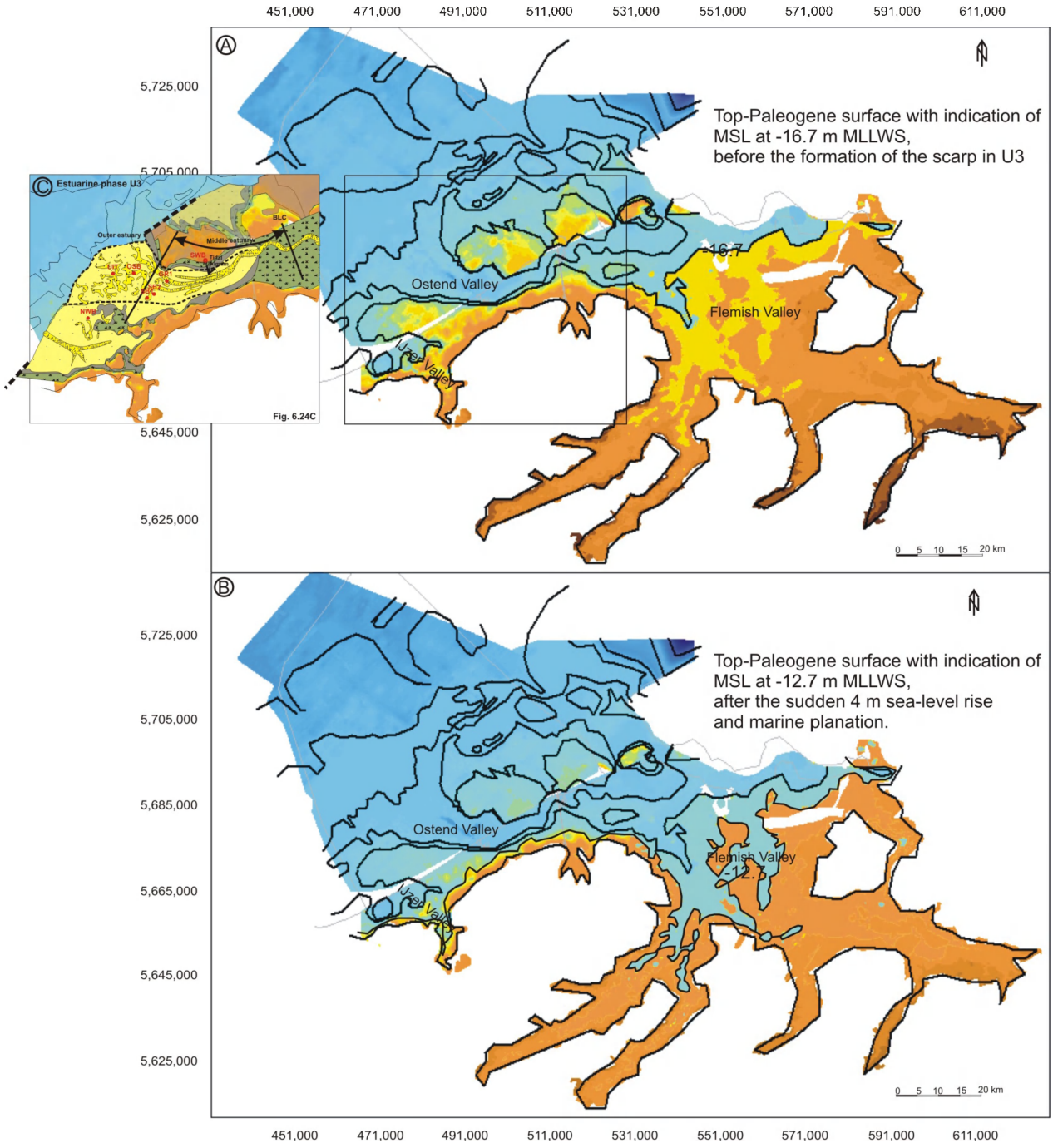

Fig. 6.28 (A) Situation when MSL was about -16.7 m MLLWS (boundary blue-yellow = marine-continental), i.e. the time when the lower shoreface of the scarp in U3 was formed, shortly after the infilling of the Ostend Valley (visualised in (C)). Note that before the upper planation of the scarp, the interfluves next to the Ostend Valley were possibly still higher than presently preserved. This is visualised in (C) as the orange transparent areas. (B) Situation when MSL was about -12.7 m MLLWS (boundary blue-yellow). Due to an abrupt 4 m sea-level rise, the interfluves in the present-day offshore area and coastal plain became soon completely drowned, and the low located Flemish Valley and its tributaries became inundated. An area up to the Flemish Valley was completely exposed to open marine erosion (bluish area), so it is unlikely that the estuarine marine sand body of the Ostend Valley (in (C)) had time to migrate all the way land inward up the Flemish Valley, with rising sea level. Note that at this time the present offshore area probably does resemble the topography of that time. In the Flemish Valley, however, it is possible that the marine influence did not reach as far inland due to alluvial infillings. (C) Paleo-reconstruction of estuarine phase U3, when MSL was about -16 m MLLWS (Fig. 6.24C), the area corresponds to the frame in (A).

What is possible though, is that continental, alluvial sediments found in the more upstream part of the Flemish Valley, especially in the Lys (Leie) Valley (formation of Oostwinkel, De Moor and Heyse 1974, De Moor and Van De Velde 1995), and at the NW valley wall (Figs. 6.29A and C after De Moor and Heyse 1978), have also been present in the further downstream and central part of the Flemish Valley, and represented the meandering, more clayey part of the contemporary Ostend Valley estuary, i.e. the fluvial-tidal transition or fluvial section according to the model of Dalrymple and Choi (2007) (Fig. 6.3). They would have been eroded though, by the later marine incursion, represented by the marine or estuarine deposits of the formations of Kaprijke, Moerkerke and Meetkerke. The continental sediments have been interpreted as fluvial to marshy, and partly perimarine deposits, formed by settling of suspension matter in the alluvial plain around meandering channels (De Moor and Heyse 1974, De Moor et al. 1996).

Link eastern Coastal Plain-Ostend Valley

In the eastern Coastal Plain, which forms the transition from the Ostend Valley to the Flemish Valley, rather thick mud-flat sequences and sandy tidal-gully deposits are overlain by open-marine nearshore sediments. The base of the open-marine sedimentation rises landward from -15 m to -5 m (OL ~MLLWS) (Fig. 6.29B), and connects offshore perfectly to the depth of the upper marine planation surface in the present-day offshore area, which changes landward from -20 m to -16 m. So these marine infillings in the eastern Coastal Plain represent the continuation of the shoreface retreat after the 4 m acceleration in the sea-level rise. So at the time of this marine transgression, also the eastern Coastal Valley estuary, as continuation of the Ostend Valley estuary, was already completely infilled. The maximum landward extent of the Eemian open marine conditions in the Coastal Plain was about 7 km south of the present-day coastline (Mostaert and De Moor 1989) (Fig. 6.29A). In the Flemish Valley the marine influence reached far more inland into the low-lying tributaries, about 40 km inland (De Moor et al. 1996). In the Coastal Plain, such as in the Flemish Valley, open marine deposits do exist. The fact that open-marine deposits do not exist in the Ostend Valley has two causes. Firstly, the marine incursion in the Ostend Valley happened very quickly and little marine sediment accumulated as the coastline retreated. The Flemish valley and Coastal Plain were flooded at the end of the Eemian transgression, practically during the highstand, when transgression had slowed and more sediment was available for the build-up of a transgressive sand sheet. Secondly, thin marine units in and around the Ostend Valley would have been vulnerable to later erosion as the coastline migrated landward of the Valley during both the Eemian and the Holocene.

Fig. 6.29 (page 129) Composition of own data and literature concerning the Eemian highstand in the Ostend-Flemish Valley area. (A) Supposed situation in the Flemish Valley and eastern Coastal Plain during the Eemian highstand, when MSL was about 0 m MLLWS. Bluish colours represent the extent of the marine influence, yellow to orange colours represent the areas that would still be located above MSL. Note that the boundary is visualised as a contour of the Top-Paleogene surface, so not taking into account any Pleistocene infillings. In two selected areas the Eemian infillings are visualised after Mostaert and De Moor (1989), and De Moor and Heyse (1978). (B) Synthetic vertical section through the eastern Coastal Plain, showing the Eemian sequences (after Mostaert and De Moor 1989). (C) Conceptual model of the sediment structure of the central part of the Flemish Valley (after De Moor 1996). Note that the original drawings (maps and vertical sections) showed only the depositional environments, and that the formation names are added based on texts of De Breuck et al. (1969), Tavernier and De Moor (1974), De Moor and Heyse (1974), and Afb. 3.14 from De Moor (1996). On the basis of vertical section (C), the map in (A) was slightly modified (formation of Meetkerke added, striped contour).

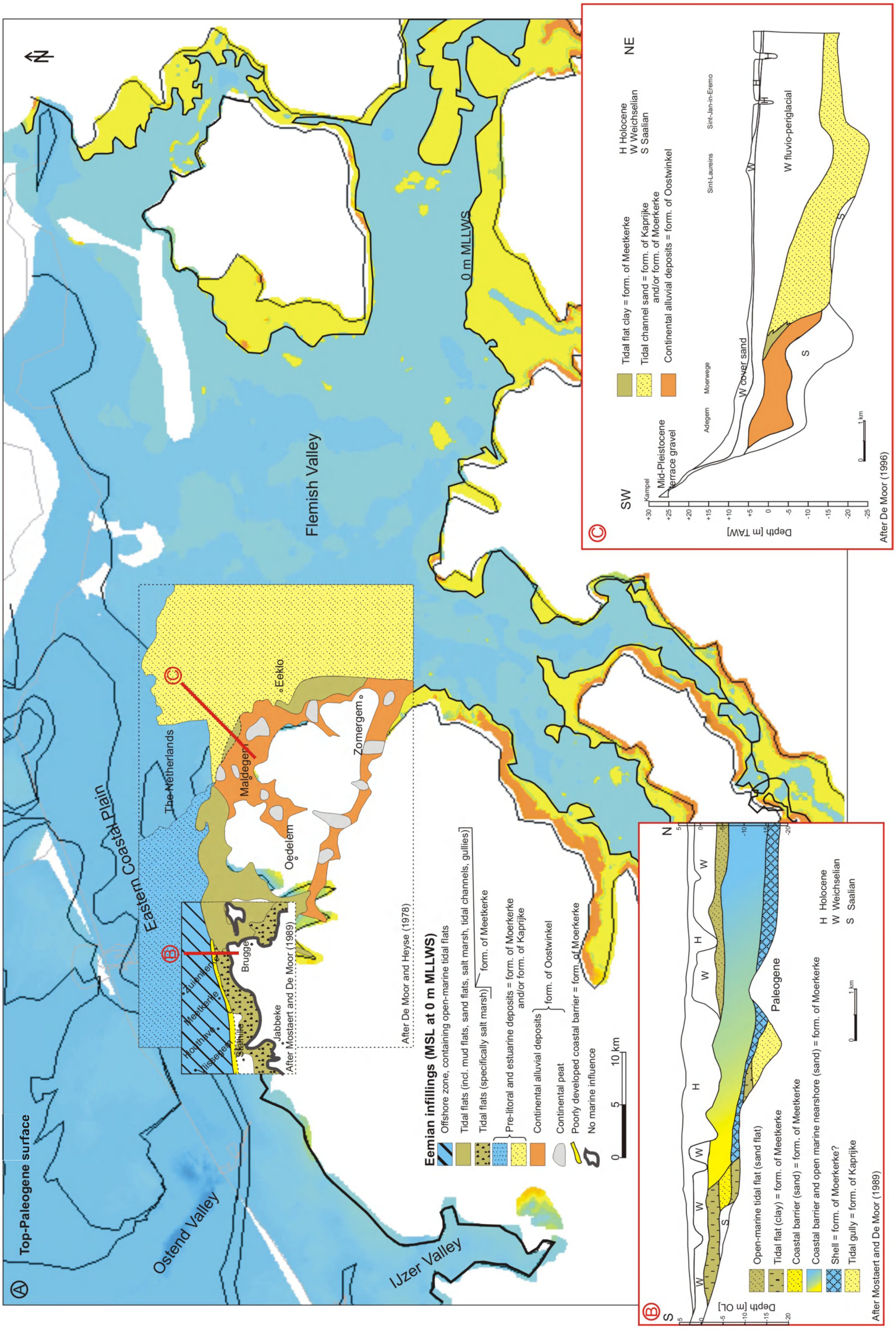
A
Top-Paleogene surface
N
Ostend Valley
IJzer Valley
Eastern Coastal Plain
The Netherlands
Flemish Valley
0 m MLLWS
Maldegem
Eeklo
Zomergem
Oedelem
Brugge
Jabbeke
Stalhille
Zuienkerke
Meetkerke
Houthave
Lissewege
After Mostaert and De Moor (1989)
After De Moor and Heyse (1978)
Eemian infillings (MSL at 0 m MLLWS)
Offshore zone, containing open-marine tidal flats
Tidal flats (incl. mud flats, sand flats, salt marsh, tidal channels, gullies)
Tidal flats (specifically salt marsh)
form. of Meetkerke
Pre-litoral and estuarine deposits = form. of Moerkerke and/or form. of Kaprijke
Continental alluvial deposits
form. of Oostwinkel
Continental peat
Poorly developed coastal barrier = form. of Moerkerke
No marine influence
0 5 10 km
C
SW
NE
Kampel
Mid-Pleistocene terrace gravel
Adegem
Moerwege
Sint-Laureins
Sint-Jan-in-Eremo
W cover sand
W fluvio-periglacial
Depth [m TAW]
Tidal flat clay = form. of Meetkerke
Tidal channel sand = form. of Kaprijke and/or form. of Moerkerke
Continental alluvial deposits = form. of Oostwinkel
H Holocene
W Weichselian
S Saalian
After De Moor (1996)
B
S
N
Depth [m OL]
Paleogene
Open-marine tidal flat (sand flat)
Tidal flat (clay) = form. of Meetkerke
Coastal barrier (sand) = form. of Meetkerke
Coastal barrier and open marine nearshore (sand) = form. of Moerkerke
Shell = form. of Moerkerke?
Tidal gully = form. of Kaprijke
H Holocene
W Weichselian
S Saalian
After Mostaert and De Moor (1989)

In the eastern Coastal Plain, the final phase in the Eemian succession is represented by the development of exposed (open-marine) tidal flats (Mostaert and De Moor 1989) (Fig. 6.29B), most likely formed during the Eemian highstand when the coastline regressed. Indeed, during highstand, when an estuary becomes filled and ceases to exist, the site becomes a delta if the sediment is supplied directly by the river, or a straight prograding coast (strand plain or open-marine tidal flats), if the sediment is delivered to the area by marine processes (waves or tides, respectively) (Dalrymple et al. 1992).
The lowermost part of the thick mud flat sequences and the sandy tidal gully deposits below the open marine deposits in the eastern Coastal Plain (Fig. 6.29B), might represent the more landward estuarine infillings, contemporary with the U3 infilling phase in the Ostend Valley (Fig. 6.24C). While the upper tidal flats could have built up behind a poorly developed barrier during the shoreface retreat, after the Ostend Valley section was completely infilled.

Depositional and incisional depth

During the Eemian transgression in the Flemish Valley, the Paleogene substrate was locally incised to depths of -20 m TAW (De Moor and Van De Velde 1995) with extremes of -25 m (Fig. 2 in: Verbruggen et al. 1991, Fig. 6.29C De Moor 1996). For comparison, the central channel in the Ostend Valley was incised to depths of -56 m (MLLWS).
In the Flemish Valley, the shallowest Eemian, i.e. marine or coastal deposits, occur up to an elevation of +2.5 m MLLWS (De Moor and Heyse 1974), whereas in the Ostend Valley, the shallowest occurrence of the Eemian estuarine deposits is only -16 m MLLWS. This relatively large depth of the shallowest Eemian deposits in the Ostend Valley is probably due to its more seaward position, the marine planation during the Eemian transgression, and the absence of open-marine or open tidal-flat deposits, which do occur in the Coastal Plain where they developed during the Eemian highstand.

Weichselian glaciation

At the beginning of the Weichselian period (Early Glacial 116ka-73ka BP, MIS 5d-5a (http://nl.wikipedia.org/wiki/Weichselien, Verbruggen et al. 1991), Fig. 6.27), sea-level lowered again in response to ice-mass expansion, due to detoriating climatic conditions. In our regions the climate became relative cold, but with a very high humidity (Verbruggen et al. 1991), which induced an intense and deep fluvial incision, as no permafrost was established yet. The Flemish Valley became deeply incised to depths of -17 m (Tavernier and De Moor 1974) (-15 m in: De Moor et al. 1996, and on: Fig. 6.29C after De Moor 1996; and -20 m on Fig. 2 in: Verbruggen et al. 1991), which removed most of the Eemian sediments. These incisional depths are very similar to the renewed incision observed in the Ostend Valley (-21 m MLLWS). During the Weichselian the river incised less than during the Saalian glaciation, because the subsurface is much more horizontal than before the Eemian marine planation. On plainer surfaces rivers tend to incise less, or even deposit sediments in case the offshore slope inclines less than the coastal plain slope, even under regressive circumstances (Blum and Törnqvist 2000). We can presume that before the Eemian marine planation, the seafloor/subsurface was steeper inclined, because marine planation can only occur when the dynamic base of the wave action is less steep than the subsurface (King 1963).

During the Early Pleniglacial (72ka-61ka BP, MIS4 (Blaser 2007), Fig. 6.27), characterised by a very cold and humid periglacial climate, extensive fluvioperiglacial accumulation took place. The presence of permafrost restricted the incisional depth, and the limited vegetation allowed an intensified runoff of meltwater, by which large amounts of sediment were swept away to the thalwegs. The rivers evolved into braided river systems. This continued during the milder Middle Pleniglacial (61ka-25ka BP, MIS3 (Blaser 2007), Fig. 6.27) and the valley complex of the Flemish Valley and her distributaries became filled to a level between 0 and +10 m TAW (De Moor and Van De

Velde 1995, Fig. 2 in: Verbruggen et al. 1991). This leaves at least 20 m of Weichselian deposits in the Flemish Valley (De Moor and Van De Velde 1995, De Moor et al. 1996), while in the Ostend Valley no fluvial sediments at all were found in the renewed valley incision (sea below).

During the Late Pleniglacial (25ka-13ka BP, MIS2 (Blaser 2007), Fig. 6.27), the climate turned very cold and dry, and vegetation became exceedingly scarce. Eolian processes began to dominate and exposed older fluvial sediments were reworked into cover-sand ridges, gradually damming the Flemish Valley. The whole northward-oriented braided drainage system of the Flemish Valley was forced to branch off eastward, along the Lower-Scheldt (De Moor and Van De Velde 1995). From then on, the Ostend Valley was no longer connected to the Flemish Valley, and no longer active as a river valley.

On the transition from Pleniglacial to Late Glacial, but mostly during the Late Glacial (=Tardiglacial, 13ka-10ka BP (Verbruggen et al. 1991, De Moor and Van De Velde 1995)), a warmer climate changed river discharge, regime and sediment load. In response, meandering rivers replaced the braided rivers of the Flemish Valley and connected lows (De Moor and Van De Velde 1995, Verbruggen et al. 1991), incising the previously infilled surface to depths in the range of -2 to +5 m (Fig. 2 in: Verbruggen et al. 1991, Fig. 6.29C after De Moor 1996, De Moor et al. 1996). At the beginning of this period of intense morfo-sedimentological change, sea-level was still lower than -50 m as the permafrost disappeared, which enhanced the intensity of the vertical erosion of the rivers. Because the Ostend Valley was no longer connected to the Flemish Valley, this episode in the river evolution is not present in the Ostend Valley fills.

The question remains why we do not find 20 m of Weichselian braided river infillings in the Ostend Valley, just like in the Flemish Valley and its tributary river valleys. Multiple reasons can be proposed. Owing to the Eemian marine planation (-20 to -16 m MLLWS), the paleo-surface was very low, so a Weichselian incision to a depth of -21 m, similar to that in the Flemish Valley, would have been able to accommodate a fill of no more than 5 m in thickness, which could easily have been removed by later erosion. Possible processes were eolian action, after the river was cut off from the Flemish Valley by the cover sand ridges, leaving a deflation surface (gravel) at the base of U4, and tidal-channel scouring during the Holocene transgression, prior to the formation of the tidal flats (U4). In this latter case, the coarse base of U4 would represent tidal-channel lags or thin remnants of the Weichselian river fills.

Holocene interglacial

Finally, during the Holocene transgression, a tidal-flat environment developed above the Ostend Valley fill, on top of the marine-planation surface and Weichselian incision. Tidal flats also developed in the present-day Coastal Plain, where the Weichselian fluvio-periglacial surface of the Flemish Valley slopes down so much in the direction of the North Sea, that it became inundated during the Holocene transgression (De Moor and Van De Velde 1995).

6.4 Limitations, innovations and recommendations

6.4.1 Difficulties and limiting factors

A number of difficulties and limitations made this investigation quite a challenge. First of all the Quaternary cover is maximum 45 m thick but the average is less than 10 m. Because of the almost complete lack of subsidence (D'Olier 1981, Kiden et al. 2002, Vink et al. 2007), the BCS provided very little accommodation space to accumulate and preserve Quaternary sediments. This is in contrast to the northern Dutch shelf, where the Quaternary cover is locally more than 600 m thick in a linear through corresponding to the Central Graben of Mesozoic and Tertiary age (Caston 1977). Moreover, on the BCS the Quaternary cover is not continuous, the deposits are preserved in isolated sandbanks and in a single valley, incised in the Paleogene substrate offshore Oostende (Fig. 5.4). In order to investigate the oldest Quaternary deposits on the BCS, the analyses had to focus primarily on the Ostend Valley, and also on some isolated patches below the Hinder Banks north of the Offshore Scarp.
A second limitation was the availability of core data. Because of the depth and thickness of the deposits in the Ostend Valley, only a limited number of boreholes reached the lowermost units. Moreover, no unreworked datable material was present in the available cores, so it was not possible to obtain reliable absolute ages.

To reconstruct the fill and evolution of the Ostend Valley from this fragmented record and limited dataset of boreholes, all available data were analysed in an integrated way, using sequence-stratigraphic principles, estuarine-facies models and the onshore record as guidelines. The Ostend Valley infillings are mainly sandy with occasional clay laminae, which is typical for a tide-dominated estuary, as shown in estuarine models (Dalrymple and Choi 2007). However, we are aware that these models are idealised end members and that in nature estuaries typically show a mixed influence of tides and waves.

The facies variability within estuaries is enormous, a function of the presence of (deep) subtidal, intertidal and supratidal environment and of lateral and temporal changes in wave and tidal characteristics. Given this variability, it is no surprise that the few cores penetrating the estuarine fill are insufficient to fully understand and reconstruct the development of the Eemian estuary. Studies in the present-day nearby Western Scheldt and other modern estuaries should be used to refine the reconstructions, and to shed light on the diachronous nature of the seismic facies that form the fill of Ostend Valley.
Nevertheless, the generalised estuarine-facies models of Dalrymple and Choi (2007) and Dalrymple and al. (1992) have facilitated the environmental and sequence-stratigraphic subdivision and interpretation of the Eemian fill, providing a useful framework in interpreting the few cores.
In the paleo-geographical reconstructions, the lateral position of the different estuarine environments during each developmental phase was inferred from their typical relationship to the high- and low-water levels. Frame of reference was the elevation range of tidal–channel fills (entirely subtidal), which are easily recognisable on the seismic data. The tidal range in the Ostend Valley during the Eemian is not known, but a mean tidal range of 4 m was used. This value was chosen because it is the present-day mean tidal range in Oostende, and does not take into account variations within the estuary due to valley convergence and friction. Spatial and temporal variability in the tidal range would have had an effect on the location and surface area of environments such as mud flats and salt marshes. Any deviations from the paleo-geography shown do not change the overall picture of a landward-migrating estuary that is filled in the course of time and then truncated on its seaward side.

Because of the absence of reliable datable material in the cores, the time of incision and the age range of the Ostend Valley fill had to be inferred from indirect evidence. We are aware that for deducing the timeframe, strong focus was put on the absolute values of the global sea-level curves and on the succession of sea-level lowerings and rises, not taking into account the reaction time of rivers to sea-level and climatic changes, local influences such as the position of the shelf edge, or tectonic events in the headward part of the river. A few clues were provided by minimum ages of shells from the estuarine fill and by data from the Dutch Continental Shelf. Thanks to the dense seismic network, the order of intersection of the different drainage systems on the BCS could be determined, helping to establish a relative chronology.

6.4.2 Innovations

The jumble of interpretations and supposed ages of the fills of the Ostend Valley (Liu et al. 1993, Trentesaux 1993, Berné et al. 1994, Trentesaux et al. 1999) has finally been sorted out. For the first time an attempt was made to define depositional environments within the Ostend Valley. Vague terminology as 'valley infilling' could now be narrowed down to more precise interpretations such as 'a tidal-channel fill in a middle-estuarine environment'.
Furthermore, there is now convincing evidence that the Ostend Valley was linked with the Flemish Valley. Except for the statement, that the Ostend Valley was probably not incised before Saalian times, which was based on observations from the Flemish Valley, it is important to say that the tentative dating of the Ostend Valley fills is based on clues from the Ostend Valley itself (depositional depths of seismic units, erosional surfaces, etc.), and not deduced from the fills of the Flemish Valley as was done before (Liu et al. 1993). It has also become clear that the Flemish and Ostend Valley do not have necessarily the same infilling history, although they are strongly interconnected. For example, in the upstream part of the incised river valley, more Weichselian braided-river deposits have been preserved, compared to the Ostend Valley. In contract, more and thicker Eemian estuarine deposits have been preserved in the downstream part of the system (-56 to -16 m = 40 m) than in the Flemish Valley (-25 to +2.5 = 27.5 m). The thickness of the fills decreases in the depositional direction, landward for the estuarine deposits, and seaward for the fluvial deposits.

6.4.3 Recommendations

The present analysis of the incision and infilling of the Ostend Valley can only be improved if additional information becomes available. Better seismic coverage is needed to better understand the architecture of the estuarine fill. In light of the scale of sedimentary and morphological features in modern estuaries, a line spacing of 500 m is recommended to be able to map individual tidal channels, tidal flats and salt marshes. Both transverse and longitudinal seismic profiles are advised. Using such a dense seismic network, one can perform a pseudo-3D analysis, which is important to capture the interrelationships between tidal channels, shoreface migration and ravinement surfaces. Extra attention should be paid to the transition between sea and land, in shallow water where no seismic data have been collected to date.

Additional core data are needed to identify and characterise lithological changes along and across the axis of the valley, and in the vertical succession. New cores must be collected at locations where the seismic data suggest the presence of important units or boundaries. In addition to the available boreholes in the Ostend Valley, some extra cores

at the margins of the valley are highly recommended. Also, the sea-land transect along the longitudinal axis of the valley needs to become denser in order to better understand lateral variability.

Seismic units are notorious for their diachronicity, and any further understanding of the three units identified in the Ostend Valley fill will require at least some absolute chronological control. Because of their transgressive setting, incised valley estuaries are usually characterised by strong reworking of the sediments, so finding unreworked datable material will be a challenge.
If the fill is young enough, ^{14}C analyses on articulated shells in life position might be considered, as well as on *in situ* salt-marsh deposits. For older deposits, luminescence dating techniques may be useful. Pre-depositional signal bleaching is a requirement for accurate luminescence ages, but even where bleaching is incomplete, the resulting, overestimated ages may still be useful to distinguish deposits from consecutive ice ages or interglacials.

6.5 Conclusion

The Ostend Valley was incised during the final phase of Saalian glaciation MIS6, when a proglacial lake, formed in front of the Saalian ice sheet, drained, and the tributaries of the Flemish Valley sought their way to the receding lake shoreline, with dropping base level. The Ostend Valley was incised to a depth of -27.5 m MLLWS. Saalian deposits in the Flemish Valley consist of medium to coarse sand with many silex boulders, and are interpreted as high-energy fluvial sediments, deposited under fluvioperiglacial circumstances during sea-level lowstand by rivers with large capacities. However, at the transition of the full glacial stage to the following warmer period (Eemian) renewed erosion took place. Global warming and the disappearance of the permafrost at the beginning of the Eemian interglacial caused a new incision before the rising sea reached the area. During this time, lots of material was eroded from the Flemish Valley. This renewed fluvial incision is probably also the reason why hardly any fluvial sediments were recognised beneath the estuarine fill in the Ostend Valley, except for the thin gravelly units at the top of the Paleogene surface with a maximum thickness of 0.5 m.

During the Eemian sea-level rise, the Ostend Valley developed into a tide-dominated estuary, as inferred from the typical funnel shape of the valley and the sandy deposits present within the entire estuary. Wave-dominated estuaries typically show a distinct tripartite facies distribution with a muddy central part.
During the early stages of the Eemian transgression, when the sea invaded the pre-existing river valley (estuarine phase U1, MSL -27 m MLLWS), tidal scouring deepened parts of the valley floor. Extreme scour depths of 30 m into the original valley floor (to depths of -56 m MLLWS) probably developed near the tidal maximum of the narrow estuary at that time. Locally, the tidal currents removed the Saalian gravel lag, and the channels were partially infilled with a coarse-grained channel lag and with lateral-accretion deposits (seismic unit U1). In this initial stage, the estuary was still very narrow with steep valley flanks, so there was little room for the development of extensive salt or freshwater marshes, which could explain the absence of humic or organic material in unit U1. Seismic unit in U1 in the Ostend Valley represents the middle part of the estuary at this stage.
With continuing rising sea level, the estuary widened, and more extensive mud flats and salt marshes could develop (estuarine phase U2, MSL -19 m MLLWS). By then, probably enough time had passed for the development of freshwater marshes at the landward end of the estuary, which explains the presence of peat fragments in the unit U2 lithofacies.

Seismic unit U2 represents the seaward part of the middle estuary during estuarine phase U2, which was located farther landward than in phase U1.
During the third phase (U3, MSL ca. -16 m MLLWS), the estuarine environment penetrated even farther inland. Seismic unit U3 represents the seaward part of the middle estuary and the outer estuary of that time. More landward sections of that estuary have most likely been partly preserved on the present-day Coastal Plain. There, thick mud-flat sequences and sandy tidal-gully deposits are present below subsequently deposited open-marine sediments. In the Flemish Valley, thick continental facies are interpreted as fluvial to marshy, and partly perimarine deposits, formed by settling of suspended matter in an alluvial plain fringing meandering channels. These deposits may have accumulated in the upstream meandering part of the contemporary Ostend Valley estuary, i.e. in the fluvial-tidal transition or fluvial section.

After the Ostend Valley gradually had infilled, open-marine processes began to modify the area, starting in the west. Here, the upper-estuarine sediments and adjacent Paleogene interfluves were eroded as the coastline was forced eastward by the rising sea. A (4 m) stepped marine planation surface formed in a period when mean sea-level changed rapidly, from about -17 m to -13 m MLLWS. At these sea levels the interfluves in the present-day offshore area and Coastal Plain were soon completely drowned and the low-lying Flemish Valley and its tributaries became inundated. An area up to the Flemish Valley was completely exposed to open-marine erosion. In the present-day Coastal Plain, a poorly developed barrier formed and tidal flats built up behind it, while in the Flemish Valley a new estuary developed. The maximum landward extent of the Eemian open marine conditions in the Coastal Plain was about 7 km south of the present-day coastline. In the Flemish Valley the marine influence reached far more inland into the low-lying tributaries, about 40 km. In the eastern Coastal Plain, the final phase in the Eemian succession is represented by the development of exposed (open-coast) tidal flats during the Eemian highstand when the coastline prograded.

At the beginning of the Weichselian period, sea-level fell again in response to a new ice age. In our region the climate became relatively cold. Intense and deep fluvial incision marked this period, as no permafrost was established yet. Most of the Eemian sediments in the Flemish Valley were removed. The Ostend Valley also experienced renewed incision, but most of the Eemian fill was preserved. During the Early Pleniglacial, characterised by a very cold and humid periglacial climate, extensive fluvioperiglacial accumulation took place. The presence of permafrost restricted fluvial incisional, and the limited vegetation facilitated an intensified runoff of meltwater, which swept large amounts of sediment to the thalwegs. Braided-river systems developed, which persisted during the milder Middle Pleniglacial. During this time, the Flemish Valley and her distributaries became filled to a level between 0 and +10 m TAW. In the Ostend Valley, however, no Weichselian fluvial sediments are present in the Weichselian valley incision. During the Late Pleniglacial, a cold and dry climate created an environment in which vegetation was scarce. Eolian action took over and older fluvial sediments were reworked into cover-sand ridges, gradually damming the Flemish Valley and separating it from the Ostend Valley. The whole northward-oriented braided drainage system of the Flemish Valley was forced to branch off eastward, along the Lower-Scheldt. Since then, the Ostend Valley has no longer been connected to the Flemish Valley and has no longer been active as river valley.

The Ostend Valley fill is a simple fill, the result of a landward-migrating (transgressive) estuary during a single sea-level cycle. The erosional unconformities separating the seismic units, correspond to local tidal ravinement surfaces, separating the different depositional environments within an estuary. During transgression, the facies within the tide-dominated estuary shifted landward. In the process, migrating tidal channels and

with wave action on the shoreface eroded much of the estuarine deposits, leaving an incomplete record of U1, U2 and U3.
In the most complete succession, a simple incised-valley fill consists of lowstand and/or transgressive fluvial deposits (LST), overlain by transgressive estuarine sediments (TST), and highstand progradational deposits (HST), either deltaic or open-coast tidal. Remarkably, nearly the entire Ostend Valley infill represents the Transgressive Systems Tract. Only a very thin Lowstand Systems Tract is present, provided the gravel lag found on top of the Paleogene surface does represent Saalian fluvial deposits. No Highstand Systems Tract has been recognised. In the Coastal Plain though, prograding open-coast tidal flats are present, and these represent the Highstand Systems Tract.
Interpreting the incised-valley system of the connected Flemish and Ostend Valleys in terms of the sequence-stratigraphic model of Zaitlin et al. 1994, the Ostend Valley represents segment 1. This is the most seaward part of the system, which initially experiences (lowstand-to-transgressive) fluvial and estuarine deposition but is transgressed by the shoreline so that the estuarine deposits are overlain by marine sands and/or shelf muds. The eastern Coastal Plain is home to segment 2. This is the middle portion of the valley, which is occupied by the estuary at the time of maximum transgression. The lower part of the valley fill consists of a transgressive, fluvial-to-estuarine succession like in segment 1, but it is overlain by a progradational fluvial succession that accumulated during the sea-level highstand. The Flemish Valley corresponds to segment 3. This is the most landward part of the valley, which lies beyond the limit of marine influence. It remained fluvial throughout its history, and is marked by terrestrial deposits. Note, however, that the Flemish Valley segment of the estuary was still functioning when the Ostend Valley and Coastal Plain had been infilled and truncated by shoreface erosion.

7.
Holocene transgression, evolution of a back-barrier basin, and formation of storm-generated sand ridges

After the Eemian estuarine infilling of the Ostend Valley, the Eemian marine transgression and the renewed Weichselian incision, the Ostend Valley embayment had changed into a linear coastline. This chapter will focus on the evolution of such a coastline during the Holocene sea-level rise. It comprises the formation of a coastal barrier, the development of a back-barrier basin behind it, and the growth of sand ridges in front (seaward) of it. During the Holocene, this barrier has migrated landward and seaward under the changing influences of accommodation space, sediment budget, storm influence, and human impact. This coastline evolution will be discussed in detail, taking into account the history of the western Belgian Coastal Plain as well.

7.1 Introduction: evolution of a coastline

At the onset of the Holocene, the Ostend Valley was completely infilled, and apart from a small renewed incision during the Weichselian, the embayed coast of the Eemian had changed into a linear coastline. Depending on the ratio sediment supply over accommodation space, and the relative influence of wave and tidal power, a linear coastline can take on different shapes of depositional environments (Fig. 7.1A after Boyd et al. 1992).
According to this model, if tidal power dominates over wave power, open tidal flats will develop, which migrate landward when the created accommodation space due to sea-level rise is larger than the available sediment supply (transgression), and will start prograding if the sediment supply exceeds the created accommodation space (regression). In case wave power dominates over tidal power, a barrier will form protecting a lagoon or marsh in case the created accommodation space exceeds the sediment supply, when the sediment supply exceeds the created accommodation space, the barrier will start prograding and evolve into a strandplain or barrier complex.

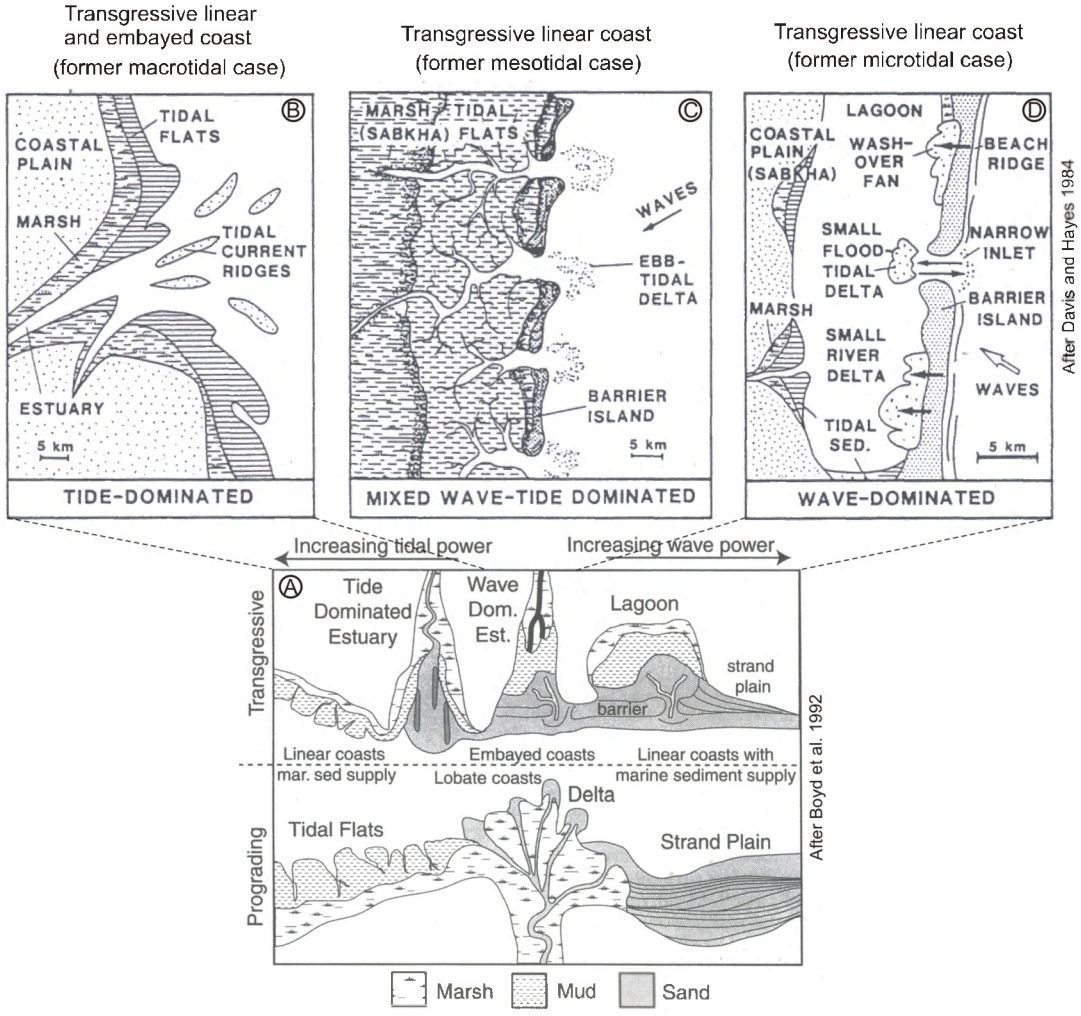

Fig. 7.1 (A) Maps of idealised coastal depositional environments, showing the relationship between wave and tidal power, prograding and transgressive environments, and different geomorphic types (after Boyd et al. 1992). (B) Example of a transgressive linear coastline adjacent to an embayed coastline in tide-dominated circumstances (former macrotidal case). (C) Example of a transgressive linear coastline in mixed wave-tide dominated circumstances (former mesotidal case). This depositional environment of a linear coast line with mixed energies is missing in (A). (D) Example of a transgressive linear coastline in wave-dominated circumstances (former microtidal case). (B), (C) and (D) adapted after Davis and Hayes (1984).

7.1.1 Formation of a barrier

During most of the Weichselian, the North Sea was dry land, but around 12,500 cal BP rising sea water entered the southern part of the North Sea again, through the Strait of Dover in the south and through channels along the Dogger Bank in the north (van der Molen and van Dijck 2000). According to van der Molen and van Dijck (2000), the land bridge between northern Holland and Britain (Texel Spur-Norfolk Banks) was flooded around 8500 BP (9500 cal BP). The tidal energy from the northern North Sea could enter the Southern Bight, and barrier islands with back-barrier basins formed along the eastern shore of the Southern Bight prior to 8000 BP (9000 cal BP), due to the predominance of westerly winds and the low gradient of the pre-transgressive, Pleistocene surface. According to Beets and van der Spek (2000), however, the Southern Bight was still isolated from the northern North Sea at 8500 BP (9500 cal BP), but was at that time already sufficient in size to produce waves at its eastern shores capable of building a protective barrier behind which a complex of estuaries and tidal basins could develop. Indeed, barrier islands form when abundant sediment, proper coastal processes, and a generally low gradient profile are present (Davis 1994, Glaeser 1978 in: Galloway and Hobday 1996). The formation of barrier-lagoon-estuary systems is a common response to transgression on shelves flanked by coastal plains incised by their drainage systems during Pleistocene sea-level falls (Swift et al. 1991).

Davis (1994) defines a 'barrier island' as an elongate, essentially shore-parallel, island composed dominantly of unconsolidated sediment, which protects the adjacent land mass and is separated from it by some combination of wetland environments. This definition includes sandy barriers that have never been separated from the mainland. A barrier island system includes numerous distinctly different but closely related sedimentary environments. The most seaward of these environments is the beach/nearshore, which extends from across the surfzone up to the seaward limit of vegetation at the base of the dunes. The dune environment represents the only totally subaerial element of the barrier system, although both the beach and washover fan environments typically have some supratidal component. Some barriers have no true dunes, due to lack of sediment or rapid sea-level rise which creates too much overwash (Roy et al. 1995). Landward of the dunes are washover fans which, in combination with the dunes and beach/nearshore environments, comprise the sand-dominate systems of the barrier island itself. Most barrier islands are breached at various locations by subtidal channels, i.e. tidal inlets. These tidal inlets can include three distinctive sedimentary environments: flood-tidal deltas, inlet channel fill, and ebb-tidal deltas. The wetlands that separate the barrier island from the adjacent mainland commonly include both intertidal and subtidal environments. The upper part of the intertidal zone may be vegetated as a salt marsh. Below this elevation is the tidal-flat and the tidal-channel environment, which borders both the landward side of the barrier island and the mainland coast.

7.1.2 Barrier morphology under different wave and tidal conditions, and influenced by embayment geometry

Relative wave and tide influence

It is generally assumed that barrier islands and associated environments only develop along microtidal (<2 m) and mesotidal (2-4 m) coasts, and are absent on macrotidal coasts (>4 m) (Hayes 1979, Reinson 1992, Boggs 1995, Galloway and Hobday 1996). Microtidal coasts are characterised by well-developed, narrow and long, nearly continuous barriers, with few and unstable tidal inlets, which have typically small or no ebb-tidal deltas but large flood-tidal deltas (Fig.7.1D). The barrier islands are separated from the mainland by a lagoon (Reinson 1992, Davis 1994). Lagoons are back-barrier

bays that have little or no freshwater influx and that are not influenced by tidal circulation (Davis 1994). Mesotidal barrier islands tend to be wide, shorter and stunted, characterised by large well-developed tidal inlets and tidal deltas (Reinson 1992). As the tidal range increases, so does the ease of sediment transport (Swift et al. 1991). And abundant sediment is transported via the numerous inlets from the shoreface into the back-barrier, where it aggrades as broad tidal flats and shoals cut by numerous tidal channels (Galloway and Hobday 1996) (Fig. 7.1C). So the barrier islands are not separated from the mainland by a lagoon, but by tidal flats or marshes, i.e. a tidal estuary which experiences tidal processes but with no appreciable freshwater input via a river (Davis 1994). Along macrotidal coasts extreme tidal ranges cause wave energy to be dispersed and dissipated over too great a width of shore zone to effectively form barriers (Boggs 1995, Galloway and Hobday 1996) (Fig. 7.1B).
But, according to Davis (1994), it is the *relative* role of wave and tidal processes which is the critical factor in the development of the overall coastal morphology, including, but not restricted to, barrier islands (Davis 1994). It are not the *absolute* values of wave height or tidal range that are significant, only the relative influence is. Whether a region has a microtidal or macrotidal range, if the wave energy is insufficient to overcome the tidal currents and/or the tidal prism is large (Hayes 1979, Davis and Hayes 1984 in: Dalrymple et al. 1992), the region is tide-dominated and barrier islands will not develop (Davis 1994). Wave-dominated coasts typically have well-developed barrier islands (the former believed microtidal case) and tide-dominated coasts have no barrier islands (the former believed macrotidal case). Mixed-energy coasts where both waves and tides have significant influence also have barrier islands (the former mesotidal case) (Fig. 7.1BCD). Indeed, barrier islands are mostly absent on macrotidal coasts, but e.g. in the Bay of Fundy at Scots Bay, a wave-dominated coast developed where the tidal range is nearly 10 m (Davis and Hayes 1984 in: Davis 1994). Conversely, the Big Bend and the Ten Thousand Islands areas of the Gulf Coast of Florida are tide-dominated and without barriers, although their tidal range is well within the microtidal range (Davis 1988 in: Davis 1994).

The situation on the BCS during the barrier formation: mixed wave-tide processes

Around 9500 cal BP a barrier formed on the BCS, behind which a complex of estuaries and tidal basins could develop. Often, these tidal basins formed in the paleo-valleys of an existing drainage pattern with rising sea level (e.g. the IJzer). Baeteman et al. (1999) consider these tidal basins as small tide-dominated estuaries, in the sense of Dalrymple et al. (1992). This would imply again an embayed coastline during the Holocene comparable to the Eemian (Fig. 7.1B). However, these estuaries were much smaller and shallower than the tide-dominated estuary of the Ostend Valley. E.g. their widths were ten times smaller then the Ostend Valley (2 km *vs* 20 km). Moreover, the low-lying divides between the thalwegs were easily drowned by the rising sea level, which caused soon the disappearance of the typical funnel shape of a tide-dominated estuary and the transformation of the small estuaries in larger tidal basins (Beets and van der Spek, 1999). But especially the presence of a coastal barrier points to a linear coastline, even when the barrier is cut by numerous tidal inlets (Fig. 7.1C or D). The coastline during the Holocene is therefore considered linear, in contrast to the situation during the Eemian.

According to Baeteman (1999) a lagoonal environment was never installed in the Belgian Coastal Plain, as no evidence of lagoonal sedimentation was ever found. Instead, vegetation horizons formed on supratidal flats. This indicates that the Belgian Coastal Plain has always been characterised by a sediment supply that was sufficiently high to fill the created accommodation space in the back-barrier area to at least an intertidal level, even during rapid relative sea-level rise (Baeteman 1999). So, most likely, mixed wave-tide processes prevailed during the formation of the barrier in our regions (Fig. 7.1C).

Under combined influence of both waves and tidal currents, barrier islands are only a few kilometres long (up to 15-20 km, Davis 1992), inlets are numerous and rather stable in size and location, and ebb-tidal deltas are prominent (Davis 1994). The relative large tidal prism or tidal budget causes formation of a substantial ebb-tidal delta. The general form is that of a seaward-extending, arcuate morphology that impacts upon incident wave direction and energy. Waves are refracted around the ebb delta causing a local reversal of longshore current direction on the downdrift side of the tidal delta. As a result of this divergence of longshore currents, a considerable part of the littoral drift sediment budget is trapped in the lee of the ebb-tidal delta, causing that end of the barrier to be a sediment sink. The consequence of this divergence of littoral drift is that some of the sediment is robbed which would otherwise be carried downdrift to the opposite end of the barrier island. This causes a shortage of sediment to that end of the island and typically it experiences washover due to lack of a wide beach and dunes.
In a situation of combined wave and tidal currents, waves cause erosion, permit deposition, and provide temporary suspension for sediment which can then be transported by currents. Tidal currents may cause erosion and deposition as well, but especially carry sediment through the inlet systems (Davis 1994). Wave-generated longshore currents represent an important distributing mechanism for sediments along the beach and nearshore zone. Waves may also overtop barriers and create landward directed currents.

Embayment geometry influence

Apart from wave and tidal currents, the barrier shape is also influenced by embayment geometry and accommodation space. Even with similar barrier sand volumes, very different surface morphologies are produced in embayments with shallow, gently sloping substrates, compared with embayments with deeper and steeper slopes, which probably experience higher energy waves. In case of a shallow, gently sloping substrate, as is the situation on the BCS, where the Top-Pleistocene has a slope of less than 0.5° (between 0.018° and 0.042°), the barrier is wide but thin (in height), and the back-barrier area is shallow and narrow. In case of a steep substrate, the barrier is narrow, but thick (high), and the back-barrier area is wide and deep (Roy et al. 1995).

7.1.3 Barrier migration in function of sea-level rise and sediment supply

The balance between the rate of relative sea-level rise and sediment supply defines whether a coast recedes (retreats), is stable or progrades (Beets and van der Spek 2000). In a tide-dominated back-barrier basin, the tidal prism, and consequently the transport capacity is directly affected by changes in accommodation space. And as all or most sand brought into the back-barrier basis is derived form the shoreface of the barrier, an increase in accommodation space means erosion and retreat of the barrier.
The size of the back-barrier basin, which is function of the slope of the pre-transgressional surface, and the rate of the relative sea-level rise are the main factors defining the accommodation space (Beets and van der Spek 2000). As long as there is accommodation space in the back-barrier basin, the tidal prism sets up tidal currents that bring sand and mud to fill up this space. If insufficient sand is supplied to the shoreface by longshore and cross-shore transport to compensate for this sediment loss, the shoreline is forced to recede.

Along the Belgium coast, prior to 7500 cal BP, sediment supply did not outrun the created accommodation space created by the rapid relative sea-level rise (0.7 cm/a), as the barrier retreated, but was high and constant enough to prevent the barrier from drowning and to put off the creation of a lagoon in the back-barrier area. The barrier transgressed in a dynamic equilibrium with rising sea level, by the landward transfer of

sand, eroded from the shoreface to the back-barrier. When the rate of relative sea-level rise dropped to 0.4-0.25 cm/a around 7500 cal BP, sediment supply could gradually catch up with the relative sea-level rise, resulting in the closure of associated tidal inlets, stabilisation and later even progradation of the adjacent coast (Beets and van der Spek 2000). Around 5500 cal BP the rate of relative sea-level rise decreased to less than 0.1 cm /a, and almost the entire Belgian Coastal Plain changed into a freshwater marsh with peat formation. In the western Coastal Plain, the barrier started retreating again from 2400 cal BP onwards (Baeteman 2005b), as the sediment supply was insufficient to compensate for the created accommodation space. The accommodation space was this time not created by the relative sea-level rise, since after 5500 cal BP the relative sea-level still rose with the same strongly reduced trend, but due to compaction of the peat which induced an increase in tidal prism (Baeteman 2005b).

7.1.4 Barrier transgression (retreat)

Barrier roll-over mechanism

Barriers do not remain in place, but migrate landward as relative sea-level rises rapidly with respect to the rate of sediment input. The process of barrier migration is well described in Swift et al. (1991). Migration of a barrier is accomplished by a movement of sand described as 'barrier roll-over' (Leatherman 1983) (Fig. 7.2). Sand eroded from the shoreface moves on to the beach under the impulse of wave surge. Sand is blown from the beach across the barrier onto the back-barrier environment, and also storms transport sand landward as washover fans (Fig. 7.3A). The net effect of these processes is an upward building of the barrier. The cycle, however, has also an important horizontal component (Leatherman 1983), in which sand moves along the surf zone of the barrier and into an inlet, where it is stored in a tidal delta (Fig. 7.3A). Inlets may migrate down-drift, and new inlets form as others close. Eventually much of the back-barrier area consists of joined tidal deltas of varying ages, which extend the barrier landward, forming a back-barrier platform (Fig. 7.2B). Movement of the barrier's shoreline tends to be discontinuous over time-scales of several thousand years. When eventually a major event erodes back the shoreface, former washover fans re-emerge at the shoreface (Fig. 7.3A). Much of the resulting sand is dumped on, i.e. 'rolls over', the barrier top and back-barrier platform (Fig. 7.2C). And the cycle of platform building and inlet formation then begins anew. The erosional surface cut by the retreat process is the shoreface ravinement surface.

Barrier sediment sources

Migrating barriers mainly obtain their sand from the substrate over which they migrate, and not from the barrier shorefaces, which are only secondary sources, as the erosional retreat mainly recycles washover sand originally deposited at the back of the barrier (Swift et al. 1991) (Fig. 7.3A). The lower portion of the barrier shoreface may erode into back-barrier muds that have been overridden in the retreat process, but it generally cannot reach the antecedent substrate (Fig. 7.3B). Tidal inlets, however, commonly are primary sources of sand. They may scour down as deep as 15 or 30 m, make contact with the antecedent substrate, and release large amounts of sand from the previous depositional cycle (Fig. 7.3A).
An additional sand source is the along-shore flux. During every storm, sand is moved off the beach, but tends to return during fair-weather periods, carrying contributions from along-shore flux with it (Fig. 7.3A). However, during peak storm flow, sand may be swept down the shoreface to be incorporated into the leading edge of the transgressive sand sheet on the shoreface ravinement surface (i.e. 'sawdust' due to shoreface erosion as Swift et al. 1973 express it), where it is permanently lost from the littoral system (Swift et al. 1991) (Fig. 7.3A).

The fine-sediment dispersal in the back-barrier environment is coupled only loosely to the coastal sand budget. The immediate source of fine sediment is the nearshore turbid zone on the adjacent shelf where it is kept in suspension by wave stirring, and is trapped against the coast by baroclinic coastal currents and by the weak estuarine circulation characteristics of the inner shelf (Swift et al. 1991). The ultimate source is the ebb-tidal effluent of upstream estuaries and inlets, and shoreface erosion of older Holocene lagoonal or tidal-flat deposits overrun by the barrier (Fig. 7.3B).

It is calculated by Beets and van der Spek (2000) that all clastic sediments in the coastal plain of Belgium and the Netherlands is derived form only three sources: an alluvial source, the Pleistocene basement eroded during recession of the shoreline, and the North Sea by tide-induced shore-normal currents. The contribution of rivers hardly surpasses 10%, while 90% of the sediment stored in the coastal plains is derived from the Pleistocene basement and the North Sea.

Barrier sediment distribution

Both the sand and fine-grained sediment which were brought into the back-barrier area, are redistributed via a complex back-barrier dispersal system (Fig. 21 in: Swift et al. 1991), and are used for the upsilting of mud and sand flats up to supratidal level, and the infilling of tidal channels. The upper part of the intertidal zone and the supratidal zone may be vegetated as a salt marsh. In a final phase, even fresh-water marshes can develop, in areas no longer influenced by the tide (when upsilted above spring tide).

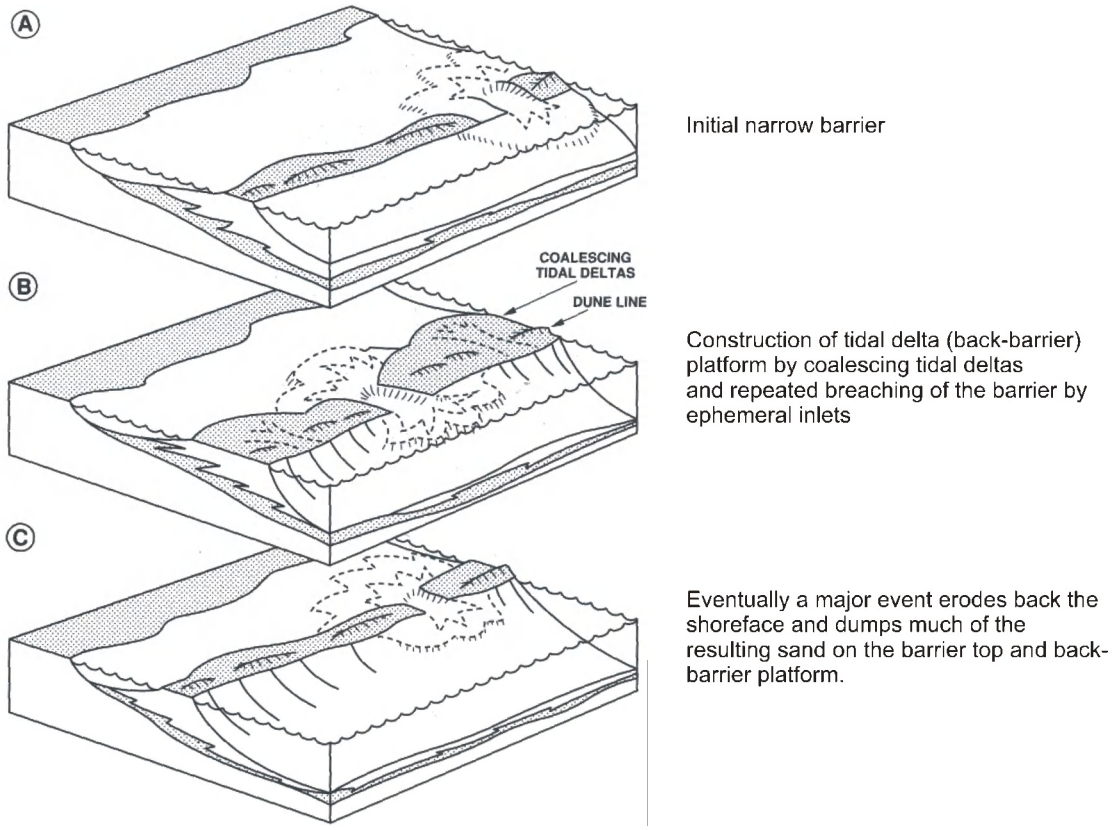

Fig. 7.2 Subsequent steps in he process of barrier migration accomplished by a movement of sand described as 'barrier roll-over' (Leatherman 1983 in: Swift et al. 1991).

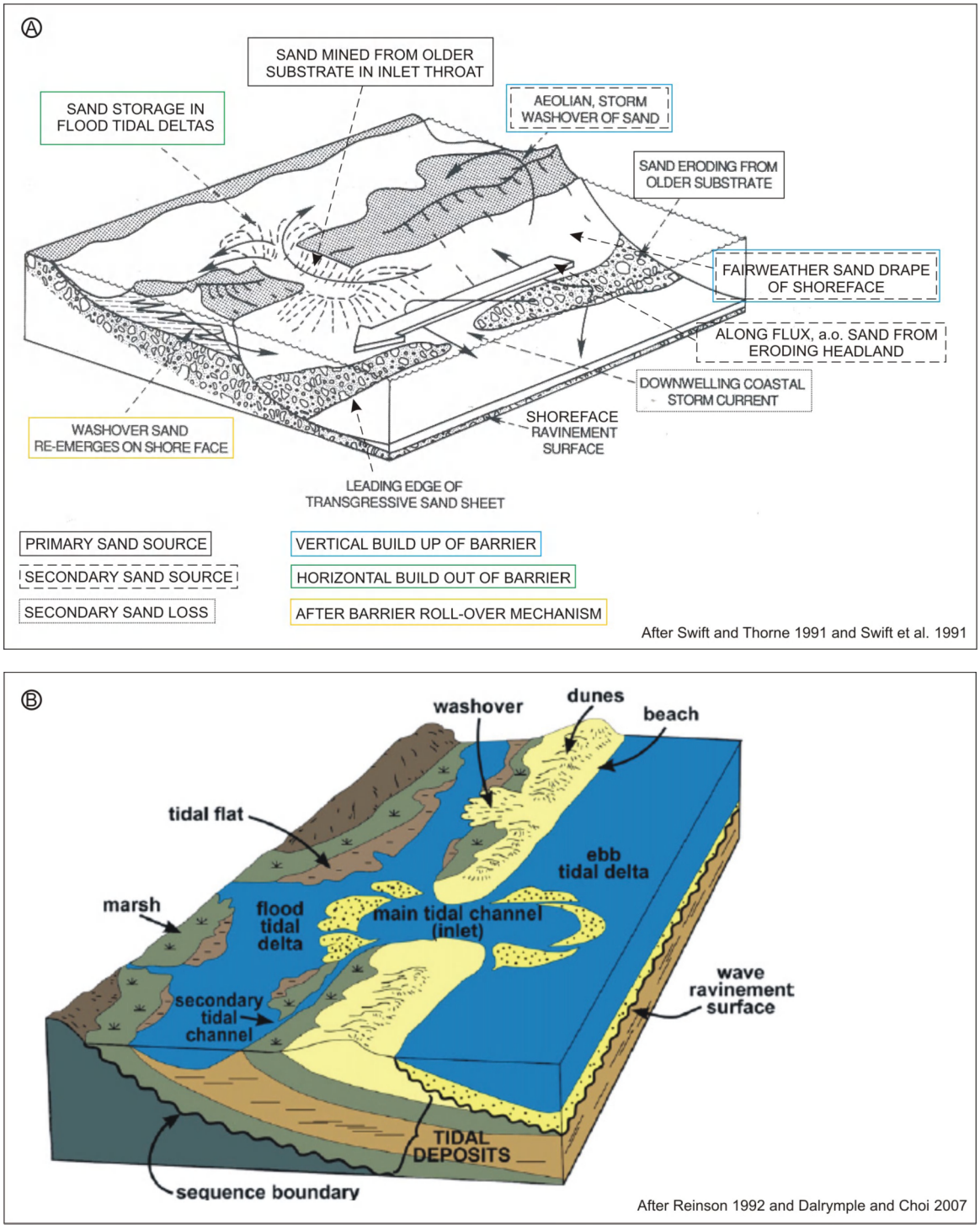

Fig. 7.3 Sand budget of a migrating barrier. Rising sea-level causes an upward and landward translation of the shoreface profile. The barrier top cycles in roll-over fashion by storm washover, burial, and re-emergence on the shoreface. Sand is eroded from the shoreface by downwelling along-coast storm currents. Storm-eroded sand is swept over the barrier and into the inlet. It also moves seaward to join the leading edges of the transgressive shelf sand sheet. But part of it tends to return during fair-weather periods, carrying contributions from along-shore flux with it. Migrating barriers mainly obtain their sand from the substrate over which they migrate (A), or in case overridden back-barrier muds still cover the substrate (B), from tidal inlets which deeply scour into the antecedent substrate. Whether former back-barrier muds are preserved after barrier transgression depends on the rate of relative sea-level rise, the slope of the substrate and the sediment budget. (A) Adapted after Swift and Thorne (1991) and Swift et al. (1991). (B) Adapted after Reinson (1992) and Dalrymple and Choi (2007).

Influence of rate of relative sea-level rise, slope and sediment budget on barrier retreat

The rate of relative sea-level rise determines the preservation potential of back-barrier deposits after shoreface ravinement (Reinson 1992, Davis 1994). Assuming all other factors to be constant, if sea-level rise is slow, the barrier system may be completely destroyed. The only stratigraphic record will be a thin layer of back-barrier facies resting unconformably on older sediments, truncated by the ravinement surface, which in turn are overlain by offshore storm deposits. While rapid sea-level rise permits nearly total preservation and in place drowning of the barrier, so that almost complete transgressive sequences are preserved.
Roy et al. (1995) deduced that the rate of sea-level rise determines the continuity of barrier migration. Barrier migration is fairly continuous when sea level is rising relatively rapidly, but may become intermittent, with hiatuses of many hundreds of years, when it slows down.

According to model results of Roy et al. (1995), the barrier retreat rate strongly depends on the substrate slope. On gentle slopes, rates of coastal recession are high and there is an onshore transfer of sand with the migration of transgressive barriers. In contrast, on relatively steep substrates, the coast is in encroachment mode and rates of coastal recession are slow. Sediment moves offshore to the lower shoreface, and is lost to the barrier which consequently loses volume.

A migrating barrier is supplied with sediment from relatively short-lived point sources (tidal inlets and the substrate), as only 1-10% is extracted form the littoral drift, which is in the same order as the loss during peak storm flows. When local sand sources are not available, the barrier must rely on its banked sand supply to balance offshore and back-barrier losses. As it withdraws this capital, the barrier becomes lower and thinner. And if a new source of sediment supply is not reached in time, the stored sand of the barrier is exhausted, an the barrier is overstepped (Swift et al. 1991).
Also Roy et al. (1995) investigated the role of sediment budget on a migrating barrier. In case of a balanced sediment budget the dimensions of the transgressive barrier and its rate of landward migration remain constant with time, provided that the substrate slope and rate of relative sea-level rise are unchanged. The ravinement surface in case of a balanced sediment budget corresponds closely to the original land surface. With a negative imbalance and the same boundary conditions, landward barrier migration occurs at a similar rate, but the toe of the shoreface erodes into the underlying substrate, and the barrier is significantly smaller. The reverse is true for a positive sand imbalance. Excess sand, originally deposited in back-barrier environments, is left as a sand sheet on the shelf surface after the transgression passes and the barrier itself is considerably larger.

7.1.5 Barrier progradation

If sediment supply outruns the relative sea-level rise, barriers start to prograde seaward and form a regressive barrier or barrier complex. A regressive barrier, composed of multiple parallel beach ridges, is similar to a strandplain, but the latter is much wider and connected to the mainland. Strandplains also lack extensive enclosed lagoonal environments and tidal channels. As regressive barriers build seaward, the associated lagoon, estuary or marsh and tidal channels commonly fill in, and the barrier develops into a strandplain (Reinson 1992). The regressive or prograded part of the barrier is composed of sand winnowed from the adjacent shelf and/or carried along by littoral currents. If the slope over steepens, breakdown can occur (Roy et al. 1995)

7.2 Observations

7.2.1 Seismic-stratigraphy

After the general description of the main observations in Chapter 4, seismic units U4, U5 and U6 are described in more detail in this chapter. These units all three extend outside the incised valley over large parts of the BCS and are located in the nearshore area (<30 km offshore), which has the highest density of seismic data and core distribution. Therefore this area can be described and discussed in great detail.

Seismic unit U4: extensive sheet-like deposit

Unit U4 is the first of the discussed seismic units with a large lateral extent. Its distribution is no longer determined by the presence of the Ostend Valley, as was the case with units U1 to U3, but it extends over the entire width of the BCS and up to the present-day coastline. Despite its regional distribution, it is a relative thin unit: 53% of the unit is less than 3m thick, which makes it difficult to define its original form and its internal facies. The shape and thickness of this unit are strongly determined by the shape and depth of the underlying surface, which is a combination of the upper bounding surface of U3 and QT, i.e. the Top-Pleistocene surface. Furthermore, the upper boundary of U4 clearly bears the imprint of the overlying unit U5 (Fig. 7.5BC) and the present-day bathymetry, formed under the modern hydrodynamic conditions (Fig. 7.5D).

As discussed in the previous chapter (section 6.3.2), the morphology of the Top-Pleistocene surface is characterised by a distinct scarp and by a shallow remnant of a river incision (Fig. 7.4A). On the one hand, these features determine the shape of seismic unit U4 (e.g. U4 is relative bulkier above the scarp than north or south of it (Fig. 7.4C)), but on the other hand, also U4 itself determines the shape of the Top-Pleistocene surface by the channels that are incised into it (Fig. 7.4B). Between De Panne and Nieuwpoort, the Top-Pleistocene surface shows a depression which is -at least partly- formed due to incisions by internal channels of U4. Near the Vlakte van de Raan, U4 is too thin for channels or other erosional features to be discerned by the seismic data, but also here a depression is present in the Top-Pleistocene surface below U4. So either this depression was already formed during the Pleistocene before U4 was deposited, or it was formed during deposition of U4. At the Ostend Valley, some of the channels of U4 coincide with the remnant depression in U3, which was interpreted as the Weichselian renewed river incision in the Ostend Valley (Fig. 7.4A), but elsewhere this depression is clearly not related to the channels of U4. Most likely the channels of U4 followed the easiest course of an earlier river bed.

Fig. 7.4 (page 147) (A) The Top-Pleistocene surface, composed of QT and the top bounding surface of U3, with indication of internal channels of overlying unit U4. The surface shows a number of depressions below U4 (contour dark blue). So, either these depression were already formed during the Pleistocene before U4 was deposited, or they were formed during/due to the deposition of U4. At the Ostend Valley, some of the channels of U4 coincide with the depression in U3 interpreted as the Weichselian renewed river incision. Most likely the channels of U4 followed the easiest course of an earlier river bed. So U4 clearly influences the shape of the Top-Pleistocene surface. (B) An example of an internal channel of U4 incising into the Pleistocene substrate. (C) On the other hand, U4 itself is also influenced by the shape of the Top-Pleistocene surface. North of the slope break (scarp) in the Top-Pleistocene surface, U4 is much thicker than south of it. (B) and (C) are interpreted seismic profiles. The original seismic profiles are shown in Figs. 4.6A and 4.6C, respectively.

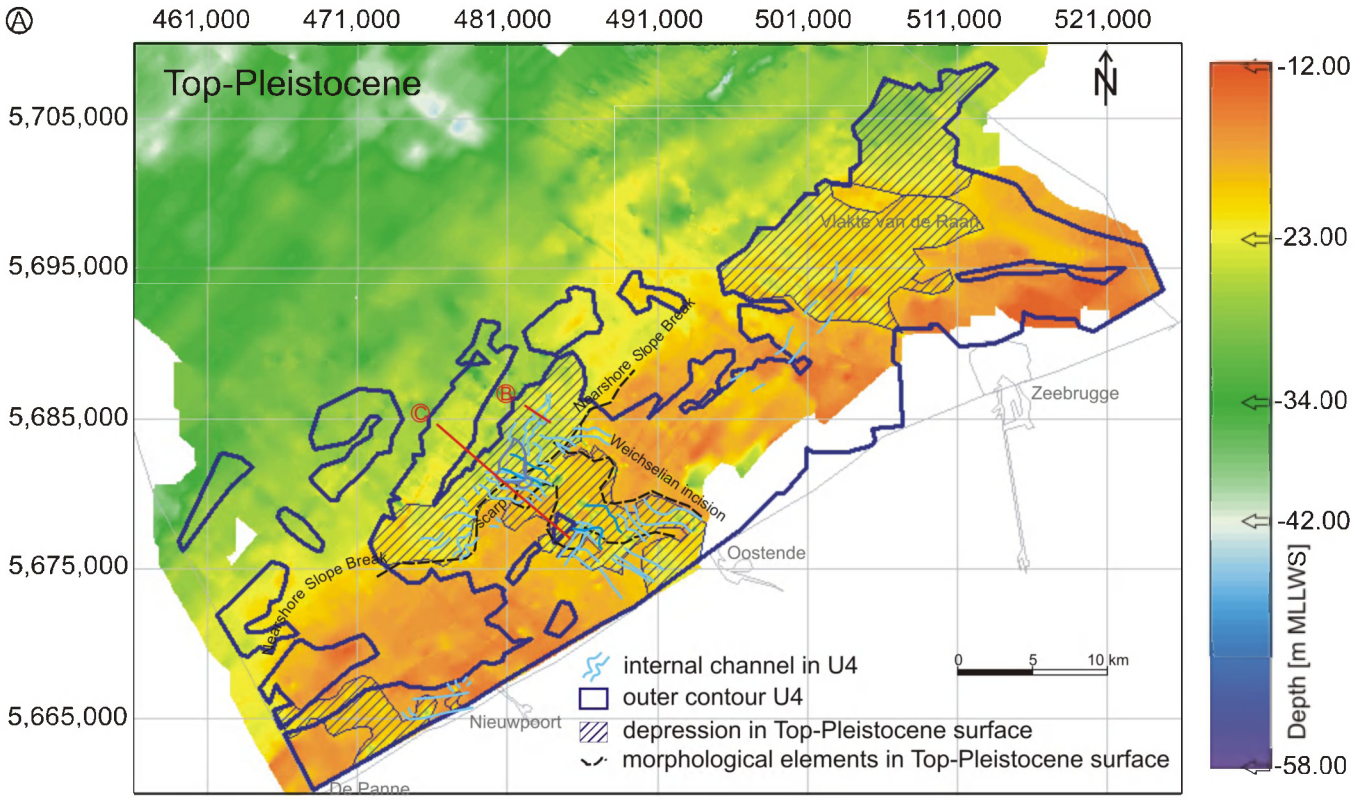
Ⓐ
461,000
471,000
481,000
491,000
501,000
511,000
521,000
5,705,000
5,695,000
5,685,000
5,675,000
5,665,000
Top-Pleistocene
Vlakte van de Raan
Nearshore Slope Break
Weichselian incision
Scarp
Nearshore Slope Break
Zeebrugge
Oostende
Nieuwpoort
De Panne
internal channel in U4
outer contour U4
depression in Top-Pleistocene surface
morphological elements in Top-Pleistocene surface
0 5 10 km
-12.00
-23.00
-34.00
-42.00
-58.00
Depth [m MLLWS]

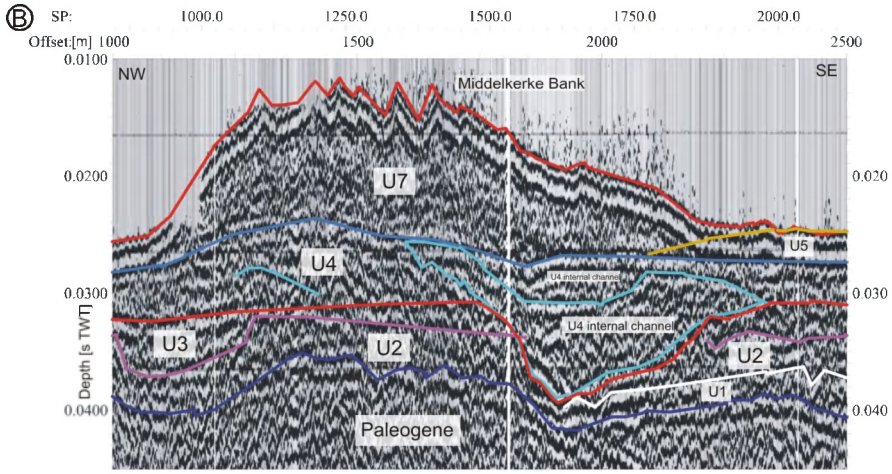
Ⓑ
SP:
Offset:[m]
NW
SE
Middelkerke Bank
U7
U4
U5
U3
U2
U1
U4 internal channel
Paleogene
Depth [s TWT]

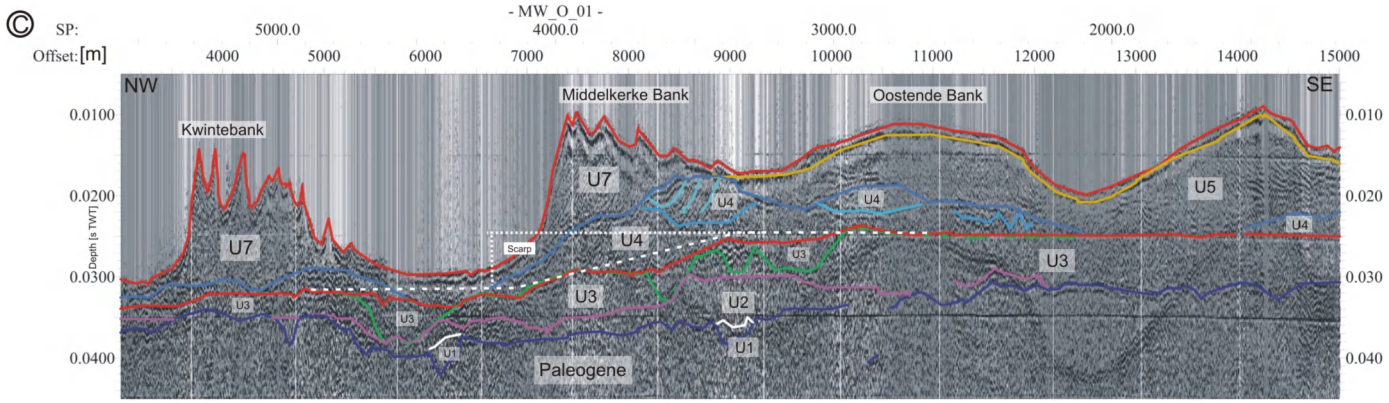
Ⓒ
- MW_O_01 -
SP:
Offset:[m]
NW
SE
Kwintebank
Middelkerke Bank
Oostende Bank
U7
U4
U5
U3
U2
U1
Scarp
Paleogene
Depth [s TWT]

In addition to these depressions, the Top-Pleistocene surface is also characterised by the presence of some highs. These also determine the shape of U4. E.g. offshore Zeebrugge and Nieuwpoort, the Top-Pleistocene surface lies shallow (-15 to -13 m MLLWS), and there U4 is very thin (2 m) or even absent.

Another reason for the limited thickness or even absence of U4 in some places, is the strong erosion by the overlying units, or before deposition of the overlying units. Fig. 7.5 shows the topography of the top bounding surface of U4 with the indication of i) where the overlying unit U5 fills in deep impressions in U4 (Fig. 7.5B), ii) where U6 seems to truncate U4 (Fig. 7.5B), and iii) where the upper unit U7 lies directly on top of U4 and seems to erode U4 (Fig. 7.5D). The figure also shows i) the areas where U4 is absent, but where it is expected to have been present based on the surrounding areas, and ii) which unit (U5 or U7) overlies U4 (and might be (partly) responsible for the erosion of U4. As Fig. 7.5 illustrates, little is preserved of the original top surface of U4. The modern hydrodynamic regime strongly influences the distribution of U4, and the scarp observed in the top bounding surface of U4 is clearly linked to the presence of unit U5 (Fig. 7.5C), which will be discussed in detail in the next section.

So, U4 is thickest and best preserved where U4 shows deep incisions, where the Top-Pleistocene surface lies deep enough, and where subsequent erosion before or during deposition of the overlying units was less severe, e.g. below the crests of the present-day sandbanks.
Where U4 is at least 4 m thick, internal structures could be observed (Fig. 7.6A). Some isolated channel structures are present in the coastal area near Nieuwpoort and 8 km offshore between Zeebrugge and Oostende. More continuous channels and large areas of prograding reflectors occur offshore Oostende. The internal structures could not be fully mapped in 3D or correlated over large areas, due to the limited thickness of unit U4, due to problems with the data quality and multiples, due to the presence of gas in the nearshore area, and due to the fact that several generations of overlapping channels occur, which cross each other or occupy the same thalweg (Figs. 7.6CD).
Fig. 7.6B shows the course of the channels and the direction of the prograding reflectors in the area offshore Oostende. The channels are restricted to two zones, separated by an area where U4 is less than 1.5 m thick. One zone is situated within 7 km from the present-day coastline, and a second zone between 10 and 15 km offshore. Two types of channel structures occur: i) NW-SE oriented channels, and ii) NE-SW oriented channels. The NW-SE channels in the coastal near zone have a width between 300 and 1500 m and a depth ranging between 5 and 16 m. Neighbouring channels alternately deepen in shoreward and seaward direction to depths of –20 to –27 m.

Fig. 7.5 (page 149) (A) The relief of the top bounding surface of U4 is strongly influenced by the overlying units (U5, U6, U7). There is also a zone defined where U4 does not occur (white background), but where it is expected to have been present based on the surrounding areas. Here U4 is most likely eroded by the next overlying unit. For U7, a distinction is made between erosion in the swales or erosion below the sandbanks. (B) The above lying unit U5 left locally deep imprints in U4. Before (or due to) the deposition of U6, U4 was sharply, horizontally truncation. (C) shows how the 'scarp' in the surface of U4 is clearly linked to the presence of U5. (D) Also the modern hydrodynamics strongly influence the extension and topography of U4. This mainly appears from the lacking of U4 in the swales between the sandbanks. But also below the sandbanks, the constructing hydrodynamic forces of U7 seem to have eroded part of U4. Fig. 4.12A illustrated this as well.

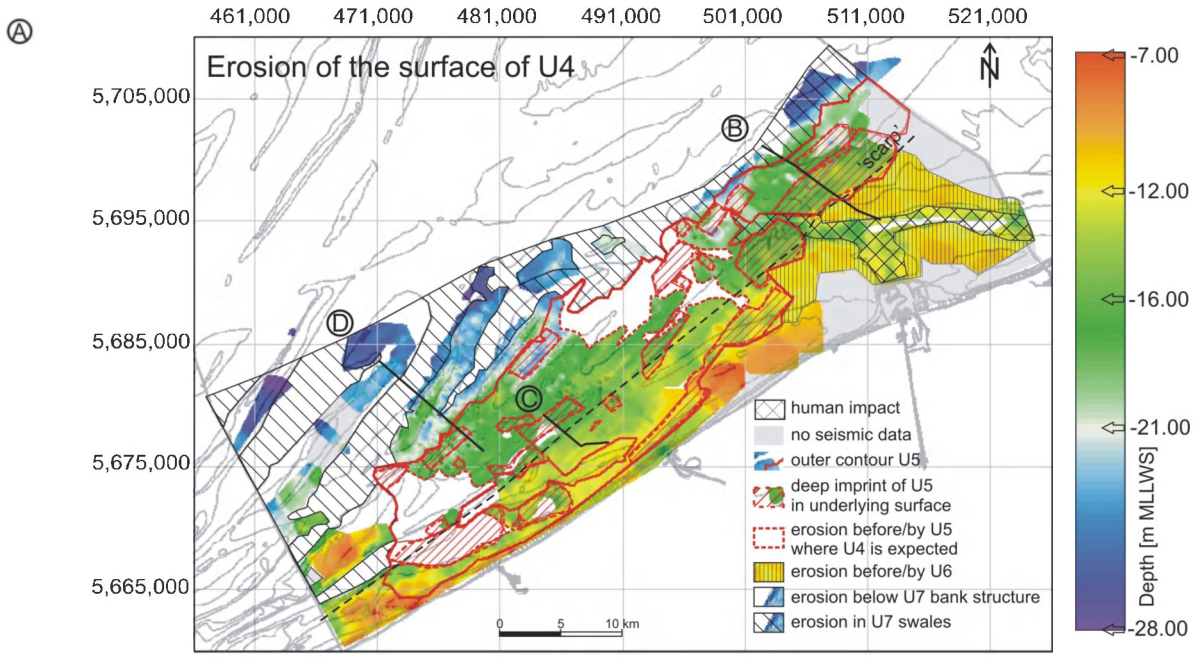
Ⓐ
461,000
471,000
481,000
491,000
501,000
511,000
521,000
5,705,000
5,695,000
5,685,000
5,675,000
5,665,000
Erosion of the surface of U4
Ⓑ
Ⓒ
Ⓓ
Scarp
human impact
no seismic data
outer contour U5
deep imprint of U5 in underlying surface
erosion before/by U5 where U4 is expected
erosion before/by U6
erosion below U7 bank structure
erosion in U7 swales
0 5 10 km
-7.00
-12.00
-16.00
-21.00
-28.00
Depth [m MLLWS]

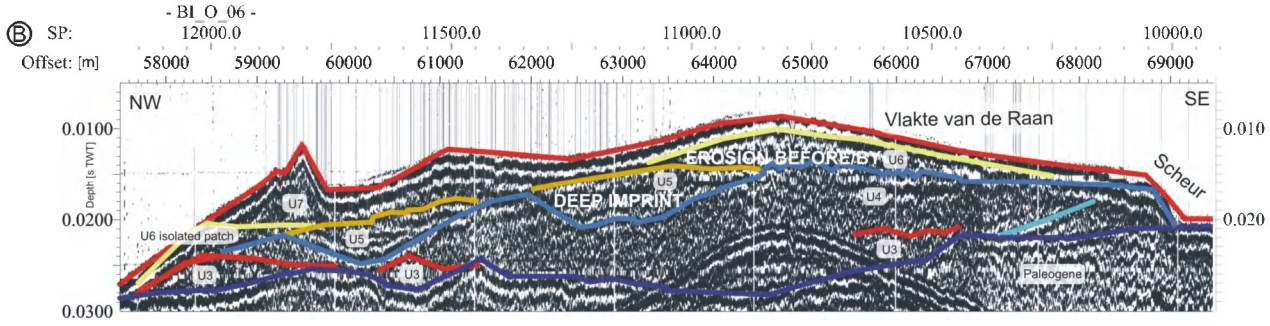
Ⓑ
- BI_O_06 -
SP:
12000.0
11500.0
11000.0
10500.0
10000.0
Offset: [m]
58000
59000
60000
61000
62000
63000
64000
65000
66000
67000
68000
69000
NW
SE
Vlakte van de Raan
EROSION BEFORE U6
DEEP IMPRINT
Scheur
U6 isolated patch
U7
U6
U5
U4
U3
Paleogene
Depth [s TWT]
0.0100
0.0200
0.0300
0.010
0.020

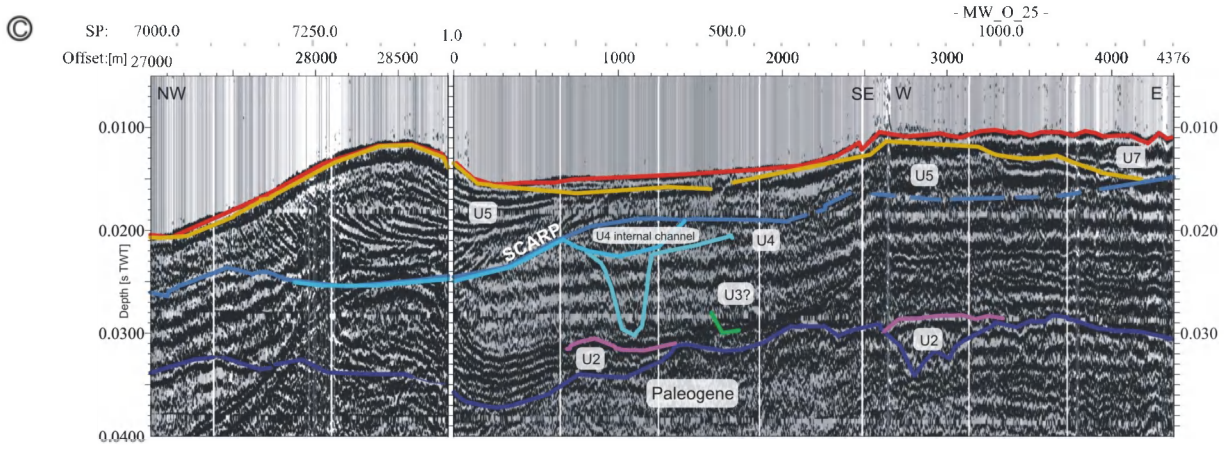
Ⓒ
- MW_O_25 -
SP:
7000.0
7250.0
1.0
500.0
1000.0
Offset:[m]
27000
28000
28500
0
1000
2000
3000
4000
4376
NW
SE
W
E
SCARP
U4 internal channel
U3?
U2
Paleogene
Depth [s TWT]
0.0100
0.0200
0.0300
0.0400
0.010
0.020
0.030

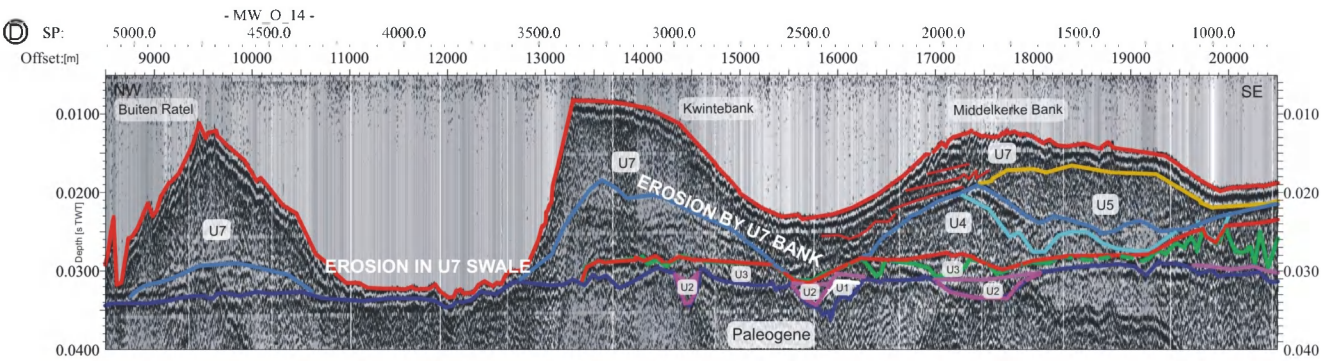
Ⓓ
- MW_O_14 -
SP:
5000.0
4500.0
4000.0
3500.0
3000.0
2500.0
2000.0
1500.0
1000.0
Offset:[m]
9000
10000
11000
12000
13000
14000
15000
16000
17000
18000
19000
20000
NW
SE
Buiten Ratel
Kwintebank
Middelkerke Bank
EROSION BY U7 BANK
EROSION IN U7 SWALE
Paleogene
Depth [s TWT]
0.0100
0.0200
0.0300
0.0400
0.010
0.020
0.030
0.040

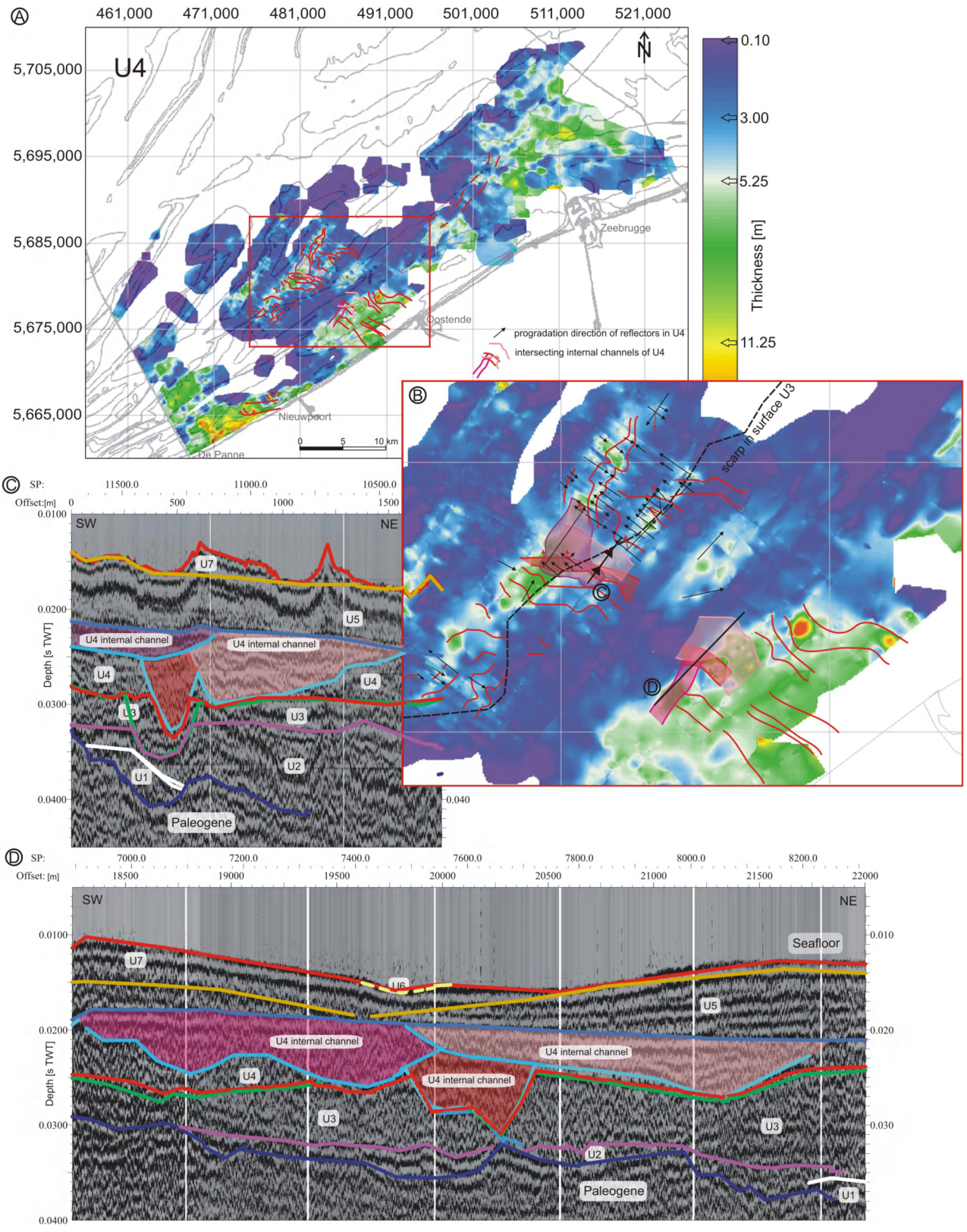

Fig. 7.6 (this page and next) (A) Isopach map of U4. Where U4 is at least 4 m thick, internal structures could be observed. (B) Detail of isopach map of U4, offshore Oostende, with indication of internal channels and prograding reflectors. The presence of a prograding reflection pattern on a seismic profile is indicated with a black arrow along the seismic line; the length of the arrow indicating the stretch over which this pattern is visible and the direction being indicative of the apparent dip direction. At the tie-points of two intersecting seismic lines the true dip direction is indicated with a little red arrow.

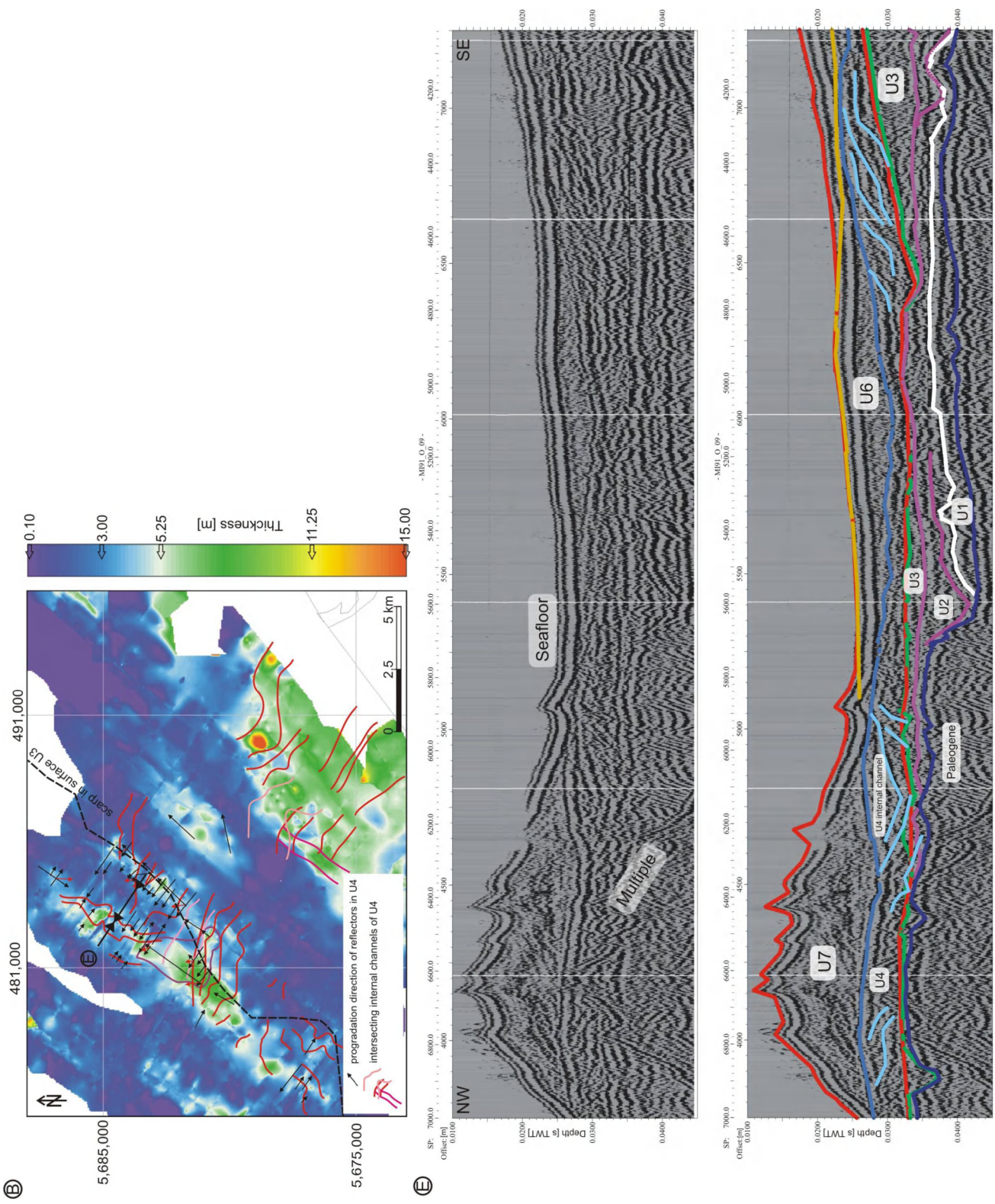

(C) Seismic section showing several overlapping channels. (D) Seismic section showing several overlapping channels. The offshore channel configuration (C), i.e. a deep incised narrow channel (red) alongside a wide shallow channel (light pink), is very similar to the one in the nearshore zone (D). Both configurations lie exactly in line, only separated from each other by thinning of U4 (cf. B). (E) A Seismic section, showing prograding reflection patterns on both sides of a channel and along the slope of the scarp in the underlying unit U3. The top section is the original seismic profile, the bottom section is the interpreted seismic profile. For positioning is referred to (B).

In the second zone, three NE-SW oriented channels occur. The channels are 600-1000 m wide, 3-10 m deep, and incised to depths of -22 to –30 m. There are also NW-SE channels, with a width of 400-1000 m, a depth of 3-9 m below the unit's surface, and incised from –20 to –26 m. Some of the offshore NW-SE channels (Fig. 7.6C) show a configuration that is very similar to that of the channels in the nearshore zone (e.g. a deep incised narrow channel alongside a wide shallow channel, Fig. 7.6D), and they lie exactly in line with the latter, only separated from them by a region where U4 is thinner (Figs. 7.6 BCD).

In the offshore zone, seismic unit U4 comprises also prograding reflectors outside the channels, in addition to the prograded fill in the channels. One of the most prominent zones of prograding reflectors is located along both sides of two NE-SW oriented channels (Figs. 7.6BE), where they apparently slope in the direction of the channels, although the true slope direction is overall northward. Another area with prograding reflectors is along the slope of the scarp in the underlying unit U3 (Figs. 7.6BE).

Seismic unit U5: local sequence of bank-shaped deposits

Seismic unit U5 is present along almost the entire present-day coastline of the BCS. It is the first seismic unit that directly underlies the present-day seafloor over a large area. Unit U5 occurs mainly in bank- and lens-shaped external geometries with a prograding (tangential and parallel oblique) or channel-like internal seismic reflection pattern, while in the nearshore zone the unit is more sheet-like or very thin and a transparent reflection configuration dominates. From a detailed 3D reconstruction of seismic unit U5, taking into account directions of internal reflectors and the depth of each structure, it became clear that the bank-like structures, lenses and sheets of which U5 consists, belong in fact to three parallel 'bank' structures in juxtaposition, which extend over the entire width of the BCS.

Fig. 7.7 shows how the sandbank-like structures change laterally into lenses, due to erosion either before or during deposition of the overlying unit or by the present-day hydrodynamic regime. In some places, a distinct bank shape has been preserved (Fig. 7.7H), while in other places only a lens of seismic unit U5 remains from the former structure (e.g. Fig. 7.7A).
Of the three parallel bank structures, two exhibit in transverse sections asymmetrical profiles with an offshore-facing gentle side and a landward-facing steep side. While the third, most landward bank-like structure, shows an offshore-facing gentle side as well, but no steep side (Fig. 7.7). Instead, the top of the bank is horizontal and forms a plateau that almost reaches the present-day coastline near Nieuwpoort (Fig. 7.7K). The three banks are smoothly connected.

Fig. 7.7 (page 153) Pseudo-3D reconstruction of seismic unit U5, consisting of 14 interpreted seismic profiles (U5 in colour) and a map presenting the topography of the surface of U5. The figure shows how the bank-like structures, lenses and sheets of which U5 consists, belong in fact to three parallel 'bank' structures in juxtaposition, which extend over the entire width of the BCS (in yellow: the outer bank, in orange: the middle bank, in brown: the nearshore plateau). In some places a distinct bank form is still visible (e.g. H), while in other places only a lens of seismic unit U5 is a witness of the former structure (e.g. A). Based on the characteristics of the most complete banks (position of the crest in relation to the form of the base and the internal reflection pattern), the contours of the original bank form of the remnants could be reconstructed (cf. Fig. 7.9). The supposed original bank form is indicated with an orange dashed line.

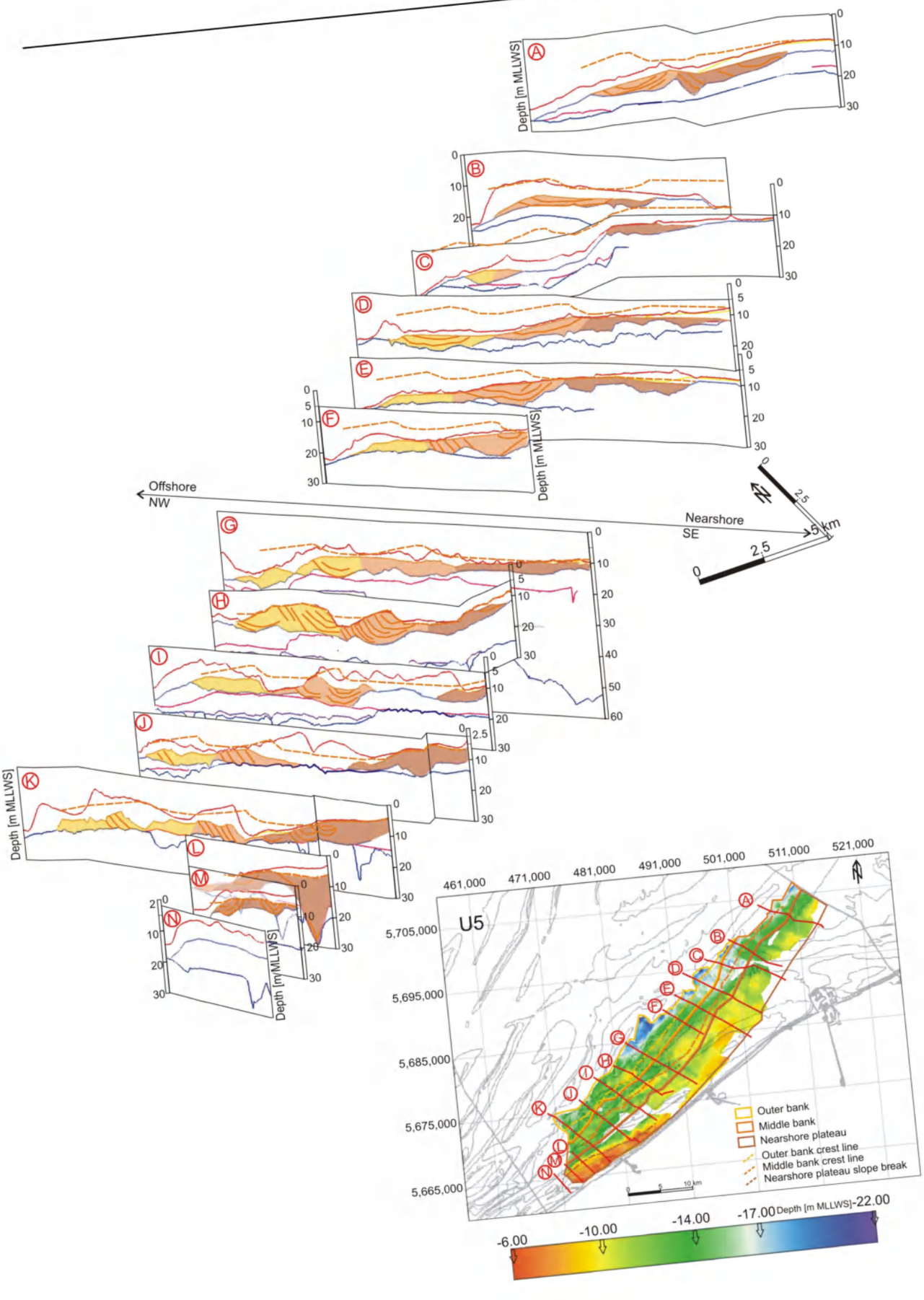
Depth [m MLLWS]
Offshore
NW
Nearshore
SE
5 km
U5
461,000
471,000
481,000
491,000
501,000
511,000
521,000
5,705,000
5,695,000
5,685,000
5,675,000
5,665,000
Outer bank
Middle bank
Nearshore plateau
Outer bank crest line
Middle bank crest line
Nearshore plateau slope break
-6.00
-10.00
-14.00
-17.00
Depth [m MLLWS]
-22.00

Assuming that the most completely preserved bank structures occur in the shallowest part of U5 (e.g. Figs. 7.8AC), a rough estimate of the depositional depth and of the geomorphological dimensions could be made (Fig. 7.8B). The depth of the bank crest lines decreases landward. The most offshore bank has a crest up to -9 m (-12 ms TWT) MLLWS, the middle bank has a crest up to -7.5 m (-10 ms), and the landward plateau culminates at -7.5 to -6 m (-10 to -8 ms) MLLWS. The depth of the interbank zones changes in landward direction from -12 to -10.5 m (-16 to -14 ms).

The best preserved parts of the outer, most offshore bank are 4 to 4.7 km wide, with a height of 8 m, measured below the crest. The middle bank is typically 2.5 to 3 km wide, with a height of 11-12.5 m. The distance between the crests of the outer and middle bank, measured along the seismic profiles, is 2.5-3 km. The third bank or plateau is 3.5 to 5 km wide and 7.5 to maximum 10 m high. The distance from the crest line of the middle bank to the start of the plateau is about 3 km. The slope of the gentle slopes, measured nearly perpendicular to the strike direction of the banks, is typically around 0.30% (0.17°), the steeper slopes dip at an angle of around 0.70% (0.40°) (Fig. 7.8B).

The bank structures show several different types of cross-sections (Fig. 7.9). Apart from the constantly changing top of the bank due to erosion, also the base of the bank changes laterally. The base can be flat and horizontal beneath most of the bank, slightly rising in landward direction below the steep slope (Fig. 7.9A), or the base can be wavy with the deepest part either located beneath the steep or beneath the gentle side (Figs. 7.9BC), or with similar depth below both sides (Fig. 7.9D). But apart from a few exceptions, the base below the steep slope always rises up in landward direction (Figs. 7.9ABCDE), also in the coastal-near, plateau-like bank (Fig. 7.7).
The internal structures of U5 consist of parallel straight, landward-prograding reflectors below the gentle slope of the bank, downlapping against the base reflector of the bank, and truncated at the top. These internal reflectors become progressively more tangential towards the middle of the bank, beneath the crest, until they appear as curved reflectors below the crest and steep side of the bank, onlapping on the rising base reflector (Fig. 7.9B), and finally as fully channel-like reflectors, more or less parallel with the base reflector, and truncated at the top. So, below the steep side of the bank, above the landward-rising base reflector, the internal reflectors can show a seaward prograding pattern (Fig. 7.9E). The landward prograding reflectors have a dip of about 1° (2%) below the gentle side, become progressively less steep (0.5° or 1%) to horizontal below the crest and steep side, and finally become seaward-sloping with a dip of about 0.5% (Fig. 7.9E) (all measured nearly perpendicular to the strike direction of the banks).

This typical seismic reflection pattern, and the characteristic form of the base of the bank, enabled us to trace the bank structures along almost the entire width of the BCS, from the practically complete bank structures between the Oostende Bank and the Stroombank, to the isolated lenses in the Vlakte van de Raan area.

Based on the characteristics of the most complete banks (position of the crest in relation to the form of the base and the internal reflection pattern), also the presumed crest lines of the remnants were reconstructed (e.g. Figs. 7.9BCD, Fig. 7.10). The crest line of the middle bank runs over a distance of 24 km in NE direction, after which it turns to the NNE over a distance of 25 km. The crest line of the most offshore bank is nearly parallel to that of the middle bank. The distance between the two varies between 2.5 and 5 km. The nearshore bank shows no crest, as no steep side is present, but the slope break of the plateau is indicated on Fig. 7.10.

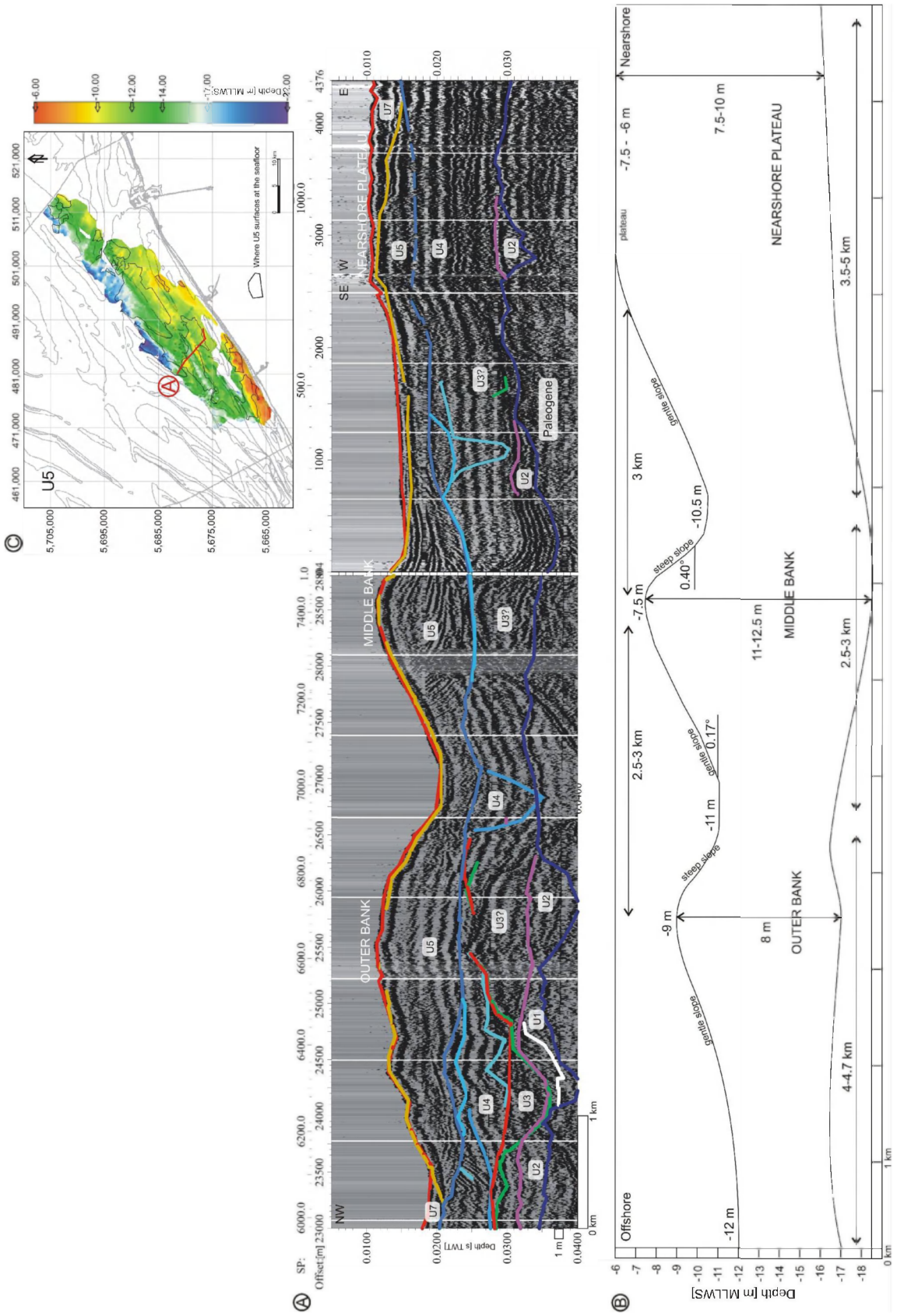

Fig. 7.8 (A) Example of a seismic profile showing three parallel bank structures in U5. This profile comprises the shallowest parts of U5 (cf. (C)), which are presumed to be least eroded. (B) The generalised depositional depth and geomorphological dimensions of the three bank structures, based on what was presumed to be the most complete bank structures. (C) Isobath map of the surface of U5, with positioning of seismic profile (A). Note the different horizontal and vertical scales in (A) and (B).

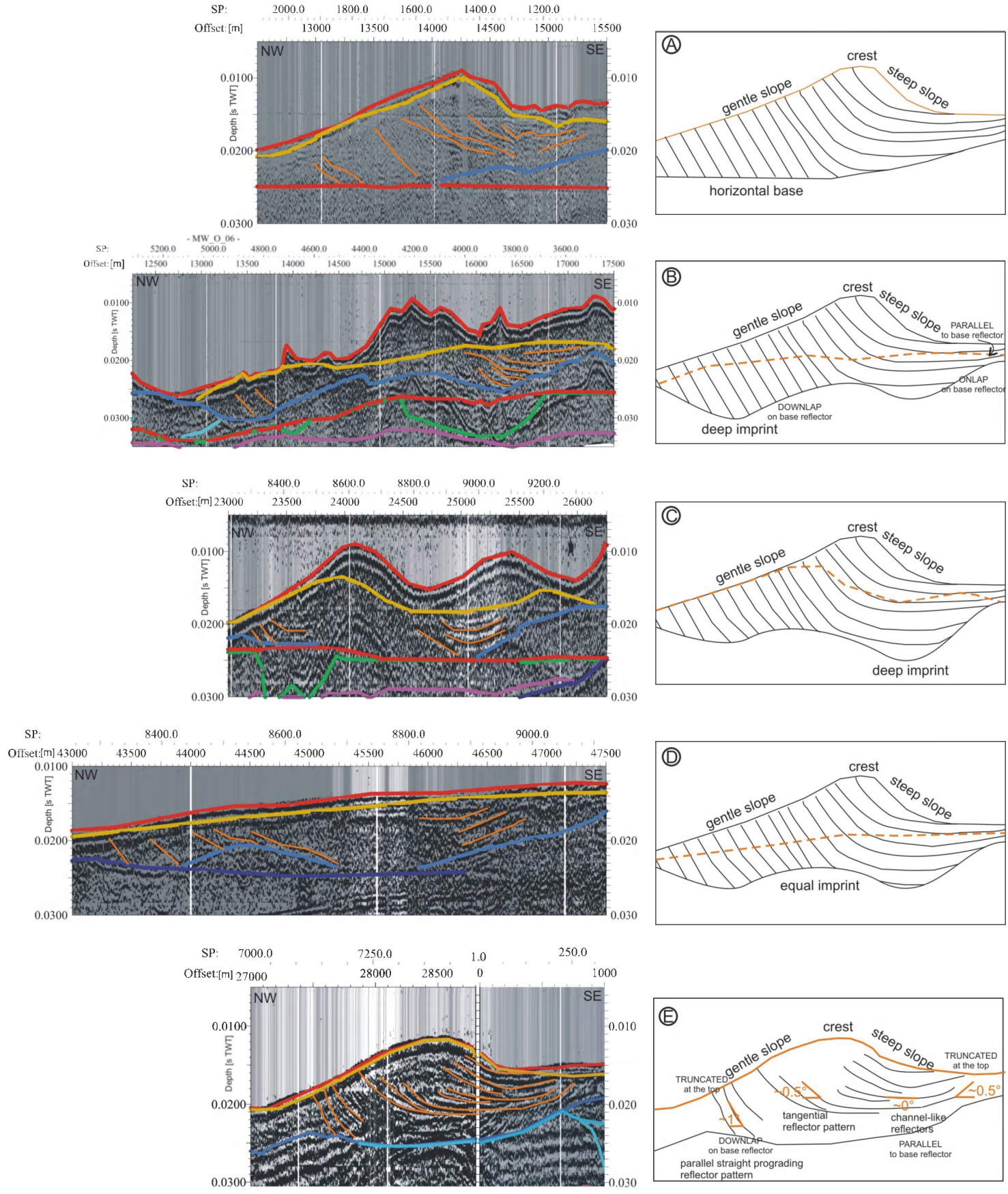
SP:
Offset: [m]
NW
SE
Depth [s TWT]
- MW_O_06 -
A
crest
steep slope
gentle slope
horizontal base
B
PARALLEL
to base reflector
ONLAP
on base reflector
DOWNLAP
on base reflector
deep imprint
C
D
equal imprint
E
TRUNCATED
at the top
~0.5°
~0°
~1°
tangential
reflector pattern
channel-like
reflectors
parallel straight prograding
reflector pattern

Fig. 7.9

Fig. 7.9 (page 156) Several types of cross-sections of the U5 bank structures. Apart from the constantly changing top of the bank due to erosion, also the base of the bank changes laterally over different cross-sections. (A) The base can be straight beneath most of the bank with a landward rising below the lee side. (B) The base can be wavy with the deepest section located beneath the gentle slope. (C) The base can be wavy with the deepest section located beneath the steep slope. (D) Or the base can be wavy, but equally deep below both sides. But apart from a few exceptions, the base below the steep side always rises up in landward direction. (E) Typical reflection configuration in a U5 bank structure, even when the bank structures are reduced to lenses, due to erosion (e.g. (B) and (D)). Left panels represent interpreted seismic sections, the right panels represent the corresponding schematised situation. Based on the characteristics of the most complete banks (position of the crest in relation to the form of the base and the internal reflection pattern), also the contours of the original bank form of the remnants could be reconstructed. The idealised reflection patterns in the right panels of (A), (B), (C) and (D) are based on the real situation in (E). Position of the seismic sections is indicated on Fig. 7.10.

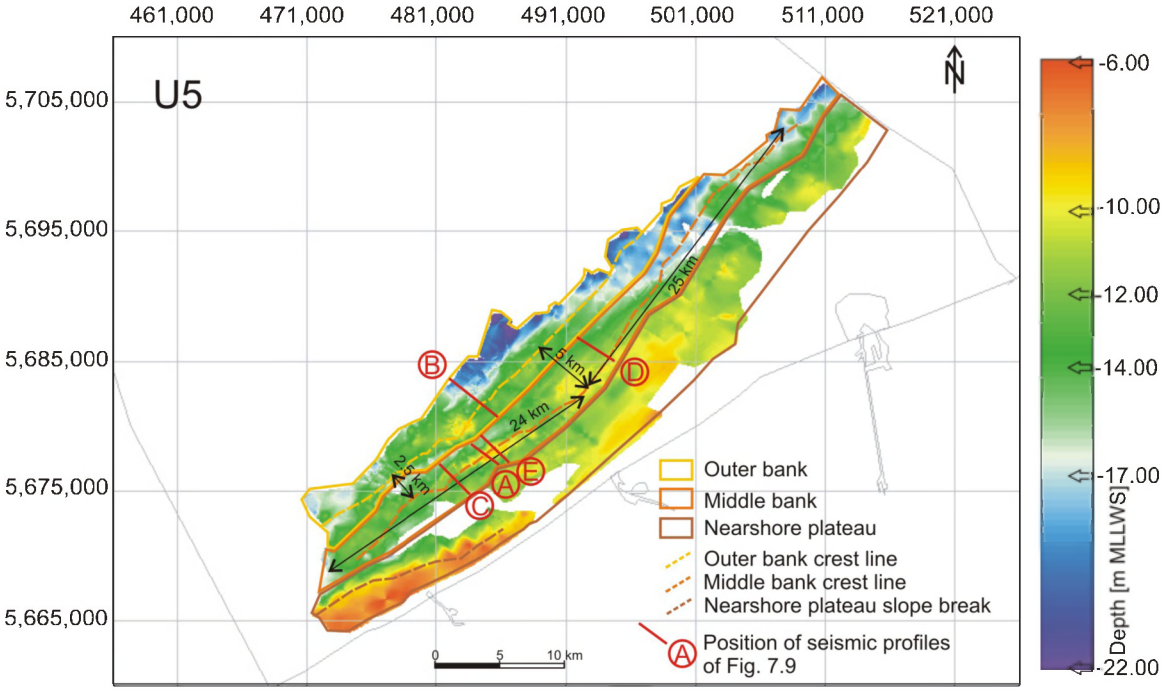

Fig. 7.10 Isobath map of the surface of U5, with indication of the three bank-like structures and the corresponding presumed crest lines. The presumed crest lines of the remnants could be reconstructed based on the characteristics of the most complete banks (position of the crest in relation to the form of the base and the internal reflection pattern). The coastal-near bank shows no crest as no lee side is present, but the slope break of the plateau is indicated on.

Fig. 7.11 (page 158) (A) An isobath map of the surface on which U5 lies, composed of the surfaces of QT, U3 and U4 (the contours of the extend of unit U5 are indicated in red). Along the stretch of the banks, the base has a wavy, undulating course. Not the base of the bank as a whole, but alternately below the gentle and steep side of the bank, the base has a deeper imprint in the subsurface. The colour bar is set up as such that the structural features in the nearshore area are enhanced. (B) Example of a seismic section showing how below the nearshore plateau depressions alternate with zones where U4 emerges. Note the channel-like internal reflectors in U5 in this area. (C) Seismic section almost parallel to the stretch of the middle bank. The internal reflection pattern is here a SW sloping progradation with only slightly dipping (<0.2%) reflectors.

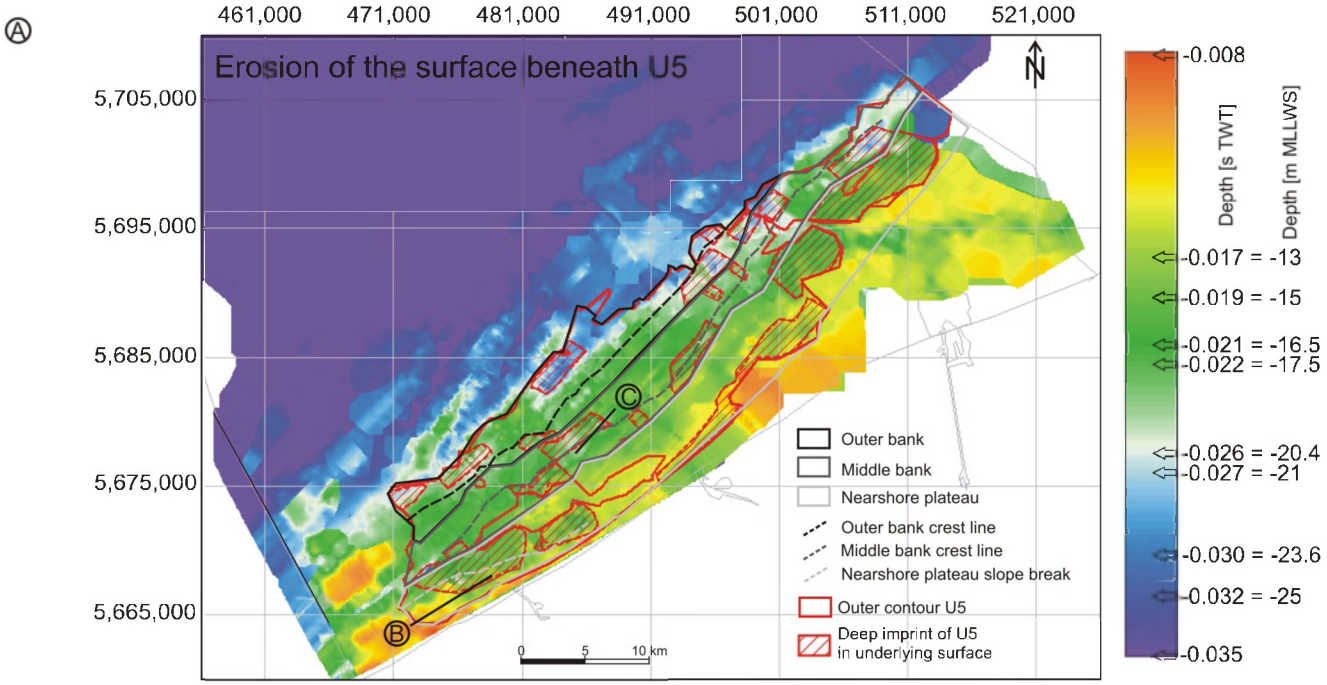
Ⓐ
461,000
471,000
481,000
491,000
501,000
511,000
521,000
5,705,000
5,695,000
5,685,000
5,675,000
5,665,000
Erosion of the surface beneath U5
N
Ⓒ
Ⓑ
0 5 10 km
Outer bank
Middle bank
Nearshore plateau
Outer bank crest line
Middle bank crest line
Nearshore plateau slope break
Outer contour U5
Deep imprint of U5 in underlying surface
-0.008
Depth [s TWT]
Depth [m MLLWS]
-0.017 = -13
-0.019 = -15
-0.021 = -16.5
-0.022 = -17.5
-0.026 = -20.4
-0.027 = -21
-0.030 = -23.6
-0.032 = -25
-0.035

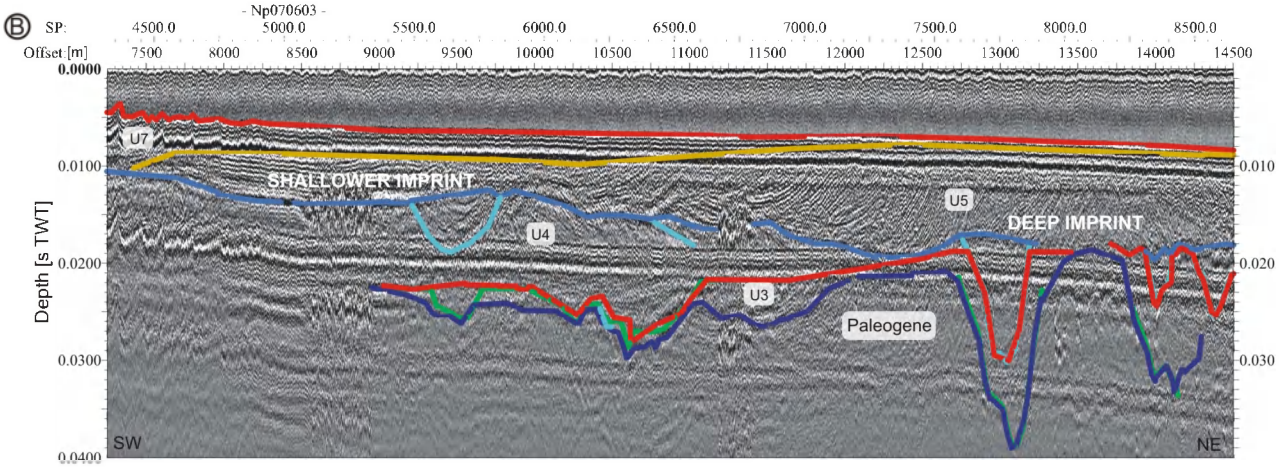
Ⓑ
- Np070603 -
SP:
4500.0
5000.0
5500.0
6000.0
6500.0
7000.0
7500.0
8000.0
8500.0
Offset [m]
7500
8000
8500
9000
9500
10000
10500
11000
11500
12000
12500
13000
13500
14000
14500
0.0000
0.0100
0.0200
0.0300
0.0400
Depth [s TWT]
U7
SHALLOWER IMPRINT
U4
U5
DEEP IMPRINT
U3
Paleogene
SW
NE

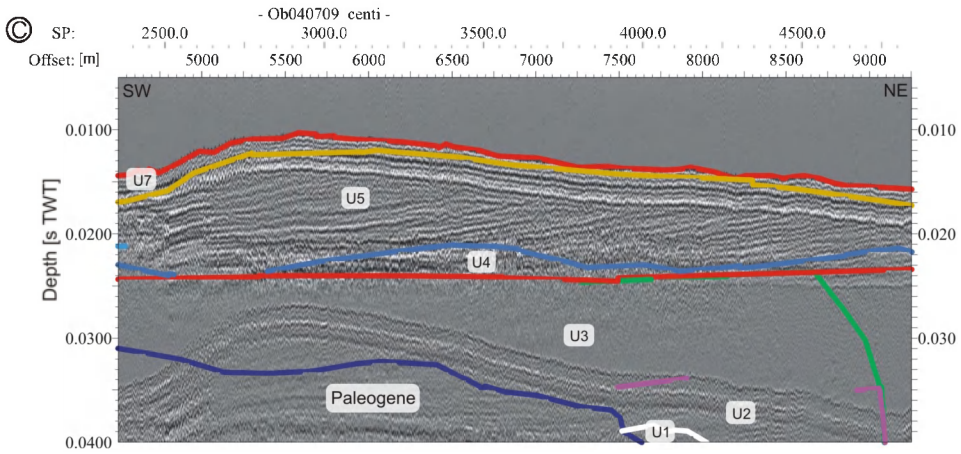
Ⓒ
- Ob040709_centi -
SP:
2500.0
3000.0
3500.0
4000.0
4500.0
Offset [m]
5000
5500
6000
6500
7000
7500
8000
8500
9000
SW
NE
0.0100
0.0200
0.0300
0.0400
Depth [s TWT]
U7
U5
U4
U3
Paleogene
U2
U1

Fig. 7.11A represents a map of the surface on which U5 lies, which is composed of the surfaces of QT, and the upper bounding surfaces of U3 and U4.
Along the length of the banks, the base has a wavy, undulating morphology. Not the base of the bank as a whole, but alternately below the gentle and steep side of the bank, the base depresses (erodes) deeper in the subsurface, over distances of about 5-6 km. At the transition between the two situations, the bases below the steep and gentle sides are equally deep. Below the gentle side of the outer bank, the depth ranges between -22 and -32 ms (-17.5 and -25 m MLLWS). Below the steep side, depth ranges between the extremes of -30 ms and -21 ms (-23.6 m and 16.5 m). In the middle bank, the depth below the gentle side ranges between -26 and -21 ms (-20.4 and -16.5 m). Below the steep side, depth ranges between -27 and -19 ms (-21 and -15 m).
Also beneath the nearshore bank, depressions alternate with zones where U4 emerges. The depth of the deepest imprints below the nearshore bank ranges between -26 and -17 ms (-20.4 and -13 m). An example of the wavy pattern of the base of U5 along the strike direction of the banks is shown in Fig. 7.11B. The internal reflection pattern along the stretch of the banks is a SW sloping progradation with only slightly dipping (<0.2%) reflectors (Fig. 7.11C). An exception is the nearshore area offshore Nieuwpoort, where channel-like reflectors are present (Fig. 7.11B).

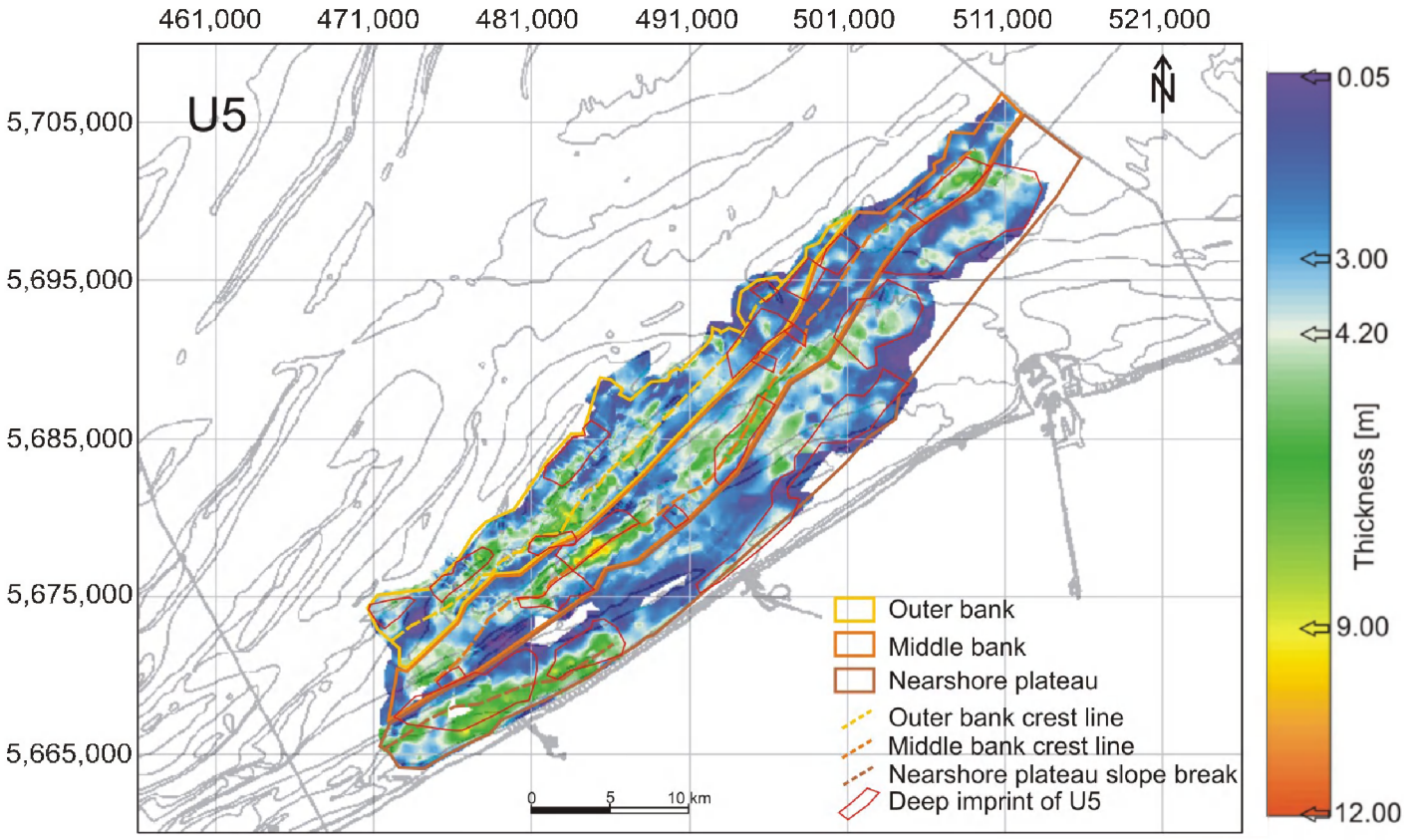

Fig. 7.12 Isopach map of U5. The parts below the crest lines of the bank structures are thickest and stand out, while the alternating depressions below stoss and lee side (in red) can not be distinguished. The thickness of U5 is particularly determined by the depth and shape of the upper surface, and not by the depth of the base (cf. Fig. 7.13).

The isopach map of U5 (Fig. 7.12) clearly illustrates that the parts below the crest lines of the bank structures are thickest and stand out, while the alternating depressions below the gentle and steep sides of the banks structures can not be distinguished. The thickness of U5 is particularly determined by the depth and shape of the upper surface, and much less by the depth of the base. Fig. 7.13 shows the morphology of the upper bounding surface of U5, with indication of the zones where the original bank shape is eroded. Assuming that the best-preserved banks structures of U5 resemble the original bank shapes, as described above, Fig. 7.13A shows that only 20% (120 km²) of the entire surface of U5 (565 km²) still has its original shape. This observation supports our approach to trace the bank structures across the BCS using the *base* of the bank and the internal reflection pattern, rather than using the surface of the bank, which is strongly affected by erosion.

Seismic unit U6: the uppermost, nearshore sheet-like structure

As described in Chapter 4, seismic unit U6 is a thin unit covering the nearshore parts of units U4 and U5. The unit is restricted to a 14 km wide strip along the present-day coastline near the Dutch border, which narrows to 2.5 km near Middelkerke and eventually disappears further along the coastline to the SW. Some isolated remnants occur further offshore, but these have been deduced from lithological evidence rather than from seismic data.

The surfaces of both units U4 and U5 have been strongly affected by, or before, deposition of the overlying units U6 and U7. Indeed, the basal reflector of U6 truncates the internal reflectors of the underlying units and thus represents an erosional surface. Over a large area offshore Zeebrugge and near the Vlakte van de Raan, this erosional surface is more or less horizontal, at a depth of -12 m MLLWS (-15 ms) (Figs. 7.14AB). In the area between the Wenduine Bank and the present-day coastline, where the latter changes in general orientation, the erosional surface occurs at a much shallower depth though, i.e. -9 to -7.5 m (-12 to -10 ms) (Fig. 7.15B). Further offshore, in an area connecting the western end of the Wenduine Bank and the eastern end of the Stroombank, the erosional base of U6 shows an elongated depression, down to -12 m (-15 ms). The isolated patches of U6 offshore, have no horizontal erosional basal surface, but follow the underlying topography of remnants of U5 and are located at depths of -15 m (-20 ms). This seems to suggest that the area offshore Zeebrugge, and the elongated area between the Wenduine Bank and the Stroombank have been more intensively eroded before deposition of U6 than the shallower located area between the Wenduine bank and the present-day coastline. It also seems that the isolated patches of U6 offshore have not been preceded by an intensive erosional phase, and are simply draped on the underlying surface.

Overall, U6 forms a kind of ‘cap’ on the highest parts of the Vlakte van de Raan and the area near the Wenduine Bank (Figs. 7.14B and 7.15A). Its surface slopes down in seaward direction and towards incisions like the Scheur. In the area of the Stroombank and the Wenduine Bank, U6 is locally eroded by, or before, the deposition of the overlying sandbanks of unit U7 (Fig. 7.15B).

Fig. 7.13 (page 161) (A) The isobath map of the top surface of U5, with indication of the zones where the original bank shape is eroded by the overlying units or before deposition of the overlying units. (B) Example of a seismic section showing erosion of U5 before the deposition of U6. (C) Example of a seismic section showing erosion of U5 by the overlying unit U7, or the modern hydrodynamics. A distinction is made between erosion in the swales or erosion below the sandbanks of U7. (D) Example of a seismic section in an area where U5 is presumed to be least eroded. The presumed original bank shapes are indicated with a dashed orange line.

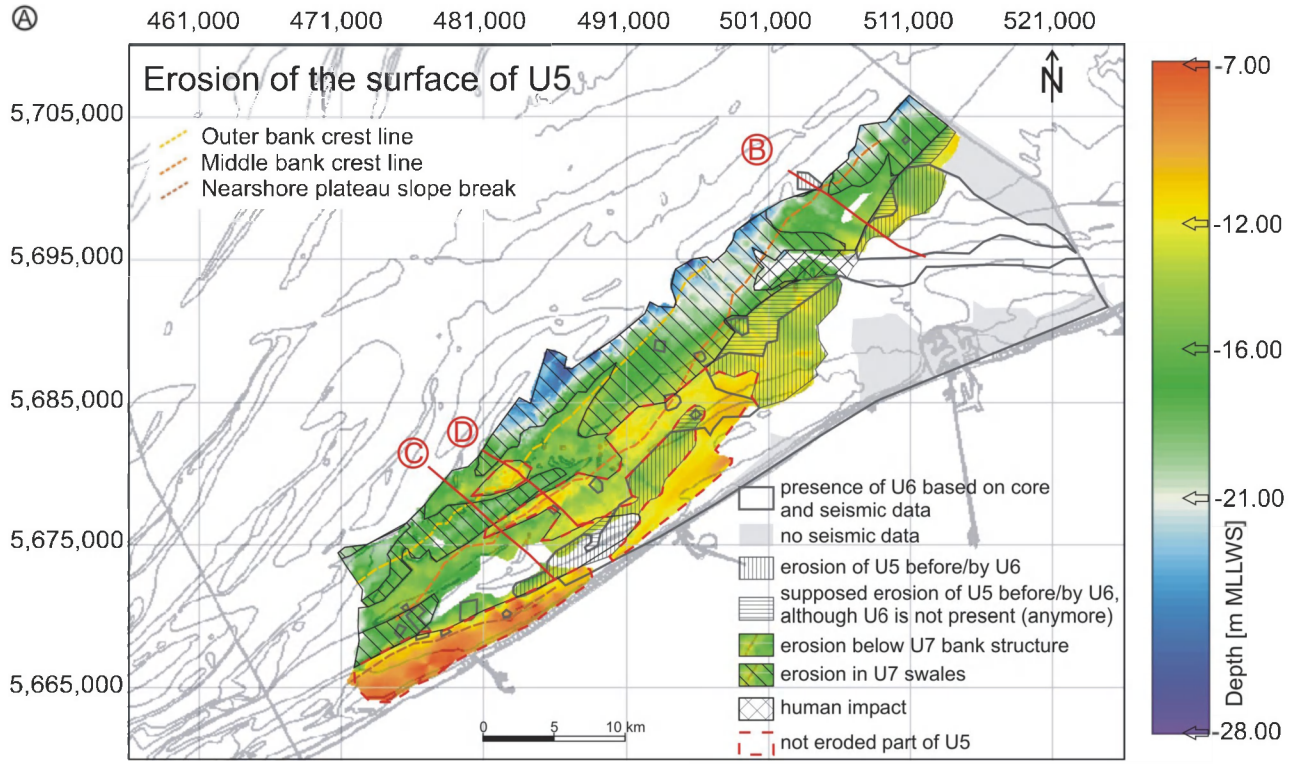
Ⓐ
461,000
471,000
481,000
491,000
501,000
511,000
521,000
5,705,000
5,695,000
5,685,000
5,675,000
5,665,000
Erosion of the surface of U5
Outer bank crest line
Middle bank crest line
Nearshore plateau slope break
N
B
C
D
presence of U6 based on core and seismic data
no seismic data
erosion of U5 before/by U6
supposed erosion of U5 before/by U6, although U6 is not present (anymore)
erosion below U7 bank structure
erosion in U7 swales
human impact
not eroded part of U5
0
5
10 km
-7.00
-12.00
-16.00
-21.00
-28.00
Depth [m MLLWS]

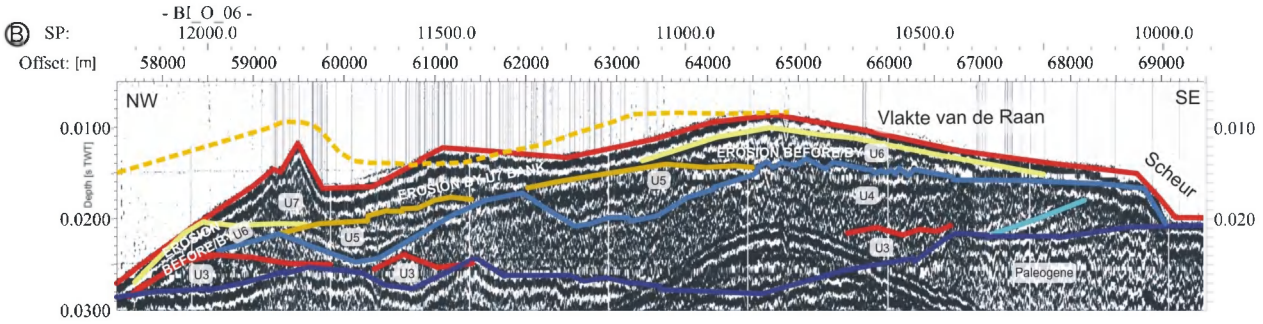
Ⓑ SP:
- BI_O_06 -
12000.0
11500.0
11000.0
10500.0
10000.0
Offset: [m]
58000
59000
60000
61000
62000
63000
64000
65000
66000
67000
68000
69000
NW
SE
Vlakte van de Raan
Scheur
EROSION BEFORE/BY U6
EROSION BY U7 BANK
Paleogene
U3
U4
U5
U6
U7
0.0100
0.0200
0.0300
0.010
0.020

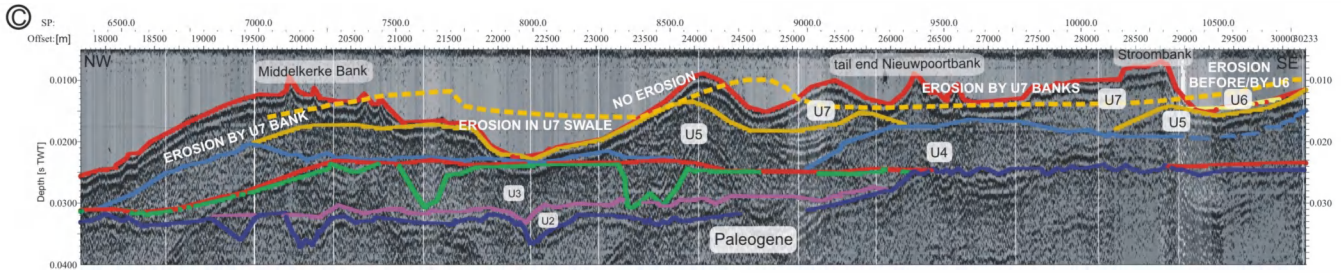
Ⓒ
NW
SE
Middelkerke Bank
tail end Nieuwpoortbank
Stroombank
ERODED BY U7 BANK
EROSION IN U7 SWALE
NO EROSION
EROSION BY U7 BANKS
EROSION BEFORE/BY U6
Paleogene
U2
U3
U4
U5
U6
U7

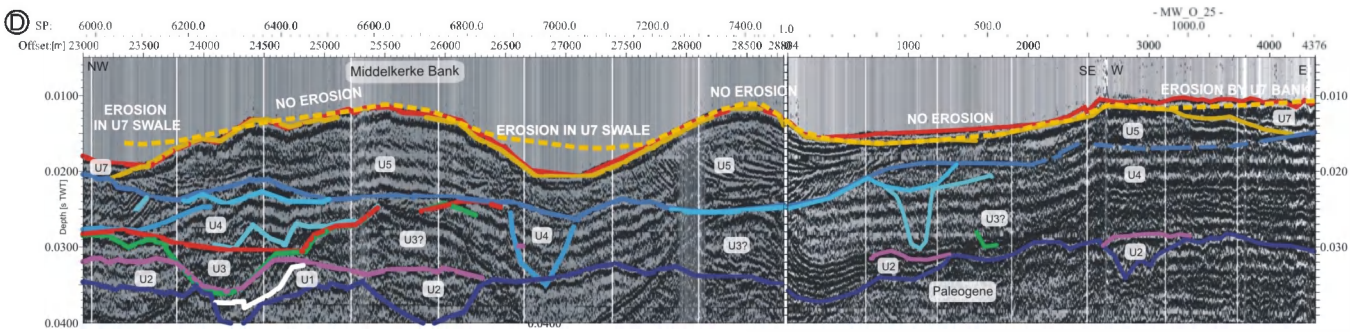
Ⓓ SP:
- MW_O_25 -
NW
SE
W
E
Middelkerke Bank
EROSION IN U7 SWALE
NO EROSION
EROSION BY U7 BANK
Paleogene
U1
U2
U3
U3?
U4
U5
U7

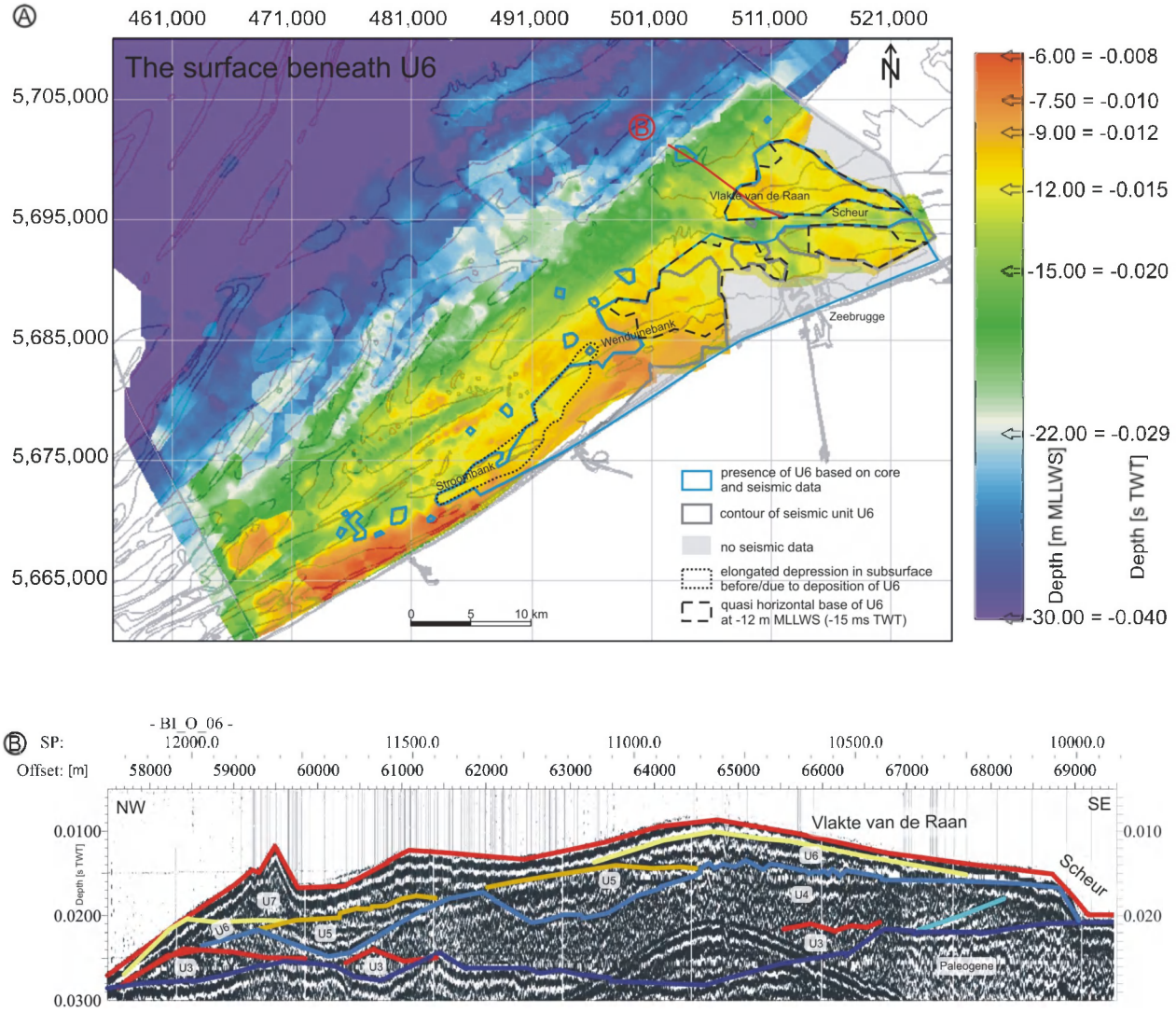

Fig. 7.14 (A) Isobath map of the surface on which U6 lies, composed of the surfaces of QT, U4 and U5. The contours of seismic unit U6 are indicated in grey. Based on core data, the coverage of U6 is extended to the area limited by the light blue border. The surfaces of both units U4 and U5 have been strongly altered by, or before deposition of the overlying units U6 and U7. Indeed the basal reflector of U6 cuts off the internal reflectors of the underlying units and probably represents an erosional surface, which is over a large area offshore Zeebrugge and near the Vlakte van de Raan quasi horizontal, and emerges in the area between the Wenduine Bank and the present-day coastline. (B) Seismic profile showing the horizontal base of U6 in the Vlakte van de Raan area. Also note how U6 forms a 'cap' on the highest parts of the Vlakte van de Raan; its surface slopes down in seaward direction and towards incisions like the Scheur. The isolated patches of U6 offshore, show no horizontal erosional basal surface, but follow the underlying topography. It seems that the isolated patches are not preceded by an intensive erosive phase, and are simply draped on the underlying surface.

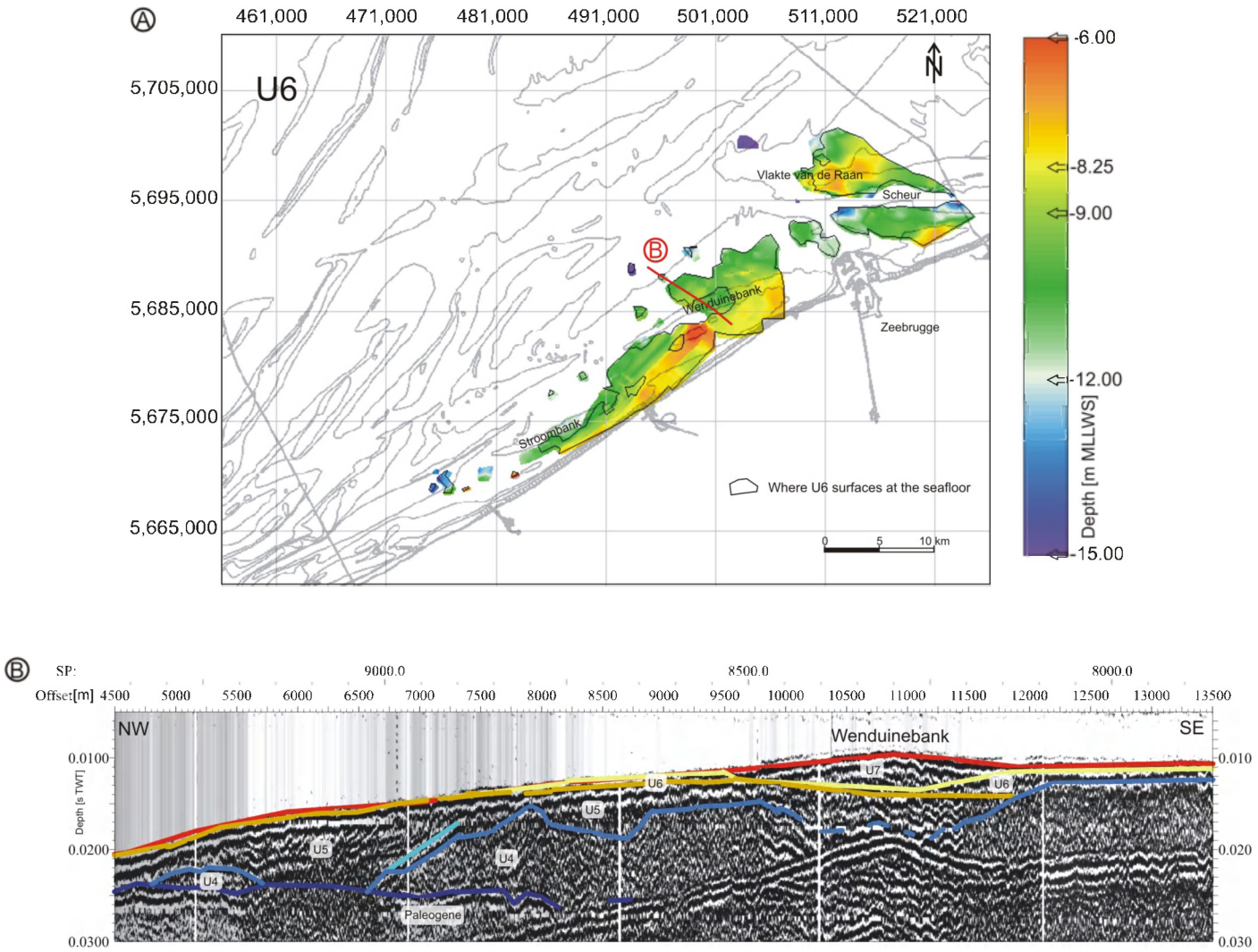

Fig. 7.15 (A) Isobath map of the surface of U6, showing how the unit forms a 'cap' on the highest parts of the Vlakte van de Raan and near the Wenduinebank. (B) Seismic section showing how in the area of the Wenduine Bank U6 is locally eroded by (of before) the deposition of the overlying sandbank.

7.2.2 Lithostratigraphy

Seismic units U4, U5 and U6 occur close to the seafloor (U5 and U6 are partly exposed at the seafloor), and are therefore encountered in many cores. Unit U4 occurs in 180 cores, unit U5 in 166 and unit U6 in 131 cores.

Some specific lithofacies were recognised, but it soon became clear that a single lithofacies can correspond to different seismic units and could represent different sedimentation environments. Therefore was opted to discuss the lithology only in function of characterising the three seismic units. The different lithofacies were not mapped separately, nor were sedimentation environments deduced from the lithological data alone. Both lithological and morphological (seismic) clues were always considered together. As a result, a comprehensive description of the lithology follows in the discussion (7.3.1), where the cores are correlated with the seismic units. In advance though, some photos of typical lithological phenomena are presented: a clay-sand-silt lamination (Fig. 7.16); a thick coarse-grained shell concentration (Fig. 7.17); a light grey, medium fine sand with shell accumulations in silt lenses (Fig. 7.18); a homogeneous grey-brown, fine sand containing sea-urchin debris (Fig. 7.19); and a black clay with some sand layers (Fig. 7.20).

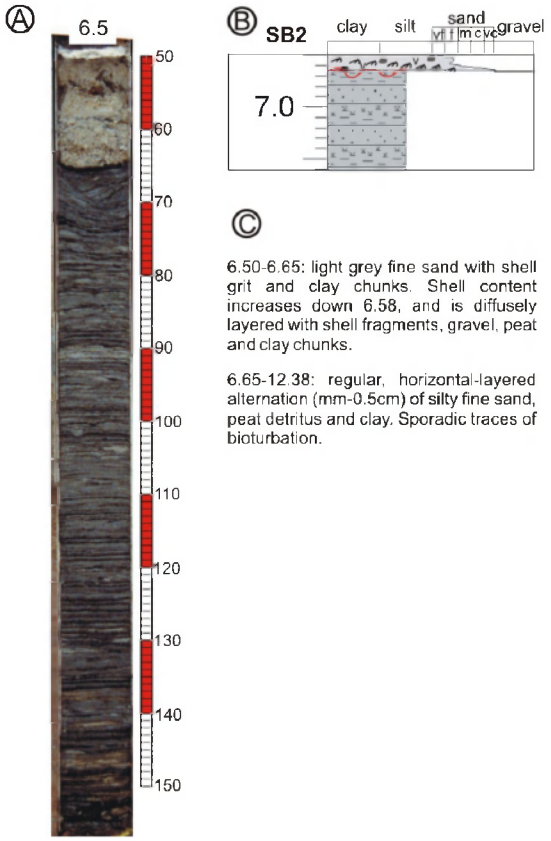

Fig. 7.16 An example of a clay-sand-silt lamination (core SB2). (A) photograph, (B) corresponding litholog, (C) lithological description.

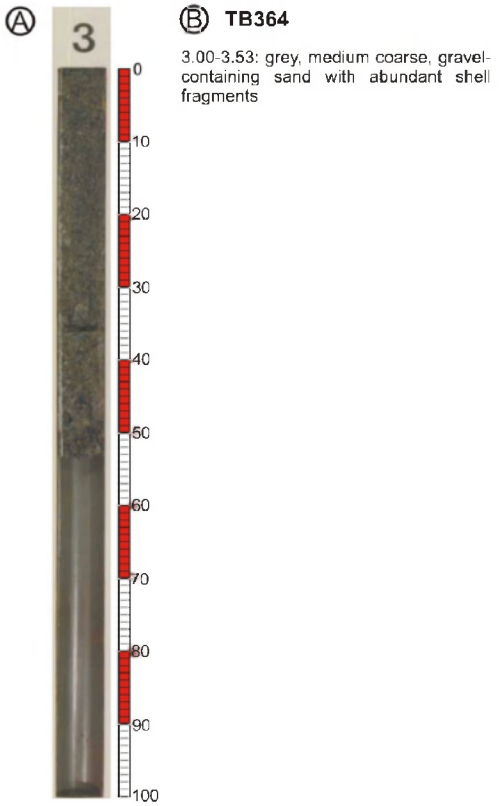

Fig. 7.17 An example of a shell bank (core TB364). (A) photograph, (B) lithological description.

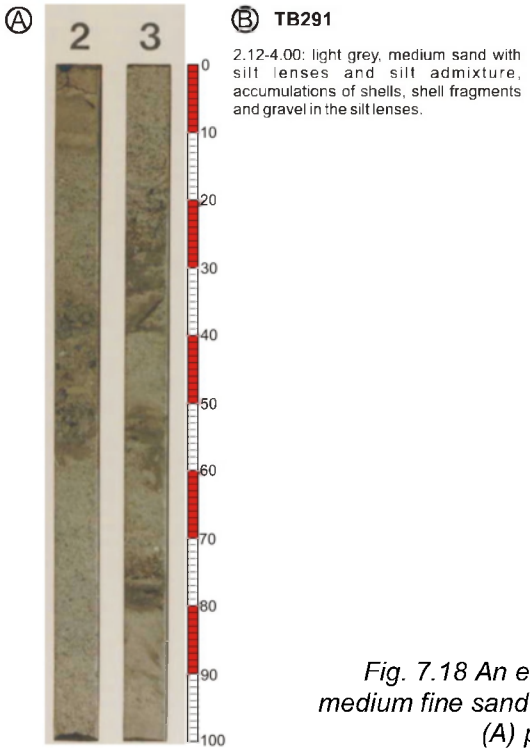

Fig. 7.18 An example of an often occurring lithology: light grey, medium fine sand with shell accumulations in silt lenses (core TB291). (A) photograph, (B) lithological description.

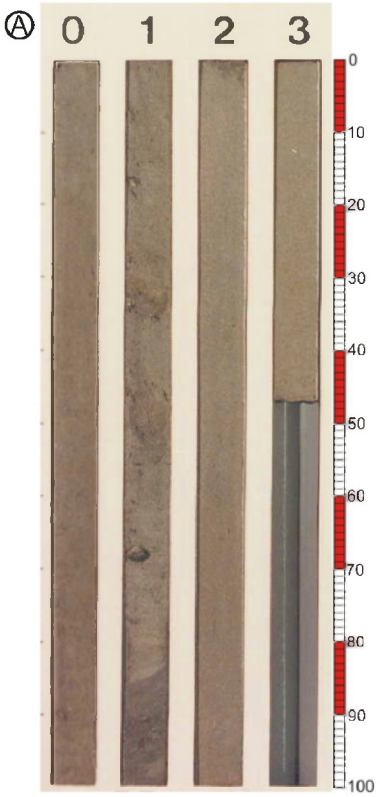

Ⓑ **TB451**

0.00-2.00: grey-brown fine sand, poorly sorted at the top, with sea-urchin fragments, and few shell fragments.
2.00-3.46: grey-brown fine, well sorted sand, with very few sea-urchin needles, and no shell fragments.

Fig. 7.19 An example of an often occurring lithology: homogeneous grey-brown, fine sand containing sea-urchin debris (core TB451). (A) photograph, (B) lithological description.

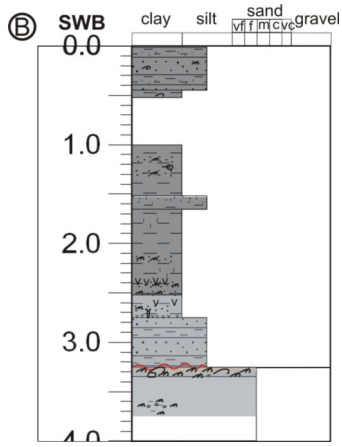

Ⓒ 0.00-0.45: originally black (brown-grey after drying) alternation of silty soft clay and fine sand containing little very fine shell grit, and some little whole shells.

0.45-1.65 (0.52-1.00 lacks): black soft clay with irregular sand lenses. 0.49: concentration of shells.
1.27-1.29: laminae of fine silty sand with shell grit and fragments, on top sea-grass remnants and other organic material
1.52-1.65: alternation of strongly silty fine sand with shell fragments, fine sandy silt, and silt and clay in a diffuse horizontal layering.
1.65-2.52: black slightly silty, soft clay, with regularly cm thick sand layers with shell grit. Between 2.41-2.44: rather much peat detritus in the clay.

2.52-2.75: dark grey soft clay, slightly silty, with lots of fine peat detritus. 2.60-2.66: zone with fine silty sand. Bioturbation structures at 2.66-2.70. 2.74: cm horizontal layering of concentrated peat detritus
2.75-3.25: same clay as above, with some thin (mm to cm) horizontal sand layers.

3.25-3.35: grey and brown-grey heterogeneous mixture of shells, shell grit, sand and clay chunks, gravel.
3.35-4.00: grey medium sand with fine shell grit.

Fig. 7.20 An example of an often occurring lithology: black clay with some sand layers (core SWB). (A) photograph, (B) lithological description.

7.3 Discussion

7.3.1 Integration of seismic data and lithology: genetic interpretation of the seismic units

By considering every core within the boundaries of a seismic unit, the lithological characteristics of each unit could be determined. It was attempted to find a main lithology for each seismic unit. In case of a heterogenic character, however, patterns were sought in the sediment distribution, and possible relations with the morphology of the unit, or the relative position of the cores, were tested.
Based on both the lithological (including diatom results) and the morphological characteristics of the unit (the latter derived from the seismic data), an interpretation in terms of depositional environment could be given to each seismic unit.

Seismic unit U4

Main lithology

Based on 180 core descriptions, basically two main litho-facies were identified as characteristic for U4. In one third of the cores the main facies of U4 is clayey and consists of an alternation of clay, sand and/or silt laminae, while in the remaining two thirds, U4 mainly consists of sand.

Laminated clayey facies

The U4 heterolithic sediments consist typically of an alternation of grey clay and grey fine sand layers, containing fine shell grit and sporadic whole shells. When mentioned, the lamination is of millimetre to centimetre scale, but more often the layer thickness is not defined in the core descriptions. In some cores, grey silt layers and black layers with peat detritus are present in equal amounts as the basic layers, but mostly peat is present as an occasional layer, or as peat fragments and detritus associated with the clay or silty layers. Coarse material is rarely observed within the heterolithic sediments. Only in one core, a layer of gravel-containing coarse sand is present.
In cores TB48, TB40, and TB55, a substantial layer of brown silt lies below the grey clay-sand laminations. In cores TB258, TB400, TB415, and Tr112, the clay and silt layers are not grey, but brown to brown-grey. In core Tr118, besides brown clay, also grey-green clay layers are present, while in TB25, the sand is green-grey glauconitic.

Sandy facies

The sandy facies, observed in 110 cores, is characterised by light-grey to grey, occasional glauconitic (in: TB11, TB65, TB71, TB19, TB91), fine to medium-fine sand, containing fine shell grit, occasional whole shells, shell fragments of bivalves (oysters, *Spisula solida, Macoma, Cardium)* and small gastropods (*Hydrobia*), and a sporadic gravel fragment. In 41 cores, clay occurs as a secondary component, either in the form of occasional layers, flasers, strings, clay balls (nuts) or lenses. Occasionally (in 9 cores) U4 also contains admixtures of silt, silt layers, or lenses. In 49 of the 110 cores, sporadic peat detritus horizons and peat fragments are also present, mostly distributed over the entire unit. Although in some cores the humus content is typically restricted to the clay horizons, and especially the silt layers. In 10 cores, unit U4 comprises thick layers of coarser-grained material, which show up on the seismic profiles as high-amplitude reflections. This coarser material can appear as shell banks, consisting of more than 50% of shells and shell fragments, and small gravel fragments (Fig. 7.17). Two of these coarse-grained layers, contain less shell fragments, but more and coarser gravel, and contain clay balls, they correspond to channel floors (UIT in Fig. 7.21, Tr21 in Fig. 7.22).

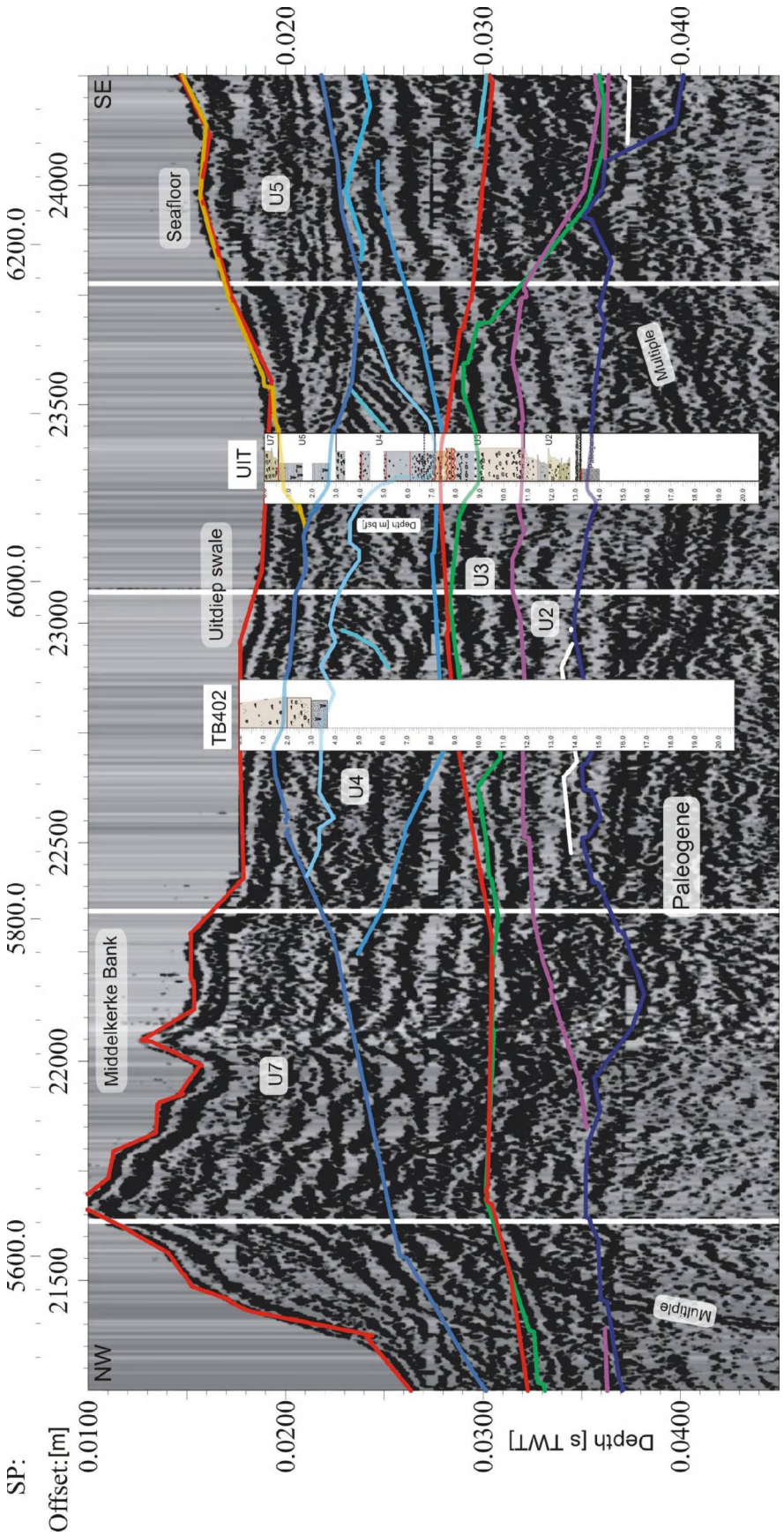

Fig. 7.21 Seismic section integrated with cores UIT and TB402, showing the lithology of an internal channel of U4. Tidal channels typically have a coarse-grained channel floor, containing gravel, abundant shell fragments and clay balls, while the top part of the channels consist of more fine grained sediments, often clay-sand alternations. For more detailed logs is referred to Appendix B.

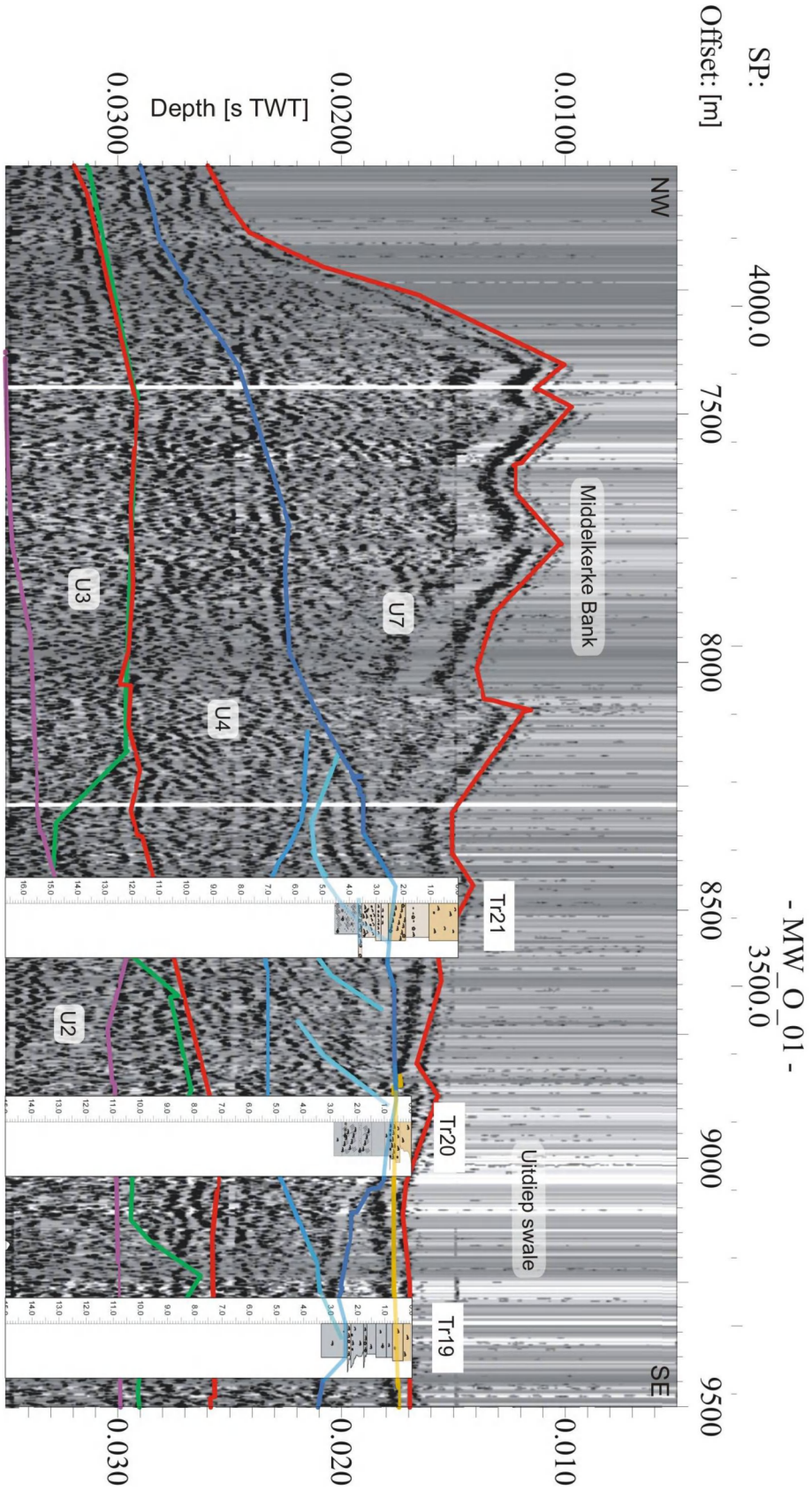

Fig. 7.22 Seismic section integrated with cores TR19, Tr20 and Tr21, demonstrating the coarse-grained basal infilling of a tidal channel in U4 (Tr21), and how the adjacent prograding reflectors correspond to fine sands showing cross stratification (with some shells and mud following this layering). It could represent a tidal bar or sand flat adjacent to the tidal channel. For more detailed logs is referred to Appendix B.

In the grey sandy facies the silt (in: TB44, TB133, TB420, SWB, Tr109, Tr120 and Tr27) and clay (in: TB333 and Tr120) layers are occasionally brown, and the sand itself can be grey-green due to the glauconite content (TB257, TB08, TB34 and TB350).

Apart from the laminated clayey facies and the sandy facies, U4 consists in six cores entirely of coarse material, i.e. shell banks consisting of abundant shell fragments (a.o. oyster and gastropods), whole shells, and gravel in a grey medium-coarse sand, with an occasional brown, silt or fine sand layer with plant fragments.
In another four cores, U4 is characterised by a silty facies. In core TB340, U4 consists entirely of light, green grey silty sand with dark green silt layers and rust-coloured patches. While in cores TB36 and TB39, brown silt was encountered similar to the one below the grey clay-sand lamination in cores TB48, TB40, and TB55 (as described above) and located at the same depth. In core TB358, U4 consists of green silt with brown patches, overlain by a brown-coloured well developed peat horizon (cf. Appendix B and C for detailed litholog and photos). Neighbouring core 78H10 shows brown moss peat at a similar depth.

Diatom results

Five sediment samples, corresponding to seismic unit U4, were taken from cores SWB, SB1, OSB and UIT for diatom analysis in order to determine the unit's depositional environment. Diatoms were, however, sparse. Fragments of *Paralia* and *Rhaphoneis* sp. indicated a probable marine-brakish environment with sandy tidal flats. Only in one sample (SWB) abundant species were present typical for muddy tidal flats and a few species indicative of a marine influence. The assemblage suggests e.g. lower tidal flats.

Interpretation

The diatom assemblages, together with the presence of peat remnants, oysters and *Hydrobia*, suggest a nearshore shallow-water environment, while the almost total absence of sea-urchin debris argues for a restricted environment with limited circulation with the open sea. The heterolithic bedding with rapid and repeated alternations of clay, sand and silt layers might represent portions of tidal rhythmites. Thus, unit U4 is interpreted as a tidal-flat environment, possibly protected by a barrier.
Also the seismic evidence, with the occurrence of a seismic unit over such a large area, the maze of prograding reflection patterns and several overlapping channel systems, points in the direction of a dynamic tidal-flat environment. Tidal environments are characterised by complex networks of tidal channels and bars, and by the migration and stacking of successive channels, the architecture of the deposits is often very complex (Dalrymple and Choi 2007).
The channels typically have a coarse-grained channel floor, containing gravel, abundant shell fragments and clay balls as shown in Figs. 7.21 and 7.22. The top part of the channels consists of clay-sand alternations (TB402 in Fig. 7.21), which is a typical assemblage for upsilted tidal channels (Boggs 1995, Galloway and Hobday 1996, Baeteman 2007a). The prograding reflectors parallel to the channel on Fig. 7.22 correspond with fine sands showing cross stratification (with some shells and mud following this layering), and could represent tidal bars or sand flats adjacent to the tidal channel. On Fig. 7.23 the section with prograding reflectors corresponds to a zone with coarse-grained sediments showing cross stratification, containing shell and gravel concentrations. This probably indicates the migration of a tidal channel, rather than a sand flat. The part of U4 with the prograding reflection pattern, leaning against the scarp in U3 (Fig. 7.6E), might represent a sand flat or tidal bar attached to the slope of U3.

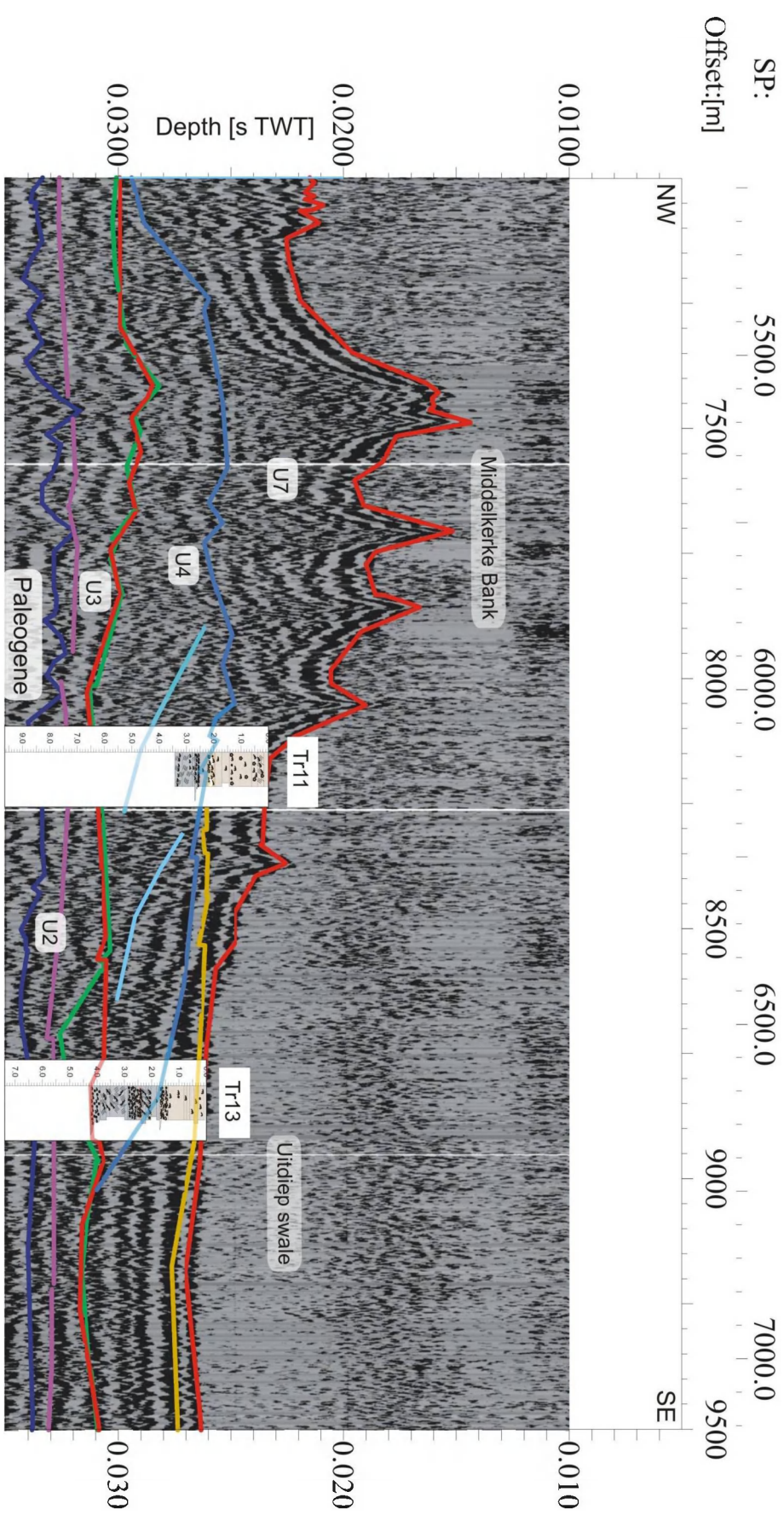

Fig. 7.23 Seismic section integrated with cores Tr11 and Tr13, demonstrating how the prograding reflectors of U4 correspond to a zone with coarse-grained sediments showing cross stratification with shell and gravel concentrations. This might indicate the migration of a tidal channel, rather than a sand flat as in Fig. 7.22. For more detailed logs is referred to Appendix B.

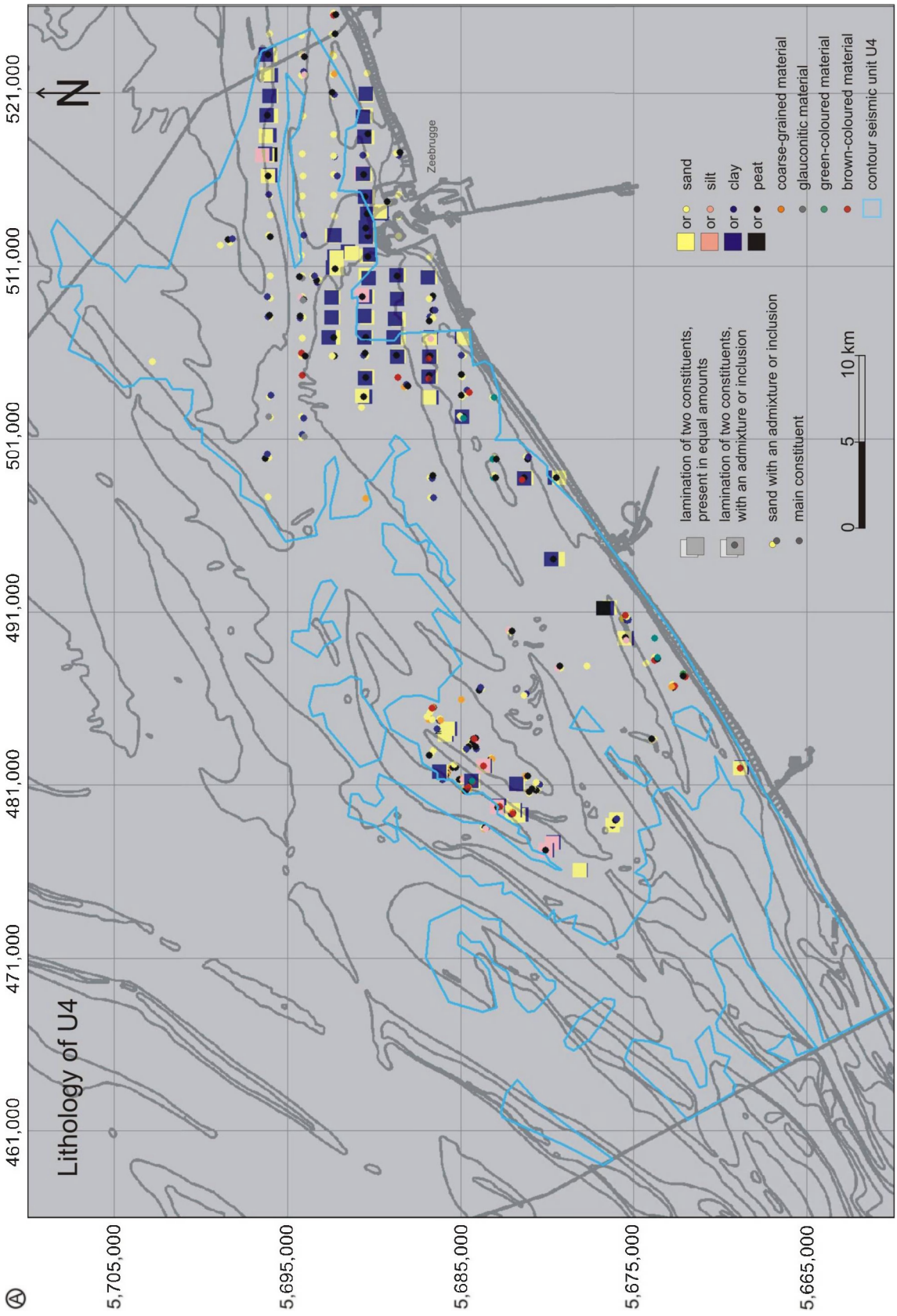

Fig. 7.24 (A) The lithology of seismic unit U4 in each of the 180 cores. The light blue contour represents the outer boundary of seismic unit U4. Note how U4 is also encountered offshore Zeebrugge, where no seismic data are available.

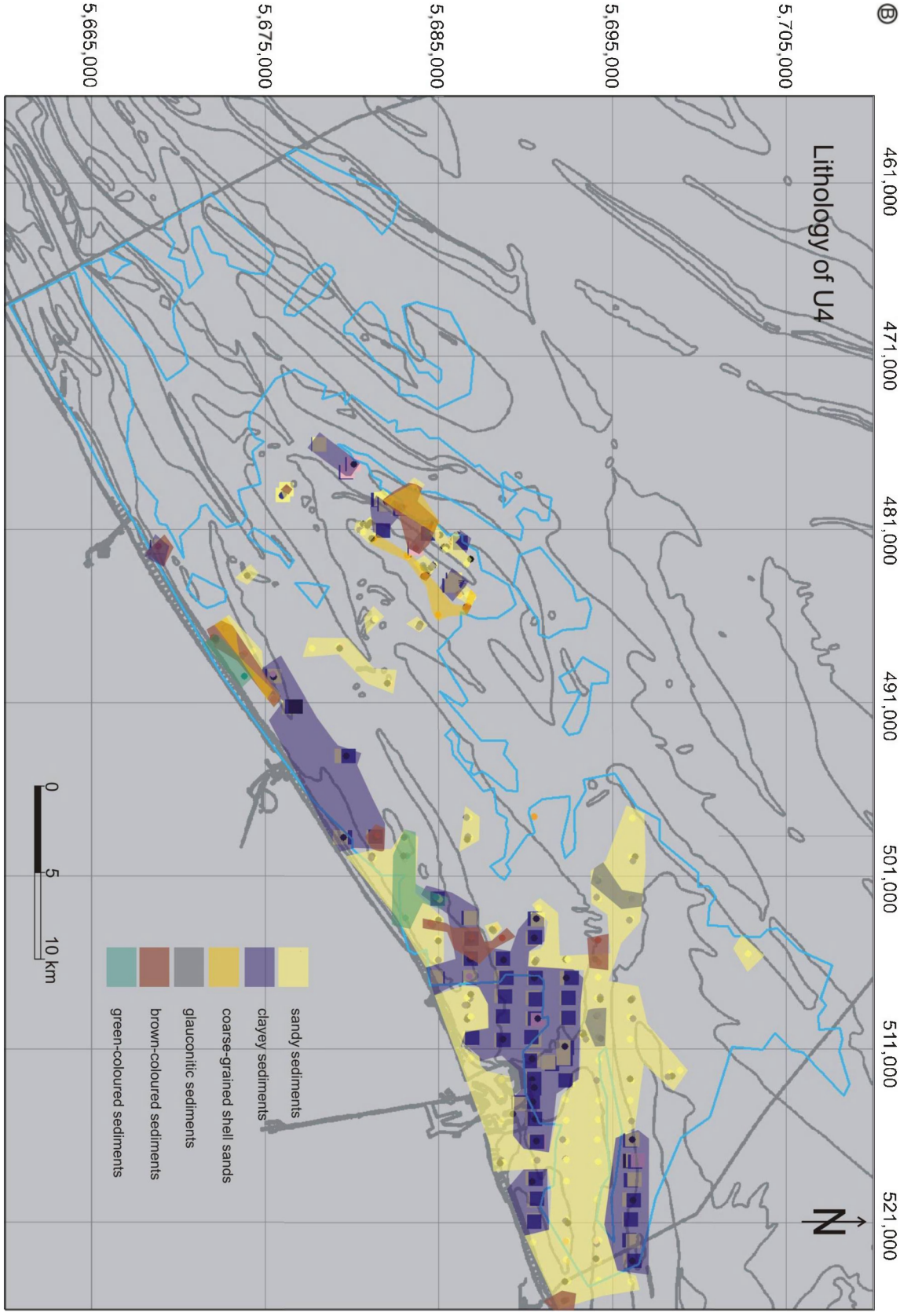

Fig 7.24 (B) The areal distribution of the different lithofacies of unit U4.

The areal distribution of the different lithofacies of unit U4 is presented in Fig. 7.24. Offshore Zeebrugge, there is a number of clearly outlined areas of similar lithology. A sandy area with a definite channel-like shape is bordered on both sides by vast areas of clayey sediments. The sandy zone most likely represents the infill of a main tidal channel or inlet, where the tidal energy is strongest, with adjacent sand flats. The presumed tidal channel partly corresponds to the present-day Scheur, i.e. the entrance to the Western Scheldt, and could represent a precursor of it.
The clayey parts represent mud flats and the typical heterolithic infilling of smaller tidal creeks or gullies, i.e. branches of the main tidal channel. These creeks are less energetic and carry finer-grained sediments. The rhythmic alternations of sand layers with thin mud drapes represent transportation and deposition of sand by flood and ebb-tidal currents, followed by the settling of suspended mud during the slack-water periods (Dalrymple 1992).
Between the Stroombank and Wenduine Bank another clayey area occurs, adjacent to marked out areas with green and brownish sediments, which contain well developed peat horizons. The latter most likely represent high silted-up areas where freshwater marshes developed, the brown oxidation colour being indicative of the supra-tidal position.
The area near the Middelkerke Bank is less evident to interpret, because only the cores in the adjacent swales reached as deep as seismic unit U4, and the relation between structures observed in the seismic unit and the lithology is not straightforward. It is a zone with several clayey and sandy patches, an extensive area of deposits containing brown clay and silt layers, and two vast areas representing shell banks.

Seismic unit U4 was originally identified starting from the seismic interpretation of the Middelkerke Bank by Trentesaux et al. (1999), who interpreted this section in the sandbank as a subtidal, lagoonal or tidal-flat deposit. Based on the depth of rootlets and comparison with similar deposits in the Netherlands (Elbow Formation), an early Holocene age was proposed for these deposits in the Middelkerke Bank (Heyse et al. 1995, Trentesaux et al. 1999). The evidence of diatom samples and 140 new core descriptions now confirm that the interpretation of Trentesaux et al. (1999) has a regional validity, and that a tidal-flat environment extended over the entire width of the BCS. Interpreting the unit as consisting of lagoonal deposits is, however, doubtful, as no evidence for lagoonal sedimentation has been found in the present-day Coastal Plain. The Belgian Coastal Plain has always been characterised by a large sediment supply from the sea by shoreface erosion, sufficient to fill the created accommodation space to an intertidal level, even during rapid relative sea-level rise (Baeteman 1999).

Basal gravel lag

A gravel lag occurs occasionally at the base of U4. The presence of this lag highlights the strong erosional processes during the Eemian transgression, which prevailed before deposition of this unit. Remarkably, of the 40 cores that reached the base of U4, 10 cores show no gravel lag or coarsening at the base of U4 at all. Together with 7 other cores without a gravel lag, but which do show a coarsening of the sand and shell content at the base of U4, these cores are all (but 3) located in the sandy area offshore Zeebrugge (Fig. 7.25). The absence of the lag deposit in these cores could have three causes: (1) there was locally little gravel available in the underlying unit, (2) a gravel lag was present, but was locally removed, or (3) there was little gravel supplied by the Eemian transgression to the areas above the scarp.

(1) In the cores without gravel lag, U4 is almost always located on top of the Paleogene substrate, while in the cores that do contain a gravel lag at the base of U4, U4 directly overlies U3. It might be that fewer gravel fragments were present in the Paleogene sediments than in the outer-estuary deposits of U3, and that

less gravel accumulated when the fines were washed out by the Eemian transgression. But then again, SWB does contain a 70 cm thick gravel lag at the base of U4 on top of QT (cf. litholog and photos in Appendices B and C). However, in the area where SWB is located, the Aalter Formation and Gentbrugge Formation outcrop below U4, and these contain several layers of sandstone, which are most likely the origin of the sandstone gravels in the gravel lag of SWB (Fig. 7.26, Le Bot et al. 2003). In the area where the other cores are located, the Maldegem and Zelzate Formations outcrop below U4, and these consist of blue-grey clays and clayey sands without sandstone or other gravely layers (Le Bot et al. 2003).

(2) On the other hand, it is not impossible that in the sandy area of U4 offshore Zeebrugge, the basal gravel lag was removed by tidal channels, as was also the case in cores GR1 and OSB, discussed in the previous chapter. In these cores, the Paleogene substrate is not overlain by a gravel lag, but the overlying unit U1 shows tidal channels with a shell-rich channel floor.

(3) It is possible, that during the Eemian transgression less gravel was supplied to the areas above the scarp in U3. The massive gravel lag encountered in SWB would then have a local origin, derived from the extensive erosion of the Paleogene headland on which the core is located.

And most likely, a combination of the three factors played a role.

In 14 of 17 cores that contain brownish silt, brown clay or brown fine sand layers plus organic remnants, the plant fragments (wood, peat) occur only in the brownish sediments. Peat remnants also occur in the overlying grey clay-sand alternation only in three cores, and in an additional six cores no plant remnants are present at all. Of eight cores that also contain a gravel lag at the base of U4, seven are located in the Middelkerke Bank area, where the plant-fragment-containing brown silt or fine sand is always located directly on top, or within a metre above this gravel lag. Only one core that contains both a gravel lag and brown sediments is located near the present-day coastline (SWB) (Fig. 7.25). In 15 brown-sediment containing cores, mostly located more nearshore (of which 7 show the close association of peat with brown deposits, 5 contain no peat, and 3 contain also peat in the overlying grey sediments), the base of U4 was not reached, so it is not known whether the brownish sediments are associated with the gravel lag at the base of U4, in that area.
The relation between plant remnants and brown sediments has also been observed in the form of a brown peat horizon in TB358, the occurrence of brown-grey silt layers alternating with grey clayey lamina, with rootlet penetrations in a salt marsh deposition in NWB, the occurrence of brown moss peat in core 78/H10, and the presence of (fresh water marsh/terrestrial) wood fragments in brown fine sand (e.g. Tr13, TB133). Trentesaux et al. (1999) observed in the Middelkerke Bank area a large amount of pollen in the brown-grey clay with interbedded silts and fine sands, and interpreted the clay as indicative of a low-energy environment, probably situated very close to the coast.
The brown colour is probably due to oxidation of ferrous oxide (FeO; black) into ferric oxide (Fe_2O_3; red). It occurs only in supra-tidal areas above the mean high-water line and in strictly terrestrial zones, where respectively salt marshes and fresh-water marshes (peat) develop. It is possible that the plant-fragment-containing brown silts and fine sands on top of the gravel lag, are reworked remnants of a basal peat that developed, when after the Weichselian lowstand the area was affected by a rising ground-water table, in reaction to the Holocene relative sea-level rise. Alternatively, the brown deposits could also correspond to reworked remnants of salt marshes that built up at the landward edges of a tidal-flat area, which developed when the tidal influence reached this area. Or they could represent reworked remnants of soils developed during the Weichselian lowstand.

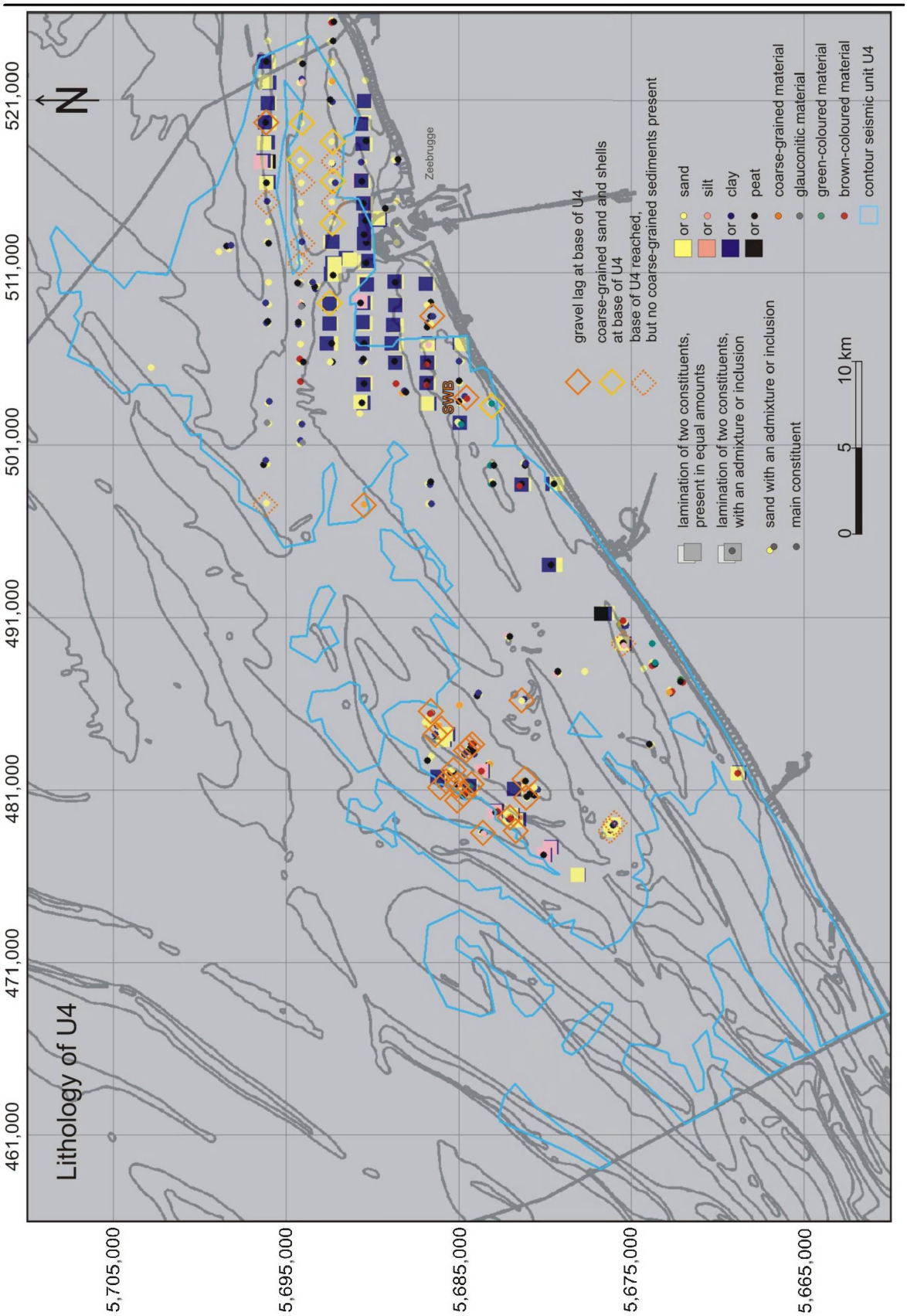

Fig. 7.25 The lithology of seismic unit U4. The cores indicated with a diamond reach as deep as the base of U4. Full dark orange diamond: the cores showing a gravel lag at the base of U4; full light orange diamond: the cores showing no gravel lag, but a coarsening of the sand and shell content at the base of U4; and the dotted dark orange diamonds: the cores that show no coarsening at the base of U4 at all.

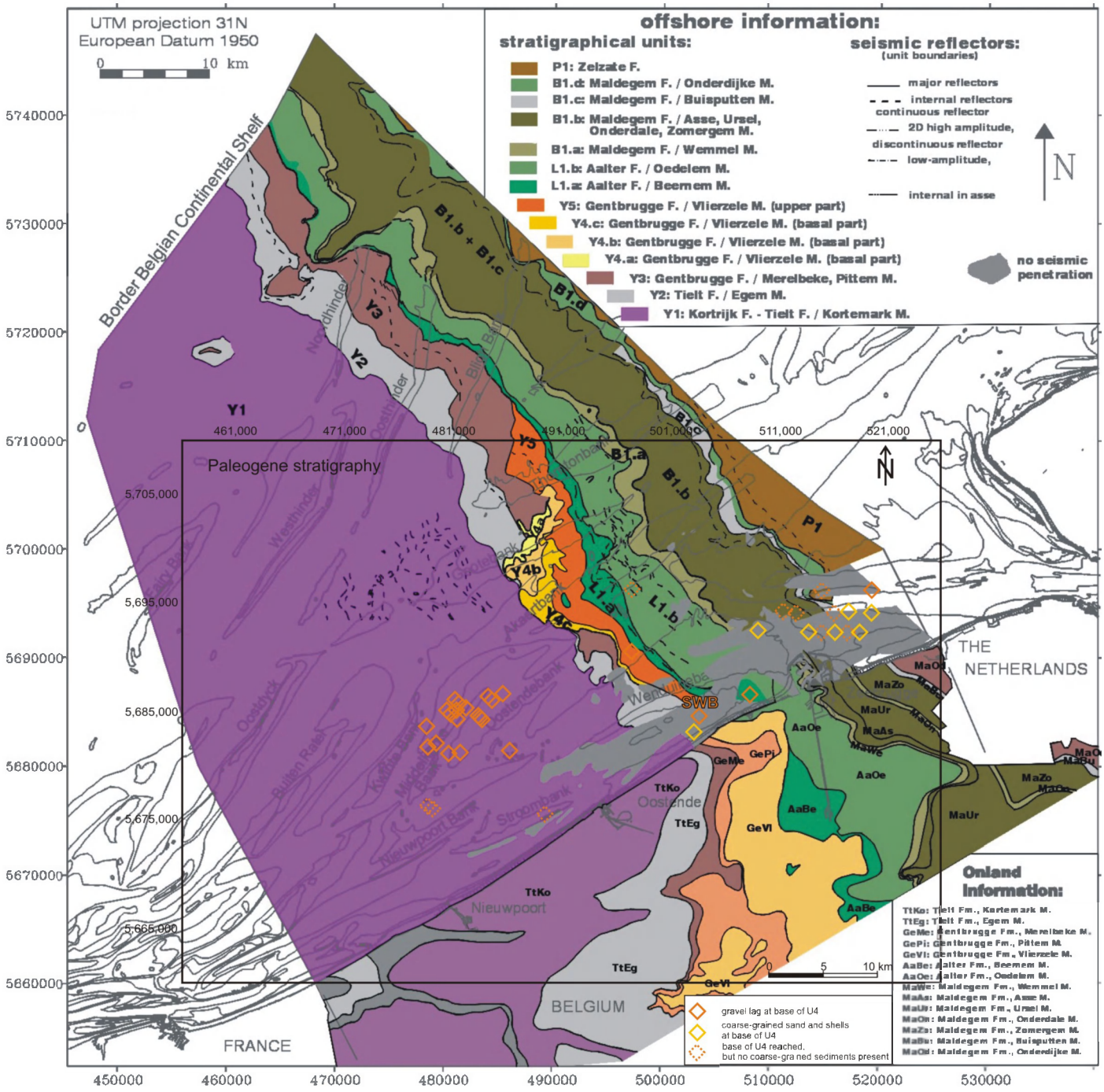

Fig. 7.26 Stratigraphy of the Paleogene deposits (adapted after Fig. 7 in: Le Bot et al. 2003), with indication of the cores that reach the base of U4. In the cores without a gravel lag, U4 is almost always located on top of the Paleogene substrate, while in the cores that do contain a gravel lag at the base of U4, U4 directly overlies U3. It might be that less gravel fragments were present in the Paleogene sediments than in the outer-estuary deposits of U3, and that less gravel accumulated when the fines were washed out by the Eemian transgression. SWB, however, does contain a 70 cm thick gravel lag at the base of U4 on top of QT (cf. litholog and photos in Appendices B and C). This could however be explained by the fact that in the area where SWB is located, the Aalter Formation and Gentbrugge Formation outcrop below U4, which contain several layers of sandstone, which are most likely the origin of the sandstone gravels in the gravel lag of SWB.

Additional remarks

The green silt and glauconitic sands have often been interpreted as Pleistocene deposits, solely based on their colour. Nevertheless, in all but three cores (Tr96, Tr102, Tr95) in which seismic units U1, U2 and U3 were encountered, the sediments are typically grey, brown or brown-grey, apart from sediments directly overlying the green Paleogene deposits (U3 gravel lag in SB2, U2 in UIT).
In some areas the green and glauconitic sediments are located 0-3.5 m from the underlying Paleogene boundary (TB34, TB25, TB08, and possibly also TB257), and most likely obtained their greenish colour from erosion of the green, glauconitic sands and clays of the Paleogene substrate. A series of five cores, four located within the sandy area near the Scheur and one in the harbour of Zeebrugge, contain glauconitic but grey sands. Also here, the Paleogene substrate is located less than 1.5 m below the cores, and could be the source for the glauconite.
On the other hand, Fig. 7.24 shows how zones with green-sediment-containing cores are located near areas with brown-sediment-containing cores. This suggested relation is also observed in cores where greenish silt or clay layers are associated with the presence of brown silt or clay layers. E.g. in core TB358 a green silt with brown stains is overlain by the brown peat horizon; in TB350 greenish silt layers are present within a grey-brown silt layer which contains rusty spots, i.e. possibly erosional fragments of the peat layer in TB358; in TB258 the top of a clay-sand alternation is characterised by green clay layers (interpreted as U6), while from 50 cm below the seafloor the layers become brown downward; in Tr118 grey-green clay layers overlie the brown-grey clay layers on top of a gravel lag.
In several core descriptions it was noted also that fresh dark-grey to black sediments can become brown-grey after drying, while other dark-grey sediments became grey after drying (TB420). And some mice-grey (light-grey) sediments became green-grey.
Possibly there is a close chemical relation between the green and brown layers, and not all of the greenish sediments are related to the nearby presence of glauconitic Paleogene deposits. Greenish-blue-grey colours are typical for reducing environments, while reddish, yellow or brown colours are indicative of oxidation (Gildersleeve 1932, Nichols 1999, Ameryckx et al. 1995). The colour of sediments can be very misleading. A sediment may be deposited in a reducing environment but if the pore waters passing through the sediment long after deposition are oxidising, then any iron minerals are likely to be altered to iron oxides. Conversely, reducing pore waters may change the colour of a sediment from red to green. In fine-grained sediments reduction spots may form around particles of organic matter: the breakdown of the organic matter draws oxygen ions from the surrounding material and results in a localised reduction of oxides from red to green.

Based on the available seismic data, there is no evidence that Pleistocene deposits come as close to the seafloor as was sometimes suggested in previous interpretations of the core descriptions. Preliminary interpretations of age were often based on remarkable colour differences (green vs brown or grey), or based on the presence of typical Eemian or Weichselian mollusc fauna, but without taking into account the possibility of reworking, in spite of the fact that they did consider the possibility of fall in of Holocene shells during coring.
The lithological and seismic data show that unit U3, interpreted as the final Eemian estuarine infilling, is separated from the overlying tidal-flat deposits of unit U4, only by the marine transgressive or shoreface ravinement surface, sometimes represented by a gravel lag, and that no Weichselian sediments are present. On the seismic profiles, there are no indications that in between seismic units U3 and U4 an extra unit would be present. Even in areas with high gas content, obliterating the seismic signal, the top boundaries of U3 and U4 show nonetheless strong reflections, and no additional reflector is observed in between them.

Seismic unit U5

Main lithology

Analysis of 52 cores shows that the outer bank of seismic unit U5 consists of brown-grey to grey, mostly fine, but occasionally medium-coarse, well-sorted to medium-sorted sand. Characteristically, U5 in the outer bank is very homogenous and contains few shell fragments (e.g. Fig. 7.19, Tr19 in Fig. 7.22, Tr13 in Fig. 7.23), except for accumulations in loamy/silty lenses, frequently at the base of the unit (e.g. Fig. 7.18). Typically, sea-urchin needles are abundant. In two areas (in 13 cores), between the Kwinte and Middelkerke Bank (Negenvaam), and SW of the Vlakte van de Raan, occasionally clay lenses and clay laminae occur (Fig. 7.27A), typically in areas where the base of U5 shows a depression. The cores in the area SW of the Vlakte van de Raan are taken in the channel-like structure below the steep slope of the bank, while the clayey area in the Negenvaam is situated at the gentle side. There is no consistency in the distribution of the more silt-containing cores. In three clay-containing cores also peat fragments or humic-rich layers were encountered.

Also in the middle bank structure, U5 consists mainly out of brown-grey to grey, fine to medium fine, well to poorly-sorted sands, which contain few shell fragments, except for accumulations in loam/silt lenses. Also sea-urchin needles are abundant here. There is a clear difference between the lithology at the gentle side and at the steep side of the bank (Fig. 7.27B), which was not the case with the outer bank. Below the gentle side of the middle bank, the sediments are clearly more sandy, while below the steep side the sands contain typically more silt lenses with shell accumulations, hold frequently peat remnants and occasionally clayey laminae. Of the 39 cores, 17 are located at the steep side, 17 at the gentle side, and 3 on the crest line. Of the 19 cores with shell accumulations in silt lenses, 12 are located at the steep side, as also 9 of the 12 peat-containing cores (in some cores both are present). Also 4 of the 6 coarsest, shell-containing cores are located at the steep side. Of the 6 clay-containing cores, 3 are located at the steep side, and 3 at the crest, while of the 11 sand-containing cores (with only occasional shell fragments), 10 are located at the gentle side of the middle bank.

In the nearshore, plateau-like bank, 30 out of 75 cores consist only of light-grey to brown-grey, medium-fine to fine, well-sorted to poorly-sorted sand, containing very few to few shell fragments, occasionally very fine shell grit and sea-urchin needles. Out of these 75 cores, 28 contain besides that also silt lenses, layers or silty patches, mostly present in confined zones within the cores, and are highly frequently associated with concentrations of sea-urchin needles and shell fragments. Out of 75, 12 cores contain occasional clay lenses or clay layers, and 5 cores hold coarse material with occasional small gravels and thick layers of shell fragments (shell banks). Of the 75 cores, 25 contain also humus in the form of lenses, specks and fine layers, which are (except for 6 cores) always found in association with the silt or clay lenses, silt patches or silt layers in the confined zones of the core. In the six other cases, the humus fragments are not related to clayey or silty areas, or appear scattered throughout the core. The humus-containing cores occur over a large area in the most coastward part of the nearshore bank (Fig. 7.27B). The silt-containing cores are not restricted to, or associated with, certain zones of the bank, but occur in joined narrow zones. The cores containing clay and coarse material are scattered.

Diatom results

Four sediment samples were taken from the sections representing seismic unit U5 in cores NWB, OSB and UIT, in order to determine its depositional environment.
Although diatoms were sparse, the sample from the coarse-grained base of U5 in OSB (5.68 m) suggests deposition in marine shallow water and sandy tidal flats, although

sponge spicules indicate a marine influence. The sparse species from UIT (2.4 m) suggest a more marine setting (planctonic *Paralia sulcata*, sponge spicules, and *Rhaphoneis surirella*). The abundant species present in OSB (5.4 m) and NWB (8.3 m) would suggest a sandy tidal-flat environment.

Interpretation

Seismic unit U5 consists of two, partly eroded, parallel sandbanks or ridge-like structures, with an asymmetrical cross-section and a landward-facing steep slope, parallel to a more plateau-like structure, subparallel to the present-day coastline. These three structures have a spacing of 2.5-5 km, a height of 7.5-12 m, a length of at least 50 km, and their slopes are less than 1°. The diatom results and abundant presence of sea-urchin debris point to a shallow-water, open-marine setting, so the bank-like structures have to be interpreted as some type of shallow-marine large-scale bedforms.

Based on their dimensions, the bank-like structures of seismic unit U5 do not represent sand waves or sand dunes, nor can they represent features that are common on beach profiles, such as wave breakpoint bars, 'ridge and runnel' features, or swash bars. Even if sand waves can have heights up to 12-18 m and a spacing of more than 1000 m, according to the classification table of shallow marine large-scale bedforms of Ashley (1990), the height/spacing ratio of the structures in U5 is much larger (ca. 1/300) than the values of 1/30 to 1/100 that are commonly encountered in sand waves. Also the height-spacing relationship of Flemming (1980), which is typical for transverse subaqueous bedforms, is not valid for the features of U5.
Wave breakpoint bars are offshore submerged sand bars (there may be as many as three or four subparallel bars separated from each other by troughs) that parallel the shoreline and underlie the breaking point of waves (Weise and White 1980). Although their description fits the situation of the bank structures in U5, the dimensions of wave breakpoint bars (maximum height of 2 m) are much smaller than the structures in U5 (Kroon et al. 2008).
Also an interpretation as 'ridge and runnel' topography or swash bars can be excluded. Swash bars are described as low, elongate bars of sand, formed along and parallel to the beach (King 1972), but are typically only a few metres wide and high. E.g. a swash bar deposited during a hurricane had an average width of 15 m and a height of 1.5 m. Also ridge and runnel features found on beaches with considerable tidal range have heights of only 0.5-1 m (Masselink et al. 2006).

We can also rule out the possibility that U5 is composed of a series of active tidal sandbanks, or open shelf ridges following the classification of Dyer and Huntley (1999). Firstly, large parts of the bank-like structures in U5 are strongly eroded and not active anymore. And secondly, although the best preserved sections of the ridge-structures in U5 have dimensions that are slightly smaller, but comparable to those of tidal sandbanks - which are typically tens of kilometres long (up to 80 km), on average 13 km wide, asymmetrical, and tens of metres high- the steep slope of an active tidal sandbank is typically 6° (Dyer and Huntley 1999), while the steeper sides of the structures in U5 have slopes of less than 1°.
Sandbanks are maintained by circulatory movement of sand over and around a bank by mutually evasive ebb-flood channels, but they grow to be moribund if they become isolated from their sediment source or when the peak currents are insufficient to move the seabed sand (Dyer and Huntley 1999). Moribund sand ridges or tidal sandbanks have a less distinct morphology, more round crested cross sections, have no large sand waves on their flanks and their slopes are generally only 1° (Yang 1989, Dyer and Huntley 1999), which describes exactly the morphology of the U5 bank structures. So, U5 could be interpreted as consisting of a series of moribund open-shelf ridges, in accordance with the classification of Dyer and Huntley (1999).

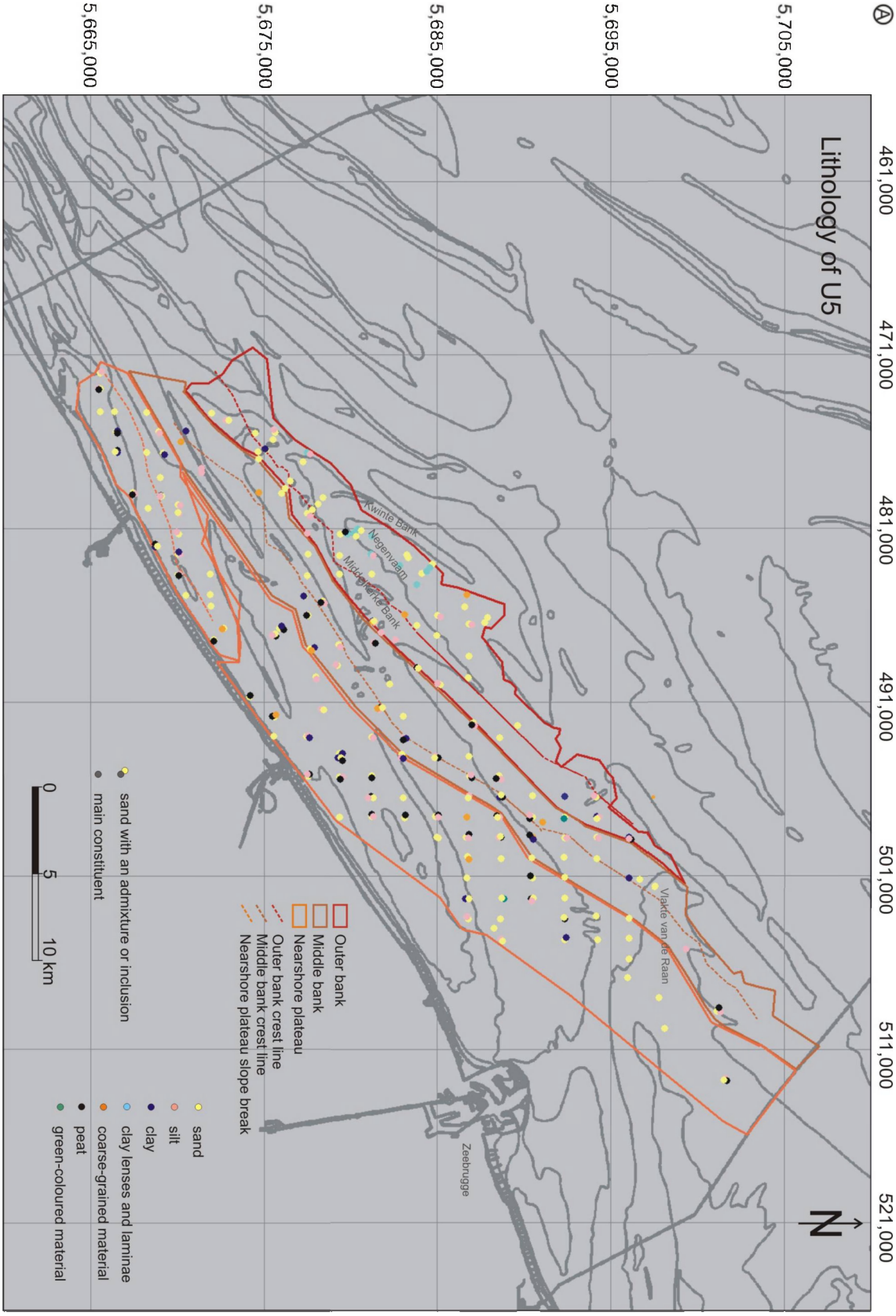

Fig. 7.27 (A) The lithology of seismic unit U5 in each of the 166 cores. (B) (next page) The areal distribution of the different lithofacies of unit U5.

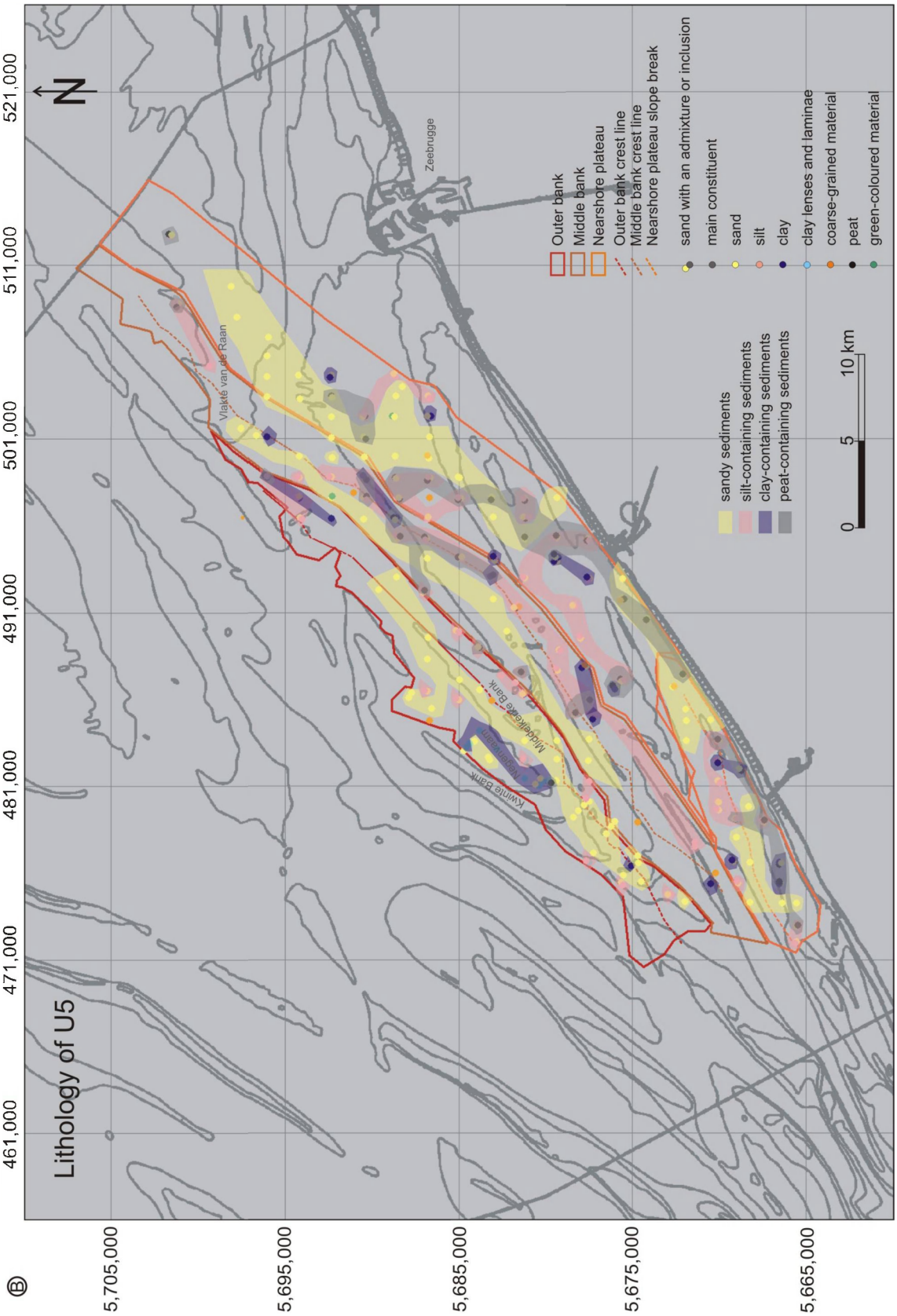
Lithology of U5
N
Zeebrugge
Vlakte van de Raan
Middelkerke Bank
Kwinte Bank
Outer bank
Middle bank
Nearshore plateau
Outer bank crest line
Middle bank crest line
Nearshore plateau slope break
sand with an admixture or inclusion
main constituent
sand
silt
clay
clay lenses and laminae
coarse-grained material
peat
green-coloured material
sandy sediments
silt-containing sediments
clay-containing sediments
peat-containing sediments
0
5
10 km
461,000
471,000
481,000
491,000
501,000
511,000
521,000
5,705,000
5,695,000
5,685,000
5,675,000
5,665,000

On the other hand, the dimensions and gentle slopes of the structures of U5 also fit the proportions of shoreface-connected ridges (synonyms: shoreface-attached ridges, shoreface-detached ridges, storm-generated sand ridges and linear shoals). This type of sand ridges are up to 10 m high, 2-5 km apart, and their crestlines can extend for tens of kilometres. Side slopes are rarely more than 1° (Dyer and Huntley, 1999).
Also Trentesaux et al. (1999) interpreted the lens structure below the Middelkerke Bank (their seismic unit U6), which is part of our unit U5, as the remains of a coastal sandbank. The coastal sandbank was defined as a type of sandbank intermediate between a tide-dominated and a storm-dominated bank. Trentesaux et al. (1999) too observed the similarities in morphology with the storm-generated shoreface-connected ridges that occur along the Atlantic coast of the USA (Swift et al. 1973), but remarked that a tidal influence cannot be excluded on the BCS. Although shoreface-connected ridges have been considered as a special class of storm-generated ridges, shoreface-connected ridges along the Dutch coast are found in a setting where tidal currents and storms are both important. This suggests that a storm-dominated setting is not essential for the formation of shoreface-connected ridges (van de Meene and van Rijn 2000).

Shoreface-connected ridges typically converge with the coast at angles of 25-35° along a trend that is intermediate between the dominant direction of storm wave approach and the coast parallel trend of storm currents (Dyer and Huntley 1999). Some banks are, however, detached as the coast retreats to form fields of isolated ridges. These do not connect to the coastline anymore, but they appear to have still the same characteristics and movement as the attached ones, although a reorientation can occur under the influence of the hydraulic regime on the shelf. Ridges further offshore can move into parallelism with the shoreline (Swift et al. 1973). At the north coast of the Netherlands and Germany, the ridges do not connect to the beach, but disappear into the shoreface sand sheet, presumably because of the higher tidal current and wave regime, and a reduction in shoreface retreat rate (Dyer and Huntley 1999). According to Trentesaux et al. (1999) coastal banks are parallel or slightly oblique to the coast, in contrast to tidal sandbanks, which have an angle of around 20° with regard to the coastline.
It is not possible to determine whether the ridge structures of U5 are shoreface connected or not, or at what angle they are oriented with respect to the coastline, as the former coastline is not visible any more. It is possible though, that the most nearshore bank structure, which is more plateau-like, forms the transition to a former coastline, and might represent part of the former shoreface.

The bank-like structures of U5 could thus either represent moribund open shelf ridges (tidal sandbanks), or storm-dominated (shoreface-connected) ridges. However, both have distinct lithological characteristics. Moribund ridges are separated from each other by sandy or muddy floors, rather than by clean gravel as is the case for active open shelf ridges. In shoreface-connected ridges, sands are coarsest in the landward trough and become finer up the landward flank to the crest, where they are well sorted, and down the seaward flank where they become increasingly fine.
For what concerns the structures in U5, only in the middle bank structure a difference was observed between the lithology of the steep and gentle side. Elsewhere, the density of cores was insufficient to draw any conclusions. And even over the middle bank structure, the cores did not cover an entire cross-section from trough, over crestline, to trough. In the middle bank, the landward side is characterised by the coarsest sediments, contains also the most shell accumulations in silt lenses, but also the most clayey layers and peat fragments, while the gentle side is characterised by a more homogenous sandy lithology, with few shell fragments. The sparse available data thus show a seaward sorting and fining, which allows us to interpret the bank-like structures of U5 as remnants of storm-dominated ridges.
The internal reflectors of coastal banks, which parallel the steep side of the banks, probably represent storm-induced growth layers (Trentesaux et al. 1999). Most likely the

frequent shell accumulations in silt lenses represent storm layers, which could be an extra indication for the storm control on the deposition of unit U5.

There are also significant morphological differences between tide-dominated sandbanks and storm-dominated sand ridges (Belderson 1986, van de Meene and van Rijn 2000). The orientation of the tidal sandbanks is related primarily to the peak tidal-current direction, while the orientation of the storm-dominated sand ridges is related primarily to the orientation of the coastline. Tidal sandbanks are generally higher than storm sand ridges: the former have heights up to 43 m, while the latter range between 3 and 12 m. Tidal sandbanks may be steeper than storm-dominated sand ridges and they generally have sharper crests. Tidal sandbanks have a larger spacing than storm-generated ridges and they are generally longer. Typical spacings range between 2 and 30 km for tidal sandbanks and between 0.5 and 7 km for storm-dominated sand ridges (Belderson 1986, van de Meene and van Rijn 2000).
So, based on lithological and morphological evidence, the bank-like structures in U5 most likely represents remnant of a series of storm-generated ridges, with a possible tidal influence.

Basal gravel lag/coarse-grained base

In 17 out of 79 cores, in which the base of U5 was encountered, U5 is separated from the underlying unit U4 by a gravel lag (e.g. Tr13 in Fig. 7.23). The seismic data show the internal reflections of U4 to be truncated at the top of the unit. Both observations are indicative of an intensive erosional phase before the deposition of U5. The gravel lag consists of a heterogeneous mixture of (silex) boulders, shell fragments and whole shells in a sandy matrix.
In 33 cores, U5 shows an increase or coarsening in shell content towards the base of the unit (overlying U4, U3 or QT) (e.g. Tr19 in Fig. 7.22), which might indicate that the deposition of U5 had also an erosional character itself, in other words: a high-energy environment existed during the initial phase of deposition of U5. The locally undulating character of the base of U5 is an extra argument that suggests that U5 itself is also eroding the underlying units. Because a strong erosional phase before the deposition of U5 alone (without local erosion by U5 itself), would have left a regional planation surface similar to the Eemian transgressive surface.
In 26 cores, the base of U5 shows no coarsening, although the contact with the underlying unit (U4, U3 or QT) is mostly sharp. In six of these cores, U5 is separated from the underlying unit U4 by a thin (2-10 cm) clay layer. These cores are located between the Kwinte and Middelkerke Bank (Negenvaam) (Fig. 7.28), below the gentle side of the outer bank, where a depression is visible at the base of U5, and where U5 shows occasionally clay lenses and clay laminae. Possibly this depression represents an initially sheltered area where fine-grained sediments could settle down, before the deposition of the U5 bank. Alternately, the clay might originate from erosion of the underlying deposits of U4, although in these six cores the remnants of U4 show no clay content.

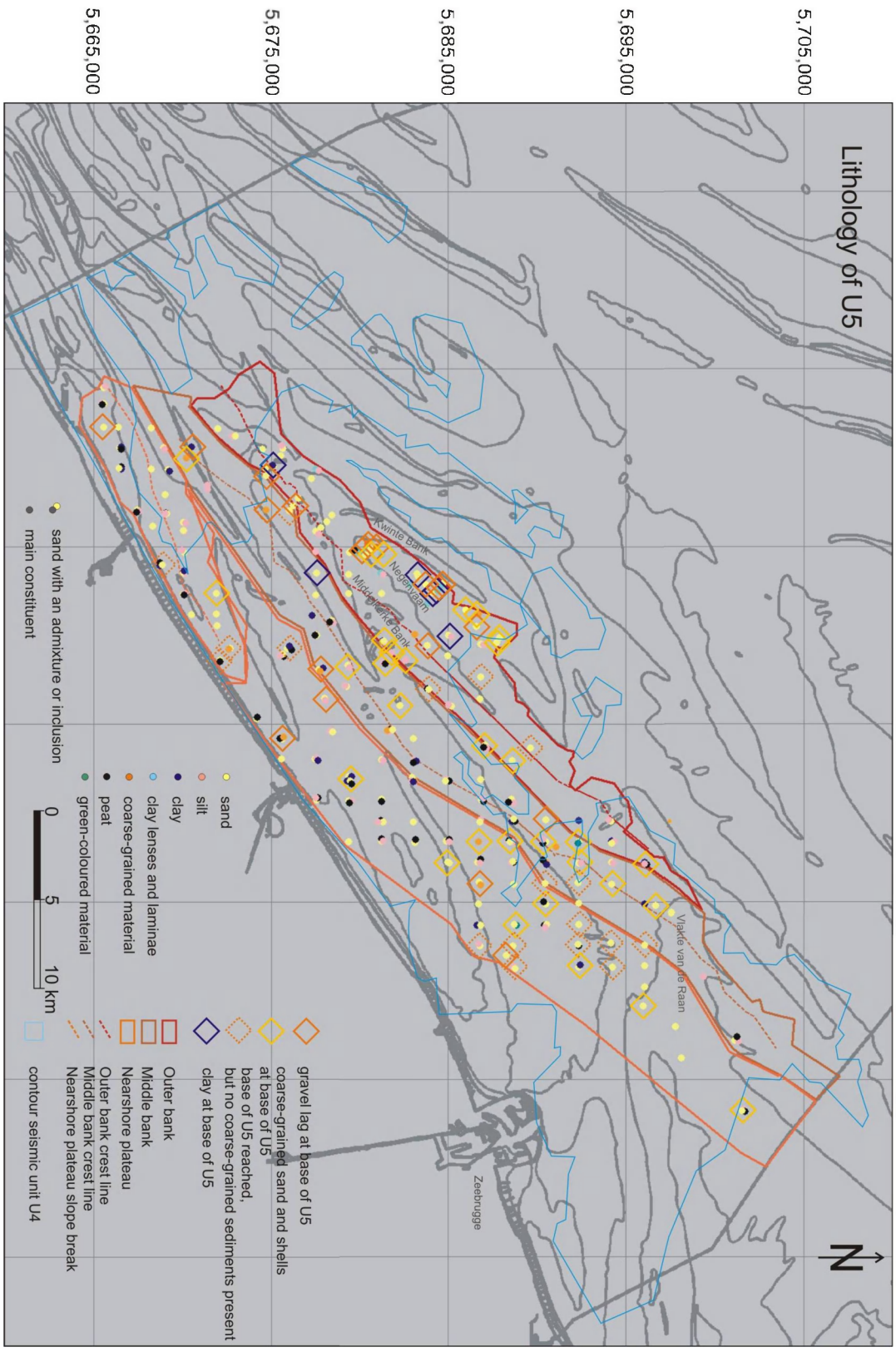

Fig. 7.28 The lithology of seismic unit U5. The cores indicated with a diamond reach as deep as the base of U5. Full dark orange diamonds: the cores showing a gravel lag at the base of U5; full light orange diamonds: the cores showing no gravel lag, but a coarsening of the sand and shell content at the base of U5; the dotted dark orange diamonds: the cores that show no coarsening at the base of U5 at all; and the dark blue diamonds: represent cores with a clay layer at the base of U5. The contour of seismic unit U4 is indicated (blue) to show two large areas, around the Nieuwpoort Bank and NE of the Oostende Bank, were no unit U4 is present, and U6 rests directly on top of U3 or QT.

In two large areas, around the Nieuwpoort Bank and NE of the Oostende Bank, no unit U4 is present, and U5 rests directly on top of U3 or QT (Fig. 7.28). This could indicate three things: i) U4 was never deposited there, which is unlikely because in the immediate surroundings it does occur; ii) U4 has been eroded before deposition of U5; or iii) U4 has been removed by erosion by unit U5 itself.
In three of thirteen cores (NWB, 83A04, TB273), in which the base of U5 was encountered on top of U3 or QT, a gravel lag was present, which could represent two erosional phases: i) the Eemian transgression, or ii) the intensive erosional phase which removed U4. Most likely its was a combination of the two. In seven of these cores an increase or coarsening in shell content was observed towards the base of U5, and in three cores no coarsening was observed at all above QT or U3.

Additional remarks

Often, the lithology of U5 strongly resembles the lithology of the underlying unit U4. This can be interpreted as another indication that U5 is largely built up of sediments eroded from unit U4. E.g. in many cores in the nearshore, plateau-like bank offshore Zeebrugge, U5 consists of light-grey medium-fine quartz sand, containing very few to few shell fragments and occasionally very fine shell grit, while U4 in the sandy area also typically consists of light-grey, fine to medium-fine sand, containing fine shell grit, occasional whole shells and shell fragments. In some cases, the only difference between both units is the presence of sea-urchin debris in U5, which is absent in U4. Another example is core TB39, in which U5 contains a grey layer of strong calcareous silt at its base, and overlies U4, which consists entirely of brown, strong calcareous silt. Also the diatom assemblages of U5, which indicate a sandy tidal-flat environment, might be (partially) reworked from eroded U4 tidal flats.

Seismic unit U6

Main lithology

Integration of seismic and core data reveals that seismic unit U6 is mainly characterised by an alternation of black clay and grey fine sand layers (Figs. 7.20 and 7.29). An additional 30 cores close to the shore and Zeebrugge, which could not be correlated with seismic profiles, show this typical clay-sand alternation as well (together, 90 out of 131 cores). This allowed mapping the extent of U6 beyond where it was observed on the seismic data (Fig. 7.30A). The clay fraction mostly dominates, is occasionally very soft and has a typically black, blue-black or dark-grey colour, and a high content in organic matter (humic dry-weight percentage is 2-5%, compared to 0.2-0.5% in other layers). The sand layers are blue-grey, dark-grey or grey. In some cores, also grey clay occurs (20/90), or only grey clay is present, but alternating with blue-grey to dark-grey sand (11/90). It has to be noted, however, that when opening the cores, the typical black reduction colour turns into (rust) brown, green-grey (in TB255, TB266, and probably also TB312) or light-grey due to dehydration and oxidation.
The heterolithic, clay-sand alternation often contains shell grit, shell fragments and whole shells (especially *Abra alba*, *Spisula subtruncata*, *Spisula elliptica*, *Angulus tenuis*, but also *Cerastoderma*, juvenile gastropods, and mussels), sea-urchin fragments, and sporadically humus specks or peat detritus (in 18 out of 90 cores). In one core, the sand is glauconitic (TB06). In 14 of the 90 cores with a clay-sand alternation, also silt layers, lenses, patches or silt admixtures occur. Strikingly, the siltiest parts show a micro-layering in colour after drying; seemingly homogeneous grey silt, becomes an alternation of light and dark-brown fine silt laminae after drying. In 4 of these 14 cores, the silty sand matrix or silt patches show shell accumulations, as was also observed in U5.

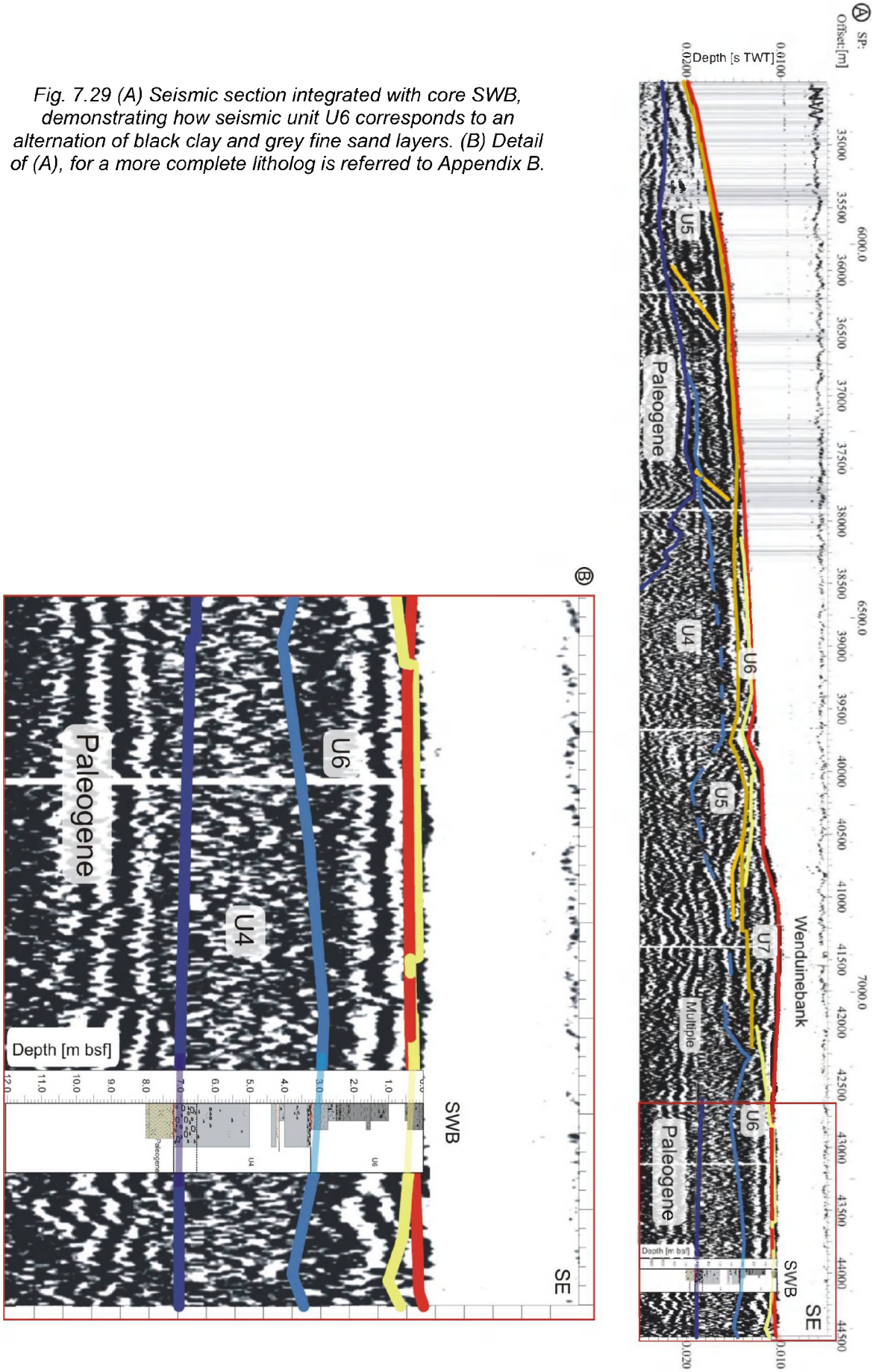

Fig. 7.29 (A) Seismic section integrated with core SWB, demonstrating how seismic unit U6 corresponds to an alternation of black clay and grey fine sand layers. (B) Detail of (A), for a more complete litholog is referred to Appendix B.

Where U6 is only a few cm to dm thick, the unit consists entirely of black clay (12 cores) (Fig. 7.30B). Exceptionally, several metres of continuous black clay can occur as well. Sometimes sporadic shell inclusions, or an occasional fine sand layer are present (3 additional cores).

In three more cores, U6 consists of an alternation of initially blue-black, silt layers and grey fine sand layers with sporadic shell fragments, humic particles or peat layers. These silt layers typically turn brown-grey after opening the cores, and probably also the green-grey clay at the base of one of the cores, was originally black. In one other core, U6 is a 15 cm thick black silt layer with shell accumulation.

The remaining 22 cores (of the total of 131), are characterised by a lithology of black or blue-grey fine sand, often with silt admixture or silt lenses (9/22 cores), containing shell grit, fragments, whole shells, sea-urchin debris, and (black) clay strings or clay balls (7/22 cores). The shell fragments are often (6/9) accumulated in the silty zones (as observed in U5) (Fig. 7.30B). Three cores also contain humus. The transition of this sandy lithology to the underlying units is often vague.

The areal distribution of the different lithofacies of unit U6 is presented in Fig. 7.30B. The figure shows that the heterolithic clay-sand and pure black clayey sediments are located closer towards the coast, while the sandy deposits are located near the more offshore margins of U6 and in the isolated patches at the SW end, where U6 is merely draped over the underlying units. Also the silt-containing sediments (both in sandy and heterolithic cores) occur mostly in these SW isolated patches, although the silt also occurs in the other isolated patches offshore. Also the shell accumulations in silty matrix, which were interpreted as storm horizons in U5, generally occur in these SW patches.

Diatom results

Two sediment samples were taken from the sections representing seismic unit U6 in cores SEWB and SWB, in order to determine its depositional environment.
Abundant diatoms were preserved in both samples, and the assemblages suggest a marine-littoral (marine sandy tidal-flat) environment for U6 (Sue Dawson, pers. comm.) (Table 7.1). Although some species (*Paralia sulcata*, *Rhaphoneis amphiceros*, *Nitzschi punctata*, *Nitzschia navicularis*) are typical for intertidal mud flats (Vos and de Wolf 1993).

SEWB_2.40 m	SWB_1.43 m
Paralia sulcata	*Cocconeis scutellum*
Cocconeis scutellum	*Rhaphoneis surirella*
Rhabdonema minutum	*Rhaphoneis amphiceros*
Rhaphoneis surirella	*Nitzschia punctata*
Rhaphoneis amphiceros	*Nitzschia navicularis*
Nitzschia punctata	*Nitzschia panduriformis*
Nitzschia navicularis	*Cosconodiscus* fragments
Cosconodiscus marginatus	
Coscinodicus radiatus	

Table 7.1 Overview of diatom species present in U6.

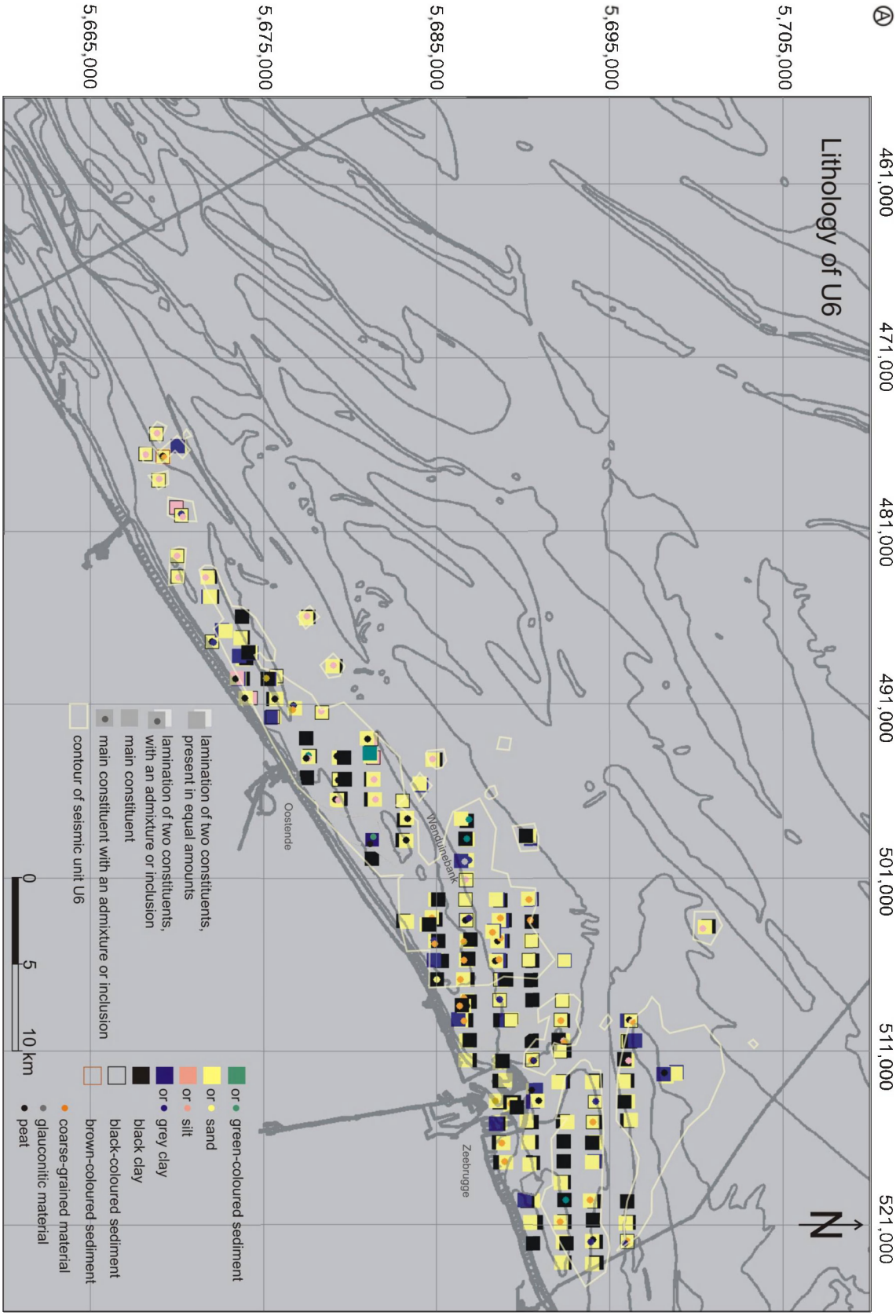

Fig. 7.30 (A) The lithology of seismic unit U6 in each of the 131 cores. Note how U6 is also encountered offshore Zeebrugge, where no seismic data are available. (B) (next page) The areal distribution of the different lithofacies of unit U6.

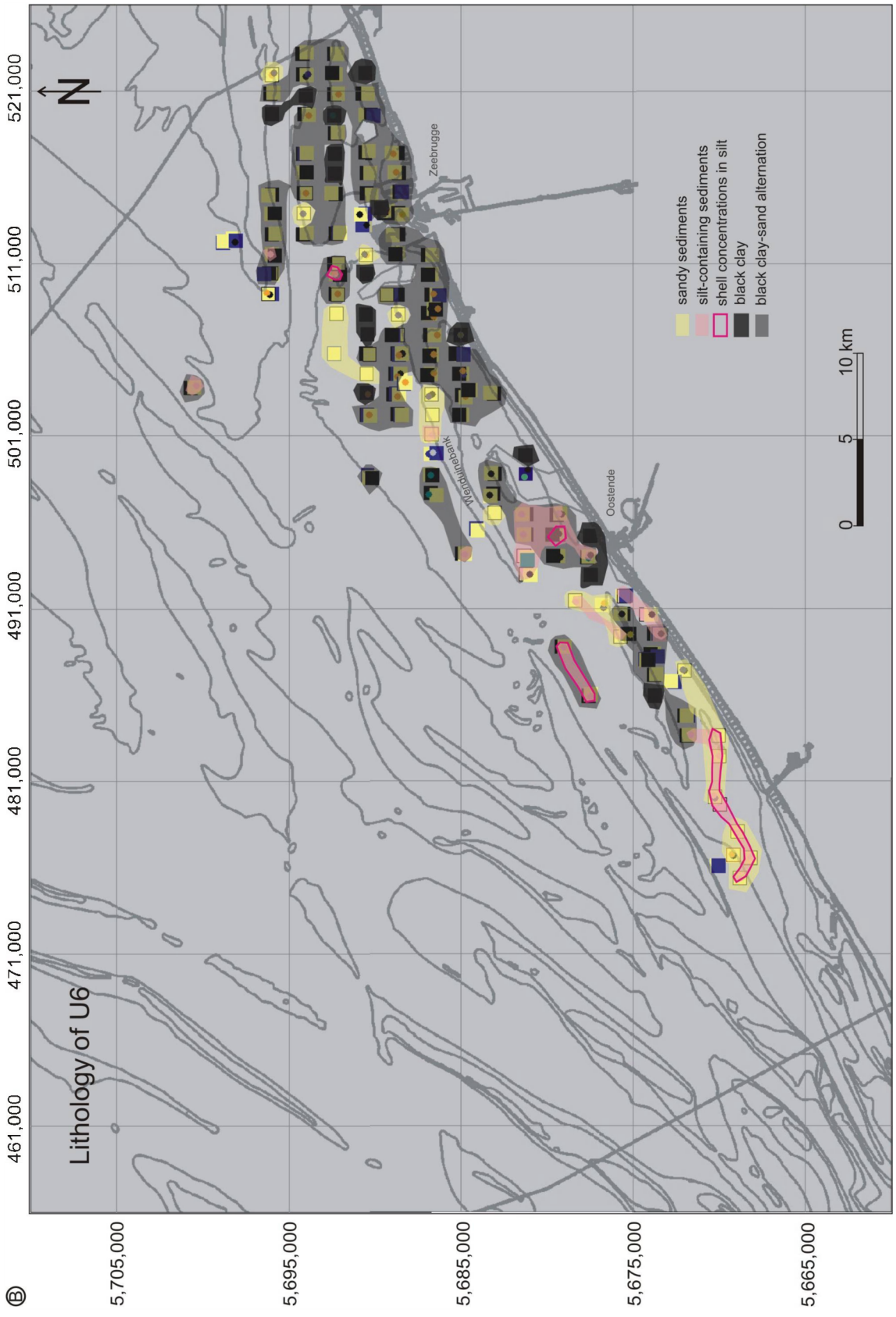
Ⓑ
Lithology of U6
N
Zeebrugge
Oostende
Wenduinebank
sandy sediments
silt-containing sediments
shell concentrations in silt
black clay
black clay-sand alternation
0
5
10 km
461,000
471,000
481,000
491,000
501,000
511,000
521,000
5,705,000
5,695,000
5,685,000
5,675,000
5,665,000

Interpretation

Interpretation of the depositional environment of unit U6 is not straightforward. The mainly clayey lithology is indicative of a low-energy environment, but also the interbedded silt and sand layers, and possible storm horizons have to be taken into account.
The high content in organic matter in the black clays, the presence of peat fragments and occasional juvenile gastropods suggest an upsilted tidal-flat environment. But on the other hand, the presence of abundant sea-urchin debris and mollusc fauna argue for a marine sublittoral environment below the low water line, or a frequent circulation with the open sea. The diatom assemblages are typical marine-littoral species (Tornqvist et al. 2000) and suggest a marine sandy tidal-flat environment (Sue Dawson, pers. comm.), although some species indicate an intertidal mud flat environment. As the diatom species are mostly strongly silicified, they can be reworked (Koen Sabbe, pers. comm.).

Unit U6 is therefore interpreted as a deposit of reworked tidal flats, clayey material that settled in a sublittoral environment below wave action, possibly still protected by e.g. coastal-near banks, but frequently disturbed by storm action.

Base of U6

The seismic data indicate that the area offshore Zeebrugge has been intensively eroded before deposition of U6, while the isolated patches offshore are not preceded by an intensive erosional phase, and are simply draped on the underlying surface. This is confirmed in the core data. In the area offshore Zeebrugge, the transition of the heterolithic facies of U6 to the underlying units (U5 or U4) is mostly sharp and erosional, while in areas where U6 is merely draped over the underlying units, the transition of the sandy lithology to the underlying units is often vague. This difference is even more underlined by the fact that in a distinct area west of Zeebrugge, U6 shows a coarsening and increase of shell content towards its base (no gravel lag) (Fig. 7.31A). These cores are mostly located at the transition between the seemingly more intensely eroded area offshore Zeebrugge, and the shallower area between the Wenduine Bank and the break in orientation of the present-day coastline (Fig. 7.31B). Boreholes SB1 and SB2, located offshore Oostende, represent two exceptions, in which U6 also shows a heterogenic coarse-grained base, overlying U4. They are, however, also located in a deeper, possibly more eroded, part in the subsurface of U6.

Additional remarks

Remarkably few cores through unit U6 contain organic matter or humic particles. In fact, organic matter and humic particles were only reported from cores, which had been described in great detail (i.e. the long borings of the GSB and TB250-TB464). This suggests that the detail of description may have played a role in identifying the presence of organic matter, especially since the black organic matter is difficult to discern in the black or dark-grey background sediments. Black clays in cores TB01 to TB142 showed a higher humic content (a few % compared to < 1% in other layers), but in the descriptions peat detritus or humic fragments were not mentioned being present in the black clays.

The one core with glauconitic sand is located next to the green-grey mud-containing cores, which were originally black (Fig. 7.30A). Is it possible that the green colour of glauconitic clay is only visible when dried (even if glauconite tends to become brownish due to oxidation)?

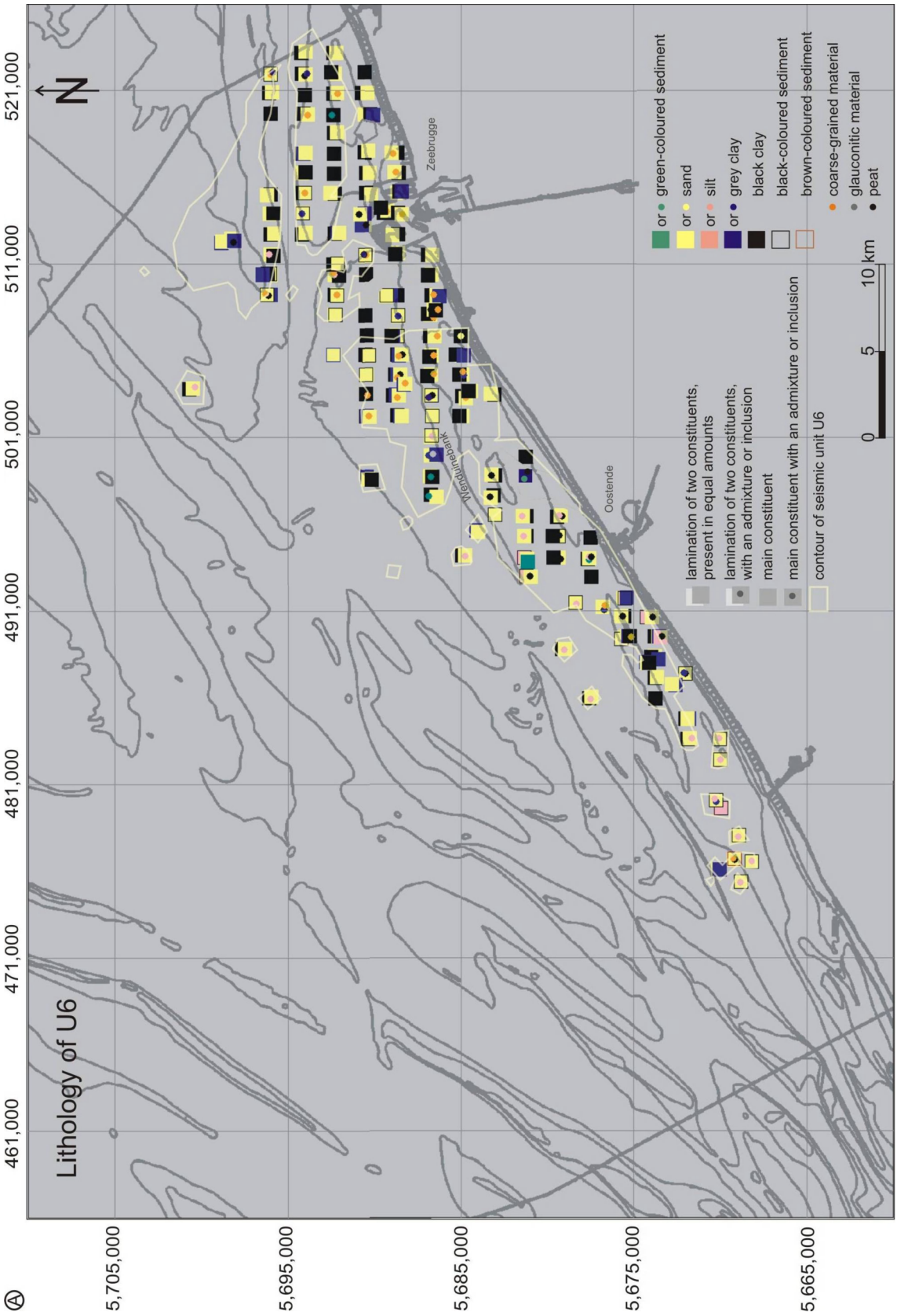

Fig. 7.31 (A) The lithology of seismic unit U6. The cores indicated with a diamond contain coarse-grained sands with shells. The dark orange diamonds represent the cores with the coarse-grained sands at the base of U5. The light orange diamonds represent cores which show no coarsening of the sand and shell content at the base of U6. All other cores show no coarse-grained sands at all.

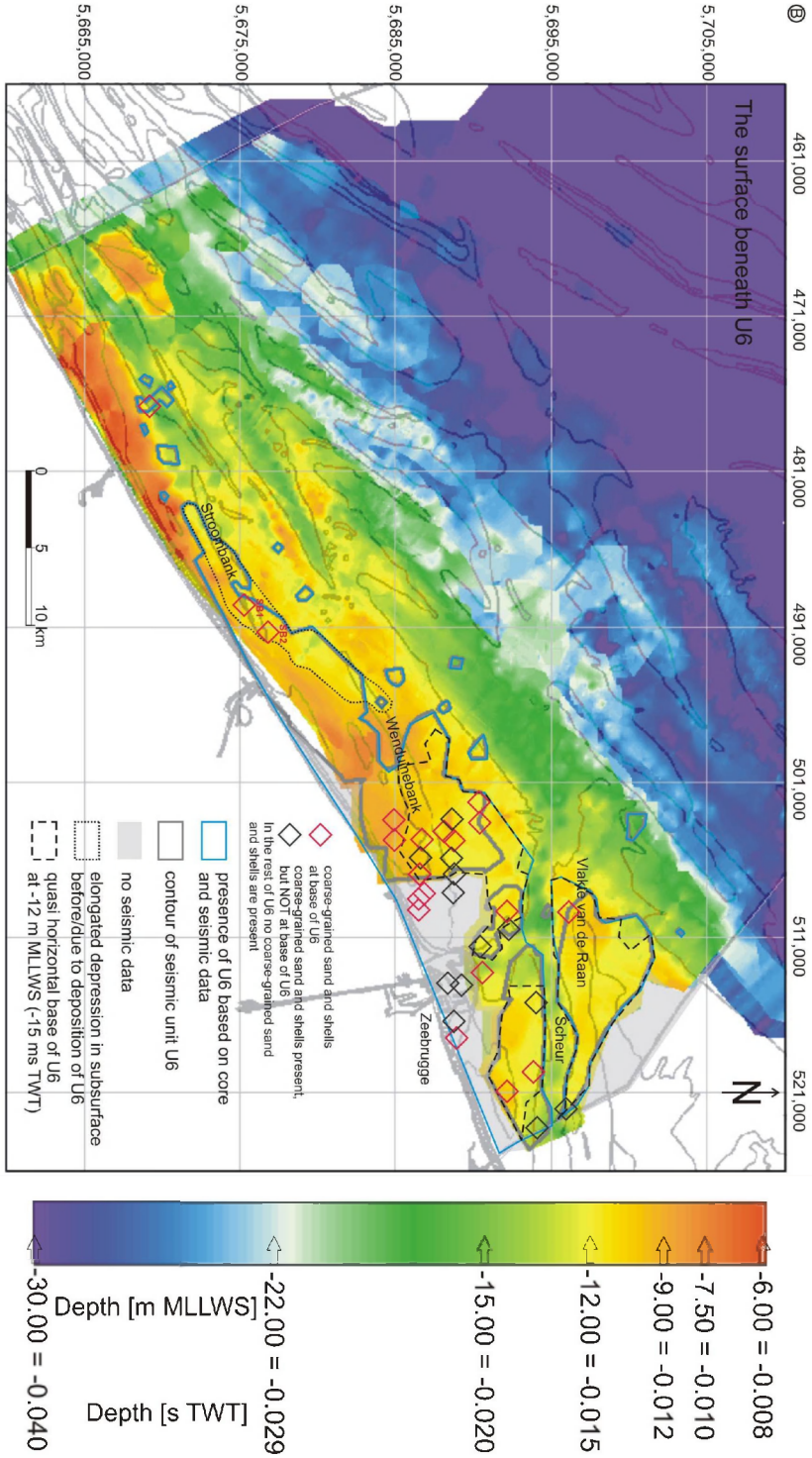

Fig. 7.31 (B) The core data confirm what was already suggested based on the seismic data, that the area offshore Zeebrugge is intensively eroded before deposition of U6, while the higher located areas below U6 and the areas of the isolated patches offshore are probably not eroded as intensively. In the area offshore Zeebrugge, the transition of the heterolithic facies of U6 to the underlying units (U5 or U4) is mostly sharp and erosional, and the cores show often a coarsening and increase of shell content at its base (no gravel lag). Note how these cores are mostly located at the transition between the seemingly more intense eroded area offshore Zeebrugge, and the shallower area between the Wenduine Bank and the present-day coastline. In the area where U6 is merely draped over the underlying units, the transition of the sandy lithology to the underlying units is often vague, and the cores show mostly no coarse-grained base at all. Exceptions are SB1 and SB2 which are located offshore Oostende, in which U6 also shows a heterogenic coarse-grained base, overlying U4. They are however also located in a deeper, possibly more eroded, part in the subsurface of U6.

Also note that the green-grey mud-containing cores are located near the area in which U4 contains green layers as well (near the Wenduinebank in Fig. 7.24B), although there is further no direct correlation between the lithology of U4 and the overlying U6. E.g. where U4 is sandier, the overlying U6 contains as much black clay as in the areas where U4 is more clayey.

7.3.2 Interpretation of erosional surfaces

From the lithology and seismic data it is clear that some intensive erosional phases occurred between the Eemian marine transgression, i.e. after the final infilling of the Ostend Valley (U3), and the deposition of U6. The surfaces moulded by these erosional phases will be discussed here, as well as the basal surface that was present at the onset of the Holocene transgression, i.e. the Top-Pleistocene surface.
Fig. 7.32 gives an overview of the (straight) borings and shows the erosional phase to which each contact between units corresponds. It demonstrates that an erosional contact between units can have resulted from multiple erosional phases, separated in time. Gravel lags that are encountered in different cores – and that were deposited during the same erosional phase- do not necessarily have to have the same lithology, as the latter depends on the local lithology (e.g. availability of gravel) of the underlying unit as well.

The Top-Pleistocene: the Eemian marine transgressive surface and imprint of the Weichselian lowstand, base of the Holocene relative sea-level rise

After the final estuarine infilling of the Ostend Valley (phase U3) during the initial part of the Eemian, the shoreface erosion during the ensuing Eemian relative sea-level rise was so severe that seismic unit U3 was completely eroded down to the level of the Top-Paleogene surface, so that remnants of U3 were only preserved in the depressions within this Top-Paleogene substratum. E.g. in the Hinderbank area, the only preserved Eemian deposits, are found below (north of) the Offshore Scarp on the Offshore Platform, while just south of (above) the scarp they were completely removed down to the Paleogene clays (Fig. 7.33 and 7.34B) (possibly not only due to the Eemian transgression in this area, but in combination with the later Holocene transgression). During the subsequent Weichselian lowstand, only a small sinuous river incised in the Eemian marine transgressive surface, where previously the Ostend Valley existed. No Weichselian cover sands were encountered above this marine transgressive surface. Instead, it was directly overlain by early-Holocene tidal-flat deposits (Heyse et al. 1995, Trentesaux et al. 1999). The base of the Holocene, or the Top-Pleistocene surface, can thus be composed by merging the Paleogene surface (QT) with the top surface of the Eemian deposits (i.e. U3 and IVDB Eemian, where present). Fig. 7.34A shows the morphology of this surface, merged with the Top-Pleistocene surface of the Coastal Plain.

Note that this Top-Pleistocene surface represents the base of the Holocene deposits as it occurs in the present-day subsurface, and not a reconstruction of the real topography at that time. E.g. in the Hinderbank area, the present-day bank-swale topography can clearly be distinguished in the Top-Pleistocene surface. Also in the Coastal Plain, one has to be careful not to take incisions by Late Holocene tidal channels for the original Pleistocene topography.
As already described above (7.2.1), also the tidal channels of U4 left imprints in the underlying Pleistocene surface (Fig. 7.4). There are also areas where U5 is located directly on top of U3 or QT, and thus where the Pre-Holocene surface might have been modified by the storm-dominated banks of U5 (Fig. 7.5, where U5 extends outside the contours of U4). Except for the Hinderbank area, the imprint of the present-day hydrodynamic processes on the topography of the Top-Pleistocene surface in the

offshore region is less obvious. Nevertheless, the Pre-Holocene surface lies systematically higher below the present-day sandbanks, than in the adjacent swales, which suggests that the original surface has been eroded in the swales (Fig. 7.34B).

For the paleo-reconstructions in the next section, this Top-Pleistocene or Pre-Holocene surface will be used as the reference surface representing the topography of the landscape at the time of the Holocene sea-level rise, but always bearing in mind the later imprints.
The Top-Pleistocene surface slopes down in NW direction, from +7m TAW in the Coastal Plain, where the Paleogene substrate emerges in the hinterland, to -42 m GLLWS in the NW corner of the BCS. In the eastern Coastal Plain, the surface ranges from +7 m at the more landward side, to -7 m at the coastline west of Zeebrugge. East of Zeebrugge, near Knokke-Heist (Het Zwin) and the Dutch border Late-Holocene tidal channels incised the Pleistocene surface (Vos and van Heeringen 1997).
In the western Coastal Plain, the Pre-Holocene surface shows incisions from the former IJzer from -7 m inland, to -18 m at the present-day coastline, which seem to continue offshore to -21 m. The shallowest occurrence of the Top-Pleistocene surface offshore, is west and east of Zeebrugge where the Paleogene substrate reaches up to -13 m (in SWB) and -12 m (profile BI_06), respectively, below tidal-flat deposits of U4. The surface slopes down to -20 m at around 13.5 km offshore (slope ~0.05% or 0.029°) where the Nearshore Slope Break occurs (slope 0.27°), and the surface drops down to a depth of -24 m. About 10-14 km further offshore, a second, but less obvious scarp/slope break occurs, i.e. the Middle Scarp (Liu et al. 1992), where the surface drops from about -27 m to -29 m. Apart from these scarps, the surface also shows a Weichselian renewed incision to a depth of –21 m in the area of the former Ostend Valley. This renewed river incision is, however, not present in the Pleistocene surface of the Coastal Plain. Most likely, the river found its course in the nearshore area off Zeebrugge, where no seismic data are available, and few cores reach as deep as the top of the Pleistocene.
Further offshore, the Pre-Holocene surface gradually slopes down from -29 m to -43 m (slope ~0.03% or 0.018°), although intensively impacted by the present-day bank-swale hydrodynamics. In this area, the surface coincides largely with the Top-Paleogene surface. Also, no Holocene tidal-flat deposits (U4) are present here, so that the offshore part of the Pre-Holocene surface may have been moulded by both the Eemian and Holocene transgressions, removing most of the Eemian (U3 and IVDB) and all of the Holocene U4 deposits (if ever deposited there). This also implies that in the Hinder Banks area, the Eemian deposits found north of the Offshore Scarp on the Offshore Platform, have probably been levelled with the Top-Paleogene substratum of the Middle Platform by both the Eemian and the Holocene transgressions, as on top of the Eemian remnants only present-day tidal sandbanks are present (U7), and no early Holocene deposits from before the transgression like tidal flats or basal peats.

The polygenetic Top-Pleistocene surface is punctuated and overlain by a gravel lag, which occurs at the base of both U4 and U5, where U5 is located directly on top of U3 or QT. As will be shown below, this gravel lag is also present at the base of U7, where U7 unit is located directly on top of U3 or QT (cf. 8.3.1). Indeed, all gravel lags found at the contact between the Pleistocene surface, which is composed of U3 and QT, and U4, were deposited during the same erosional phase of the Eemian transgression (Fig. 7.32). Where U4 is not present, the basal gravel lag of any other overlying unit (i.e. U5 or U7) can most likely be attributed to this phase as well. Although probably influenced by the erosional phase that removed U4, or U5 in those cases where U7 directly overlies U3 or QT. In other words, the gravel lag encountered in borehole NWB at the base of U5, which directly overlies the outer estuarine deposits of U3 (at -15.8 m MLLWS), is deposited during the same time frame as the gravel lag found in SWB (at -13.2 m) at the base of U4, which overlies QT.

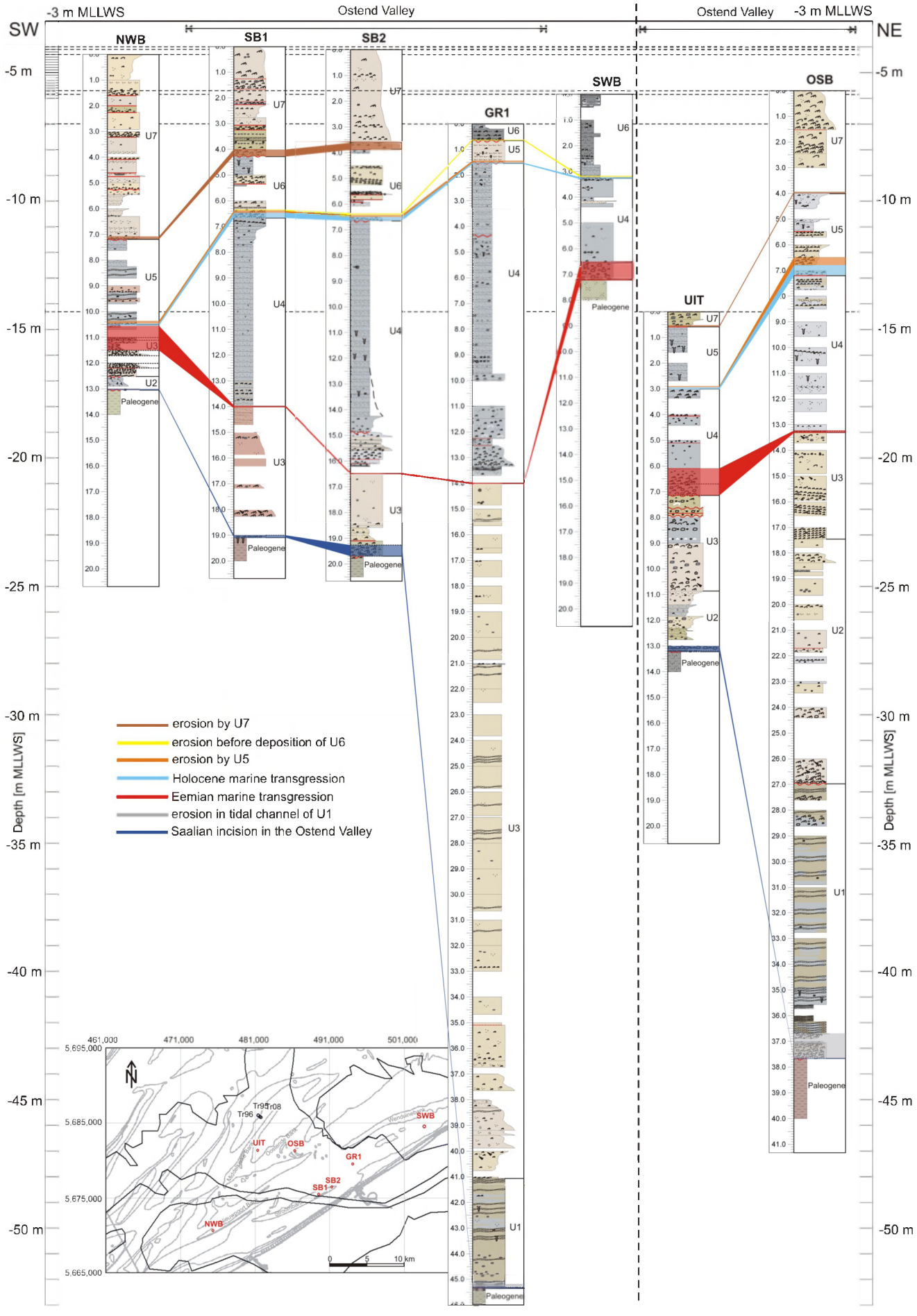
SW
NE
-3 m MLLWS
Ostend Valley
NWB
SB1
SB2
GR1
SWB
UIT
OSB
U1
U2
U3
U4
U5
U6
U7
Paleogene
-5 m
-10 m
-15 m
-20 m
-25 m
-30 m
-35 m
-40 m
-45 m
-50 m
Depth [m MLLWS]
erosion by U7
erosion before deposition of U6
erosion by U5
Holocene marine transgression
Eemian marine transgression
erosion in tidal channel of U1
Saalian incision in the Ostend Valley
461,000
471,000
481,000
491,000
501,000
5,695,000
5,685,000
5,675,000
5,665,000
Tr95
Tr08
Tr96
0
5
10 km

Fig. 7.32 (page 195) Composition of Figs. 6.14B and 6.15B, showing to which erosive phase each contact between units corresponds. It demonstrates that an erosional contact between units can be related to multiple erosive phases in time. And gravel lags in different cores, deposited during the same erosive phase, do not have necessarily the same lithology, as one has to take into account the lithology (availability of gravel) of the underlying unit as well. For more detailed lithologs is referred to Appendix B. The thickness of the coloured band at the erosional boundary represents the thickness of the related gravel lag or coarse-grained base.

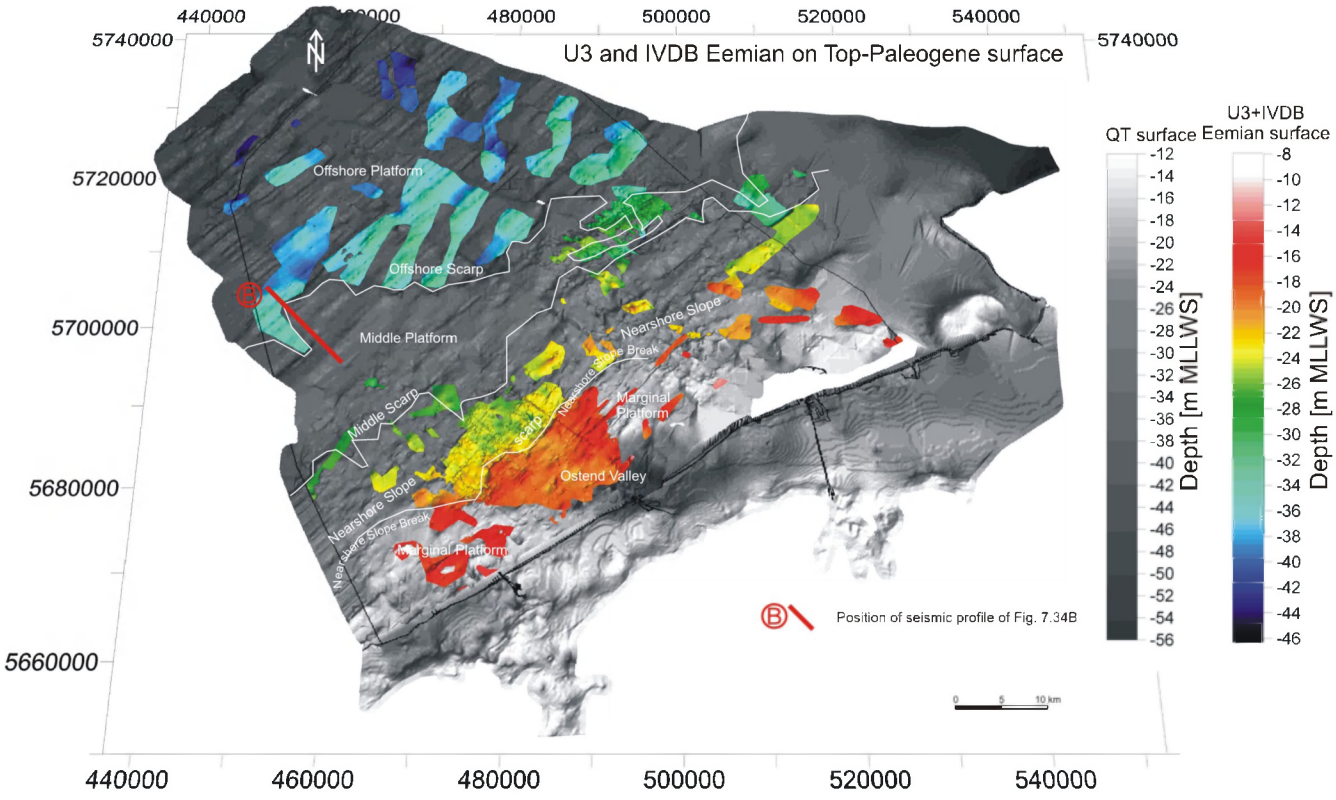

Fig. 7.33 Isobath map of the top surface of seismic unit U3 and IVDB Eemian deposits (in colour). The surface is shown in 3D on top of the underlying Top-Paleogene surface (QT reflector, in grey). After the final estuarine infilling of the Ostend Valley (phase U3), the shoreface erosion during the Eemian relative sea-level rise was that severe, that seismic unit U3 and IVDB Eemian deposits were completely levelled with the Top-Paleogene surface, and remnants were only left in depressions in the Top-Paleogene substratum. E.g. in the Hinderbank area, the only Eemian deposits left, are found below the Offshore Scarp on the Offshore Platform, while just south of the scarp they are completely removed down to the Paleogene clays.

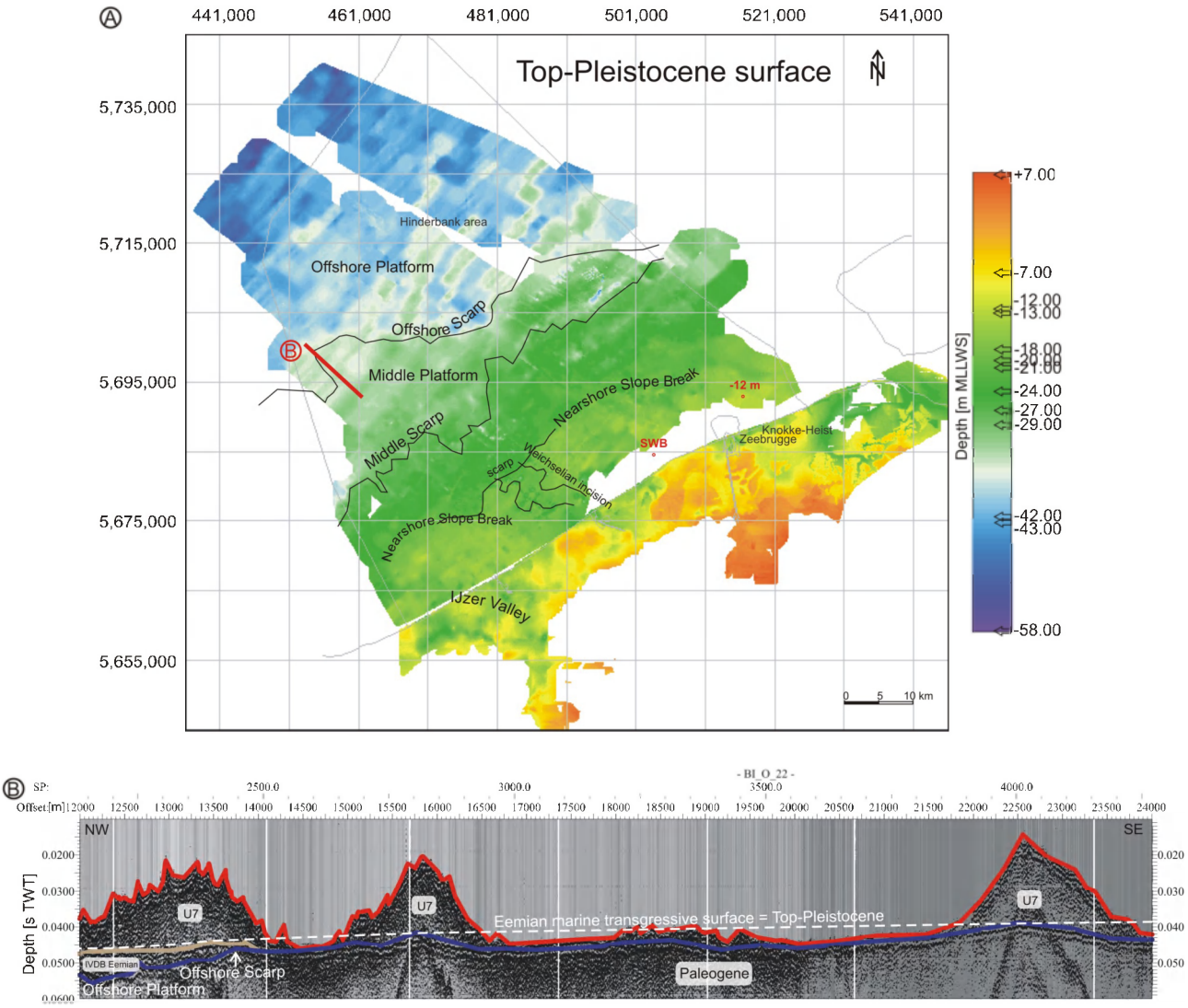

Fig. 7.34 (A) Top-Pleistocene surface composed of the QT, U3 and IVDB Eemian surfaces. Note that this surface is the Top Pleistocene as it is found in the present-day subsurface, and not a reconstruction of the reality at that time. (B) Seismic section showing the impact of the present-day hydrodynamic processes on the Top-Pleistocene surface. The Top-Paleogene surface on the seismic profile, corresponds as well to the Eemian marine transgressive surface, as the Eemian deposits are levelled together with this surface during the Eemian relative sea-level rise (this is also the Top-Pleistocene surface as no younger Pleistocene deposits have been encountered). The surface lies systematically higher (even when corrected for velocity effects) below the present-day sandbanks, than in the adjacent swales, which implies that the original Top-Pleistocene surface has been eroded in the swales.

As discussed above, the gravel lag is most pronounced offshore, in the area of the Middelkerke Bank, where it overlies U3, instead of QT, as it does in the nearshore area. It is likely that during the Eemian transgression less gravel was supplied to the areas above the scarp in U3. The massive gravel lag encountered in SWB (above the scarp) would then have a local origin, derived from the underlying sandstone-layer-containing Paleogene clays. Also in NWB, located above the scarp, a 1 m thick gravel lag is encountered below the base of U5. These gravels are probably (at least partly) derived from the immediately underlying coarse-grained outer-estuary deposits of U3 (cf. 6.3.3 Paleo-landscape reconstructions). An admixture of gravel supplied by the Holocene transgression, which possible removed U4 in the area of NWB, can, however, not be excluded either. So the local availability of gravel in the underlying layers is an important factor determining the distribution of a gravel lag on a marine transgressive surface. This

is underscored by the fact that the gravel lag in SWB, located on top of QT shows many similarities with the gravel lag at the base of U3 on top of QT in SB1 and SB2 (Fig. 7.32 and Appendix B for detailed lithologs). Although deposited at different times, they all contain reworked Paleogene shells and silex fragments, most likely derived from the underlying Paleogene substratum. Conversely, gravel lags deposited during the same period (e.g. during Eemian transgression in NWB and SWB, both above the scarp), do not necessarily have the same lithology (cf. Appendix B for detailed lithologs of NWB and SWB).
It thus appears that during the Eemian shoreface erosion, high-energy hydrodynamic processes (wave action, storm, tidal action) were on the one hand able to transport gravel from offshore towards the shoreface, in front of which it accumulated during the slowdown or acceleration in sea-level rise (which formed the Nearshore Slope Break or scarp in U3), and on the other hand, to wash out the fines from the underlying deposits, which created a gravel lag in areas where gravel was locally available.

The Holocene marine transgressive surface

Seismic unit U4 has been interpreted as having been deposited in a tidal-flat environment, probably landward of a coastal barrier. According to van der Molen and van Dijck (2000), the land bridge between northern Holland and Britain (Texel Spur-Norfolk Banks) was flooded at around 8500 BP (9500 cal BP). The tidal energy from the northern North Sea could enter the Southern Bight, and barrier islands with back-barrier basins formed along the eastern shore of the Southern Bight prior to 8000 BP (9000 cal BP), due to the predominance of westerly winds and the low gradient of the pre-transgressive, Pleistocene surface. According to Beets and van der Spek (2000), however, the Southern Bight was still isolated from the northern North Sea at 8500 BP (9500 cal BP), but was nevertheless already sufficient in size to produce waves at its eastern shores capable of building a protective barrier behind which a complex of estuaries and tidal basins could develop. Sand to fill the basins was derived from the shoreface adjacent to the tidal inlets and from the ebb-tidal deltas. As insufficient sediment was supplied to the shoreface by along-shore and cross-shore transport to compensate for this sediment loss, the shoreline was forced to recede (Beets and van der Spek 2000), while eroding the underlying deposits. Shoreface erosion by receding barriers leaves a sand sheet on the shelf, seaward of the barrier (Swift et al. 1973, Swift and Thorne 1991). From this sandy layer storm-generated or shoreface-connected ridges can be formed under influence of storm and tidal forces (Swift et al. 1973, van de Meene and van Rijn 2000).

The erosional surface at the top of U4, clearly recognised on the seismic data (truncation of internal reflectors of U4) as well as in the lithological data (gravel lag and coarse-grained shell lag at the base U5), was thus most likely formed by the regional shoreface erosion of the receding barrier during the Holocene transgression, followed by local erosion related to the formation of storm-generated ridges (U5).

As discussed above, little is preserved of seismic unit U4, and its surface shows imprints of U5, U6 and U7 (swales and banks) (Fig. 7.5). Note that the erosional phases associated with the deposition of U6 and U7 also affect U5 (Fig. 7.13), which means they took place *after* the deposition of U5. They will be discussed in the next sections. In this section, the Holocene marine transgressive surface or barrier shoreface ravinement surface is discussed, which is present above the tidal-flat deposits of U4 and below the storm-generated ridges of U5 (Fig. 7.35). In areas where U5 is not present, the Holocene marine transgressive surface corresponds to the base of U6, and where that unit is not present, to the base of U7. In these cases, an extra imprint on the marine transgressive surface is possible by the erosional phases related to the deposition of U6 and U7. Where unit U4 is not present, U5 or U7 directly overly U3 or QT, and the Holocene marine transgressive surface coincides with the Eemian marine transgressive surface.

Although it is not sure that the tidal flats of U4 have ever been deposited in the offshore area, the Holocene transgression set in after the Last Glacial Maximum, when the relative sea level was about 120 m lower than today, and so has affected the entire BCS. The example of the Hinder Bank area has already been given. The Eemian deposits found below (north of) the Offshore Scarp on the Offshore Platform, have probably been levelled with the Top-Paleogene substratum by both the Eemian and Holocene transgressions, as on top of the Eemian remnants only present-day tidal sandbanks are found (U7). It can, however, not be determined which erosional phase was the most intensive and reached deepest, whether the Holocene shoreface erosion removed only initial Holocene deposits, or whether it also levelled the Eemian deposits of the Offshore platform with the Top-Paleogene surface of the Middle Platform.

The surface of U4 slopes down in NW direction from –7 m to –28 m MLLWS, with a sudden drop of 3-4 m (from about –12 m to –16 m), at a distance of 5-13 km offshore the present-day coastline (13 km in the most north-eastern part of U4) ('scarp' on Figs. 7.5A and 7.35). Further offshore the surface coincides with the Top-Pleistocene surface, described above, so the focus lies on the nearshore part where U4 occurs. There are a number of features that affect the surface of U4, such as depressions, occurring over distances of about 5-6 km, alternately under the steep and gentle sides of the U5 storm-generated ridges, and zones where U4 is completely removed (Fig. 7.35).
At first sight, the sudden drop in the Holocene marine transgressive surface seems not to be related to a slowdown, stillstand or acceleration in the relative sea-level rise, as is the case for the scarp in the Eemian marine transgressive surface, but appears to be related to the presence of U5 (Fig. 7.5BC). Where the surface of U4 expresses the 'scarp'-morphology, U5 leans against the emerging surface of U4.
The depressions that alternate with zones where U4 emerges beneath the nearshore bank, which have been described before (Fig. 7.11B), could be related to the presence of tidal inlets, separating the barrier islands which migrated over U4. The large depression in the surface of U4, below the nearshore bank offshore Nieuwpoort, where U4 is almost entirely eroded, might be formed by the strong tidal currents in a tidal inlet. This is supported by the fact that in the nearshore bank above the depression in U4, channel-like structures are present in U5, which could represent flood and ebb channels in the tidal inlet (Fig. 7.11B). In that case, the western part of the nearshore bank of U5 would be part of a barrier. This depression in U4 lies in line with a zone offshore, where U4 is completely removed (Fig. 7.35). It is possible that during the Holocene transgression, when the barrier continuously migrated landward over earlier deposits of U4, that these were completely removed in the strong erosional areas of the along-landward-shifting tidal inlets. A similar process could have occurred in the area between the Oostende Bank and the Vlakte van de Raan, where U4 is also completely removed in a large area. However, in the area offshore Nieuwpoort, the elevated Marginal Platform is present below U4. Most likely only thin tidal-flat deposits could have developed on top of it, which would sooner be completely removed than in areas where U4 is more massive. Thus, the presence of local strong erosional processes as in tidal inlets, is not the only possible explanation for the almost complete removal of U4 in certain areas.
The much smaller depressions in the U4 surface, alternately below the gentle and steep side of the offshore and middle storm-generated ridges, are probably due to natural rhythms in the hydrodynamic processes, which lie at the origin of the formation of these sand ridges.

The Holocene marine transgressive surface is sedimentologically mainly characterised by an increase and coarsening of the shell content. Also gravel lags occur, encountered at the base of U5 and U7 (where U7 is located directly on top of U4, cf. 8.3.1). The base of U6 shows no gravel lags, only coarse-grained shell layers.

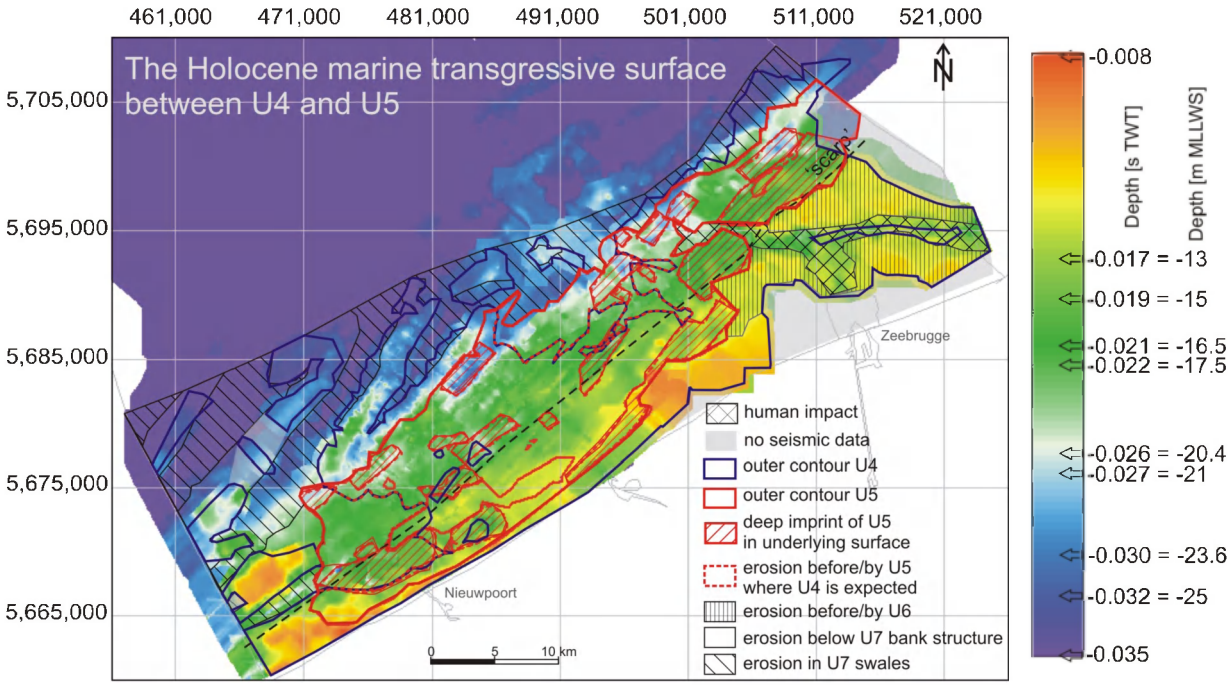

Fig. 7.35 Isobath map of the Holocene marine transgressive surface. It is a polygenetic surface, with imprints of eroding storm-generated sand ridges (U5), and impacts of later erosion before deposition of U6, and erosion by the present-day hydrodynamic processes (U7 banks and swales). This makes it difficult to reconstruct the original depth of the shoreface erosion, and from this the related relative sea-level and deduced age. The colour bar is set up as such that the structural features in the nearshore area are enhanced.

Indeed, all coarse-grained lags found on top of the Holocene marine transgressive surface (i.e. the top of U4, or the top of U3 or QT in case U4 is removed) and at the base of U5, have been deposited during the same erosional phase of the Holocene transgression (Fig. 7.32). Although a contribution by later local erosion (e.g. at the base of U5) is possible. If U5 is not present, the basal coarse-grained lag of any other overlying unit (i.e. U6 or U7) most likely corresponds to the Holocene marine transgression phase as well. Probably also influenced by the erosional phases that removed U5, and U6 in case U7 directly overlies U4. In areas where U4 is not present (i.e. because it was removed down to the underlying Top-Pleistocene surface), remnants of the Eemian transgressive phase probably also contribute to the basal coarse-grained lag (e.g. in NWB).

The coarse-grained layers at the base of U5 have possibly multiple origins. The gravel lags are interpreted as an indication of an intensive erosional phase before deposition of U5, i.e. the shoreface erosion during Holocene transgression. But, the presence of a gravel lag does not necessarily imply that in that area the original transgressive surface is still present, because of the possible reworking during the later deposition of unit U5.
The coarse-grained shelly base of U5 rather points to an additional erosive character of the storm-generated sand ridges itself, or a high-energetic phase in the initial deposition of U5, e.g. storm layers. Especially the local, undulating character of the base of U5 suggests that also U5 itself is eroding the underlying units. If only the Holocene transgression had occurred before the deposition of U5, it would have left a regional planation surface similar to the Eemian shoreface ravinement surface, rather than local depressions alternately below steep and gentle sides. Most likely, shells have been accumulated by storms and strong currents in some areas, while in local depressions finer sediments settled (cf. 7.3.1 discussion basal gravel lags of seismic unit U5), before deposition of the sand ridges. Alternately, the coarse-grained shell lag could have been

created during the growth and development of the sand ridges: i.e. currents in the adjacent troughs washed out the finer material from the underlying units used for building up the ridges, leaving behind a coarse-grained shell lag at the base of the (migrating, growing) ridge. This would also explain the similarities between the lithologies of U5 and U4, i.e. U5 is actually composed of material eroded from U4.

Most of the cores that contain a gravel lag at the base of U5 are located near the Middelkerke Bank. The reason why only the cores in this area contain a gravel lag at the base of U5 is probably because generally little gravel was available in the underlying units; i.e. especially U4 contains only coarse material in tidal-channel infillings. The gravel occurrences near the Middelkerke Bank are therefore probably due to the fact that in that area U4 is very thin and closely located to the Eemian marine transgressive surface (top of U3), characterised by pronounced gravel lags. Alternately, gravel could have been brought to that area by the Holocene shoreface ravinement processes, from the nearby offshore area, where possibly the underlying unit U4 was very thin or absent and the Eemian marine transgressive surface (with gravel lag) was exposed.

The Holocene marine transgressive surface, as it is present in the subsurface, is a polygenetic surface, with imprints of eroding storm-generated sand ridges (U5), and impacts of subsequent erosion before deposition of U6, and by the present-day hydrodynamic processes (banks and swales of U7). This polygenetic origin makes it difficult to reconstruct the original depth of the shoreface erosion, and to derive from it the exact sea level and –using published relative sea-level curves- the age of the transgression.

Surface of barrier progradation and subsequent landward retreat

The presented surface corresponds to an erosional phase which influenced both the top of the storm-generated sand ridges of U5 in front of a barrier, and the tidal-flat deposits of U4 in the back-barrier environment. The surface is located below the U6 deposits (Fig. 7.14AB).

Prior to 7500 cal BP, the sand supply from shoreface erosion was insufficient to balance the rapid relative sea-level rise, and the shoreline was forced to recede. According to Baeteman (2004), the decrease in the rate of relative sea-level rise after 7500 cal BP, resulted in a sand surplus and consequently in the silting up of the tidal basins of the western Coastal Plain and the onset of stabilisation of the coastal barrier. Between 6800 and 6000 cal BP, the relative sea-level rise lost its driving force (Baeteman and Declercq 2002), sediment supply exceeded the accommodation space created by the rising sea level, and this induced the coastal barrier to prograde (Baeteman and Declercq 2002, Baeteman 2005a). Between 5500-5000 cal BP, the rate of relative sea-level rise decreased again, and the area behind the protecting coastal barrier of the western Coastal Plain changed into a freshwater marsh with peat accumulation. At that time, the barrier prograded beyond the present-day coastline. After 2000-3000 years of uninterrupted peat growth, a tidal system was again installed in the western Coastal Plain between 3000 and 2400 cal BP (Baeteman 2004). Shoreface erosion and shoreline retreat occurred, and peat areas were again transformed into sub- and intertidal flats.
In accordance with the evolution in the western Coastal Plain, the erosional surface at the top of U5 and U4 might represent a shoreface ravinement surface, due to barrier progradation and subsequent retreat, following the development of the U5 sand ridges in front of a stabilised coastal barrier. The barrier progradation could have caused the erosion of the storm-generated ridges (U5) and the retreat caused the erosion of earlier back-barrier deposits (U4) and surface peat, and these eroded sediments settled on the ravinement surface as U6.

As this erosional phase only affected U5 and U4 (up to the present-day coastline), only the nearshore section of the presented surface, underlain by U5, U4 and U3, and by QT, will be discussed (Fig. 7.36).
The surface slopes down in NW direction ranging from -6 m in the west (where shallow U5 remnants are present) and -10 m in the east (where the top of U4 forms the surface), to -17 to -22 m offshore, with a sudden drop of 8 m (from about –6 to –14 m) at a distance of 2-4 km offshore the present-day coastline in the SW, and a drop of 5 m from about –12 to –17 m at a distance of 10 km offshore in the NE. Both drops in the morphology are actually related to the formation of the swales and banks under the modern hydrodynamic conditions (U7) (Fig. 7.36), and will therefore be discussed in the next chapter.
In a large area offshore Zeebrugge and near the Vlakte van de Raan, the erosional surface above U5 and U4 is nearly horizontal, and lies at a depth of -12 m MLLWS (-15 ms) (Fig. 7.14AB). In the area between the Wenduine Bank and the present-day coastline, where the latter changes in general orientation, the erosional surface is located much shallower, at depths of -9 to -7.5 m (-12 to -10 ms). Further along the coastline in SW direction, between Nieuwpoort and De Panne, the surface even reaches heights of -6 m. Further offshore, in an area connecting the ends of the Wenduine Bank and Stroombank, the erosional base of U6 shows an elongated depression to -12 m (-15 ms). The isolated patches of U6 offshore show no horizontal erosional basal surface, but follow the underlying topography of the U5 remnants and are located at depths of -15 m (-20 ms).

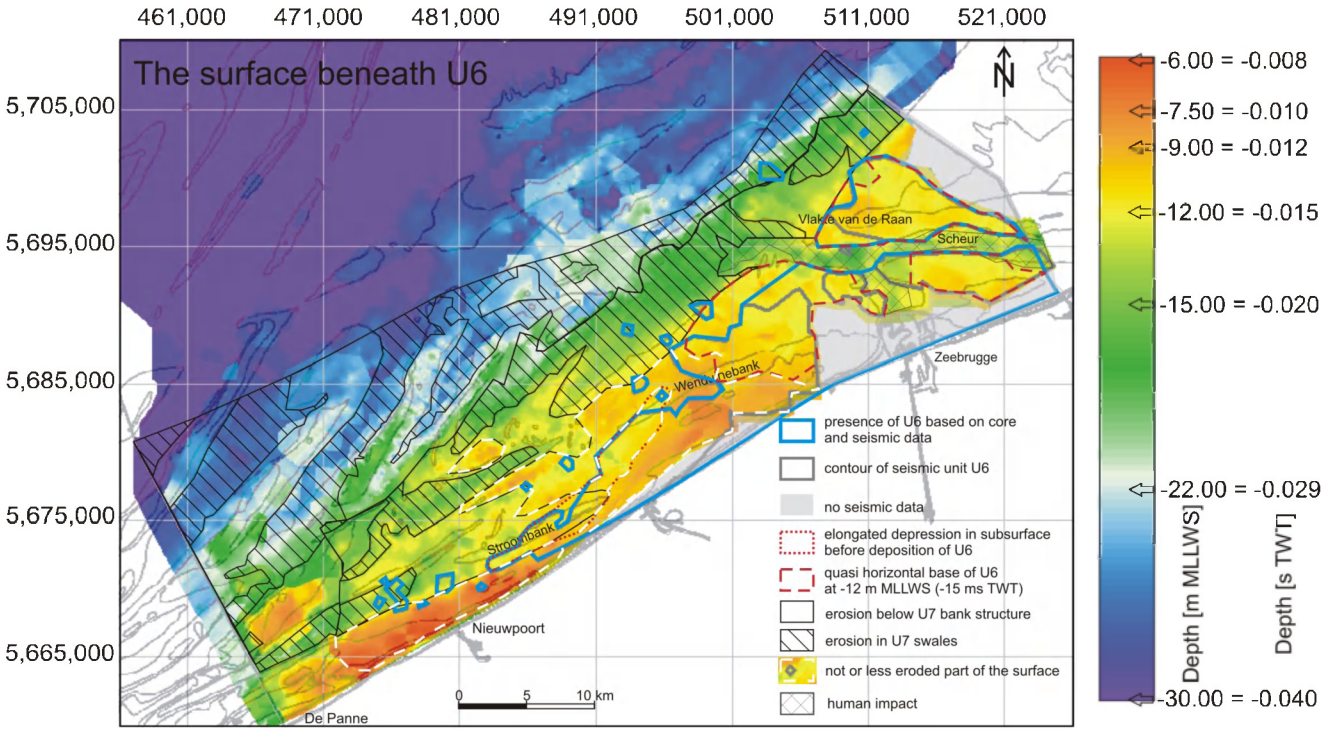

Fig. 7.36 Isobath map of the surface below seismic unit U6. It is a polygenetic surface, with erosion by the present-day hydrodynamic processes (U7 banks and swales), and evidence of erosion before deposition of U6. Over a large area offshore Zeebrugge and near the Vlakte van de Raan, the erosional surface below U6 is nearly horizontal, in the area between the Wenduine Bank and the present-day coastline, however, the erosional surface is located much shallower. Further along the coastline in SW direction, between Nieuwpoort and De Panne, the surface reaches even higher. Further offshore, in an area connecting the ends of the Wenduine Bank and Stroombank, the erosional base of U6 shows an elongated depression.

The surface also shows offshore nearly coast-parallel highs of about -11 m, the shallowest parts (up to -8 m) representing the almost original shapes of the storm-dominated sand ridges of U5 (Fig. 7.36). Large parts have, however, been eroded under the modern hydrodynamic processes and the formation of tidal sandbanks and swales, as will be discussed in the next chapter.

In the light of the proposed model of barrier progradation and retreat, the horizontal eroded section in the area offshore Zeebrugge (over U5 and U4), might represent the erosional surface of a receding barrier (after progradation over the sand ridges of U5), similar to the planation surface (or shoreface ravinement surface) that was left by the landward-migrating coastline during the Eemian marine transgression. The shallower part of the surface, between the Wenduine bank and the knick point in the present-day coastline, might represent the hinge point of the recession: i.e. near the Dutch border, the barrier retreated drastically over a distance of several kilometres, while the amount of retreat and the intensity of the associated erosion becomes gradually less towards this hinge point. The elevated area further SW along the coastline, between Nieuwpoort and De Panne, has probably not been eroded because U5 shows no clear erosional surface: internal reflectors are not truncated, and the surface is not characteristically horizontal, but smoothly undulating. The difference in erosional depth between the area offshore Zeebrugge (to -12 m) and the coastal-near shallow areas to the SW (-9 to -6 m), and the details on the origin of this surface will be discussed in '7.3.3 Paleo-reconstructions and chronostratigraphic framework'.

The deep elongated area between the Wenduine Bank and the Stroombank, which seems to be also intensively eroded, although not by barrier retreat, might represent a channel in front of the barrier, scoured by storm and tidal currents. It seems that the offshore isolated patches of U6 have simply been draped on the underlying surface. These sediments are probably transported to that area by longshore currents or storm events.

The described erosional surface corresponds in the area offshore Zeebrugge to a mostly sharp and erosional contact between unit U6 to the underlying unit, while in the other areas the transition of the underlying unit into the sandy lithology of U6 is often vague. This difference is even more underlined by the fact that in a distinct area west of Zeebrugge, U6 shows a coarsening and increase of shell content at its base (no gravel lag). The cores in which this is observed are all located at the transition between the area eroded by barrier recession and the area probably not eroded by barrier recession, i.e. at the inferred hinge point of the barrier retreat. The heterogenic coarse-grained bases, observed in SB1 and SB2, are located in the elongated channel, which was probably deposited or washed out by strong storm and/or tidal currents.

Little is preserved of the original shape of the U5 storm-generated sand ridges. Most of it has been eroded by modern hydrodynamic processes with the formation of swales and tidal sandbanks (U7), but also a large part of its surface, together with the surface of U4, has been modified by the barrier progradation and subsequent retreat. As the erosional surface, which separates units U5 and U4 from U6, partly makes up the boundary between back-barrier tidal-flat deposits (U4) and open-marine deposits (U6), it actually is also part of the Holocene marine transgression surface.

The formation of tidal sandbanks and swales

All previous discussed erosional surfaces, as well as the top of U6, show an imprint of, or are affected by the formation of tidal sandbanks and swales under the modern hydrodynamic conditions, which will be discussed in the next chapter.

7.3.3 Paleo-reconstructions and chronostratigraphic framework

In this section, the above-discussed evolution of a back-barrier basin up to the development of storm-generated banks will be illustrated by means of a series of reconstruction maps. These maps have been generated, based on the presented results (i.e. integration of seismic and lithology data, interpretation of erosional surfaces) and taking into account information from literature. By linking depositional depths with the Holocene relative sea-level curve (Denys and Baeteman 1995, Baeteman 2004), the paleo-reconstructions will also be fit in a chronostratigraphic framework.

Depositional phase U4: development of a back-barrier basin and barrier retreat

The results

- On top of the Eemian marine transgressive surface and Weichselian renewed river valley incision, tidal flats (U4) developed behind a coastal barrier.
- The U4 tidal-flat deposits extend to the present-day coastline, and range (vertically) between -7 and -28 m MLLWS.
- In cores TB358 and 78/H10 *in situ* peat horizons occur at a depth of -12 m and -11 m MLLWS, respectively. Near the Middelkerke Bank, possible remnants of a basal peat occur at a depth of about -25 m, on top of U3.

To take into account from literature

- At 9500 cal BP, the Southern Bight was already sufficient in size for the building of a barrier with estuaries and tidal basins behind it (Beets and van der Spek 2000, van der Molen and van Dijck 2000). Sand to fill the basins was derived from the shoreface adjacent to the tidal inlets and from the ebb-tidal deltas. As insufficient sediment was supplied to the shoreface to compensate for this sediment loss, the shoreline was forced to recede (Beets and van der Spek 2000), while eroding the underlying deposits.
- Based on the depth of rootlets and comparison with similar deposits in the Netherlands (Elbow Formation), an Early-Holocene age was proposed for subtidal, lagoonal or tidal-flat deposits in the Middelkerke Bank (Heyse et al. 1995, Trentesaux et al. 1999). This unit is included in our seismic unit U4.
- The different landscapes in a tidal-flat environment are typically related to certain water levels. Mud and sand flats are intertidal deposits that occur between high water at neap tide, and mean low water level. For convenience it is assumed that sand flats occur to a level in the middle of the intertidal flats, exactly in between high water at neap tide and mean low water. Salt marshes develop in supratidal conditions, above high water at neap tide. Tidal channels always stay in subtidal position, below mean low water at spring tide, and peat (freshwater marshes) can develop above the high water level at spring tide. In accordance to the present-day situation, a mean tidal range of 4 m can be assumed for the period during which unit U4 was formed, with a tidal range of 4.5 m during spring tide and of 3 m during neap tide (Fig. 6.23). So, peat can develop from 2.25 m above mean sea level (MSL), salt marshes from 1.5 to 2.25 m above MSL, mud flats from 0.25 m below to 1.5 m above MSL, sand flats from 2 m below to 0.25 m below MSL, and tidal channels are located below 2 m below MSL.
- Fig. 7.37 represents the Holocene relative mean sea-level curve as reconstructed by Denys and Baeteman (1995). It shows the envelope of the minimal level by the highest mean high water levels at spring tide (MHWS), and the envelopes (error bands) of the upper and lower relative mean sea level (MSL) limits, expressed in metre TAW. Between 10,000 and 6000 cal BP, the relative MSL curve (in red) is reconstructed based on MSL values obtained from literature (fig. 3.18 in: Baeteman 2004, Baeteman 2005a); the part between 6000 cal BP and present is based on the

position of the Upper and Lower MSL curves from Denys and Baeteman (1995). To compare depositional depths derived from seismic data (converted to metre MLLWS) with the relative sea-level curve, it is assumed that TAW is equal to MLLWS. Although the difference between both datums can be up to 70 cm in Dunkerque, 40 cm in Oostende and 20 cm in Zeebrugge, it can be considered negligible compared to the seismic resolution and as sufficient for the detail of the reconstructions.

- It is also important to know to what depth sediments are being eroded, at a certain moment in time. Sediments are stirred by wave action, to a depth half the wave length, which corresponds to the depth of closure of a beach profile. The portion of the seafloor that lies below everyday (fair-weather) wave base, which is the depth at which sediments are not stirred anymore by wave action, is called the lower shoreface. Along the Belgian present-day coastline, the lower shoreface is located at an average depth of -5 m MLLWS (-7.3 m MSL) (IMDC 2007). In the following reconstructions, the position of the lower shoreface, i.e. the depth to which sediments are eroded, is assumed to be 5 m below the mean lowest low water line at spring tide for a certain time, in correspondence with the present-day situation. Bearing in mind though, that mean wave heights increased up to 0.5 m since 7500 years BP (~8300 cal BP) (van der Molen and de Swart 2001b), so the depth of erosion, or the lower shoreface is overestimated, deduced mean sea levels could be slightly lower, and corresponding ages somewhat older.

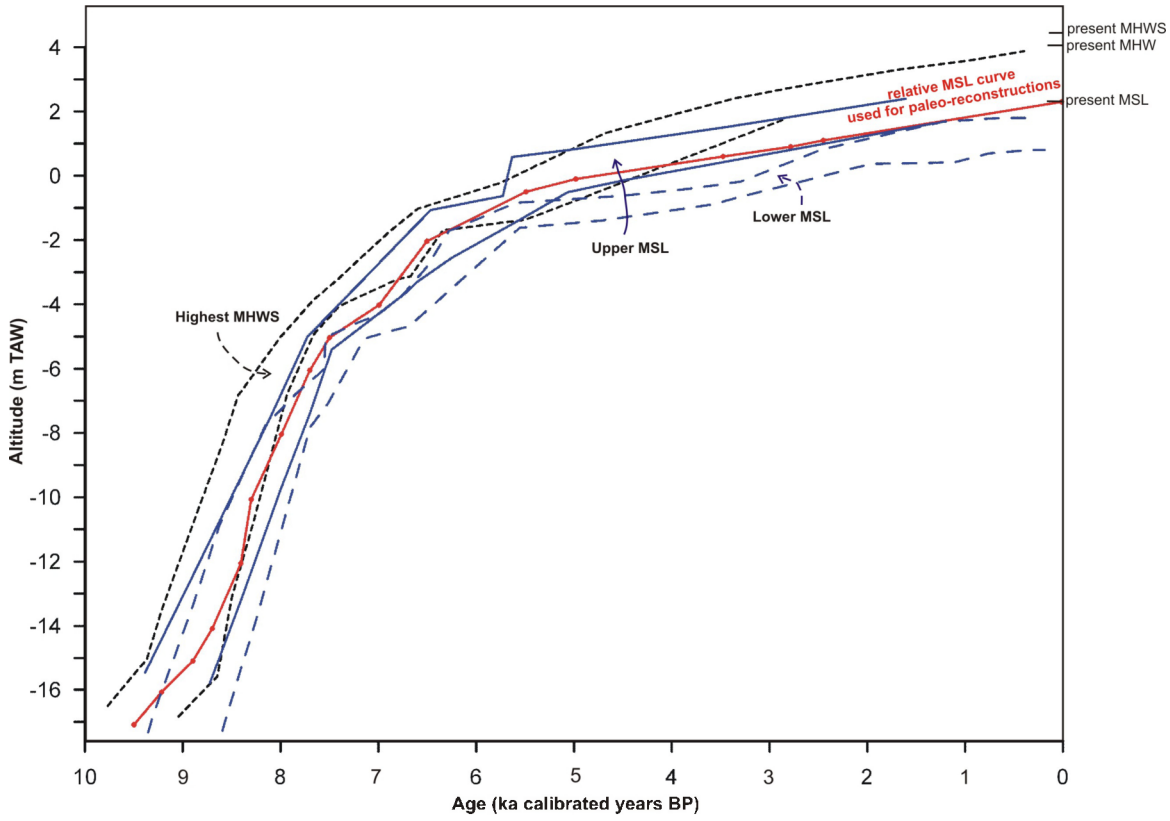

Fig. 7.37 Relative mean sea-level curve (MSL in red) for the Holocene. Adapted after Denys and Baeteman (1995) and Baeteman (2004). MHWS = mean high water at spring tide, MSL = mean sea level, MHW = mean high water. The (red) relative mean sea-level curve between 10 and 6 ka cal BP, is reconstructed based on MSL values obtained from literature (fig. 3.18 in: Baeteman 2004, Baeteman 2005a); the part between 6 ka BP and present is based on the position of the Upper and Lower MSL curves from Denys and Baeteman (1995).

Paleo-reconstruction and dating of the deposits of U4

The fact that the Eemian marine ravinement surface is overlain by shallow-water deposits (tidal flats) confirms that at least a sea-level lowering has taken place. The fact that these tidal-flat deposits occur above the renewed Weichselian river valley incision implies moreover that they were formed as a result of a new relative sea-level rise after the regression, as tidal flats are rarely encountered inside an incised valley, or over such a large area, during a relative sea-level lowering. In conclusion, the back-barrier deposits of U4 are logically Holocene in age. This is in agreement with the dating of the subtidal deposits below the Middelkerke Bank, which are included in our seismic unit U4, as Early Holocene (Heyse et al. 1995, Trentesaux et al. 1999).

Development of the oldest preserved deposits of U4

Based on the comparison of the depositional depth of unit U4 and the relative sea-level curve, the tidal-flat deposits of U4 were probably formed between 10,950 cal BP and 7600 cal BP.
As it is not known to which specific landscape (mud or sand flats, salt marsh, etc.) the deepest and shallowest deposits of U4 correspond, they could have been deposited somewhere between 2.25 m above and 2.25 m below MSL, i.e. between low water and high water level during spring tide. It is hereby assumed that these deposits do not belong to the base of a tidal channel (i.e. there were no seismic-stratigraphic indications for this on the seismic data), and that they do not correspond to fresh-water marsh deposits. The deepest deposits of U4, located below the Oostdyck and Buiten Ratel at -28 m MLLWS, were probably formed in times when MSL was somewhere between -26 and -30 m MLLWS. On the sea-level curve of Siddall in Fig. 6.27, this corresponds to 9400 BP and 9600 BP respectively, or 10,450 cal BP and 10,950 cal BP.
However, these tidal-flat deposits formed in a back-barrier basin. The time at which the coastal barriers formed thus provides an additional constraint on the possible age of the tidal-flat deposits of unit U4. Beets and van der Spek (2000) and van der Molen and van Dyck (2000) postulated that coastal barriers could not have developed before 9500 to 9000 years ago, when the Southern Bight was sufficiently large to produce waves at its eastern shores capable of building a protective barrier behind which a complex of estuaries and tidal basins could develop. With these constraints, there are three possibilities for the interpretation of the occurrence of deposits of U4 at a depth of -28 m:

(1) it could be remnants of infillings of deep-incised tidal channels which formed behind an initial barrier, 9500 years ago, when MSL was at -17 m and channels infillings developed below -19 m.
(2) the isolated remnant of U4 below the Oostdyck and Buiten Ratel does indeed represent a tidal-flat environment formed between 10,450 and 10,950 cal BP, but not in a back-barrier basin, but one that is bordering the coastline, comparable to the present-day German Bight (Toro et al. 2005). According to Eisma et al. (1981) before 8100 BP (9050 cal BP), and probably between 10,000 and 8000 BP (11,450-8860 cal BP), a brackish water area, presumably a tidal flat, existed in the present Deep Water Channel.
(3) the seismic interpretation of the isolated patches below these outer banks is wrong, and they actually represent remnants of deposits of Eemian age (U3).

In Fig. 7.38 situation (2) is shown, where the most offshore deposits of U4 represent tidal flats bordering the coastline, deposited around 10,450 cal BP, when MSL was around -26 m and a fringe of basal peat could develop (above -24 m).
In fact, in both situations (1) and (2), the reworked plant remnants in brown silt found at a depth of -25 m near the Middelkerke Bank (Fig. 7.24B) (closely overlying U3, as described in 7.3.1) could represent remnants of a basal peat, fringing the tidal flats at their landward margin (Fig. 7.38). Intervening peat layers only occurred after 7500 cal BP (Baeteman and Declercq 2002).

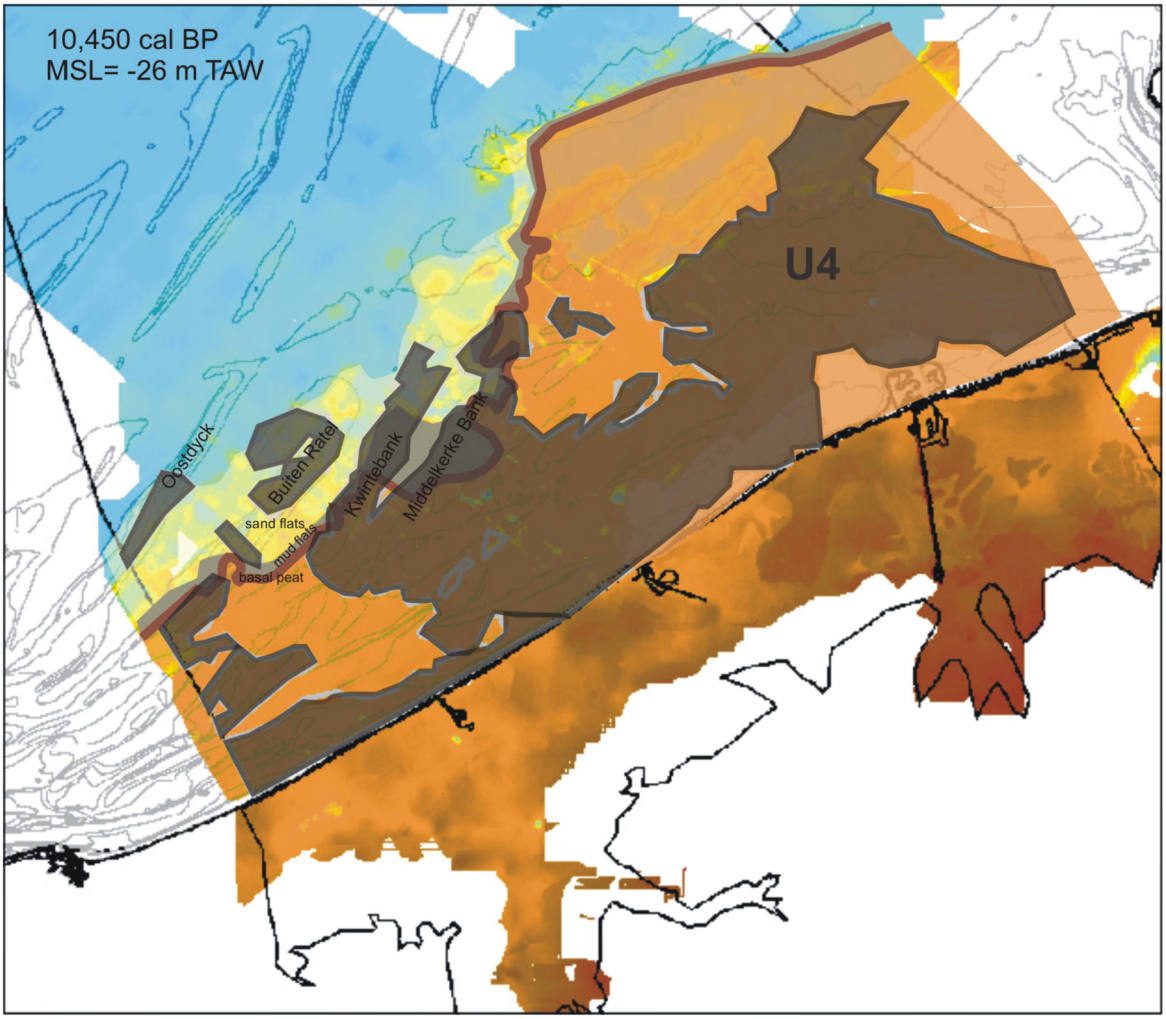

Fig. 7.38 Paleo-reconstruction of the situation around 10,450 cal BP, when MSL was -26 m MLLWS. Part of the deepest (oldest) deposits of seismic unit U4, located below the Oostdyck and Buiten Ratel at -28 m MLLWS, have developed at that time. These deposits might represent remnants of an open (exposed) tidal flat environment, not located behind a barrier, comparable to the present-day German Bight (Toro et al. 2005). A fringe of basal peat (brown line) bordered the tidal flats (grey: mud flats and yellow: sand flats). Orange to brown area is land. The orange transparent overlay represents the presumed Pleistocene surface located higher than presently preserved (due to erosion in the swales between the present-day banks). The transparent dark grey area represents the position of seismic unit U4.

Initial formation of the coastal barrier, 9500 cal BP

Fig. 7.39 illustrates the paleo-geographic situation 9500 years ago, at the time when coastal barriers started to form in the Southern Bight (Beets and van der Spek 2000). Mean sea level at that time was about -17 m MLLWS (Baeteman 2005a, Fig. 7.37), and tidal deposits could develop behind the barrier between about -19 and -15 m. The most offshore deposits of U4 at a depth of -19 m are located below the Kwintebank, and probably represent the first deposits formed behind the barrier. So when the initial barrier developed, it was located (at least) 15 km off the present-day coastline. The isolated patches of presumed U4 below the Oostdyck and Buiten Ratel are drowned tidal flats from a time between 10,450 to 10,950 cal BP. In the western Coastal Plain, the paleo-channel of the IJzer was flooded since 9500 cal BP (Baeteman 2005a), but more to the east, offshore Middelkerke, the first evidence of flooding only occurs around 8700 cal

BP. In core TB358, an *in situ* peat horizon is located at a depth of -12 m (cf. Appendix B and C for detailed litholog and photo), which implies a MSL at about -14.25 m (or deeper), which corresponds to a time 8700 years ago. As intervening peat layers only occur after 7500 cal BP and surface peat only started growing around the second slowdown in relative sea-level rise (6400-5500 cal BP) (Baeteman 2005a, Denys 2007), this peat layer most likely represents a basal peat, which formed when the groundwater level rose with the sea level. This implies that the underlying green silt layer at -12.3 m MLLWS is of Pleistocene age, which is in agreement with the shallowest occurrence of the Top-Pleistocene surface offshore in SWB (-13 m) and on profile BI_06 (-12 m) (cf. 7.3.2 Fig. 7.34).

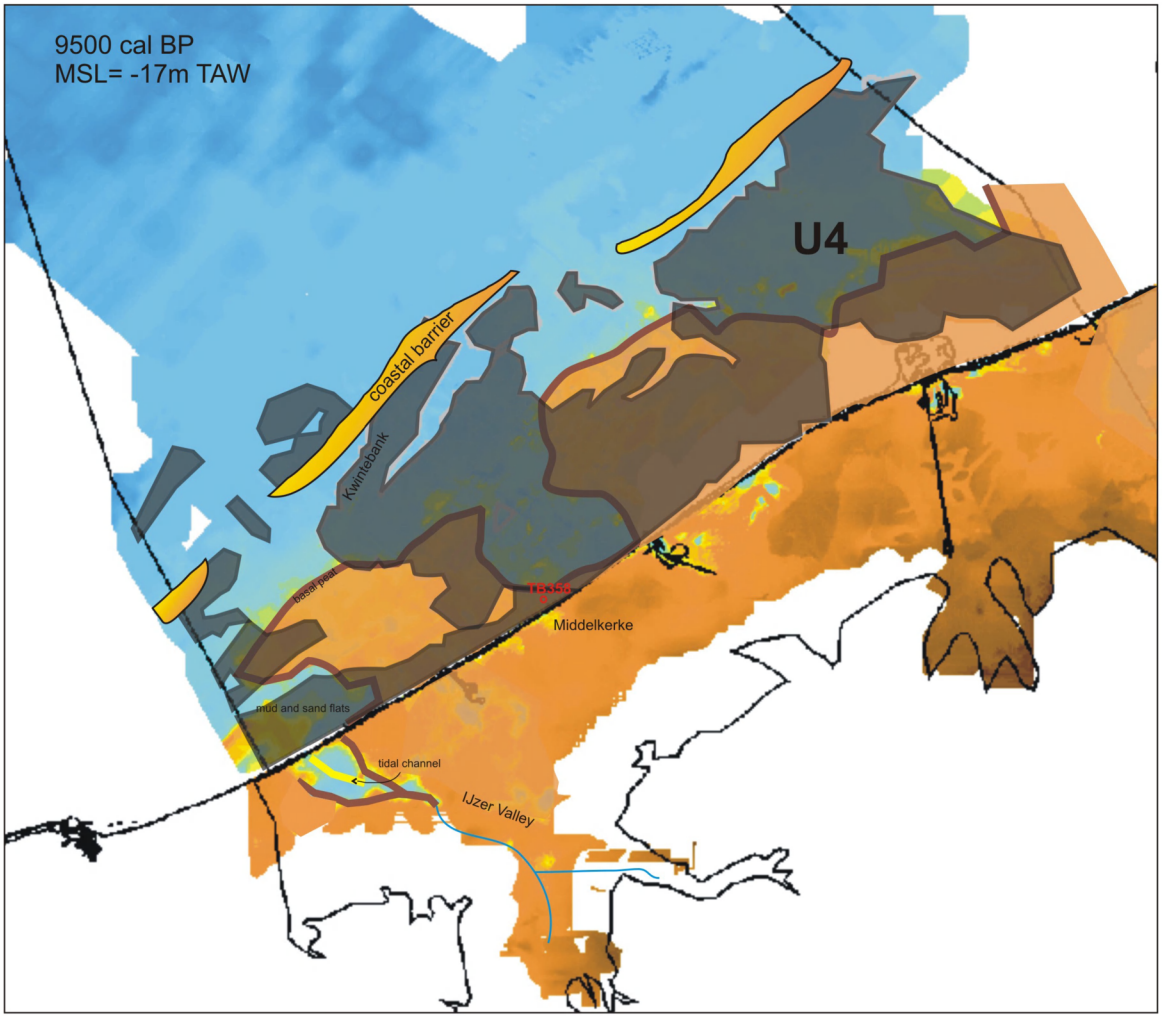

Fig. 7.39 Paleo-reconstruction of the situation around 9500 cal BP, when coastal barriers started to form in the Southern Bight (Beets and van der Spek 2000). Mean sea level at that time was about -17 m MLLWS (Baeteman 2005a, Fig. 7.37). The first deposits formed behind the barrier (at a depth of -19 m) are located below the Kwintebank. So when the initial barrier developed, it was located (at least) 15 km off the present-day coastline. The isolated patches of U4 below the Oostdyck and Buiten Ratel are in this figure drowned open tidal flats. The situation in the Western Coastal Plain is adapted after Baeteman (2005a). There, the paleo-channels of the IJzer have been flooded since 9500 cal BP (Baeteman 2005a), but more to the east, offshore Middelkerke, the first evidence of flooding is probably around 8700 cal BP, which shows from the presence of basal peat at a depth of -12 m in TB358 (indicating a MSL of about -14 m). A fringe of basal peat (brown line) borders the tidal flats (in blue, distinction between mud and sand flats not specified here). Orange to brown area is land. The orange transparent overlay represents the presumed Pleistocene surface located higher than presently preserved. The transparent dark grey area represents the position of seismic unit U4.

Position of coastal barrier, 8000 cal BP

The shallowest sediments of U4 occur close to the present-day coastline, offshore between De Panne and Nieuwpoort, at a depth of -7 m MLLWS (Fig. 4.8A). Assuming that they consist of back-barrier tidal-flat deposits comparable to the other deposits of U4, they have to have been deposited when MSL was between -9 and -5 m MLLWS. This corresponds to an age between 8100 cal BP and 7500 cal BP (Fig. 7.37). However, the barrier had already reached the present-day coastline in the western Coastal Plain at 8000 cal BP (Baeteman 2004, 2005a), so the youngest date for the formation of back-barrier deposits in that location can be rejected. It also means that these back-barrier deposits (in the present offshore area) were already overridden by the retreating barrier by 8000 cal BP.
The remnants of these deposits at a depth of -7 m (by then located offshore) would thus have been located above mean sea level, which was at that time -8 m. This is rather unlikely, as one would expect erosion at least to a depth of -15 m at the lower shoreface (ca. 5 m below low water level, in agreement with the present-day situation) (Fig. 7.40B). This implies that, unless there would be a good explanation for the preservation of back-barrier deposits at that depth, these shallow remnants of U4 do not consist of tidal-flat sediments deposited in a back-barrier environment. The shallowest back-barrier deposits that could have been preserved in the above scenario should not have been located any shallower than -15 m, which coincides with the top of the underlying unit at this location (U3 or QT) (Fig. 7.42BC). In this area, most of the former back-barrier deposits were thus probably completely removed by the barrier retreat down to the Pleistocene surface, as is presented in schematic cross-sections of the adjacent coastal plain (Fig. 7.42D, adapted after Baeteman and Declercq 2002). This was facilitated by the shallow position of the Pleistocene surface and the consequently thin back-barrier cover, which is in contrast to the situation offshore Oostende, where the renewed river-valley incision lowered the Pleistocene surface and back-barrier deposits were initially thicker.
The question then rises what type of deposits these shallow sediments of unit U4 represent, if the depth at which they occur is inconsistent with an origin as back-barrier tidal-flat deposits. They could only have been deposited and preserved at around 5500-5000 cal BP, when MSL was -0.5 to 0 m MLLWS, and the lower shoreface about -7 m. At that time the barrier had already prograded and migrated seaward from the present-day coastline position, so these shallow sediments most likely represent the advance of the barrier. In that case, the overlying nearshore bank structure of U5 in that area is probably not built up of remnants ('sawdust') after barrier retreat, but of sediments deposited after the barrier progradation. The paleo-geographic reconstructions that represent this local re-interpretation of the upper part of U4 and U5 will be discussed in the next section.
In this section, the situation around 8000 cal BP is presented (with the corrected contour of U4) (Fig. 7.40A), when the barrier reached for the first time the present-day coastline. The situation in the western Coastal Plain is adopted from the reconstructions of Baeteman (2005a) and Baeteman and Declercq (2002). The eastern coastline is reconstructed based on the -15 m contour in the Holocene transgressive surface, assuming that this line represents the approximate position of the barrier at that time. Deposits seaward of this line were eroded to the depth of the lower shoreface (-15 m), while deposits landward of this line were still developing in a back-barrier position, and were eroded at a later stage, when relative sea level was higher (Fig. 7.40B). The shallowest back-barrier deposits of U4 occur between the Wenduine Bank and the present-day coastline, at a depth of -7.5 m MLLWS. As these sediments were deposited between 2.25 m above and 2.25 m below MSL, they probably have an age between 8200 and 7600 cal BP, when MSL was about -9.5 and -5.5 m, respectively. The landward extent of the back-barrier as drawn in Fig. 7.40A, was determined by plotting the presumed high water level at spring time of that time on the Top-Pleistocene surface. However, corrections were made in the eastern Coastal Plain, where presumably Late-Holocene tidal channels changed the Top-Pleistocene surface, e.g. in the Zwin area.

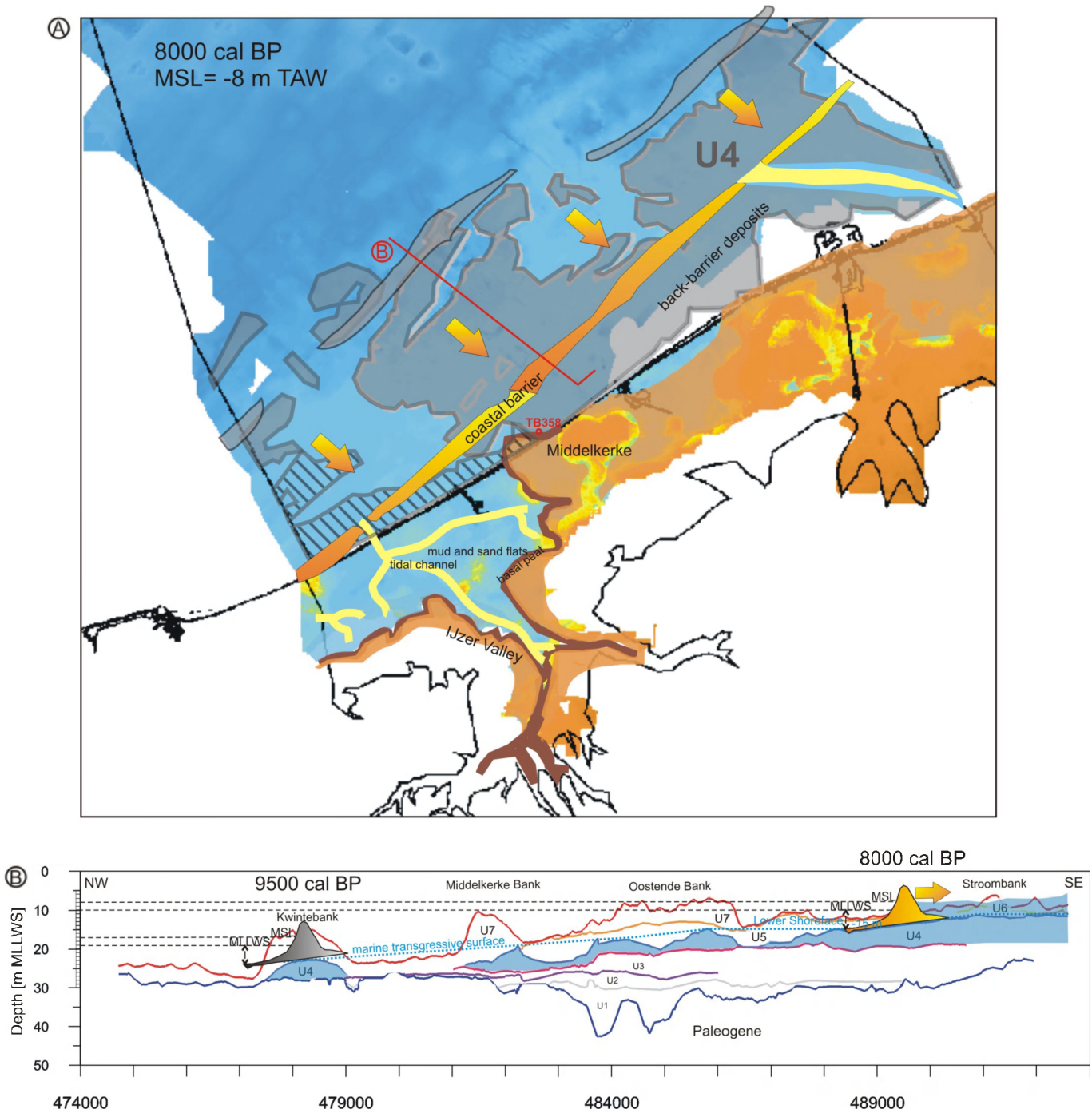

Fig. 7.40 (A) Paleo-reconstruction of the situation around 8000 cal BP, when the coastal barrier reached the present-day coastline in the west for the first time. Mean sea level at that time was about -8 m MLLWS (Baeteman 2004, Fig. 7.37). Seaward of the barrier, former tidal flats have been eroded (in the west, they are even completely removed), landward of the barrier, the tidal environment is still developing. A fringe of basal peat (brown line) borders the tidal flats (in blue, distinction between mud and sand flats not specified here). Orange area is land. The orange transparent overlay represents the presumed Pleistocene surface located higher than presently preserved. The transparent grey area represents the position of seismic unit U4, the hatched areas are no longer interpreted as U4 (cf. Fig. 7.42). The situation in the Western Coastal Plain is adapted after Baeteman (2005a). (B) The eastern coastline is reconstructed based on the -15 m line in the Holocene marine transgressive surface. It is assumed that this line represents the approximate position of the barrier at 8000 cal BP. Deposits seaward of this line have been eroded to the depth of the lower shoreface (i.e. ca. 5 m below low water level, following the present-day situation = -15 m), while deposits landward of this line are still developing in back-barrier position, and are eroded later, at a higher relative sea level. Also the position of the initial barrier is indicated (9500 cal BP, MSL = -17 m).

Summary

When sea level started rising after the Last Glacial Maximum, a tidal-flat environment developed at the borders of the receding coastline. Around 9500 cal BP, the Southern Bight was wide enough to produce waves at its eastern coastlines, so that barriers formed, behind which tidal basins developed. Sand to fill the basins was derived from the shoreface adjacent to the tidal inlets and from the ebb-tidal deltas. As insufficient sediment was supplied to the shoreface by along-shore and cross-shore transport to compensate for this sediment loss, the shoreline was forced to recede (Beets and van der Spek 2000), while eroding the underlying deposits and previous back-barrier sediments. Evidence of this is found at the top of U4 in the form of a gravel lag. Remnants of the back-barrier deposits seaward of the barrier ended up in a marine position, while tidal flats continued to develop in the back-barrier area. In the west, the U4 back-barrier deposits were completely removed down to the shallow Pleistocene subsurface, when the barrier reached the present-day coastline at around 8000 cal BP. In the sandy remnants left on top of the Holocene marine ravinement surface, storm-generated ridges formed erosively, leaving a deep imprint in the U4 surface.

Depositional phase U5: barrier stabilisation, progradation, and formation of storm-generated sand ridges

The results

- Seismic unit U5 is interpreted as a series of three parallel storm-generated sand ridges. The depth of the troughs ranges between -12 and -10.5 m, the crests of the banks culminate at -9 to -6 m. The most landward bank shows an offshore facing gentle side, but no steep side. Instead, in the west, the top of the bank is horizontal and forms a plateau. The shallow occurrence of this nearshore bank and its typical form suggests that it formed the transition to, or made part of, a former barrier.
- U5 is restricted to a NE-SW-oriented 12 km wide strip along the present-day coastline in the SW, and narrowing to 6 km wide at 12 km off the present-day coastline in the NE, in line with the coastline of the Dutch island Walcheren. As U5 represents sand ridges that have formed seaward of the barrier, the most landward limit of U5 represents the minimal landward position of the barrier. The barrier reached at least to that limit, but could have migrated further landwards.
- The horizontal eroded section of U5 in the area offshore Zeebrugge might represent the erosional surface of a receding barrier (after progradation over the U5 sand ridges). The high elevated area further along the coastline to the SW, was probably eroded less intensively and over only a short distance by the prograding and subsequently retreating barrier. The deep elongated area between Wenduine Bank and Stroombank was not eroded by barrier retreat, but might represent a channel in front of the barrier, scoured by storm and tidal currents.

To take into account from literature

- As U5 has been deposited seaward of the coastal barrier, the knowledge of former positions of the barrier at certain moments can help to determine the age of U5. E.g. the evolutionary history of the western Coastal Plain (Baeteman 2004) contains important clues. It also has to be taken into account that in contrast to the western part, the eastern Coastal Plain does not show an extensive barrier complex, formed during barrier progradation (Baeteman 2007b, Denys 2007, Fettweis et al. 2007). This suggests that the barrier in the east did not retreat as far as the present-day coastline, before barrier progradation took place.
- Barrier movements known from the evolutionary history of the western Coastal Plain: The decrease in the rate of relative sea-level rise after 7500 cal BP resulted in a sand surplus and consequently in the silting up of the tidal basins and the onset of

stabilisation of the coastal barrier (Baeteman 2004). Between 6800 and 6000 cal BP, the relative sea-level rise lost its driving force and sediment supply exceeded the accommodation space created by the relative sea-level rise, inducing the coastal barrier to prograde (Baeteman and Declercq 2002, Baeteman 2005a). Between 5500-5000 cal BP, the rate of relative sea-level rise decreased again, and the area behind the protecting coastal barrier of the western Coastal Plain changed into a freshwater marsh with peat accumulation. At that time, the barrier prograded beyond the present-day coastline. After 2000-3000 years of uninterrupted peat growth, a tidal system was again installed in the western Coastal Plain between 2800 and 2400 cal BP (Baeteman 2004, Baeteman 2005b). Shoreface erosion and shoreline retreat occurred, and peat areas were again transformed into sub- and intertidal flats.

- Another important clue is that shoreface-connected ridges appear to build to about a third of the water depth, and that the associated troughs are similarly excavated to a third of the water depth below the level of mean sea bed. Based on the dimensions of the sand ridges, former water depths, related MSL and corresponding ages can be deduced using the Holocene relative sea-level curve (Fig. 7.37, Denys and Baeteman 1995, Baeteman 2004).

Paleo-reconstruction and dating of the deposits of U5

Barrier stabilisation

Also after 8000 cal BP, sediment supply could not compensate for the fast relative sea-level rise and the shoreline kept receding. At around 7500 cal BP, the rate of relative sea-level rise decreased from 0.7 cm/a to 0.4-0.25 cm/a, resulting in a sand surplus and consequently in the upsilting of the back-barrier tidal basins and the onset of stabilisation of the coastal barrier (Baeteman 2004).
The stabilisation of the coastal barrier around 7500 cal BP is illustrated in Fig. 7.41A. In the western Coastal Plain, the paleo-geography is adopted from the reconstructions of Baeteman (2005a) and Baeteman and Declercq (2002). The barrier stabilised there, about 3 km inland of the present-day coastline. To determine the situation in the eastern part of the area, several aspects had to be taken into account. For example, in contrast to the west, the eastern Coastal Plain does not show an extensive barrier complex formed during the subsequent barrier progradation. This suggests that the barrier in the east did not retreat as far as the present-day coastline before barrier progradation took place (Denys 2007, Fettweis et al. 2007). At the time of stabilisation, MSL was about -5 to -4 m (Baeteman 2004, Fig. 7.37), which implies a lower shoreface possibly at about -12 m (-15 ms). The -12 m isohypse of the Holocene marine transgressive surface was thus used to reconstruct the approximate position of the barrier at that time. Deposits seaward of this isohypse were eroded to the depth of the lower shoreface, while deposits landward of it still developed in a back-barrier position, and were eroded only later, at a higher relative sea level, when the barrier retreated again.

Fig. 7.41 (page 213) (A) Paleo-reconstruction of the situation around 7500 cal BP, when the relative sea-level rise decreased, resulting in a sand surplus and consequently in the upsilting of the back-barrier tidal basins and the onset of stabilisation of the coastal barrier. Mean sea level at that time was about -5 m MLLWS (Baeteman 2004, Fig. 7.37). The situation in the Western Coastal Plain is adapted after Baeteman (2005a). The transparent grey areas represents the position of seismic units U4 and U5. (B) The eastern coastline is reconstructed based on the -12 m line in the Holocene marine transgressive surface. It is assumed that this line represents the approximate position of the barrier at 7500 cal BP. Deposits seaward of this line have been eroded to the depth of the lower shoreface (i.e. ca. 5 m below low water level = -12 m), while deposits landward of this line are still developing in back-barrier position. At the location of core TB358, of U4 only the basal peat on top of the Pleistocene surface was left after shoreface erosion. Note that because TB358 is projected on the nearest seismic profile, the seafloor (-7 m) does not correspond to the top of the core (-10 m). The former position of the barrier around 8000 cal BP is indicated (MSL = -8 m) as well. (C) Detail of core TB358.

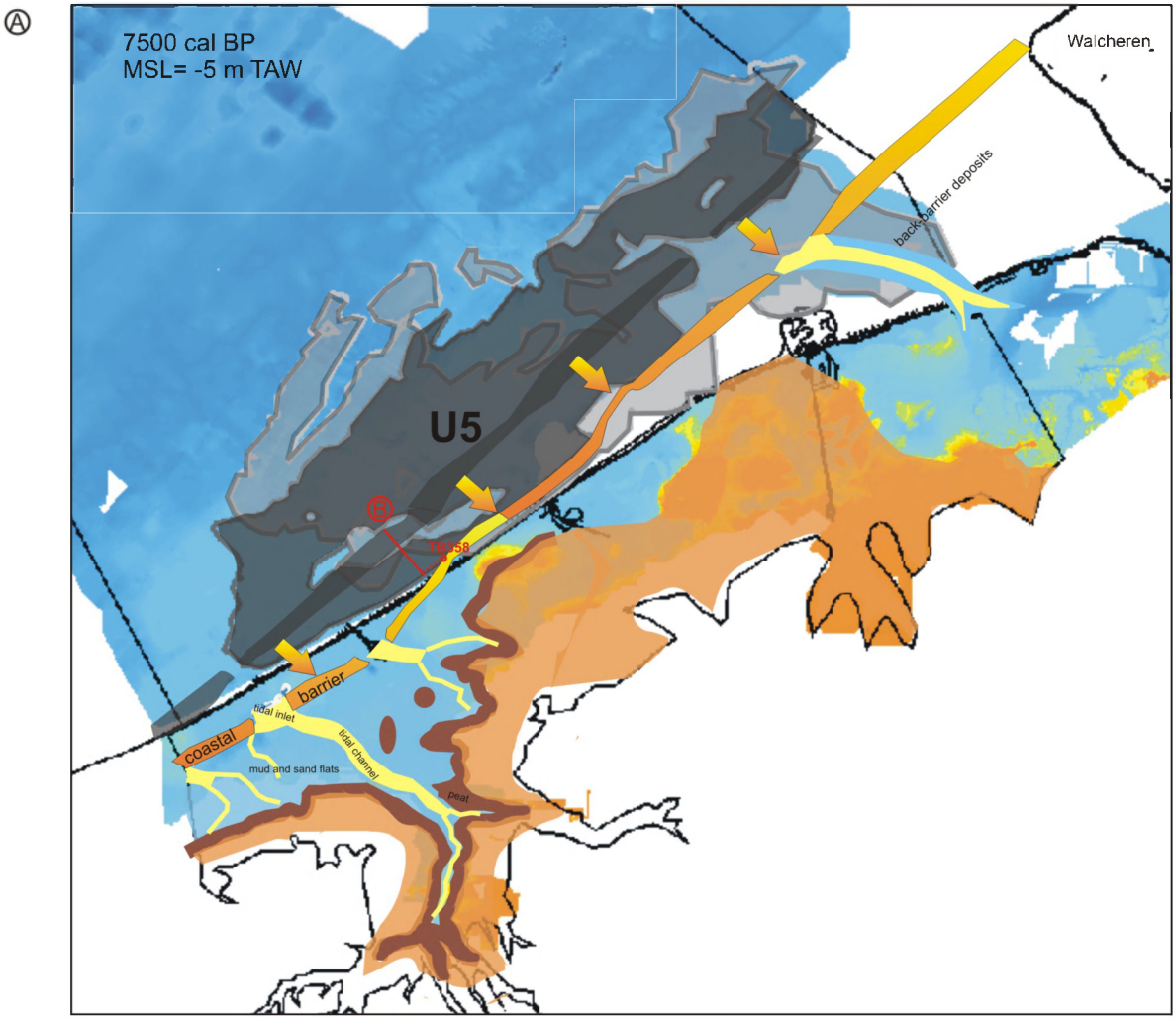

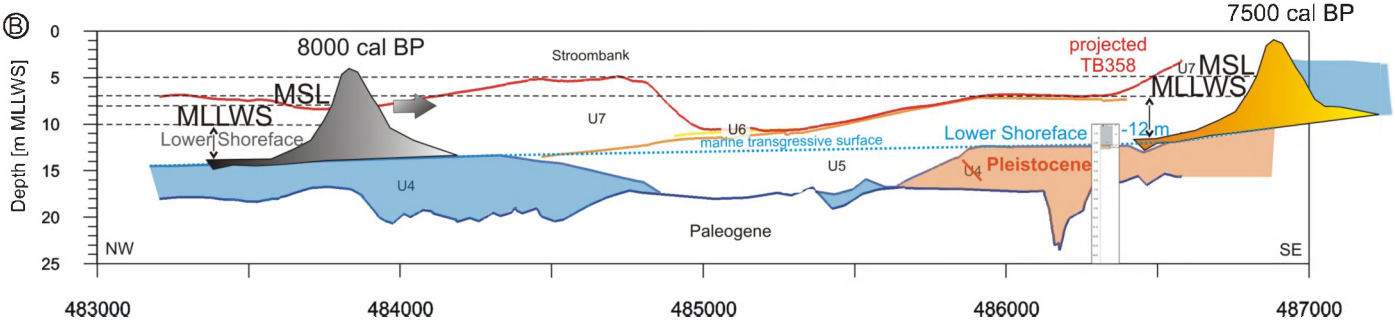

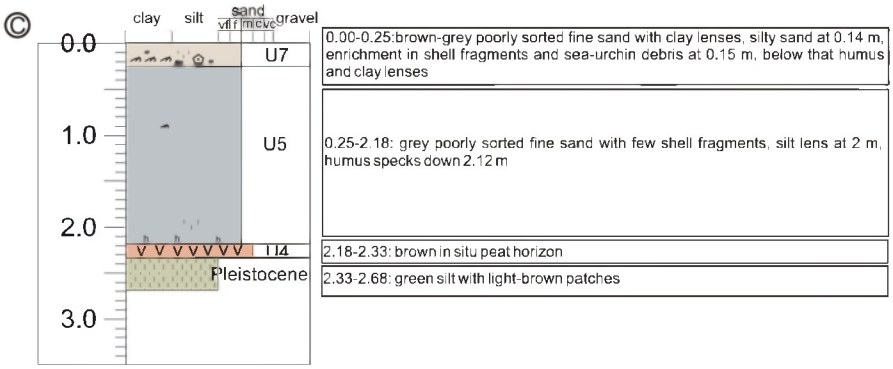

Core: TB358
Date: 19/09/1986
Location: offshore Middelkerke
UTM position (ED50): E 487,431.016 m
N 5,672,368.105 m
Core length: 2.68 m
Water depth: -10 m MLLWS

In core TB358 (Figs. 7.41BC), between Nieuwpoort and Middelkerke, U4 consist only of a basal peat on top of the Pleistocene surface, cut off at the top at -12.2 m, and overlain by deposits of U5. Most likely, the barrier was located not far landward of that core at around 7500 cal BP, which resulted in the erosion of the earlier back-barrier deposits at the lower shoreface to a depth of -12 m, leaving only the basal peat.
Apart from the decrease in the relative sea-level rise and the consequent sand surplus, an additional reason for the barrier to stabilise in that place might have been the presence of the sudden rise in the Pleistocene subsurface near TB358. Also, coastlines tend to develop towards a straight line. At around 7500 cal BP, the barrier thus formed a straight line between the Pleistocene rise and the headland of Walcheren. This interpretation is supported by the existence of a coastal barrier system at the seaward side of the present-day shoreline of Walcheren, at the maximum landward extend of this transgression in Zeeland (Vos and van Heeringen 1997). In this position, the retreat distance between 8000 and 7500 cal BP is the same in the eastern part as it is in the west.

Barrier progradation

After stabilisation at 7500 cal BP, the barrier started to prograde in the western Coastal Plain around 6800 cal BP (Baeteman and Declercq 2002), when the relative sea-level rise lost its driving force. A barrier complex formed with seaward migrating tidal inlets, remnants of which are still present in the present-day western Coastal Plain (Fig. 7.42A, adapted after Baeteman 2007b). Since 5500 cal BP, the barrier extended seaward of the modern coastline. Mean sea level at that time was about -0.5 m, and the lower shoreface was probably located around -7.5 m. Remnants of this barrier are present offshore De Panne. In earlier interpretations, these were before erroneously interpreted as part of U4 (back-barrier deposits) (Figs. 7.42A, B and C). This barrier is built up to a depth of -7 m MLLWS, which corresponds to the depth of the lower shoreface at 5000 cal BP. The deposits of U5 found on top of this barrier complex, fill a large depression in this barrier (as described in section 7.2.1 Seismic unit U5) (Fig. 7.11A). Unit U5 is here characterised by channel structures (Fig. 7.11B). These lie exactly in line with tidal-inlet deposits observed in the Coastal Plain (Fig. 7.42A), which belong to a tidal channel that formed around 7500 cal BP (near Nieuwpoort) and migrated seaward with the prograding barrier (Figs. 7.41A and 7.43A) (Baeteman 2005a). The deposits of U5 therefore correspond most likely to (reworked) ebb-tidal-delta sediments related to this tidal inlet (Fig. 7.42A), and possibly to a second one nearby (Fig. 7.41A). By 5000 cal BP, apart from some tidal channels the major part of the tidal inlet was probably already filled in. Unit U5, which forms this infill, built up to a depth of -7 m, which corresponds to the lower shoreface at 5000 cal BP. Offshore Nieuwpoort, U5 even built up to a depth of -6 m, which corresponds to the lower shoreface at 2800 cal BP. After the progradation of the barrier (until about 5000 cal BP), ebb-tidal deltas were probably redistributed forming the infilling of the tidal inlet represented by U5, which continued building up to about 2800 cal BP. At around 2800 cal BP, when MSL was +1 m, and the lower shoreface was around -6 m, the barrier retreated again. However, the deposits were not always built up to that level before the renewed retreat. It is possible that a sediment decrease towards the shoreface prevented some parts of the barrier from building upwards.

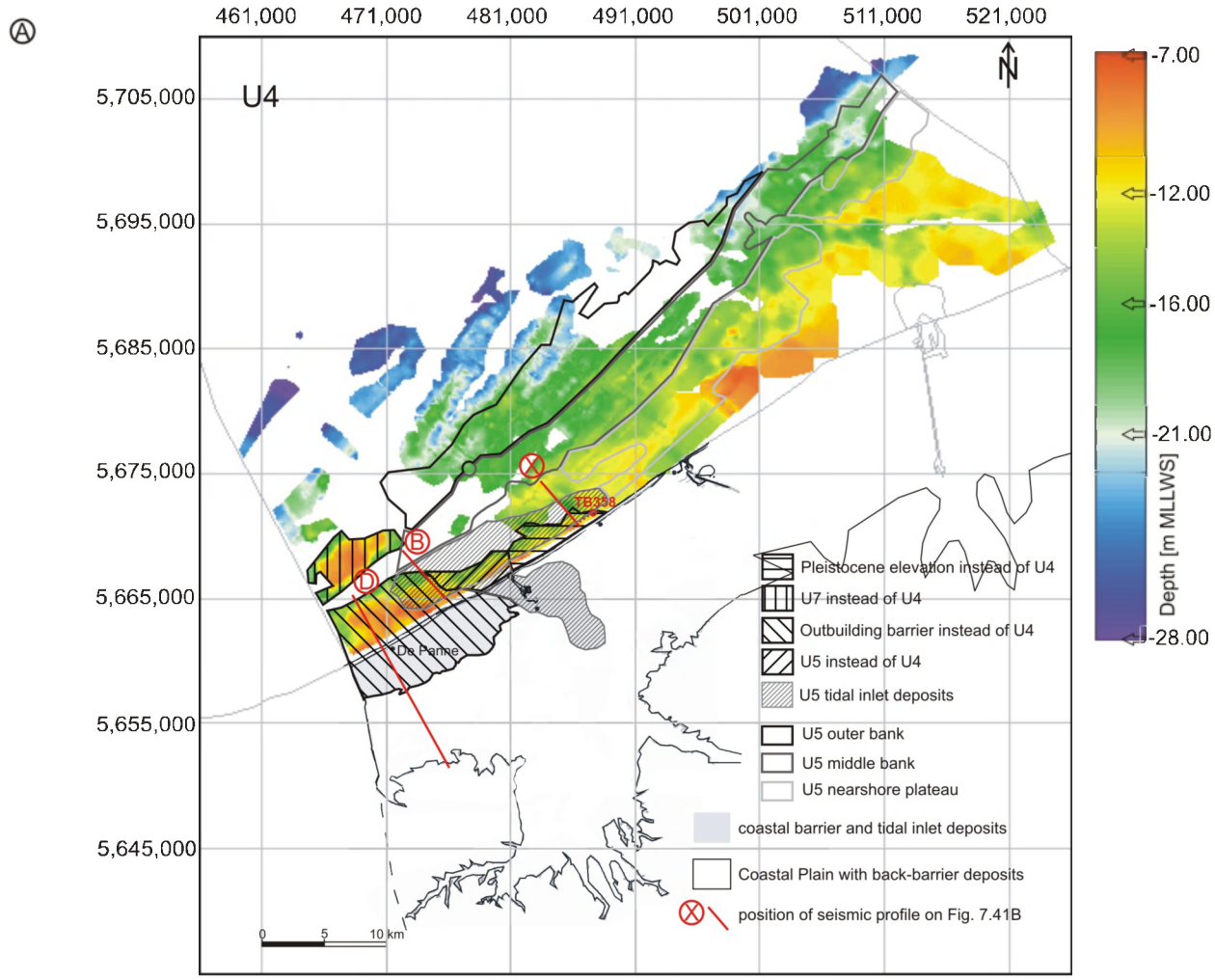
Ⓐ
461,000
471,000
481,000
491,000
501,000
511,000
521,000
5,705,000
5,695,000
5,685,000
5,675,000
5,665,000
5,655,000
5,645,000
U4
N
-7.00
-12.00
-16.00
-21.00
-28.00
Depth [m MLLWS]
De Panne
Pleistocene elevation instead of U4
U7 instead of U4
Outbuilding barrier instead of U4
U5 instead of U4
U5 tidal inlet deposits
U5 outer bank
U5 middle bank
U5 nearshore plateau
coastal barrier and tidal inlet deposits
Coastal Plain with back-barrier deposits
position of seismic profile on Fig. 7.41B
0
5
10 km

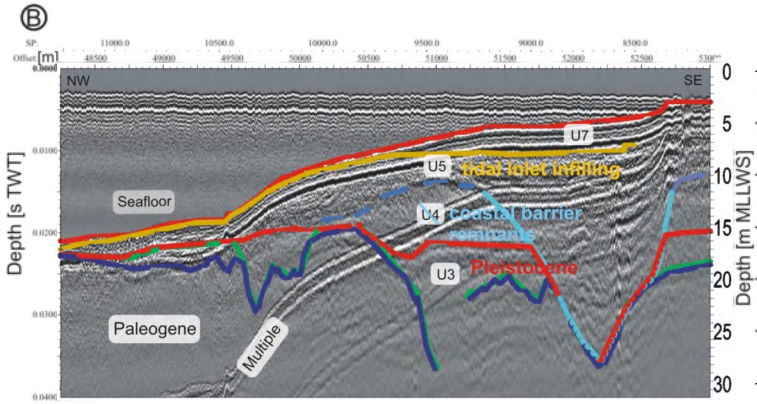
Ⓑ
NW
SE
U7
U5
tidal inlet infilling
Seafloor
U4
coastal barrier remnants
U3
Pleistocene
Paleogene
Multiple
Depth [s TWT]
Depth [m MLLWS]
0
5
10
15
20
25
30

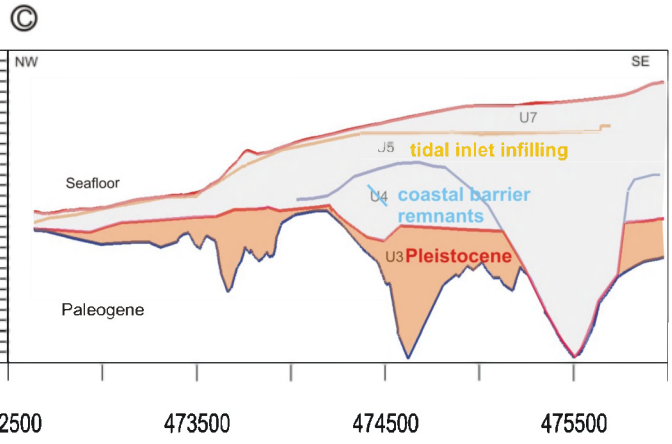
Ⓒ
NW
SE
U7
U5
tidal inlet infilling
Seafloor
U4
coastal barrier remnants
U3
Pleistocene
Paleogene
472500
473500
474500
475500

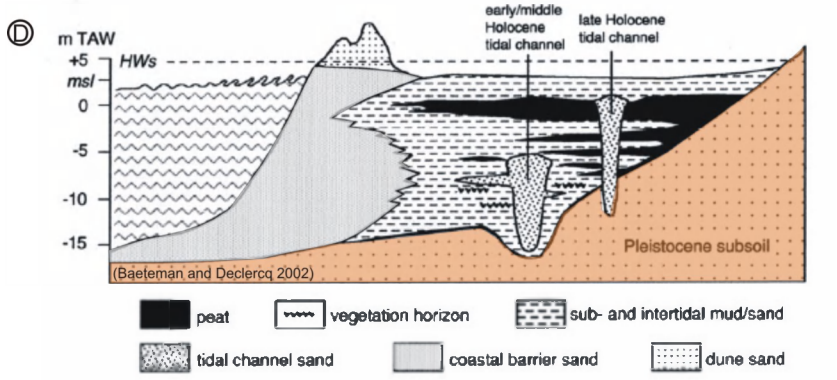
Ⓓ
m TAW
+5
msl
0
-5
-10
-15
HWs
early/middle Holocene tidal channel
late Holocene tidal channel
Pleistocene subsoil
(Baeteman and Declercq 2002)
peat
vegetation horizon
sub- and intertidal mud/sand
tidal channel sand
coastal barrier sand
dune sand

Fig. 7.42 (page 215) (A) Isobath map showing the corrections in the interpretation of seismic unit U4. The shallow nearshore part offshore De Panne belongs in fact to the barrier complex which formed during the barrier progradation, following the stabilisation of 7500 cal BP. Based on core TB358 a small area is now interpreted as Pleistocene deposits. The onshore part is adapted after Baeteman (2007b). (B) Example of a seismic section showing the new interpretation of U4 in this specific area. (C) Line drawing (depth in metre) of the presented seismic section. Note how the former back-barrier deposits are completely eroded below the barrier down to the Pleistocene surface, which is now in agreement with the schematic cross-section of the Coastal Plain. The barrier is in reality, however, much more complex (with tidal inlet infillings and a plateau around -5 m) than shown in (D). (D) Schematic cross-section through the sedimentary sequence of the coastal Holocene (after Baeteman and Declercq 2002).

Fig. 7.43A illustrates the paleo-geographic setting when the coastline reached its maximal seaward extent, between 5000 and 2800 cal BP. It is also illustrated by five typical cross-sections (Fig. 7.43B-F). In the western part of the area (Fig. 7.43B), offshore De Panne, the maximal seaward extent was determined based on the position of the shallowest barrier deposits at -7 m (5000 cal BP). Fig. 7.43C shows the situation offshore Nieuwpoort, in line with the tidal-inlet deposits in the Coastal Plain, where U5 represents the infilling of a former tidal inlet from -15 to -6 m, and no other barrier deposits are present. As U5 continued up-building to this depth, i.e. the lower shoreface at about 2800 cal BP, the adjacent barrier did probably not prograde seaward of these deposits of U5 after 5000 cal BP.

East of Nieuwpoort, no barrier complex deposits were encountered either above the Pleistocene subsurface covered with basal peat, but U5 has build up to -7 m (Fig. 7.43D). In this area, U5 lies not in line with the tidal inlet, and most likely represents reworked ebb-tidal-delta deposits, transported from the SW. In this area east of Nieuwpoort, the barrier did most likely not prograde after 7500 cal BP, but stayed there in a stable position. With rising relative sea-level the lower shoreface gradually built up with material originating from nearby ebb-tidal deltas until about 5000 cal BP. After that time, the barrier did not prograde either, as the top of U5 does not represent a clear erosional surface, but a smoothly rounded crest like that of a sand ridge. Around 2800 cal BP, a sediment deficiency (due to renewed opening of the tidal channels) caused the barrier to retreat again (which will be discussed later). It is probably only when the barrier finally stabilised at the present-day shoreline, that the (lower) shoreface was built up again, i.e. the present unit U7, which has been deposited to a depth of -5 m MLLWS and shallower.

Also further to the east, offshore Oostende, no direct evidence of a barrier was encountered either (Fig. 7.43E). Seismic unit U5 consists here of a thin layer of material, probably left by the earlier shoreface retreat, built up in the most nearshore part to about -10 m. The typical bank form of U5 is not present, and a large part of U5 has been eroded. This erosion most likely has a dual origin. On the one hand there is the presence of the local gully or channel, discussed in 7.3.1 (Fig. 7.31B). On the other hand, the composition of core SB2 indicates that the barrier was located seaward of this core, and that part of U5 was also eroded by shoreface progradation followed by retreat. Unit U4 in SB2 is characterised by a typical tidal-channel infilling, with a coarse-grained sandy base, but gradually becoming more clayey upwards, showing a heterolithic cm-scale alternation of clay, sand and peat detritus layers at the top (cf. Appendix B and C for a detailed litholog and photos). The presence of such large amounts of peat detritus implies that the channel was formed after the development of the surface peat, so after 2800 cal BP. This means that the core was still located landward of the coastal barrier at that time. Thus, after the stabilisation around 7500 cal BP, landward of the present remnants of U5 (which built up to at least -10 m, so possibly to about 6700 cal BP when MSL was -3 m), the barrier prograded over U5 to a position seaward of SB2.

Near the Vlakte van de Raan (Fig. 7.43F), U5 is strongly flattened. Most likely here the barrier *did* prograde, after which the renewed shoreface retreated around 2800 cal BP, and removed all of its remnants. Why the renewed shoreface retreat eroded U5 and U4 to a depth of -12 m, while the lower shoreface at that time was only -6 m, will be discussed later in the section concerning the final barrier retreat.

Formation of storm-generated sand ridges (U5)

Although the bank-like structures above U4 all belong to the same seismic unit U5, and have all been interpreted as (parts of) storm-generated sand ridges based on their morphology and dimensions, they were not necessarily formed at the same time or have the same origin. The shallow western nearshore plateau-like bank, between De Panne and Middelkerke, is partly composed of a tidal-inlet infilling and partly of a sand ridge formed of redistributed ebb-tidal-delta remnants, probably during or shortly after the barrier progradation. Conversely, the more central and eastern remnants of U5, found at the Vlakte van de Raan, in line with the nearshore plateau-like bank, were most likely been formed from/in remnants left behind after the first barrier retreat, before barrier progradation.

Sand ridges formed from ebb-tidal-delta sediments have been classified by Dyer and Huntley (1999) as Type 2B (i) or (ii), depending on whether they were formed in relation to barrier retreat (ii) or not (i). Since the western nearshore plateau-like bank lies in line with a tidal inlet that formed after stabilisation, and since the bank is located on top of the barrier build out of around 5000 cal BP, the plateau-like bank was not formed in relation to barrier retreat, but after barrier progradation. The western shallow nearshore bank thus possibly corresponds to Type 2B (i), which are banks formed close to tidal inlets of a stable barrier, as ebb and flood deltas.
The rest of U5 corresponds most likely to sand ridges that were formed when the coast was retreating. The sand ridges near the Vlakte van de Raan were eroded by the prograding barrier and thus must have been formed earlier, i.e. during the barrier retreat or during stabilisation. Two types can be recognised: sand ridges as products of ebb-tidal deltas of a receding barrier (i.e. Type 2B (ii) of Dyer and Huntley (1999)) or sand ridges moulded in a transgressive shelf sand sheet, left after barrier retreat (Swift et al. 1973, Swift and Thorne 1991). Ebb deltas at the tidal inlets of a retreating barrier form a primary source of sand to the nearshore region, which can become modified by storm flows into ‘shore-attached ridges’. But sand ridges can also be moulded in the surface of a discontinuous sand sheet that is built up of the debris of shoreface erosion after barrier passage: i.e. the transgressive shelf sand sheet (Swift et al. 1973, Swift and Thorne 1991). The storm-generated ridges originate at the shoreface and, as the shoreface retreats landwards due to sea-level rise, eventually become detached and isolated, thus evolving into nearshore and offshore ridges. Because of the higher tidal-current regime on the BCS, the ridges most likely did not connect directly to the barrier beach, but disappeared into the shoreface sand sheet, as is also the case at the northern coast of the Netherlands (Snedden et al. 1994 in: Dyer and Huntley 1999).

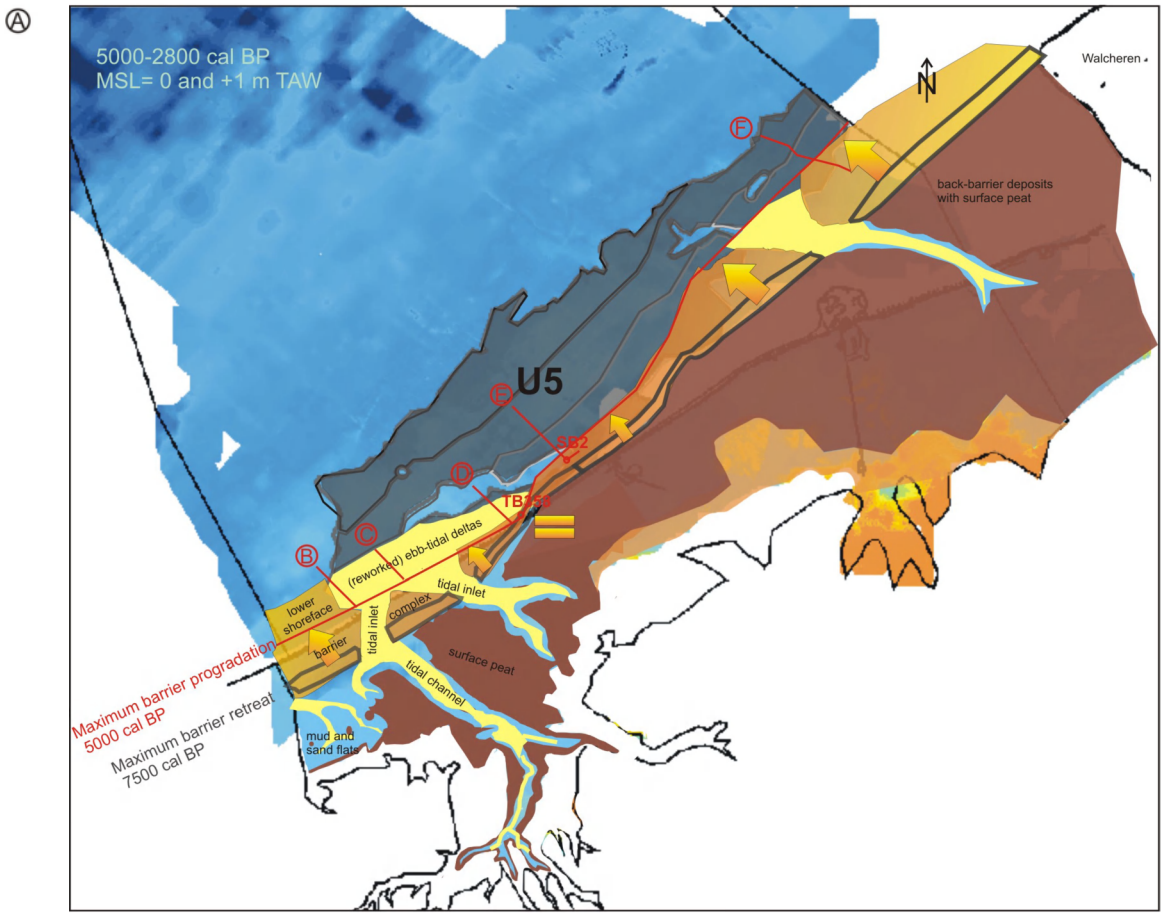

Fig. 7.43 (A) Paleo-reconstruction of the situation between 5000 and 2800 cal BP, when the coastal barrier reached its maximal seaward extend since it started prograding around 6800 cal BP, and before a second barrier retreat set in. Mean sea level in that period rose from 0 m to +1 m MLLWS (Baeteman 2004, Fig. 7.37). The situation in the Western Coastal Plain is adapted after Baeteman (2005a). The transparent grey area offshore represents the position of seismic units U5. The position of the coastline is reconstructed based on the height and the erosional character of the surface of seismic unit U5. Five representative cross-sections (depth in metre) from SW to NE: (B) The coastal barrier built up to -7 m MLLWS, which corresponds to the lower shoreface around 5000 cal BP. Seismic unit U6 represents here reworked ebb-tidal delta deposits and tidal inlet infillings, built up to -6 m, i.e. the lower shoreface around 2800 cal BP. As U6 kept on developing until 2800 cal BP, the barrier did not prograde over these units after 5000 cal BP. Between 5000 and 2800 cal BP the barrier stayed in a stable position. (C) Shows the situation offshore Nieuwpoort, in line of the tidal inlet deposits in the Coastal Plain, where U6 represents the infilling of a former tidal inlet from -15 to -6 m, and no other barrier deposits are present. (D) East of Nieuwpoort, no barrier complex deposits have been encountered either above the Pleistocene subsurface covered with basal peat, but U6 has build up to -7 m. In this area U6 lies not in line with the tidal inlet, and most likely represents reworked ebb-tidal delta deposits, transported from the SW. In this area, most likely the barrier did not prograde after 7500 cal BP, but stayed there in place, in a stable position. With rising relative sea-level the lower shoreface gradually build up with material originating from nearby ebb-tidal deltas until about 5000 cal BP. After that time, the barrier did not prograde either, as U6 does not show an erosional surface, but a smoothly rounded top like a sand ridge. (E) Offshore Oostende, no direct evidence of a prograded barrier is present. Core SB2, however, contains indications that the barrier was located seaward of this core. The presence of lots of peat detritus in a tidal channel implies that the channel was formed after or during the development of the surface peat, i.e. between 5500 and 2800 cal BP. Which means that the core was still located landward of the coastal barrier at that time. A large part of former deposited U6 is eroded, due to later renewed barrier retreat or due to the presence of a local longitudinal channel (Fig. 7.45A).

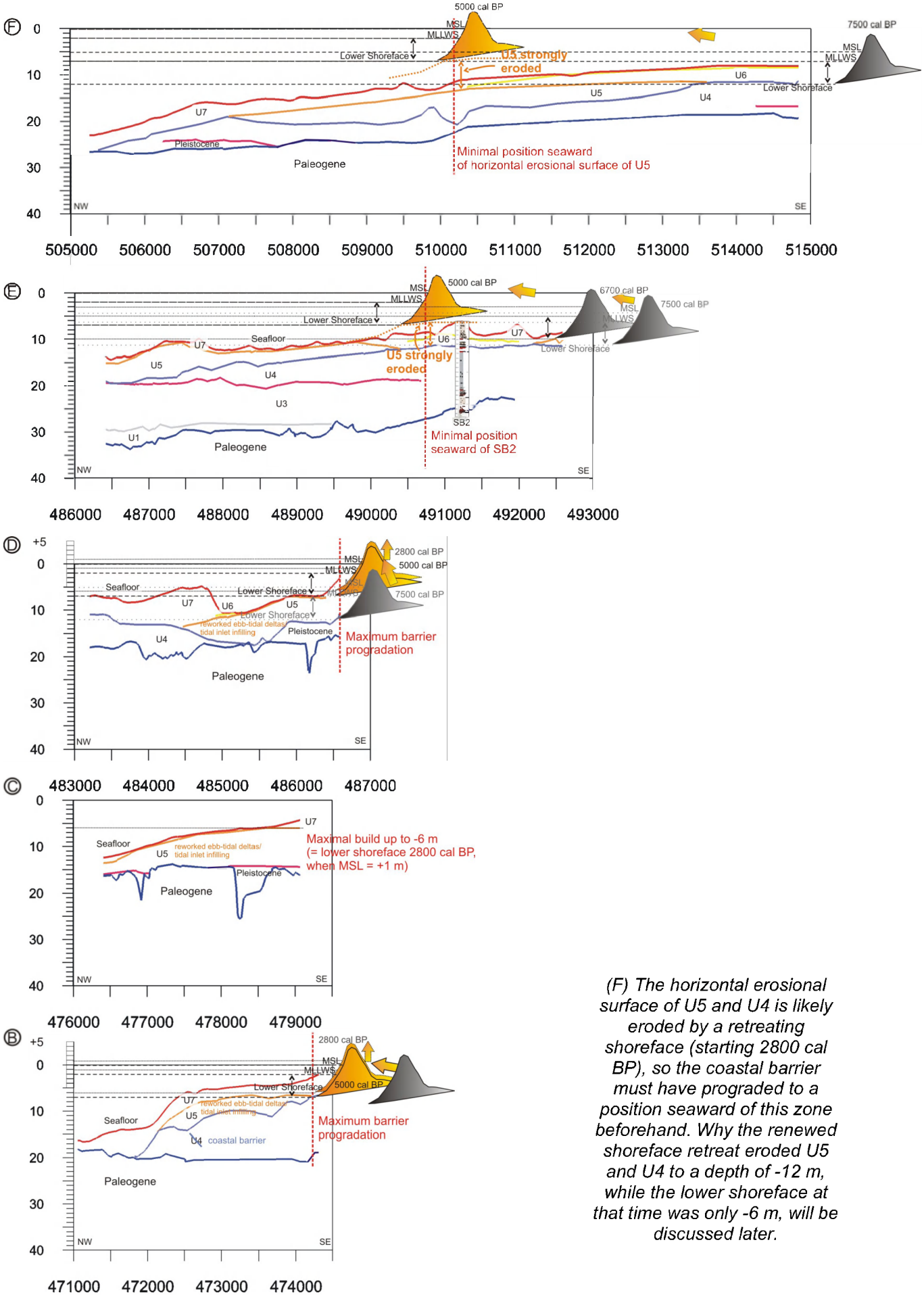

(F) The horizontal erosional surface of U5 and U4 is likely eroded by a retreating shoreface (starting 2800 cal BP), so the coastal barrier must have prograded to a position seaward of this zone beforehand. Why the renewed shoreface retreat eroded U5 and U4 to a depth of -12 m, while the lower shoreface at that time was only -6 m, will be discussed later.

How much of the sand ridges of U5 consists of reworked ebb-tidal-delta deposits near tidal inlets of a receding coastline or of a reworked transgressive shelf sand sheet (or shoreface sand sheet) is not clear. In a large area between the Oostende Bank and the Vlakte van de Raan, U4 has been completely removed (Fig. 7.42A). It is possible that during the Holocene transgression, when the barrier continuously shifted landward, the earlier deposits of U4 were completely removed in a strong erosional zone of landward shifting tidal inlets. Thus, it is not completely excluded that also the bank remnants at the Vlakte van de Raan were formed from redistributed ebb-tidal-delta sediments from a tidal inlet, as is the case for the shallow western nearshore plateau (Fig. 7.43A)). Both origins are probably valid: i.e. where tidal inlets were present, sand ridges were formed from redistributed ebb-tidal-delta sediments, while in intervening areas, sand ridges were formed in the transgressive sand sheet, or 'sawdust', left by shoreface retreat (e.g. offshore Oostende where U5 is a widespread, thin sand layer). The ridges have diverse origins but are probably in most cases initiated by the impact of storm currents on the shoreface and adjacent shelf. This involved scour and down-cutting in the troughs, eroding the underlying deposits of U4, with simultaneous aggradation of the ridge crests. The sand ridges are locally erosional rather than constructional responses to the hydraulic regime, as is clear from the coarse-grained shell lag at the base of U5, and the sometimes deep imprints of U5 in U4. This was also observed by Duane et al. (1972) (in: Swift et al. 1973) concerning linear shoals on the Atlantic shelf.

Based on the height and dimensions of a sand ridge, the corresponding water depth and MSL can be determined, as Type 2B (ii) ridges appear to build to a third of the water depth and the troughs are likewise excavated to a third of the water depth below the mean seabed level (Dyer and Huntley 1999). A possible age can thus be determined for the best preserved outer and middle bank structures. The most offshore bank has a trough at -12 m and a top at -9 m (Fig. 7.8B). The elevation in between corresponds to 2/3 of the water depth (Fig. 7.44), so the bank, as it is preserved now, was formed when MSL was -6 m (in case the water depth is referred to the MSL, if the water depth is referenced to the MLLWS, the MSL would be 2.3 m higher), so around 7700 cal BP. The middle sand ridge with a trough depth of -11 m and a height of -7.5 m would be formed when MSL was about -4 m, which was at about 7000 cal BP. It has to be noted, however, that these ages correspond to the final phase of the bank development, when the banks had already heights corresponding to what is preserved at the moment. Around 7700 cal BP, when the outer bank stopped developing, the coastline was already located about 6 km landward from the bank, and around 7000 cal BP the coastline was located 2-4 km from the middle bank. So, most likely, the start of the bank development began much earlier, when the presumed coastline was closer to the position of the outer and middle ridges. This could have been at around 8400 cal BP for the outer ridge, and at around 8000 cal BP for the middle ridge, based on the position of the reconstructed coastlines of 9500 and 8000 cal BP. These are, evidently, rather rough estimations. The central and western part of the nearshore ridge have been too strongly eroded to deduce any final age for this ridge, but based on its position it probably started forming around 7500 cal BP, which is when the barrier stabilised (Fig. 7.41). Sand ridges developing seaward of a prograding shoreface have been observed before (Galloway and Hobday 1996). Most likely the development continued until the barrier prograded over the central and western nearshore sand ridge.
The above reasoning can also be followed for the eastern part of the western shallow nearshore bank, even though it is a Type 2B (i) bank. This bank has a through depth of -12 m and a top depth of -6 m. This implies that the bank would have formed when MSL was 0 m, so around 5000 cal BP, which corresponds to the age suggested before. The sand-ridge systems formed diachronously, in response to a steady change in conditions, such as flooding of the area and shoreface retreat due to sea-level rise (van de Meene and van Rijn 2000).

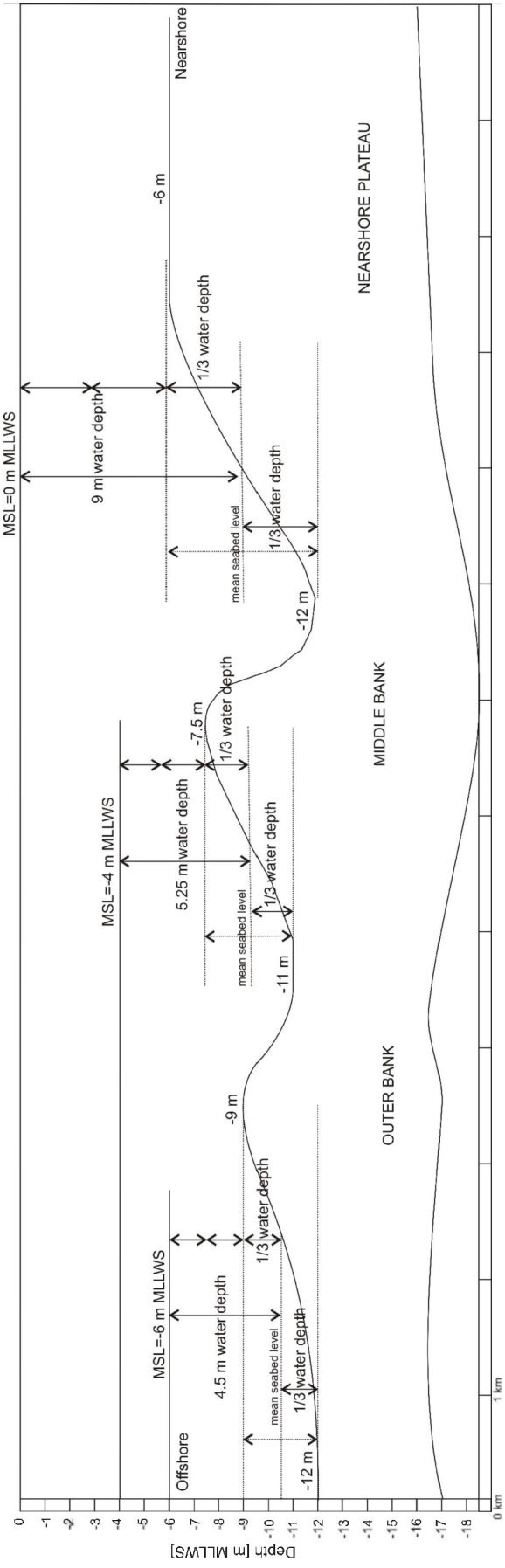

Fig. 7.44 Based on the height and dimensions of a sand ridge, the corresponding water depth and MSL can be determined, as ridges appear to build to a third of the water depth and the troughs are likewise excavated to a third of the water depth below the mean seabed level (Dyer and Huntley 1999).

Summary

The coastal barrier continued retreating with rising sea-level until 7500 cal BP. At that time, a first slowdown in the relative sea-level rise occurred and the barrier stabilised. During the barrier recession, the outer and middle sand ridges were shaped in a transgressive sand sheet left behind after the barrier retreat, or from ebb-tidal-delta sediments near a tidal inlet. From about 6800 cal BP, the barrier started to build out in seaward direction (except at the central part of the coastline, near Middelkerke, which stayed in place). In the NE part, in the area offshore Zeebrugge, the barrier prograded far across the former storm-generated sand ridges. At around 5000 cal BP, the barrier progradation stabilised. Ebb-tidal deltas had been redistributed, forming the tidal-inlet infillings as well as the western nearshore bank, represented by U5, which continued building up to about 2800 years ago.

Depositional phase U6: final barrier retreat up to the present-day coastline

The results

- Unit U6 is restricted to a 14 km wide strip along the present-day coastline near the Dutch border. This strip narrows to 2.5 km near Middelkerke and eventually disappears further along the coastline to the SW.
- Close to the coast, U6 mainly consists of an alternation of black clay layers with high organic content and grey fine sand layers. More sandy and silty deposits occur at the most offshore margins of U6 and in the isolated patches at the SW end, which also contain shell accumulations interpreted as storm horizons. U6 is interpreted as reworked tidal-flat deposits, consisting of clayey material that settled in a sublittoral environment below wave action, but frequently disturbed by storm action.
- U6 is located on top of a horizontal erosional surface at a depth of -12 m MLLWS offshore Zeebrugge. In the area between the Wenduine Bank and the present-day coastline the erosional surface is located at much shallower depth, ranging from -9 to -7.5 m. Further along the coastline in SW direction, between Nieuwpoort and De Panne, the surface even rises to a depth of -6 m. Further offshore, in an area connecting the ends of the Wenduine Bank and Stroombank, the erosional base of U6 shows an elongated depression to -12 m. Isolated patches of U6 occur offshore. These show no horizontal erosional basal surface, but are simply draped on the underlying surface.
- On top of U6, present-day tidal sandbanks have formed.

To take into account from literature

- The evolutionary history of the western Coastal Plain presented by Baeteman (2004, 2005a) and Baeteman and Declercq (2002) is used as a framework to develop the presented paleo-reconstructions.
- As the evolutionary history reaches modern ages, human involvement can not be excluded and also historical data have to be taken into account (e.g. Coornaert 1989, Augustyn 1995, Termote 2006).

Paleo-reconstruction and dating of the deposits of U6

Barrier retreat in the western Coastal Plain

Between 2800 and 2400 cal BP (Baeteman 2004, Baeteman 2005b), a tidal system was again installed in the back-barrier area of the western Coastal Plain, and peat areas were transformed into sub- and intertidal flats. The surface peat growth ended during the Roman occupation between 2400 cal BP (450 BC) in the seaward part and 1500 cal BP (450 AD) in the most landward area of the western Coastal Plain. The renewed expansion of the tidal system was not the result of a sea-level rise, as sea-level was still

rising with the same strongly reduced trend as during the period of peat growth (0.7 m/ka). Re-entrance of the tidal system was probably induced by the cleaning of older channels due to an increased rainfall and excessive run-off from the continent, related to a climatic change around 2800 cal BP and human activity (Baeteman 2005b). Due to compaction of the peat and collapse of the channel banks, a lowering of the ground level occurred, which induced an increase of the tidal prism of the tidal channels and, consequently, deep vertical incision. Possibly also peat digging induced compaction, and thus intensified the process of tidal inundation (Baeteman 2007b). Human activity during Roman occupation is, however, considered a secondary cause for the renewed expansion of the tidal environment, while climate change was most likely the initial trigger (Baeteman 2005b). The resultant barrier retreat will therefore be called 'natural' later in the text.
The sediment needed to fill the deep incised channels came from the early and mid-Holocene channels and the eroding shoreface. This resulted in a landward migration of the coastline (barrier retreat) and erosion of the tidal flats in the present-day offshore area. It was not until 1400-1200 cal BP (550-750 AD) that sediment supply and tidal prism became in equilibrium with the sea-level rise in the western Coastal Plain. The newly formed channels came in intertidal position (infilling phase), and the major part of the plain evolved again in a supra-tidal environment. By 1000 cal BP (900-1000 AD) most of the tidal-flat areas between the channels were silted up to high-tide level and people started to build dikes to protect the newly formed salt marshes (Baeteman 1999, Beets and van der Spek 2000).

Most likely the back-barriers in the central and eastern Coastal Plain (including the present-day offshore parts) started evolving in a similar way and with a comparable timing as in the western Coastal Plain, since the driving force for the barrier retreat was of climatic origin and should have had a regional impact. The exact timing of the further development, however, depended on the timing, the degree and the extension of the collapse of the surface peat, which in turn depended on the incision of tidal channels and the peat digging during Roman occupation. These two controlling factors were not identical over the entire plain. As little is known about these controlling factors in the central and eastern Coastal Plain, the initial climatic trigger of 2800 cal BP is used as the starting date for the renewed entrance of the tidal system.
In the area of Zeeland it is known that the time range for the renewed installation of the tidal environment is comparable to the one in the western Coastal Plain (2400 cal BP - 450 AD). The marine influence increased there locally around 2550 cal BP, and the peat areas on Walcheren and Zeeuws-Vlaanderen were flooded by the sea shortly after 300 AD, as indicated by the Middle Roman finds on the peat (Vos and van Heeringen 1997). Also the moment when the tidal channels came in intertidal position again (around 1200 cal BP or 750 AD in the western Coastal Plain) is the same in Zeeland. There, channels started silting up around 750 AD, a process which ended in the 9th and 10th century (Vos and van Heeringen 1997), similar as in the western Coastal Plain.

Barrier retreat (until 1200 cal BP) and the situation in the central Coastal Plain in the Early Middle Ages

With the cleaning of former up-silted tidal channels around 2800 cal BP and the lowering of the surface due to compaction of mud and peat, the marine environment could enter the back-barrier area of the central Coastal Plain again, and tidal channels incised deeply. Because a large supply of sediment was needed to fill these channels, the tidal deltas and shoreface were eroded, and the barrier was forced to recede (Fig. 7.45).
Most likely, the zebra-like alternations of sand, clay and peat laminae, present in core SB2, represent the infilling of a channel that incised deeply in the underlying sediments and surface peat, with the new tidal expansion around 2400 cal BP in the most seaward part of the back-barrier. The channel has incised to a depth of -20.6 m, which is not an

exception. In the western Coastal Plain, incisions of late Holocene tidal channels have been observed to depths of -23 m TAW, but the basal depth of channels usually varies between -15 and -20 m TAW in the seaward part of the Coastal Plain (Baeteman 2004). Around 2400 cal BP, MSL was about +1.1 m TAW, and as tidal channels fill up to below mean low-water level, about 2 m below MSL, more than 9.8 m of the back-barrier deposits were eroded since then, for the present-day top of the channel lies at -10.7 m. Most likely, the major part of the channel was eroded at the shoreface of the retreating barrier, but an additional deepening took place in the elongated depression offshore Oostende (Fig. 7.45A), probably due to storm or tidal currents parallel with the receded barrier.

By around 1200 cal BP (750 AD), the back-barrier was completely upsilted again after the re-instalment of the tidal environment. As almost no sediment was needed anymore for the further infilling of remaining tidal channels, the barrier retreat probably slowed down or even stopped. The paleo-geographic setting in the Early Middle Ages (9^{th}-10^{th} century) in the area of Oostende, is illustrated in Fig. 7.45B. The plain has silted up to high-tide level, except from some tidal channels, which remained open. In that period an 'island' surrounded by tidal channels, 'Testerep', was located near the present-day coastline, on which former settlements of Westende (in the west), Oostende (in the east), and Middelkerke (in the middle) have been found. The medieval town of Oostende remained located offshore the present-day coastline to at least the storm surge of 1393 (Fig. 7.45D, Augustyn 1995).

Fig. 7.45 (page 225) (A) Paleo-reconstruction of the situation between 2800 cal BP and 1400 AD. After 2000-3000 years of uninterrupted peat growth, a tidal system was again installed in the back-barrier area. Peat areas were transformed into sub- and intertidal flats and re-opened tidal channels vertically incised. The sediment needed to fill the deep incised channels came from the early and mid-Holocene channels and the eroding shoreface. This resulted in a landward migration of the coastline (barrier retreat) and erosion of the tidal flats in the present-day offshore area. Around 1200 cal BP (750 AD), the back-barrier was completely upsilted again, and as almost no sediment was needed anymore for the further infilling of remaining tidal channels, the barrier retreat probably slowed down or even stopped. A wide dune belt formed in a gradual curve from Nieuwpoort to the western corner of the island Walcheren. Unit U6, which is for the major part located within the back-barrier area of 5000 cal BP, most likely represents remnants of the back-barrier deposits and surface peat of that time, which have been eroded during the natural barrier retreat since 2800 cal BP. And on the other hand, it represents remnants of newly upsilted areas since 1200 cal BP (750 AD), which have been eroded in the early 15^{th} century by intensive storm surges. (B) The situation in the Early Middle Ages (9^{th}-10^{th} century) in the area of Oostende (http://nl.wikipedia.org/wiki/Testerep). The plain had silted up to high-tide level, except from some tidal channels which remained open. In that period an 'island' surrounded by tidal channels, 'Testerep', was located near the present-day coastline on which former settlements of Westende (in the west), Oostende (in the east), and Middelkerke (in the middle) have been found. The medieval town of Oostende remained located offshore the present-day coastline to at least a storm surge of 1393 AD. (C) The map shows the situation in the east before 1300 AD (Augustyn 1995), when the wide dune belt was still intact. The blue dashed line indicates the coastline around 1300 AD when the dune belt was largely degraded by human impact (Coornaert 1989). Until eventually, in 1404, a north-westerly storm almost completely destroyed this chain of dunes. The large isle of Wulpen, situated off Cadzand, submerged in the sea, which resulted in irreversible hydrographic changes in the course of the Zwin and Westerschelde (Augustyn, 1995, Vos and van Heeringen 1997). (D) A map of the situation near Oostende shows that after the storm surge in 1393, little remained of the original 13^{th} century town of Oostende. The last remnants completely submerged in the sea between the 16^{th} century and today (Augustyn, 1995).

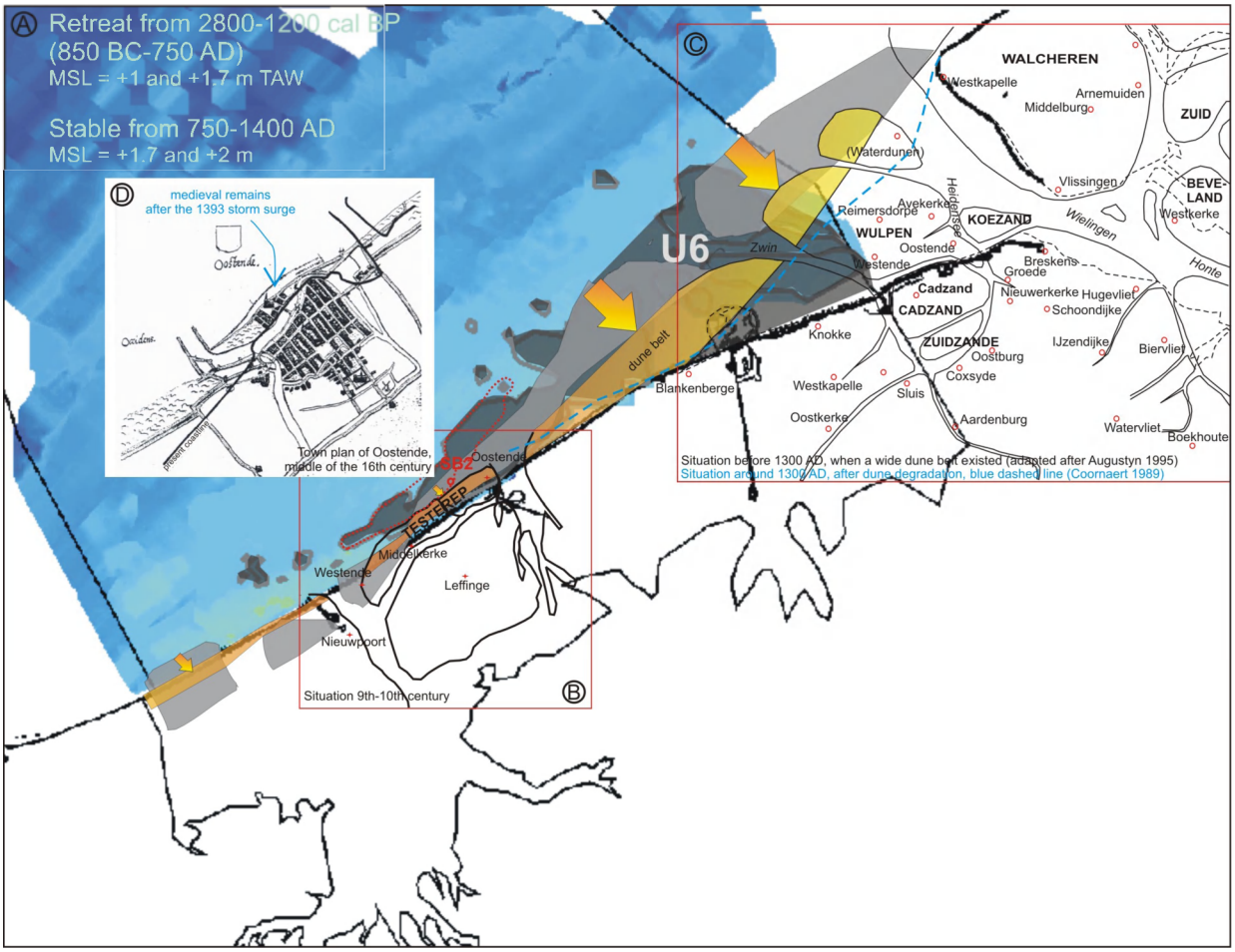

Barrier retreat (until 1200 cal BP) and the situation in the east around 1300 AD

Fig. 7.45C shows the paleo-geography of the coastline near the present mouth of the Western Scheldt around 1300 AD, which is based on the reconstruction map of Augustyn (1995). It is in agreement with the amongst historians, geologists and geographers, increasingly accepted hypothesis of a dune belt in line with the barrier on the western Coastal Plain, which links Nieuwpoort in a gradual curve with the western corner of the island Walcheren (Termote 2006). Although based on the main areal surface of parishes at that time, the reconstruction of the island Wulpen according to Augustyn is somewhat too large, while others are too modest, e.g. the reconstruction of Buntinx of 1968 (Termote 2006), comparable to the 1300 AD reconstruction map of Beekman (1921) in Vos and van Heeringen (1997). The surface area of Wulpen, reconstructed by Coornaert (1989) and indicated on the figure with a dashed line seems to be more correct (Termote 2006). It is thought that the reconstruction of Augustyn represents in fact a situation before 1300 AD, when the wide dune belt had not yet disappeared (Termote 2006).

Also in this area, the coastal barrier had not retreated yet up to the present-day coastline by 1300 AD. At that time, a large tidal channel, the Zwin, existed connecting the North Sea with Brugge. On the map of Augustyn (1995) (Fig. 7.46B), its position coincides perfectly with the position of the sandy channel-like section of U4 (Fig. 7.46A). Most likely, the sandy remnants at the top of U4 represent a renewed incision of a tidal channel, starting around 2800-2400 cal BP, when the tidal environment entered the back-barrier area again. The sandy section of U4 shows a widening, exactly at the barrier position of 2800 cal BP, and probably represents the seaward most sand flat of the back-barrier area or part of a tidal inlet at that time (Fig. 7.46). The tidal channel of

U4 probably forms the seaward extension of the Zwin channel, which became shorter with the receding barrier since 2800 cal BP.

In the area offshore Zeebrugge, U4 lays between -20 and -12 m MLLWS. Therefore the channel must have incised here at least 11.1 m and up to 19.1 m, as the MSL then was ca. +1.1 m and tidal channels fill to about 2 m below MSL. This corresponds to the values found in the western Coastal Plain (Baeteman, 2004). Tidal channels incised deeply because of the increase in the tidal prism due to compaction of the peat and collapse of the channel banks.
It is possible that the tidal channel of U4 re-incised in a former channel, because late-Holocene tidal channels tend to occupy the same location as early- and mid-Holocene channels since their infill consisted of easily erodible sands. Such a former tidal channel probably existed before 5500 cal BP, and became gradually upsilted since then when the back-barrier turned into a freshwater marsh. It is even possible that a predecessor of this channel existed during the first barrier retreat, before 7500 cal BP, when the barrier was located more seaward. This is inferred from the lithology distribution map of U4, which shows a sandy extension seaward of the 5000-2800 and 7500 cal BP barrier positions, in line with the sandy channel. Seaward of the barrier U4 fills in incisions in the Top Paleogene surface.
The erosion of U5 outside the maximal seaward position of the barrier of 5500-2800 cal BP is recent, due to present-day hydrodynamics in the Scheur. Possible former positions of tidal channels have been sketched in the above-discussed reconstruction maps.

Due to the 11-19 m deep incision of the Zwin channel, about 2800-2400 years ago, a large supply of sediment was needed to fill in. As the offshore sediment source was probably nearly exhausted due to the previous barrier progradation (Baeteman 2008), the coastal barrier retreat was most likely associated with an intensive and deep shoreface erosion. Probably also in the eastern plain the back-barrier was upsilted again at around 1200 cal BP (750 AD). Since almost no sediment was needed for the further infilling of remaining tidal channels, the barrier retreat probably slowed down or even stopped, and the barrier did not retreat much further until it reached the situation around 1300 AD (Fig. 7.45C). From historical writings its is known that the barrier consisted initially of a range of high dunes, several kilometres wide, which were overgrown and even wooded (Augustyn 1995). This is also illustrated on the map (Fig. 7.45C). Likely, this dune belt developed during the slowdown or stabilisation of the barrier retreat from 1200 cal BP (750 AD) onwards. Also on the island Walcheren, the upsilting of the back-barrier area and infilling of the tidal channels resulted in the development of a continuous barrier system covered with a chain of dunes. From the 9th century, even a regressive process (barrier progradation) may have occurred again in Zeeland. It did, however, not continue, as occasional flooding occurred during storm tides in the 11th and 12th century (Vos and van Heeringen 1997).

Fig. 7.46 (page 227) The position of the Zwin tidal channel, which existed around 1300 AD (B), coincides perfectly with the position of the sandy channel-like section of U4 on the lithofacies distribution map (A). Most likely the sandy remnants at the top of U4 represent a renewed deep incision of a tidal channel, when around 2800 cal BP the tidal environment re-entered the back-barrier area. The widening in the sandy section probably represents the most seaward sand flat of the back-barrier area or part of a tidal inlet at that time. As late-Holocene tidal channels mostly occupy the same location as early- and mid-Holocene channels (their infill consisting of easily erodible sands), this tidal channel is likely incised in a former channel, which existed before 2800 cal BP. It is even possible that a predecessor of the Zwin channel existed during the first barrier retreat, before 7500 cal BP, when the barrier was located more seaward. This because the lithology distribution map of U4 shows a sandy extension, more seaward of the 5000-2800 and 7500 cal BP barrier positions. The position of a possible tidal channel is indicated in Figs. 7.43A, 7.41 and 7.40.

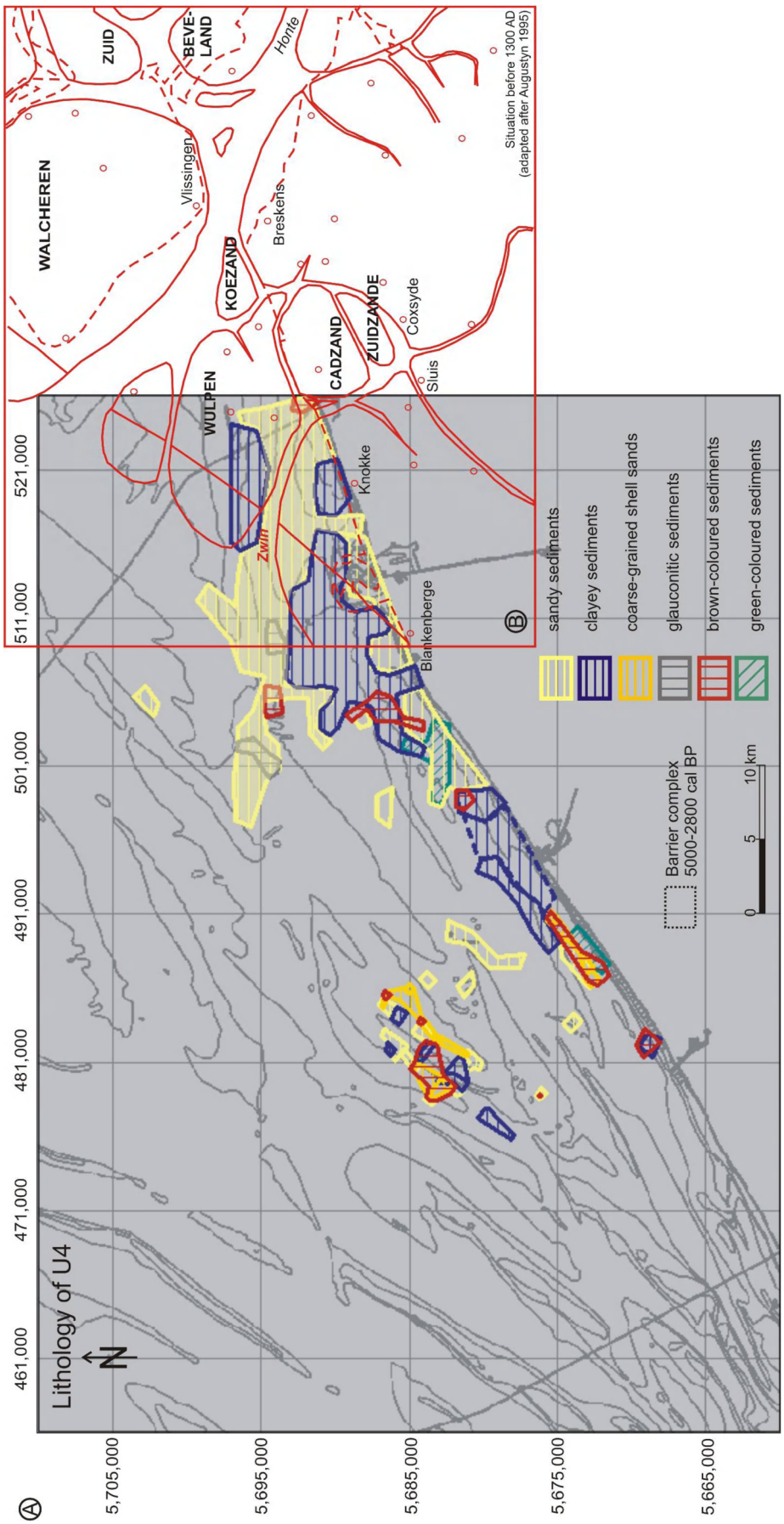
Lithology of U4
N
WALCHEREN
ZUID
BEVE-LAND
Vlissingen
Breskens
Hontе
KOEZAND
WULPEN
CADZAND
ZUIDZANDE
Coxsyde
Sluis
Knokke
Zwin
Blankenberge
Situation before 1300 AD (adapted after Augustyn 1995)
sandy sediments
clayey sediments
coarse-grained shell sands
glauconitic sediments
brown-coloured sediments
green-coloured sediments
Barrier complex 5000-2800 cal BP
0
5
10 km
461,000
471,000
481,000
491,000
501,000
511,000
521,000
5,705,000
5,695,000
5,685,000
5,675,000
5,665,000

Barrier retreat in the eastern Plain after 1300 AD

As stated above, around 1300 AD the coastal barrier had not yet retreated up to the present-day coastline. Since 750 AD, the back-barrier was silted up again, and the barrier retreat slowed down or even stopped. So what caused the further retreat of the coastal barrier up to the present-day coastline?
According to Augustyn (1995), the further coastal retreat did not have a natural origin, but was a consequence of human intervention. Until the 11th-13th century, the Flemish lowlands were protected from the sea by a high and wide range of dunes, which was completely overgrown and which formed a solid natural barrier. Storm surge dikes along the coastline were not required in those days. Various factors, such as harbour construction and urbanisation activities in the dunes, which involved deforestation and levelling of the dunes, as well as the almost total conversion of the dunes from a natural landscape into a man-made landscape, mainly intended for breeding cattle, led to a slow but irreversible degradation of the dunes from the 12th century onwards. This degradation reached such an extent that in the beginning of the 14th century seawalls had to be built in some locations to take over the protective function of the dunes. Furthermore, violent north-westerly storms got a grip on the dune landscape and accelerated the degradation of the dune landscape until, by the late 14th/early 15th century, little more was left but the small unstable drift-sand dunes we still know today. However, in 1404, a north-westerly storm, known as the first Saint Elisabeth Flood, almost completely destroyed this chain of dunes, leaving only a small stretch of dunes in the western Coastal Plain. During this storm surge the dunes and polders were flooded up to about 15 km inland. The Western Scheldt estuary was the region in which most land was lost to the sea, since here the north-westerly storm swept across the land from two sides (Augustyn 1995, Termote 2006). The large isle of Wulpen, situated off Cadzand, submerged in the sea. During the Saint Clemens Flood of 1334, which also ravaged the towns of Oostende and Blankenberge, the dune range of the isle of Wulpen had already been severely damaged, facilitating the complete flooding in 1404, and, consequently, irreversible hydrographic changes in the course of the Zwin and Western Scheldt (Augustyn 1995, Vos and van Heeringen 1997).
A paleo-geographic map of the region of Oostende shows that after a storm surge in 1393 little remained of the original 13th century town of Oostende (Fig. 7.45D). The last remnants completely submerged in the sea between the 16th century and today (Augustyn 1995).
According to Vos and van Heeringen (1997), the drowning of the islands in the mouth of the present Western Scheldt and large parts of Zeeuws-Vlaanderen originates from a mismanagement, not of the dunes, but of dikes and embankments, which had been built since the 11th century in the area of Zeeuws-Vlaanderen. Dike breaches were difficult to close and could not be dammed anymore because of limits of medieval technology, and as a consequence the inundated areas were lost. As was also suggested by Augustyn (1995), such large losses of land occurred after storm surges at the end of the 14th century, and the Saint Elisabeth Flood of 1404, and caused the tidal volume of the Western Scheldt to increase (Vos and van Heeringen 1997).

The deposition of U6

Unit U6 is for the major part located within the back-barrier area of 5000 cal BP (Fig. 7.45A). Most likely, it partly consists of remnants of the back-barrier deposits and surface peat of that time, which were eroded during the natural barrier retreat between 2800 and 1200 cal BP. Unit U6 also consists of remnants of newly upsilted areas since 1200 cal BP (750 AD), which have been eroded in the early 15th century by intensive storm surges. So, U6 would mainly be made up of muds from the eroded mud flats (polder clays) and salt marshes, sand from eroded tidal channels, and remnants of the surface peat, which is consistent with the lithology of U6.

This unit is, however, deposited on an erosional surface at a depth of -12 to -10 m offshore Zeebrugge, and at a depth of -9 to -7.5 m further to the SW, which does not correspond to the erosional depth or lower shoreface position at that time. Mean sea level between 2800 cal BP and 1400 AD is around +1 m to +2 m, and the lower shoreface is thus expected to be around -6 to -5 m. The erosional surface lies thus much deeper than the expected lower shoreface. The presumed position of the lower shoreface represents, however, the fair-weather base, not taking into account storms. But even considering the storm base, this would probably not account for the large discrepancy.

It might be suggested that the erosional depth of -12 m originates from the presence of the deeply incised Zwin channel, which needed a large sediment supply for its infilling, while its offshore sediment source was probably nearly exhausted due to the previous barrier progradation (Baeteman 2008). These both factors might have caused the barrier to recede with intensive and deep shoreface erosion, in areas where tidal inlets were present. In the areas further to the SW along the present-day coast, where the erosional surface is located at -9 and -7.5 m, no or smaller tidal inlets might have been present, or less sediment was needed to fill smaller tidal channels, or more sediment supply was still available offshore. Another possibility is that the erosion offshore Zeebrugge is due to a landward shifting of a deep channel parallel with the barrier, as is also present offshore the shallow remnants, that formed under storm and tidal currents. However, in that case the question rises why that channel did not migrate landward with the retreating barrier in the shallow areas.
If the erosional surface at -12 m is created simultaneously with the barrier retreat, U6 could have been directly deposited in the form of ebb-tidal deltas or as 'sawdust' on top of this shoreface erosional surface. But as all the available sediments were used to infill the channels, most likely only small ebb-tidal deltas could have formed, and probably a thin layer of eroded back-barrier deposits, i.e. 'sawdust' after barrier retreat, could have settled in the offshore area below the lower shoreface on the shoreface erosional surface.
This scenario, with the proposed reasons for a deep located shoreface erosional surface, is, however, only possible for the 'natural' barrier retreat between 2800 and 1200 cal BP, offshore Wulpen.

During the subsequent storm-induced coastline retreat, tidal channels were already upsilted, so there was no need for a large sediment supply, which could have caused the intensive and deep shoreface erosion. Moreover, in the area of the former isle of Wulpen, U6 could not have been deposited immediately after the coastline retreat due to the 1404 flooding. Because the erosional surface at a depth of -12 to -10 m, on which U6 was deposited, was only formed at least 150 years later. At the time when the map of the isle of Wulpen in the Scheldt delta (shown in Fig. 7.45C) was drawn up, i.e. in the middle of the 16th century, it was still possible to trace the contours of the island. More than 150 years after the disaster, the ruins of the villages that were submerged during the flood, still surfaced at low tide (Augustyn 1995).
As the island was covered by polders, the surface of which reached at least +2.5 m TAW within the dikes (Termote 2006), and as 150 years after the flooding, the ruins on top of this surface were still visible at low tide, the drowned island surface was certainly not located at -10 m, as it is now the case. This means that since the flooding of 1404, when the island surface was about +2.5 m, at least 12.5 m of material must have been eroded, but not before the middle of the 16th century. The widening of the mouth of the Western Scheldt estuary with the disappearance of the isle of Wulpen, resulted in a bigger water volume and a higher flow rate in this coastal inlet (Augustyn 1995, Peters 2006). The hydrographic changes caused strong tidal currents and an increasing flood inflow in the funnel-shaped mouth of the Western Scheldt (Peters 2006), and probably also in the

area offshore Zeebrugge in line with it (Fig. 7.47), which corresponds exactly with the area where the surface below U6 has been eroded down to -12 m.

So, most likely, the horizontal erosional surface below U6 is a combination of shoreface erosion (wave action) and tidal erosion. Due to changes in the hydraulic regime associated with the disappearance of the isle Wulpen, and the consequently stronger tidal currents near the entrance of the widened Western Scheldt, the original shoreface erosional surface was deepened, until equilibrium was reached under the new hydraulic regime. After that, the fine-grained remnants of the eroded upsilted islands and redistributed sediments of former 'sawdust' could finally settle down in a sheltered area between the isle of Walcheren and the shallower area between the Wenduine Bank and the present coastline, forming U6. It is possible that during the settling of the fine sediments of U6, several storms occurred, represented by the sandy layers, which redistributed the black muddy sediments of U6 further offshore where they draped over the underlying surface and in the elongated channel.

U6 can have an age that ranges from as old as 2800 cal BP, to somewhat younger than 1550 AD. It possibly partly consist of 'sawdust' associated with the barrier retreat of 2800 to 1200 cal BP. However, most of U6 is probably composed of remnants of flooded areas which had been upsilting until 1200 cal BP, but which could only settle after an equilibrium was reached under the new hydraulic regime since the 1404 flood, which was probably only after the middle of the 16th century. This corresponds well with the date suggested by Termote (2006) for the removal of the island group in the Western Scheldt mouth at around 1500 AD. That parts of U6 were still being deposited during the 16th century is confirmed in core 83A04, located near the Nieuwpoort Bank. The deposit of U6 contains a shell of *Mya arenaria*, which only appeared at the European coasts from the 16th to 17th century onwards (Wartel and Vansieleghem 1985). There is, however, also a constrain on the upper limit of the age of U6. On top of U6, the shore-attached Wenduine Bank and the 7-m-high, near-coastal Stroombank have formed. This process must have taken some time as well.

Fig. 7.47 (page 231) The widening of the mouth of the Westerschelde estuary with the disappearance of the isle of Wulpen around 1400 AD, resulted in a bigger water volume and a higher flow rate in this coastal inlet (Augustyn 1995, Peters 2006). The hydrographic changes caused strong tidal currents and an increasing flood inflow in the funnel-shaped mouth of the Westerschelde (Peters 2006) (B), and probably also in the area offshore Zeebrugge in line with it (A), which corresponds exactly with the area where the surface below U6 is deepest eroded, down to -12 m. So most likely the horizontal erosional surface below U6 is a combination of shoreface erosion (wave action) and tidal erosion. Due to changes in the hydraulic regime associated with the disappearance of the isle Wulpen, and the consequently stronger tidal currents near the entrance of the widened Westerschelde, the original shoreface erosional surface was deepened, until an equilibrium was reached under the new hydraulic regime. After that, the fine-grained remnants of the eroded upsilted islands and redistributed sediments of former 'sawdust' could finally settle down in a sheltered area between the isle of Walcheren and the shallower area between the Wenduine Bank and the present coastline, forming U6. It is possible that during the settling of the fine sediments of U6, several storm events occurred, represented in the sandy layers, which redistributed the black muddy sediments of U6 further offshore where they draped over the underlying surface and in the elongated channel.

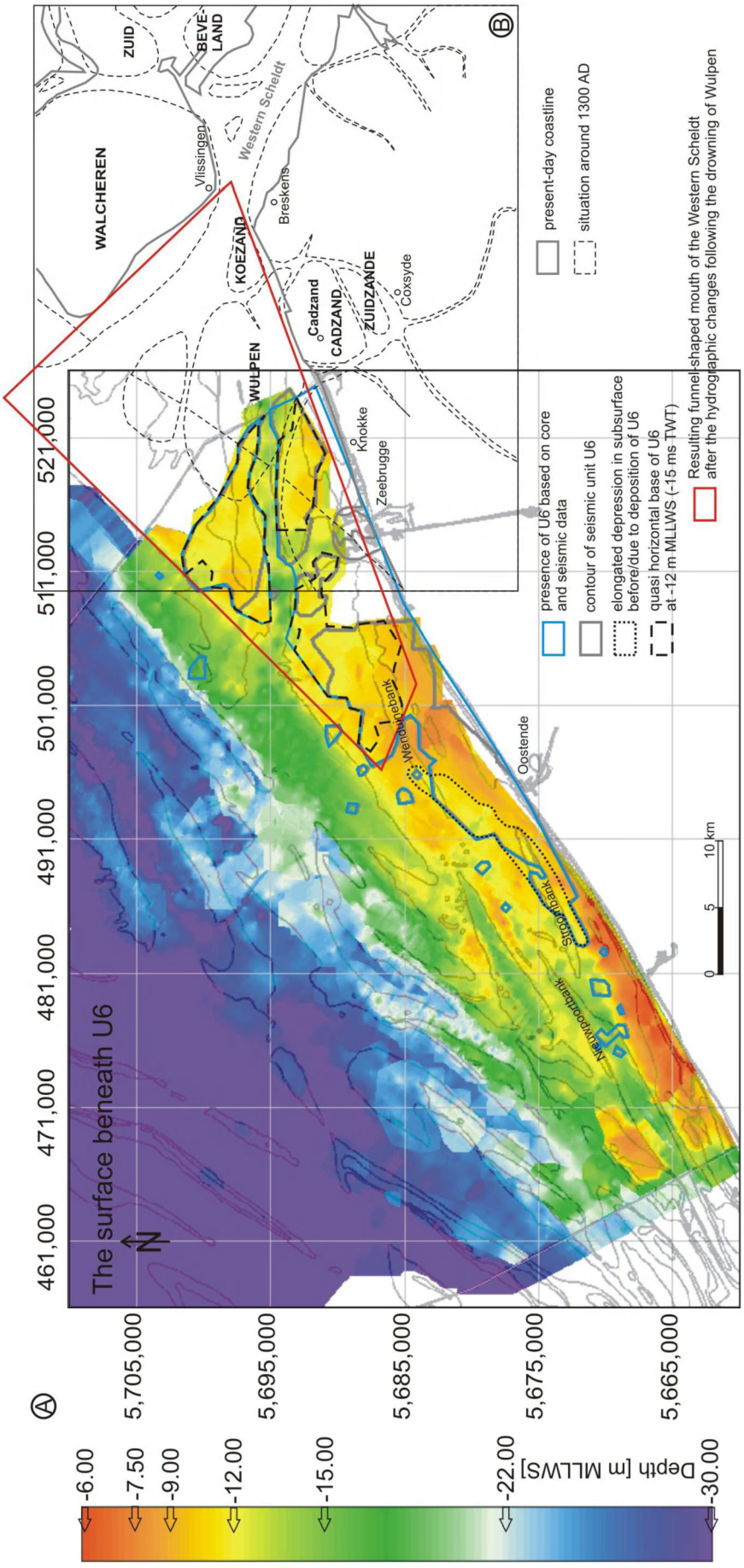
Ⓐ
Ⓑ
The surface beneath U6
N
461,000
471,000
481,000
491,000
501,000
511,000
521,000
5,705,000
5,695,000
5,685,000
5,675,000
5,665,000
Depth [m MLLWS]
-6.00
-7.50
-9.00
-12.00
-15.00
-22.00
-30.00
WALCHEREN
ZUID
BEVE-LAND
Vlissingen
Western Scheldt
Breskens
KOEZAND
WULPEN
Cadzand
CADZAND
ZUIDZANDE
Coxsyde
Knokke
Zeebrugge
Oostende
Wenduinebank
Stroombank
Nieuwpoortbank
0
5
10 km
present-day coastline
situation around 1300 AD
presence of U6 based on core and seismic data
contour of seismic unit U6
elongated depression in subsurface before/due to deposition of U6
quasi horizontal base of U6 at -12 m MLLWS (-15 ms TWT)
Resulting funnel-shaped mouth of the Western Scheldt after the hydrographic changes following the drowning of Wulpen

Summary

After 2000-3000 years of uninterrupted peat growth, a tidal system was once more installed in the back-barrier area, starting sometime between 2800 and 2400 cal BP. Peat areas were again transformed into sub- and intertidal flats, associated with deep vertical incision of tidal channels, e.g. a predecessor of the Zwin channel offshore Zeebrugge, and the channel near SB2. Because a large sediment supply was needed to fill these channels and because the offshore sediment source was probably nearly exhausted due to the previous barrier progradation, the barrier was forced to recede. The eroded sediments were mostly used to fill the channels, so most likely only small ebb-tidal deltas were formed. Possibly a thin layer of eroded back-barrier deposits, i.e. 'sawdust' after barrier retreat, settled in the offshore area below the lower shoreface on the shoreface erosional surface, and in a deep elongated barrier-parallel depression, in front of the barrier.
Between 1400 and 1200 cal BP the tidal channels came in intertidal position, and by 1200 cal BP (750 AD) the back-barrier area was upsilted again in supratidal position. Because almost no sediment was needed for the further infilling of remaining tidal channels, the barrier retreat probably slowed down or even stopped, and a large chain of dunes was formed. At that time, the coastline in the east was still located in line with the most seaward limit of Walcheren. The shoreface erosional surface, formed during the barrier retreat of 2800-1200 cal BP, probably still approximated -6 to -5 m MLLWS, although a slightly deeper position was possible due to storms, or intense erosion in tidal inlets and channels parallel with the barrier. In the back-barrier, e.g. on the island Wulpen, the upsilted area reached +2.5 m within the dikes.
The second part of the barrier retreat, up to the present-day coastline, was mainly a consequence of human intervention. Harbour construction and the almost total conversion of the dunes from a natural landscape into a man-made landscape, mainly intended for breeding cattle, led to a slow but irreversible degradation of the dunes from the 12th century onwards (Augustyn 1995). Violent north-westerly storms got a grip on the dune landscape and accelerated the degradation of the dune landscape until, by the late 14th/early 15th century, little more was left but small unstable drift-sand dunes. Eventually, in 1404 AD, a major north-westerly storm almost completely destroyed this chain of dunes, leaving only the small stretch of dunes in the western Coastal Plain. During this storm surge the large isle of Wulpen, completely submerged in the sea, which caused irreversible hydrographic changes in the mouth of the Western Scheldt. According to Vos and van Heeringen (1997), however, it was mainly the mismanagement of dikes and embankments that induced the inundation and losses of large areas of Zeeland, and the consequent hydrographic changes in the Western Scheldt.
After the storm surge, the drowned island surface of Wulpen was still visible at low tide. But, tidal currents increased in the estuary mouth and its seaward extent, which caused further deep erosion (of the shallow remnants left after the natural and storm-induced shoreface retreat) in the area offshore Zeebrugge, until an equilibrium surface with a depth of -12 to -10 m was reached. After that, at least after the middle of the 16th century, the eroded muddy sediments (of former back-barrier deposits) settled, alternated with sandy storm layers, and represents U6. Due to storm and tidal currents, sediments of U6 have been found on top of the U5 nearshore deposits on which they have been draped. The shallower position of the erosional surface before deposition of U6, along the coastline to the SW (-9 to -7.5 m), is probably because of weaker tidal currents away from the Western Scheldt, even if an erosional depth of -9 to -7.5 m is still deeper than the expected lower shoreface position of -6 to -5 m at that time (2800 cal BP to present). The differences in barrier retreat along the coastline (such as diverse erosional depths and receded distances) will be discussed in more detail in the next section.

7.3.4 Coastline retreat and advance during the Holocene sea-level rise

The movement of a barrier, whether it stabilises, advances or retreats, depends on the equilibrium between the rate of relative sea-level rise, the sediment supply towards the barrier shoreface and the sediment need (proportional to the tidal prism or accommodation space) of the back-barrier area. The importance of each factor did not only change in the course of time, but each factor did also show differences along the coastline at a certain moment in time. In this section, the focus lies on the local differences and processes involved with the movement of the barrier during the Holocene transgression.

Barrier retreat until 7500 cal BP and stabilisation until 6800 cal BP

The positions of the barrier could quite accurately be reconstructed for the period between 8000 and 7500 cal BP. During this period, the barrier in the western section, from De Panne to Westende receded about 4 to 5 km; in the central section, between Westende and Oostende, 3.5 to 4.5 km; and in the eastern section, 5 to 5.5 km (Fig. 7.48A). This corresponds to a barrier retreat rate of between 700 and 1100 m per 100 years, or on average 920 m per 100 years. These values are fully in agreement with simulation results of the shoreface translation model of Roy et al. (1995). For a substrate slope of 0.05°, the shoreface translation rate is 1100 m per 1.0 m rise in sea level. The rate of relative sea-level rise before 7500 cal BP is 7 m/ka (Baeteman 2004). So, between 8000 and 7500 cal BP, the relative sea-level has risen about 3.5 m, which would induce a shoreface translation of 3.85 km in simulated circumstances. Taking into account that the slope of the Top-Pleistocene surface on the BCS is even less than 0.5° (0.018°-0.042°), the reconstructed barrier retreat distances of 3.5-5.5 km are reasonably accurate.

The numbers clearly show that the barrier in the west did not retreat faster or over a larger distance than the barrier in the east. The barrier in the east did not stop retreating before the barrier in the west because of an elevated Pleistocene headland. This has, however, always been proposed, based on the more landward position (with respect to the present-day coastline) of the coastline in the west around 7500 cal BP, and on the presence of a barrier complex in the western Coastal Plain, in contrast to the complete absence of a barrier complex in the eastern Coastal Plain (Baeteman 2007b, Denys 2007, Fettweis et al. 2007). In fact, the entire coastline retreated constantly over its entire length. The retreat stopped at a given moment because sediment supply became able to compensate the created accommodation space, which became reduced due to an overall deceleration in sea-level rise.
Indeed, the western part is characterised by a major paleo-valley, incised to about -18 m TAW (Baeteman and Declercq 2002, Baeteman 2004, Fig. 7.42D). Contrarily, it is known from unpublished borehole data that the top of the Pleistocene in the Coastal Plain near Zeebrugge is at an elevation of about -2 m TAW (Fettweis et al. 2007). Because of this high elevation of the Pleistocene deposits, the inundation started much later in the eastern part (at least in what is now the Coastal Plain), than in the western part, which was inundated by the tidal environment as from 9500 cal BP (Fettweis et al. 2007). It has also been suggested that the accommodation space in the western part was much larger than in the east because of the deeper located pre-Holocene surface, which would have caused a much faster and more southward barrier retreat, as more sediment would have been needed for the infilling (Baeteman 2005a, Denys 2007).

In the eastern, presently *offshore* part, however, the Pleistocene surface is located at depths between -22 and -13 m TAW. So around 8000 cal BP, the inundated areas behind the barriers in the western and eastern parts (Fig. 7.48B) had about the same area and volume. In the west, the back-barrier had a surface area of 260 km², deeply penetrating landward, while the surface area behind the central and eastern part was 360 km², elongated and narrow, reaching up to about the present-day coastline, and both areas had comparable depths.

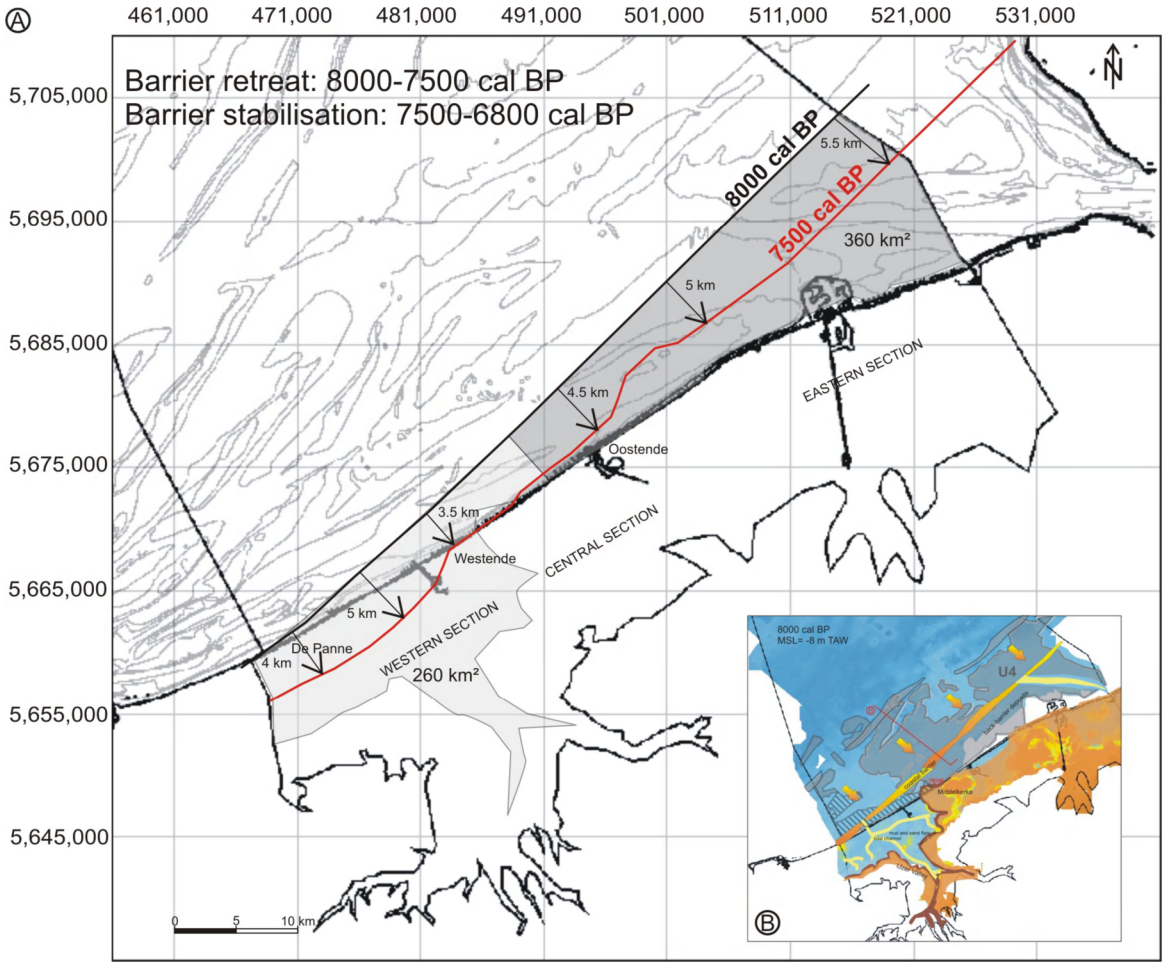

Fig. 7.48 (A) Quantification of the barrier retreat between 8000 and 7500 cal BP. The numbers show how the barrier retreated constantly over its entire length. And did not stop retreating earlier in the eastern section as was supposed by Denys (2007) and Baeteman (2005a). They suggested that because of the deeper located pre-Holocene surface in the west, the accommodation space there was much larger than in the east, which would have caused a much faster and more southward barrier retreat, as more sediment would have been needed for the infilling. The inundated areas behind the barriers in W and E around 8000 cal BP, however, had about the same surface area and depth, so similar accommodation space. (B) The back-barrier area is determined from the paleo-reconstruction of 8000 cal BP (Fig. 7.40).

The accommodation space in the western part was thus not much larger, and the barrier did not retreat much faster than in the eastern part. In fact, the barrier retreated more or less parallel with its former position, keeping a straight coastline, but with an angle to the present-day coastline, which caused the seemingly more landward position of the barrier in the western Coastal Plain. The orientation of the initial barrier was most likely predominantly determined by the strike direction of the pre-transgressive surface, and transgressed more or less constant over its entire length to its position of 7500 cal BP.

The Holocene marine transgressive surface rises gradually (not including later erosion associated with the deposition of U5 and U7) from -19 m in the most offshore position between the Kwinte Bank, over -15 m in the 8000 cal BP position, to -12 m in the 7500 cal BP position. The erosional depth is more or less constant over the entire coastline length, which seems contrary to the fact that in the western part, a 7 km wide strip of the back-barrier deposits (U4) has been completely eroded down to the Pre-Holocene surface (U3 and QT). This is explained by the shallow position of the Pre-Holocene surface in that area, between -19 and -15 m (later erosion associated with the deposition of U5 and U7 not included).

The decrease in the rate of relative sea-level rise after 7500 cal BP resulted in a sand surplus and consequently in the stabilisation of the coastal barrier (Baeteman 2004). Between 6800 and 6000 cal BP, sediment supply exceeded the accommodation space created by the relative sea-level rise, inducing the coastal barrier to prograde (Baeteman and Declercq 2002, Baeteman 2005a).

Barrier progradation until 5000 cal BP and possible stabilisation until 2800 cal BP

Since 6800 cal BP the barrier in the western part started outbuilding over 4-4.5 km, until it probably stabilised again around 5000 cal BP, just offshore the present-day coastline (Fig. 7.49A). A stabilisation has been assumed because the top of the outbuilding barrier remained at about -7 m, which corresponds to the lower shoreface at 5000 cal BP. After that, the infilling ebb-tidal-delta sediments were redistributed and built up to -6 m, which corresponds to the supposed depositional depth at 2800 cal BP (when MSL was 1 m), when the barrier started receding again. As the top surface shows no clear evidence of erosion, the origin of the growth stop has to be sought in sediment deficiency, which impeded the barrier from building out further seaward. Surface peat started developing between 6400 and 5500 cal BP (Baeteman and Declercq 2002, Baeteman 2008), which means that tidal channels were infilled and had already fallen out of use by then. Because of the upsilting of the tidal channels, ebb-tidal deltas became inactive, and got redistributed, infilling the tidal inlets and forming the western part of the nearshore sand ridge. Due to this redistribution, the shoreline got locally lined up again, and the longshore current could not be trapped anymore for the supply of sediments required for the further outbuilding of the barrier between 5000 and 2800 cal BP. In this scenario, the suggested time frame for the formation of the western part of the nearshore sand ridge, i.e. around 5000 cal BP based on the depositional depth, corresponds well with the time frame of the development of the surface peat and related closure of the tidal channels, which permitted the ebb-tidal-delta redistribution.
An alternative explanation for the sediment deficiency responsible for the stabilisation of the barrier, is that the offshore sediment supply was simply exhausted due to the barrier progradation (Baeteman 2008). From 7000 cal BP onwards, when the shoreward net sand-transport pattern changed to a pattern of along-shore transport, also a sand divergence zone developed between Zeeland and Britain. This led to the reversal of sediment transport along the Belgian coast, causing the sand supply to the coast to decrease. This process was enhanced by a decrease in the suspension of sand by wind waves as the sea became deeper (van der Molen and van Dijck 2000). Initially, this decrease in sand supply must have been slow enough compared with the decrease in sea-level rise to cause a temporary sand surplus (and consequently initial barrier stabilisation and even progradation), but this sand surplus soon decayed to a slight deficit as the decrease in supply and the rise in sea level continued, initiating stabilisation again. Most likely the barrier expansion continued until supply from all these sediment sources together (eroding ebb-tidal deltas, along-shore transport, cross-shore transport) did no longer exceed the effects of sea-level rise.

In the central part, offshore Westende, the barrier only prograded about 500 m in the period between the stabilisation of 7500 cal BP and the renewed barrier retreat of 2800 cal BP. Further eastwards, however, the distance of progradation gradually increases again from 1.5 km offshore Oostende, to 6.5 km offshore Zeebrugge (Fig. 7.49A).
The progradation (or not) of a barrier depends on the equilibrium between the rate of relative sea-level rise, the sediment supply towards the barrier shoreface and the sediment need (proportional to the tidal prism or accommodation space) of the back-barrier area.
So in the central part near Westende, the sediment supply did not exceed the accommodation space created by the relative sea-level rise, but reached an equilibrium which made the barrier remain in a more or less stable position, instead of prograding as was the case in the west and east, between 6800 and 5000 cal BP. There was thus either less sediment available at the shoreface, compared to the western and eastern barrier, or there was more sediment needed in the central back-barrier area. The latter can be ruled out, as the central back-barrier area near Westende is rather narrow because of the shallow position of the Pleistocene surface (Fig. 7.49B).

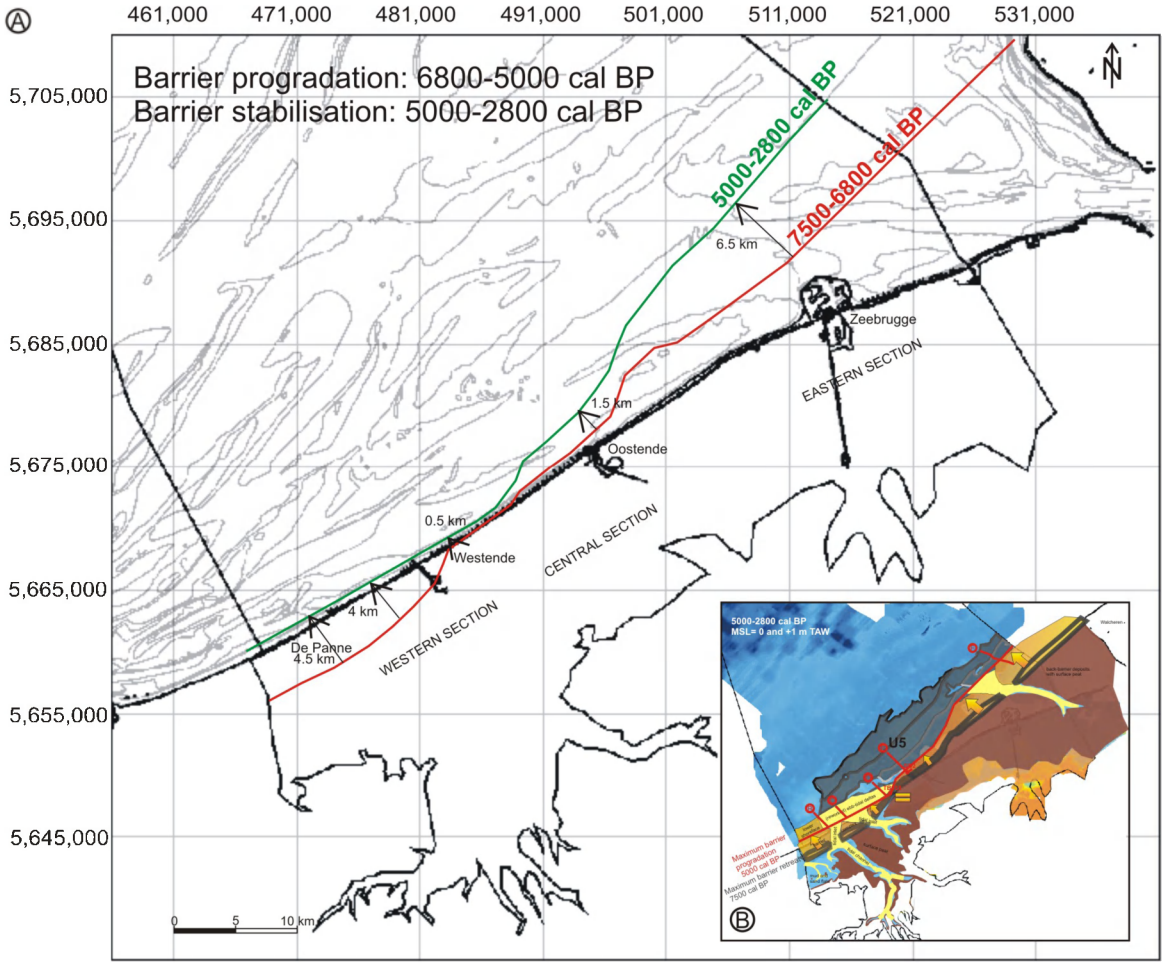

Fig. 7.49 (A) Quantification of the barrier progradation between 6800 and 5000 cal BP. The numbers show how the central section stayed in an almost stable position, while the western and eastern sections prograded several kilometres. There was either less sediment available at the shoreface in the central part, or there was more sediment needed in the central back-barrier area. The latter can be ruled out, as the central back-barrier area near Westende is rather shallow and narrow, as shown in (B), because of the elevated position of the Pleistocene surface.

The changing net sand-transport pattern since 7000 cal BP might have influenced the relative sediment deficiency in the central section compared to the eastern and western ones, or a sediment surplus in the eastern and western section, compared to the central part, which was in balance. Although the large-scale model of van der Molen and van Dijck (2000, Fig. 7) is not ideal for predicting small-scale changes in the coastal-near zone, it shows deposition, a sediment surplus, in the eastern section, following the transport-direction change. Also the formation of the middle storm-generated sand ridge and the development of tidal sandbanks since 7000 cal BP (cf. Chapter 8), might have influenced the local hydrogeography (deviation of tidal and storm currents) and might have caused the differences in progradation along the coastline.
It should also be noted that one barrier island, only a few kilometres in length, can produce both regressive (prograding) and transgressive or stable sequence models. At one end of the island, the barrier progrades due to the build out of ebb-tidal deltas, while this causes sediment decrease at the downdrift end. The presence of tidal channels and related ebb deltas in the west, still intact at the onset of the barrier progradation around 6800 cal BP, might thus have caused the stabilisation in the central, downdrift, section of the coastline.

Barrier retreat until 1200 cal BP (750 AD) and possible stabilisation until late 14th /early 15th century

Between 2800 and 2400 cal BP, a tidal system was again installed in the back-barrier area coupled with deep vertical incision of tidal channels. The sediment needed to fill the deep incised channels came from the early- and mid-Holocene channels and the eroding shoreface. As the offshore sediment supply was probably reduced, this resulted in a landward migration of the coastline in the western and eastern plain. This ended at about 1200 cal BP (750 AD), when the back-barrier area was upsilted again in supratidal position and the barrier retreat probably slowed down or even stopped.

In the western section of the area, the barrier retreated over a distance of only about 1 km up to the present-day coastline; in the central part, between Westende and Middelkerke, the barrier did not retreat since its former position at 5000-2800 cal BP; further eastwards, the barrier retreated progressively from 1 km to more than 5.5 km towards its position of around 1200 cal BP (Fig. 7.50A).
Three reasons are suggested for this extreme discrepancy in retreat distance between the western and eastern coastline for the period 2800 to 1200 cal BP. As the rate of relative sea-level rise is constant along the coastline, the dissimilarities have to be sought in the differences in sediment supply towards the barrier shoreface and differences in sediment need (accommodation space) of the back-barrier.

(1) As the barrier retreat is stimulated by the infilling of deeply incised late-Holocene tidal channels, the difference in barrier retreat between the eastern and western section might be sought in a difference in size and/or number of tidal channels, or the time the tidal channels were open in both areas. In the westernmost part of Zeeuws-Vlaanderen, and in the Zwin area, young Holocene tidal channels exist that are incised to more than -13 m TAW (Vos and van Heeringen 1997), and an additional large tidal channel existed in the present Western Scheldt mouth (reconstruction maps in: Vos and van Heeringen 1997). So, in the eastern section, the number of tidal channels and incisional depths were at least comparable to the situation in the west. However, in the east, the barrier retreat might have been encouraged by the peat digging and artificial drainage by Romans, which lowered the ground level, which resulted in an increased accommodation space and sediment need. In the western Coastal Plain the renewed tidal channels followed the course of their mid- and early-Holocene predecessors, but in Zealand, located adjacent to the eastern plain, the newly

formed tidal channels followed the course of the artificial drainage patterns of the Roman peat excavations (Vos and van Heeringen 1997). What concerns the timing, in the western Coastal Plain, the tidal channels progressively migrated landwards from 2400 to 1500 cal BP. In the eastern part, however, the exact timing of the opening and closure of the tidal channels is not known. It is possible that the retreat distance in the eastern plain was larger because the tidal channels were opened for a longer period of time.

(2) As the natural compaction of the surface peat covering the back-barrier area induces an increase in accommodation space, i.e. an increase in tidal prism, it induces the sediment need for the particular area. So, the surface area of the back-barrier region might be an indication for the potential accommodation space created between 2800 and 1200 cal BP, and the consequently needed sediment supply (which induced the barrier retreat). The potential back-barrier surface area is determined by the most seaward boundary of the surface peat (Fig. 7.50B), and the most landward boundary of the Coastal Plain (which is by definition the most landward extent of the Holocene deposits). In the eastern section, the back-barrier area is 600 km², while that is only 460 km² in the western part of the area (Fig. 7.50A). Due to this difference in surface area, the accommodation space created in the eastern section, with the renewed expansion of the tidal-flat environment, was probably larger than in the west, which might partially explain the more extensive barrier retreat in the east, compared to the west. In the central part, between Westende and Middelkerke, the barrier remained in position. The sediment supply was just sufficient to compensate the newly created accommodation space, which was much smaller (150 km²) than in the western and eastern back-barrier areas. The smaller accommodation space induced a smaller tidal prism, possibly causing the tidal channels to close sooner.

Note, however, that in this reasoning the thickness of the surface peat was not taken into account. Thin peat layers, e.g. where the Pleistocene substrate lies high, will create less accommodation space. Neither the presence of tidal channels was taken into account. The potential for the surface peat to incline, depends largely on the presence of nearby channels which cause the drainage and consequent compaction of the peat. Apart from the location of some large tidal channels in the eastern plain, little is known about the smaller channel networks.

(3) Possibly, also a factor of differential sediment supply should be taken into account as was suggested by Denys (2007). Before 7500 cal BP, the barrier migrated constantly over its entire length and formed a straight line. But since 5000 cal BP (and not since the early Holocene as was suggested by Denys 2007), the eastern plain protruded a few kilometres further seaward than the central plain, and formed a kind of 'headland' (Fig. 7.49A). According to Denys (2007) this 'headland' could have intercepted the along-shore net sediment transport which was oriented NE-ward, causing a larger sediment deficiency in the east compared to the west, inducing the eastern barrier to retreat further landward. The western barrier receded less because more sediment was available there, due to the interception of the longshore drift by the further NE located 'headland'.

The presence of the elongated erosional depression, parallel to the coastline, where it forms the 'headland', confirms the presence of strong currents along this 'headland'. No sediment deposits have, however, been found upstream of the headland, but were probably immediately used for the infilling of the western and central back-barrier. The sediment supply was sufficient for the central barrier which remained stable, but still insufficient for the western barrier which did recede.

Around 1200 cal BP (750 AD), when the barrier stabilised, the coastline had developed towards a straight line once more. With the disappearance of the 'headland', the longshore sediment drift was no longer intercepted and possibly the available sediment surplus could be used to build a wide chain of dunes.

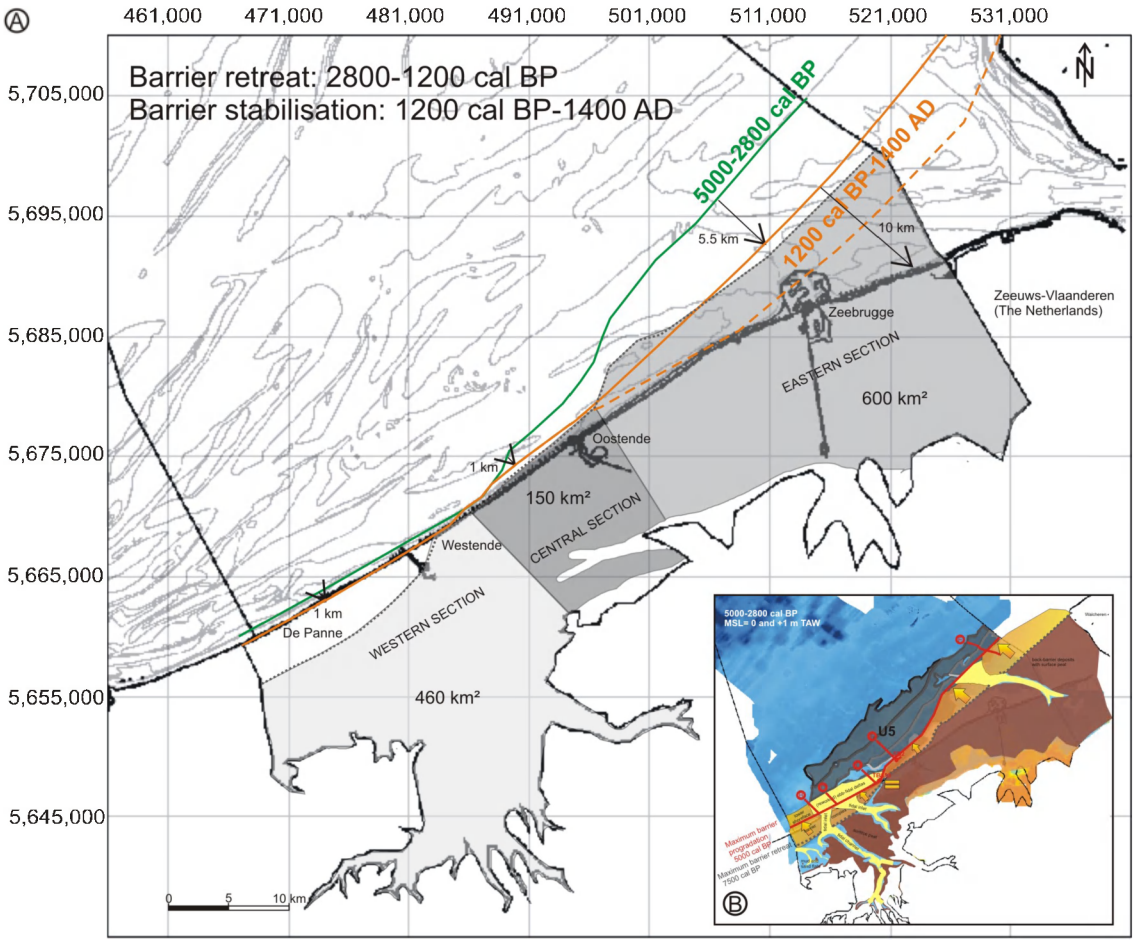

Fig. 7.50 (A) Quantification of the barrier retreat between 2800 and 1200 cal BP. The presence of a large back-barrier area in the east, might partially explain why the eastern part of the barrier retreated much further than the western one. This, because a larger accommodation space needs more infilling, which induces the barrier to retreat further. The back-barrier surface area is determined by the most seaward boundary of the surface peat (B), and the most landward boundary of the Holocene Coastal Plain (grey areas, black contour includes Pleistocene Coastal Plain). The dashed line indicates the coastline around 1300 AD when the dune belt was largely degraded by human impact (Coornaert 1989).

Final barrier retreat up to the present-day coastline

During the second part of the barrier retreat, the large isle of Wulpen completely submerged in the sea, which caused irreversible hydrographic changes in the mouth of the Western Scheldt. Tidal currents increased in the estuary mouth and its seaward extend, which caused further deep erosion (of the shallow remnants left after the natural and storm-induced shoreface retreat) in the area offshore Zeebrugge, until an equilibrium surface with a depth of -12 to -10 m was reached.

The differences in erosion intensity, since the barrier retreated from its stable position between 5000 and 2800 cal BP until the present-day position, between different sections of the coastline are remarkable. In the eastern section, the erosional surface is located at depths between -12 and -10 m, while further to the SW the erosional depth is -9 to -7.5 m in the area between the Wenduine Bank and the present coastline, -11 m offshore Oostende near core SB2, and -7 m in the area offshore Nieuwpoort and De Panne (Fig. 7.36)
The deep position of the Holocene marine transgressive surface north of Zeebrugge, is probably due to intensive shoreface and tidal-inlet erosion of the extended Zwin channel during the initial barrier retreat, because of the large sediment demand in the back-barrier area and the shortage of sediment supply from offshore, but mainly due to the increased tidal currents that were adjusting to the renewed hydrographic situation after the further, human induced, barrier retreat of 1404 AD. The deeply eroded section lies exactly in line with the funnel-shaped mouth of the Western Scheldt (Fig. 7.47).
As the deep erosional surface offshore Zeebrugge, truncating U5 and U4 and located below U6, is mainly formed by the re-adjusting tidal currents in the mouth of the Western Scheldt since 1404 AD, one might wonder whether the barrier did prograde as much forward between 6800 and 5000 cal BP, eroding first U5 and subsequently U4 with the retreat, in the first place. It can be assumed that it did, because the barrier must have been located seaward of its position of 1300 AD, the assumed prograded distance is comparable to the one in the western section (Fig. 7.49A), and because the sandy section of U4 shows a widening exactly at this former position (Fig. 7.46), which probably represents the most seaward sand flat of the back-barrier area or part of a tidal inlet at the time of its maximal seaward extent.

The shallower position of the erosional surface more to the SW is probably due to the weaker tidal currents away from the Western Scheldt. Nevertheless, the erosional depth of -9 to -7 m is still deeper than the expected lower shoreface position of -6 to -5 m at that time (2800 cal BP to present). However, one has to bear in mind that the supposed lower shoreface represents the fair-weather base, and not the storm wave base, which could have been much deeper. The position of -11 m near core SB2 probably originates from shoreface erosion at the retreating barrier with an additional deepening in the elongated depression offshore Oostende (Fig. 7.45A), probably due to storm or tidal currents parallel with the receding barrier.

In the western Coastal Plain, the present-day coastline was possibly already reached during the initial, natural barrier retreat, as it was the only section of the coastline where the chain of dunes was not destroyed during the storm of 1404 AD (possibly because they were less damaged by human activity), so the coastline did probably not retreat any further. In the central part of the Coastal Plain, between Westende and Middelkerke, the barrier stayed in a more or less stable position since the minor progradation since 6800 cal BP, forming the western seaward boundary of the area which later became 'island' Testerep. Between Middelkerke and Oostende, the barrier did prograde since 6800 cal BP, past the location of SB2, and retreated again over about 600-1000 m since 2800 cal BP, to form the eastern part of the seaward boundary of the area Testerep (Fig. 7.45B). This area became known as an 'island' when the plain was dissected by tidal channels around 2000 cal BP (Denys 2007). This 'island' was still located offshore the present coastline until at least the Early Middle Ages (9^{th}-10^{th} century). It retreated about 1.5 km during the storms in the 14^{th}/15^{th} century, so that by the 16^{th} century, the old town of Oostende was almost completely drowned (Fig. 7.45D), and the present coastline was more or less reached. In the east, after the initial, natural retreat of 5.5 km, the barrier receded another 10 km (Fig. 7.50A). Most land was lost to the sea in the Western Scheldt estuary, because there the NW storm swept across the land from two sides (Augustyn 1995, Termote 2006), because the island was surrounded by two large channels, i.e. the Zwin and the Western Scheldt. The Western Scheldt existed since the

progressively eastward migrating tidal channel 'Honte' connected the Scheldt with the North Sea (although the age of this connection is still under debate) (Fig. 7.45C).

Differences between the barrier retreat of 9500-7500 cal BP and 2800 cal BP-present

Although the coastal barrier retreated twice, i.e. during the period between 9500 and 7500 cal BP and during the period of 2800 cal BP to present, there are some remarkable differences (Table 7.2).

During the initial barrier retreat (9500-7500 cal BP), it was the fast relative sea-level rise that forced the barrier to recede. Sediment supply did not outrun the created accommodation space, as the barrier retreated, but was high and constant enough to prevent the barrier from drowning, to put off the creation of a lagoon in the back-barrier area, and to allow the formation of ebb-tidal deltas and a transgressive sand sheet in which afterwards sand ridges formed (U5). The barrier transgressed in a dynamic equilibrium with rising sea level, by the landward transfer of sand, eroded from the shoreface to the back-barrier.
During the second retreat (especially from 2800 to 1200 cal BP), the barrier retreat was forced by sediment deficiency, as relative sea-level remained almost constant. During this period all available sediments were used to infill tidal channels in the back-barrier, only small ebb-tidal deltas could be formed. And possibly only a thin layer of eroded former back-barrier deposits, the 'sawdust' after barrier retreat, could settle in the offshore area below the lower shoreface. Most of U6 was probably deposited after equilibrium was reached under the new hydraulic regime since the 1404 AD flood.

PERIOD	**9500-7500 cal BP**	**2800 cal BP- present** (2800-1200 cal BP + 1400 AD-present)
CAUSE	natural	natural induced human induced
DRIVING FORCE	relative sea-level rise	sediment need storm surges hydrographic balancing
OFFSHORE REMNANTS AFTER RETREAT	transgressive sand sheet sand ridge formation (U5)	clay-sand alternation (U6)

Table 7.2 Characteristic differences between the barrier retreat of 9500-7500 cal BP and 2800 cal BP- present.

The difference in lithology between the deposits of U5 and U6, both deposited after a barrier retreat, is quite remarkable as well. U5 consists of grey fine sands with occasional shell accumulations and peat fragments, while U6 mainly consists of organic-rich black clays alternating with thin sandy layers. The difference lies partly in the fact that the back-barrier just before the 2800 cal BP retreat, was completely upsilted to supratidal level and consisted of extensive muddy sediments and fresh-water marshes. Contrarily, before 7500 cal BP, organic matter only occurred as local vegetation horizons and basal peat, and the back-barrier area was probably upsilted to a lesser degree and therefore consisted mainly out of sandy sediments. So, the lithology of the remnants deposited after barrier retreat could have been determined by the difference in substrate.

However, things are not that straightforward. During a coastline retreat, a transgressive sand sheet originates in the first place from downwelling storm currents, eroding the barrier shoreface, which is built up of sandy material. This sandy material originated from the eroded substrate supplied by wave action from offshore, from erosion in tidal inlets and from longshore transport (Swift et al. 1991).
In the case of the barrier retreat prior to 7500 cal BP, a large part of the substrate was eroded. It consisted of U4 (offshore De Panne erosion even cut down to the Pleistocene surface), which is mainly characterised by sandy sediments. This was especially true in the areas where tidal inlets eroded the underlying substrate, as in a mixed wave-tide dominated environment tidal inlets tend to be stable and lock on previous tidal inlets and channels, which consist almost entirely of sandy material. This sand was supplied to the barrier, which fed the transgressive sand sheet during peak storms, from which subsequently the storm-generated ridges of U5 were built up. This might explain (apart from the erosive character of storm ridges itself) why the sands of the U5 storm-generated ridges, show so much similarities with the sands of U4.
In the case of the barrier retreat between 2800 and 1200 cal BP, the eroded material at the shoreface of the barrier consisted initially predominantly out of sands, previously supplied during the preceding barrier progradation. In tidal inlets and at the lower shoreface also the muddy substrate of the previously upsilted back-barrier with surface peat was possibly reached and released. But, although it is possible that a part of the eroded muds and sands could settle offshore as a thin layer beyond the reach of storm waves, most likely most of the released material was used for the infilling of the back-barrier area, which was the driving force of the barrier retreat at that time.
The largest part of U6 was deposited much later, after the second, human-induced phase of the coastline retreat, when the erosional surface below U6 became much deeper due to the impact of storm surges and intensive tidal currents, re-adjusting to the changed hydrographic situation since the late 14th/early 15th century floods. It was only then, that most of the clayey and organic-rich material of the former back-barrier deposits was eroded and could settle in the sheltered area between Walcheren and the shallow area near the Wenduine Bank.
The difference in lithology between U5 and U6, although they were both deposited after barrier retreat, is therefore not only determined by the difference in substrate over which the barrier receded, but also by the fact that they are deposited under different hydrodynamic circumstances. U5 is deposited after barrier retreat under sea-level-rise forcing. While U6 is mainly deposited after tidal erosion, following coastline retreat under storm forcing. Only a minor part of U6 could deposit after the initial, natural barrier retreat, as the barrier retreated under 'sediment-need' forcing.

Possibly, the differences in lithology *within* unit U6, between the SW part, which is more sandy, and which contains more silt with shell accumulations, and the offshore Zeebrugge part, which is more heterolithic and clayey, can be explained by the different hydrographic evolution as well. In the SW, the silty, sandy sediments could represent storm-related deposits of the late 14th/early 15th century, while offshore Zeebrugge they have been reworked and removed by the subsequent strong tidal currents, after which the more clayey sediments settled.
Another difference between units U5 and U6 is that sand ridges formed in the sand sheet of U5, while this was not the case in U6. The clayey sediments of U6 evidently did not lend themselves for the formation of ridges. Although, in a later phase, nearshore sand ridges did form *on top* of U6.

Summary: changes in relative sea-level rise, sediment supply, and accommodation space during the Holocene sea-level rise

The data suggest that between 9500 and 7500 cal BP, during the period of fast relative sea-level rise, the retreat of the coastal barrier was more or less uniform over its entire length (Fig. 7.51A), while after the first (Fig. 7.51B) and second slowdown (Fig. 7.51C), local factors seem to have played a more important role, causing differences in barrier migration between the different sections (west, centre, east). During the initial period, the rate in relative sea-level rise was the determining factor for the position of the barrier. Sediment supply was directed towards the shore and more or less constant. It was insufficient to avoid the barrier from receding, but sufficient to prevent the barrier from drowning, and to put off the creation of a lagoon in the back-barrier area. Landward migration was through a process of erosional shoreface retreat as the barrier adjusted to changing sea level.

After the first slowdown in the relative sea-level rise, around 7500 cal BP, the sediment supply was in equilibrium with the created accommodation space, and the barrier stabilised (Fig. 7.51A). From about 7000 cal BP, the shoreward-directed net sand-transport pattern changed into a pattern of along-shore transport. At the same time a sand divergence zone developed between Zeeland and Britain, and the transport along the Belgian coast changed, causing the sand supply to the coast to decrease, which was enhanced by a decrease in the suspension of sand by wind waves as the sea became deeper (van der Molen and van Dijck 2000) (Fig. 7.51B). The decrease in the rate of relative sea-level rise could, however, compensate for the reduced sediment supply and resulted in a sand surplus. From 6800 cal BP, the relative sea-level rise lost even more of its driving force and the barrier started to prograde. In this period, the sediment supply was the determining factor of the barrier position. Probably due to local hydrographic processes (i.e. presence of ebb deltas updrift, development of Flemish Banks) and due to the development of the sand divergence zone, the sediment supply towards the central barrier shoreface was much less than towards the western and eastern section, which prograded much further (Fig. 7.51B).

Despite the second slowdown in relative sea-level rise, around 5500-5000 cal BP, the barrier did not continue prograding, but stabilised (Fig. 7.51C). This was caused either because the longshore net sand transport could not be trapped anymore due to the redistribution of the ebb-tidal deltas, or because the offshore sediment supply was simply exhausted due to the barrier progradation (Baeteman 2008). It is, however, more likely that the sand supply was not exhausted (as later dunes could still form when sea-level was more or less stable), but continued decreasing after 7000 cal BP, leading to a sand deficit with continuing sea-level rise. This is in contrast to the earlier situations, when the decrease in sand supply was slow enough compared to the decrease in sea-level rise causing even a temporary sand surplus (and consequently barrier progradation).

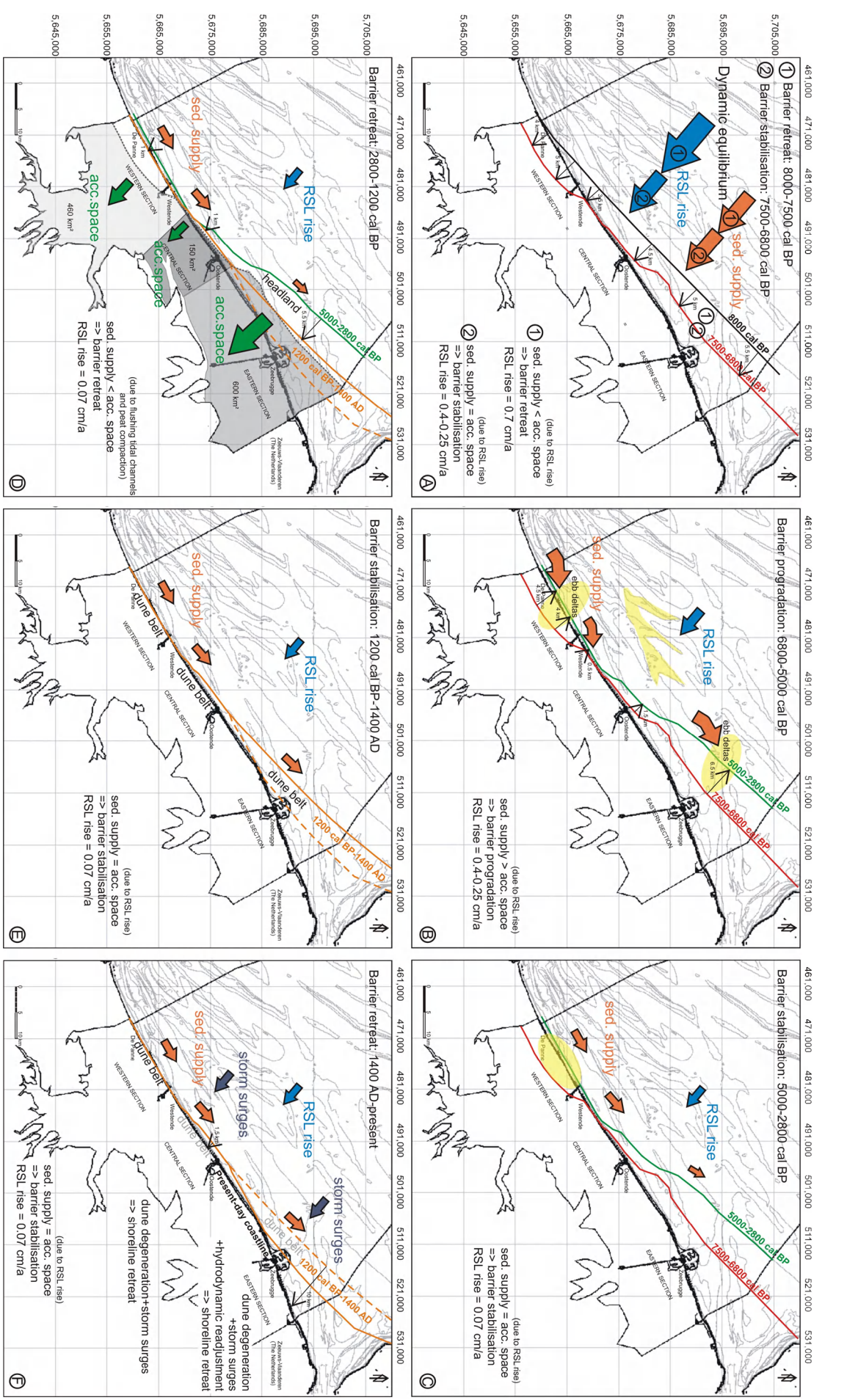
① Barrier retreat: 8000-7500 cal BP
② Barrier stabilisation: 7500-6800 cal BP
Dynamic equilibrium
RSL rise
sed. supply
8000 cal BP
7500-6800 cal BP
① sed. supply < acc. space (due to RSL rise)
=> barrier retreat
RSL rise = 0.7 cm/a
② sed. supply = acc. space (due to RSL rise)
=> barrier stabilisation
RSL rise = 0.4-0.25 cm/a
Barrier progradation: 6800-5000 cal BP
ebb deltas
5000-2800 cal BP
7500-6800 cal BP
sed. supply > acc. space (due to RSL rise)
=> barrier progradation
RSL rise = 0.4-0.25 cm/a
Barrier stabilisation: 5000-2800 cal BP
sed. supply = acc. space (due to RSL rise)
=> barrier stabilisation
RSL rise = 0.07 cm/a
Barrier retreat: 2800-1200 cal BP
headland
5000-2800 cal BP
1200 cal BP-1400 AD
150 km²
600 km²
460 km²
acc.space
sed. supply < acc. space (due to flushing tidal channels and peat compaction)
=> barrier retreat
RSL rise = 0.07 cm/a
Barrier stabilisation: 1200 cal BP-1400 AD
dune belt
sed. supply = acc. space (due to RSL rise)
=> barrier stabilisation
RSL rise = 0.07 cm/a
Barrier retreat: 1400 AD-present
storm surges
present-day coastline
dune degeneration
+storm surges
+hydrodynamic readjustment
=> shoreline retreat
dune degeneration+storm surges
=> shoreline retreat
sed. supply = acc. space (due to RSL rise)
=> barrier stabilisation
RSL rise = 0.07 cm/a
WESTERN SECTION
CENTRAL SECTION
EASTERN SECTION
Oostende
Westende
De Panne
Zeeuws-Vlaanderen (The Netherlands)
Zeebrugge

Fig. 7.51 (page 244) Overview of the changes in relative sea-level rise (RSL rise), sediment supply (sed. supply), and accommodation space (acc. space) during the Holocene, which gave rise to differential barrier movements along the coastline. The accommodation space can be created either by the RSL rise or by peat compaction and tidal channel incision. The transport direction of the sediment supply (orange arrows) diverts from onshore to alongshore around 7000 cal BP. The RSL rise shows two decreases: around 7500 cal BP and 5000 cal BP. The size of the arrows, representing the RSL rise (blue), sed. supply and acc. space, is proportional to the relative contribution of the aspect in the system, through time and along the coastline. Meaning yellow areas see text.

In the period between 2800 and 1200 cal BP, it was sediment demand (i.e. accommodation space created in the back-barrier) that was the major determining factor for the position of the barrier, although also differential sediment supply due to the presence of a headland could have played a role (Fig. 7.51D). As the eastern section had prograded further than the central part, the eastern plain formed a headland, which could have intercepted the along-shore sediment drift. Therefore, the western and central parts probably received more sediment than the eastern plain. Sediment supply in the central section, between Westende and Middelkerke, was just sufficient for the infilling of the small back-barrier area, and the barrier remained stable, while in the western section, it was insufficient, making the barrier retreat. In the eastern plain, the largest back-barrier area received the least sediment and therefore retreated the furthest. Since 1200 cal BP (750 AD), the back-barrier has been upsilted to supratidal level, the barrier has stabilised, and the coastline developed towards a straight line once more (Fig. 7.51E). With the disappearance of the 'headland', the longshore sediment drift was no longer intercepted and the available sediment surplus was used to build a wide chain of dunes.

In the final phase, it was mainly the human interventions which determined the landward shift of the barrier up to the present coastline (Fig. 7.51F). The destruction of the dune complex, mismanagement of dikes, and lowering of the back-barrier area due to drainage for land reclamation, determined how far inland the land was flooded during storm surges. After the flooding the tidal currents took over the area if it was not reclaimed by man again.

7.4 Limitations, innovations and recommendations

7.4.1 Difficulties and limiting factors

The BCS is an accommodation-dominated shelf where the accumulation rate is low. On such sediment-starved shelves, sediment is repeatedly reworked. The resulting transgressive deposits are thin and discontinuous, commonly coarse-grained (sandy) and heterogeneous. Discontinuous units that consist primarily of reworked material make it difficult to reconstruct the distribution of depositional environments, and to make a stratigraphic classification based on core data alone. Lithologically similar material commonly belongs to highly different depositional environments. Seismic data was indispensable for the identification of important erosional surfaces, and for the delineation of former boundaries of different depositional environments. The dense seismic network was indispensable in correlating isolated lens and bank structures forming the three parallel storm-generated sand ridges of U5.

For the creation of the paleo-reconstructions after 9500 cal BP, the position of former coastlines was constrained using the depth of the erosional upper bounding surface of seismic unit U4. This surface is considered the Holocene marine transgressive or shoreface-ravinement surface, which was created by erosion at the shoreface of a coastal barrier that migrated landward over the former U4 back-barrier deposits. With rising sea-level, the vertical position of the lower shoreface (the erosion base) rose as well. For a certain point in time and a known MSL, the position of the coastline was drawn as a contour on the Holocene transgressive surface, assuming a fixed depth of the lower shoreface of that time. Deposits of U4 below (seaward of) this contour were eroded to the depth of the lower shoreface, while deposits above (landward of) this line were still developing in the back-barrier and will be eroded at a later stage with continuing rising sea level.
This approach has two limitations: (1) the original Holocene flooding surface has to be known (i.e. the passive flooding surface before parts of it were eroded), and (2) the depth of the lower shoreface in relation to the MSL has to be known. Owing to the constant reworking of *in situ* available sediments the surface of U4 has strongly been altered during (or before) the deposition of overlying units. An envelope was drawn connecting the highest preserved parts of U4 to approach the original surface. However, if the original marine flooding surface was located even higher, the reconstructed coastlines should be located farther seaward.
To overcome the second limitation, it was assumed that the lower shoreface was located about 7 m under the MSL level of that time. This is in concordance with the present-day situation where the lower shoreface is on average located 5 m below MLLWS (which is about 2 m below MSL). We are aware that this is an oversimplification. The position of the lower shoreface varies in depth and time as it is determined by many local factors such as sediment availability, seasonality, storm frequency and wave height. Since the wave height has increased since the beginning of the Holocene (van der Molen and de Swart 2001b), it might be suspected that the toe of the shoreface was located at shallower water depths below MSL than today. In that case the proposed coastlines should be located farther landward than drawn. In this light, it must be noted that the depth of closure for the Belgian coast, as taken to define the toe of the modern shoreface, is an imperfect proxy. During long-term coastline transgression, both the shoreface and the associated ridge-and-swale systems migrate landward. It may well be that the migrating base of swales seaward of the most landward shoreface-connected ridge forms the ravinement recognised on seismic profiles. In the Netherlands, depth of closure is easier to define where shoreface-connected ridges are absent. There, it is located below -15 m MSL.

For the indirect age determination of the deepest (i.e. oldest) deposits of U4, a fictitious mean tidal range was used in agreement with the present-day situation to asses a MSL and corresponding age. It is known from model results though that the tidal range in the early Holocene in the Southern Bight was microtidal (about 1 m around 8000 BP or 8900 cal BP, van der Molen and de Swart 2001a). However, in this early Holocene period relative sea-level rose quickly. Thus, when inferring ages from depositional depths, mistakes in depositional depth lead to only minor age variations. In the paleo-reconstruction of 10,450 cal BP, the sand- and mud-flat zones would be narrower in case of a smaller tidal range.
Around 9500 cal BP (MSL = -17 m MLLWS), when the first barrier islands formed, the first deposits to develop in the back-barrier basin would have been located at a depth of about -17.5 m in case of a microtidal range, instead of -19 m as was proposed. So the initial barrier could have been located slightly farther landward than indicated in Fig. 7.39.

Another limiting factor in the reconstruction of the Holocene coastline evolution is the absence of high-quality seismic data and deep boreholes in the nearshore area. This

area is crucial when it comes to reconstructing the Holocene (and especially historical) coastline evolution. As an example, the evolution of the Holocene Coastal Plain involved a part of the area that is presently offshore. The Belgian nearshore area, however, is characterised by the presence of gas, which strongly attenuates the seismic signal. The draught of the RV Belgica was an additional restriction.

A final constraint is the absence of detailed studies of the Late-Holocene evolution in the central and eastern Coastal Plain. We had to assume that the back-barriers in the central and eastern Coastal Plain (including the present-day offshore parts) started evolving in a similar way and with a comparable timing as in the western Coastal Plain. The driving force for the barrier retreat was of climatic origin and should be reflected as a regional pattern, but local governing factors did undoubtedly overprint this regional pattern. The exact timing of local coastal changes depended laterally and spatially on variable sediment supply and wave and tidal processes. Furthermore, the degree and the extent of the collapse of the surface peat depended on the incision of tidal channels and the peat digging during Roman occupation. These two controlling factors were not synchronous over the entire plain. As little is known about local controlling factors in the central and eastern Coastal Plain, the initial climatic trigger of 2800 cal BP was used as the starting date for the renewed entrance of the tidal system.

7.4.2 Innovations

Despite the difficulties of a sediment-starved shelf and the limited data on the eastern Coastal Plain, some innovative results can be presented.
Scattered tidal-flat deposits and coastal barriers have been recognised before within certain sandbanks on the BCS (Maréchal and Henriet 1983, 1986). In this new study, the entire Holocene barrier system, consisting of remnants of back-barrier tidal-flat deposits and storm-generated sand ridges moulded in the transgressive sand sheet left after barrier retreat, has been mapped. More importantly, former coastline (barrier) positions have been reconstructed and are presented in paleo-reconstructions.

A first step has been taken in linking the Holocene evolution of the entire Belgian coastline with the evolutionary history of the western Coastal Plain (Baeteman 1999, 2004, 2005ab, Baeteman and Declercq 2002). Holocene geological and archaeological reconstructions of Zeeland (The Netherlands) (Vos and van Heeringen 1997) and historical coastline reconstructions of the Western Scheldt area (Coornaert 1989, Augustyn 1995, Termote 2006) have also been taken into account. This integration of offshore and onland information has contributed to a better understanding of the onland evolution. The proposed stabilisation of the coastal barrier around 5000 cal BP, a new hypothesis, must now be confirmed by independent evidence and absolute dates.

A new insight comes from the coastline reconstructions of 8000 and 7500 cal BP, which suggest that the barrier in the east did not stop retreating before the barrier in the west. Such a diachronicity had always been expected in light of the presence of a Pleistocene high in the subsurface of the eastern offshore area (Baeteman 2007b, Denys 2007, Fettweis et al. 2007). In the eastern present offshore area, the Pleistocene high has not been found. It is more likely that the entire coastline retreated constantly over its entire length, and stopped simultaneously when sediment supply became sufficient to compensate accommodation space created by decelerating sea-level rise. The accommodation space in the western part was not much larger, and the barrier there did not retreat much faster than its eastern part. The barrier retreated parallel to its original position, maintaining an overall straight coastline, but at an angle to the present-day coastline, causing the seemingly more landward position of the barrier in the western

coastal plain. The orientation of the initial barrier was determined by the strike of the pre-transgressive surface.

In the framework of several projects (a.o. MOCHA: Mud Origin, Characterisation and Human activities; Fettweis et al. 2007) mud deposits and high concentrations of suspended particulate matter between Oostende and the Western Scheldt estuary have been intensively investigated. The origin of the mud and the human impact on its distribution and transport have received particular attention. This mud corresponds to seismic unit U6. Hence, the interpretation of U6 and the supposed timeframe provide an important new context to these projects.

7.4.3 Recommendations

Again, on a sediment-starved shelf it is important to aim for a pseudo-3D seismic study, in order to be able to trace and interpret the strongly reworked deposits. Extra attention should be paid to the transition between sea and land, in shallow water where no seismic data have been collected to date. Unfortunately, the data can be overprinted by the presence of a shallow seafloor multiple or by blanking caused by shallow gas.
Additional core data are needed to help explain the abrupt transition from a Pleistocene high in the present-day onshore area to a near absence of Pleistocene deposits in the present offshore area. New cores must be collected at locations where the seismic data suggest the presence of important units or boundaries.
Future work will have to focus strongly on the integration of data from offshore and various onshore regions. The evolution of the coastal plain, for example, is an essential element in reconstructing paleo-coastlines because back-barrier development and river behaviour are important governing factors in coastline change. These factors result in differentiation of coastal behaviour in regions where relative sea-level change is identical. To explain the more extensive landward retreat of the eastern coastal barrier (from 2800 to 1200 cal BP) in comparison to that of the western barrier, more data in the eastern Coastal Plain are needed. The Pleistocene subsurface should be mapped in more detail, as well as the occurrence and depth of tidal channels and the potential thickness of the surface peat, as these are the determining factors for potential accommodation space, which in turn was a factor governing shoreface retreat.
For the moment, the explanations for shoreface retreat and progradation of the Belgian coastline are sought in the processes on the nearby BCS and in sediment supply or demand from the BCS and the adjacent Coastal Plain. Of course, processes are not bounded by country borders, so more attempts should be made to correlate and compare the Quaternary evolution of the BCS with that of the French and Dutch shelves and coastal zones.
A good exercise that is recommended for future investigations, is calculating volumes of seismic units and checking whether or not certain structures can be completely built up of locally available sediment alone (e.g. the storm-generated sand ridges). Another useful exercise is calculating the volume of sediment that disappeared with the drowning of the island Wulpen and the subsequent tidal erosion until a new hydrodynamic equilibrium was reached. Such a calculation is needed to find out how much of the eroded sediment settled to form U6, and how much disappeared to the Dutch shelf or was transported to the west to form the Coastal Banks and other bedforms (cf. Chapter 8).

7.5 Conclusion

When sea-level started rising after the Last Glacial Maximum, a tidal-flat environment developed at the borders of the receding coastline. Around 9500 cal BP, the Southern Bight was wide enough to produce waves at its eastern coastlines, so that barriers formed, behind which tidal basins developed. Sand to fill the basins was derived from the shoreface adjacent to the tidal inlets and from the ebb-tidal deltas. As insufficient sediment was supplied to the shoreface by cross-shore transport to compensate for this sediment loss, the shoreline was forced to recede, while eroding the underlying deposits and previous back-barrier sediments. Evidence of this erosion is found at the top of seismic unit U4 in the form of a gravel lag. Remnants of the back-barrier deposits seaward of the barrier ended up in a marine position, while in the back-barrier area, tidal flats continued developing. In the west, the back-barrier deposits of U4 were completely removed down to the shallow-located Pleistocene subsurface. Also in the most offshore parts of the BCS, no U4 tidal-flat deposits have been preserved, indicating that the initial Holocene sea-level rise was associated with intense erosion, which might have caused also the complete removal of former Eemian marine sands.

Where tidal inlets were present in the coastal barrier, sand ridges were formed from redistributed ebb-tidal-delta sediments, while in the areas in between, sand ridges were formed in the 'sawdust' left by the shoreface retreat, i.e. in the marine transgressive sand sheet. The ridges of seismic unit U5 have diverse origins but were probably in most cases initiated in response to storm currents on the shoreface and adjacent shelf. This involved scour and down-cutting in the troughs, eroding the underlying deposits of U4, with simultaneous aggradation of the ridge crests. The formation of the sand ridges is locally an erosional rather than a constructional response to the hydraulic regime, as is clear from the coarse-grained shell lag at the base of U5, and the sometimes deep imprints of U5 in the surface of U4.
Three sand ridges were formed. The outer ridge probably started developing around 8400 cal BP, based on the position of the reconstructed coastlines of 9500 and 8000 cal BP, and reached its present-day preserved elevation around 7700 cal BP. The middle ridge started developing around 8000 cal BP and reached its present-day preserved elevation around 7000 cal BP. The central and western part of the nearshore ridge were too severely eroded to deduce any final age for it, but based on its position it probably started forming around 7500 cal BP, which is when the barrier stabilised.

Until 7500 cal BP, the barrier retreated more or less parallel with its former position, keeping a straight coastline, but with an angle to the present-day coastline. This caused the seemingly more landward position of the barrier in the western Coastal Plain. The orientation of the initial barrier is in the first place determined by the strike direction of the pre-transgressive surface. The barrier in the west did not retreat faster or over a larger distance than the barrier in the east. Also, the barrier in the east did not stop retreating before the barrier in the west because of a high-elevated Pleistocene headland, although this was previously proposed based on the more landward position (i.e. with respect to the present-day coastline) of the coastline in the west around 7500 cal BP, and the presence of a barrier complex in the western Coastal Plain, in contrast to the complete absence of a barrier complex in the eastern Coastal Plain.

A decrease in the rate of relative sea-level rise around 7500 cal BP resulted in a sand surplus and consequently in the silting up of the tidal basins and the onset of stabilisation of the coastal barrier. Between 6800 and 6000 cal BP, the relative sea-level rise lost its driving force, sediment supply exceeded the accommodation space created by the relative sea-level rise, and induced the western and eastern parts of the coastal barrier

to prograde. A barrier complex formed with seaward migrating tidal inlets and channels, the remnants of which are still present in the present-day western Coastal Plain.

The barrier in the western part built out over 4.5 km, until it stabilised again around 5000 cal BP, just offshore the present-day coastline. A stabilisation was inferred because the top of the outbuilding barrier remained at about -7 m, which corresponds to the lower shoreface of 5000 cal BP. After that, the infilling ebb-tidal-delta sediments were redistributed and built up to -6 m, which corresponds to the supposed depositional depth at 2800 cal BP (when MSL was +1 m), when the barrier started receding again. As the top surface shows no clear evidence of erosion, the origin of the growth stop has to be sought in sediment deficiency, making it impossible for the barrier to build out further seaward.
Due to the slowdown in relative sea-level rise, the tidal channels got infilled and fell out of use, so surface peat started developing. Because of the upsilting of the tidal channels, ebb-tidal deltas became inactive, and got redistributed, forming tidal-inlet infillings and the western part of the nearshore sand ridge. Due to this redistribution, the shoreline got locally lined up again, and the longshore current could not be trapped anymore for the supply of sediments required for the further build out of the barrier between 5000 and 2800 cal BP. Another possibility for the sediment deficiency is that the offshore sediment supply was simply exhausted due to the barrier progradation. From 7000 cal BP onwards, when the shoreward net sand-transport pattern changed to a pattern of along-shore transport, a sand divergence zone developed between Zeeland and Britain. The sediment transport along the Belgian coast reversed, causing the sand supply to the coast to decrease. This was enhanced by a decrease in the suspension of sand by wind waves as the sea became deeper. As only 1-10% of the sediment needed for the supply of a migrating barrier is extracted from the along-shore littoral drift, the diminishing of the *shoreward* sand supply must have had a large impact on the barrier development. Initially, this decrease in sand supply must have been slow enough compared with the decrease in sea-level rise to cause a temporary sand surplus (and consequently initial barrier stabilisation and even progradation), but this sand surplus soon decayed to a slight deficit as the decrease in supply and the rise in sea level continued, initiating stabilisation again around 5000 cal BP.
The central part of the barrier prograded only about 500 m in the period between the stabilisation of 7500 cal BP and the renewed barrier retreat of 2800 cal BP. The eastern section of the coastal barrier prograded about 6.5 km offshore Zeebrugge, eroding a large part of the former nearshore storm-generated sand ridges. In the centre, the sediment supply did not exceed the accommodation space created by the relative sea-level rise, but reached an equilibrium which made the barrier remain in a more or less stable position between 6800 and 5000 cal BP. Only a smaller sediment availability at the central shoreface, compared to the western and eastern barrier, could explain this difference in barrier migration. The changing net sand-transport pattern since 7000 cal BP might have influenced the sediment supply. Additionally, the formation of the middle and nearshore storm-generated sand ridges and the development of tidal sandbanks since 7000 cal BP (cf. Chapter 8), might have influenced the local hydrogeography (i.e. deviation of tidal and storm currents) and might have caused the differences in progradation along the coastline. Also the presence of tidal channels and related ebb deltas in the west, still intact at the onset of the barrier progradation around 6800 cal BP, might have caused the stabilisation in the central, downdrift, section of the coastline.

After the stable period since 5000 cal BP, a tidal system was once more installed in the back-barrier area, starting between 2800 and 2400 cal BP. Re-entrance of the tidal system was probably induced by the cleaning of older channels due to an increased rainfall and excessive run-off from the continent, related to a climatic change around 2800 cal BP and human activity. Due to compaction of the peat and collapse of the channel banks, a lowering of the ground level occurred, which induced an increase of the

tidal prism of the tidal channels and consequently, deep vertical incision. Because a large sediment supply was needed to fill these channels, and because the offshore sediment source was probably nearly exhausted due to the previous barrier progradation, the barrier was forced to recede. The eroded sediments were used to fill the channels, so most likely only small ebb-tidal deltas were formed. Possibly, a thin layer of eroded back-barrier deposits, i.e. 'sawdust' after barrier retreat, settled in the offshore area below the lower shoreface on the shoreface erosional surface, and in a deep elongated barrier-parallel depression, in front of the barrier (part of seismic unit U6). In contrast to the initial barrier retreat (9500-7500 cal BP), where it was the fast relative sea-level rise that forced the barrier to recede, the barrier retreat was now forced by sediment deficiency, as relative sea level rose only mildly. The sediment deficiency was now caused by an increased accommodation space, i.e. a sediment demand from the back-barrier, in contrast to the stabilisation around 5000 cal BP, when the sediment deficiency was caused by a reduced sediment supply towards the coast.

In the western section, the barrier retreated over a distance of only about 1 km up to the present-day coastline. In the central part, between Westende and Middelkerke, the barrier did not retreat since its former position at 5000-2800 cal BP. Further eastwards, the barrier retreated progressively from 1 km to more than 5.5 km. As the rate of relative sea-level rise is constant along the coastline, these dissimilarities have to be sought in the differences in sediment supply towards the barrier shoreface and differences in sediment need (accommodation space) of the back-barrier.
As the barrier retreat is stimulated by the infilling of deeply incised late-Holocene tidal channels, the difference in barrier retreat between the eastern and western section might be sought in a difference in size and/or number of tidal channels, or the time the tidal channels were open in both areas.
As the natural compaction of the surface peat covering the back-barrier area induces an increase in accommodation space, i.e. an increase in tidal prism, it induces the sediment need for the particular area. So, the surface area of the back-barrier region might be an indication for the potential accommodation space created between 2800 and 1200 cal BP, and the consequently needed sediment supply (which induced the barrier retreat). Note, however, that in this reasoning the thickness of the surface peat is not taken into account. Thin peat layers, e.g. where the Pleistocene substrate lies high, will create less accommodation space. Neither the presence of tidal channels is taken into account. The potential for the surface peat to incline, depends largely on the presence of nearby channels which cause the drainage and consequent compaction of the peat. Apart from the location of some large tidal channels in the eastern plain, little is known about the smaller channel networks.
Possibly, also a factor of differential sediment supply should be taken into account as was suggested by Denys (2007). Before 7500 cal BP, the barrier migrated constantly over its entire length and formed a straight line. But since 5000 cal BP (and not since the early Holocene as was suggested by Denys 2007), the eastern plain protruded a few kilometres further seaward than the central plain, and formed a kind of 'headland' (Fig. 7.49A). According to Denys (2007) this 'headland' could have intercepted the along-shore net sediment transport which was oriented NE-ward, causing a larger sediment deficiency in the east compared to the west, inducing the eastern barrier to retreat further landward.
Around 1200 cal BP (750 AD), when the barrier stabilised, the coastline had developed towards a straight line once more. With the disappearance of the 'headland', the longshore sediment drift was no longer intercepted and possibly the available sediment surplus could be used to build a wide chain of dunes.
Between 1400 and 1200 cal BP (550-750 AD) sediment supply and tidal prism reached equilibrium with the sea-level rise and the tidal channels came in intertidal position. The back-barrier area evolved again in a supra-tidal environment, and because almost no sediment was needed anymore for the further infilling of remaining tidal channels, the

barrier retreat slowed down or even stopped. The coastline had developed towards a straight line once more. With the disappearance of the 'headland', the longshore sediment drift was no longer intercepted and possibly the available sediment surplus was used to build a wide chain of dunes. Except for the western part, the coastal barrier had not yet retreated up to the present-day position at that time. In the central section, the city of Oostende was still positioned offshore the present-day coastline, and in the west, several islands existed where now the mouth of the Western Scheldt is.

The second phase of barrier retreat, up to the present-day coastline, was a consequence of human intervention. The mismanagement of dikes and embankments, harbour construction and the almost total conversion of the dunes from a natural landscape into a man-made landscape, led to a slow but irreversible degradation of the dunes from the 12th century onwards. Violent north-westerly storms got a grip on the dune landscape and accelerated the degradation of the dune landscape until, by the late 14th/early 15th century, little more was left but small unstable drift-sand dunes. Until eventually, in 1404, a north-westerly storm almost completely destroyed this chain of dunes, leaving only the small stretch of dunes in the western Coastal Plain. During this storm surge the large isle of Wulpen, completely submerged in the sea, which caused irreversible hydrographic changes in the mouth of the Western Scheldt.
Tidal currents increased in the estuary mouth and its seaward extent, which caused further deep erosion in the area offshore Zeebrugge, until an equilibrium surface was reached. Shallow back-barrier remnants of the natural and storm-induced shoreface retreat were completely removed, such as large parts of the former deposits of U5, leaving only unrecognisable lenses of the eastern nearshore storm-generated sand ridge. After that, at least after the middle of the 16th century, the eroded muddy sediments (of former back-barrier deposits) settled, alternated with sandy storm layers, i.e. seismic unit U6.
The destruction of the dune complex, mismanagement of dikes, and lowering of the back-barrier area due to drainage for land reclamation, determined how far inland the land was flooded during storm surges. After the flooding the tidal currents took over the area if it was not reclaimed by man again.

In the western part of the Coastal Plain, the present-day coastline was possibly already reached during the initial, natural barrier retreat, as it was the only section of the coastline where the chain of dunes was not destroyed during the storm of 1404 AD. In the central plain, between Westende and Middelkerke, the barrier stayed in a more or less stable position after the minor progradation since 6800 cal BP. Between Middelkerke and Oostende, the barrier prograded since 6800 cal BP, and retreated about 500-1000 m since 2800 cal BP. Oostende was still located offshore the present coastline until at least the Early Middle Ages (9th-10th century). During the storms in the 14th/15th century, the coastline retreated again about 1.5 km, so that by the 16th century, the old town of Oostende was almost completely drowned, and the present coastline was almost reached. In the east, after the initial, natural retreat of 5.5 km, the barrier receded another 10 km. Most land was lost to the sea in the Western Scheldt estuary, because there the NW storm swept across the land from two sides because the island was surrounded by two large channels, i.e. the Zwin, and the Western Scheldt. The Western Scheldt existed since the progressively eastward migrating tidal channel 'Honte' connected the Scheldt with the North Sea.

From the lithology and the seismic data it is clear that some intensive erosive phases occurred between the Eemian marine transgression, after the final infilling of the Ostend Valley (U3), and the deposition of U6. Two main erosional phases can be distinguished on a region scale: the Holocene marine transgression, and an intense erosive phase, which removed large parts of U5 and U4 offshore Zeebrugge, before deposition of U6.

But on a local scale, there is also the impact of erosive storm-generated sand ridges (U5).
An erosional contact between units, and its associated coarse-grained (gravel) lag, can be related to multiple erosive phases in time. Nevertheless, gravel lags deposited in a different time frame or under different circumstances (fluvial incision, marine transgression, tidal scouring) can be lithologically quite similar because of the lithology and composition of the underlying unit. Also the inverse is true, gravel lags in different cores, deposited during the same erosive phase, do not have necessarily the same lithology, because of the different lithology (availability of gravel) of the underlying unit.

8.
Holocene tidal sandbanks

Seismic unit U7 is the uppermost and final unit. It consists of bank-like structures and thin sand sheets in the adjacent troughs. The unit makes up the top part of the most prominent features on the present-day seafloor: i.e. ‘sandbanks’ and swales. An overview is given of the many different theories that exist on the origin of sandbanks, and their formation and maintenance mechanisms. A summary of the prevailing hydrodynamic processes, however, would be too far-reaching for this thesis.

8.1 Introduction: the present BCS, a tide-dominated shelf

The North Sea is a typical, tide-dominated shelf (Dalrymple 1992). Tide-dominated shelves are distinguished by the presence of tidal currents with velocities ranging from about 50 to 150 cm/s (Dalrymple 1992, Boggs 1995), and are characterised by mesotidal or macrotidal ranges (Davis 1992). The major influence of a large tidal range is, however, not to cause appreciably faster currents, but to increase the area that experiences strong tidal influence (Dalrymple 1992). Such conditions give rise to considerable sediment transport over extensive periods of time and in a regular cyclic fashion. The North Sea is also subject to intense storm wave energy. Nevertheless, the tides exert a stronger influence on sediment transport and patterns than the storm waves (Davis 1992). Tide-dominated shelves are characterised particularly by the presence of sand bodies of various types and dimensions.

8.1.1 Morphological distinction between various types of sand bodies (sand dunes, tidal ridges and shoreface-connected ridges) on a tide-dominated shelf

The most striking features on tide-dominated shelves are large, long ridges of sand. These have originally been described in detail by Off (1963), who called them tidal ridges (Davis 1992). Tidal sand ridges or tidal sandbanks (no distinction is made here) are high-relief bar macroforms that are nearly parallel to the flow, although always oriented at a small angle (< 20°) with respect to the prevailing flow as required by the Huthnance stability model (Huthnance 1982a). Their formation requires large volumes of sand and *surface* tidal current velocities exceeding 50 cm/s (Galloway and Hobday 1996). According to Belderson (1986), however, tidal sandbanks are associated with mean spring *near-surface* peak tidal currents of 90 cm/s or more, corresponding to a *near-bottom* velocity of about 55 cm/s in water 30 m deep. According to Davis (1992) and Dalrymple (1992) tidal sand ridges require maximum current velocities exceeding 100 cm/s (not distinguishing between surface or bottom speed) to maintain themselves. In areas with lower current velocity, sand ridges do not form and the dominant bedforms are sand waves (Swift 1976). Finally, Dyer and Huntley (1999) mention the 50 cm/s lower limit (not distinguishing between surface or bottom velocity either), and the necessary presence of sand for the formation of sand ridges

The modal amplitude of tidal ridges is typically 10-15 m, according to Galloway and Hobday (1996) or 20-30 m, according to Belderson (1986), but tidal sand ridges up to 40 m high (43 m, according to Belderson (1986) and van de Meene and van Rijn (2000)), 5 km wide and 60 km long have been reported on the North Sea shelf (Boggs 1995). According to Dyer and Huntley (1999), tidal sandbanks can be up to 80 km long, 13 km wide and are tens of metres high. They are asymmetrical in cross section, having slopes of about 6° on the steeper side, and less than 1° on the gentler side (Dyer and Huntley 1999). Like sand dunes, tidal ridges occur in swarms with regular spacing ranging up to several kilometres (Galloway and Hobday 1996). Typical spacings range between 2 and 30 km (Belderson 1986, Dalrymple 1992, van de Meene and van Rijn 2000).

The present, tide-dominated shelf systems include both active and moribund examples. Ridges can become moribund –or 'inactive'- due to increasing water depth or due to an altered current regime. They become increasingly symmetrical, with low-angle beds draping the ridge flanks (Galloway and Hobday 1996), and display a rather featureless surface (Dalrymple 1992, Davis 1992). Active ridges can be recognised by the presence of extensive, apparently mobile bedforms on the surface. The migration of large bedforms contributes to the development of foreset stratification and indicates that large volumes of sediment are being transported (Davis 1992). Under those circumstances in which tidal currents decrease in strength, such as occurs during a rising sea level, the ability of these currents to produce large bedforms and transport large volumes of sediment is gradually lost.

Less prominent features are sand waves or sand dunes (Ashley 1990). They are flow-transverse structures with asymmetrical shapes, a few metres to more than 20 m in height and with wave lengths of tens to hundreds of metres, and typically occur in fields on a tide-dominated shelf (Boggs 1995). Sand waves occur also on the surface of active sand ridges and in the interridge swales. The sand wave asymmetry is generally oriented differently on either side of the ridge as a result of the differences in dominance between the ebb and flood currents. This typical sand wave orientation on either side of the sand ridges implies that there is a convergence of sand at the crest of the bank (Caston 1972 In: Dalrymple 1992, Galloway and Hobday 1996, Dyer and Huntley 1999).

In addition to sand dunes, ridges and ribbons, tide dominated shelves may also comprise sand sheets, sand patches and gravel sheets, characterised by small-scale bedforms and patches of bioturbated muds in areas sheltered form tidal currents and waves (Boggs 1995). The association of sandbanks with such strong currents implies that, in the absence of sufficient sand to construct tidal sandbanks, a gravel sheet or scoured pavement should exist in the place of sandbanks, rather than a sand sheet. Such a gravelly floor usually occurs in the troughs between active sandbanks (Belderson 1986). Ridges migrate onto the swales, thus they commonly overlie an erosion surface or hardground and basal lag (Galloway and Hobday 1996).

In the nearshore area on the BCS, bank structures (i.e. the Coastal Banks) have been observed that are smaller than the average tidal sand ridges. They, in fact, show more resemblance to the storm-generated shoreface-attached ridges of a storm-dominated shelf. Most likely the nearshore area of the BCS has a mixed storm-tide regime. Although shoreface-connected ridges have been considered a special class of storm-generated ridges, shoreface-connected ridges along the Dutch coast are found in a setting where tidal currents and storms are both important. This suggests that a storm-dominated setting is not essential for the formation of shoreface-connected ridges (van de Meene and van Rijn 2000).
There are significant morphological differences between active tide-dominated sandbanks and storm-dominated/shoreface-connected sand ridges (Belderson 1986, van de Meene and van Rijn 2000). The orientation of the tidal sandbanks is related primarily to the peak tidal current direction, while the orientation of the storm sand ridges is related primarily to the orientation of the coastline. According to Swift et al. (1991) on the other hand, storm-built/shoreface-connected ridges are typically oriented obliquely with respect to the prevailing flow, like tidal ridges. Shoreface-connected ridges are typically 5 to 10 m high, smooth crested, spaced 2-5 km apart, with side slopes that rarely exceed more than 1°, and with crestlines that can extend for tens of kilometres (Galloway and Hobday 1996, Dyer and Huntley 1999, van de Meene and van Rijn 2000). Tidal sandbanks are thus generally higher than storm sand ridges or shoreface-connected ridges, they may be steeper and they generally have sharper crests. Tidal sandbanks have larger spacings than storm ridges and they are generally longer. Typical spacings range between 0.5 and 7 km for storm sand ridges (Belderson 1986, van de Meene and van Rijn 2000).
According to Belderson (1986) there is no general continuum between the strongly tidally influenced (plus storm-affected) sandbank bed forms and the storm-dominated (weakly tidally influenced) sand ridges. Instead, in areas of intermediate surface peak tidal currents (i.e. 50-90 cm/s, equivalent to 30-55 cm/s at 1 m from the seafloor in water 30 m deep) there is an interval occupied by fields of sand waves (i.e. the offshore tidal sand sheet). The author sees this as an argument that tidal sandbanks and storm-generated sand ridges have different origins.

8.1.2 Classification and origin of sand ridges

Descriptive classifications and theories about the formation of sandbanks

As sandbanks are the most prominent features on the present-day seabed, a lot of studies have been carried out to describe and understand their morphology, processes of formation, growth and maintenance, and how they interact with the coastline. This resulted in many different theories from various points of view. A number of different types of banks have been defined in terms of their location and morphology (e.g. in embayments, on the open shelf or at the lee side of headlands (Swift 1985, Swift 1975 in: Dyer and Huntley 1999)). Sometimes a distinction was made on the basis of the dominant hydrodynamic force (e.g. tide- or storm-built banks (Amos and King 1984)), the sediment source (e.g. seabed or coastline (Swift 1985)), the bank orientation (Pattiaratchi and Collins 1987), or their origin and maintenance.

The above-mentioned descriptive distinction between tidal sandbanks, sand dunes and shoreface-connected ridges is only an initial approach, that can be made when only the outer dimensions of the ridges are known (e.g. from bathymetric charts, single-beam, multibeam or echosounder data). However, when also seismic and core data are available, revealing the internal structure of the ridges, also the long-term evolution and regional setting can be unravelled, making it possible to categorise the sandbanks following a more sophisticated classification, which takes into account not only the morphology, but also the formation mechanisms, origin, evolution and setting of the ridges (e.g. the classification of Dyer and Huntley (1999)).
Dyer and Huntley (1999) developed a descriptive classification scheme to unify all the different approaches of marine geologists and physical oceanographers, which emphasises the formation and present hydrodynamic setting in their long-term development. They consider regional topographical and dominant hydrographical forces, the sediment source and the strength of coastline retreat. The resulting classification proposes a generic relationship between banks in the light of their origin and development (Dyer and Huntley 1999). They identify open-shelf ridges (Type 1), linear ridges formed in mouths of wide estuaries (Type 2A) (called tidal sand bars by Dalrymple 1992, cf. Chapter 6), banks formed close to the mouth of narrow-mouthed estuaries as ebb and flood deltas (Type 2B (i)), shoreface-connected ridges formed from similar ebb and flood deltas but at a retreating coastline (Type 2B (ii)) (they are also called shoreface-attached ridges, shoreface-detached ridges, storm-generated ridges or linear shoals; Dyer and Huntley 1999), banner banks at headlands (Type 3A), and, when the headland is retreating, alternating or 'en-echelon' ridges can be formed (Type 3B). Banner banks may become alternating ridges given time and further headland retreat, and finally approach Type 1 open-shelf ridges. Most types appear to have moribund as well as active types.
Open-shelf ridges (Type 1) can be created in three ways (Dyer and Huntley 1999): (1) ridges are created by an excess of sand supply, with their growth depending on a greater supply being added to the head than being lost from the tail; (2) ridges are remnants of a larger deposit which is being whittled away by selective transport; or (3) they are an expression of an equilibrium with the ridges maintained within an active sand transport path. Some ridges appear to have a relict core of material that may be the remnant of transgressive conditions (Houbolt 1968, Berné et al. 1994).
Groups of linear en-echelon or V- or S-shaped alternating ridges (Type 3B) have also been called shoal-retreat massifs. At present there are two theories for the origin of en-echelon ridges, and it is possible that shoreface-connected ridges form by similar processes (Swift et al. 1991, Dyer and Huntley 1999). The theories are based on: (1) shoreline retreat, and (2) ridge multiplication (Caston 1972). In many ways these two are related, since the source of the sand requires shoreline retreat, and the multiplication of the sandbanks implies an offshore movement and modification of the outermost bank,

which is aided by retreat of the shoreline (Dyer and Huntley 1999). The multiplication theory, however, does not account for the initial generation of the banks, but may explain part of the adjustment of the banks to the offshore hydrodynamic regime (Dyer and Huntley 1999).

Also Berné et al. (1994) proposed a descriptive classification on the basis of an initial classification and observations of Houbolt (1968). Berné et al. (1994) discern two types of tidal sandbanks and link the internal structure of the bank (i.e. the presence of an internal core or rather a flat base) with a formation mechanism. The two types comprise:

(1) banks formed by sand accumulation only, resting on an essentially flat surface and showing no internal core. Those banks consist entirely of Holocene deposits (late Holocene in case of active sandbanks).
(2) banks with an internal core, which consists of eroded fluvial or estuarine sediments of early Holocene or Pleistocene age, or of erosional bedrock morphology. The banks are partly formed by erosion of older deposits and are not shaped by accumulation only.

Quantitative theories about the formation of sandbanks

Some theories for sandbank formation and maintenance involve quantitative predictions of sandbank characteristics, instead of the above-presented essentially descriptive ideas on their formation. An overview of both the descriptive and quantitative (modelling) theories on the formation of sandbanks, as well as a summary of classifications is given in Dyer and Huntley (1999). Pattiaratchi and Collins (1987) provide a chronologic overview of the different theories and models on sandbank formation.
According to Dyer and Huntley (1999), the existing mathematical models to explain the existence of sandbanks fall into three generic types: (1) those based on secondary flows assumed to produce a convergence of sediment transport towards a sandbank crest; (2) those considering long period wave motion with length scales similar to sandbank scales; and (3) those based on stability analysis of the coupled hydrodynamic and morphodynamic system (Dyer and Huntley 1999). The latter type of theories would be very promising as an explanation for Type 1 open-shelf ridges, while the first one could be relevant for explaining the formation of Type 3A banner sandbanks at headlands. Long-period flows are unlikely to be relevant for sandbanks (Dyer and Huntley 1999). The first type of theories comprises helical flows (a.o. Houbolt 1968), phase lag between bed stress and bed topography, and headland eddies. The third type or seabed-stability theories, comprises theories considering the interacting system of water and sand (a.o. Huthnance 1982a, 1982b), the sand response being an integral part of the theory, instead of considering the sandbank the result of sand response to hydrodynamic effects, which is the case for the first and second type theories.

Summary

Theories for the origin and maintenance of sandbanks generally fall into two broad categories: (1) the sandbanks are relict features created during the post-glacial sea level rise, or (2) the sandbanks are formed as a response to hydrodynamic and sediment regimes that are similar to those presently active (Dyer and Huntley 1999, van de Meene and van Rijn 2000).
In the first category, the theories consider the regional setting in which the banks have developed. They are based on descriptive, geomorphological and geological field observations, and are usually lacking any theoretical or observational hydrodynamical basis. The origins depend on the source of sediment being mainly created by coastal retreat and coastal erosion.
Whereas in the second category, the shape of the sandbanks is considered in equilibrium with the present-day processes. These are mathematical models, using well-established sets of mathematical formulations, describing the evolution of the seabed as

a result of interactions between water motion, sediment transport and bed-level changes. The theories do not take into account recession of the coastline, and assume that the sediment source is the bank itself and the immediate surrounding seabed, which implies that the bank is more or less in the same position as when it formed.

Although many studies have focussed on the morphodynamic behaviour of sandbanks, there is no general consensus on the processes that may be responsible for their formation and their present-day maintenance (van de Meene and van Rijn 2000). It is apparent that there are several possible origins for sandbanks. It is also possible that banks may lose the characteristics of their origin once they are separated from the initial sediment source, and tend to converge towards equilibrium with the tidal hydrodynamics (Dyer and Huntley 1999, van de Meene and van Rijn 2000).

8.1.3 Distinction between a sand ridge or sandbank s.l. and a tidal sand ridge or tidal sandbank s.s.

One has to take care not to confuse the term 'sandbank', with the term 'tidal sandbank'. In common language, the term 'sandbank' (synonym of sand ridge) is merely used as a morphological term for describing an elevation, i.e. a ridge or bank-like structure, on the seafloor, e.g. on a bathymetric chart, of which at least the surficial sediments consist of sand. The bank-like structures on the BCS have been called in the past 'tidal sandbanks', implying that the entire bank structure was formed by strong tidal currents, accumulating sand in an open-shelf environment. Seismic data revealed, however, that in some cases only the top part of the bank structure had the characteristics of a tidal sandbank, while the base or internal core of the structure was composed of estuarine or tidal-flat deposits, deposited under very different hydrodynamic circumstances and potentially consisting of material different from sand.
In this chapter, all general bank structures (i.e. in the broad sense of an elevation from the present-day seafloor) will be referred to as 'sandbanks s.l.' (*sensu lato*), 'sandbanks', or 'sand ridges'. These terms do not hold a genetic connotation. All references to tidal sandbanks (i.e. in the strict sense of a sandbank structure formed by strong tidal currents in an open-shelf environment) will be made as 'sandbanks s.s.' (*sensu strictu*) or as 'tidal sandbanks' (using the prefix 'tidal'). Seismic unit U7 consists of tidal sandbank structures, gravely sand sheets in the interridge swales, and of nearshore shoreface-attached ridges or storm-dominated ridges. The unit is exposed at the seafloor and makes up the uppermost seismic unit in the sandbanks s.l.

8.1.4 Sandbanks on the Belgian Continental Shelf

On the Belgian Continental Shelf, four groups of sandbanks s.l. are classically distinguished, mainly on the basis of their orientation (Fig. 8.1).

(1) In the north, the Hinder Banks are more or less oriented in NNE-SSW direction. They consist of the Noordhinder, Westhinder, Oosthinder, Blighbank and Fairy Bank.
(2) In the west, the Zeeland Ridges are more or less oriented parallel to the present-day coastline in a more NE-SW direction. The group consists of the Thorntonbank, the 'Bank Zonder Naam' (BZN, 'Bank Without a Name') north of the Thorntonbank, the Gootebank and the Akkaertbank. These are, in fact, part of a larger group of sandbanks s.l. that covers also a part of the Dutch sector.
(3) The Flemish Banks occur further to the west, and are oriented at an angle between the Hinder Banks and Zeeland Ridges (closer to the Hinder Banks). They consist of the Oostdyck, Buiten Ratel, Kwintebank, Middelkerke Bank, Oostende Bank and Smalbank.

(4) The banks closest to the shore are the Coastal Banks, oriented parallel to the coastline with a NE-SW direction. The larger sandbanks of this group consist of the Nieuwpoort Bank, the Stroombank and Wenduinebank.

Only the top part of these banks s.l. consists of seismic unit U7, which comprises the deposits that are typical for a tidal sandbank s.s. or a shoreface-connected ridge. In some banks the underlying seismic units, however, also stand out from the seafloor due to additional erosion in the swales and form the base of the sandbank s.l.

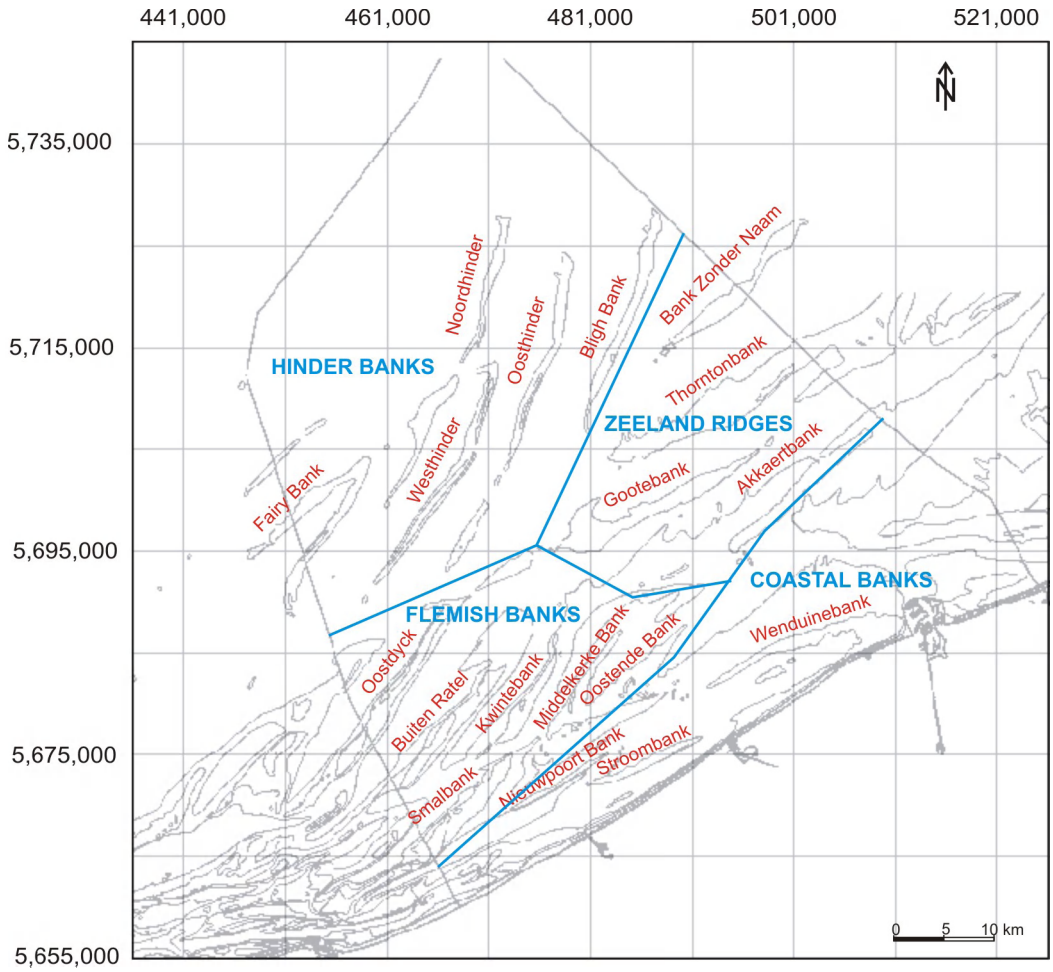

Fig. 8.1 Positioning of the sandbanks (s.l.) on the Belgian Continental Shelf. Four groups of sandbanks have been distinguished, mainly on the basis of their orientation: the Hinder Banks, the Zeeland Ridges, the Flemish Banks and the Coastal Banks.

Banks often store large quantities of the available sand on a shelf, and appear to be hydraulically maintained sand traps of a high order of efficiency. Since banks occur in areas with currents strong enough to move sand, there is the implication that there must be a circulation of sediment around the bank that ensures that it does not get more widely dispersed (Dyer and Huntley 1999). One fundamental process to create a regional sand accumulation appears to be the presence of mutually evasive ebb-flood channels. These cause a circulatory movement of sand over and around the bank, which helps to maintain quasi-stability. There is normally an asymmetry in the current strengths on either side of the banks with maximum currents being in the ebb direction on one side and in the flood direction on the other, causing sediment accumulation (Dalrymple 1992, Dyer and Huntley 1999). This is because sandbanks make a small angle with the tidal flow, which tends to make one side of the ridge more exposed to the flood flow, and the

other more exposed to the ebb, thus helping to produce flood and ebb dominance on alternate sides (Dyer and Huntley 1999). Also deformation of the tidal wave and interaction of the currents with the bottom topography produces inequalities between the flood and ebb currents. As a result, many areas experience a net or residual transport of sediment in the direction of the stronger (dominant) current (Dalrymple 1992).

Numerical model results of the hydrodynamics on the BCS show that the tidal current velocities (not distinguishing between surface and near bottom current velocities) reach their maximum value during flood (in NE direction) in the near coastal zone, along most of the Flemish Banks and Zeeland Ridges region (Fig. 6 in: Lanckneus et al. 2001) (schematically visualised in Fig. 8.2). The maximum current velocity along the Hinder Banks is in the ebb direction (in SW direction). In some of the swales of the Flemish Bank region, the maximum currents are also oriented to the SW. High currents of up to 160 cm/s are modelled in the Western Scheldt estuary mouth and are directed from SE to NW. High currents of up to 140 cm/s occur to the north of the BCS, towards the main channel (Channel Deep) of the Southern Bight of the North Sea (Lanckneus et al. 2001). The fact that current ellipses are highly rectilinear and that the currents are relatively strong in some of the near-coastal swales means that a considerable amount of sediment can be advected along the swales and can act as a source of material for the sandbanks (Lanckneus et al. 2001).

Results of a sediment transport model (Van den Eynde 2001, Fig. 11 in: Lanckneus et al. 2001) show that the sediment transport (total load) on the sandbanks is clockwise: to the NE on the W flank of the banks, and to the SW on the E flank of the banks. In de coastal zone (i.e. taken to be 20 km wide) the transport direction is towards the NE (Fig. 8.2), and in the Scheur towards the W. In open sea, north of the sandbanks, the sediment-transport direction is towards the SW.
A comprehensive study of the residual sediment transport directions on the basis of the asymmetry of bedforms (i.e. small, medium and large sand dunes, not sandbanks) provides more detail (Lanckneus et al. 2001).

The Flemish and Hinder Banks receive sand from both adjacent swales. The residual flood current from the SW commands the residual sand transport on the western flanks and the eastern part of the swale, while a residual ebb current from the NE is responsible for the sand transport on the eastern bank flank and the western part of the swale. So the residual sand transport is in clockwise direction, as predicted by the sediment transport model. As a result, sand is moving residually in each swale along two opposite directions. This causes an up-piling of sand on the bank summit.
The strongest tidal current (ebb or flood) tends to erode one flank of the bank maintaining the steep slope (Lanckneus et al. 2001). So, the steep side of the bank corresponds with the flank that is subdued to the highest current-topography interaction (Lanckneus et al. 2001). In the Hinder Banks region, where a clockwise sediment transport is valid (the western flank of a bank is flood-dominated and the eastern flank is ebb-dominated), the ebb-tidal current predominates, and the eastern flank is indeed steepest (Fig. 8.2). The same principle applies to the Flemish Banks. The steepest side is here the western flank, which corresponds to the flood-dominated flank, which is the strongest tidal current in the Flemish Banks region (Fig. 8.2).
However, in the Coastal Banks nearshore region, where also the flood current is generally strongest (Lanckneus et al. 2001), the steep slope occurs at the eastern side. So, if the strongest current tends to erode one flank of the bank maintaining the steep slope, as proposed by Lanckneus et al. (2001), the eastern flank should be flood-dominated and the western flank ebb-dominated, which would imply an anti-clockwise sand transport direction (Fig. 8.2). Van Lancker (1999) confirms that the strongest current is flood-directed and along the eastern steep side of the Nieuwpoort Bank and Stroombank. However, on the one hand the sediment sorting over the Nieuwpoort Bank

and Stroombank is clearly unidirectional toward the NE, so one can not speak of a clockwise or anti-clockwise sediment transport (Van Lancker 1999). And on the other hand, sediment transport has been observed from the flood channel east of the Nieuwpoort Bank towards the Stroombank, which *does* imply a clock-wise sediment transport (Van Lancker 1999).
In the Zeeland Ridges region, modelled maximal tidal currents are flood-dominated and the modelled sand transport direction (total load) is also directed towards the NE in this zone. However, on a regional scale, the outlined main bedload transport near the Gootebank is directed to the SW, and also on a large scale, large dunes just NE of the Flemish Banks are ebb-dominated (near the Zeeland Ridges). If the flood current is strongest in the Zeeland Ridges region, the sand transport direction would be anti-clockwise, as the steepest flank, supposedly maintained by the strongest current, is the eastern flank (Fig. 8.2).
This implies that the Coastal Banks and the Zeeland Ridges represent an anomalous situation in comparison to the rest of the banks on the BCS. Either the strongest current in the Zeeland Ridge area is not flood directed or the sand transport direction is anti-clockwise, or the steepest flanks of the sandbanks are not caused by the strongest tidal current and have a different origin.

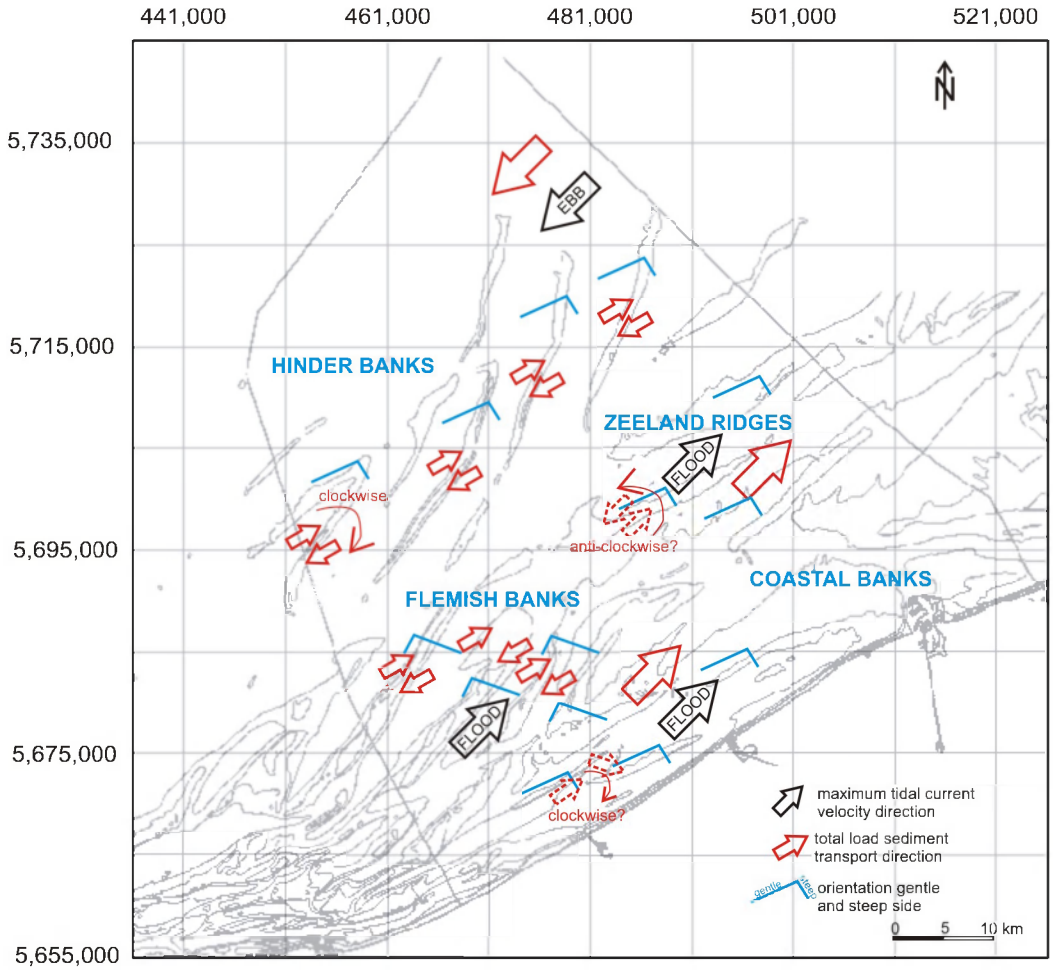

Fig. 8.2 Schematic visualisation of the maximum tidal current velocity direction, and the total sediment transport direction (data from Lanckneus et al. 2001). In the Hinder and Flemish Banks region, the strongest tidal current (ebb or flood) maintains the steep slope of the bank. In the Zeeland Ridges region, however, the modelled strongest tidal current (flood) does not correspond to the steep slope of the banks, presuming a clockwise sediment transport direction. So, either the sediment transport direction is anti-clockwise, or the strongest current in the Zeeland Ridges region is not flood directed. Or the steepest flanks of the Coastal Banks and Zeeland Ridges are not maintained by the strongest tidal current and have a different origin.

8.2 Observations

8.2.1 Seismic-stratigraphy

After the general seismic-stratigraphic description in Chapter 4, seismic unit U7 is described here in more detail. The complete (digital) seismic grid available on the BCS was applied to describe and discuss this unit. The boundaries of seismic unit U7 confine the area where the distance between the seafloor reflector and the underlying surface (composed of U4, U3 (and IVDB cf 5.3.1), and QT) is more than 1.5 m.

Seismic unit U7 is the uppermost seismic unit and covers almost the entire BCS, underlying most of the present-day bathymetry. Unit U7 consists mainly of bank forms, separated by sheet-like deposits in the swales in between the banks, and at the extremities of some banks. The bank structures of U7 make up the top section of the sandbanks s.l., which can be sub-divided into the Coastal Banks, the Flemish Banks, the Hinder Banks and the Zeeland Ridges on the basis of their orientation (Fig. 8.2). Note that elevations of reflectors below the sandbanks (s.l.) are real and not
due to 'velocity-effects (i.e. pull-ups)', as after time-to-depth conversion of the seismic profiles the elevations are still present. Nevertheless, on seismic profiles with a vertical scale in seconds TWT time, the elevations are slightly exaggerated.

External form of seismic unit U7

The Hinder Banks

In the north, the U7 structures of the Hinder Banks mostly have a landward-facing steep side, and an offshore-facing gentle side. An exception is U7 in the unnamed bank located to the NW of the Fairy Bank, which shows an offshore-facing steep side, similar to the SW extremity of the Westhinder. Contrarily, the NE extremities of U7 in the Noordhinder, Oosthinder and Bligh Bank, the SW extremities of the Oosthinder, the extension of the Noordhinder and the Fairy Bank all show symmetrical cross-sections (Fig. 8.3). The steep side of the banks can be either straight or convex, with an average slope angle of 2-4°. The gentle sides are characteristically 0.5-1°, and mostly convex upward. The banks s.s. are sharp-crested, and are often covered by sharp, 4-8 m high structures, interpreted as sand dunes (Lanckneus et al. 2001). These dunes can occur on the top, on the steep and on the gentle side (Fig. 8.3BCD). In most of the Hinder Banks, the quality of the seismic data was too poor to distinguish any internal reflectors in U7. In the Westhinder and Blighbank, however, parallel-oblique prograding reflectors are visible in U7, dipping with an angle of 0.5-1.9°, in the same direction as the steep side (landward).

Fig. 8.3 (A) (page 265) Overview map presenting the external morphology of the U7 tidal sandbanks of the Hinder Banks. The (vertical) cross-sectional outline of U7 is defined along every available seismic profile by the position of the steep and gentle side, if present. (B), (C), (D) Examples of seismic profiles showing the internal structure of the sandbanks s.l., and how the vertical cross-section of a tidal sandbank varies along its length.

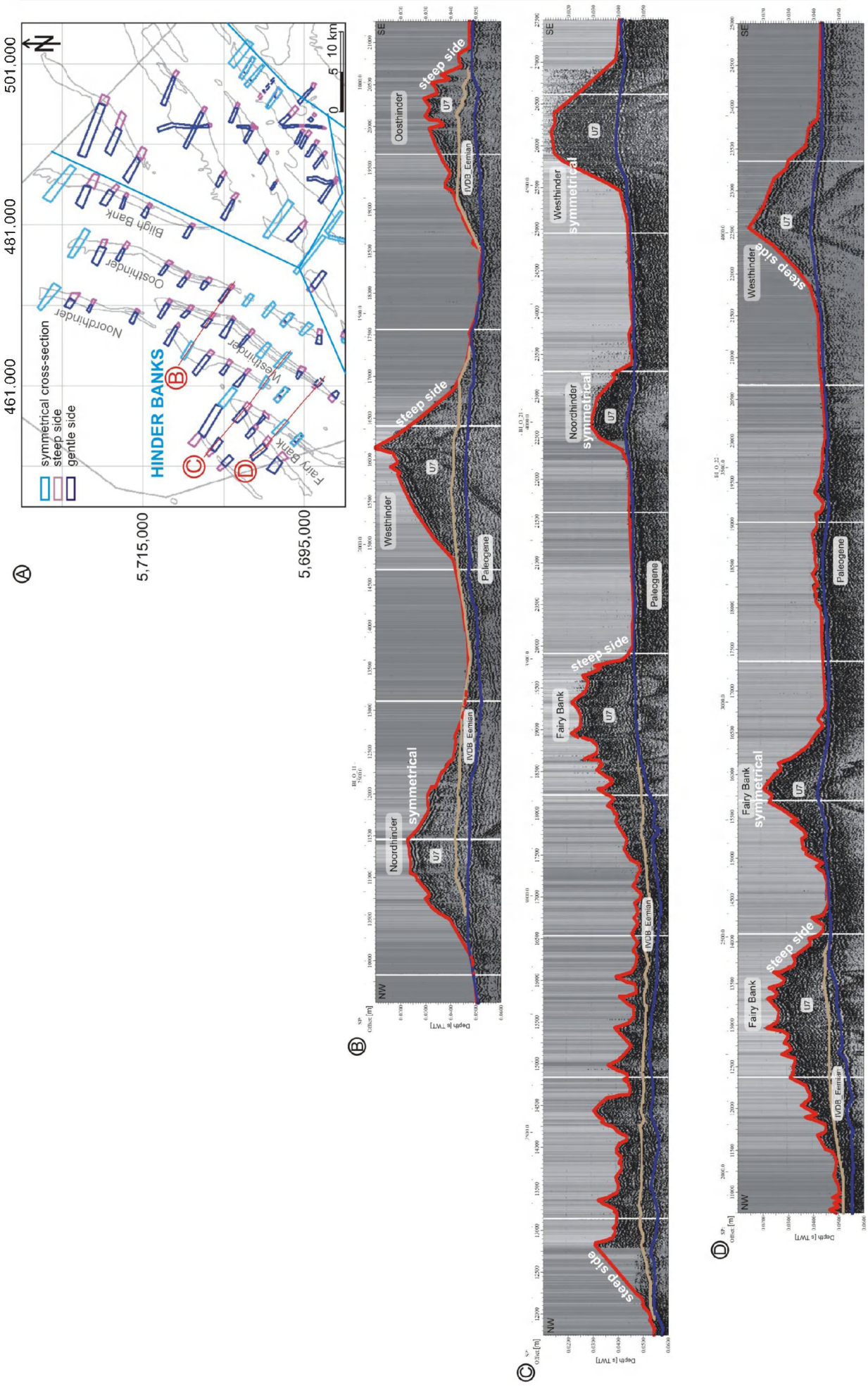
A
501,000
481,000
461,000
5,715,000
5,695,000
N
0 5 10 km
symmetrical cross-section
steep side
gentle side
HINDER BANKS
Bligh Bank
Oosthinder
Noordhinder
Westhinder
Fairy Bank
B
C
D
B
NW
SE
Noordhinder
symmetrical
Oosthinder
steep side
Westhinder
U7
IVD8_Eemian
Paleogene
C
NW
SE
Noordhinder
symmetrical
Westhinder
symmetrical
Fairy Bank
steep side
U7
IVD8_Eemian
Paleogene
D
NW
SE
Fairy Bank
symmetrical
steep side
Westhinder
steep side
U7
IVD8_Eemian
Paleogene

The Zeeland Ridges

Also the structures of U7 in the Zeeland Ridges, in the north-east, mostly have a landward-facing steep side, and an offshore-facing gentle side (Fig. 8.4). Exceptions are the SW extension of the Gootebank and the NE extremity of the Akkaertbank, in which U7 shows an offshore-facing steep side. Most of U7 in the Gootebank, and especially in the broad section of the structure, is not really characterised by a bank form, but instead consists of a series of sand dunes or a simple sand sheet (Fig. 8.4G). U7 in the Akkaertbank consists mainly of a rounded asymmetrical bank with landward-facing steep side and landward-dipping prograding internal reflectors. Toward the NE, this gradually evolves first into a sharp-crested bank form, then into a symmetrical bank with still landward-sloping internal reflectors, then into a bank with offshore-facing steep side and landward-sloping internal reflectors, and finally into a rounded, thin sand sheet, still with the same reflector configuration (Fig. 8.4G to B). U7 at the NE end of the Akkaertbank changes into the sheet-like structure of U7 on the Vlakte van de Raan. The slope of the steep side varies between 0.5-0.9° in the Akkaertbank, 0.7° in the 'Bank Zonder Naam', 1.3° in the Gootebank and 3.5° in the Thorntonbank. The slopes are mostly concave or straight. The slope of the mostly convex-upward or straight gentle side is 0.1-0.3°. Apart from the Thorntonbank, in the Zeeland Ridges the U7 structures are mostly more rounded than in the Hinder Banks, and mostly the gentle side and the top are covered by sharp, 2-4 m high sand dunes. Internal structures that could be distinguished in seismic unit U7 (especially in the Akkaertbank) comprise parallel-oblique landward-prograding reflectors with a dip angle of 0.5-2°.

The Flemish Banks

In contrast to the Hinder Banks and Zeeland Ridges, the U7 structures in the Flemish Banks have an offshore-facing steep side, and a landward-facing gentle side (Fig.8.5). An exception is the SW end of the Smalbank, in which U7 shows a landward-facing steep side, while the transition between the two shows a symmetrical cross-section (Fig. 8.5BCD). In the Smalbank, U7 changes from a broad bank with a straight, steep (5°) landward-facing side (adjacent to the deepest part of the Westdiep swale), a concave to convex, gentle (1.4°) side, and a more or less horizontal (0.075°) top section (Fig.8.5B), over a symmetrical broad bank with gentle sloping sides (1.2 and 1.6°) and horizontal top (Fig. 8.5C), to a more sharp-crested bank with a relative steep (1.15-1.2°), concave, offshore-sloping side and a gentle (0.13-0.9°) convex, landward-facing side (Fig. 8.5D). Internal reflectors could not be identified.
Also in the Kwintebank, U7 shows a symmetrical cross-section at its SW end (Fig. 8.5E). U7 in the Kwintebank changes from a bank with a straight to concave short and steep (2.7-3.4°), offshore-facing side and a straight to typically convex, long and gently sloping (0.4-0.6°) side in the NE (Fig. 8.5GHI), over a bank with a relative steep (1°), offshore-facing side, but which is convex and long, and a gentle (0.35°), landward-sloping side, which is long and concave at the SW kink in the Kwintebank (Fig. 8.5F). Further to the SW, the bank becomes symmetrical (Fig. 8.5E) and finally shows again a straight, short, steep, offshore-facing side and a convex, long, gentle sloping side, although the bank is more rounded and smaller at the SW extremity (Fig. 8.5D). Internal reflectors could not be identified.

Fig. 8.4 (page 267) (A) Overview map presenting the external morphology of the U7 tidal sandbanks of the Zeeland Ridges. The (vertical) cross-sectional outline of U7 is defined along every available seismic profile by the position of the steep and gentle side, if present. (B) to (G) Examples of seismic profiles showing the internal structure of the sandbanks s.l., and how the vertical cross-section of a tidal sandbank varies along its length.

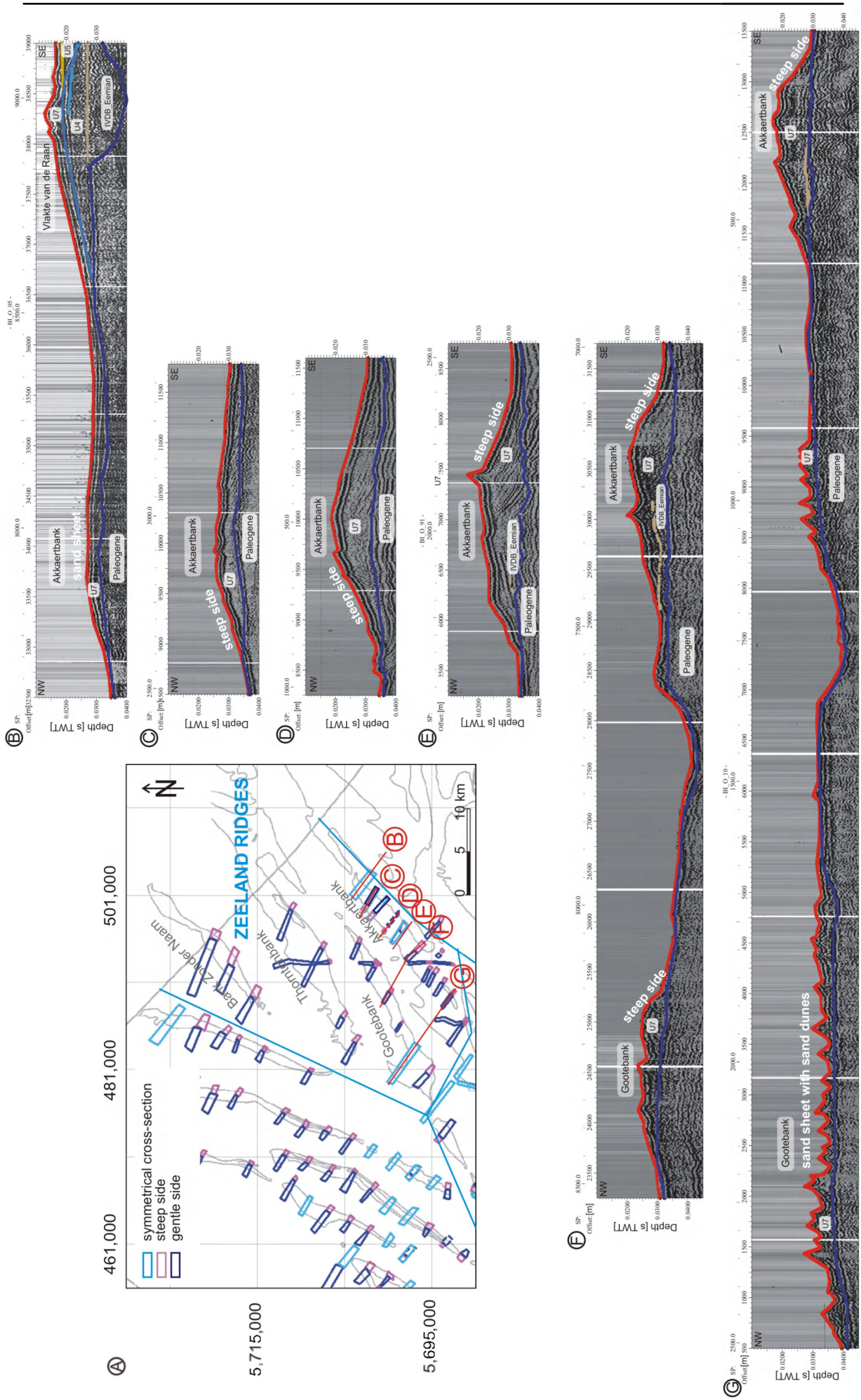
A
461,000
481,000
501,000
5,715,000
5,695,000
N
0
5
10 km
ZEELAND RIDGES
symmetrical cross-section
steep side
gentle side
Akkaertbank
Goodebank
Thornton bank
Bank Zuider Noam
B
C
D
E
F
G
Vlakte van de Raan
sand sheet
Akkaertbank
Paleogene
U7
U5
U4
IVDB_Eemian
steep side
Gootebank
sand sheet with sand dunes
NW
SE
SP
Offset [m]
Depth [s TWT]

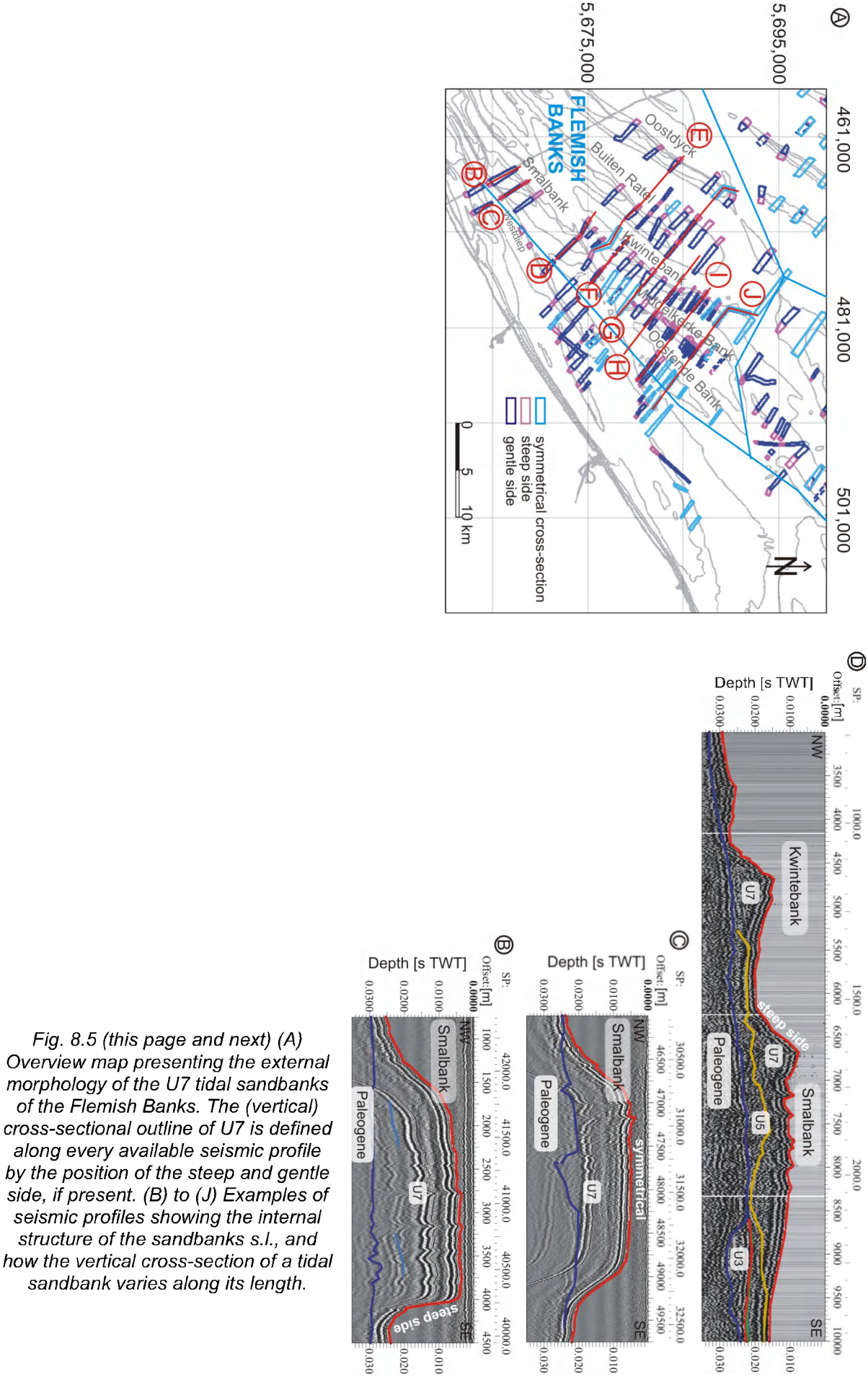

Fig. 8.5 (this page and next) (A) Overview map presenting the external morphology of the U7 tidal sandbanks of the Flemish Banks. The (vertical) cross-sectional outline of U7 is defined along every available seismic profile by the position of the steep and gentle side, if present. (B) to (J) Examples of seismic profiles showing the internal structure of the sandbanks s.l., and how the vertical cross-section of a tidal sandbank varies along its length.

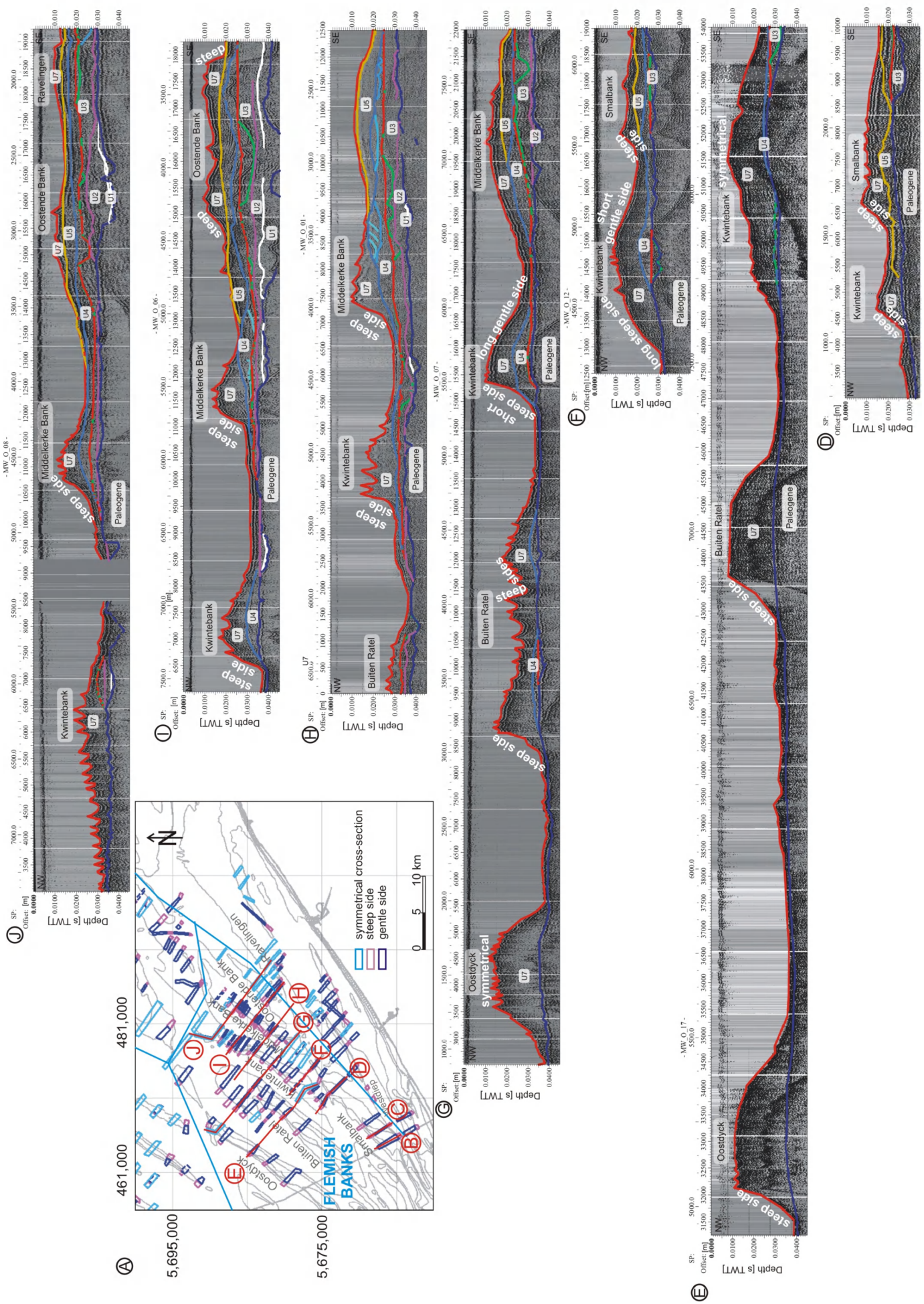
A
461,000
481,000
5,695,000
5,675,000
FLEMISH BANKS
Oostdyck
Buiten Ratel
Kwintebank
Middelkerke Bank
Oostende Bank
Ravelingen
Smalbank
symmetrical cross-section
steep side
gentle side
0 5 10 km
B
C
D
E
F
G
H
I
J
- MW_O_08 -
- MW_O_06 -
- MW_O_01 -
- MW_O_07 -
- MW_O_12 -
- MW_O_17 -
Depth [s TWT]
steep side
short gentle side
long steep side
long gentle side
symmetrical
Paleogene
U1
U2
U3
U4
U5
U7

U7 in the Middelkerke Bank changes from a rounded, sheet-like structure in the SW (Fig. 8.5G), where it is merely draped over the underlying units, with an offshore-facing slope of 0.5° and a slightly landward-sloping top of 0.075°, to a sharp-crested bank with a steep offshore-sloping side of 2.6° and a landward-sloping side of 0.2-0.5° (Fig. 8.5HI). Towards the NE extremity, the bank cross-section becomes more and more symmetrical (Fig. 8.5J). Internal reflectors dip in the same direction as the steep side, with a dip angle between 0.5° in the SW sheet-like part and 1.9° in the more NE part.
In the Oostende Bank, as defined on the bathymetric charts, U7 consists in fact of two bank-like structures with opposite steep slope directions (Fig. 8.5I). There is the offshore bank with an offshore-sloping steep side (1.1°) and a nearshore bank with a landward-sloping steep side (3°). The slope of the intervening gentle sides are 0.4° and 0.1° respectively. Towards the NE, the two bank structures merge to one sheet-like structure with an offshore slope of 0.15° and a horizontal top section covered with sand dunes, in order to finally become two separate sheets with sand dunes (the nearshore structure corresponds to the area 'Ravelingen', and shows a steep landward side again) (Fig. 8.5J).
U7 in the Oostdyck and Buiten Ratel shows more consistent cross-sections, with a straight to concave, offshore-facing steep side (4.3° and 1.8-2.7° respectively), and a convex, landward-facing gentle side (0.9° and 0.6-1.3° respectively) (Fig. 8.5E). The Buiten Ratel U7 bank structure transforms towards the NE in a broad sand sheet covered by a dune field (Fig. 8.5GH). Internal reflectors in U7 in the Buiten Ratel dip in offshore direction, with a dip angle of 1.5°.
Sand dunes are not very common on the Flemish Banks, and are often only 2-3 m high. Most of them occur on the top of the Smalbank and the Kwintebank, and on the gentle sides of the Oostdyck, Buiten Ratel, Middelkerke Bank and Oostende Bank. At the transition between the Kwintebank and the Akkaertbank of the Zeeland Ridges, U7 consists of a sheet with sand dunes (3-4 m high) (Figs. 8.4G and 8.5J).

The Coastal Banks

In the nearshore area offshore De Panne-Nieuwpoort, U7 consists of a thin sheet-like structure draped over units U4 and U5. It is locally (offshore De Panne) moulded into a bank-like structure with a straight landward-facing steep side (1.5°), and a convex offshore-facing gentle side (becoming less steep towards the crest; 0.9-0.14°) (Fig. 8.6B). More to the NE, U7 consists of the Nieuwpoort Bank, Stroombank and part of the Wenduine Bank. Just as in the Hinder Banks and the Zeeland Ridges, also in the Coastal Banks U7 has a landward-oriented steep side.
U7 in the Nieuwpoort Bank is sharp-crested (but smoother than in the Hinder and Flemish Banks) with a straight to concave steep side with a slope of 1.5-1.6°, and a straight gentle side, with a slope of 0.17-0.2° (Fig. 8.6CD). The internal reflectors show a tangential-oblique reflection pattern parallel to the steep slope. Towards the NE, the bank becomes more rounded and symmetrical (Fig. 8.6EF), and finally changes into a thin sheet structure.
Offshore, adjacent to the NE extremity of the Nieuwpoort Bank, another small rounded bank exists, with an offshore-directed steep slope adjacent to a deep swale (NE of the Noordpas) (Fig. 8.6E). This small bank structure becomes also more symmetrical towards the NE, where it finally merges with the middle sand ridge of the underlying unit U5 (Fig. 8.6F).

Fig. 8.6 (page 271) (A) Overview map presenting the external morphology of the U7 tidal sandbanks of the Coastal Banks. The (vertical) cross-sectional outline of U7 is defined along every available seismic profile by the position of the steep and gentle side, if present. (B) to (H) Examples of seismic profiles showing the internal structure of the sandbanks s.l., and how the vertical cross-section of a tidal sandbank varies along its length.

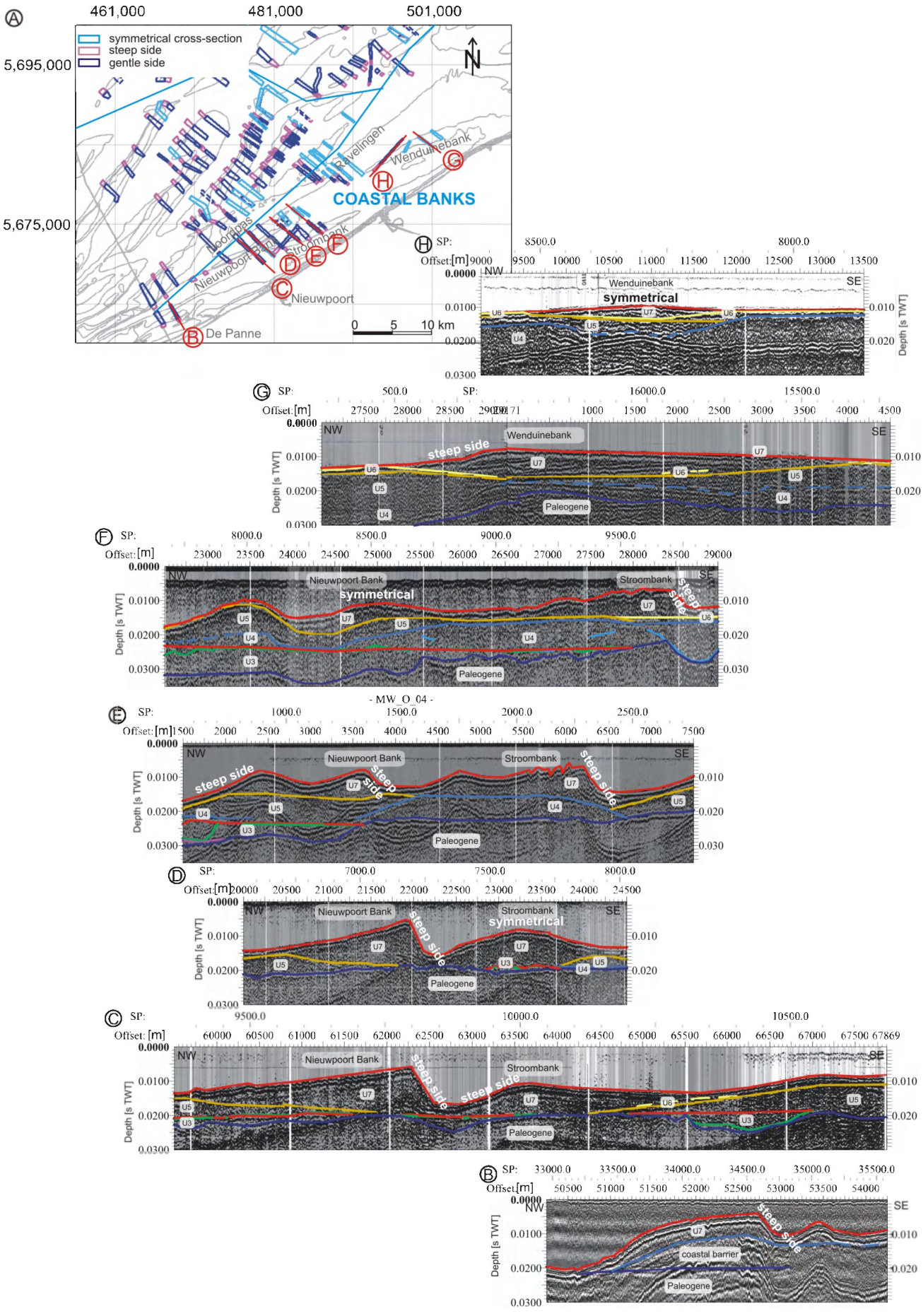
A
461,000
481,000
501,000
5,695,000
5,675,000
symmetrical cross-section
steep side
gentle side
N
Raveling
Wenduinebank
COASTAL BANKS
Noordpas
Nieuwpoort Bank
Stroombank
Nieuwpoort
De Panne
0 5 10 km
H SP:
Offset:[m]
NW
SE
Wenduinebank
symmetrical
U4
U5
U6
U7
Depth [s TWT]
G SP:
steep side
Paleogene
F SP:
Nieuwpoort Bank
Stroombank
- MW_O_04 -
E SP:
D SP:
C SP:
Offset: [m]
B SP:
coastal barrier

U7 in the Stroombank changes in SW direction from a sharp-crested bank with landward-oriented concave steep side (1.5°) and an offshore-oriented straight gentle side (0.2°) (Fig. 8.6FE), into a rounded symmetrical bank (slope 0.2-0.4°) (Fig. 8.6D). At its most SW extremity, the bank's steep and gentle sides (0.4° and 0.07° respectively) face opposite directions (Fig. 8.6C). Throughout the bank the internal reflection pattern stays the same, i.e. landward-sloping tangential-oblique prograding reflectors, parallel to the main steep side of the bank.
U7 of the Wenduine Bank is grafted onto the underlying seismic unit U6. It consists of a thin sheet-like layer (Fig. 8.6H), and changes in SW direction into a bank structure with a landward-facing concave steep side (0.38°), an offshore-sloping gentle side (0.08°), and a tangential-oblique prograding reflection pattern, parallel to the steep slope (Fig. 8.6G).
The seismic data show except from some small sand dunes on the top of the Stroombank (1.5 m high), no other sand dunes on the Coastal Banks. A detailed overview of the presence and dimensions of sand dunes on the BCS is given in Lanckneus et al. (2001).

Depositional depth and the U7 bank dimensions (height, length, width and spacing)

The Hinder Banks

In general, the depth of the crest lines of the banks decreases landward (Fig. 8.7). In the most offshore bank, the Noordhinder, U7 has a crest up to -20 m MLLWS (-15 m, including the sand dunes at the top), U7 in the outward arm of the Fairy bank reaches up to -17 m (-13.5 m including sand dunes), in the Westhinder to -14 m (-7.5 m, including sand dunes), and in both the Oosthinder and Bligh Bank U7 reaches up to -12 m. Exceptionally, in the landward arm of the Fairy Bank, U7 reaches depths of -10 m. The swales in between the banks occur at depths between -40 m in the more offshore parts and -30 m MLLWS landward of the Bligh Bank. The U7 bank structures in the Hinder Banks have a length of 15 km (the Noordhinder) to 26 km (in the Westhinder), and a width of 1.5 to 4 km (on average 2.3 km), the broadest section mostly being located at the NE end of the banks. The maximum height of the individual banks, measured below the crest lines, ranges between 17 m (in the Blighbank) and 24 m (in the Fairy Bank), with an average of 20 m. The spacing between the banks varies between 4 and 7 km.

The Zeeland Ridges

The depth of the crest lines of the U7 banks in the Zeeland Ridges decreases landward, with the exception of U7 in the Thorntonbank, which rises above the other banks. In the most offshore bank, the 'Bank Zonder Naam' (BZN), U7 has a crest up to -19.5 m MLLWS (-15 m including the sand dunes at the top), in the Gootebank it reaches up to -18 m (-16 m including sand dunes), in the Akkaertbank to -14 m, and in the Thorntonbank U7 reaches up to -12 m (-8 m including the sand dunes). The swales in between the banks lie at depths between -34 m (between the Bligh Bank and the BZN), and -21 m landward of the Akkaertbank. The depth of the swales decreases from offshore the Hinder Banks in landward direction (Fig. 8.7). Individual banks are 19 to 34 km long, 1 to 6 km wide, with an average of 3 km, and maximal 6-18 m high with an average of 8 m, the spacing between banks ranges between 5 and 7.5 km. In general the U7 banks in the Zeeland Ridges do not rise as high as in the Hinder Banks and they are also thinner, but in the Zeeland Ridges they are wider and slightly longer.

The Flemish Banks

The depth of the crest lines of U7 in the Flemish Banks again decreases in landward direction, with the exception of the Middelkerke Bank, in which U7 is slightly deeper than the surrounding banks. In the most offshore bank, the Oostdyck, U7 has a crest up to -7.5 m MLLWS. In the Buiten Ratel, the Kwinte and Oostende Bank, U7 reaches up to -6

m, while in the Middelkerke Bank in between it reaches up to -7.5 m. In the Smalbank U7 has a crest up to -3 m. The swales in between the banks lie at depths of -31.5 m (between the Westhinder and Oostdyck), but this shallows to depths of -15 m and -13 m, landward of the Smalbank and Oostende Bank, respectively. This again reflects the gradually higher position of the swales from offshore the Hinder Banks (-40 to -30 m) over the Flemish Banks (-31.5 to -13 m) towards the coastline. The swale depths in between the Flemish Banks correspond very much with the swale depths in between the Zeeland Ridges at similar distances offshore (Fig. 8.7). However, the crest lines of U7 in the Zeeland Ridges at similar distances offshore are located much deeper than those of the corresponding Flemish Banks (e.g. in the Thorntonbank at -12 m versus the Oostdyck at -7.5 m, in the Akkaertbank at -14 m versus the Kwintebank at -6 m). Individual banks of the Flemish Banks are 12 to 26 km long, 1 to 5 km wide, with an average of 2.3 km, and have a maximum height of 8.5-21 m (increasing offshore with each bank), with an average of 11 m. The spacing between banks ranges between 4 and 7 km. The U7 bank structures in the Flemish Banks have a very similar spacing, and similar widths and lengths as in the Hinder Banks, while in the Zeeland Ridges they are wider and slightly longer, and more widely spaced. In the Flemish Banks, the U7 banks are thinner (8.5-21 m, 11 m on average) than in the Hinder Banks (17-24 m, 17 m on average), but higher than in the Zeeland Ridges (6-18 m, 8 m on average).

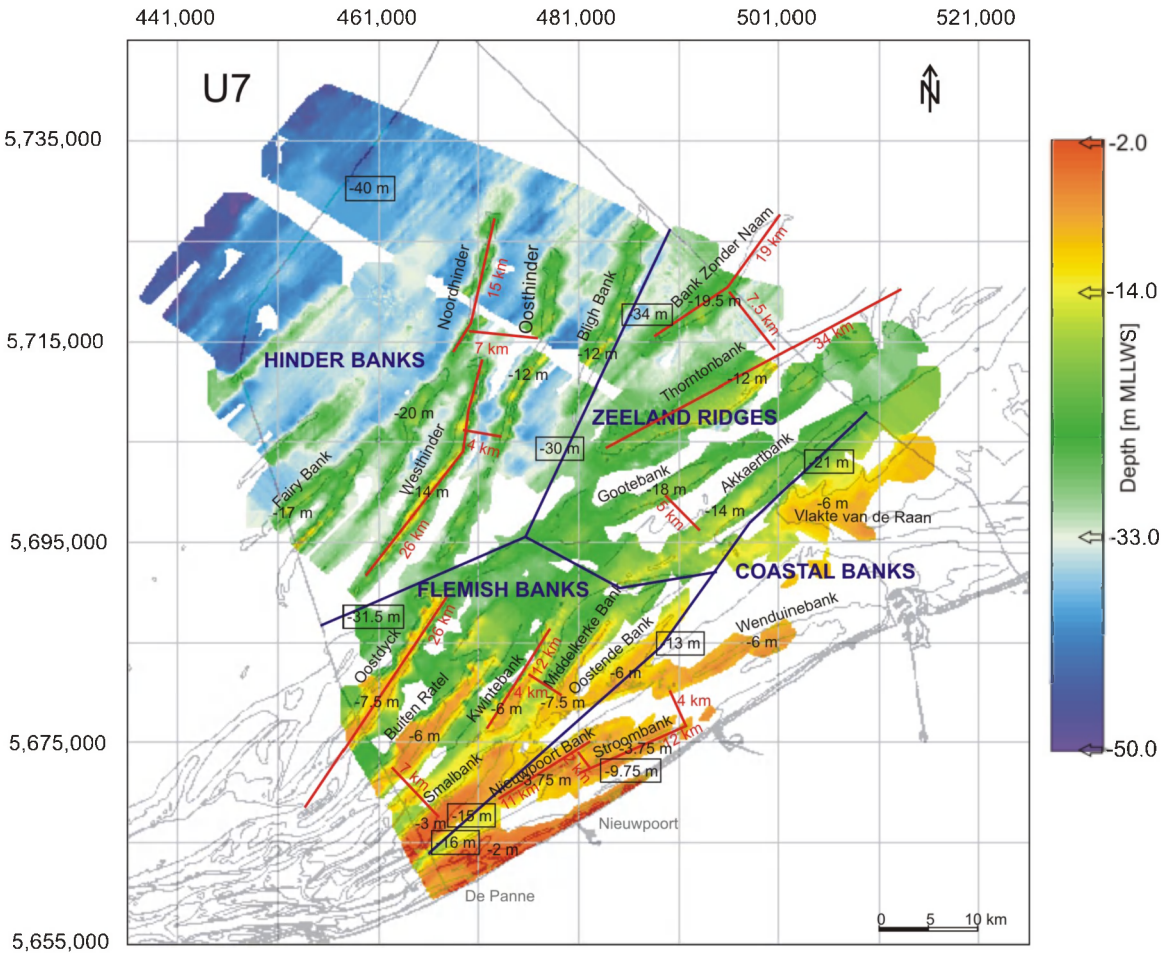

Fig. 8.7 Isobath map of seismic unit U7, with indication of maximum height of each bank (number in black) and the maximum and minimum bank length and spacing for each of the four sandbank groups (in red). For each sandbank group also the depth limits of the swales are given (boxed numbers).

The Coastal Banks

Again, the depth of the crest lines of the Coastal Banks becomes shallower closer towards the coastline, with the exception of U7 in the Wenduinebank, which is slightly deeper. In the most outward bank of the Coastal Banks, the Nieuwpoort Bank, U7 has a crest up to -3.75 m MLLWS, similar to that of the Stroombank, while in the Wenduinebank it reaches up to -6 m (Fig. 8.7). The nearshore sheet of U7 offshore De Panne-Nieuwpoort reaches up to -2 m, while on the Vlakte van de Raan the depth is -6 m. The swales in between the banks lie at depths that range between -16 m (between the Smalbank and the nearshore sand sheet) and -9.75 landward of the Stroombank, again reflecting the gradually shallowing of the swales from offshore the Hinder Banks (-40 to -30 m) over the Flemish Banks (-31.5 to -15 à -13 m), towards the coastline (-16 to -9.75). Individual banks are 11 to 12 km long, 0.9 to 3 km wide, with an average of 2 km, and 7 to 12 m high, with an average of 8 m. The spacing between banks ranges between 2 and 4 km. In general the U7 bank structures of the Coastal Banks have heights similar to the ones of the Zeeland Ridges (6-18 m, with an average of 8 m), but they are narrower than the Zeeland Ridges (1-6 km, 3 km on average), and show more resemblance to the Hinder Banks (1.5-4 km, 2.3 km on average) and to the Flemish Banks (1-5 km, 2.3 km on average). Concerning the length, the U7 structures in the Coastal Banks are much shorter than in the Hinder Banks, the Flemish Banks and the Zeeland Ridges.

Base of seismic unit U7

Not only the external form of the U7 banks shows differences along its length and between the banks (e.g. the orientation of the steep side), but also the base of the bank structures of U7 shows variations. On the basis of the slope of the basal reflector of U7, and whether the width of the bank s.s. corresponds to the width of the bank s.l., four main types of cross-sections of banks s.l. can be distinguished, with a few variants: types A, B, C and D (Fig. 8.8). The boundaries of the bank structure s.l. are defined by the transition of bank to swale, where the slope of the bank flank becomes suddenly more horizontal (visually determined). The boundaries of the U7 bank structure (s.s.), are also determined by the slope change, or the lateral extension of seismic unit U7.
In types A and B, the upper boundary of a bank s.l., deduced from the bathymetric map, corresponds entirely with seismic unit U7 (bank s.s.). It is the tidal sandbank alone that forms the elevation above the seafloor (Fig. 8.8AB). In types C and D, however, the bank s.l., is wider than U7 only, and the flanks of the bank s.l. consist not only of U7 but also of another seismic unit at its base (Fig. 8.8CD). In the situation where U7 has a flat, quasi-horizontal base, a sort of 'basal layer' is present below U7 (i.e. type D), while in the situation where U7 shows a sloping base, there exists some sort of 'core' below U7 as well (i.e. type C). The distinction between types A and B is also made based on the presence or not of a 'core' below U7. In case the base of U7 is flat (i.e. type B), the bank structure does not contain a core, while in case the base of U7 is sloping, there is another seismic unit present below the outer bank form of U7, so the bank holds a core (i.e. type A).
In case of a sloping U7 basal boundary, internal reflectors (when visible) always incline in the same direction. E.g. Fig. 8.9 presents how in the Akkaertbank two sets of internal reflectors, with an opposite direction, slope in the direction of the basal boundary, which shows an opposite slope orientation below the flanks of the bank.

Variations on the scheme comprise an intermediate situation between types A and C, where U7 coincides at one flank with the bank s.l. (is considered to belong to type C), and an intermediate type between A and B, or C and D, where the base of U7 is partly sloping and partly flat (considered being A or C). A variant between types B and D does exist as well, where the base of U7 is entirely flat and where U7 coincides at only one flank with the bank s.l. (is considered being type D).

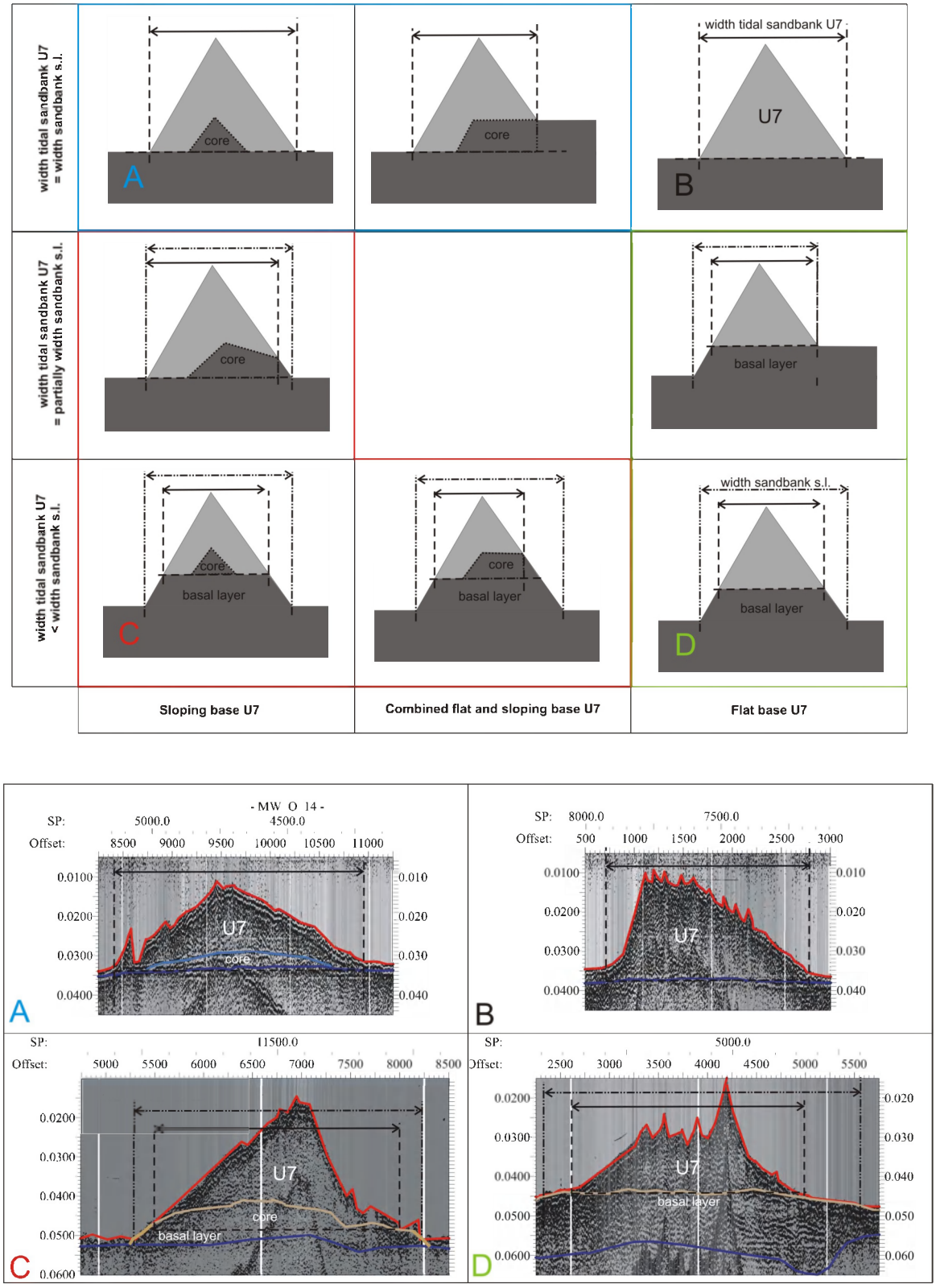

Fig. 8.8 On the basis of the slope of the basal reflector of U7, and whether the width of the U7 tidal sandbank, i.e. the bank s.s., corresponds to the width of the bank s.l., four main types of cross-sections of banks s.l. can be distinguished (A B C D), with a few variants. At the top: a schematic scheme. U7 in light grey, underlying units in dark grey. For detailed explanation see text. At the base: an exemplary seismic profile for each main cross-sectional type.

In types A, C or D the 'core' or 'basal layer' can consist of Paleogene, Pleistocene or Holocene deposits depending on the seismic unit underlying U7. Fig. 8.10 shows a map of the cross-sectional types of each bank (s.l.) (red contour), and for each bank the seismic unit on which U7 (black contour) rests. There is remarkable contrast between the northern part which is characterised by mainly types-C and type-D cross-sections and an IVDB Eemian subsurface, and the southern part which is characterised by mainly type-A and type-B cross-sections, and a Paleogene or Holocene subsurface, with the Offshore Scarp as a sharp boundary in between, cutting through the Hinder Banks and the Thorntonbank. It is clear that along one bank different cross-sectional types can occur, and that in general an entire bank can not be classified under one type.

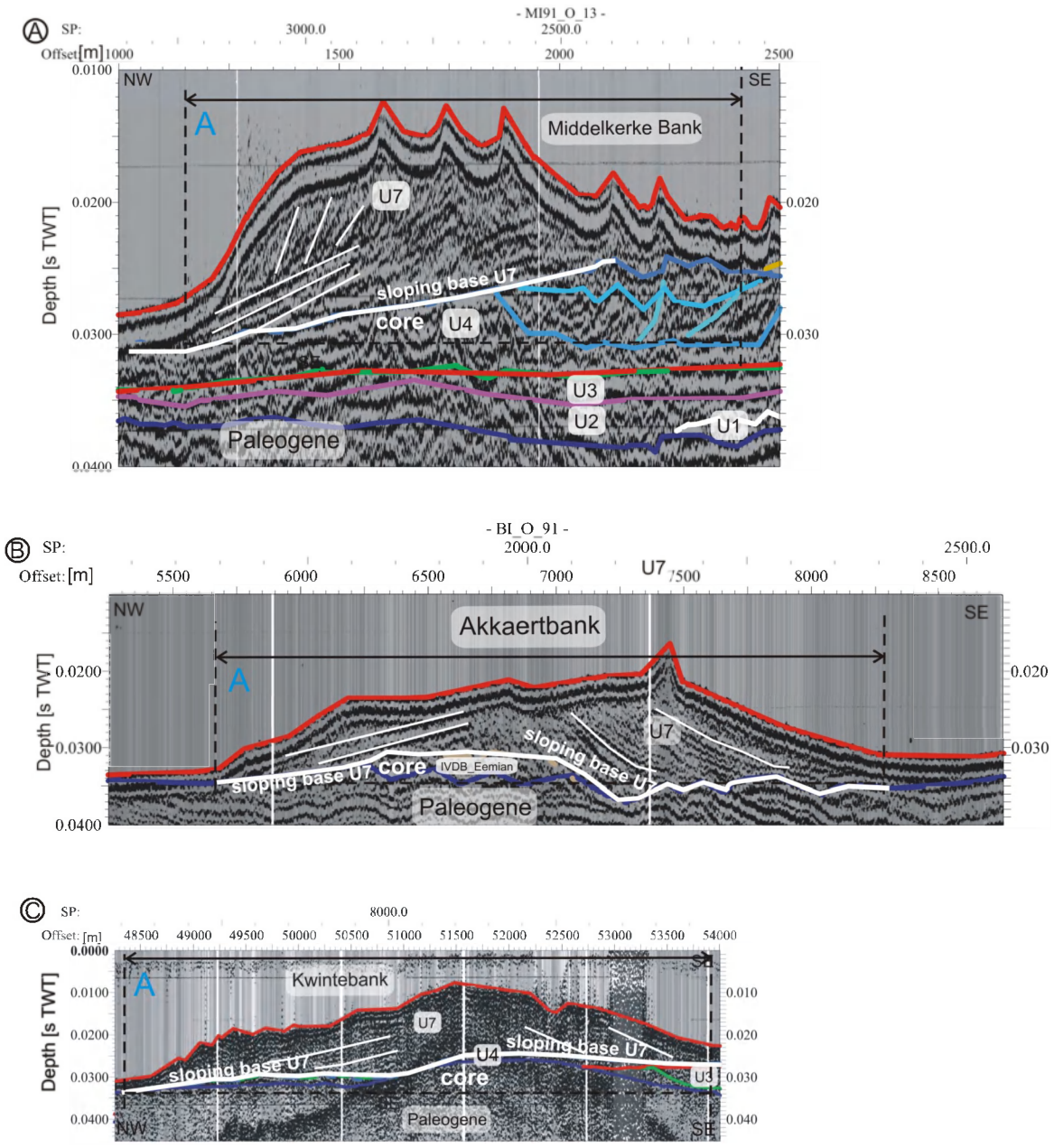

Fig. 8.9 (A), (B), (C) Exemplary seismic profiles showing how in case of a sloping U7 basal boundary, internal reflectors (when visible), always incline in the same direction. All three examples are of type A: the width of the U7 sandbank, i.e. the bank s.s., corresponds to the width of the bank s.l., and the base of U7 is sloping, so that a 'core' exists below U7.

The Hinder Banks

The Noordhinder consists entirely of type-D cross-sections. This means that U7 has a flat lower boundary, and rests on top of a basal layer which is incised itself, which makes it stand out from the seafloor as part of the bank. The bank s.l. consists of a basal layer of IVDB Eemian deposits with a U7 tidal sandbank on top. The bank in the south-western prolongation of the Noordhinder, the cross-sections belong to type A and C, and becomes entirely type A south of the Offshore Scarp, where it is the Paleogene substrate that forms a core or elevation below U7. The NW arm of the Fairy Bank in line with this bank consists mostly of cross-sections of type A and B, although it is located north of the Offshore Scarp. The bank consists of a U7 tidal sandbank, with an IVDB Eemian core underneath in type A. The SE arm of the Fairy bank, located south of the Offshore Scarp, consists of type-A cross-sections, with a Paleogene core below the U7 tidal sandbank. In an inlet in the Offshore Scarp, the SE arm shows locally a type-B cross-section, where the U7 bank lies flat on the IVDB Eemian subsurface. The Westhinder comprises type C and D north of the Offshore Scarp, where the bank s.l. consists of an IVDB Eemian basal layer with a U7 bank on top of it. In case of type C, an Eemian core is present below U7. South of the Offshore scarp, the Westhinder is entirely type A, with U7 resting directly on the Paleogene substrate which forms an internal core below the deposits of U7. The same applies to the Oosthinder. The Bligh Bank, located entirely north of the Offshore Scarp, consists of type-C and type-D cross-sections, with an Eemian basal layer. So, the parts of the Hinder Banks that are located north of the Offshore Scarp mainly consist of a basal layer of IVDB Eemian deposits with U7 on top (type D), sometimes with a core below U7 (type C). The basal layer is incised itself, and makes part of the bank s.l. The parts of the Hinder Banks that are located south of the scarp on the other hand, mainly consist of a tidal sandbank U7 only, with a small elevation of the substrate underneath (type A). This is –exceptionally- also the case for the NW side of the Fairy Bank, in line with the south-western prolongation of the Noordhinder, but to the north of the Offshore scarp. There, the small elevation is, however, of Eemian origin, while south of the scarp, the small core is formed by the Paleogene substrate.

The Zeeland Ridges

The main part of the Thorntonbank, located north of the Offshore Scarp, is a type-C bank, while the SW section of the bank, located south of the scarp, has a typical type-A cross-section. North of the scarp, the bank s.l. consists of an Eemian (IVDB) (to possibly Weichselian or even Holocene) layer and core below the U7 tidal sandbank, while south of the scarp the bank s.l. consists of the U7 tidal sandbank on top of the Paleogene substrate, which forms an internal elevation below U7. The Gootebank is mainly characterised by a type-A cross-section, which means that the bank s.l. consists entirely of U7, located over a small elevation of the Paleogene substrate underneath. A small section in the central part of the bank forms an exception. Here the bank s.l. is slightly wider than U7, and U7 overlies an Eemian or Paleogene basal layer and core. A distinct part of the Akkaertbank consists entirely of tidal sandbank U7, without any internal core (type B) overlying a flat Top-Paleogene surface. Towards the NE, however, a possible Eemian internal core occurs (type A) and finally the U7 bank forms the top part of a larger bank structure (type C). The base and internal elevation below U7 of this larger bank is made up of the Paleogene substrate, which stands out from the seafloor.

The Flemish Banks

In some parts the Oostdyck consist entirely of the U7 tidal sandbank, overlying the flat Paleogene surface (type B), while in other sections the Paleogene subsurface forms a small elevation below U7. The Buiten Ratel is entirely characterised by type-A cross-sections, consisting of the U7 tidal sandbank, overlying a core of a different seismic unit.

This is also the case in the Kwintebank (except from two cross-sections of type C), the Middelkerke Bank, the Oostende Bank and Smalbank. In the Buiten Ratel the U7 bank is located over a core of possibly U4 Holocene tidal-flat or of U3 Eemian deposits. In the Kwintebank, the U7 tidal sandbank overlies a core of U4 tidal-flat deposits, U3 estuarine sediments, and Paleogene deposits. Near the two type-C cross-sections the lower part of the bank s.l. is formed by a U4 core. Below the U7 tidal sandbank in the Middelkerke Bank and the Smalbank, a core of U4 tidal-flat deposits and U5 storm-generated sand ridges is present. In the Oostende Bank U7 overlies a core of only U5 storm-generated sand ridges.

The Coastal Banks

Also the Nieuwpoort Bank, Stroombank and Wenduinebank all consist of type-A cross-sections, i.e. the banks s.l. consist completely of the tidal sandbank U7 overlying a core of U5 sand ridges or of U6.

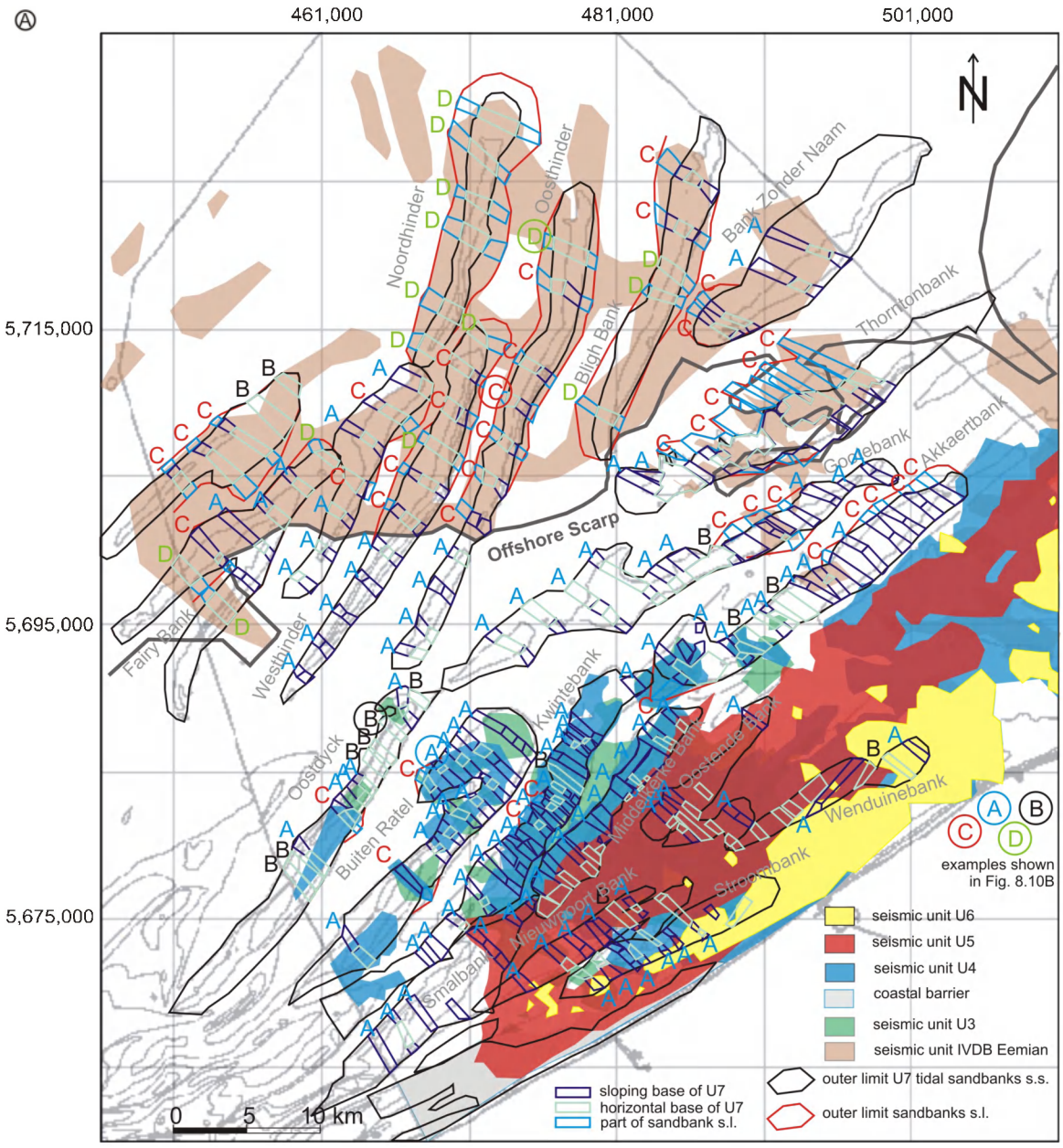

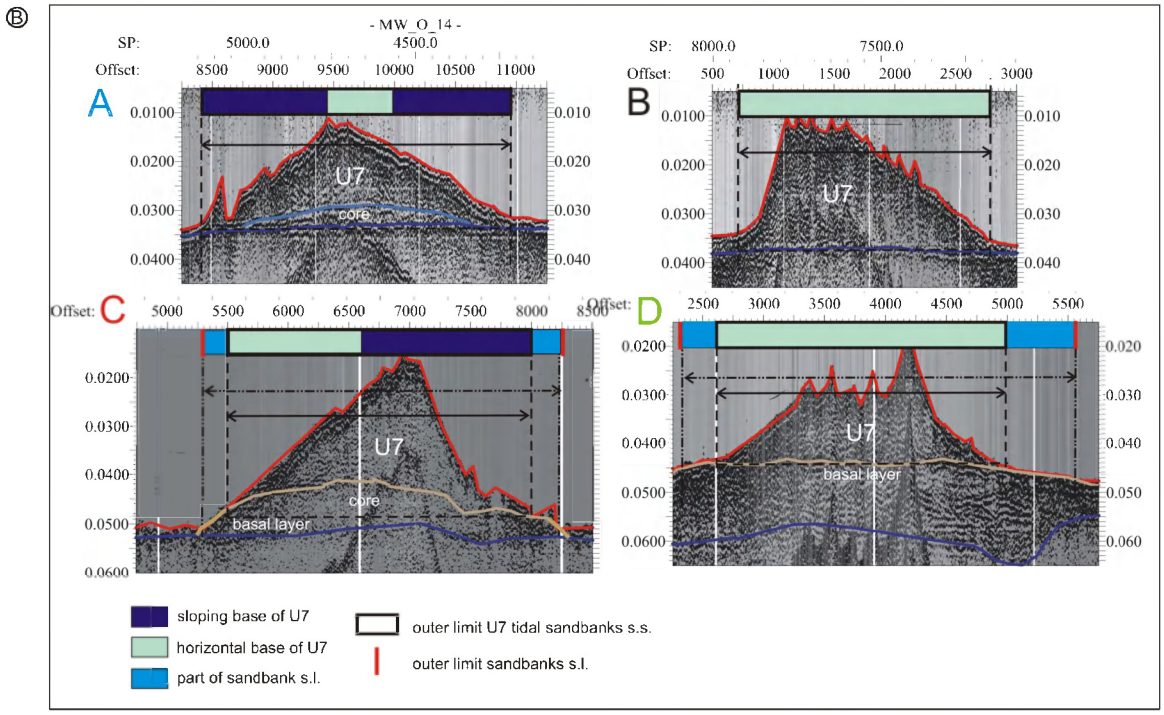

Fig. 8.10 (this and previous page) (A) Map showing the cross-sectional types of each bank (s.l.) (red contour), and for each bank the seismic unit on which U7 (black contour) is positioned. Where no seismic unit is present (white background), the Paleogene lies directly below U7. (B) Examples of the four main cross-sectional types, in order to explain the colour codes and the terms 'sloping base of U7', 'horizontal base of U7', and the remaining 'part of sandbank s.l.' as used in (A).

Thickness of seismic unit U7

The Hinder Banks

The maximum thickness of U7 is reached in the Fairy Bank, where it amounts up to is 24 m. The thickness decreases in landward direction from 22 m in the Westhinder, 21 m in the Oosthinder and 17 m in the Blighbank. In the Noordhinder, the maximum thickness if U7 is only 18 m (Fig. 8.11).

The Zeeland Ridges

U7 in the Thorntonbank (s.s.) has a maximum thickness of 18 m, not taking into account the presence of a deep incised channel which seems to be infilled entirely by U7 deposits. Unit U7 would be 35 m thick, if these channel deposits would be included. U7 in the Gootebank (s.s.) is thinnest, with a maximum thickness of 6 m, and U7 in the Akkaertbank is at most 14 m thick (Fig. 8.11).

The Flemish Banks

The thickness of U7 below the Flemish Banks decreases in landward direction from 21 m in the Oostdyck, over 20 m in the Buiten Ratel, 12 m in the Kwintebank, 11 m in the Middelkerke Bank, to 8.5 m in the Oostende Bank. U7 is exceptionally 14 m thick in the Smalbank (Fig. 8.11).

The Coastal Banks

U7 in the Nieuwpoort Bank has a thickness of 12 m, U7 in the more landward located Stroombank has a maximum thickness of 10 m and U7 in the Wenduinebank is 7 m thick at most (Fig. 8.11).

In general the thickness of the U7 banks decreases in landward direction, and banks at similar distances from the shore have similar thicknesses (i.e.12 m in the Kwintebank versus 14 m in the Akkaertbank, 21 m in the Oostdyck versus 18 m in the Thorntonbank). In the swales, the thickness of U7 ranges between 0 and 5 m.

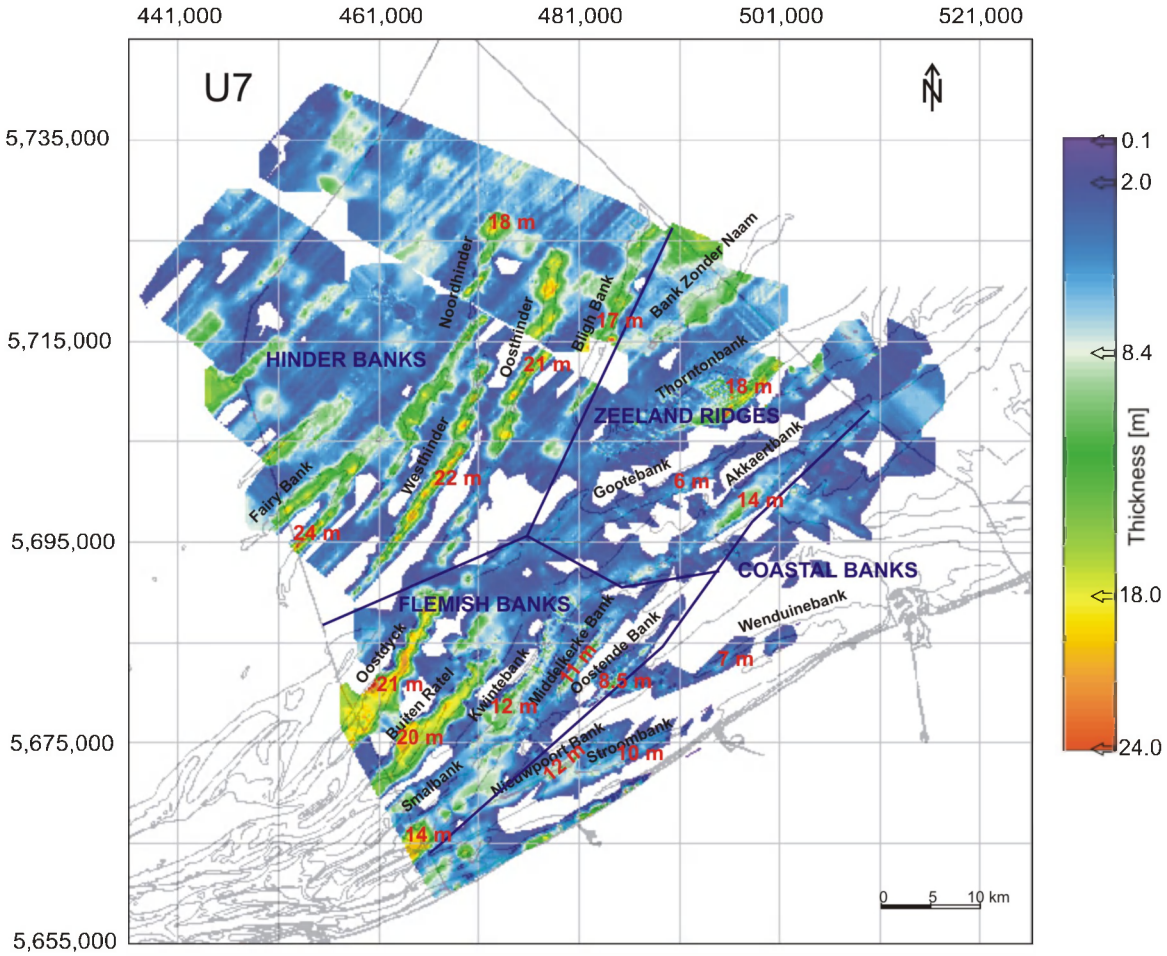

Fig. 8.11 Isopach map of seismic unit U7, with indication of maximum thickness of each bank (number in red). In general, the thickness of the U7 banks decreases landward, and banks at similar distances from the shore have similar dimensions (12 m below the Kwintebank versus 14 m under the Akkaertbank, 21 m below the Oostdyck versus 18 m below the Thorntonbank). In the swales U7 ranges between 0 and 5 m.

8.2.2 Lithology

A large part of the core data set (266 cores) was applied to describe and discuss unit U7. As U7 is virtually absent in the nearshore area (where U5 and U6 are exposed at the seafloor), mostly offshore core data were used, which are, however, mostly old flush cores, and therefore less detailed, in contrast to the nearshore vibrocores.
Some photos of typical lithologies of U7: a bioclastic sand (Fig. 8.12A), a homogeneous sand with very few shell fragments (Fig. 8.12B), a gravel lag at the base of U7 on top of the Paleogene surface (Fig. 8.12C), a coarse-grained gravel lag at the base of U7 on top of U4 (Fig. 8.12D), a typical sequence in a swale (Fig. 8.12E).

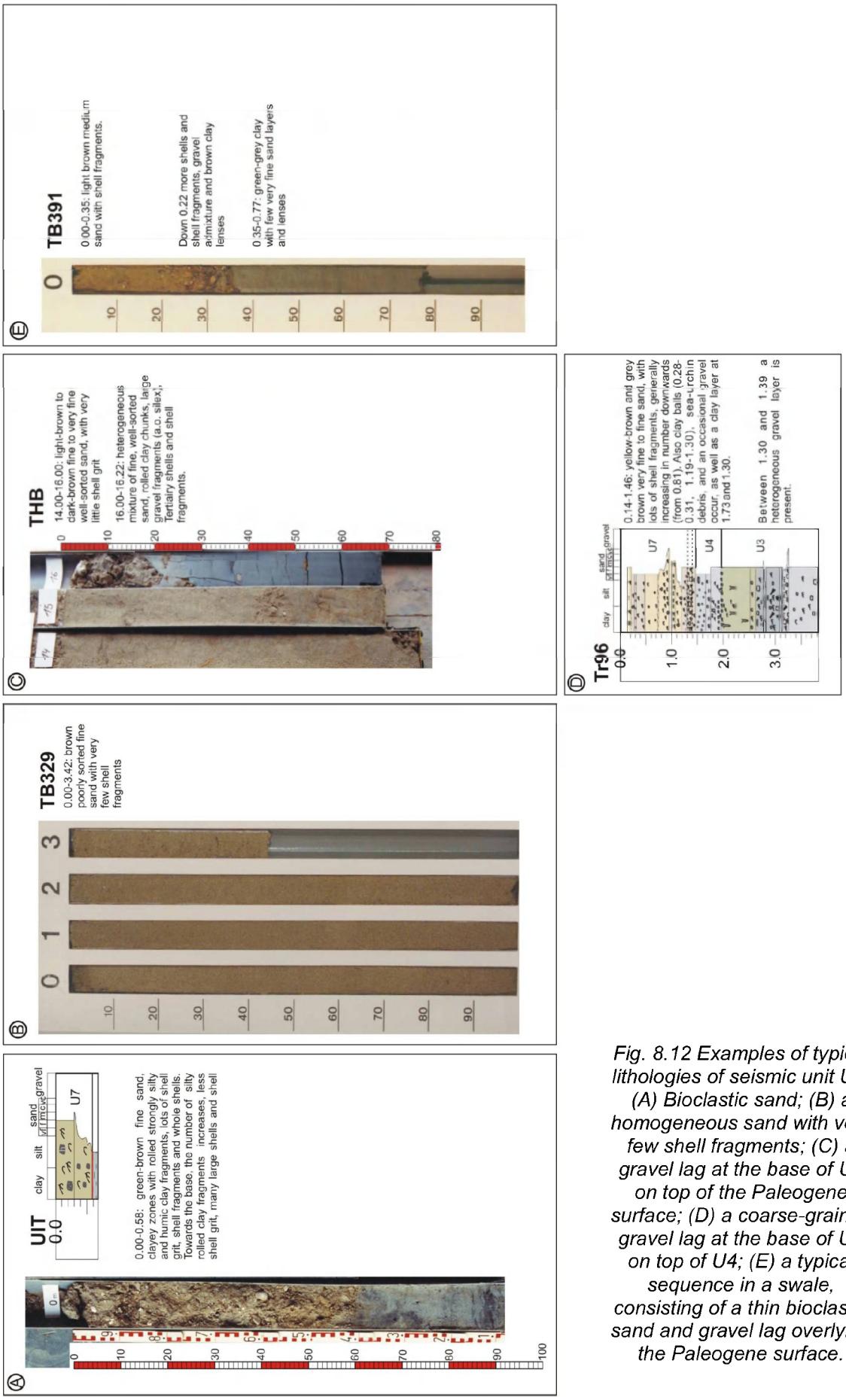

Fig. 8.12 Examples of typical lithologies of seismic unit U7. (A) Bioclastic sand; (B) a homogeneous sand with very few shell fragments; (C) a gravel lag at the base of U7 on top of the Paleogene surface; (D) a coarse-grained gravel lag at the base of U7 on top of U4; (E) a typical sequence in a swale, consisting of a thin bioclastic sand and gravel lag overlying the Paleogene surface.

8.3 Discussion

8.3.1 Integration of seismic data and lithology: genetic interpretation of the seismic unit

Main lithology

In general seismic unit U7 consists of brown, brown-grey or grey, fine to coarse sands (Fig. 8.17), frequently containing shells, shell fragments and sea-urchin needles, although zones with very low shell content occur as well. Some cores contain a significant silt component (in 55 out of a total of 266 cores that sampled U7), often associated with local shell accumulations, and as many cores contain clay layers or clay chunks. Only 11 cores hold humic particles or plant fragments (Fig. 8.17). A detailed description of the surficial sediments of the BCS is given in Lanckneus et al. (2001).

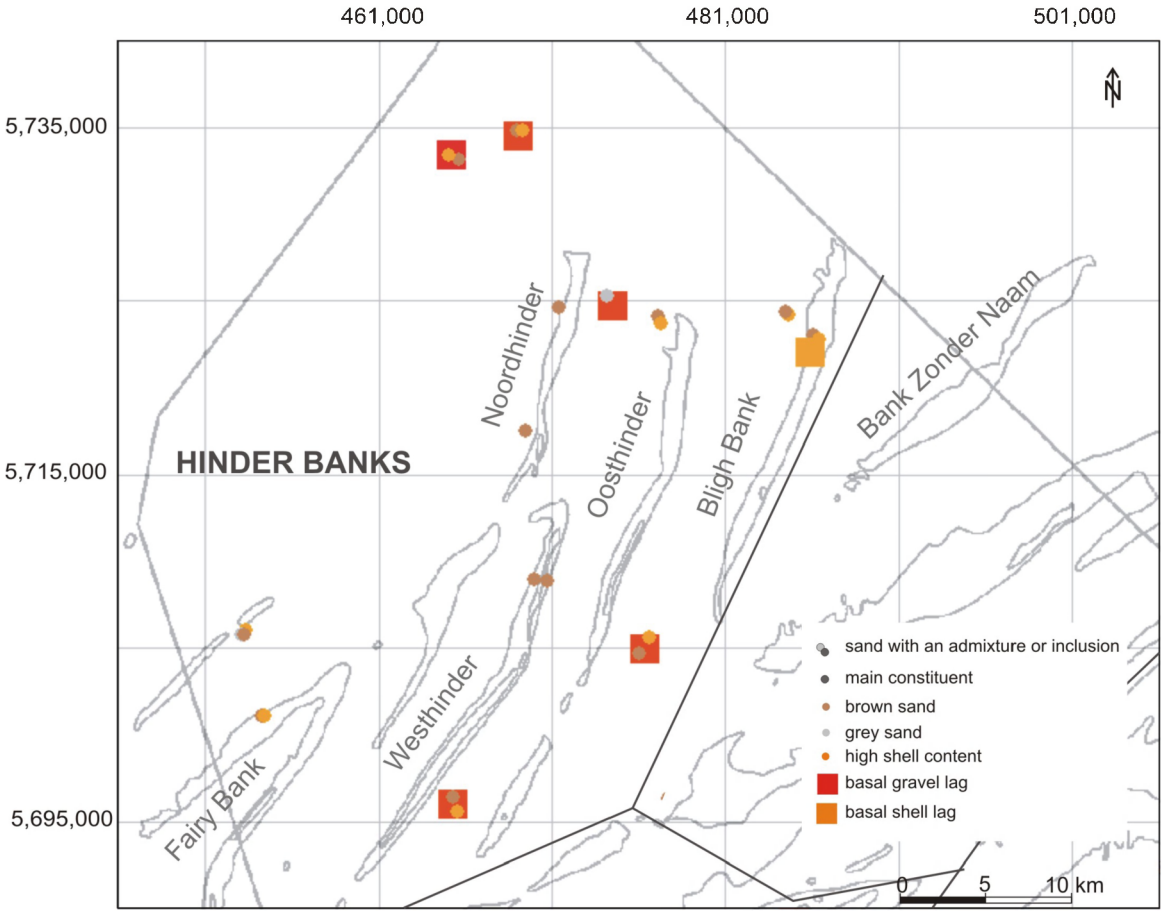

Fig. 8.13 The lithology of seismic unit U7 in the area of the Hinder Banks. Whether or not a gravel lag or coarse-grained layer is present at the base of U7 is indicated as well.

The Hinder Banks

Only a few cores cover the area of the Hinder Banks and these are mostly flushcores of which only one sample per metre section was taken for the core description. The base of U7, or the transition to the underlying unit, was consequently often missed in these cores.
In the Noordhinder, U7 consists of brown coarse sand, containing shell grit and sea-urchin debris (Figs. 8.13 and 8.17). U7 in the area north of the Noordhinder is characterised by sand dunes, consisting of green-brown to brown-grey and brown-yellow gravely coarse sand, containing abundant shells, shell grit and sea-urchin debris. In one core, U7 overlies the Top-Paleogene surface and shows a basal gravel lag with abundant gravel and shells. Gravel is also present in anther core, this time on top of IVDB Eemian deposits.
In the Westhinder, U7 shows many similarities with the Noordhinder. It is characterised by brown coarse sand, containing shell grit and sea-urchin debris.
U7 within the Oosthinder and the Blighbank consists of brown, medium fine to coarse-grained sand as well, but it contains more shell fragments and sea-urchin debris. The swale in between the Noordhinder and Blighbank contains light grey medium fine sand on top of a medium coarse basal gravel lag with abundant shell fragments and gravel (5 cm diameter). The gravel lag overlies Eemian IVDB deposits. The swale between the Westhinder and Oosthinder contains brown-grey coarse sand with gravel and shell fragments erosionally overlying the Paleogene clay. Yellow-brown coarse sand, with abundant shell grit and shell fragments at the top, is present in the swale between the Oosthinder and Blighbank. The base, overlying IVDB Eemian deposits, consists of shell fragments, silex and sandstone gravel in a coarse grained sandy matrix.
U7 in the Fairy bank is characterised by brown coarse sand containing shells, shell fragments and sea-urchin debris. North of the Fairy Bank, the sand dunes consist of yellow-brown coarse sand, little gravel, and shell grit (*Angulus pygmaeus* fauna), while the basal part of U7 consists of grey coarse sand, containing fragments of the *Angulus pygmaeus* fauna as well.

The Zeeland Ridges

In the 'Bank Zonder Naam', U7 consists of yellow-brown to grey coarse to medium fine sand with shell fragments (*Angulus pygmaeus*), shell grit and sea-urchin debris. In the swale in between the BZN and the Thorntonbank, U7 consists of yellow-brown, medium fine to very coarse sand with few shells, on top of a very coarse sand with gravel and shells erosionally overlying the Top-Paleogene surface (Figs. 8.14 and 8.17).
In the Thorntonbank, U7 consists of brown, fine to medium coarse sand, with very few shell fragments or shell grit, some silty zones and clay lenses. The base of U7 on top of QT is represented by fine sand, containing large gravel, shell fragments and clay chunks.
In the swale between the Thorntonbank and the Gootebank, U7 consists of grey or brown, well- to poorly-sorted, fine- to medium-grained sand with few shell fragments, overlying a basal gravel lag consisting of a heterogeneous mixture of gravel (sandstone), large shell fragments, and occasional clay lenses on top of QT.
U7 in the Gootebank consists of brown to brown-grey, well to poorly sorted, fine to medium coarse sand, with very few shell fragments at the SW broad part of the bank (but sea-urchin debris is present), and more shell fragments and sea-urchin debris in the rest of the bank. At the NW side of the bank (gentle side) U7 contains silty and clayey patches. The base of U7, on top of QT, is mostly characterised by sandy gravel with abundant shell fragments, silex cobbles up to 8 cm in diameter, and occasional clay chunks. However, in some cases only a shell accumulation occurs or even no clear coarser-grained base is present (Fig. 8.14).
In the swale between the Gootebank and Akkaertbank, U7 is characterised by a thin layer of brown medium sand with a base containing lots of shell fragments, sea-urchin debris, gravel, and occasional clay lenses on top of QT.

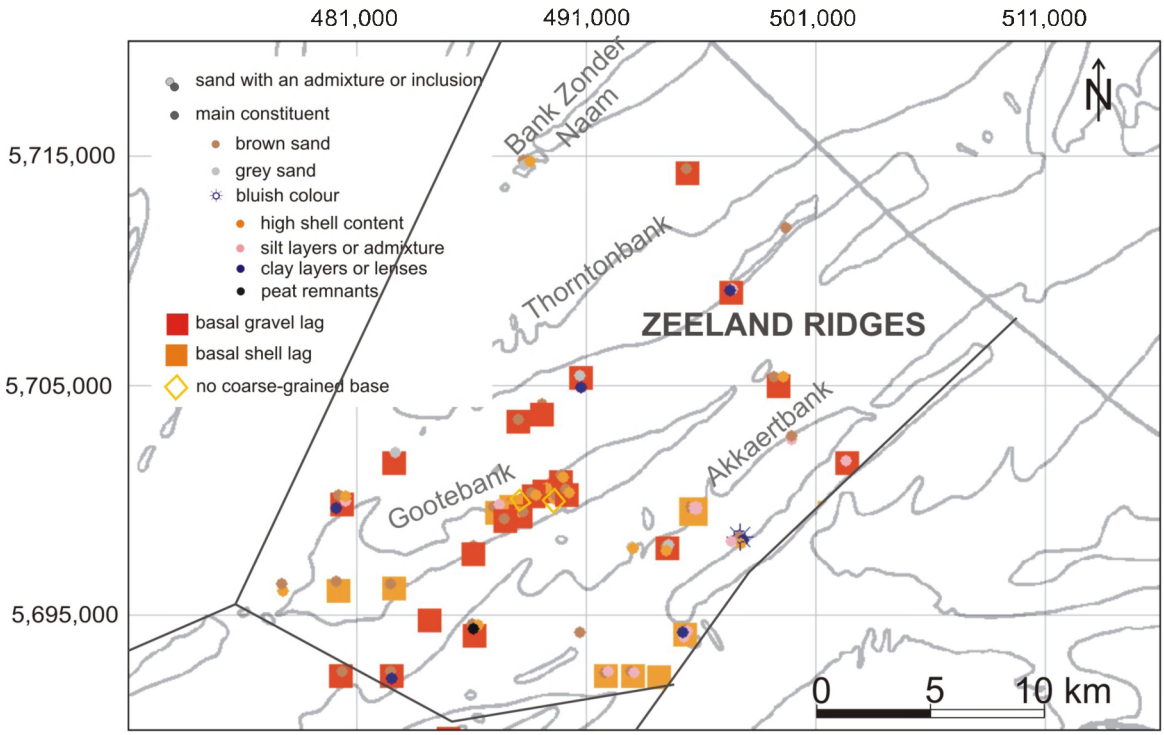

Fig. 8.14 The lithology of seismic unit U7 in the area of the Zeeland Ridges. Whether or not a gravel lag or coarse-grained layer is present at the base of U7 is indicated as well.

In the Akkaertbank, U7 consists of brown to grey, fine to medium sand with few shell fragments, although locally shell accumulations can occur. In one core in the SW, humic lenses are present, and the NE section of the bank presents silty and clayey patches. U7 in the swale between the Akkaertbank and Vlakte van de Raan consists of greenish brown silt overlying a basal gravel lag on top of QT, containing Paleogene shells and gravel in a silty sand matrix. The base of U7 under the bank is characterised by a similar gravel lag (with silex), or a shell accumulation.
In general, U7 in the Zeeland Ridges is finer grained than in the Hinder Banks and contains less shell fragments.

The Flemish Banks

The Oostdyck and Buiten Ratel have only been sampled by one core each (Figs. 8.15 and 8.17). U7 in the Oosdyck consists of yellow-brown fine sand with generally few shell fragments, but with an occasional shell accumulation. The base of U7 on QT consists of grey fine sand with abundant gravel (> 5 cm diameter), shell fragments and clay chunks. While in the Buiten Ratel, U7 is characterised by yellow-brown, medium to very coarse sand with abundant shell fragments and the base of U7 on QT shows an increase in shell content and few gravel.
In the swale between the Buiten Ratel and Kwintebank, U7 consists of yellow-brown medium fine sand with abundant shell fragments and gravel (up to 9 cm in diameter), erosionally overlying the Paleogene clays.
U7 in the Kwintebank consists of well-sorted grey fine sand with very few shell fragments, but a little shell grit. Towards the NE, U7 consists of a brown medium fine sand with few sea-urchin or shell fragments.
In the swale between the Kwintebank and Middelkerke Bank, U7 is characterised by dark grey, yellow-brown or brown, rather well to poorly-sorted fine to medium sand with few shell fragments or sea-urchin debris (although locally more shell fragments can be present), overlying a base of sandy gravel with lots of shell fragments on top of U4, U3 or

QT. In two cores, U7 contains an admixture of silt, but more often clay layers or lenses occur close to the Middelkerke Bank.
In contrast to the Kwintebank, in the Middelkerke Bank U7 is mainly characterised by brown-grey, yellow-brown to grey-brown fine to medium fine sand with some shell fragments and sea-urchin debris. In the central part, shell content is abundant, although some zones with very few shell fragments exist as well. At the most SW end of the bank, at the flank facing the Kwintebank, U7 becomes, however, grey coloured towards the base, clay and silt layers occur and very few shell fragments and sea-urchin debris are present. Also at the most NE end of the Middelkerke Bank, at the flank facing the Kwintebank, some cores consist of yellow-grey sand in stead of brownish sand, or U7 becomes grey coloured towards the base. Over the entire length of the Middelkerke Bank, the flank of U7 facing the Kwintebank is characterised by the presence of occasional clay layers and clay chunks.
In the swale between the Middelkerke Bank and the Oostende Bank, U7 consists of dark grey to yellow-brown well sorted fine to medium fine sand, with few shell fragments or sea-urchin debris (although locally more shell fragments can be present), frequently with a coarse-grained shell accumulation or basal gravel lag at its base, erosionally overlying U4 or U5. However, more often no coarse-grained base is present at all on top of U5. Occasionally clay chunks are present in the gravel lag. When encountered within the Middelkerke Bank itself, the base of U7, overlying QT, U4 or U5, mostly consists of brown-grey sandy gravel, containing sea-urchin debris and abundant shell fragments (in 16 cores), or a coarse-grained shell accumulation (in 15 cores). In some cases U7 shows no coarse-grained base at all (in 8 cores).

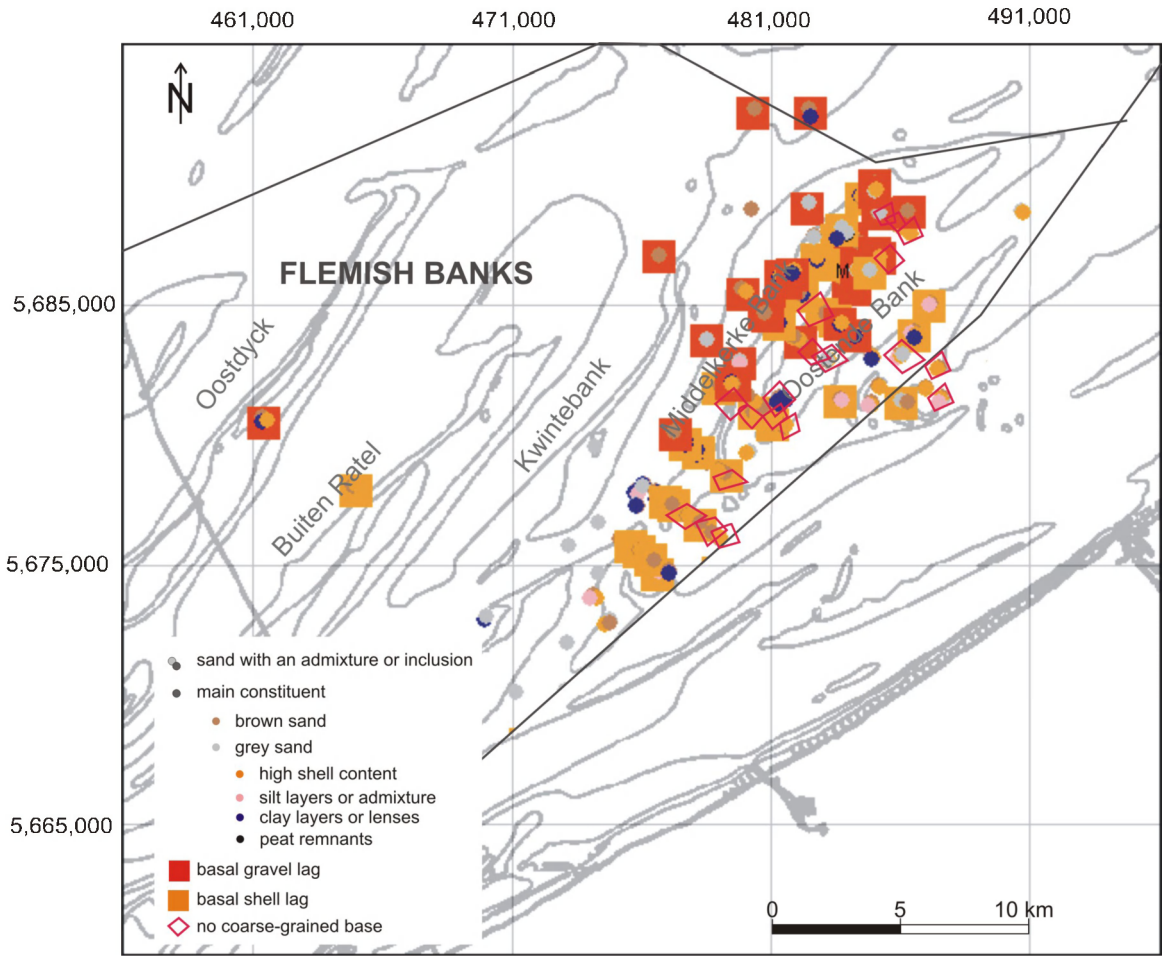

Fig. 8.15 The lithology of seismic unit U7 in the area of the Flemish Banks. Whether or not a gravel lag or coarse-grained layer is present at the base of U7 is indicated as well.

Both U7 bank structures within the Oostende Bank mainly consist of grey-brown, poorly-sorted fine to medium fine sand, with shell fragments or sea-urchin debris (occasionally very few), and frequently an admixture of fine gravel. The more offshore bank is characterised by clay and silt layers, silt patches or silt admixture, which are characterised by local shell accumulations. In some sections U7 consist of dark grey sands (brown-grey after drying), or becomes grey towards the base in some cases. The base of U7 in the Oostende Bank is characterised by either a poorly-sorted shell accumulation or by no coarse-grained base at all, but merely a facies change.
The main body of U7 in the Smalbank consists of dark grey, rather well-sorted fine sand with very few shell fragments or sea-urchin debris. In one core at the offshore flank of the bank, thin mud layers occur. In the swales between the Smalbank, the Nieuwpoort Bank and the near-coastal zone, however, U7 consists of brown-grey, rather well-sorted fine to medium sand, with shell and sea-urchin accumulations in silty patches, and an occasional clay layer. The base of U7 was not reached below the Smalbank, but when encountered in the swales, a coarse-grained shell accumulation overlies U5 or QT.

The Coastal Banks

The U7 tidal sandbank in the Nieuwpoort Bank mainly consists of dark-grey, rather well-sorted fine sand with very few shell fragments or sea-urchin debris (Figs. 8.16 and 8.17). The offshore-oriented gentle side is characterised by clay and silt patches. The NWB core, however, shows a yellow-brown to grey-brown fine sand with shell accumulations with small gravel and with the presence of peat remnants and clay lenses. In the NE prolongation of the Nieuwpoort Bank, U7 is yellow-brown to grey-brown, well-sorted, strongly silt-containing fine sand, with very few shell or sea-urchin debris. The base of U7 below the Nieuwpoort Bank consists of a coarse-grained shell accumulation on top of U5 or U3, a basal gravel lag with abundant shell and sea-urchin debris and gravel on top of U5, or a more gradual transition towards U5.

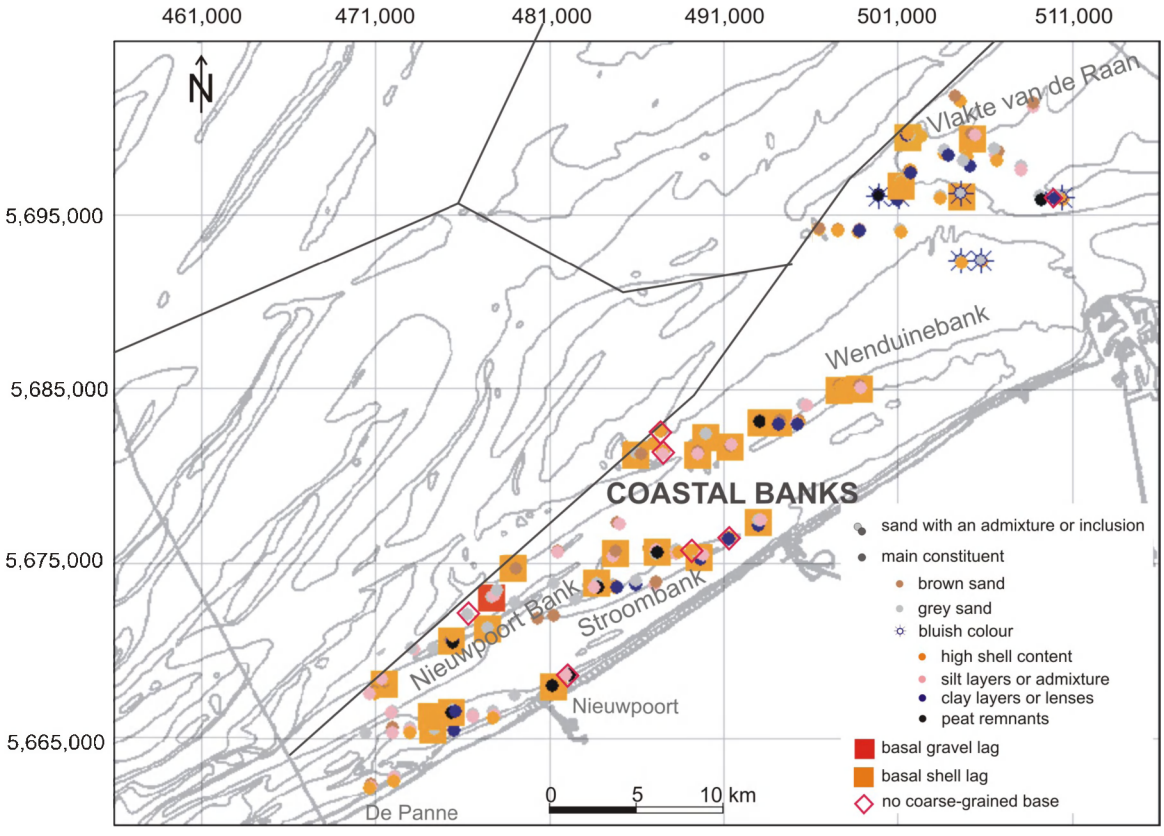

Fig. 8.16 The lithology of seismic unit U7 in the area of the Coastal Banks. Whether or not a gravel lag or coarse-grained layer is present at the base of U7 is indicated as well.

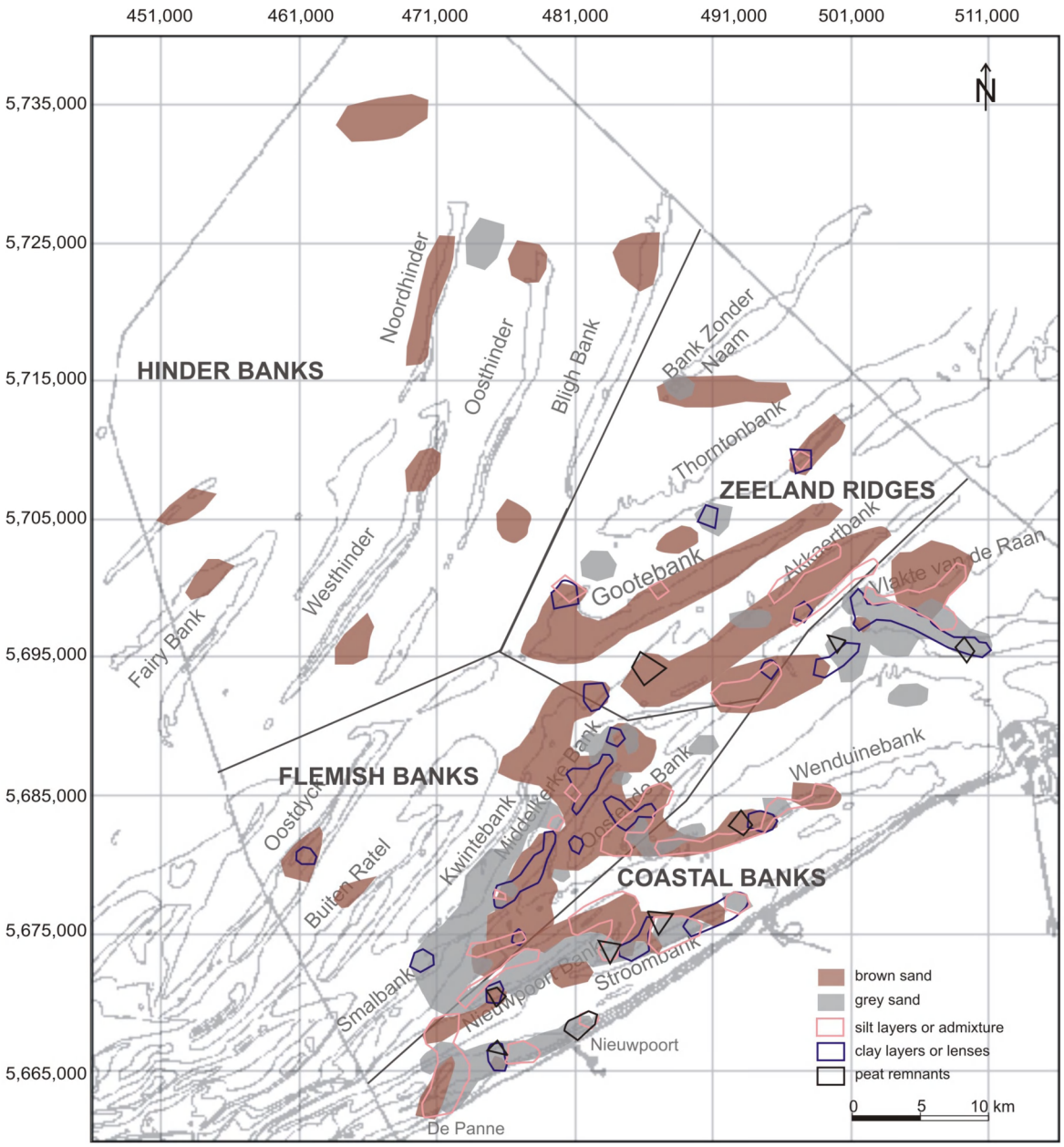

Fig. 8.17 The areal distribution of the different lithofacies of seismic unit U7.

U7 in the Stroombank is characterised by both yellow-brown and dark-grey well- to poorly-sorted fine to medium fine sand, with very few shell or sea-urchin fragments. Sometimes, U7 contains clay layers or lenses, and silt admixture. The base is characterised by shell accumulations with occasional humic spots or layers in silt lenses and clay lenses on top of U5 or U6, or by no coarse-grained base at all above U6.
U7 in the Wenduinebank consists predominantly of brown, well- to poorly-sorted fine sand with very few shell fragments and lots of silt lenses (with local shell accumulations), and an occasional clay or humus lens. Towards the base, U7 shows an increase in shell content, and coarser sand on top of U5.

The U7 near-coastal sand sheet offshore De Panne-Nieuwpoort consists predominantly of grey, well- to poorly-sorted fine sand with few shell fragments, but more sea-urchin debris, often containing silt admixtures or silt lenses with local shell accumulations. Locally some clay layers and humus particles are present in this area as well. Where the base of U7 is reached, it shows an increase in shell content in coarser-grained sand, with often the presence of clay lenses and humus particles on top of U5

In general the U7 near-coastal banks and sand sheet are characterised by grey to brown fine sands with few shell fragments, apart from their base on top of U5 and U6, and local accumulations in silt lenses, which are common (also in the Oostende and Akkaertbank). Also most of the humus containing cores are located in this area.

The U7 sand sheet near the Vlakte van de Raan and Scheur consists of distinct areas of (bluish) grey and brown fine to medium fine sands (Figs. 8.16 and 8.17), with often a higher content of shell fragments than the nearshore sand sheet offshore De Panne-Nieuwpoort. Frequent silt and clay admixture, patches and layers, and occasional humic particles are also present. The base of U7 on top of QT, U4, U5, or U6, is characterised by a coarse-grained shell accumulation.

Interpretation

Seismic unit U7 consists of large-scale bank-like structures and sand sheets that are exposed at the present-day seafloor and subjected to a macrotidal environment. The Hinder Banks (s.s.) have a spacing of 4-7 km, a maximum height of 17-24 m, a length of 15-26 km, and a width of 1.5-4 km. They are sharp-crested, covered with sand dunes and are in general asymmetrical with a steep slope of 2-4°, and a gentle slope of 0.5-1°. The Zeeland Ridges (s.s.) have a spacing of 5-7.5 km, a maximum height of 6 m in the Gootebank, 14 m in the Akkaertbank and 18 m in the Thorntonbank, and a length of 19-34 km. The U7 bank in the Thorntonbank is sharp-crested, covered with sand dunes and is asymmetric with a steep slope of 3.5°. The other Zeeland Ridges (s.s.) are more rounded, covered by sand dunes, in general asymmetrical with a steep side of only 0.5-1.3°. The gentle slope of the U7 banks in the Zeeland Ridges ranges between 0.1-0.3°. The Flemish Banks (s.s.) have a spacing of 4-7 km, a height of 8.5-21 m (increasing in offshore direction), a length of 12-26 km, and a width of 1-5 km. They are mostly sharp-crested, covered with sand dunes and are in general asymmetrical with a steep slope of 2.6-5° and a gentle slope of 0.4-1.4°. The Coastal Banks (s.s.) have a spacing of 2-4 km, a height of 7-12 m, a length of 11-12 km, and a width of 0.9-3 km. They are rather sharp-crested (but smoother than the Hinder and Flemish Banks s.s.), not covered with sand dunes, and are asymmetrical with a steep slope of 0.38-1.6°, and a gentle slope of 0.08-0.9°.

On the basis of their dimensions, morphological characteristics and position, U7 within the Hinder Banks, Flemish Banks, and within the Thorntonbank (Zeeland Ridge) are interpreted as active tidal sandbanks or active open-shelf linear ridges (Type 1) following the classification of Dyer and Huntley (1999). The banks are not related to the presence of wide- (Type 2A) or narrow-mouth estuaries (Type 2B), nor to the presence of a headland (actively eroding (Type 3A) or not (Type 3B)). However, Dyer and Huntley (1999) suggest that the Flemish Banks and the ridges in the Baie de la Somme may have been formed during the widening of the Dover Straits and erosion of the coastline to the east and the west of Cap Gris Nez (Type 3B).
Active tidal sandbanks or open shelf linear ridges (Type 1) are generally higher and longer than storm-generated ridges or shoreface-connected ridges (Type 2B (ii)) (van de Meene and van Rijn 2000). The former can be up to 80 km long, and hundreds of metres (Galloway and Hobday 1996) or several kilometres wide (Belderson 1986), and are tens of metres in height. The modal height of tidal banks is 10-15 m (20-30 m according to Belderson 1986), but maximum heights reach 40-50 m (Galloway and Hobday 1996). They are asymmetrical having slopes of about 6° on the steeper side, and less than 1° on the gentler side (Dyer and Huntley 1999), which is steeper than storm-generated ridges (van de Meene and van Rijn 2000). The bank crests are flat in shallow water (e.g. the Smalbank located at -3 m), but are sharp when water depth is large enough to limit

wave effects (Dyer and Huntley 1999). Typical spacings range between 2 and 30 km for tidal sandbanks (Belderson 1986, van de Meene and van Rijn 2000).

The features of the U7 bank structures in the Coastal Banks closely resemble the characteristics of (active) shoreface-connected ridges, or of storm-generated ridges, in more general terms. These are typically 5 to 10 m high, smooth crested, 2-5 km apart, with side slopes rarely more than 1°, and crestlines which can extend for tens of kilometres (Galloway and Hobday 1996, Dyer and Huntley 1999, van de Meene and van Rijn 2000). Also the lithology of U7 in the Coastal Banks is in agreement with that expected in shoreface-connected ridges, which are generally coarsest in the landward through and become finer up the landward flank to the crest, where they are well sorted, and down the seaward flank where they become increasingly fine (Dyer and Huntley 1999). The U7 Coastal Banks, and especially U7 in the Nieuwpoort Bank, show indeed clay and silt inclusions at their offshore side.
The Coastal Banks occur close to the present-day coastline. The Wenduine Bank shows a clear connection to the shoreface on the bathymetric map. And also the Stroombank was connected to the present-day coastline before the digging of the harbour entrance of Oostende around 1900 AD (Verwaest 2008). Only the Nieuwpoort Bank shows no direct link with the coastline. Shoreface-connected ridges can, however, become detached as the coast retreats to form fields of isolated ridges. At that stage, they are not connected to the coastline anymore, but they appear to retain the same characteristics and dynamics as the attached ones, although a reorientation can occur under the influence of the shelf hydraulic regime (Dyer and Huntley 1999). This could be the case for the Nieuwpoort Bank.
U7 within the Wenduine Bank s.l. is not connected to the beach but to an elevation in U6, which might resemble the situation at the northern coast of the Netherlands and Germany, where the ridges disappear into the shoreface sand sheet, presumably because of the higher tidal-current and wave regime (Dyer and Huntley 1999). Although shoreface-connected ridges have been considered a special class of storm-generated ridges, shoreface-connected ridges along the Dutch coast are found in a setting where tidal currents and storms are both important. This suggests that a storm-dominated setting is not essential for the formation of shoreface-connected ridges (van de Meene and van Rijn 2000). Most likely the Coastal Banks (s.s.) represent shoreface-connected ridges, which developed in the both high tidal and wave regime of the Belgian coastline.

The remaining Zeeland Ridges (s.s.) are more difficult to interpret. Although located far from the present-day coastline, the Akkaert and Gootebank have characteristics that resemble the Coastal Banks, which are interpreted as shoreface-connected ridges. The Akkaert (s.s) and Gootebank (s.s.) have comparable heights (6-14 m versus 7-12 m), are only slightly broader (2.6 km versus 2 km on average) and more widely spaced (5 km versus 2-4 km). They have similar steep slopes around 1°, but are much longer (22 km versus 11-12 km). Large parts of these two banks are, however, clearly rounded, so they could represent moribund ridges as well. Moribund ridges are found where the present-day peak currents are insufficient to move the sea bed sand. They have more round-crested cross-sections and slopes of only 1° as the crest has been progressively eroded an the material spread out on its slopes (Stride 1989, Dyer and Huntley 1999). But, in contrast to the Coastal Banks, these two banks are covered by sand dunes. Large parts of U7 in the Gootebank are even that thin that they seem to consist of solely sand dunes on top of the Paleogene substrate, while moribund ridges do not have large sand waves (dunes) on their flanks (Dyer and Huntley 1999), as sand waves are only associated with evolving sandbanks (Stride 1989). Moribund ridges are also separated by sandy or muddy floors, rather than clean gravel (Dyer and Huntley 1999). Only a very thin layer of sand is present on top of the gravel lag overlying the Top-Paleogene surface in the swales between the Thorntonbank, Gootebank and Akkaertbank, which suggests that

the Gootebank (s.s.) and Akkaertbank (s.s.) are not moribund but still active under the present-day tidal regime.
The central part of U7 in the Akkaertbank (Fig. 8.4EF) closely resembles the dimensions and internal structure of U7 in the Coastal Banks (Fig. 8.6EF) and the storm-generated ridges of U5 (Fig. 7.8A), although the steep side is less steep and the crest is more rounded. Towards the extremities, the bank structure is even more rounded until only a thin sand sheet exists in the NE, with the internal configuration remaining the same (Fig. 8.4). So, this bank most likely represents a former shoreface-connected or storm-generated sand ridge which lost its original form, becoming rounder, slightly wider, and longer due to the redistribution of sediments, and transformed partly into a sand sheet, probably when it became moribund and detached from a former coastline with rising sea level and changing hydrodynamic conditions. At this deeper position, away from the coast and associated wave and storm currents, active sand dunes could develop on top of the moribund ridge, and the surrounding swales got cleaned by the prevailing strong tidal currents.
Although in the central part of the Gootebank (s.s.) a small bank form may be distinguished (Fig. 8.4F), most of the bank consists of sand dune fields or a thin sand layer. It is possible that the Gootebank was formed in a similar way as the Akkaertbank, but that because of its more offshore position, the original bank form was almost completely removed before it became covered by sand dunes.

Although the U7 bank structures part of the Flemish Banks have been interpreted as active tidal sandbanks or open-shelf linear ridges because of their general sharp crestline and steeper steep side, parts of U7 in the Kwinte, Middelkerke, and Oostende Bank are rounded, mostly symmetrical, with slopes of not more than 1°, and reach further into the swales as if material is being redistributed in the swales. Examples are: the SW end of the Kwintebank (Fig. 8.5E); a large section at the SW end of the Middelkerke Bank where U7 is a thin draped sand sheet (Fig. 8.5G) instead of the sharp-crested bank further to the NE (Figs. 8.5HI); as well as the NE part of the Oostende Bank (Fig. 8.5J) and the Middelkerke Bank. Also in the offshore arm of the Oostende Bank U7 has only a steep side slope of 1°, while the nearshore arm has a steep side slope of 3° (Fig. 8.5I).
This might suggest that certain parts of the sandbanks are not active (moribund) and are not maintained (anymore), while adjacent areas (still) are. Nevertheless, in some sections, sand dunes are present on top of this redistributed sand in the swales (e.g. NE Middelkerke Bank, relative small ones on the SW Middelkerke and Kwintebank in Fig. 8.5FG). This might indicate an active redistribution of the sand into the swales, or a reactivation after redistribution.
It is true that normally sharp-crested tidal sandbanks can develop flat tops as they grow close to the sea surface, where they come under the influence of wave action, and grow wider (Belderson 1986, Dyer and Huntley 1999). A nice example is the broad and shallow (-3 m MLLWS), flat-topped Smalbank s.s. (Fig.8.5BC). In the Middelkerke Bank, however, the sharp crest of U7 has a shallower position than the rounded SW end. According to Caston (1981, in: Dyer and Huntley 1999), ridges are often relatively broad and flat at one end, and narrower and pointed at the other end, because of sand joining the ridge at the broad end, and leaving it at the narrow end, the broad end being considered the upstream end as far as the sand transport is concerned. This might explain the rounded SW extremities of U7 in the Kwinte and Middelkerke Bank, as it is known that in the area of the Flemish Banks residual sediment transport is directed towards the NE (Lanckneus et al. 2001), so the broad ends are located upstream. The rounded extremities of U7 in the Kwinte and Middelkerke Bank are therefore not considered moribund, but active under different hydrodynamics than the sharp-crested parts of the banks.

Basal gravel lag

In 115 out of 147 cores that sampled the base of U7, the base is characterised by a coarse-grained layer, consisting of a shell accumulation or gravel lag. Where U7 directly overlies the Top Paleogene, the Eemian deposits (U3 and IVDB), or the Holocene tidal flats (U4), the basal layer could represent the coarse-grained remnants or gravel lags left by the Eemian and Holocene transgressions. But also on top of U5 and U6, which are not influenced by the Holocene marine transgression, the U7 tidal sandbank shows a coarse-grained basal layer, sharply overlying the underlying units. This suggests that the formation and expansion of the tidal sandbanks is coupled with a high-energy environment, eroding the underlying deposits. Therefore, the coarse-grained base of U7 on top of QT, U3 or U4 could represent a reworking of the original transgressive coarse remnants during the erosive formation and expansion of the U7 tidal sandbank.
The cores that do not show a coarse-grained layer at the base of U7, are predominantly located at the landward-facing gentle side and adjacent swale of the Middelkerke Bank (Fig. 8.15). There the U7 tidal sandbank is very thin, and most likely the sediments just settled on top of U5.

Additional remarks

Often, the lithology of U7 strongly resembles the lithology of the underlying unit U5 (and therefore also U4), which is another indication that U7 is most likely built up of sediments eroded from underlying units (e.g. U7 in Fig. 8.12B and U5 in Fig. 7.19). U5 consists of brown-grey to grey, fine to medium fine sand, containing very few to few shell fragments (except for accumulations in silty lenses) and abundant sea-urchin needles, while U7 in the Kwintebank, Smalbank, Nieuwpoort Bank, Stroombank and the nearshore sand sheet also consists of brown-grey to grey, fine to medium fine sand with very few shell fragments but more sea-urchin debris, except for local shell accumulations in silt lenses.

The difference in colour between the greyish near-coastal and Vlakte van de Raan sand sheets, the greyish near-coastal banks (such as U7 in the Smalbank, Nieuwpoort Bank, Stroombank and Kwintebank), and the brown more offshore banks (Fig. 8.17) could have different causes. It could be due to a difference in original source material of the U7 sandbanks. Also the colour of the present shell grit can determine the appearance of U7. As brown-coloured sediments mostly indicate oxidised circumstances, there could be a difference in pore-water fluxes, or active reworking of the sediments. Sediments reworked during storms are expected to be more oxidised. If both grey and brown sediment occur in one core, the sediments become greyish towards the base, away from the active and oxygen rich upper surface. However, some sand dunes, which are considered to be the active migrating and moving parts of the banks, can be completely grey coloured. The colour differences could also be due to inconsistencies in the description of the cores, as it was not always indicated in which condition, wet or dry, the cores were described. Typically, fresh (dark-)grey sands tend to become brown-grey or brown after drying.

Also strong differences in shell content occur within seismic unit U7. Especially the greyish nearshore banks (U7 in the Coastal Banks, Smalbank, Kwintebank), the swale between Middelkerke en Oostende, the Oostdyck and the Zeeland Ridges are characterised by a low content in shell or sea-urchin debris. In the Hinder Banks, the Buiten Ratel, the Middelkerke and Oostende Bank, as well as in most swales, shells and shell fragments are abundant. This is possibly due to differences in source material (availability of shells), as well as differences in hydrodynamic conditions during the formation of the banks. The presence of abundant coarse shell fragments indicates a high-energy environment (Trentesaux et al. 1999). However, in some sand dune fields (e.g. in the Gootebank), which are considered to have formed under high-energy

circumstances (current velocities of 55-90 cm/s at surface peak flow, Belderson 1986), few shell fragments are present. So most likely also the availability of shells plays a role. According to Berné et al. (1994) coarse layers (consisting of shells and pebbles) correspond to the prograding inclined reflectors on the seismic data and represent alternating phases of erosion and deposition at the flank of the bank. Each coarse layer could correspond to the beginning of a storm period, which was subsequently followed by the deposition on the flank of finer sediment eroded from the top of the bank (Berné et al. 1994).

8.3.2 Origin and evolution of tidal sandbanks s.s. and banks s.l.

Types of sandbank cross-sections and their origin: in general

Over the years, several studies have addressed the processes involved in the initiation of the formation of tidal sandbanks. From the day that reflection seismic investigation revealed the presence of internal reflectors in sandbanks, it was suggested that an initial 'core', acting as a sort of nucleation point, was necessary in the build-up process of the sandbanks (Laban and Schüttenhelm 1981; Maréchal and Henriet 1983; De Maeyer et al. 1985; De Moor 1985a, 1985b; Maréchal and Henriet 1986). Houbolt (1968) and Berné et al. (1994) described the existence of two basic types of (tidal) sandbanks:

(1) banks formed by sand accumulation only, resting on an essentially flat surface and showing no internal core. Those banks consist entirely of Holocene deposits (late Holocene in case of active sandbanks).
(2) banks with an internal core, which consists of eroded fluvial or estuarine sediments of early Holocene or Pleistocene age, or of erosional bedrock morphology. The banks are partly formed by erosion of older deposits and are not shaped by accumulation only.

Sandbank s.s. versus s.l.

It is, however, not always clear whether the authors in previous studies made a distinction between a 'bank s.l.', i.e. an elevated structure above the seafloor, and a 'bank s.s.', i.e. a real tidal sandbank. When the authors discuss 'banks' with an internal core, it is not entirely clear whether that refers to a core below a tidal sandbank is meant (the proposed types A and C in 8.2.1, Fig. 8.8), or merely to a 'basal layer' below a tidal sandbank, being the 'core' of a bank s.l (type D). E.g. the Noordhinder (s.l.) consists of a basal layer of IVDB Eemian deposits covered by a U7 tidal sandbank with a flat lower boundary (Figs. 8.10A and 8.19B). So the bank s.l. represents a "type 2 bank" (*sensu* Houbolt (1968) and Berné et al. (1994)) with an internal core consisting of Pleistocene sediments, partly formed by erosion of the Eemian deposits in the swales. It is a core as defined by Houbolt (1968): i.e. older deposits occurring in a ridge at a level above the surrounding seafloor. The Noordhinder tidal sandbank s.s. (U7), however, rests on an essentially flat surface, shows no internal core, consists entirely of Holocene deposits, and is probably formed by sand accumulation only, which would classify it as a "type 1 bank" (*sensu* Houbolt (1968) and Berné et al. (1994)).
In order to avoid this confusion, a new classification scheme with four types of cross-sections (types A, B, C and D) was developed for this study (Fig. 8.8). It was already presented and discussed above in 8.2.1 'Base of seismic unit U7'.

The base of a tidal sandbank

On the BCS, the base of the tidal sandbanks of U7 often slopes down towards the adjacent swale, and the overlying deposits often contains prograding reflectors sloping in the same direction (Fig. 8.9). This can be in opposite directions below each flank of the bank (Figs. 8.9B and C), in one direction below a single flank (while the other has a flat base) (Fig. 8.10B, type C), or in one direction below the entire bank (Fig. 8.9A). The

inclined basal surface of U7 is clearly erosional as it cuts through the original form of the underlying units (i.e. the marine transgressive surfaces of U3 and U4, the sand ridge form of U5). In addition, the base of the tidal sandbanks are commonly characterised by a coarse-grained layer or gravel lag, erosionally overlying the underlying units (even if U7 is not located on top of a marine transgressive surface). This implies that the tidal sandbank is governed by an erosive migration or growth over the underlying units in the direction of the prograding reflectors, which mostly coincides with the downward slope towards the adjacent swale. Such a process can happen when the substrate is relatively easily erodible and sediment supply is limited. It can be compared to the migration of transverse bedforms with a negative angle of climb (Berné 2002).

Cross-sectional types A and C

Thus, in most cases on the BCS, the core below a tidal sandbank in cross-sectional type A or C is most likely a remnant of older deposits, which have not (yet) been eroded by the overlying developing tidal sandbank, and is not a pre-existing sediment body on which the tidal sandbank accumulated (although some isolated cases do exist, cf. Akkaert and Gootebank).
It has been believed by many authors that these types of banks on the BCS were at least partly created by sand accumulation around a pre-existing sediment body (Laban and Schüttenhelm 1981; Maréchal and Henriet 1983; Van den Broeke 1984; De Maeyer et al. 1985; De Moor 1985a, 1985b; Maréchal and Henriet 1986), the core visible below the tidal sandbank being the initial topographic irregularity needed for the sandbank initiation according to the Huthnance numerical model (Huthnance 1982a). But this implies an initial modelling of the older substrate into a series of swells and swales, before the modern tidal sandbanks could accumulate on top of these cores. De Moor (1985a, 1985b) suggests a mechanism in which, tidal currents in inundated paleo-valleys adapted to the direction of former thalwegs, which evolved into tidal channels, so forming initial swales. The eroded sediments were washed from their fines and piled up on the existing interfluves, which acted as cores for the embryonic banks. This mechanism would imply, however, the presence of former thalwegs at the location of the present-day swales, while currently most swales are oriented more or less transverse to the main paleo-valley system in the area, i.e. the Ostend Valley.

It is therefore more likely that the banks and swales formed at the same time, that the hydrodynamic processes in the swales eroded the older sediments, directly providing the sand for the build up of the tidal sandbanks just next to it (as also suggested by Stride 1989). A small nucleus was indeed probably needed for the start of the bank development, but the large internal cores that are currently present below the tidal sandbanks are most likely the result of a continuing process of constantly deepening swales and increasing growth and migration of the banks towards the swales (Fig. 8.19). The tidal sandbanks form now a (temporally) protection of the older cores from further erosion by the prevailing hydrodynamics in the swales (Mostaert et al. 1989, Berné et al. 1998), as they are considered relative stable at present (Veenstra 1964, Houbolt 1968, De Moor 1985b).
In case of a cross-sectional type C, additional erosion probably occurred in the swales after the growth of the tidal bank towards the swale(s), which made the underlying older units below the tidal sandbank stand out from the seafloor as well, i.e. a sandbank s.l. (Fig. 8.19B, Oosthinder).

Cross-sectional types B and D

In case of cross-sectional types B and D, in which the base of the tidal sandbank is flat, the banks could have formed due to sand accumulation only, conform to the “type 1 banks” of Houbolt (1968) and Berné et al. (1994). In the case of type-D cross-sections, an extra erosion would be required in the swales, to make the basal layer stand out from

the seafloor as well. One has to bear in mind that, although an internal core is not present at the moment, and apparently the bank formed due to sand accumulation only, a core could have been present initially, before it got eroded due to sandbank migration as proposed by Snedden and Dalrymple (1999). So a flat base could be linked to strong erosion as well, in stead of to accumulation only.
The model for bank origin and evolution of Snedden and Dalrymple (1999) consists of: the formation of an initial irregularity by coastal or shelf processes, interaction of nearshore and/or shelf currents with the irregularity in the way described by the Huthnance hydrodynamic model (Huthnance 1982a), and subsequent evolution of the bank under continued current action. On the basis of the degree of evolution the authors categorise shelf banks into three classes: Class I – juvenile or stationary banks that retain their initial nucleus; Class II – banks that have migrated somewhat, eroding the initial irregularity, but that retain part of their nucleus; and Class III – "fully evolved" banks that have migrated sufficiently so that they contain no trace of their origin. Class I and II banks would correspond to "type 2 banks" (*sensu* Houbolt (1968) and Berné et al. (1994)): i.e. sand bodies that have migrated less than their width and thus retain part of their core, and have formed by erosion of older deposits.
A Class III bank, however, would correspond to a "type 1 bank" (*sensu* Houbolt (1968) and Berné et al. (1994)) morphostructurally (i.e. containing no internal core), but has migrated at least a distance equal to its own width, eroding the older deposits, so based on the evolutionary mechanism it would rather belong to "type 2" as well.

Distinguishing between accumulation and erosion

So disentangling the two mechanisms of accumulation and erosion, and linking the one strictly to a flat subsurface, and the other to the presence of a core, is probably an oversimplification. As accumulation can occur around a pre-existing core without the formation of the tidal sandbank being erosive (e.g. when the base of the U7 tidal sandbank is not erosional), and as extensive erosion by the tidal sandbank of older underlying deposits can leave a flat subsurface.
However, as was clear from the description of the banks on the BCS, an entire sandbank can in most cases not be classified under one type. So, the presence of different types of cross-sections along a single sandbank (s.l.) could help to distinguish between "only accumulation", or "extensive migration and erosion". In case no internal core is present on one cross-section, but present on a nearby cross-section of the same sandbank, most likely the section without the internal core was formed due to accumulation, as it is unlikely that along a linear sandbank, one part migrated over a large distance, eroding completely former deposits, while the adjacent part stayed more or less in situ, still protecting the underlying deposits. The differences in cross-sectional type can probably be explained by changes (different strengths) of the hydrodynamics in the swales along the bank (accumulation versus erosive migration towards the swales).
To distinguish between a core formed due to erosion by a migrating tidal sandbank, and a pre-existing core on which a tidal sandbank accumulated, will mostly depend on the characteristics of the base of the tidal sandbank. If the basal surface is clearly erosional, cutting through the original form of the underlying units (e.g. marine transgressive surfaces -which are erosional features themselves- or sand ridges), the core is most likely formed due to erosion by the tidal sandbank. Contrarily, if the underlying unit retains its original form, the overlying tidal sandbank is probably formed by accumulation. Initial morphologies of the underlying surface that can act as a core, and that can be more or less easily recognised are e.g. cuestas or scarps in the Top-Paleogene surface, or 'complete' storm-generated banks. The presence of a coarse-grained (gravel) lag at the base of a tidal sandbank is in some cases less suited for making the distinction between an erosive tidal sandbank or not, as scarps and cuestas in marine transgressive surfaces are covered by a coarse-grained layer anyhow.

Cross-sectional types through sandbanks and their origin: examples from the BCS

The Hinder Banks

The Hinder Banks consist north of the Offshore Scarp mostly of type C and D cross-sections, while south of the scarp the cross-sections are of type A (Fig.8.10A, Fig. 8.19B versus C). As C and D types are located next to each other, it is unlikely that one part migrated over a large distance, leaving no trace of an original core, while the adjacent part stayed more or less in situ, with a core still intact. Most likely local hydrodynamic differences in the swales caused in one location merely accumulation of the sand, while in adjacent areas the tidal currents were stronger, eroding the swales deeper, and forcing the tidal sandbanks to erosively migrate continuously deeper towards the swales.
In the bank SW in line with the Noordhinder, the northern part of U7 migrated in NW direction (based on the slope direction of the base of U7), while the southern part migrated towards the SE swale, which is still visible in the sinuous form of the bank. Also the U7 tidal sandbanks in the nearby NW arm of the Fairy Bank and the further offshore located nameless bank have migrated towards the NW according to the direction of the basal slope of U7, while the tidal sandbanks in the Westhinder and Oosthinder north of the scarp have migrated in SE direction. The southern extremity of the tidal sandbank in the Oosthinder, south of the scarp, has mainly migrated towards the NW. The southern part of the Westhinder has grown wider in opposite directions towards the swales, such as the northern part of the Blighbank and the 'Bank Zonder Naam'.
The sharp contrast between the northern sections of the Hinder Banks, which are typically characterised by type-C and type-D cross-sections with IVDB Eemian basal layers below the U7 tidal sandbanks, and the southern sections which are characterised by type-A cross-sections, in which the bank s.l. corresponds to the tidal sandbank, with a core of Paleogene material underneath (Fig. 8.10A), is due to the presence of easily erodible material in the swales north of the scarp (IVDB Eemian), while south of the scarp the platform consists of stiff clays of the Paleogene subsurface (Fig. 8.19B versus C). After the Eemian and Holocene transgression, which levelled the IVDB Eemian deposits with the Paleogene clays, the Hinder Banks s.s. and in-between swales formed across the scarp (partly as pure accumulations, and partly erosively down the swales). In the section north of the scarp, however, the swales were deeper eroded in the softer material than in the stiff clays south of the scarp, which made the banks stand out more from the seafloor in the north, forming a bank s.l. with a basal Eemian layer below the tidal sandbanks s.s. (types C and D), while in the southern part the banks s.l. correspond to the tidal sandbank s.s. overlying a Paleogene core. Due to this differential erosion, the scarp is again visible in the present-day bathymetry in the swales in between the banks, since the time it was infilled by Eemian deposits.
The difference between the northern section, often consisting of a flat surface below the tidal bank, and the southern section, which always shows a core, is most likely due to a difference in availability of sediment. In the northern section, easier erodible material is present so the banks are more often characterised by accumulation, while in the southern section probably only a thin cover of a transgressive sand sheet was present on top of the Holocene marine transgressive surface, making the sediment supply limited, causing the erosive character of these bank sections (Berné 2002).

The Zeeland Ridges

The Akkaertbank and Gootebank s.s. are moribund storm-generated or shoreface-connected ridges (the Akkaertbank with a clearly landward migration direction), which have been partly remodelled by present-day tidal currents (forming sand dunes). The initial position of these banks is not only related to the position of a former coastline, but is most likely also linked with the presence of cuestas in the Top-Paleogene surface, which are still clearly visible at the NE ends of the banks (Fig. 8.18B). The Akkaertbank and Gootebank are probably initially formed by accumulation on top or in the shade of a pre-existing Paleogene core, as was also suggested by Maréchal and Henriet (1983) and Mostaert et al. (1989). Although probably later the tidal sandbanks acted erosively as well, eroding the original marine transgressive surface and cuesta, migrating towards the swales (Fig. 8.18B). Some parts of the Gootebank s.l. and the Akkaertbank s.l. consist not only of the tidal sandbank s.s., but also of a Paleogene or Eemian layer at the base. So the tidal sandbank s.s. is formed by accumulation on an initial core, as well as erosion of older units, and makes part of a bank s.l. which is partly shaped due to additional erosion in the swales and partly by the presence of the cuestas (Fig. 8.19B).

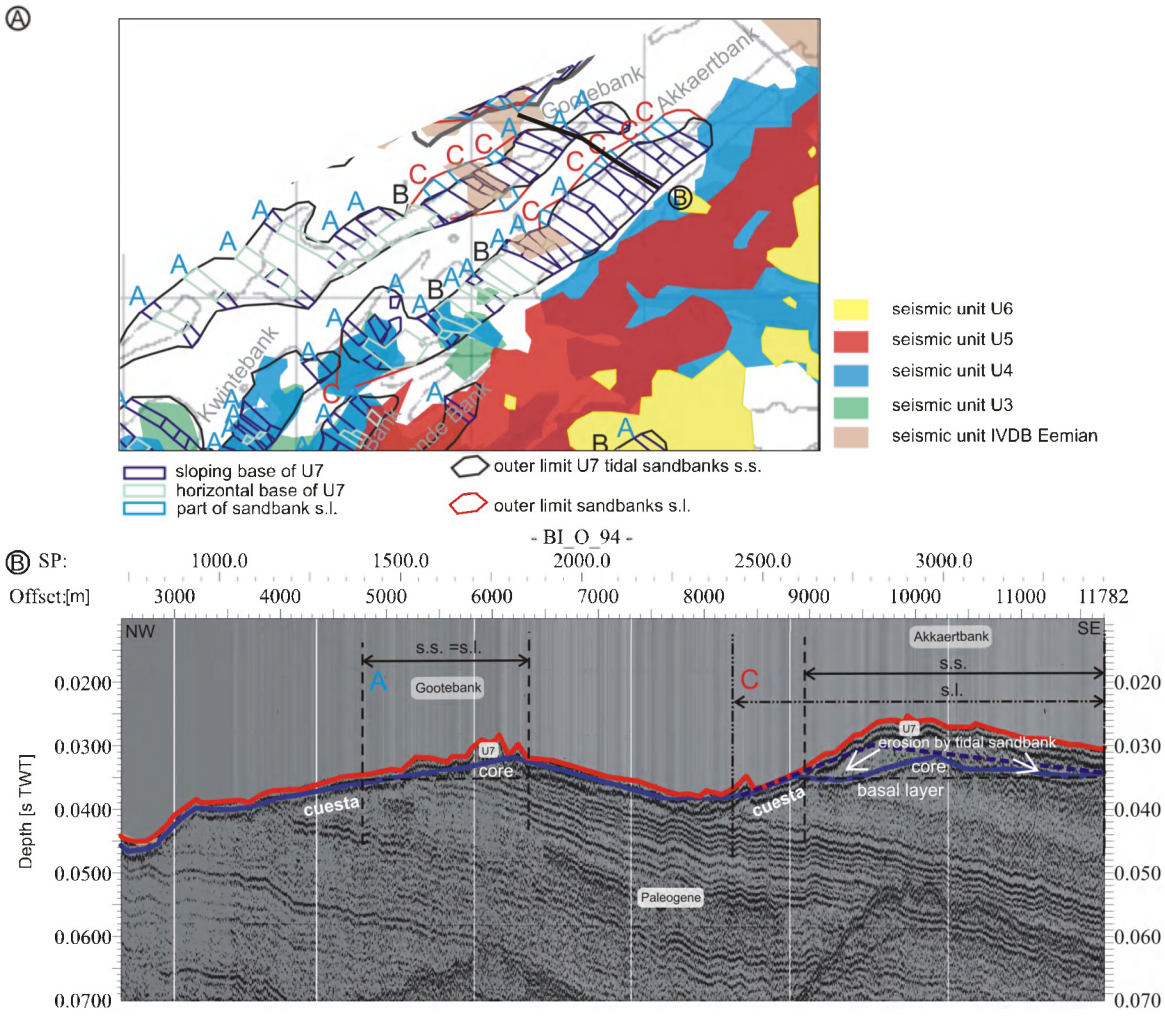

Fig. 8.18 (A) Positioning of the seismic profile presented in (B). (B) The initial position of the Akkaertbank and Gootebank is not only related to the position of a former coastline, but is also linked with the presence of cuestas in the Top-Paleogene surface. The Akkaertbank and Gootebank are initially formed by accumulation on top or in the shade of a pre-existing Paleogene core, but later the tidal sandbanks acted erosively as well, eroding the original cuesta (dark blue dashed line), migrating towards the swales.

The Thorntonbank s.s. has been clearly erosive, migrating for the major part in SE direction, and at the SW extremity in NW direction, but could as well be linked to a channel in the Top-Paleogene surface, which could have induced the initial position and accumulation of the bank.
The main part of the Thorntonbank is a type-C bank, while the SW section of the bank has a typical type-A cross-section. In the NE part, the sediments present at the base of the bank s.l. are easier erodible, consisting of Eemian (IVDB) (to possibly Weichselian or Holocene) deposits, and form a basal layer and core below the U7 tidal sandbank. While in the SW, the U7 tidal sandbank rests directly on top of the Paleogene substrate and shows no basal layer because the Paleogene is here not as much eroded in the swales as in the northern part.

The Flemish Banks

In most parts, the Oostdyck s.l. consist entirely of the U7 tidal sandbank located on a flat subsurface (type B), but in some parts the subsurface forms a small elevation below U7 (Figs. 8.10A and 8.19D). So most likely the Oostdyck tidal sandbank was for the major part formed in situ due to accumulation. As some parts still show a core below the bank, the bank could not have migrated over a long distance. Where the bank s.s. shows a sloping subsurface, it is mostly oriented in offshore direction, so most likely the bank grew in NW direction towards the offshore swale. The Buiten Ratel, however, consists almost entirely of type-A cross-sections. The U7 tidal sandbank overlies a core of U4 Holocene tidal-flat and U3 Eemian deposits, and has for the major part grown in two opposite directions towards the swales. Although the thicker main body can show a single NW-ward erosive migration as well. According to Maréchal and Henriet (1983) the initial location of the Buiten Ratel and Oostdyck might be related to slope breaks in the abrasion surface (Middle Scarp and valley wall of the former Ostend Valley).
Also the Kwintebank (except from two cross-sections of C type), the Middelkerke Bank, the Oostende Bank and Smalbank consist entirely of A type cross-sections, in which the sandbank s.l. consists only at the top of the U7 tidal sandbank, while the underlying core consists of older e.g. tidal-flat deposits (Figs. 8.10A and 8.19D). The U7 tidal sandbank in the Kwintebank migrated in two opposite directions towards the swales, such as in the Oostende Bank, where the two opposite sloping banks occur. In the Smalbank on the other hand, the tidal sandbank has an overall NW oriented migration direction, such as in the Middelkerke Bank, which only shows opposing migration directions at its most NE extremity. It is possible that the U7 tidal sandbank in the Middelkerke Bank initially formed at the higher positioned U5 deposits at its SW end (Fig. 8.10A), prograded offshore, and grew progressively longer towards the NE in the direction of the dominating flood current. According to Trentesaux et al. (1999), over a long period, the northern end can become detached, giving rise to an isolated tidal sandbank.

Although between the Kwintebank, Middelkerke Bank and Oostende Bank easily erodible sediments are present (U5, U4, U3), the banks have a typical A-type cross-section and not C- or D-type as was the case in the Hinder Banks (except for the two profiles through the Kwintebank Fig. 8.5G). The swales between the Kwintebank, Middelkerke Bank and Oostende Bank are less deep incised than the swales in the Hinder Banks area (compare Figs. 8.3B and 8.5), and they show even infillings of U7 (redistributed) deposits (Fig. 8.5 FGI). Most likely the tidal currents between the offshore Hinder Banks are (have been) stronger than between these nearshore Flemish Banks, or less sediment was available in the offshore area, which caused the deeper scoured swales.

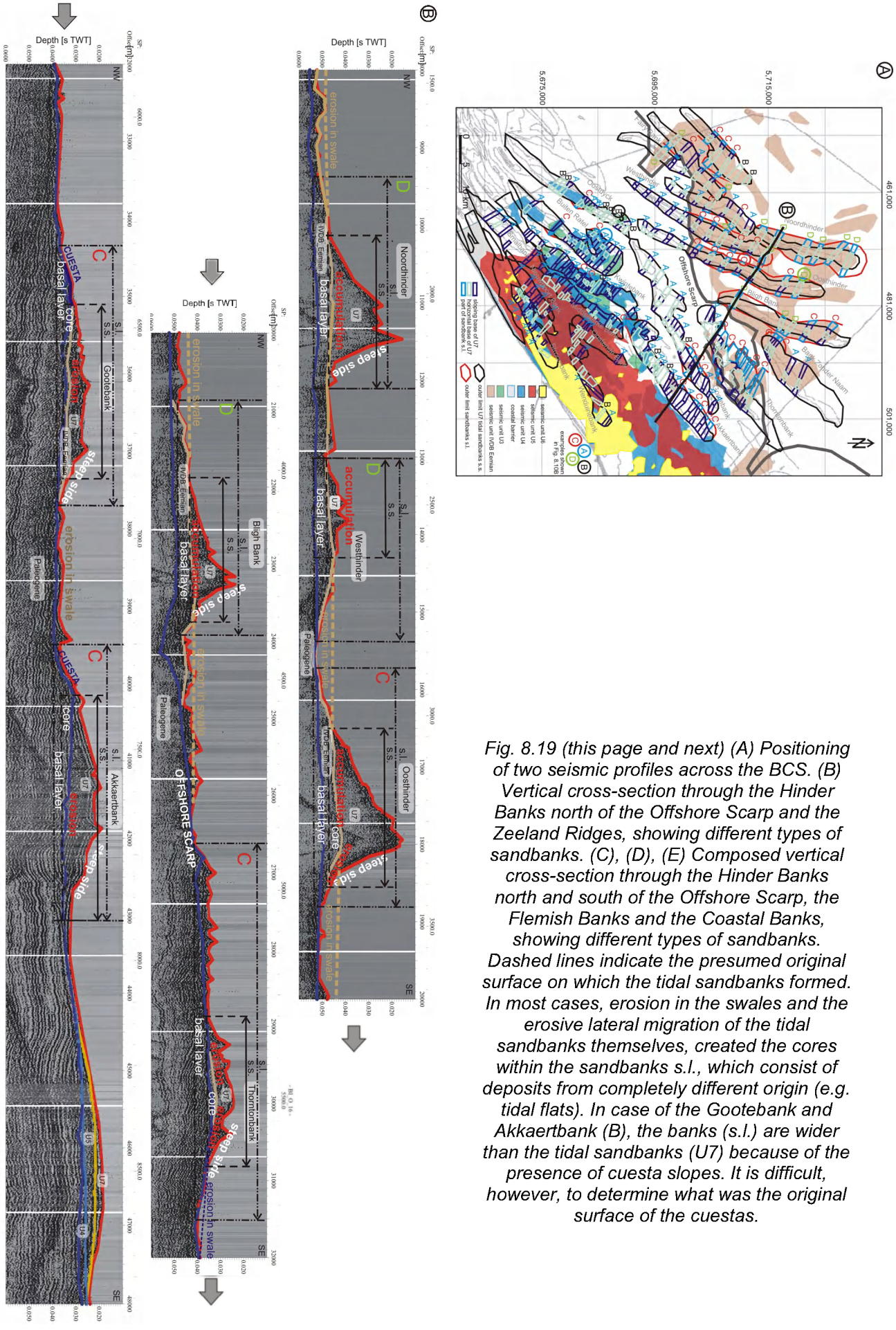

Fig. 8.19 (this page and next) (A) Positioning of two seismic profiles across the BCS. (B) Vertical cross-section through the Hinder Banks north of the Offshore Scarp and the Zeeland Ridges, showing different types of sandbanks. (C), (D), (E) Composed vertical cross-section through the Hinder Banks north and south of the Offshore Scarp, the Flemish Banks and the Coastal Banks, showing different types of sandbanks. Dashed lines indicate the presumed original surface on which the tidal sandbanks formed. In most cases, erosion in the swales and the erosive lateral migration of the tidal sandbanks themselves, created the cores within the sandbanks s.l., which consist of deposits from completely different origin (e.g. tidal flats). In case of the Gootebank and Akkaertbank (B), the banks (s.l.) are wider than the tidal sandbanks (U7) because of the presence of cuesta slopes. It is difficult, however, to determine what was the original surface of the cuestas.

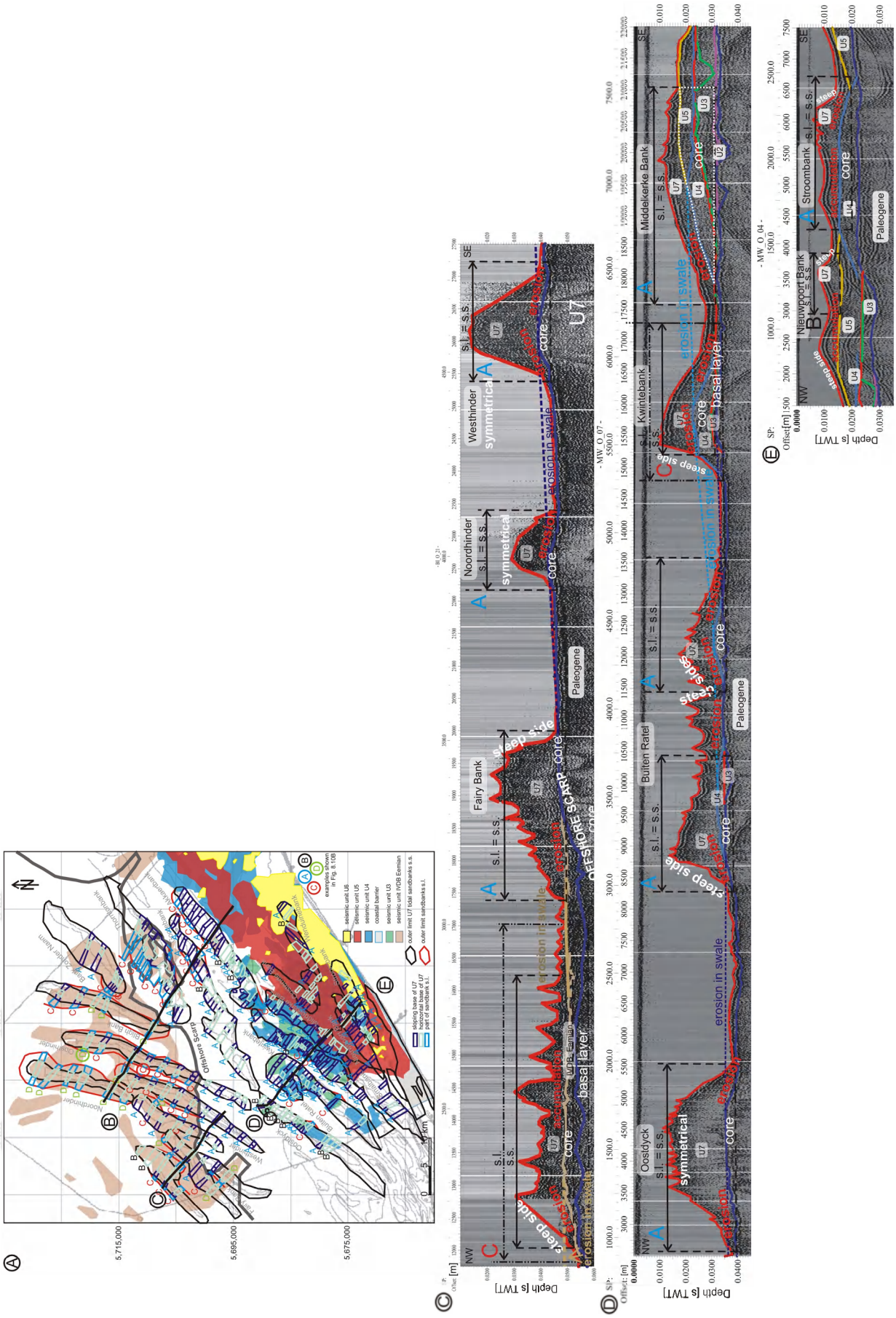
A
B
C
D
E
Oostdyck
Buiten Ratel
Fairy Bank
Noordhinder
Westhinder
Middelkerke Bank
Kwintebank
Nieuwpoort Bank
Stroombank
Paleogene
basal layer
core
erosion in swale
steep side
symmetrical
s.l. = s.s.
Depth [s TWT]
Offset [m]
SP:
NW
SE

The Coastal Banks

The Nieuwpoort Bank, Stroombank and Wenduinebank s.s. represent shoreface-attached ridges with a clearly landward-oriented migration direction, based on the internal prograding reflectors. They almost completely consist of A type cross-sections, i.e. the bank s.l. consists entirely of the sandbank U7 covering a core of U6, U5 sand ridges or U4. The Wenduinebank and Stroombank s.s. are (or recently have been) connected to the shoreface, but the Nieuwpoort Bank s.s. lies about 5 km offshore the present-day coastline. An option for the formation of this bank is the process of ridge multiplication, from e.g. the Stroombank s.s.. But as ridge multiplication implies an offshore movement and modification of the outermost bank, mostly aided by retreat of the shoreline (Dyer and Huntley 1999), this option can be rejected because the Coastal Banks s.s. show a clear shoreward prograding (growing) reflection pattern. Neither could the Nieuwpoort Bank s.s. start off as a shoreface-connected ridge, becoming detached as the coast retreated, because the bank overlies the U5 middle ridge which developed until 7000 cal BP, and at that time the coastline was already located far more landward. So most likely the Nieuwpoort Bank s.s. developed simultaneously with the Stroombank and Wenduinebank s.s. as a response of the sea bed to a suitable hydraulic regime of wave (storms) and tide. The latter formed on top of U6, which started depositing after the mid 16th century.

From the seismic data it was observed that the Stroombank s.s. changes in SW direction from a sharp-crested bank with landward-oriented steep side and offshore-oriented gentle side, into a rounded symmetrical bank, whereas at its most SW extremity adjacent to the Westdiep Swale, the bank has an opposite facing steep and gentle side (Fig. 8.6FEDC). While throughout the bank the internal reflection pattern stayed the same, i.e. landward-sloping prograding reflectors. This phenomenon is a confirmation that the direction of the steep side of a sandbank does not indicate the migration direction of the sandbank, but is merely dependent on the strength of the tidal currents in the adjacent swales. What does indicate the former migration or growth direction of a sandbank, is the direction of internal prograding reflectors (which on the BCS coincides with the slope direction of the erosional base of the U7 sandbank). As the innermost, lowest reflector has been formed before an overlying, more outer located reflector, the direction of the successive reflectors indicates the growth or sediment transport direction of a bank during its formation, which does not have to be the same direction as the present-day sediment transport or growth direction, as tidal sandbanks are considered stable structures nowadays (Veenstra 1964, Houbolt 1968, De Moor 1985b). In case of the Middelkerke Bank s.s., the prograding bedding represents alternating phases of erosion and deposition along the steep slope of the bank controlled by the combination of wave activity and wind-driven and tidal currents (Berné et al. 1994). Preservation of inclined reflectors requires a net deposition along the NW flank of the Middelkerke Bank s.s., while the SE flank is mainly characterised by erosion (topflat terminations), which implies a net migration of the bank. Berné et al. (1994) concluded that the orientation of the inclined reflectors within U7 in the Middelkerke Bank can be used as an indicator of the long-term movement of the bank.

Although in the past the directions of asymmetric profiles of sandbanks have been used to define the large scale sediment transport pattern for the Southern Bight of the North Sea (Kenyon et al. 1981), many arguments exist to prove that in fact the steep slope can be considered as an erosional surface and is merely created by the stronger tidal current along that flank (Houthuys 1989, Van Lancker 1999, Deleu 2001, Lanckneus et al. 2001). Another example is the Smalbank s.s., which shows an overall offshore-directed steep side, while at its SW end adjacent to the relatively deep scoured Westdiep swale, the steepest side is located landward (Fig. 8.5FDCB). Sandbanks can show an inversion of the steep side direction along their length, with a symmetrical cross-section in the

transitional section between the two, e.g. the SW ends of the Noordhinder s.s. extension, the Westhinder s.s., the Smalbank s.s., and a single cross-section through the Buiten Ratel s.s. have a steep side opposite to the general direction. This inversion is probably due to lateral changes in the strength of the tidal currents along the length of the swales adjacent to the banks, which might also explain the symmetrical NE extremities of the Hinder Banks s.s. (upstream ends of the residual sediment transport direction in the Hinder Banks).

Fig. 8.19 shows two vertical cross-section through the BCS, with an overview of the different types of sandbanks.

Origin of the sediments forming the U7 tidal and shoreface-attached sandbanks

Probably most of the material of which the U7 banks are build up originates from local erosion of underlying sediments, what can be deduced from the often erosional character of the base of the banks and the presence of deeply incised swales in between. This was also presumed by Stride (1989) for the Kwintebank (s.s.) and Buiten Ratel (s.s.), although he also suggested an additional mechanism of providing sand for the construction of the sandbanks, i.e. sand brought into the region as a result of occasional storm surges, and the slow net mean drift of water. Also Belderson (1986) states that the main effect of storm action in strongly tidal seas is to greatly supplement sand transport rates. But it was presumably the removal of much of the older Holocene deposits, as well as some underlying material that has supplied the sediment that makes up the later Holocene deposits (Stride 1989).
A suggestion of Laban and Schüttenhelm (1981), that the Dutch Zeeland Ridges (s.s.) are build up of Holocene sands originating from the English Channel is discounted by Stride (1989). The presence of Angulus pygmaeus fauna in the modern banks was cited as evidence by Laban and Schüttenhelm (1981) that these shells were probably transported from the English Channel, where they are relatively common, along with sand, pebbles of chalk and chert. Stride (1989) suggests, however, that the fauna could have entered the Southern Bight as spat, carried there by the known slow northerly drift. Moreover because the shells are too fragile to be transported over such a long distance, especially together with pebbles.

In the nearshore part, the underlying deposits being eroded by the tidal sandbanks and shoreface-connected ridges mainly consist of Eemian U3 estuarine, Holocene U4 tidal-flat and U5 sand ridge sediments, the latter formed in the nearshore part of the Holocene transgressive sand sheet. While further offshore, the banks consist most likely only of remnants of a former transgressive sand sheet left after the Holocene transgression. This sheet itself probably consisted of remnants of the earliest Holocene tidal-flat deposits and maybe of underlying remnants of the former Eemian transgressive sand sheet (if not removed during the Weichselian lowstand), which were reworked by the Holocene open marine transgression during the initial fast relative sea-level rise. An additional amount of material was available north of the Offshore Scarp in the form of easily erodible IVDB Eemian deposits below the Holocene and Eemian marine transgressive surface. While south of the scarp probably also the erosion of the Paleogene substrate contributed material.
This was also stated by Houbolt (1968, Houthuys 1989): the sand of which the Hinder Banks are composed was already present in the area before the Holocene marine transgression started and it is not derived directly from a retreating shore. Heavy mineral investigations (Baak 1936 in: Veenstra 1964, Houbolt 1968, Schüttenhelm and Laban 2005) showed that the sands making up the Hinder Banks are originally Rhine/Meuse-derived, deposited in this area by river action during periods of lower sea level. During and after the post-glacial transgression of the North Sea, the tidal currents reworked part of these deposits into the present-day sand ridges.

Possible origins for the gravelly material in the swales between the sandbanks have been suggested in Chapter 5. Former gravelly valley or lake deposits (Paleogene rivers, Elsterian proglacial lake, Saalian proglacial lake, Saalian Meuse, Ostend Valley, Weichselian Rhine/Meuse, Thames), and in situ coarse-grained material within the Paleogene substrate itself (concretions, sandstone banks) have been cut by the retreating shoreface, and redistributed by the Eemian and Holocene transgression. In general, the gravel is overlain by several metres of sand, but in areas of strong storm or tidal currents the transgressive sand sheet is discontinuous or lacking altogether. So that the basal gravels, Holocene back-barrier deposits or older Pleistocene or Paleogene deposits are exposed in windows through the sand sheet.

In the offshore area, the Pleistocene and Paleogene are exposed in the swales between sandbanks, while in the nearshore Flemish Banks region U7 shows a sand sheet in the swales. There are two possible causes: (1) less sediment was available in the offshore area, which caused the deeper scoured swales, or (2) the tidal currents between the offshore Hinder Banks are (have been) stronger than between these nearshore Flemish Banks.

(1) When during the Early Holocene (from 12,500 cal BP) rising sea water entered the southern part of the North Sea through the Strait of Dover in the south and through channels along the Dogger Bank in the north, coastward sediment transport could not keep pace with the rapid rise in sea level and the relict landscape drowned rapidly (van der Molen and van Dijck 2000). This might have caused the absence of extensive tidal-flat or storm-generated ridge deposits in the offshore area, leaving only a thin sediment sheet. This in contrast to the more nearshore area, which drowned later, at a slower pace, leaving time for the development of extensive tidal-flat deposits and storm-generated ridges. Moreover, at greater water depths, sandbanks build higher (are thicker), and more sediment was needed. And in the absence of sufficient sand to construct sandbanks, a gravel sheet or scoured pavement exists, rather than a sand sheet (Belderson 1986), such as in the swales in the nearshore area.

(2) It is also possible that in the offshore area stronger currents are active (removing more sediment) than in the nearshore area. However, in general the fastest tidal currents occur in coastal areas because onshore shallowing increases the tidal range and decreases the cross-sectional area (Dalrymple 1992). Still, strong tidal currents may also occur on the outer part of the continental shelf if the offshore increase in the volume of water flowing through any shore-parallel section is not compensated by a sufficient increase in water depth (Dalrymple 1992). This could be the case on the BCS, as it makes part of a shallow epicontinental sea without a shelf break. Model results indeed show that present-day current velocities increase towards the Deep Water Channel (Lanckneus et al. 2001).

8.3.3 Paleo-reconstructions and chronostratigraphic framework

Possible arguments for a relative dating

As absolute dating of the U7 tidal and shoreface-connected sandbanks is not possible because of the strong reworking of datable material (shells, peat fragments), indirect indications for a relative dating have to be found. The grouping of the sandbanks with similar orientation could be taken into account, assuming that all banks in one group are formed in a same time frame and in a similar setting. Also the roundness of the bank crests, the slope of the steep side, and the absence of sand dunes might give a clue about how active a sandbank group still is, and maybe give an indication on their relative age. Although we have seen that rounded banks as the Zeeland Ridges (Goote and

Akkaertbank), can be covered by active sand dunes. According to Snedden and Dalrymple (1999), the presence or absence of an internal core could make a distinction between juvenile and fully evolved banks. But here the possibility of merely local accumulation on a flat surface is not taken into account, as e.g. in the Hinder Banks. Except for the Noordhinder, all the ridges on the BCS contain an internal core to a more or lesser extent, and have formed rather locally.
The presence of the typical Angulus pygmaeus mollusc association (Spaink 1973) in the U7 tidal and shoreface-connected banks points to an Atlantic age (8000-5000 cal BP) (Laban and Schüttenhelm 1981), but does not allow a more precise age. Moreover, due to strong reworking of the sediments this age indication is only a maximal value. The presence of Petricola pholadiformis (American piddock) suggests of deposition after 1900 AD.

More reliable indications for a relative dating of the sandbanks are: (1) the positions of former coastlines. As sandbanks can only start forming seaward of a coastline, and assuming that the sandbanks on the BCS are formed rather locally, the present position of a sandbank relative to a former coastline could give a clue about its maximal age. (2) The age of the underlying sediments on which the U7 banks formed. And (3), the hydrodynamical constrains for the formation of tidal sandbanks. Tidal sandbanks can only develop when the surface tidal currents exceed 50 cm/s (Belderson 1986, Galloway and Hobday 1996). Tidal sandbanks, in equilibrium with the present-day hydrodynamic conditions, could only have started to develop about 7000 cal BP, when the tidal regime reached macro-tidal conditions similar to the present-day situation (van der Molen and van Dijck 2000). Before that time, probably smaller structures like shoreface-attached ridges could have formed close to the coastline.

A chronostratigraphic framework

Around 9500 cal BP, already all of the Hinder Banks, the Thorntonbank, Gootebank Oostdyck and Buiten Ratel would have been located offshore the coastline of that time (Fig. 8.20). Before that period, the sea invaded the Southern Bight rather fast, possibly leaving not much time for the formation of shoreface-attached ridges at the fast landward migrating coastline. Tidal regime was also microtidal, with negligible wind action, so there was little change for the formation of these banks before that time. From 9500 cal BP onward, wave action was strong enough for the formation of a barrier, so also shoreface-connected ridges might have started forming. Around 8900 cal BP, also the Akkaertbank and Kwintebank would have been located offshore the coastline of that time. And by 8000 cal BP, the coastline had already migrated landward of the position of all of the present sandbanks, except for the Coastal Banks (Fig. 8.20).

On the basis of their dimensions and morphology, the Akkaert and Gootebank s.s. have been interpreted as moribund shoreface-connected ridges or storm-generated ridges, which became detached when the coastline retreated. If their position stayed more or less the same while the shoreline receded, the Gootebank s.s. could have started to develop around 9500 cal BP when the shoreline was located in that region, and the Akkaertbank s.s. started developing around 8900 cal BP when the coastline had already retreated further landward. As the Akkaertbank s.s. lies more or less in line with the U5 outer ridge (Fig. 8.20), the Akkaert and Gootebank s.s. might belong to the same group as the U5 storm-generated ridges.

The Middelkerke Bank, Oostende Bank, and Smalbank s.s. are located on top of the U5 outer and middle storm-generated ridges which have an age of 8400-7700 and 8000-7000 cal BP respectively, hence these banks could only have formed after that time. Therefore, it is most likely that the tidal sandbanks of the Flemish and Hinder Banks started to develop around 7000 cal BP, at a time when the tidal regime reached the

present-day macrotidal range. This period was also characterised by a change in the net-sand transport pattern, before 7000 cal BP the sediment transport was mainly directed shoreward, while from that period on the tidal wave and related transport became along-shore (van der Molen and van Dijck 2000). This might explain the difference in orientation between the Zeeland Ridges which are more or less oriented coast-parallel and which were formed when the sediment transport was shoreward directed, while the Flemish Banks and Hinder Banks are oriented at an angle with the present-day coastline, and make a small oblique angle with the prevailing peak tidal flow direction (which is NE-ward in the near-coastal zone, and SW-ward along the Hinder Banks) (Lanckneus et al. 2001), which is characteristically for a tidal sandbank (0-20° but mostly 7-15° in: Kenyon et al. 1981, Belderson 1986, Dyer and Huntley 1999).
The Thorntonbank s.s. which lies parallel to the Goote and Akkaertbank s.s., but which is clearly a tidal sandbank and not a storm-generated ridge, might have started to form when the sediment transport was still directed onshore, but when tidal currents were already strong enough to form tidal sandbanks in the deeper offshore areas (shortly before 7000 cal BP?).

The Coastal Banks s.s. have only formed in a final phase, on top of U6. So after a hydrodynamic equilibrium was reached following the widening of the Western Scheldt and the settling of the U6 sediments, i.e. after the 16th century.

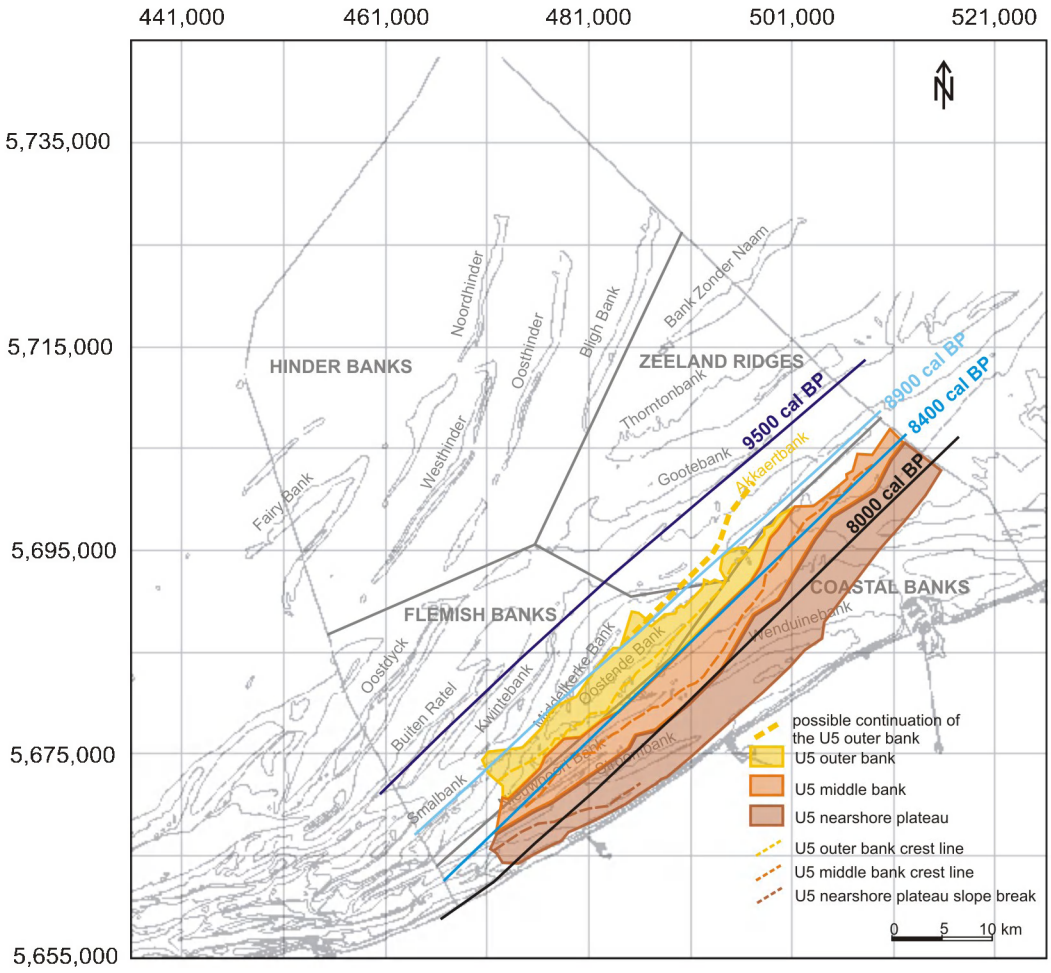

Fig. 8.20 Position of the sandbanks with respect to former coastlines. Note how the Akkaertbank lies in line with the U5 outer sand ridge. On the basis of their dimensions and morphological characteristics, the Gootebank and Akkaertbank are storm-dominated or former shoreface-connected ridges, and most likely belonged to the U5 sand ridge sequence.

For the moment the tidal sandbanks are considered stable, which appears from extensive repeated studies on the morphology of individual sandbanks over the last decades (Veenstra 1964, Houbolt 1968, De Moor 1985b). But it turns out that sand dunes on top of the banks are migrating actively, which is also demonstrated by the finding of a shampoo glass bottle at a depth of 3.5 m below the seafloor in a large dune field at the northern end of the Middelkerke Bank (Trentesaux et al. 1999).

General remarks about the time frame of the formation of the tidal sandbanks

That the Hinder and Flemish Banks s.s. likely belong to the same sandbank system, and probably have been formed from the same time onwards, might be confirmed in the fact that there seems to be a continuation between the Hinder Banks and the Flemish banks s.s., more than between the Hinder Banks and the Zeeland Ridges s.s. although located at the same distance offshore the coastline as the Flemish Banks. Not only the Hinder and Flemish Banks s.s. have similar spacings, widths, lengths and orientation, also the position of the crest lines becomes gradually shallower from the Hinder Banks s.s. over the Flemish Banks s.s. with decreasing water depth, while the Zeeland Ridges s.s. are relatively located deeper. It also confirms once more that the Zeeland Ridges s.s. have a different origin than the Hinder and Flemish Banks s.s., which are clearly related.
Indeed, according to van de Meene and van Rijn (2000), an important feature of many sandbank systems is the lateral coherence of the individual sand bodies. Shelf-sand bodies almost always occur in fields, often with a very constant spacing between the ridges. Although the factors controlling this lateral coherence are still largely unknown, three possible modes of formation of ridge fields have been recognized. (1) Sandbank systems may have formed diachronously, as a response to a steady change in conditions such as flooding of an area and shoreface retreat due to sea-level rise. This is not the case for the Hinder or Flemish Banks s.s., as the shoreface was already located much further landward by the time they could have formed (after development of U5 sand ridges). (2) Alternatively, they may have formed simultaneously, as a response of the sea bed to a suitable hydraulic regime, which is believed to have happened in the case of the Hinder and Flemish Banks, around 7000 cal BP. Or (3) by the process of `sandbank multiplication' (Caston 1972, Dyer and Huntley 1999). The latter, however, requires migration of the newly formed banks, and as most of the banks s.s. on the BCS show an internal core (with an erosional basal slope in opposing directions towards the adjacent swales), indicating that they could not have migrated very far, this process could only have been subordinate. It could have taken place, but only as an additional process, for banks s.s. with a flat base or an erosional base in only one direction (e.g. the Oostdyck, Noordhinder).

The proposed time frame for the formation of the Flemish Banks s.s. contradicts the suggestion of Dyer and Huntley (1999), that the Flemish Banks and the ridges in the Baie de la Somme may have been formed during the widening of the Dover Straits and erosion of the coastline to the east and the west of Cap Gris Nez, and represent in fact Type 3B ridges. By the time the Flemish Banks s.s. could have started to form, thus after the development of the U5 sand ridges, i.e. around 7000 cal BP, the coastline was already located far from the Flemish Banks, so they are not directly linked to coastline erosion or shoreface retreat. So in contrast to the Zeeland Ridges s.s., which are probably (reactivated) relict features created during the post-glacial sea level rise, the Flemish Banks are most likely formed as a response to the hydrodynamic and sediment regime similar to that presently active (dynamic features created by modern shelf processes). As also Belderson (1986) stated, the existence of tidal sandbanks is depending on the availability of sand in an area with surface peak tidal currents exceeding 90 cm/s (the sand ribbon zone), rather than on shoreline migration.

A time frame for the probably simultaneous start of the developing of the Hinder and Flemish Banks s.s. is proposed, but within each group it is uncertain whether some banks formed first and others last due do a process of multiplication, or whether they all formed concurrently. As already stated, the process of multiplication implies migration of the newly formed banks, and as most of the banks s.s. on the BCS show an internal core (with an erosional basal slope in opposing directions towards the adjacent swales), indicating that they could not have migrated very far, this process could only have been subordinate. It could have taken place, but only as an additional process, for banks s.s. with a flat surface or an erosional base in only one direction, e.g. the Oostdyck and Noordhinder.
But these most offshore banks (of the Flemish and Hinder Banks respectively), are not per definition the oldest, as would be the case if they were formed at a retreating coastline (e.g. the Zeeland Ridges s.s.). Although they are the thickest banks with the smallest or no core. The presence of a smaller core could be due to the very thin sheet of older sediments offshore in the first place, as few material has been deposited there during the initial very fast rising sea-level. These banks are maybe the highest because they are located in the deepest sections or where the strongest tidal currents occur, and not because they are older. According to Stride (1989) the westerly increase in the height of successive banks in the group of the Flemish Banks, and in the same direction the progressively clearer swept swales, were indications of an increasing strength of the tidal currents in that direction.

What remains a question as well, is why the Zeeland Ridges have not adapted more to the prevailing tidal currents, apart from the formation of sand dunes. As the present residual sediment transport direction over the Flemish Banks and Zeeland Ridges is in NE (flood-dominated) direction (Lanckneus et al. 2001), it is possible that most of the available sediment was captured by the Flemish Banks, and not enough sand reached the Zeeland Ridges. The orientation of the Zeeland Ridges is most likely a relict pattern of the orientation of the shoreface-connected ridges, which may locally be traced for tens of kilometres offshore (Swift et al. 1973).

8.4 Limitations, innovations and recommendations

8.4.1 Innovations

Before the present study, relatively little was known about the mechanisms and timing of the formation of the tidal sandbanks (seventh seismic unit) on the BCS, and of the 'banks' as a whole (i.e. as a morphological feature, including not only the tidal sandbank deposits at the top, but also older units at the base). Also, the reason for the differences in orientation of the four main sandbank fields (i.e. the Hinder Banks, the Flemish Banks, the Zeeland Ridges and the Coastal Banks) still remained unclear.

Over the years, several studies addressed the processes involved in the initiation of the formation of sandbanks. Houbolt (1968) and Berné et al. (1994) described the existence of two basic types of (tidal) sandbanks: (1) banks formed by sand accumulation only, resting on an essentially flat surface and showing no internal core, and (2) banks with an internal core consisting of eroded fluvial or estuarine sediments of early Holocene or Pleistocene age, which are partly formed by erosion of these older deposits and are not shaped by accumulation only.
However, disentangling the two mechanisms of accumulation and erosion, and linking the one strictly to a flat subsurface and the other to the presence of a core, is an oversimplification. A sandbank can consist of other sediments than tidal sandbank

deposits at its base (an internal core), but still the overlying tidal sandbank can be deposited by accumulation only on an originally flat surface. In that case the lower part stands out from the surrounding seafloor, i.e. forms part of a 'bank', owing to erosion in the surrounding swales. Also, accumulation can occur around a pre-existing core without any erosion related to the formation of the tidal sandbank., Finally, extensive erosion of older underlying deposits by the tidal sandbank can leave a flat subsurface as well (Snedden and Dalrymple 1999). The present, detailed study of the sandbanks on the BCS has revealed that an entire sandbank can, in most cases, not be classified under one type.
Therefore a new classification scheme with four types of cross-sections (types A, B, C and D) was developed. The classification is based on the slope of the basal reflection of U7. It furthermore distinguishes between a tidal sandbank *sensu strictu* (s.s.) (i.e. in the strict sense of a sandbank structure formed by strong tidal currents in an open-shelf environment), and a bank *sensu lato* (s.l.) (i.e. in the broad sense of an elevated morphological feature above the present-day seafloor) in which the lower part of the bank has a very different origin than a tidal sandbank (e.g. tidal flats or estuarine deposits) but stands out from the surrounding seafloor because of erosion in the surrounding swales.

The distinction between a core formed by erosion in a deepening swale and a pre-existing core on which a tidal sandbank accumulated, must be made on the basis of the characteristics of the base of the tidal sandbank. If the basal surface is clearly erosional, cutting through the original form of the underlying units (e.g. marine transgressive surfaces -which are erosional features themselves- or sand ridges), the core is most likely formed as a result of erosion by the tidal sandbank. If the underlying unit has retained its original form, the overlying tidal sandbank is probably formed by accumulation. Initial morphologies of the underlying surface that can act as a core, and that can be recognised fairly easily, include cuestas or scarps in the Top-Paleogene surface, or 'complete' storm-generated banks. The presence of a coarse-grained (gravel) lag at the base of a tidal sandbank is not always suited for making the distinction between an erosive and a depositional tidal sandbank, as scarps and cuestas in marine transgressive surfaces are commonly capped by older coarse-grained lags.

On the BCS, most of the tidal sandbanks show an erosional base sloping in opposing directions towards the adjacent swales. This systematic pattern implies that the tidal sandbanks exhibit an erosive migration or growth over the underlying units in the direction of the adjacent swales. So, probably most of the material of which the U7 banks are built up originates from local erosion of underlying sediments.
With the formation of the tidal sandbanks, the originally regionally deposited older deposits got fragmented because of erosion in the swales between the sandbanks, a clear expression of sediment reworking under sediment-starved conditions. In most cases on the BCS, the core below a tidal sandbank is most likely a remnant of older deposits that has not (yet) been eroded by the overlying developing tidal sandbank, and not, as has been generally believed, that tidal sandbanks formed on top of existing highs that had been formed beforehand. A small nucleus was indeed probably needed for the start of the bank development, but the large internal cores that are currently present below the tidal sandbanks are most likely the result of a continuing process of constantly deepening swales and increasing growth and migration of the banks towards the swales. The tidal sandbanks now act as a (temporal) protection of the older cores (Mostaert et al. 1989, Berné et al. 1998), as they are considered relatively stable at present (Veenstra 1964, Houbolt 1968, De Moor 1985b).

8.4.2 Recommendations

Absolute dating of the U7 tidal and shoreface-connected sandbanks was not possible because of the strong reworking of datable material (shells, peat fragments). Instead, indirect indications for a relative dating were used. Studies in neighbouring countries have shown that age constraints are possible by focussing on juvenile shells that are prone to damage when transported repeatedly and over significant distances. When series of ^{14}C ages are in the correct order, they can be used as semi-quantitative indicators of sandbank age. It is also recommended to conduct future studies on the origin and age of tidal sandbanks in the larger evolutionary framework of the shelf because the position of former coastlines and the age of underlying deposits can give important clues.

Furthermore, it is advised to pay attention to the continuity within and between tidal sandbank fields, by measuring and comparing in detail the tidal sandbank widths, lengths, depths of crest lines, spacing and orientation. According to van de Meene and van Rijn (2000), an important feature of many sandbank systems is the lateral coherence of the individual sand bodies. Shelf-sand bodies almost always occur in fields, usually with a very constant spacing between the ridges. This fact is confirmed for the Hinder and Flemish Banks s.s. on the BCS, which likely belong to the same sandbank system, and probably have been formed from the same time onwards. Although located at the same distance offshore the coastline as the Flemish Banks, the continuity between the Zeeland Ridges s.s and the Hinder Banks s.s. is much less obvious than that between the Hinder and Flemish Banks s.s.

The continuity within and between sandbank fields can only be established with enough seismic profiles crossing the sandbanks. Velocity effects should be avoided by converting the seismic vertical time scale into a depth scale, taking into account the different sound velocities in the water and sediment column.

A final useful exercise is the calculation of the volumes of the tidal sandbanks, in order to check whether or not they could have been formed from underlying sediments alone, and to assess to which elevation the underlying units were originally deposited.

8.5 Conclusion

Seismic unit U7 is the uppermost unit in the Quaternary sequence on the Belgian Continental Shelf, and consists of bank-like structures and thin sand sheets in the adjacent swales. We distinguish two types of U7 banks: shoreface-connected or storm-generated ridges (Zeeland Ridges: Akkaertbank and Gootebank, Coastal Banks), and tidal sandbanks (Zeeland Ridge: Thorntonbank, Flemish Banks, Hinder Banks). The former are more rounded and have more gentle slopes than the tidal sandbanks, and are mostly formed diachronously, as a response to a change in conditions such as shoreface retreat due to sea-level rise, while the tidal sandbanks formed simultaneously, as a response of the sea bed to a suitable hydraulic regime. An exception are the Coastal Banks s.s., which are shoreface-connected ridges, but which formed simultaneously when the coastline had already reached the present-day coastline.
Indirect indications were used for the relative dating of the sandbank structures: (1) the positions of former coastlines. As sandbanks can only start forming seaward of a coastline, and assuming that the sandbanks on the BCS are formed rather locally, the present position of a sandbank relative to a former coastline could give a clue about its maximal age. (2) The age of the underlying sediments on which the U7 banks formed. And (3), the hydrodynamical constrains for the formation of tidal sandbanks. Tidal

sandbanks can only develop when the surface tidal currents exceed 50 cm/s (Belderson 1986, Galloway and Hobday 1996), which happened around 7000 cal BP on the BCS (van der Molen en van Dijck 2000).

On the basis of their dimensions and morphology, the Akkaert and Gootebank s.s. have been interpreted as moribund shoreface-connected ridges or storm-generated ridges, which became detached when the coastline retreated, and which have been partly remodelled by present-day tidal currents (forming sand dunes). These banks show many similarities with the U5 sand ridges, and as the Akkaertbank s.s. lies more or less in line with the U5 outer ridge, these banks probably belong to the same system as the U5 storm-generated ridges. The Akkaert and Gootebank s.s. have been considered to make part of seismic unit U7 though, because they are covered by present-day active sand dunes.
The initial position of the Akkaert and Gootebank s.s. is not only related to the position of a former coastline, but is most likely also linked with the presence of cuestas in the Top-Paleogene surface, which are still clearly visible at the NE ends of the banks. Assuming that their position stayed more or less the same while the shoreline receded, the Gootebank s.s. could have started developing around 9500 cal BP when the shoreline was located in that region, and the Akkaertbank s.s. started developing around 8900 cal BP when the coastline had already retreated further landward.

The features of the U7 bank structures in the Coastal Banks resemble very much the characteristics of active shoreface-connected ridges or storm-generated ridges in more general terms. The Wenduine Bank still shows a clear connection to the shoreface on the bathymetric map. And also the Stroombank was connected to the present-day coastline before the digging of the harbour entrance of Oostende around 1900 AD. Only the Nieuwpoort Bank shows no direct link with the coastline. Most likely the Nieuwpoort Bank s.s. developed simultaneously with the Stroombank and Wenduinebank s.s. as a response of the sea bed to a suitable hydraulic regime of wave (storms) and tide, as the process of ridge multiplication was ruled out. The Coastal Banks s.s. formed in a final phase of the Quaternary evolution, on top of U6, i.e. after the 16th century.

The Coastal Banks s.s. and the Akkaert and Gootebank s.s. distinguish themselves not only by their dimensions and shape from the tidal sandbanks, also the sediment transport and tidal current patterns around these banks are different than for the rest of the banks on the BCS. The transport direction around e.g. the Coastal Banks s.s. is not anti-clockwise as would be expected from a flood-dominated current along the eastern steep side of the banks. So it is possible that the steepest flanks of the Coastal Banks and Zeeland Ridges s.s. are not maintained by the strongest tidal current and are merely inherited from their storm-related origin.

The Hinder and Flemish Banks s.s. likely belong to the same sandbank system, and probably have been formed from the same time onwards. An important feature of many sandbank systems is the lateral coherence of the individual sand bodies. Shelf-sand bodies almost always occur in fields, often with a very constant spacing between the ridges. In fact, there is a clear continuation between the Hinder Banks and the Flemish banks s.s., more than between the Hinder Banks and the Zeeland Ridges s.s. although located at the same distance offshore the coastline as the Flemish Banks. Not only the Hinder and Flemish Banks s.s. have similar spacings, widths, lengths and orientation, also the position of the crest lines becomes gradually shallower from the Hinder Banks s.s. over the Flemish Banks s.s. with decreasing water depth, while the Zeeland Ridges s.s. are relatively located deeper. It also confirms once more that the Zeeland Ridges s.s. have a different origin than the Hinder and Flemish Banks s.s., which are clearly related.

The Hinder and Flemish Banks s.s. could not have formed diachronously in response to a shoreface retreat due to sea-level rise, as the shoreface was already located much further landward by the time they could have formed (after development of U5 sand ridges). And also the process of sandbank multiplication was rejected, as this process requires migration of the newly formed banks. And as most of the banks s.s. on the BCS show an internal core (with an erosional basal slope in opposing directions towards the adjacent swales), indicating that they could not have migrated very far, this process could only have been subordinate. It could have taken place, but only as an additional process, for banks s.s. with a flat base or an erosional base in only one direction (e.g. the Oostdyck s.s., Noordhinder s.s.). Most likely the Hinder and Flemish Banks s.s. formed simultaneously and rather in situ, as a response of the sea bed to a suitable hydraulic regime.
This is believed to have happened around 7000 cal BP. As the Middelkerke Bank, Oostende Bank, and Smalbank s.s. are located on top of the U5 outer and middle storm-generated ridges which have an age of 8400-7700 and 8000-7000 cal BP respectively, hence these banks could only have formed after that time. Around 7000 cal BP the tidal regime reached the present-day macrotidal range and the net-sand transport pattern changed. Before 7000 cal BP the sediment transport was mainly directed shoreward, while from that period on the tidal wave and related transport became along-shore (van der Molen and van Dijck 2000).
The Thorntonbank s.s. which lies parallel to the Goote and Akkaertbank s.s., but which is clearly a tidal sandbank and not a storm-generated ridge, might have started forming when the sediment transport was still directed onshore, but when tidal currents were already strong enough to form tidal sandbanks in the deeper offshore areas, presumably shortly before 7000 cal BP.

The U7 tidal sandbank and shoreface-connected ridge deposits are actually only the top parts of what are called 'sandbanks' in a broader sense of the word (sensu lato). The lower parts of the sandbanks s.l. have a very different origin, the base or core below U7 can consist of nearshore (U6 and U5), tidal-flat (U4), estuarine deposits (U3), or even Paleogene deposits, which stand out from the surrounding seafloor, i.e. make part of a 'sandbank' in the broad sense, due to erosion in the surrounding swales.
It has been believed by many authors that these U7 banks were created by sand accumulation around a pre-existing sediment body, the core visible below the U7 sandbank being the initial topographic irregularity needed for the sandbank initiation according to the Huthnance numerical model. But this implies an initial modelling of the older sediments into swells or highs with swales in between, before the modern tidal sandbanks could accumulate on top of these cores. More likely is that the banks and swales formed at the same time, on top of originally regionally continuous older deposits, and that the hydrodynamic processes in the swales eroded the older sediments, directly providing the sand for the build up of the tidal sandbanks just next to it. Most likely a small nucleus was indeed needed for the start of the bank development, but the large internal cores below the U7 sandbanks, are the result of a continuing process of constantly deeper becoming swales and increasing growth and migration of the banks towards the swales.
The U7 sandbanks form now a (temporally) protection of the older cores from further erosion by the prevailing hydrodynamics in the swales, as they are considered relative stable at present. So the core below an U7 sandbank is a remnant of older deposits, which have not (yet) been eroded by the overlying developing tidal sandbank, and is not a pre-existing sediment body on which the tidal sandbank accumulated (although some isolated cases do exist, cf. Akkaert and Gootebank).
The erosive character of the U7 banks appears from the presence of a coarse-grained deposit or gravel lag at the base of U7, even when U7 is not overlying the Holocene or Eemian marine transgressive surface.

Thus, the material of which the U7 banks are build up originates from local erosion of underlying sediments. This explains the greatly accidented surfaces of seismic units U4, U5 and U6 (cf. Chapter 7). In the nearshore part, the underlying deposits being eroded by the U7 banks mainly consist of Eemian U3 estuarine, Holocene U4 tidal-flat and U5 sand ridge sediments, the latter formed in the nearshore part of the Holocene transgressive sand sheet. While further offshore, the banks consist most likely only of remnants of a former transgressive sand sheet left after the Holocene transgression. This sheet itself probably consisted of remnants of the earliest Holocene tidal-flat deposits and maybe of underlying remnants of the former Eemian transgressive sand sheet (if not removed during the Weichselian lowstand), which were reworked by the Holocene open marine transgression during the initial fast relative sea-level rise. An additional amount of material was available north of the Offshore Scarp in the form of easily erodible IVDB Eemian deposits below the Holocene and Eemian marine transgressive surface. While south of the Offshore Scarp probably also the erosion of the Paleogene substrate contributed material.
In the offshore area, the Pleistocene and Paleogene are exposed in the swales between sandbanks, while in the nearshore Flemish Banks region U7 shows a sand sheet in the swales. Possibly because less sediment was available in the offshore area, which caused the deeper scoured swales, and/or because the tidal currents between the offshore Hinder Banks are (have been) stronger than between the nearshore Flemish Banks.

Over the years there have been a lot of studies on the initiation of the formation of tidal sandbanks. Some studies coupled essentially flat surfaces and the absence of an internal core to a process of accumulation only, and banks with an internal core, to a process of erosion. While other studies link the absence of a core below a sandbank to a fully evolved state, in which the bank has migrated, eroded, so far that it contains no more trace of its original nucleus. This apparent contradiction proofs that breaking up two mechanisms of accumulation and erosion, and linking the one strictly to a flat subsurface, and the other to the presence of a core, is too straightforward. Moreover, it is not always clear whether a distinction is made between a ‘bank s.l.’, i.e. an elevated structure above the seafloor, and a ‘bank s.s.’, i.e. a real tidal sandbank. So when the authors discuss ‘banks’ with an internal core, it is not unambiguous whether is meant a core below a tidal sandbank, or merely a ‘basal layer’ below a tidal sandbank with a flat base, being the ‘core’ of a bank s.l. To avoid this confusion we defined four main classes of cross-sections through a sandbank (s.l.), on the basis of the slope of the basal reflector of the tidal sandbank s.s., and whether the width of the tidal sandbank corresponds to the width of the bank s.l., in order to describe a sandbank (s.l.). An entire sandbank can mostly not be classified under one type. So the presence of different types of cross-sections through a single sandbank (s.l.) can help to distinguish between merely accumulation, or extensive migration and erosion.

9.
The Quaternary evolution of the BCS, synthesis and general remarks

The Quaternary evolution of the Belgian continental shelf starts with the formation of the oldest preserved Quaternary structures, i.e. the Offshore Scarp, bounding the Offshore Platform, and the Ostend Valley. The evolutionary history ends with the formation of the most recent formed shoreface-attached Coastal Banks. The Quaternary history of the BCS is interwoven with the evolution of the Flemish Valley on land, and the Coastal Plain at the land-sea boundary, and will be presented in a larger framework of hydrodynamic changes in the Southern Bight of the North Sea.
In addition, some general remarks and thoughts will be put forward on the dissimilarities between the coastline migration during the Eemian and Holocene transgression, and the availability and origin of sediments during the discussed Quaternary period.

9.1 A Quaternary evolutionary model for the BCS

9.1.1 The Pleistocene evolution

Saalian glaciation

During the maximum ice-sheet extent of the Saalian glaciation ("Amersfoorter Stadium" during the Drente glaciation MIS6) a proglacial ice lake formed between the Scandinavian and British ice in the central North Sea area, and a ridge north of the Dover Strait (Gibbard 2007). The Rhine-Meuse system entered this proglacial lake that reached heights similar to the present mean sea-level (Busschers et al. 2007), and formed a delta close to the present-day Dutch coastline (Figs. 9.1 and 9.3).
During the following deglaciation, at the end of the Drente MIS6 ice age, the proglacial lake overtopped the ridge north of the Dover Strait, causing a break through and subsequently drained. With dropping base level, the Meuse deeply incised in the former proglacial Rhine-Meuse braidplain and sought its way south, towards the Dover Strait, forming the Offshore Platform, Offshore scarp and 'Quaternary Basin' on its way (Figs. 9.1 and 9.3). Most likely also the rivers of the Flemish Valley formed a delta entering the Saalian proglacial lake. In reaction to the dropping base level, these rivers started incising as well, moulding the eastern Coastal Valley, the Ostend Valley, and possibly smaller branches in the present-day Dutch sector (Fig. 9.1). In this period the base of the Flemish Valley reached depths to -25 m TAW, similar to the depth of the Ostend Valley (-27.5 m MLLWS). The Ostend Valley formed probably a supply route of gravelly sediments, partly still present at the valley floor, and presumably also the Meuse carried gravel towards the Offshore Platform. The bottom of the proglacial lake is presumed to have been covered by a coarse-grained layer as well.
When the meltwater outflow diminished, and only the deeper Axial Channel was still occupied as main drainage path, it is most likely that the smaller flows in the Dutch sector sought their way further to the north towards the Axial Channel and cut through the former Meuse valley flank, forming the Thornton Channel and Northern Valley. Possibly also a small stream in the Ostend Valley extended towards the Axial Channel (Fig. 9.1). Liu et al. (1992) suggested that the Ostend Valley formed the missing link between the Flemish and eastern Coastal Valley on land, and the major Axial Channel offshore, via the Northern Valley. However, most likely the Ostend and Northern Valley represent two separate drainage systems, both connecting the Flemish Valley with the Axial Channel.

Eemian interglacial

During the Eemian sea-level rise, the sea invaded the earlier incised valleys, which evolved into estuaries. Soon the Ostend Valley evolved into a typically funnel-shaped tide-dominated estuary, consisting of an outer estuary, middle estuary and fluvial-tidal transition zone according to the model of Dalrymple and Choi (2007) (Fig. 9.2D). Three seismic units (U1-U2-U3) represent the estuarine infilling of the Ostend Valley. They represent each time a more seaward section of the estuary, indicative of a landward migration of the estuarine environment. With rising sea level, the estuary continuously migrated further upstream the eastern Coastal Valley, which forms the connection between the Flemish and Ostend Valley. The estuarine deposits in the Ostend Valley became coarser and more marine upwards. In the process of transgression, landward and laterally migrating tidal channels coupled with wave action eroded part of the more landward facies, and left tidal ravinement surfaces in between the seismic units. Seismic unit U1 represents point-bar infillings of deeply-incised tidal channels (to 30 m below the average valley floor), created by initial tidal scouring in a middle estuarine environment (Fig. 9.2A). The overlying seismic unit U2 in the Ostend Valley represents the seaward part of a middle-estuary environment, while the landward part of the middle estuary and

the more clayey fluvial-tidal transition zone are located more landward, in the present eastern Coastal Plain (Fig. 9.2B). The upper unit U3 represents an outer estuary environment, while the middle estuary and fluvial-tidal transition zone have migrated even further up the eastern Coastal Valley (Fig. 9.2C). It is possible that the continental, alluvial sediments found in the more upstream part of the Flemish Valley, especially in the Lys (Leie) Valley, (Formation of Oostwinkel, De Moor and Van De Velde 1995, De Moor and Heyse 1974), formed the continuation of the meandering, more clayey part of the contemporary Ostend Valley estuary, i.e. the fluvial-tidal transition or fluvial section. In the more downstream part of the Flemish Valley, they were eroded though by the later marine incursion.

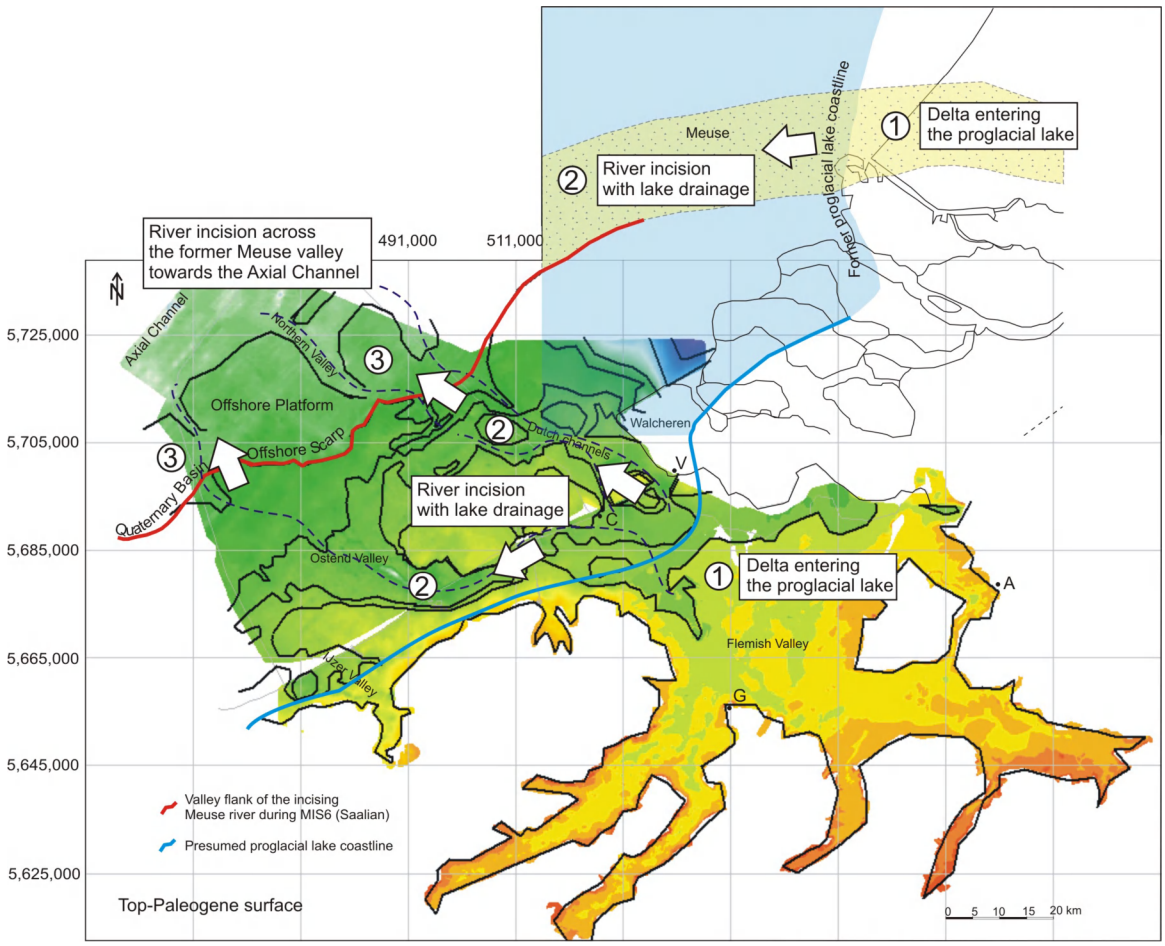

Fig. 9.1 Schematic scenario of river incision during the Saalian proglacial-lake drainage. Situation in the Dutch sector is adapted after Busschers et al. (2008).

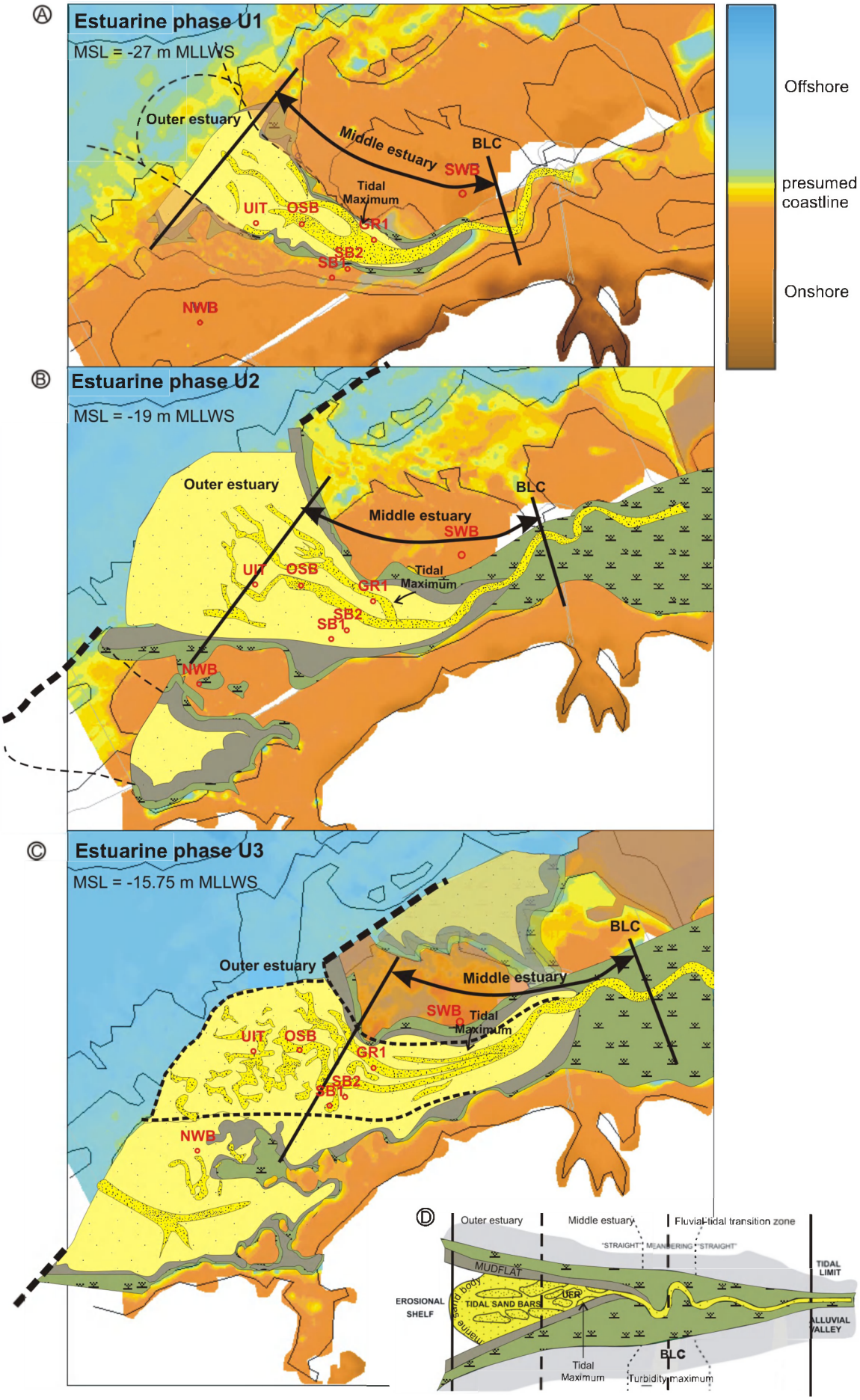
Ⓐ
Estuarine phase U1
MSL = -27 m MLLWS
Outer estuary
Middle estuary
BLC
SWB
Tidal Maximum
UIT
OSB
GR1
SB2
SB1
NWB
Offshore
presumed coastline
Onshore
Ⓑ
Estuarine phase U2
MSL = -19 m MLLWS
Outer estuary
Middle estuary
BLC
SWB
UIT
OSB
Tidal Maximum
GR1
SB2
SB1
NWB
Ⓒ
Estuarine phase U3
MSL = -15.75 m MLLWS
Outer estuary
Middle estuary
BLC
SWB
Tidal Maximum
UIT
OSB
GR1
SB2
SB1
NWB
Ⓓ
Outer estuary
Middle estuary
Fluvial-tidal transition zone
"STRAIGHT"
MEANDERING
"STRAIGHT"
MUDFLAT
TIDAL LIMIT
EROSIONAL SHELF
TIDAL SAND BARS
UER
ALLUVIAL VALLEY
Tidal Maximum
BLC
Turbidity maximum

Fig. 9.2 (page 316) Paleo-reconstructions showing the transgressive estuarine infilling of the Ostend Valley during the Eemian. (A) Estuarine phase U1, (B) estuarine phase U2, (C) estuarine phase U3, and (D) schematic map of a tide-dominated estuary with its different depositional environments, serving as legend for (A), (B) and (C) (modified after Dalrymple and Choi 2007). Orange transparent overlays represent presumed Paleogene surfaces located higher than presently preserved. BLC = bedload convergence, UFR = upper-flow-regime tidal flats. Zeebrugge harbour and BCP limit in light grey. Contours of the Ostend Valley and neighbouring platforms in (fine) black.

Meanwhile also the coastline migrated landward, and the upper surface of the estuarine infillings became truncated at the seabed by a ravinement surface formed by shoreface erosion and marine planation during marine transgression. In the offshore section erosion was that severe that remnants of former Eemian deposits were only left in depressions in the Top-Paleogene substratum (cf. Fig. 7.33). The IVDB Eemian deposits covering the Offshore Platform, have most likely been levelled with the Top-Paleogene surface south of the Offshore Scarp, starting with the Eemian open marine transgression. Also at the Ostend Valley, marine planation was that severe that seismic unit U3 was completely levelled with the Top-Paleogene surface, the resulting low relief of the sea bed belying the complexity and irregularity of the deposits lying immediately beneath. Across the Ostend Valley, a 4 m scarp (aligned with the Nearshore Slope Break) in the shoreface ravinement surface most likely represents an acceleration in the Eemian relative mean sea-level rise (from about -17 to -13 m MLLWS), leaving the previous erosional surface (lower shoreface) about 4 m below the new maximum depth of wave and tidal erosion. By the time the Eemian relative sea level reached its maximum, comparable to the present-day level, the coastline was situated 7 km inland of the present-day shoreline (near Brugge). And such as the Ostend Valley, also the eastern Coastal Valley and part of the Flemish Valley were transgressed by the retreating shoreline and completely inundated by the sea (cf. Fig. 6.29). In the Flemish Valley, the marine influence reached as far as 40 km inland into the low lying tributaries (De Moor et al. 1996), turning a large part of the Flemish Valley into an estuarine embayment. Although the infillings of the Flemish Valley are very similar to the estuarine sediments in the Ostend Valley, they do not represent the end member of the continuing upstream migration of the Ostend-eastern Coastal Valley estuary. Because the connection between the Ostend and Flemish Valley is parallel to the coast, the interconnected area drowned at once, leaving no time for a further upstream migration, instead a new estuary formed in the Flemish Valley.

The Eemian marine transgressive or shoreface ravinement surface in the present offshore area is characterised by a gravel lag. The gravel lag can originate from the retreating shoreface which cut into the gravelly valley fills originally present in the Meuse and Ostend Valley, and redistributed them as a marine basal transgressive gravel. It is also possible that the gravel lag consists of coarse-grained material winnowed out from the directly underlying Paleogene substrate (like shells, former Paleogene river infillings, concretions, sandstone banks). In general, a marine transgressive gravel lag is overlain by several metres of sand, i.e. the marine transgressive sand sheet, but in the offshore area, on top of the Eemian ravinement surface and below the initial Holocene deposits, no open marine Eemian sands are present. However, in the eastern Coastal Plain and part of the Flemish Valley, tidal flats and estuarine deposits *are* covered by open marine sediments. Possibly because in the Coastal Plain and Flemish Valley, the marine incursion happened at the end of the Eemian transgression, practically during the Eemian highstand (Fig. 9.3), when the coastline transgressed slowly, and more time (and sediment) was available for the build up of a transgressive sand sheet (see further discussion below).

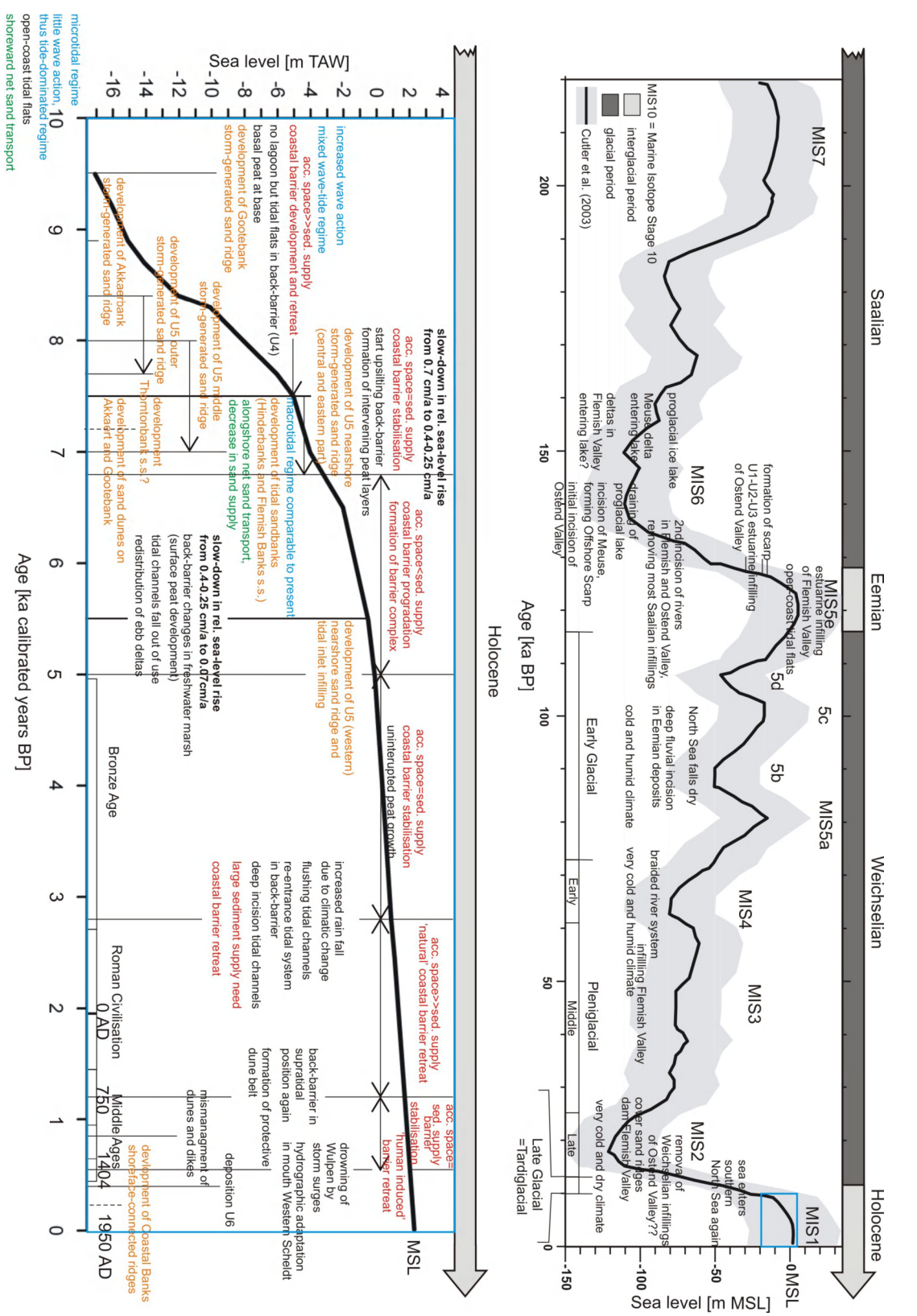

Fig. 9.3 Timeline and corresponding sea-level curve, giving an overview of the most important events since the Saalian ice age. Top: climatic changes and the related evolution of a proglacial lake and the Flemish-Ostend Valley river systems. The sea-level curve is the mean sea-level curve of Cutler et al. (2003) in Fig. 6.27. Bottom: zoom in on the Holocene period. The sea-level curve is the mean sea-level curve of Fig. 7.37. Changes in relative sea-level rise are given in bold; coastal barrier movements in response to created accommodation space (acc. space) and sediment supply (sed. supply) are indicated in red; development of U5 storm-dominated sand ridges, U7 storm-dominated and shoreface-connected ridges, and U7 tidal sandbanks in orange; tidal regime and wave action in blue; sediment transport in green; and depositional environments and events are given in black.

In both the eastern Coastal Plain and Flemish Valley, the final phase in the Eemian succession is represented by the development of exposed (open marine) tidal flats (Fig. 6.29B, adapted after Mostaert and De Moor 1989). This phenomenon is common when during highstand estuaries become infilled and cease to exist. If no sufficient sediment is supplied directly by the river, the site does not evolve into a delta, but a straight prograding coast in the form of a strandplain or open-coast tidal flats, in case the sediment is delivered to the area by marine processes (waves or tides, respectively) (Dalrymple et al. 1992).

Weichselian glaciation

At the beginning of the Weichselian period (Early Glacial 116ka-73ka BP, MIS 5d-5a, Fig. 9.3), sea level lowered due to ice-mass expansion, because of impoverished climatic conditions, and soon the North Sea floor became dry land. In our regions the climate became relative cold, but with a very high humidity (Verbruggen et al. 1991), which induced an intense and deep fluvial incision, as no permafrost was established yet (Fig. 9.3). The Flemish Valley became incised to depths of -17 m (Tavernier and De Moor 1974) (-15 m in: De Moor et al. 1996, and on: Fig. 6.29C after De Moor 1996; and -20 m on Fig. 2 in: Verbruggen et al. 1991), by which the Eemian sediments were largely removed. In the Ostend Valley, the river incised down to -21 m MLLWS.
During the Early Pleniglacial (72ka-61ka BP, MIS4), characterised by a very cold and humid periglacial climate, extensive fluvioperiglacial accumulation took place (Fig. 9.3). The presence of permafrost restricted the incisional depth, and the limited vegetation allowed an intensified runoff of meltwater, by which large amounts of sediment were swept away to the thalwegs, which evolved into braided river systems. This continued during the milder Middle Pleniglacial (61ka-25ka BP, MIS3) and the valley complex of the Flemish Valley and her distributaries became filled to a level between 0 and +10 m TAW (De Moor and Van De Velde 1995, Fig. 2 in: Verbruggen et al. 1991). This resulted in at least 20 m of Weichselian deposits in the Flemish Valley (De Moor and Van De Velde 1995, De Moor et al. 1996), while in the Ostend Valley no fluvial sediments at all were found in the renewed valley incision.
During the Late Pleniglacial (25ka-13ka BP, MIS2), the climate evolved to very cold and dry circumstances with very restricted vegetation. Aeolian action took over and earlier deposited fluvial sediments were blown into cover sand ridges, gradually damming the Flemish Valley. The whole northward oriented braided drainage system of the Flemish Valley was forced to branch off eastward, along the Lower-Scheldt (De Moor and Van De Velde 1995). Since then, the Ostend Valley was no longer connected to the Flemish Valley.
It is possible that the presumed Weichselian fluvial infillings in the Ostend Valley section were removed by aeolian action, after the river was cut off from the Flemish Valley by the cover sand ridge, leaving a deflation surface (gravel) at the base of U4. Also removal of the infillings during the Holocene sea-level rise, by tidal channels prior to the formation of the tidal flats (U4), is possible.

Also the former Meuse valley, crossing the BCS got incised again, which appears from the presence of fluvial deposits of Weichselian age found in the 'Quaternary Basin', in line with the Offshore Platform (Kirby and Oele 1975). During the Weichselian lowstand, the Meuse occupied the same position in the western Netherlands as during the Saalian lowstand, now joined with the Rhine (Busschers et al. 2007), and most likely also followed the same southward directed drainage channels offshore (Gibbard 2007).

9.1.2 Holocene evolution

Initial flooding of the southern North Sea

During most of the Weichselian, the North Sea was dry land, but around 12,500 cal BP rising sea water entered the southern part of the North Sea again, through the Strait of Dover in the south and through channels along the Dogger Bank in the north (Fig. 9.3). Coastward sediment transport could not keep pace with the rapid rise in sea level and the relict landscape drowned rapidly (van der Molen and van Dijck 2000). According to van der Molen and van Dijck (2000), around 9500 cal BP the land bridge between northern Holland and Britain (Texel Spur-Norfolk Banks) was flooded. While according to Beets and van der Spek (2000), at that time, the Southern Bight was still largely separated from the northern North Sea, although at its south-eastern side the sea had already reached the Belgian Coastal Plain via the Strait of Dover (Denys and Baeteman 1995, Beets and van der Spek 2000, Baeteman and Declercq 2002). Initially, the tides entered the basin through the Strait of Dover and propagated as a progressive, damped wave along the Belgian and Dutch coast to the north. Because of the widening of the basin to the north and dissipation in the shallow sea, the tidal amplitudes decreased rapidly away from the Strait of Dover, resulting in microtidal conditions in most of the Southern Bight (Fig. 9.3). The orientation of the tidal currents and the net sand transport was oriented towards the shore because the tides propagated to the north in the Deep Water Channel and to the east in the shallow sea between the Deep Water Channel and the coast (van der Molen and van Dijck 2000). The net tidal transports were small because of the weak currents decreasing from south to north. In this early Holocene period, most likely an exposed tidal-flat environment developed in the Southern Bight, comparable to the present-day German Bight (Toro et al. 2005) (Figs. 9.3 and 9.4). As groundwater level rose with sea level, the tidally flooded area was fringed by freshwater marshes in which peat accumulated, known as basal peat (Baeteman 2004).

Formation and retreat of a coastal barrier and back-barrier basin

As sea level rose, the basin became deeper and the dissipation was reduced, allowing the tide to penetrate further into the Southern Bight. Although according to Beets and van der Spek (2000) the Southern Bight was still isolated from the northern North Sea at 9500 cal BP, it was at that time already sufficient in size to produce waves at its eastern shores capable of building a protective barrier behind which a complex of estuaries and tidal basins (protected tidal flats, detected in seismic unit U4) could develop (Figs. 9.3 and 9.5). According to van der Molen and van Dijck (2000), barrier islands with back-barrier basins formed along the eastern shore of the Southern Bight prior to 9000 cal BP after the flooding of the northern land bridge, when tidal energy from the northern North Sea could enter the Southern Bight, so that the tidal and current amplitudes increased and the southern North Sea widened. Due to the predominance of westerly winds and the low gradient of the pre-transgressive, Pleistocene surface, barrier islands could form. Sand to fill the back-barrier basins was derived from the shoreface adjacent to the tidal inlets and from the ebb-tidal deltas. As insufficient sediment was supplied to the shoreface by alongshore and cross-shore transport to compensate for this sediment loss, the shoreline was forced to recede (Beets and van der Spek 2000), while eroding the underlying deposits and previous back-barrier sediments (Fig. 9.3). Of which evidence is found at the top of U4 in the form of a gravel lag. Like the Eemian marine transgressive surface, the gravel lag can originate from the retreating shoreface which cut into former gravelly valley fills or it can consists of coarse-grained material winnowed out from the directly underlying Paleogene substrate. And now also the underlying Eemian gravel lag can serve as a source. In contrast to the Eemian marine transgression, the Holocene marine planation was not that severe. The IVDB Eemian deposits covering the Offshore Platform, have possibly been further levelled with the

Top-Paleogene surface south of the Offshore Scarp, together with the early Holocene (exposed) tidal-flat deposits. However, below the Holocene marine transgressive surface more nearshore, remnants of former back-barrier deposits are preserved. Also in contrast to the Eemian period, the basal gravel lag was probably overlain by several metres of sand, i.e. the Holocene transgressive sand sheet, left on the ravinement surface cut by the barrier retreat process. Today, the sand is discontinuous and in areas of strong storm or tidal currents is lacking altogether, so that the basal gravels, Holocene back-barrier deposits or older Pleistocene or Paleogene deposits are exposed in windows through the sand sheet. From this sandy layer initially storm-generated or shoreface connected ridges, and later tidal sandbanks, formed erosively under influence of storm and tidal forces which left a deep imprint in the U4 surface.

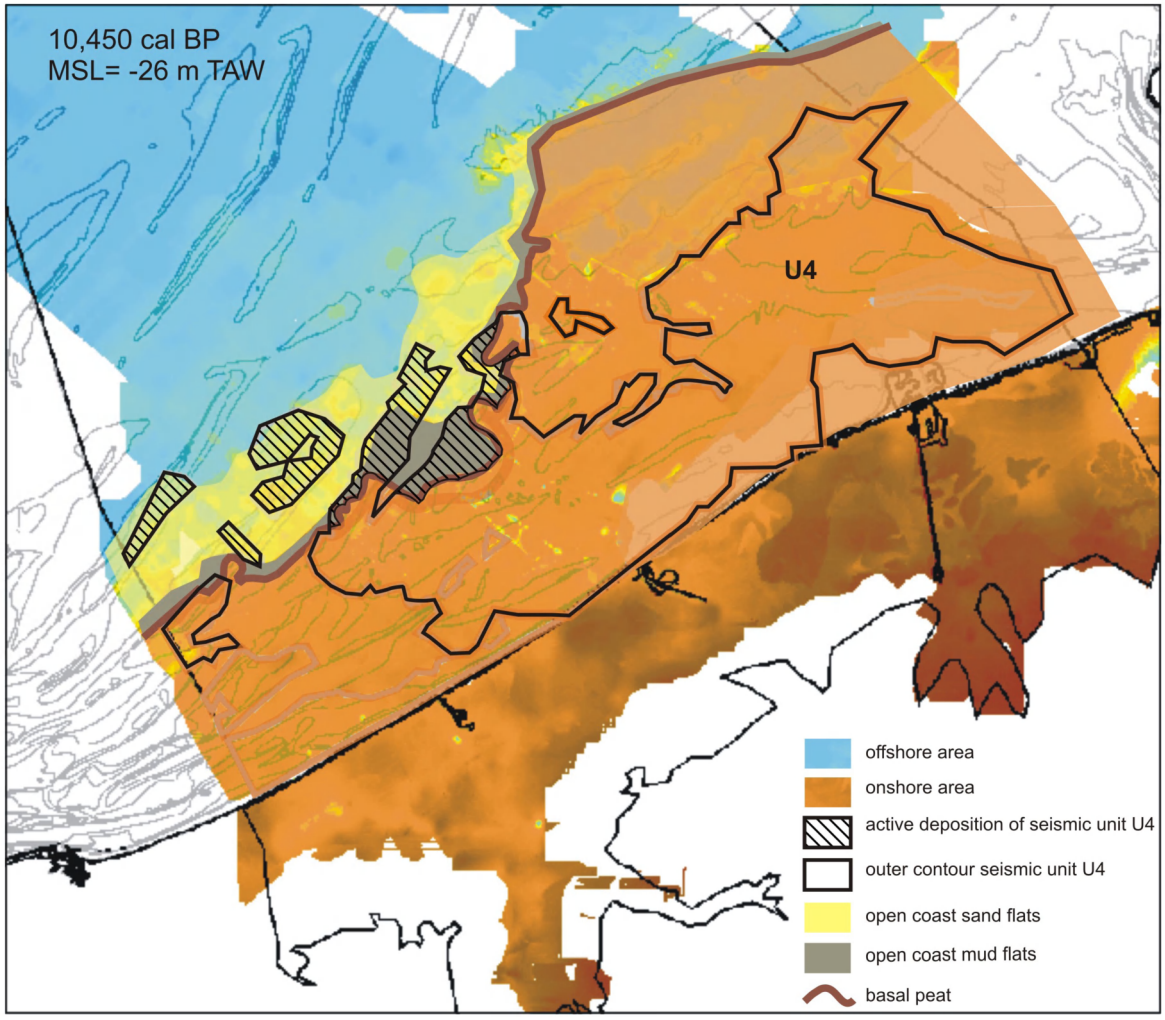

Fig. 9.4 Paleo-reconstruction of the situation around 10,450 cal BP, when MSL was -26 m MLLWS. Part of the deepest (oldest) deposits of seismic unit U4 have developed at that time. These deposits represent remnants of an open (exposed) tidal-flat environment, not located behind a barrier, comparable to the present-day German Bight (Toro et al. 2005). A fringe of basal peat bordered the tidal flats.

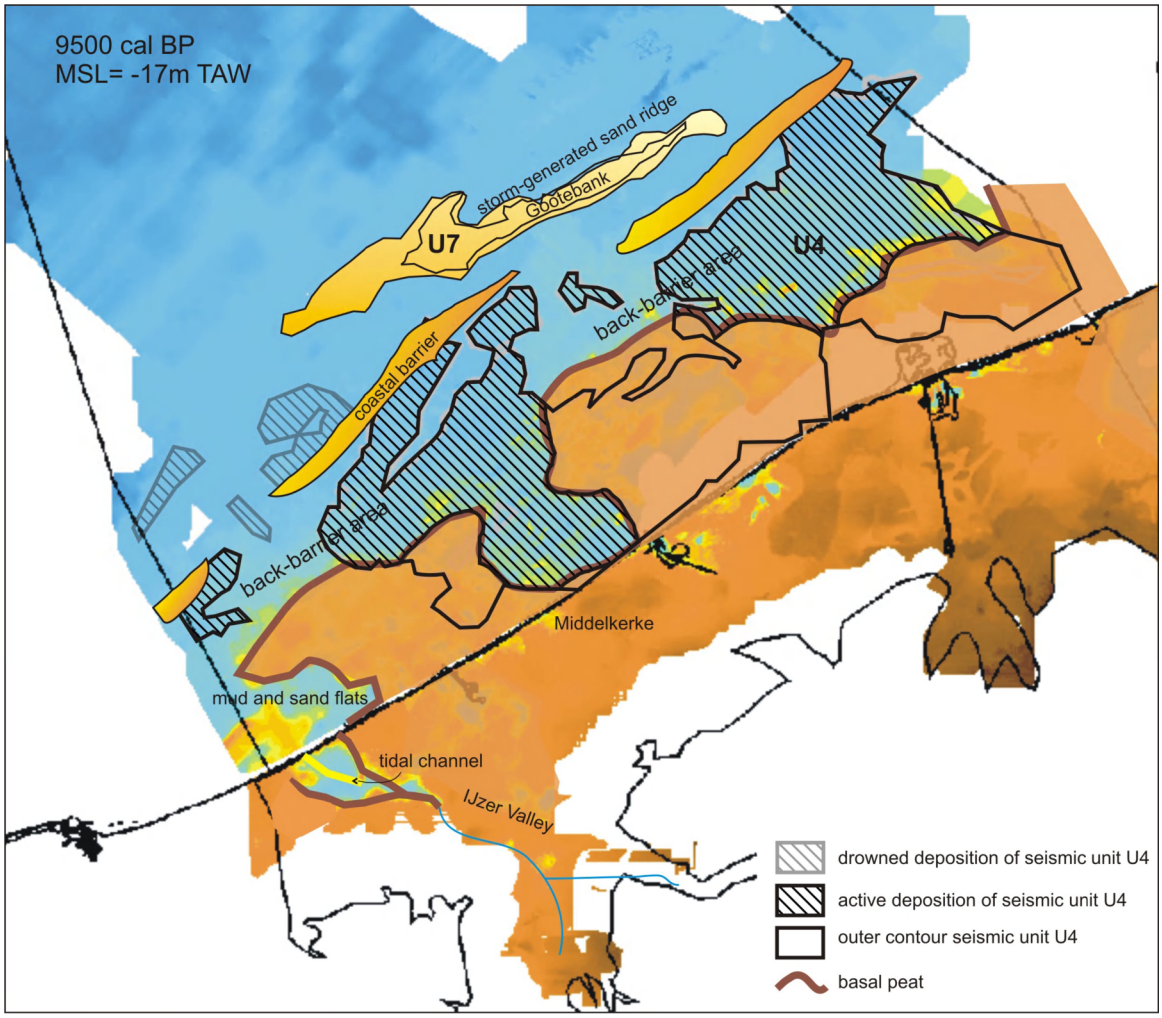

Fig. 9.5 Paleo-reconstruction of the situation around 9500 cal BP, when coastal barriers started to form in the Southern Bight (Beets and van der Spek 2000). Mean sea level at that time was about -17 m MLLWS. Behind the barrier, back-barrier sand and mud flats developed adjacent to tidal channels. A fringe of basal peat borders the tidal flats (in blue, distinction between mud and sand flats not specified here). The isolated patches of U4 below the Oostdyck and Buiten Ratel are now drowned open tidal flats. The situation in the Western Coastal Plain is adapted after Baeteman (2005a). The Gootebank storm-dominated sand ridge started forming around 9500 cal BP.

Formation of storm-generated ridges from the transgressive sand sheet

Two categories of shoreface-connected sand ridges, which formed during barrier retreat, can be recognised: shore-attached ridges as products of ebb-tidal deltas in tidal inlets of a receding barrier, i.e. Type 2B (ii) of Dyer and Huntley (1999); or sand ridges moulded in a transgressive shelf-sand sheet, left after barrier retreat (Swift et al. 1973, Swift and Thorne 1991). Probably both origins are valid: where tidal inlets were present, sand ridges are formed from redistributed ebb-tidal delta sediments, while in the areas in between, sand ridges are formed in the 'sawdust' left by shoreface retreat. The ridges have diverse origins but are probably in most cases initiated in response to storm currents on the shoreface and adjacent shelf. This involved scour and down-cutting in the troughs, eroding the underlying U4 deposits, with simultaneous aggradation of the ridge crests.

On the basis of morphological evidence, the Goote and Akkaertbank s.s. most likely represent former shoreface-connected ridges, represented by seismic unit U7. Their position with respect to former coastlines suggests that the Goote and Akkaertbank s.s.

started forming around 9500 and 8900 cal BP, respectively (Figs. 9.3 and 9.5). Shortly later, around 8400 cal BP, at a slightly higher sea level and a more nearshore position, also the outer ridge, recognised in seismic unit U5 started developing (Fig. 9.6). By 8000 cal BP, when the retreating coastline reached the present-day coastline in the most western part of the Coastal Plain, probably also the middle ridge began to form (Fig. 9.6). The central and eastern part of the nearshore ridge is least developed and probably formed around 7500 cal BP, when the barrier started stabilising (Figs. 9.3 and 9.7). With further rising relative sea level, the ridges became detached, but continued growing upwards. On the basis of the preserved dimensions of the ridges, it is suggested that the outer ridge developed until 7700 cal BP and the middle ridge until about 7000 cal BP (Figs. 9.3 and 9.7).

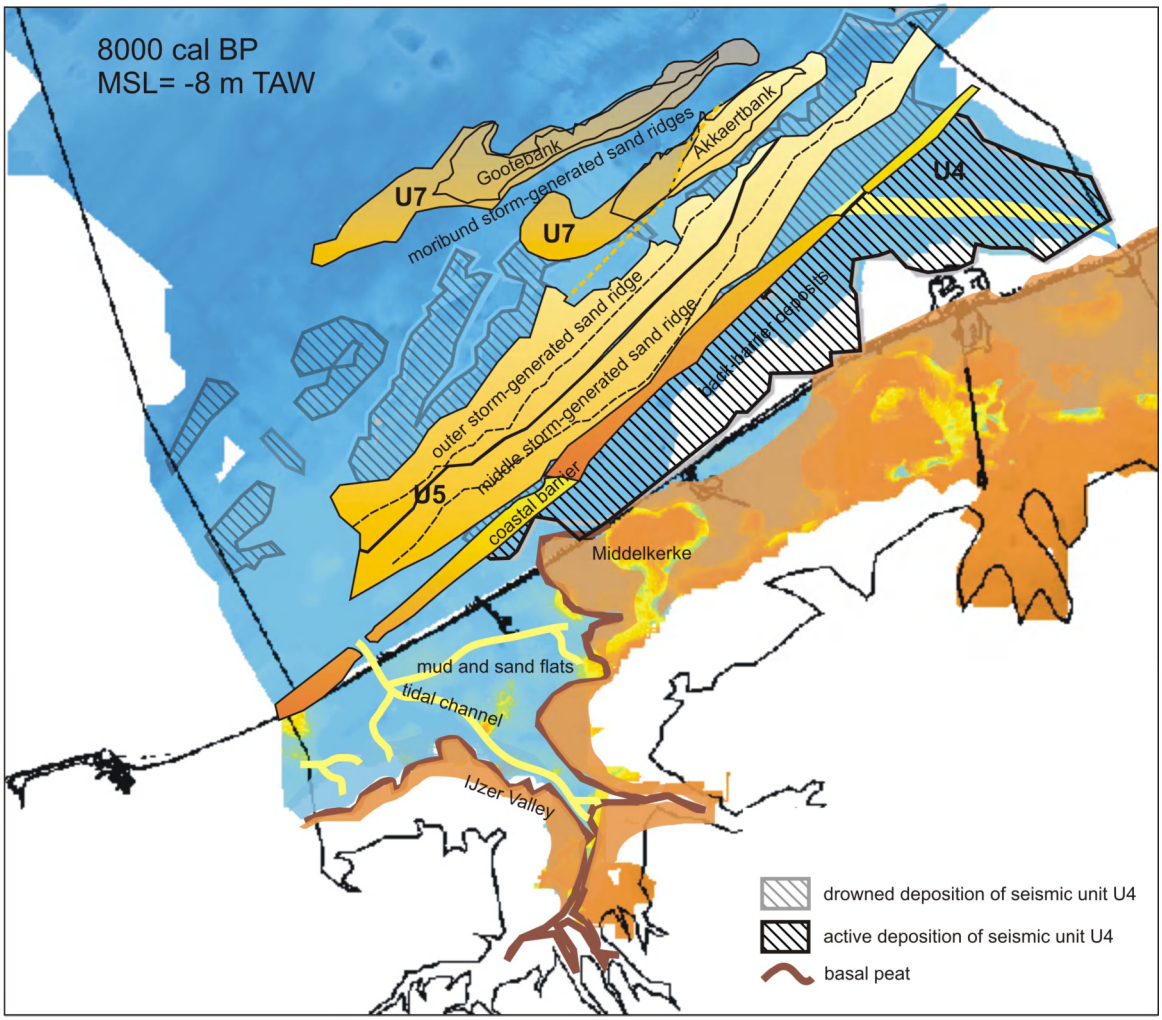

Fig. 9.6 Paleo-reconstruction of the situation around 8000 cal BP, when the coastal barrier reached the present-day coastline in the west for the first time. Mean sea level at that time was about -8 m MLLWS (Baeteman 2004). Seaward of the barrier, former tidal flats have been eroded (in the west, they are even completely removed), landward of the barrier, the tidal environment is still developing. A fringe of basal peat borders the tidal flats (in blue, distinction between mud and sand flats not specified here). The situation in the Western Coastal Plain is adapted after Baeteman (2005a).
The Akkaertbank s.s. started forming around 8900 cal BP. Some time later, around 8400 cal BP, at a slightly higher sea level and a more nearshore position, also the outer ridge of U5 started developing. By 8000 cal BP, also the middle ridge began to form. At that time, the outer ridge was still active as it continued developing until 7700 cal BP. Most likely also the part of the Akkaertbank in line with the outer ridge is still active, whereas the most offshore part is already moribund.

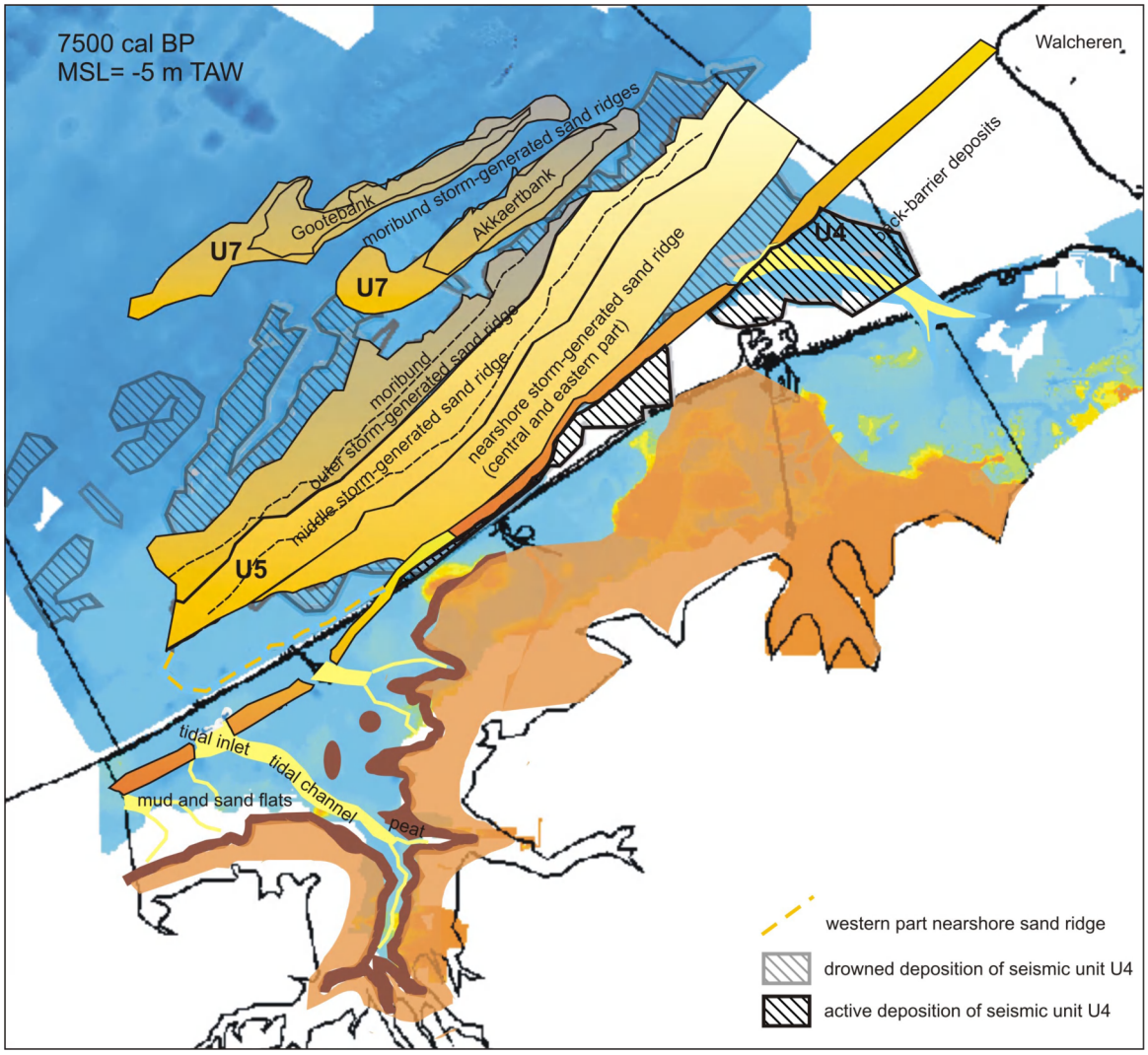

Fig. 9.7 Paleo-reconstruction of the situation around 7500 cal BP, when the relative sea-level rise decreased, resulting in a sand surplus and consequently in the upsilting of the back-barrier tidal basins and the onset of stabilisation of the coastal barrier. The upsilting of the back-barrier basins resulted in the evolution of salt marsh vegetation into reed growth (fresh water marsh), and consequently in peat accumulation, so it is not until 7500 cal BP that intervening peat layers formed. Mean sea level at that time was about -5 m MLLWS (Baeteman 2004, Fig. 7.37). The situation in the Western Coastal Plain is adapted after Baeteman (2005a). Around this time, the outer ridge had become moribund (7700 cal BP), the middle ridge continued developing (until about 7000 cal BP, based on its preserved dimensions), and the central and eastern part of the nearshore ridge started forming.

Coastal barrier stabilisation around 7500 cal BP

Since the start of the flooding of the Southern North Sea, the tidal wave propagated along the coast in deeper water, and from deeper water it propagated to the coast in the shallow zone in between. Substantial volumes of sand were eroded from the bottom of the Southern Bight, transported toward the coast by the tidal asymmetry, aided by wave suspension (van der Molen and van Dijck 2000, van der Molen and de Swart 2001b). This sand partly supplied the shoreface of the barrier. Most of the sediment supplying the barriers and back-barrier basins is, however, derived from erosion of the underlying substratum during retreat of the barriers (Beets and van der Spek 2000). Though insufficient to balance the rapid relative sea-level rise (0.7 cm/a for 10,000-7500 cal BP), the large sand supply must have slowed down the coastal retreat (van der Molen and van Dijck 2000). Around 7500 cal BP, the rate of relative sea-level rise decreased from

0.7 cm/a to 0.4-0.25 cm/a, resulting in a sand surplus and consequently in the upsilting of the back-barrier tidal basins and the onset of stabilisation of the coastal barrier (Baeteman and Declercq 2002) (Fig. 9.3). The upsilting of the back-barrier basins resulted in the evolution of salt marsh vegetation into reed growth (fresh water marsh), and consequently in peat accumulation (Baeteman 1999, Baeteman 2004). Before, due to the fast rising relative sea level, the tidal flats could be upsilted to supratidal level but only some vegetation horizons occurred, so it is not until 7500 cal BP that intervening peat layers formed. The stabilisation of the coastal barrier around 7500 cal BP is visualised in Fig. 9.7. In the western Coastal Plain the retreating shoreline reached its maximal landward position and the barrier stabilised about 3 km inland of the present-day coastline (Baeteman 2005a). Note that the barrier retreated more or less parallel with its the former position, keeping a straight coastline, but with an angle to the present-day coastline, which caused the seemingly more landward position of the barrier in the western Coastal Plain. The orientation of the initial barrier is in the first place most likely determined by the stretch of the pre-transgressive surface, and transgressed more or less constant over its entire length to its position of 7500 cal BP.

Changing hydrodynamics and formation of tidal sandbanks around 7000 cal BP

When sea level rose further, an increasing amount of tidal energy could enter the Southern Bight from the north. The tidal and current amplitudes kept increasing until 7000 cal BP. The larger water depths allowed the tide to propagate closer to the shore, changing the shoreward net sand-transport pattern from before 7000 cal BP to a pattern of along-shore transport (Fig. 9.3). At the same time a sand divergence zone developed between Zeeland and Britain. The sand transport direction along the Belgian coast reversed, causing the sand supply to the coast to decrease, which was enhanced by a decrease in the suspension of sand by wind waves as the sea became deeper (van der Molen and van Dijck 2000). The decrease in the rate of relative sea-level rise after 7500 cal BP (Denys and Baeteman 1995), could compensate the reduced sediment supply, resulting in the sand surplus and consequently in the silting up of the tidal basins as mentioned above (Baeteman 1999, Baeteman 2004). From 7000 cal BP toward the present, sea level rose about another 6 m, but the tidal system changed only little and the influence of waves on the tidal transport gradually decreased (van der Molen and van Dijck 2000) (Fig. 9.3).

So most likely from this period onwards, when the tidal system became comparable to the present one, and the outer and middle sand ridges of U5 reached their maximum preserved heights, the tidal sandbanks of the Flemish and Hinder Banks started to develop on top of these sand ridges (represented by seismic unit U7) (Figs. 9.3 and 9.8B). The change in sediment transport direction might explain the difference in orientation between the Zeeland Ridges s.s. which are more or less oriented coast-parallel and which were formed when the sediment transport was shoreward directed, while the Flemish Banks and Hinder Banks s.s. are oriented at an angle with the present-day coastline, and make a small oblique angle with the prevailing peak tidal flow direction, typical for tidal sandbanks. Possibly from 7000 cal BP on, also tidal sand dunes began developing on the now moribund shoreface-connected ridges forming the Goote and Akkaertbank. The Thorntonbank s.s. which lies parallel to the Goote and Akkaertbank s.s., but which is clearly a tidal sandbank and not a shoreface-connected ridge, might have started forming when the sediment transport was still directed onshore, but when tidal currents were already strong enough to form tidal sandbanks in the deeper offshore areas (shortly before 7000 cal BP?) (Fig. 9.3).
Most likely the Flemish and Hinder Banks s.s. formed simultaneously, as a response of the sea bed to a suitable hydraulic regime, around 7000 cal BP, and are not formed diachronously, as a response to a steady change in conditions such as shoreface retreat due to sea-level rise. `Sandbank multiplication' (Caston 1972, Dyer and Huntley 1999)

could have taken place, but only as a subordinate process. Probably most of the material of which the U7 banks are build up, originates from local erosion of underlying sediments, what can be deduced from the often erosional character of the base of the banks and the presence of deeply incised swales in between. So, the sand of which the Hinder and Flemish Banks s.s. are composed, was already present in the area before the Holocene marine transgression started and it is not derived directly from a retreating shore (Houbolt 1968). As also Belderson (1986) stated, the existence of tidal sandbanks depends on the availability of sand in an area with surface peak tidal currents exceeding 90 cm/s (the sand ribbon zone), rather than on shoreline migration.

Coastal barrier progradation from 6800-5000 cal BP

Between 6800 and 6000 cal BP, the relative sea-level rise lost its driving force (Baeteman and Declercq 2002, Baeteman 2005a), and continued to decrease to an average of 0.07 cm/a after 5500-5000 cal BP (Baeteman 1999) (Fig. 9.3). The relative sea-level rise decreased so, that even the reduced sediment supply exceeded the accommodation space created by the relative sea-level rise, inducing the coastal barrier to prograde (except for the central part of the coastline, near Middelkerke, which stayed more or less stable) (Figs. 9.3 and 9.8A). A barrier complex formed with seaward migrating tidal inlets and channels, of which the remnants are still present in the present-day western Coastal Plain (Fig. 9.8A) (Baeteman 2007b).

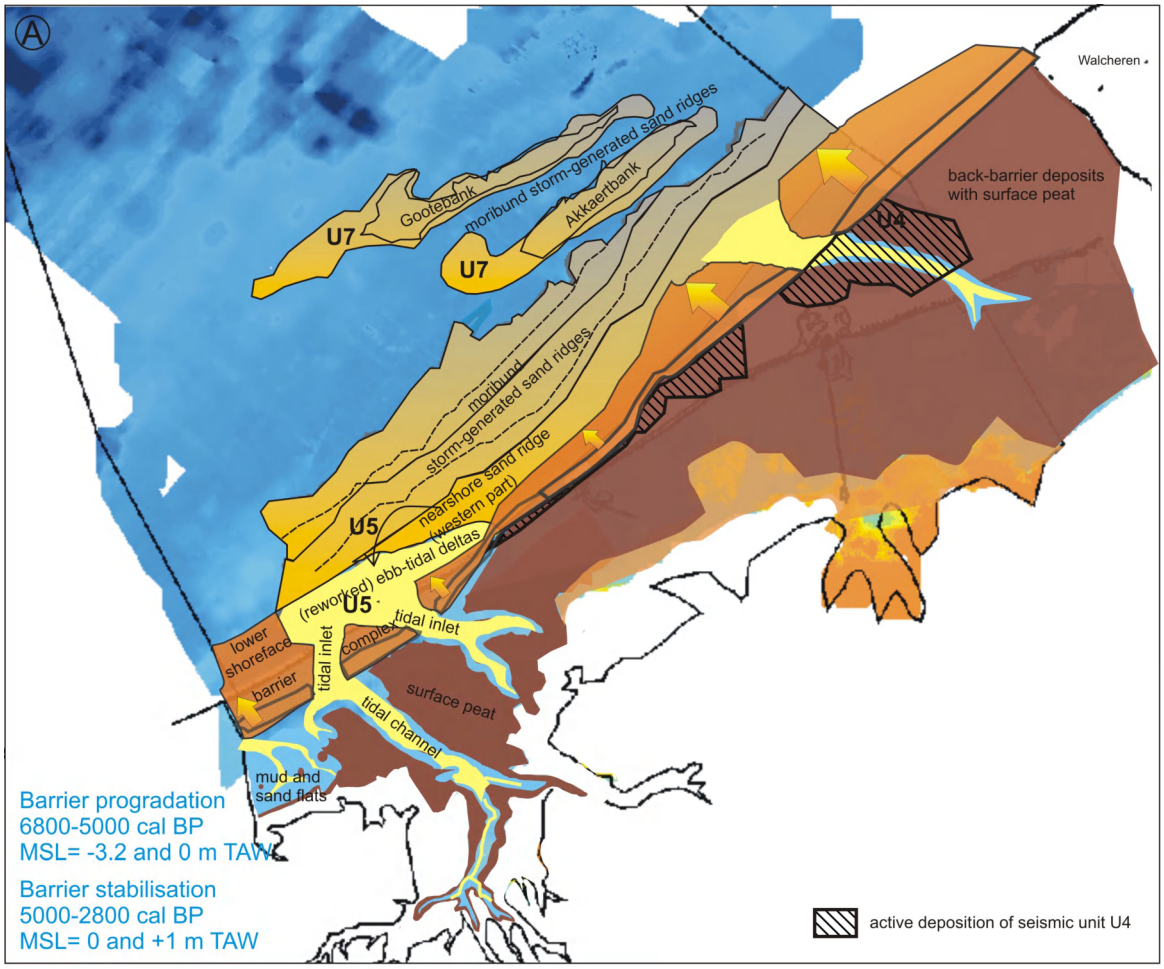

Fig. 9.8 (A)

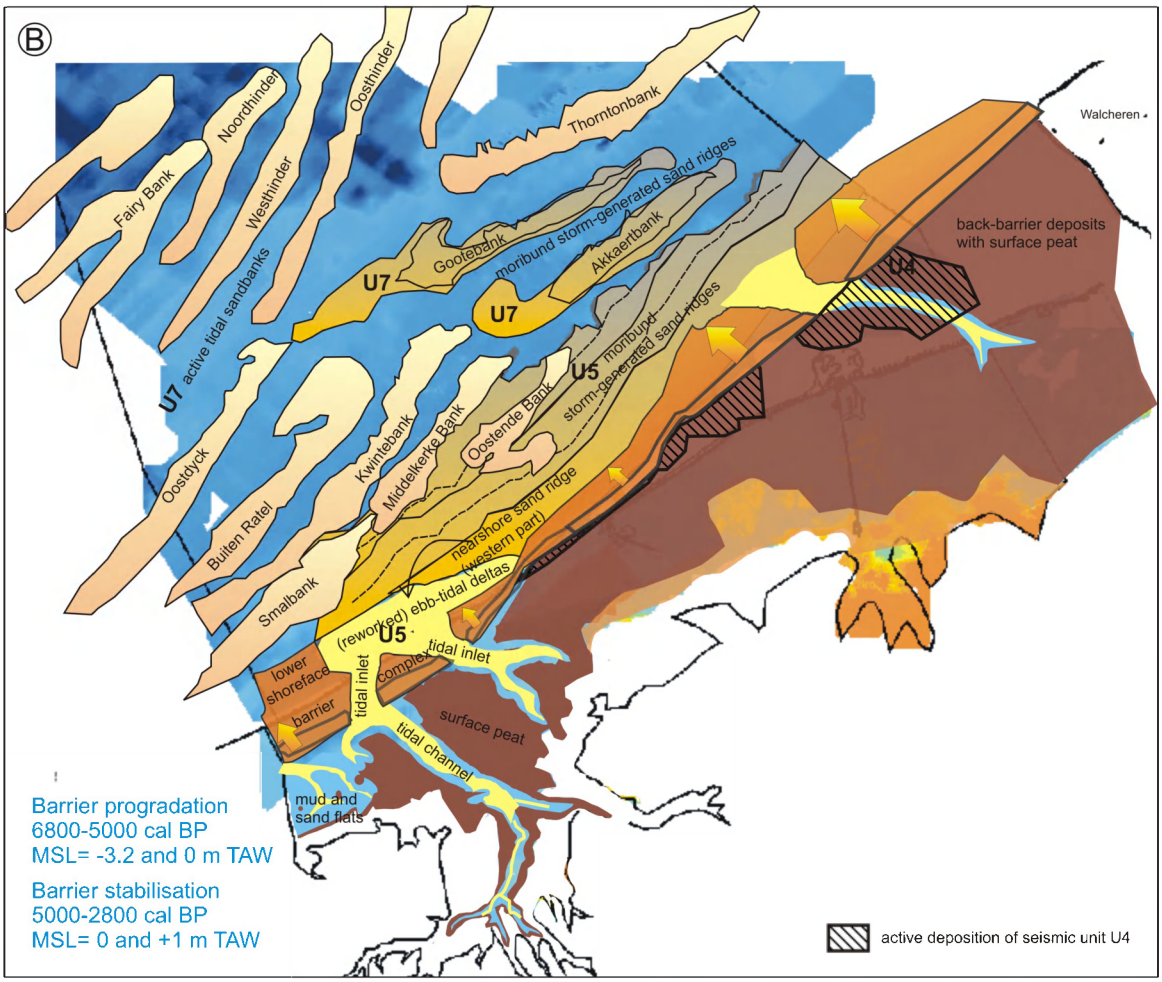

Fig. 9.8 (A) (page 326) Paleo-reconstruction of the situation between 5000 and 2800 cal BP, when the coastal barrier reached its maximal seaward extent since it started prograding around 6800 cal BP, and before a second barrier retreat set in. Mean sea level in that period rose from 0 m to +1 m MLLWS (Baeteman 2004). The situation in the Western Coastal Plain is adapted after Baeteman (2005a). Between 6800 and 6000 cal BP, the relative sea-level rise lost its driving force, so that even the reduced sediment supply exceeded the accommodation space created by the relative sea-level rise, inducing the coastal barrier to prograde. A barrier complex formed with seaward migrating tidal inlets and channels. Between 5500 and 4500 cal BP, almost the entire coastal plain had changed into a freshwater marsh with peat accumulation, the so-called surface peat. Because of the upsilting of the tidal channels, ebb tidal deltas became inactive, and got redistributed, infilling the tidal inlets and forming the eastern nearshore sand ridge. Due to this redistribution, the shoreline got locally lined up again. After 5000 cal BP the barrier complex stabilised. Either because the longshore net sand transport could not be trapped anymore due to the redistribution of the ebb tidal deltas, or because the offshore sediment supply was simply exhausted due to the barrier progradation. Also the formation of the tidal sandbanks since 7000 cal BP, which definitely triggered a change in the hydrodynamic pattern, might have played a role in the coastward sediment supply as well. At that time of stabilisation, in the west, the barrier extended again seaward of the modern coastline. In the east, the barrier had migrated seaward over the previous developed nearshore shoreface-connected ridge, so limiting its minimal age between 6800 and 5000 cal BP (period of barrier progradation).
(B) Since 7000 cal BP, the Hinder and Flemish tidal sandbanks formed simultaneously in the offshore area, on top of the moribund outer and middle U5 storm-generated sand ridges. Likely the Thornton tidal sandbank (Zeeland Ridge) formed slightly before that time, when the sediment transport direction was still directed onshore, instead of alongshore.

In spite of the second slow down in the relative sea-level rise, around 5500 cal BP, the barrier did not continue prograding, but stabilised (Fig. 9.3). At that time in the west, the barrier had extended seaward of the modern coastline. In the east, the barrier had migrated seaward over the previous developed nearshore storm-generated ridge, so limiting its minimal age between 6800 and 5000 cal BP (period of barrier progradation) (Fig. 9.8A).

Meanwhile, since 6400 cal BP, periods of peat growth lasted longer and the lateral extension of freshwater marshes became more widespread (Baeteman and Declercq 2002, Baeteman 2008). And between 5500 and 4500 cal BP, almost the entire coastal plain had changed into a freshwater marsh with peat accumulation, the so-called surface peat (Baeteman 1999, Beets and van der Spek 2000, Baeteman et al. 2002) (Figs. 9.3 and 9.8A). So by that time, tidal channels had already fallen out of use due to upsilting, which generated areas beyond tidal influence where reed peat could start to accumulate (Baeteman 2004). Major tidal channels remained open though as drainage for the peat swamp. Because of the upsilting of the tidal channels, ebb-tidal deltas became inactive and got redistributed, infilling the tidal inlets and forming the western nearshore sand ridge (being a Type 2B (i) shoreface-connected sand ridge of Dyer and Huntley (1999), i.e. a (reworked) product of an ebb-tidal delta in a tidal inlet of a barrier) (Fig. 9.8A). Due to this redistribution, the shoreline got locally lined up again, which might be part of the reason why after 5000 cal BP the barrier complex stabilised. This line up and the disappearance of ebb-tidal deltas could have caused that the longshore current could not be trapped anymore, which supposingly supplied sediments required for the build up of the barrier since 7000 cal BP.
The sediment deficiency responsible for the stabilisation of the barrier, instead of a continuing out build and vertical growth with rising sea-level, is not due to an increased sediment need for the back-barrier basin, because by 5000 cal BP, the area was virtually completely upsilted, but due to a reduced sediment supply from offshore to the shoreface. Either because the longshore net sand transport could not be trapped anymore due to the redistribution of the ebb-tidal deltas, or because the offshore sediment supply was simply exhausted due to the barrier progradation (Baeteman 2008). It is more likely that the sand supply was not exhausted, but continued decreasing after 7000 cal BP, which led to a sand deficit with continuing sea-level rise. This is in contrast to the situation before, when the decrease in sand supply was slow enough compared with the decrease in sea-level rise to cause even a temporary sand surplus (and consequently barrier progradation). Also the formation of the tidal sandbanks since 7000 cal BP (Figs. 9.3 and 9.8B), which definitely triggered a change in the hydrodynamic pattern, might have played a role in the coastward sediment supply as well. It is most likely that the barrier expansion continued until supply from all the sediment sources together (eroding ebb-tidal deltas, alongshore transport, cross-shore transport) did no longer exceed the effects of sea-level rise.

As already mentioned, the extent of the barrier progradation since 6800 cal BP was not the same over the entire coastline. In the western Coastal Plain, the barrier prograded about 4.5 km, while in the centre, offshore Westende, the barrier only prograded 500 m in the period between the stabilisation of 7500 cal BP and the renewed barrier retreat of 2800 cal BP. While further eastwards, the prograded distance gradually increases again from 1.5 km offshore Oostende, to 6.5 km offshore Zeebrugge. In the centre, the sediment supply did not exceed the accommodation space created by the relative sea-level rise, but reached an equilibrium which made the barrier remain in a more or less stable position, instead of prograding as was the case in the west and east, between 6800 and 5000 cal BP. So there was either less sediment available at the shoreface, compared to the western and eastern barrier, or there was more sediment needed in the central back-barrier area. The latter can be ruled out, as the central back-barrier area near Westende is rather narrow because of the shallow position of the Pleistocene surface. Probably due to local hydrodynamic processes, such as the formation of the Flemish tidal sandbanks or the capture of sediment by the updrift ebb-tidal deltas, the sediment supply towards the central barrier shoreface was much less than towards the western and eastern section, which prograded much further.

Renewed expansion of the tidal environment and barrier retreat from 2800 cal BP to 1200 cal BP (750 AD)

After 2000-3000 years of uninterrupted peat growth (since 6400-5500 cal BP, Baeteman and Declercq 2002, Baeteman 2008), a tidal system was again installed in the back-barrier area and peat areas were transformed into sub- and intertidal flats (Fig. 9.3). The surface peat growth ended during the Roman occupation between 2400 cal BP and 1500 cal BP (450 BC-450 AD) in the western Coastal Plain and between 2550 cal BP and 1650 cal BP (300 BC-300 AD) in Zeeuws-Vlaanderen. The renewed expansion of the tidal environment was not the result of a sea-level rise. Since the sea level still rose with the same strongly reduced trend as during the peat growth (0.7m/1 ka). Re-entrance of the tidal system was probably induced by the cleaning of older channels due to an increased rainfall and excessive run-off from the continent, related to a climatic change around 2800 cal BP and human activity (Baeteman 2005b) (Fig. 9.3). Due to compaction of the peat and collapse of the channel banks, a lowering of the ground level occurred, which induced an increase of the tidal prism of the tidal channels and consequently, deep vertical incision (e.g. a predecessor of the Zwin channel). Possibly also peat digging induced compaction, and thus intensified the process of tidal inundation (Baeteman 2007b). The sediment needed to fill the deep incised channels came from the early and mid-Holocene channels and the eroding shoreface. This resulted in a landward migration of the coastline and erosion of the tidal flats in the present-day offshore area, leaving a shoreface ravinement surface (Fig. 9.9). Most of the eroded sediments were, however, used to infill the channels, so probably only small ebb-tidal deltas were formed, but not an extensive transgressive sand sheet. Although a thin layer of eroded organic-rich back-barrier deposits could have settled in the offshore area below the lower shoreface on the shoreface ravinement surface, and in a deep elongated barrier-parallel depression, in front of the barrier (part of seismic unit U6 deposits) (Fig. 9.9).

Not until 1400-1200 cal BP (550-750 AD) sediment supply and tidal prism reached an equilibrium with the sea-level rise in the western Coastal Plain (Fig. 9.3) (750-900 AD in Zeeland). The newly formed channels came in intertidal position (infilling phase), and the major part of the plain evolved again in a supra-tidal environment. As almost no sediment was needed for the further infilling of the remaining tidal channels, the barrier retreat probably slowed down or even stopped, and did not retreat much further. When the receding barrier stabilised, the shoreline coincided with the present-day coastline in the west, in the centre it formed the seaward limit of an 'island' surrounded by tidal channels (Testerep), on which former settlements of Westende, Oostende, and Middelkerke have been found, and in the east the coastline was still located at about 10 km from the present coastline, forming the seaward boundary of the island 'Wulpen' (Fig. 9.9 presents the situation before 1300 AD). At that time the barrier still consisted of a range of high dunes, several kilometres wide, which were overgrown and even wooded (Augustyn 1995).
The reconstructions show that the coastal barrier did not retreat constantly over a same distance along its entire length. In the western section, the barrier retreated over a distance of only about 1 km up to the present-day coastline, in the central part between Westende and Middelkerke the barrier did not retreat since its former position at 5000-2800 cal BP, while further eastwards, the barrier retreated progressively from 1 km to more than 5.5 km. Three reasons are suggested for this extreme discrepancy between the western and eastern part. They are all due to differences in sediment supply towards the barrier shoreface and differences in sediment need (accommodation space) of the back-barrier, as the rate of relative sea-level rise is constant along the coastline.

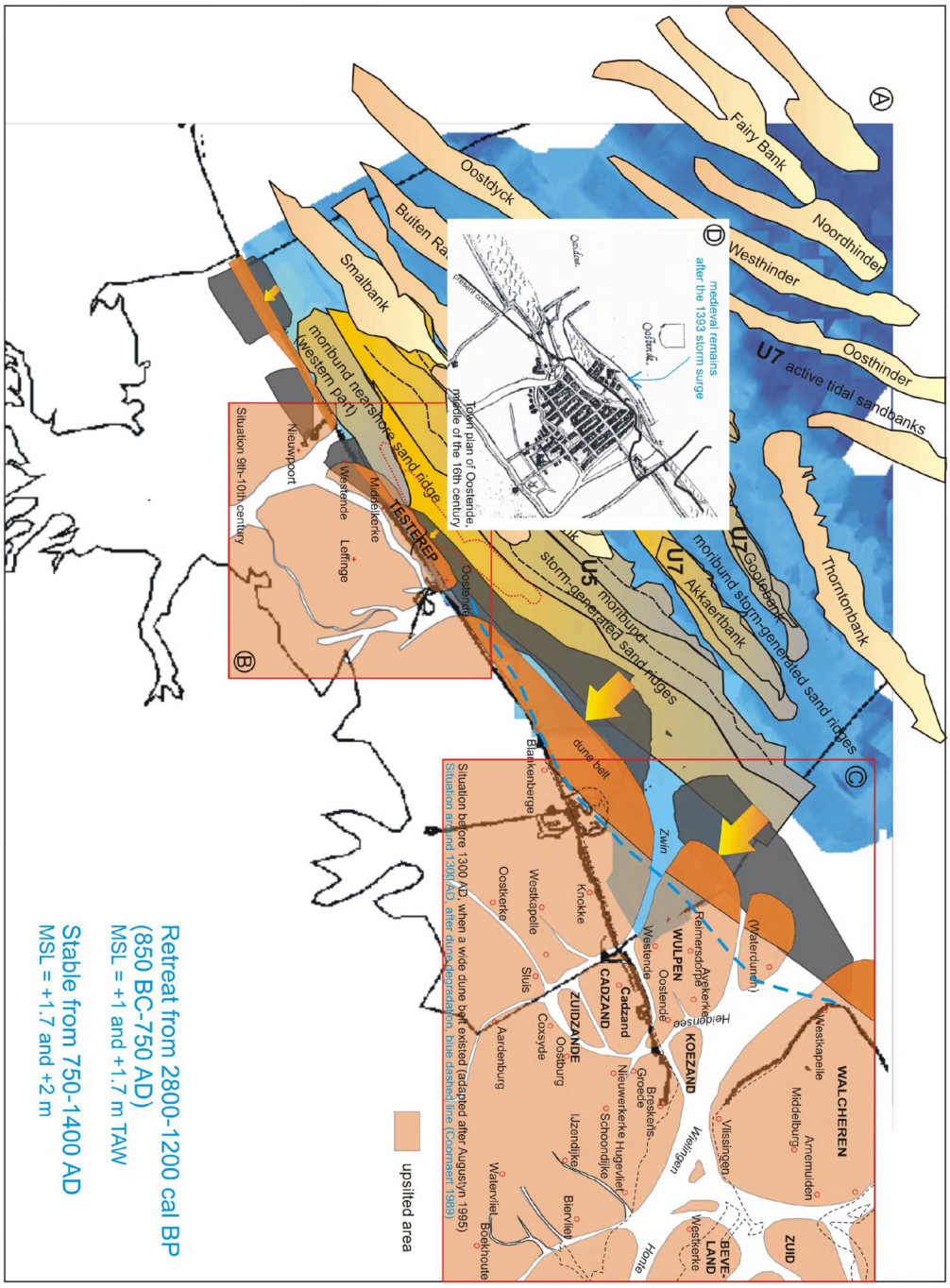

Fig. 9.9 (A) Paleo-reconstruction of the situation between 2800 cal BP and 1400 AD. After 2000-3000 years of uninterrupted peat growth, a tidal system was again installed in the back-barrier area. Peat areas were transformed into sub- and intertidal flats and re-opened tidal channels vertically incised. The sediment needed to fill the deep incised channels came from the early and mid-Holocene channels and the eroding shoreface. This resulted in barrier retreat and erosion of the tidal flats in the present-day offshore area. Around 1200 cal BP (750 AD), the back-barrier was completely upsilted again, and as almost no sediment was needed anymore for the further infilling of remaining tidal channels, the barrier retreat probably slowed down or even stopped. A wide dune belt formed in a gradual curve from Nieuwpoort to the western corner of the island Walcheren. (B) The situation in the Early Middle Ages (9^{th}-10^{th} century) in the area of Oostende (http://nl.wikipedia.org/wiki/Testerep). The plain had silted up to high-tide level, except for some tidal channels which remained open. In that period an 'island' surrounded by tidal channels, 'Testerep', was located near the present-day coastline on which former settlements of Westende (in the west), Oostende (in the east), and Middelkerke (in the middle) have been found. The medieval town of Oostende remained located offshore the present-day coastline to at least a storm surge of 1393 AD. (C) The map shows the situation in the east before 1300 AD (Augustyn 1995), when a wide dune belt was still intact. The blue dashed line indicates the coastline around 1300 AD when the dune belt was largely degraded by human impact (Coornaert 1989). (D) A map of the situation near Oostende shows that after the storm surge in 1393, little remained of the original 13^{th} century town of Oostende. The last remnants completely submerged in the sea between the 16^{th} century and today (Augustyn, 1995).

(1) As the barrier retreat is stimulated by the infilling of deeply incised late-Holocene tidal channels, the difference in barrier retreat between the eastern and western section might be sought in a difference in size and/or number of tidal channels, or the time the tidal channels were open in both areas.
(2) As the natural compaction of the surface peat covering the back-barrier area induces an increase in accommodation space, i.e. an increase in tidal prism, it induces the sediment need for the particular area. So, the surface area of the back-barrier region might be an indication for the potential accommodation space created between 2800 and 1200 cal BP, and the consequently needed sediment supply (which induced the barrier retreat). Note, however, that in this reasoning the thickness of the surface peat is not taken into account. Thin peat layers, e.g. where the Pleistocene substrate lies high, will create less accommodation space. Neither the presence of tidal channels is taken into account. The potential for the surface peat to incline, depends largely on the presence of nearby channels which cause the drainage and consequent compaction of the peat. Apart from the location of some large tidal channels in the eastern plain, little is known about the smaller channel networks.
(3) Possibly, also a factor of differential sediment supply should be taken into account as was suggested by Denys (2007). Before 7500 cal BP, the barrier migrated constantly over its entire length and formed a straight line. But since 5000 cal BP (and not since the early Holocene as was suggested by Denys 2007), the eastern plain protruded a few kilometres further seaward than the central plain, and formed a kind of 'headland' (Fig. 7.49A). According to Denys (2007) this 'headland' could have intercepted the along-shore net sediment transport which was oriented NE-ward, causing a larger sediment deficiency in the east compared to the west, inducing the eastern barrier to retreat further landward.

Around 1200 cal BP (750 AD), when the back-barrier area was upsilted in supratidal position and the barrier stabilised, the coastline had developed towards a straight line once more. With the disappearance of the 'headland', the longshore sediment drift was no longer intercepted and the available sediment surplus could possibly be used to build the wide chain of dunes (Figs. 9.3 and 9.9).

Human induced barrier retreat in early 15th century

The second part of the barrier retreat, after the upsilting and stabilisation around 750 AD, up to the present-day coastline, was a consequence of human intervention. Harbour construction and the almost total conversion of the dunes from a natural landscape into a man-made landscape, mainly intended for breeding cattle, led to a slow but irreversible degradation of the dunes from the 12th century onwards (Augustyn 1995) (Fig. 9.3). Violent north-westerly storms got a grip on the dune landscape and accelerated the degradation of the dune landscape until, by the late 14th/early 15th century, little more was left but small unstable drift-sand dunes. Until eventually, in 1404, a north-westerly storm almost completely destroyed this chain of dunes, leaving only the small stretch of dunes in the western Coastal Plain (Fig. 9.3). During this storm surge, the large isle of Wulpen completely submerged in the sea, which caused irreversible hydrographical changes in the mouth of the Western Scheldt (Fig. 9.10C). According to Vos and van Heeringen (1997), however, it was the mismanagement of dikes and embankments which induced the inundation and losses of large areas of Zeeland, and the consequent hydrographic changes in the Western Scheldt.
Due to these changes in the hydraulic regime and the consequently stronger tidal currents near the entrance of the widened Western Scheldt, the original –natural- and storm-induced shoreface ravinement surface was deepened, until an equilibrium was

reached under the new hydraulic regime. This did not happen though until the middle of the 16th century, as it was then still possible to trace the contours of the drowned island (Augustyn 1995), while the equilibrium surface adjusting to the renewed hydrographic situation reached a depth of -12 m before it was covered with sediments. So at least after the middle of the 16th century, the eroded, high-organic muddy sediments (of former back-barrier deposits) could settle, alternated with sandy storm layers, in a sheltered area between the isle of Walcheren and a shallower area between the present Wenduine Bank and the present coastline. This is represented by seismic unit U6 (Figs. 9.3 and 9.11A).

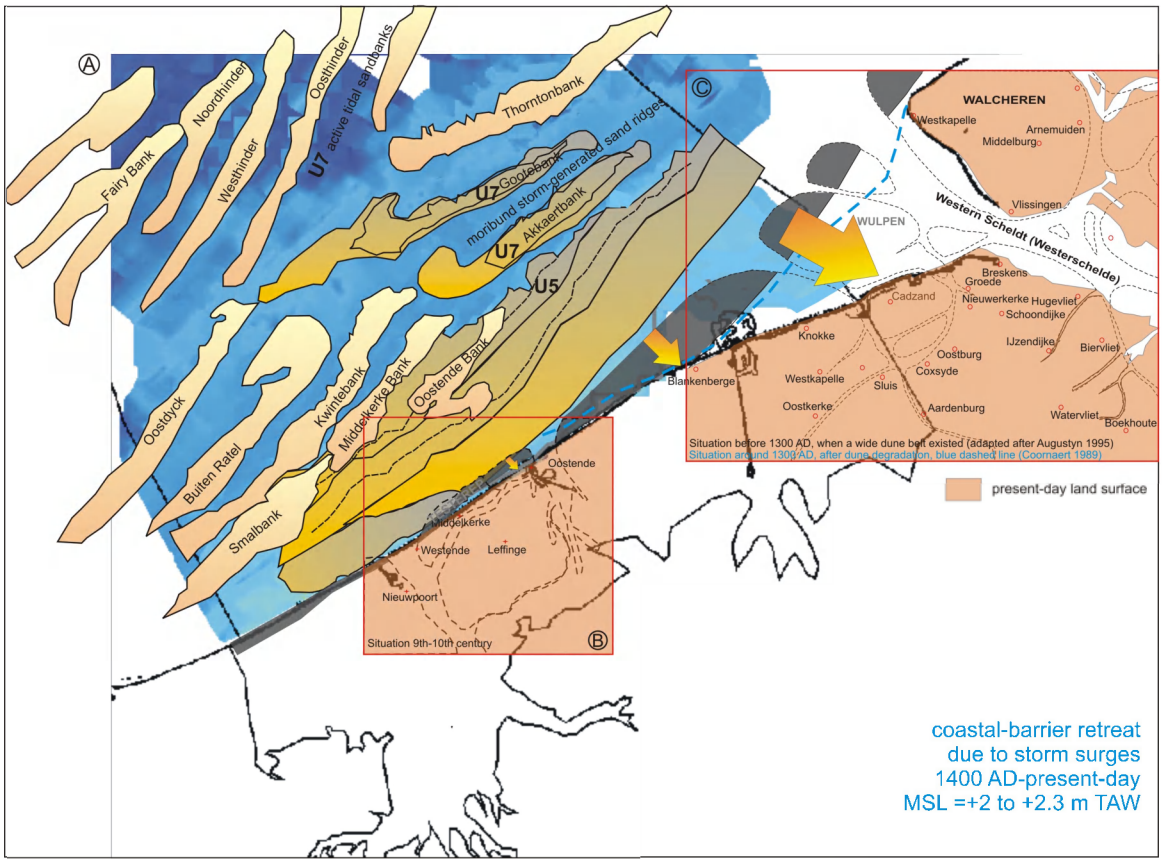

Fig. 9.10 (A) Mismanagement of dunes led to an irreversible degradation of the protective dune belt from the 12th century onwards. Violent north-westerly storms got a grip on the dune landscape and accelerated the degradation of the dune landscape until, by the late 14th/early 15th century, little more was left but small unstable drift-sand dunes. Until eventually, in 1404, a north-westerly storm almost completely destroyed this chain of dunes. (B) In the central part, the coastline retreated about 1.5 km during the storms in the 14th/15th century, so that by the 16th century, the island Testerep and the old town of Oostende were completely drowned, and the present coastline was about reached. (C) In 1404, the large isle of Wulpen submerged in the sea, which resulted in irreversible hydrographic changes in the course of the Zwin and Westerschelde. Due to these changes in the hydraulic regime and the consequently stronger tidal currents near the entrance of the widened Westerschelde, the original –natural- shoreface ravinement surface was deepened, until an equilibrium was reached under the new hydraulic regime. This, however, did not happen until the middle of the 16th century, as it was then still possible to trace the contours of the drowned island (Augustyn, 1995, 2000), whereas the equilibrium surface adjusting to the renewed hydrographic situation reached a depth of -12 m before it was covered with sediments.

In the western plain, the present-day coastline was possibly already reached during the initial, natural barrier retreat. Probably because it was the only section of the coastline where the chain of dunes were not destroyed during the storm of 1404 AD (possibly because they were less damaged by human activity), the coastline did not retreat any further. In the central part, the coastline retreated about 1.5 km during the storms in the 14th/15th century, so that by the 16th century, the island Testerep and the old town of Oostende were completely drowned, and the present coastline was almost reached (Figs. 9.9D and 9.10B). In the east, after the initial, natural retreat of 5.5 km, the barrier receded another 10 km. The Western Scheldt estuary was the region where most land was lost to the sea, because there the NW storm swept across the land from two sides (Augustyn 1995, Termote 2006), because the island was surrounded by two large channels, i.e. the Zwin, and the Western Scheldt, which existed since the progressively eastward migrating tidal channel 'Honte' connected the Scheldt with the North Sea (age is still under debate).

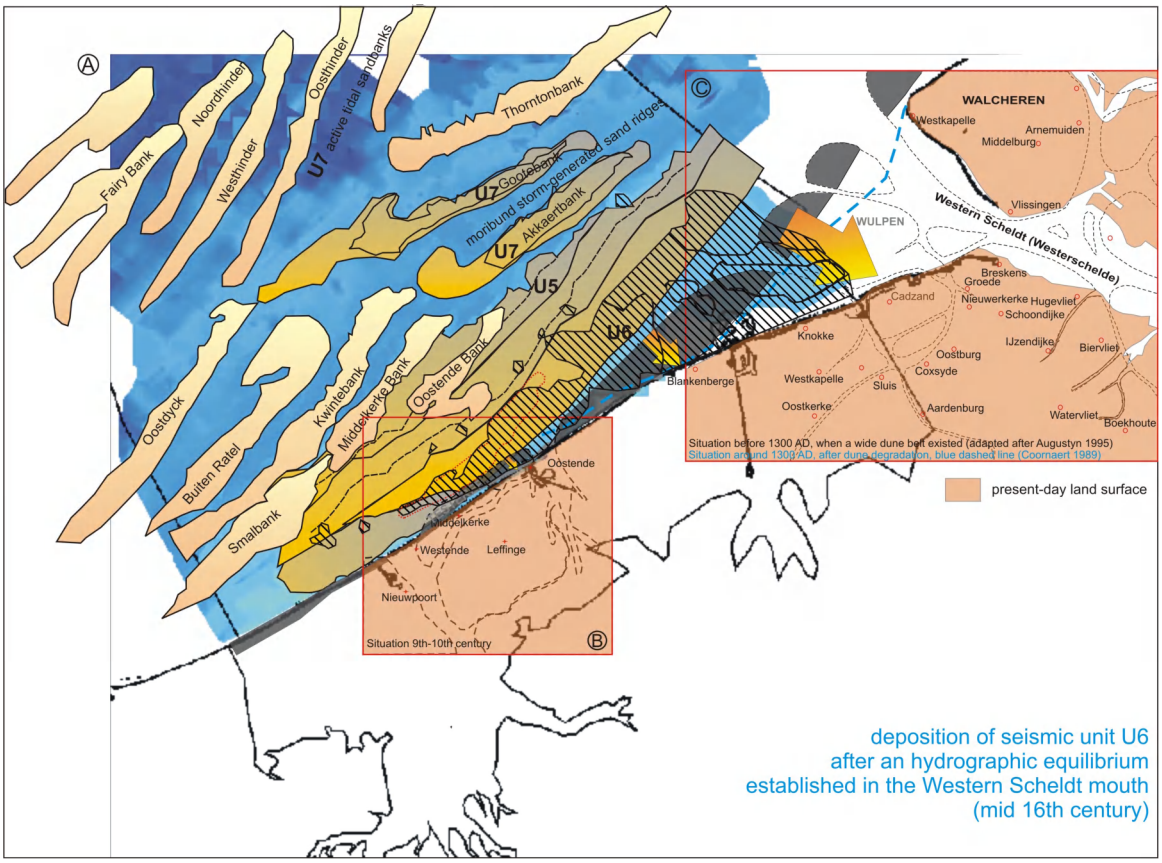

Fig. 9.11 Unit U6, which is for the major part located within the back-barrier area of 5000 cal BP (cf. Fig. 7.45), represents remnants of the back-barrier deposits and surface peat of that time, which have been eroded during the natural barrier retreat since 2800 cal BP. And on the other hand, it represents remnants of newly upsilted areas since 1200 cal BP (750 AD), which have been eroded in the early 15th century by the intensive storm surges. It was at least after the middle of the 16th century, that these eroded, high-organic muddy sediments (of former back-barrier deposits) could settle, alternated with sandy storm layers, in a sheltered area between the isle of Walcheren and a shallower area between the Wenduine Bank and the present coastline, when the hydrographic equilibrium in the Western Scheldt mouth was re-established.

Formation of the Coastal Banks s.s.

After the deposition of seismic unit U6, the Coastal Banks s.s. started developing on top of it (seismic unit U7) (Figs. 9.3 and 9.12l). On the basis of morphological evidence these banks represent shoreface-connected ridges. They developed simultaneously though, as a response of the sea bed to a suitable hydraulic regime of wave (storms) and tide, and not in relation to a retreating shoreline as the coastline had already reached the present-day position by the time they could form. The Wenduine Bank s.s. is not connected to the beach but to an elevation in U6, which might resemble the situation at the northern coast of the Netherlands and Germany, where the ridges disappear into the shoreface sand sheet, presumably because of the higher tidal-current and wave regime (Dyer and Huntley 1999). Although shoreface-connected ridges have been considered a special class of storm-generated ridges, a storm-dominated setting is not essential for the formation of shoreface-connected ridges (van de Meene and van Rijn 2000).

The difference between the Hinder Banks and Flemish Banks on the one hand, in which seismic unit U7 has been interpreted as tidal sandbanks, and the Coastal Banks and Zeeland Ridges on the other hand, in which U7 has been interpreted as shoreface-connected or storm-generated ridges, is still observed in the present-day hydrodynamics. It has been deduced by Lanckneus et al. (2001), that the strongest tidal current tends to erode one flank of the bank maintaining the steep slope. And in general the residual sand transport around a sandbank is in clockwise direction, as predicted by the sediment transport model.

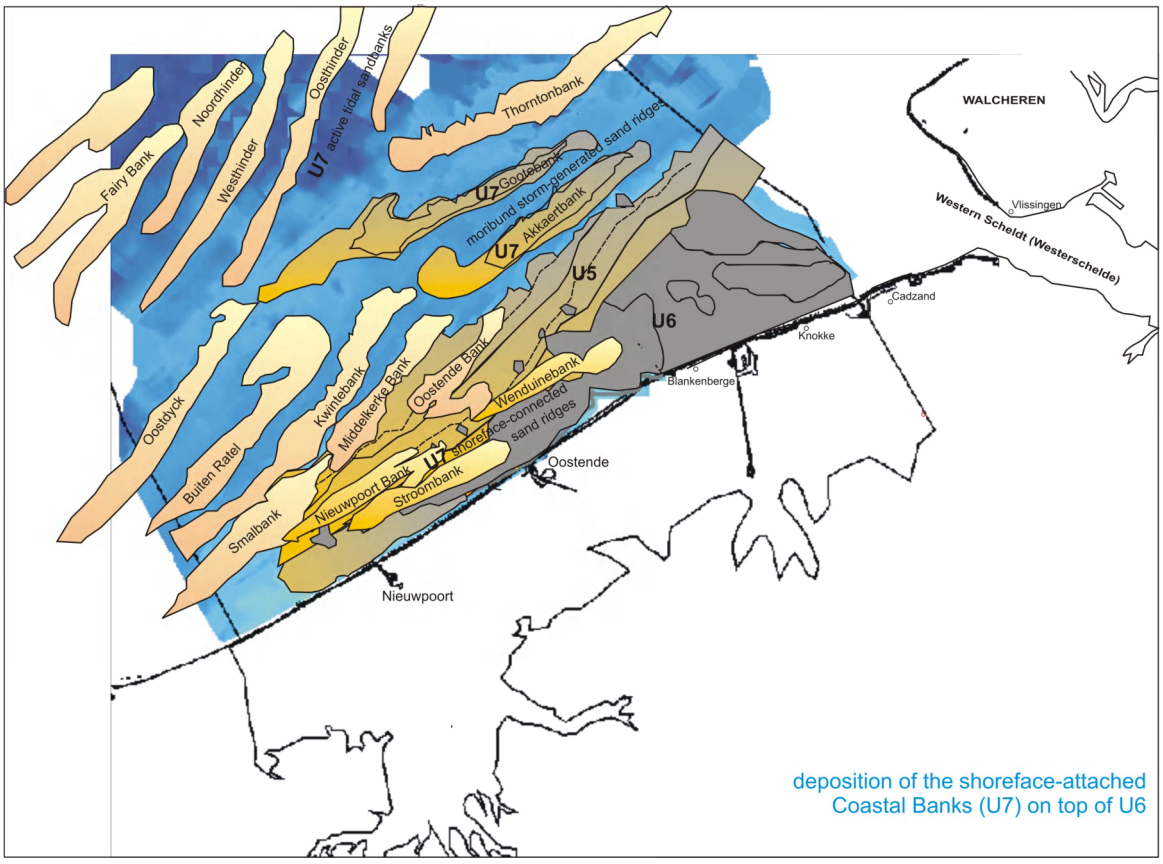

Fig. 9.12 After the deposition of seismic unit U6, the Coastal Banks shoreface-connected ridges started developing on top of it (seismic unit U7)). They, however, developed simultaneously as a response of the sea bed to a suitable hydraulic regime of wave (storms) and tide, and not in relation to a retreating shoreline as the coastline had already reached the present-day position by the time they could form.

However, in both the Coastal Banks and Zeeland Ridges area, the steep side is located at the eastern side of the banks, and modelled maximal tidal currents show a flood dominance in the areas, so implying a anti-clockwise sand transport direction. So, or the sand transport direction is anti-clockwise, or the steepest flanks of the Coastal Banks and Zeeland Ridges are not maintained by the strongest tidal current and have a different origin. The transport direction around the Coastal Banks is not anti-clockwise (Van Lankcer 1999). So, it is possible that the steep slope of the Coastal Banks and Zeeland Ridges is inherited from their nearshore formation under wave and storm action.

9.2 General remarks

9.2.1 Comparison between the Eemian and Holocene coastline migration

Contrary to the fact that the Eemian and Holocene relative sea-level curves are quite similar and reach similar heights at their highstand, the coastline evolution during these periods was rather different.

Depositional environments and tide versus wave power

During the Holocene

During the Holocene, the linear coastline evolved from a transgressive barrier with a tidal-flat back-barrier basin, from the time when the Southern Bight was large enough to form waves, to a regressive, seaward prograding barrier or strandplain when the relative sea-level lost its driving force around 6800 cal BP (Fig. 9.13B). According to the model of Boyd et al. (1992) and Davis and Hayes (1984), these deposits are typical of a transgressive mixed wave-tide and a prograding wave-dominated coastline, respectively (Fig. 9.14). Although, the prograding barrier might as well represent a mixed wave-tide environment. As literature models do not include *prograding mixed* wave-tide environments, it is not known whether a mixed-energy coastline would develop as a strandplain, as exposed tidal flats, or a combination of both.

It was generally assumed that barrier islands and associated environments only develop on microtidal and mesotidal coasts, and are absent on macrotidal coasts (Hayes 1979, Reinson 1992, Boggs 1995, Galloway and Hobday 1996). Tidal inlet width increases and barrier length decreases with increasing tidal range, until the coast passes into the macrotidal category. At that point the barriers vanish, and the shoreline is dominated by shore normal tidal channels and their ebb-tidal deltas (Swift et al. 1991). But it is known from model results (van der Molen and van Dijck 2000) that around 7000 cal BP, when there was still a barrier present on the BCS, the tidal system differed only little from the present one, and was in fact already macrotidal. In the case of the BCS, the barrier islands did not vanish, to the contrary, they merged together as tidal inlets closed with the infilling of the back-barrier basin, and the entire coastal barrier started to prograde seawards, forming a strandplain or barrier complex. Consistent with the model of Boyd et al. (1992), this system developed in a prograding wave-dominated environment (or maybe a prograding mixed-energy environment) (Fig. 9.14), even when the tidal system was macrotidal. According to the theory of Davis (1994), however, barrier islands can develop in macrotidal conditions, as it are not the absolute values of wave height or tidal range that are significant, but the relative influence. Whether a region has a microtidal or macrotidal range, if the wave energy is sufficient to overcome the tidal currents, the region is wave-dominated or mixed wave-tide influenced and barrier islands will develop. So although around 7000 cal BP the tidal range is macrotidal, the wave energy was

possibly strong enough to allow the progradation of a barrier (or strandplain) (Fig. 9.13B, tidal action < or = wave action).
This theory also explains how before the formation of the barrier coastline (9500 cal BP), when the tidal range was microtidal (van der Molen and van Dijck 2000), the BCS and Southern Bight could be tide-dominated, which appears from the presence of open-coast tidal flats (Eisma et al. 1981) (Fig. 9.13B). Even if the tidal range was microtidal, the wave energy at that time was still too weak to overcome the present tidal currents to form a barrier (Fig. 9.13B, tidal action > wave action). Probably because in the early Holocene the water surface of the initial southern North Sea was too small, so the fetch (distance of open water over which the wind blows) was to small to form waves big enough for the creation of a barrier.

The present-day coastline, although far from natural, is a more or less stabilised closed barrier. In some places one tries to reconstruct the natural situation by building artificial tidal inlets. But the inlets tend to close again as the back-barrier area is completely infilled, so the present-day natural situation, although under a macrotidal regime, is not an open tidal-flat environment, but a closed coastline with a strandplain (Baeteman 2008) (Fig. 9.13B). According to the model of Boyd et al. (1992) this would suggest a wave-dominated situation (Figs. 9.14 and 9.13, tidal action < wave action). However, plotting the present-day mean tidal range (4 m) and mean significant wave height (0.5-1 m, Van Lancker 1999), on the diagram of Davis and Hayes (1984) (in: Davis 1994), indicates tide-dominated conditions at the present-day BCS (Fig. 9.14B, tidal action > wave action!).

Three possible explanations are suggested for the present-day closed coastline in a tide-dominated environment.

(1) It might be that the situation is not in equilibrium with the present hydrodynamics and is a remnant of a time when wave or storm action were stronger and dominated over tidal currents, e.g. at the time of frequent storm surges in the late 14th/early 15th century and during the Little Ice Age from 1430-1850 AD, especially from 1530 AD when also summer storms and summer storm surges occurred (Buisman 1998-2000). For a mean tidal range of 4 m the expected mean significant wave height should have been at least 1.6 m to have mixed-energy conditions (diagram in: Davis 1994). Long-term model results for the Southern Bight (based on present-day wind climate) rule this out, as the mean significant wave height was maximal 1.3 m since 7500 a BP (8300 cal BP) (van der Molen and de Swart 2001b). However, short-term, more regional data should be consulted as well.
(2) Another option that could be considered is that in the present-day unnatural situation, there is not enough sediment supply for the formation of exposed tidal flats. It is remarkable however, that a mudflat, characterised by rapid sedimentation, developed along the IJzer estuary which has been enlarged several years ago. But even when there would be a sediment deficiency (transgression), generally still open tidal flats develop in a tide-dominated environment according to the model of Boyd et al. (1992) (Fig. 9.14).
(3) Another explanation might be that on the Belgian shelf, where the maximal tidal current in the nearshore area is oriented alongshore in NE direction, the tidal current enhances the longshore wave induced sediment drift, which normally creates the barrier in a wave-dominated setting, giving the present coastline a wave-dominated appearance under tide-dominated circumstances. This in contrast to the model of Boyd et al. (1992) which is based on tide-dominated environments where exposed tidal flats develop under tidal currents oriented *normal* to the coastline, which enhances the formation of shore normal tidal channels. E.g. Davis (1992) states that tide-dominated coasts are subjected to such extreme tidal currents, oriented essentially perpendicular to the coast, that

wave action is not effective and longshore currents are practically absent. Galloway and Hobday (1996) say that tidal currents on the shelf tend to flow parallel to open coasts, reversing with the tidal phase. But as the tidal wave propagates, tidal flow is directed toward or away from the coast, so that, in contrast to wave-driven longshore currents, tidal flows and resultant sediment transport are dominantly onshore and offshore. So the Belgian shelf occupies a rather unique position in the Southern Bight, at the narrow transition from the Dover Strait, which induces alongshore oriented tidal currents (since 7000 cal BP) instead of shore normal, which might have counteracted the formation of exposed tidal flats. Tidal current ellipses in the southern North Sea show an extreme elongation due to coastal constriction (Fig. 5 in: Dalrymple 1992). So, the proposed classification of depositional environments along a transgressive or prograding linear coastline (Boyd et al. 1992) is insufficient for explaining the present-day situation along the Belgian shore, as it appears that a closed barrier coastline can also form under tide-dominated conditions.

If the mechanism of longshore tidal currents maintaining a barrier under tide-dominated conditions is physically possible, also the situation around 7000 cal BP should be reconsidered. It was originally suggested, based on the model of Boyd et al. (1992), that the prograding barrier formed under wave-dominated or mixed-energy circumstances (Fig. 9.13B, tidal action < or = wave action), even under a macrotidal regime. Conversely, long-term model results show that mean significant wave heights were never high enough to exceed these macrotidal conditions, so suggesting a tide-dominated environment at the time of the barrier progradation (Fig. 9.13B, tidal action > wave action). However, this conclusion has to be handled with care, as the wave model results are based on present-day wind climate.

During the Eemian

In contrast to the Holocene, during the Eemian highstand open marine tidal flats did form, after the embayed coastline with the tide-dominated estuary gradually became filled and the site evolved into a prograding coast (Fig. 9.13A). Following the above proposed scenario, this would imply that during the Eemian highstand, the tidal currents were oriented normal to the coastline, and not alongshore as is now the case during the present highstand. The general morphology of the southern North Sea during the Eemian was very similar to the present-day basin geometry, i.e. connections to the Atlantic ocean in the North and via the English Channel in the south, were already established (Gibbard 2007, Gupta et al. 2007), and sea level reached similar levels. But during the Eemian the most southward margin of open marine conditions was at least 7 km more south than the most landward Holocene coastal barrier system (Mostaert and De Moor 1989), and the Flemish Valley was inundated and transformed in an estuarine embayment to about 40 km inland (De Moor et al. 1996).
This more landward and embayed coastline might have induced shore normal tidal currents, comparable to the present German Bight, Thames River and Dutch estuaries (Dalrymple 1992), as tidal effects are enhanced in coastal bights and embayments where they are drawn into (Dalrymple 1992, Galloway and Hobday 1996), in contrast to the alongshore currents of the present highstand, now the coastline is more linear and in line with the Dover Straight.

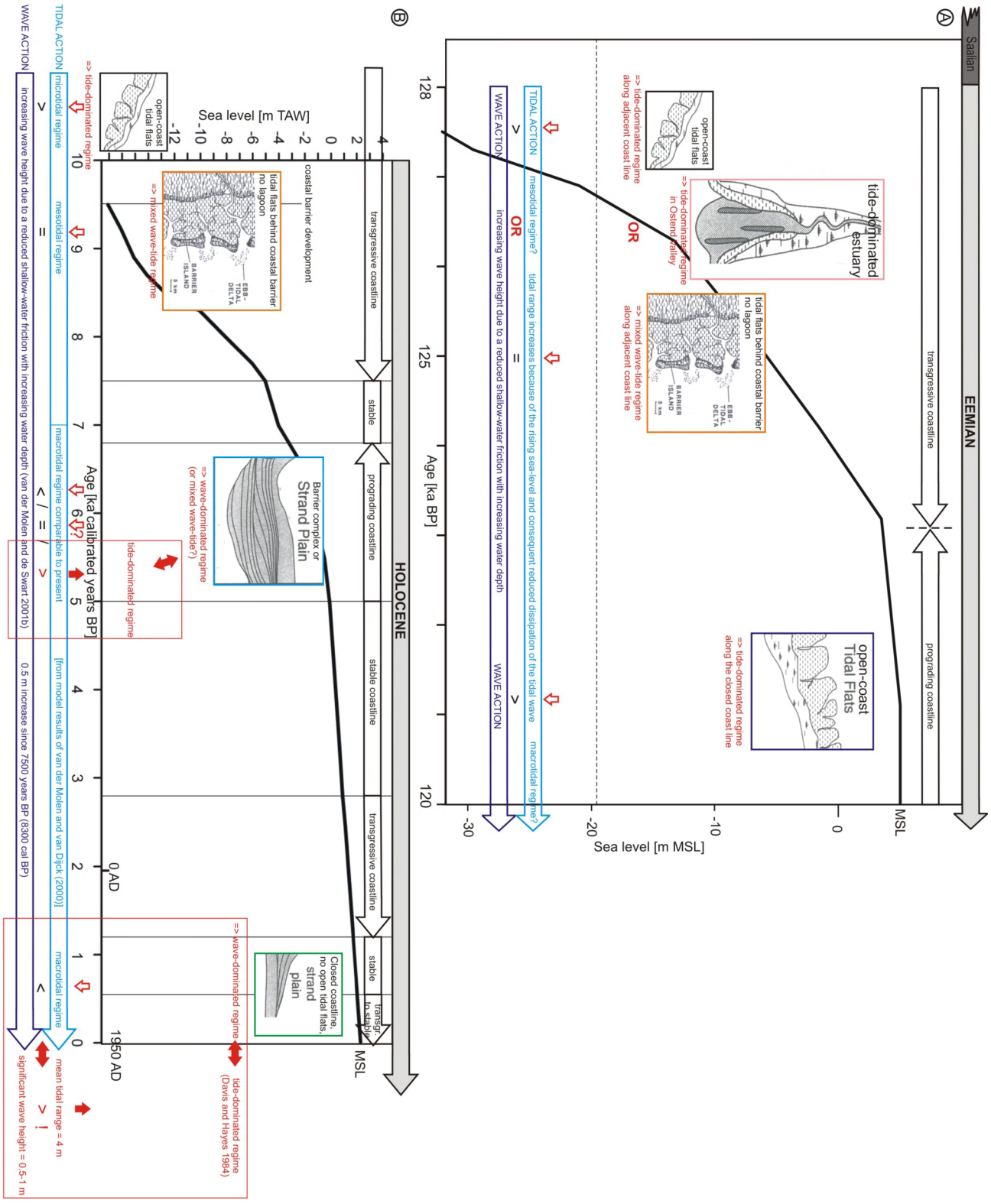

Fig. 9.13 Schematic overview of the coastline migration during the Eemian (A) and Holocene (B) sea-level rise with changing depositional environments. The tide or wave dominance (in red) for each depositional setting (coloured frame) is deduced conform the models of Boyd et al. (1992) and Davis and Hayes (1984) presented in Fig. 9.14. For each depositional setting the relative influence of the tidal and wave action is indicated: tidal action more important than wave action (>), tidal action equal to wave action (=), tidal action subordinate to wave action (<).

During the sea-level rise, the tidal range increased because of the consequent reduced dissipation of the tidal wave in the deepening basin (light blue arrow), and also the wave height increased up to the present, due to a reduced shallow-water friction with increasing water depth (dark blue arrow). The balance between created accommodation space and available sediment supply determined the direction of the coastline movement (transgressive, i.e. landwards or prograding, i.e. seawards) (black arrow). For the Eemian period, the exact moment when the transgressive coastline became prograding is uncertain (vertical dashed line). For the Holocene period is referred to Fig. 9.3. The horizontal dashed line in (A) corresponds to the lowermost value of the vertical scale in (B), which makes it easier to compare both MSL curves. The sea-level curve in (A) is from Cutler et al. (2003), the Holocene MSL curve is the one from Fig. 7.37.

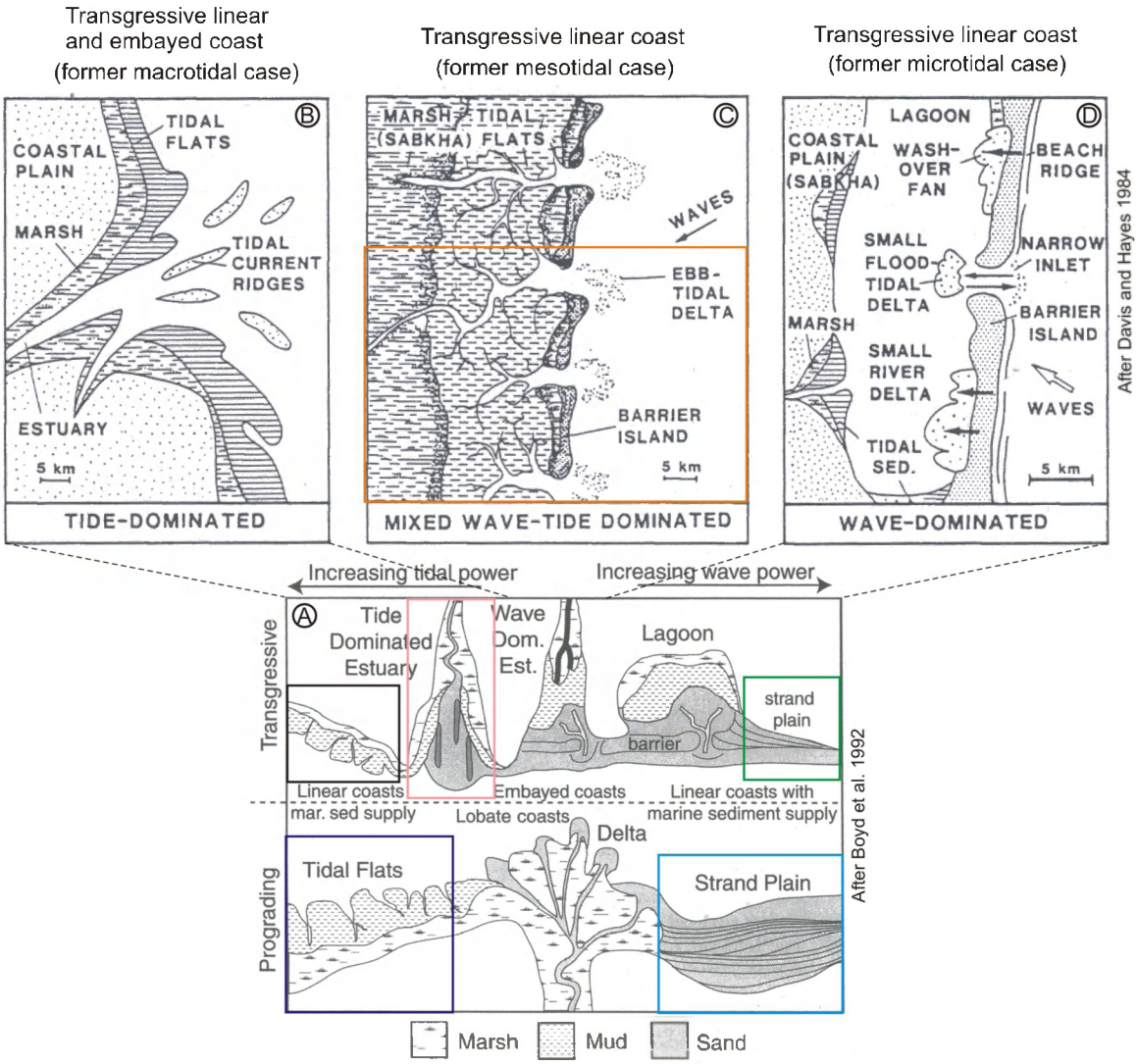

Fig. 9.14 (A) Maps of idealised coastal depositional environments, showing the relationship between wave and tidal power, prograding and transgressive environments, and different geomorphic types (after Boyd et al. 1992). (B) Example of a transgressive linear coastline adjacent to an embayed coastline in tide-dominated circumstances (former macrotidal case). (C) Example of a transgressive linear coastline in mixed wave-tide dominated circumstances (former mesotidal case). This depositional environment of a linear coast line with mixed energies is missing in (A). (D) Example of a transgressive linear coastline in wave-dominated circumstances (former microtidal case). (B), (C) and (D) adapted after Davis and Hayes (1984). The coloured frames indicate the depositional environments which prevailed on the BCS during the Holocene and Eemian sea-level rise, as indicated on Fig. 9.13.

How the coastline evolved adjacent to the Ostend Valley during the Eemian relative sea-level rise, is not known as almost nothing is preserved because of the intensive marine transgression. Some remnants in local depressions are too small to define a depositional environment from on the basis of seismic data alone. The Ostend Valley estuary was tide-dominated, what could be deduced from the funnel-shaped incision (Fig. 9.13A). But relative effectiveness of waves and tides is influenced by the shape of the basin margin (straight, narrow or broadly embayed), the nearshore bathymetry and the orientation with respect to the dominant wave approach (Galloway and Hobday 1996), so the adjacent coastlines do not necessarily have to be tide-dominated as well. Possibly the impact of the wave energy was expended on the open coasts and decreased in the Ostend Valley embayment, where tidal effects were enhanced. Even as the Ostend Valley was tide-dominated, the adjacent coastlines could have been mixed wave-tide or even wave-dominated, with the presence of a barrier instead of open-coast tidal flats (Fig. 9.13A).
The importance of wave action during the Eemian transgression was already acknowledged in a previous chapter (6.3.2 Erosional surface U3, *The scarp*), where the resemblance of the erosional surface of U3 with a wave ravinement surface was recognised. However, it is believed that the Eemian marine transgressive surface or shoreface ravinement surface was not formed by wave action only, but that a combination of tides and waves created it.

Summary

During the Eemian, the hydrodynamic situation probably changed from mixed wave-tide dominated along the straight coastlines and tide-dominated in the Ostend valley during the relative sea-level rise, to tide-dominated along the entire coastline during the relative sea-level highstand, possibly due to a relative decrease (less fast increase) in wave energy with respect to the tidal range increase because of the rising sea-level (and consequent increase in water depth) (Fig. 9.13A).
The absolute tidal range (micro-, meso-, or macro-) during the Eemian, could not be determined though, as the dominance is not determined by the absolute values of tidal range or wave height, but by their relative influence.

During the Holocene relative sea-level rise, the hydrodynamic situation was first tide-dominated with the deposition of exposed tidal flats in a micro-tidal environment, followed by a mixed wave-tide situation when a transgressive barrier with a tidal-flat back-barrier basin developed (possibly under meso-tidal regime). This barrier started prograding, either still in a wave-dominated or mixed wave-tide environment, assuming that the wave heights were larger than the models provide, and had increased enough, to compensate the tidal regime, which was macro-tidal by then. Or, the barrier prograded under tide-dominated circumstances, assuming that the alongshore tidal currents (since 7000 cal BP) replaced or enhanced the wind-wave induced longshore currents, which normally form a barrier. Finally, during the present sea-level highstand the barrier did not evolve into exposed tidal flats as is expected from the prevailing tide-dominated regime. In stead it evolved into a closed coastline, possibly because the tidal current is oriented alongshore, parallel to the wave induced longshore drift, which rather enhances a closed coastline, than shore normal tidal channels.
During the Holocene, the tidal range gradually increased because of the rising sea-level and consequent reduced dissipation of the tidal wave in the deepening basin. Also the wave height increased up to the present, due to a reduced shallow-water friction with increasing water depth (van der Molen and de Swart 2001b).

<u>The shoreface ravinement or marine transgressive surface</u>

Apart from the different depositional environments during the Eemian and Holocene sea-level rise due to differences in relative wave and tide energy, also the marine transgressive surfaces show two remarkable differences. (1) The shoreface erosion after

the estuarine infilling of the Ostend Valley, was that severe that remnants of former Eemian deposits were only left in depressions in the Top-Paleogene substratum. While during the Holocene transgression, most of the former back-barrier deposits (U4) are still present. And (2), on top of the erosional surface no Eemian, open marine deposits have been preserved on top of the basal gravel lag (neither Weichselian fluvial deposits, nor cover sands), while on top of the Holocene ravinement surface a transgressive sand sheet was preserved, in which later sand ridges formed.
That no Eemian open marine sediments are found on top of the gravel lag of the marine transgressive surface, is or because no sediments were ever deposited, or due to erosion during the following Weichselian sea-level drop and the subsequent Holocene transgression. However, the latter could only have happened in the further offshore area, as in the nearshore part U4, which represents the first Holocene deposits, lies directly on top of the Eemian marine transgressive surface (U3 and QT), so possible Eemian open marine deposits must have been eroded before the Holocene transgression and the deposition of U4. The absence of open marine deposits on top of the shoreface ravinement surface is no exception, also in the Kaiser valley on the outer Celtic Sea shelf they were not present, or at least they could not be seismically recognised. Most likely because they were removed by fluvial erosion during the succeeding lowstand (Reynaud et al. 1999). This is, however, no possible explanation for our case, as Eemian open marine deposits are absent on the entire BCS. Neither could the Eemian marine deposits have been removed by initial intensive tidal souring during the Holocene, before deposition of U4, because no evidence of tidal channels is found, which would have eroded the underlying gravel lag and scarp.
Possibly during the Eemian, less or no sediment was supplied offshore to form a transgressive sand sheet (on top of the gravelly ravinement surface), because of the presence of the Ostend Valley which demanded a large sediment supply. As river mouths becoming estuaries not only trap river sediment but also sand from the littoral current of the coast on either side of the estuary (Swift and Thorne 1991).

This is probably also the reason for the more erosional shoreface ravinement during the Eemian, which removed all former Eemian deposits. Simulation models of Roy et al. (1995) predict that variations in the marine sand budget will cause a transgressive barrier to erode the sea bed if there is a net loss of sand (e.g. to the Ostend Valley), while a sand sheet will be deposited if there is a net addition of sand.
Possibly also the initial availability of sediment played a role in the preservation of earlier deposits after shoreface ravinement. If the earlier transgressive facies successions were thin, it would have been easier to remove them completely. It is possible that during the Saalian (catastrophic) proglacial lake outflow a lot of sediment was removed from the seabed (Cohen, pers. comm. 2007), which could have induced an initial smaller availability of material for the build up of Eemian transgressive facies successions. In contrast to the Holocene transgression, which was preceded by renewed Weichselian fluvial sediment input (e.g. Rhine-Meuse origin), which was not removed by a (catastrophic) outflow.
Preservation of back-barrier systems and the thickness of transgressive facies successions also depend on the rate of relative sea-level rise (Reinson 1992, Davis 1994). Assuming all other factors to be constant, if sea-level rise is slow, the barrier system may be completely destroyed. While rapid sea-level rise permits nearly total preservation and in place drowning of the barrier, so that almost complete transgressive sequences are preserved. This implies that the Eemian transgression would have been slower than the Holocene transgression, which, however, does not show in the respectively relative sea-level curves (Fig. 9.13AB). So a different sediment budget as explanation for the more intensive erosion during the Eemian transgression than during the Holocene, is more likely.

9.2.2 Sediment budget on a tide-dominated autochthonous shelf

Most of the extensive tide-dominated shelf regions in the world that are neither carbonate nor adjacent to rivers are autochthonous (Davis 1992). The present North Sea is the best example of a tide-dominated autochthonous shelf. It has a high tidal-current energy and displays great variety and complexity in its sediment patterns. Autochthonous shelves are those on which sediment already on the shelf is reworked and redistributed to equilibrate with existing conditions. This in contrast to allochthonous shelves which derive their sediment from other adjacent environments, typically via rivers. Autochthonous shelves tend to be dominated by sand-size sediment, with some terrigenous and biogenic lag gravels but with little mud-size sediment except in areas sheltered from the tidal currents. Because of sustained, rapid currents passing over the shelf, the reworking of existing sediment is such that inherited morphology and sediment patterns are essentially nonexistent.

Apart from classification on the basis of process regime, shelves can also be classified according to stratigraphic architecture, which is determined by the balance between sediment supply (quantity and texture of sediment input) and creation of accommodation space (i.e. the sum of subsidence, eustatic sea-level change, and degree of sediment bypassing to the slope) (Swift et al. 1991, Galloway and Hobday 1996). Autochthonous settings are characterised by an accommodation-dominated configuration, which creates a transgressive coastline. The BCS typically represents a transgressive shelf where accommodation dominates supply. Even though the BCS is a relatively stable area, not affected by tectonic or (glacio)isostatic subsidence or uplift (D'Olier 1981, Kiden et al. 2002, Vink et al. 2007), and though no sediment bypassing is possible because of the absence of a distinct shelf break in the Southern Bight, the relative small created accommodation space due to only the eustatic sea-level rise during the Eemian and Holocene was still larger than the available sediment, which induced a transgressive stratigraphic architecture. Shelf units (e.g. seismic unit U5) onlap coastal strata (e.g. U4), commonly across a ravinement surface (Galloway and Hobday 1996). And sediment reworked from the shoreface and transgressed coastal deposits accumulated as widespread autochthonous sand (transgressive sand sheet). Where storm and tidal energy were sufficient, sandy bar macroforms formed along the inner shelf and became moribund as water deepened (U5 and U7).
In this accommodation-dominated regime, the accumulation rate is low. Sediment is repeatedly resuspended before final burial as high values of the accommodation/supply ratio induce a high reworking ratio (Galloway and Hobday 1996). The resulting transgressive deposits are thin, coarse-grained (sandy) and heterogeneous. The constant reworking of autochthonous, in situ available sediments appears e.g. from lithological similarities between U4, overlying U5 and U7, which are partly build up of material eroded from the underlying units, and from the strongly uneven surfaces of U4 and U5.

The material of which the U7 banks are build up originates from local erosion of underlying sediments, what could be deduced from the often erosional character of the base of the banks and the presence of deeply incised swales in between. In the nearshore part, the underlying deposits being eroded consist of Eemian U3 estuarine, and Holocene U4 tidal-flat and U5 sand ridge sediments. While offshore, the banks consist most likely only of remnants of the transgressive sand sheet left after the Holocene transgression. This sheet itself probably consisted of remnants of the earliest Holocene tidal-flat deposits and maybe of underlying remnants of the former Eemian transgressive sand sheet (if not removed during the Weichselian lowstand), which were reworked by the Holocene open marine transgression during the initial fast relative sea-level rise. An additional amount of material was available north of the Offshore Scarp in the form of easily erodible IVDB Eemian deposits below the Holocene and Eemian

marine transgressive surface. While south of the scarp probably also the erosion of the Paleogene substrate contributed material.
Seismic unit U6 sediments originate from eroded former back-barrier deposits (U4). The Holocene U4 tidal flats and the initial barrier were in turn build up of reworked early open-coast tidal flats, reworked Weichselian fluvial sediment input of Rhine-Meuse origin, possible remnants of an Eemian marine sand sheet, and of remnants of the eroded Paleogene substrate. When the shoreface was sediment starved and could no longer build out faster than the downwelling storm currents could erode it, the barrier underwent erosional retreat, and the resulting debris was swept out onto the shelf floor forming the transgressive sand sheet, or was transported along coast in the breaker zone via tidal inlets into the back-barrier basin (Swift and Thorne 1991). So the cycling barrier served as temporary storage for sand during its journey out of the substrate and on to the shelf floor. Under conditions of slow subsidence the shoreface incised into, and released deposits of a previous cycle, which served as an additional source for the build up of the barrier system.
Later shoreface-connected or storm-dominated ridges (U5) formed from/in the transgressive sand sheet.
The marine deduced material needed for the Eemian estuarine infilling of the Ostend Valley (U1, U2, U3) was derived from possibly present older Pleistocene deposits and again the underlying Paleogene substrate, by shoreface ravinement. Although it is possible that during the Saalian (catastrophic) proglacial lake outflow a lot of sediment was removed from the seabed (Cohen, pers. comm. 2007).
The gravelly material in the swales between the sandbanks originates from multiple sources: former gravelly valley or lake deposits (Paleogene rivers, Elsterian proglacial lake, Saalian proglacial lake, Saalian Meuse and Ostend Valley, Weichselian Rhine/Meuse, Thames), and in situ coarse-grained material within the Paleogene substrate itself (concretions, sandstone banks), which have been cut by the retreating shoreface, and redistributed by the Eemian and Holocene transgression. In general, due to strong tidal currents the transgressive sand sheet overlying the gravel lag is discontinuous or lacking altogether. So that the basal gravels, Holocene back-barrier deposits or older Pleistocene or Paleogene deposits are exposed in windows through the sand sheet.

So most of the material present on the BCS is originally derived from local erosion of the Paleogene substrate, or is carried into the southern North Sea basin by large rivers such as Meuse and Rhine, crossing the North Sea basin during glacial stages. It is possible that also material deposited by these rivers as far as into the English Channel, are being brought back now by tidal currents (Schüttenhelm and Laban 2005). The North Sea is a classic example of an area of palimpsest deposits, i.e. reworked sediments supplied from within the shelf environment (Jacobs 2000), which contain textural mixing of the products of deposition of different periods of time and different sources (Caston 1979). Most of the marine Holocene sand in the southern North Sea is reworked from Pleistocene fluvial deposits. As the Holocene rivers surrounding the Southern Bight only carried suspended matter to their mouths, because bed load and part of the suspended load were deposited in the alluvial plains to fill up the space created by the rapidly rising sea level (Beets and van der Spek 2000).

In contrast to progradational and aggradational shelf systems, which are characterised by thick sediment successions supplied by rivers (Galloway and Hobday 1996), the Belgian transgressive shelf system is characterised by a thin and fragmented Quaternary sediment cover, due to constant reworking of in situ available sediments, which made it very difficult to reconstruct the Quaternary evolution from. Moreover, due to the reworking of older depositional environments to construct new ones, it was not possible to make a stratigraphic classification on the basis of core data alone, as lithologically similar material could in fact belong to completely different depositional environments.

Seismic data was indispensable for the identification of important erosional surfaces and to distinguish the different depositional environments.

10.
Conclusions and outlook

10.1 Introduction

Since the late '70's, in the framework of several national and international projects, such as the extension of the harbour of Zeebrugge, and the search for potentially exploitable near-surface sediments, the Quaternary cover of the Belgian Continental Shelf (BCS) has been intensively investigated. However, apart from some detail studies on certain sandbanks and distinct research areas, where for each sandbank a new stratigraphic classification and interpretation was proposed, the available seismic and core data were never processed or interpreted in an integrated coherent way, to produce an evolutionary model of the Quaternary valid for the entire BCS. As in a time when only analogue data were available, it was not possible to correlate the complex Quaternary structure of the diverse sandbanks and research areas with one another.

Now, in this digital era, almost 30 years after their acquisition, more than 4000 km of high-resolution paper seismic recordings have been scanned, converted into digital 'SEG-Y' format, and integrated with 1300 km of modern acquired data, and ground-truthed with more than 600 core descriptions. This digital approach made it possible to develop a model for the geological evolution of the BCS during the Quaternary, which was the main goal of this thesis.

Two immense data sets of seismic profiles and core descriptions formed the foundation of this study. But also the detailed knowledge of the western Coastal Plain and Flemish Valley on land, literature on tidal and wave processes on the BCS, formation and origin of sandbanks, the morphology of the Base-Quaternary surface, the knowledge of studies on particular sandbanks on the BCS, and even archaeological evidence of former coastlines, have been considered. And all these clues have been put together as in a giant jigsaw puzzle, to come to a comprehensive model for the Quaternary history of the BCS.

10.2 Significance of digital approach

Notwithstanding the digital approach, it was still a challenge to develop a genetic model for the Quaternary evolution of the BCS, from the fragmented and thin remnants of the Quaternary record. But thanks to the digital approach all available seismic data sets could be easily integrated into one well-organised database.
On the one hand, this enabled us to get a comprehensive overview of the internal structure of the patchy Quaternary cover and to understand the interrelationships between sandbanks. Instead of interpreting paper seismic records of several metres long, entire seismic profiles could now be conjured up on screen in an instant, and looked at in a pseudo-3D setting.
On the other hand, due to the gain of time in handling the digital seismic profiles and produced maps, the interpretation of the seismic data could be performed now in more detail, to actually offer an additional value to former studies. Instead of creating a model for the Quaternary evolution of the entire BCS by merely combining copied interpretations of the former fragmented investigations, the old data were looked at in more detail in order to find well-funded arguments for more precise interpretations. A vague term as 'valley infilling' could now be specified to e.g. a tidal channel infilling in an outer-estuarine environment.
Also due to the additional, recently acquired seismic profiles in crucial areas as the Ostend Valley, made it e.g. possible to identify channel system in the lowermost units, which had not been recognised until now. What was identified before as isolated scour

hollows, could now, owing to this new seismic information, be interpreted as a continuous sinuous channel system. Another example: channel structures observed on different seismic profiles were previously considered a single channel, but belong in fact to different channel systems. Such details demand a very intensive and time-consuming study of the seismic data, but offer an important surplus in comparison to previous, more general interpretations.

10.3 The seismic-stratigraphic interpretation

The seismic-stratigraphic interpretation of the Quaternary deposits started with the centrally located Middelkerke Bank, of which the internal structure was probably most complete and its Quaternary evolution was largely unravelled by previous studies (Lanckneus et al. 1991, De Moor et al. 1993, Stolk and Trentesaux 1993, Trentesaux 1993, Berné et al. 1994, Heyse et al. 1995, Stolk 1996, Trentesaux et al. 1999). This sandbank showed a 7-unit seismic-stratigraphic subdivision, with estuarine channel infillings at the base (three units), followed by a lagoonal or sub-littoral deposit, coastal bank deposits (two units), and finally a tidal sandbank at the top (Trentesaux et al. 1999). This subdivision was used as a guideline for the seismic interpretation of the surrounding sandbanks. And when integrating the extensive sedimentological data set with the extended seismic units outside the Middelkerke Bank, the lithology of these units appeared to be consistent with the descriptions of the units within the Middelkerke Bank (Trentesaux et al. 1999), which was an indication that the seismic interpretation of the Middelkerke Bank indeed had regional validity, and opened the perspective to extend this seismic-stratigraphic subdivision to the entire BCS. It is assumed that these units were initially deposited across large parts of the BCS, but were subsequently affected by erosion and the formation of sandbanks, which created the fragmentation and irregular occurrence of the seismic units.
However, the interpretation of the seismic units by Trentesaux et al. (1999), in terms of depositional environment was not entirely accepted. On account of the far more extended seismic and core data sets applied for this thesis, more details were available, and more specific interpretations were possible. The three lowermost units (U1-U2-U3) are now interpreted as middle-estuary (point or tidal bar) deposits in a sinuous tidal channel at the base of the Ostend Valley, more seaward middle-estuary deposits, and outer-estuary deposits, respectively. The fourth seismic unit (U4) is not considered a lagoonal or sub-littoral deposit, as core data point to tidal-flat sedimentation. This was initially also proposed by Berné et al. (1994) and Stolk (1996) for the Middelkerke Bank area. In the presented study no distinction is made between the fifth and sixth seismic unit, representing coastal bank deposits in the Middelkerke Bank, they are considered one unit (U5) and is referred to as a storm-dominated or storm-generated sand ridge deposit. An additional seismic unit (U6) was observed in the present nearshore area, which was not encountered in the Middelkerke Bank, and represents reworked tidal-flat deposits. The final seismic unit (U7) corresponds with the interpretation of the seventh unit in the Middelkerke Bank, i.e. tidal sandbank (and swale) deposits.

10.4 Most important innovations in the Quaternary evolutionary model of the BCS

Apart from the fact that a comprehensive evolutionary theory for the Quaternary on the BCS has never been introduced before, there are some important novelties to highlight.

Chapter 6: Pleistocene incision and infilling of the Ostend Valley

- The jumble of interpretations and supposed ages of the infillings of the Ostend Valley (Liu et al. 1993, Trentesaux 1993, Berné et al. 1994, Trentesaux et al. 1999), has been sorted out. At the base, the Ostend Valley shows a thin gravel lag of Saalian age, possibly deposited by fluvial processes. The valley is subsequently infilled during the Eemian sea-level rise, when it transformed into a tide-dominated estuary. The lower seismic units represent the marine sand body of the middle and outer estuary portions of the estuary, consisting of tidal bars and intervening tidal channels, adjacent mud flats have not been encountered within the valley.
- It has been often suggested that the Ostend Valley represents the seaward extension of the paleo-drainage systems of the onshore Flemish and Coastal Valley (Mostaert et al. 1989, Liu et al. 1992). However, for the first time, the Ostend Valley is linked with the Flemish Valley in terms of infilling sediments, depositional environments and timing.

Chapter 7: Holocene transgression, evolution of a back-barrier basin, and the formation of storm-generated sand ridges

- Tidal-flat deposits and coastal barriers have been suggested before within certain sandbanks on the BCS (Maréchal and Henriet 1983, 1986). But now, the entire Holocene coastal barrier system, consisting of remnants of back-barrier tidal-flat deposits, and storm-generated sand ridges moulded in the transgressive sand sheet left after barrier retreat, has been mapped. In addition, former coastline (barrier) positions have been reconstructed and are presented in paleo-reconstructions.
- The Goote and Akkaertbank s.s., belonging to the Zeeland Ridges, most likely represent remnants of such storm-generated sand ridges which formed seaward of the retreating coastline.
- Not only the Quaternary evolution of the continental shelf is discussed, the Holocene evolution of the coastline has been tightly interwoven with the evolutionary history of the Western Coastal Plain (Baeteman 1999, 2004, 2005ab, Baeteman and Declercq 2002). And facts from Holocene geological and archaeological reconstructions in Zeeland (The Netherlands) (Vos and van Heeringen 1997), and historical coastline reconstructions of the Western Scheldt area (Coornaert 1989, Augustyn 1995, Termote 2006) have been taken into account. This integration of offshore and onland information has also contributed to a better understanding of the onland evolution. E.g. the stabilisation of the coastal barrier around 5000 cal BP appeared from offshore data.
- An innovative fact is that the coastline reconstructions of 8000 and 7500 cal BP show that the barrier in the east did not stop retreating before the barrier in the west because of a high-elevated Pleistocene subsurface. Although this has always been expected on the basis of the more landward position, with respect to the present-day coastline, of the coastline in the west around 7500 cal BP, and the high positioned Pleistocene in the eastern present-day Coastal Plain. Also the complete absence of a barrier complex in the eastern Coastal Plain, in contrast to the presence of a barrier complex in the western Coastal Plain (Baeteman 2007b, Denys 2007, Fettweis et al. 2007) implied this. However, in the eastern present offshore area there is no evidence of a high-positioned Pleistocene subsurface. In fact, the entire coastline retreated constantly over its entire length, and stopped simultaneously because of sediment supply compensating the created accommodation space, which was reduced due to an overall sea-level deceleration. The accommodation space in the western part was not much larger, and the barrier there did not retreat much faster than its eastern part. The barrier retreated parallel with its former position, keeping a straight coastline, but with an

angle to the present-day coastline, which caused the seemingly more landward position of the barrier in the western coastal plain. The orientation of the initial barrier is in the first place determined by the strike direction of the pre-transgressive surface.

Chapter 8: Holocene tidal sandbanks

- The Flemish and Hinder Banks s.s. probably have formed simultaneously, as a response of the sea bed to a suitable hydraulic regime, which is believed to have happened in the case of these banks around 7000 cal BP, at a time when the tidal regime reached the present-day macrotidal range (van der Molen and van Dijck 2000), and the underlying storm-generated sand ridges became moribund. Their formation is not related to a retreating shoreline, as by that time, the shoreline was located far from these banks.
- This period was also characterised by a change in the net-sand transport pattern. Before 7000 cal BP the sediment transport was mainly directed shoreward, while from that period on the tidal wave and related transport became along-shore (van der Molen and van Dijck 2000). This might explain the difference in orientation between the Zeeland Ridges, which are more or less oriented coast-parallel and which were formed when the sediment transport was shoreward directed, while the Flemish Banks and Hinder Banks are oriented at an angle with the present-day coastline.
- With the formation of the tidal sandbanks, the originally regionally deposited older deposits got fragmented because of the contemporary erosion in the swales between the sandbanks, supplying sediments for the build up of the adjacent banks. So the tidal sandbank deposit is actually only the top part of what is called 'a sandbank' in a broader sense of the word. The lower parts of the sandbanks consist of nearshore, tidal-flat and estuarine deposits, which stand out from the seafloor, i.e. form a 'sandbank' in the broad sense, due to present- day erosion in the surrounding swales. And not, as has been generally believed, that the tidal sandbanks formed on top of existing highs, implying that underlying deposits were first eroded, moulded into elevated areas, before the tidal sandbanks could form on them.
- The gravelly material in the swales between the sandbanks originates from multiple sources: former gravelly valley or lake deposits (Paleogene rivers, Elsterian proglacial lake, Saalian proglacial lake, Saalian Meuse and Ostend Valley, Weichselian Rhine/Meuse, Thames), and in situ coarse-grained material within the Paleogene substrate itself (concretions, sandstone banks), which have been cut by the retreating shoreface, and redistributed by the Eemian and Holocene transgression.

Chapter 9: The Quaternary evolution of the BCS, synthesis and general remarks

- The proposed classification of depositional environments along a transgressive or regressive linear coastline by Boyd et al. (1992), is insufficient for explaining the present-day situation along the Belgian shore, as a closed coastline formed under tide-dominated conditions instead of exposed tidal flats. A possible explanation might be that on the Belgian shelf, where the maximal tidal current in the nearshore area is oriented alongshore in NE direction, the tidal current enhances the longshore, wave-induced sediment drift, giving the present coastline a wave-dominated appearance under tide-dominated circumstances.

10.5 The challenge of a shelf with low accommodation space

The BCS typically represents a transgressive shelf where accommodation dominates supply. Even though the BCS is a relatively stable area, not affected by tectonic or (glacio)isostatic subsidence or uplift (D'Olier 1981, Kiden et al. 2002, Vink et al. 2007), and though no sediment bypassing is possible because of the absence of a distinct shelf break in the Southern Bight, the relative small created accommodation space due to only the eustatic sea-level rise during the Eemian and Holocene was still larger than the available sediment, which induced a transgressive stratigraphic architecture.
In contrast to progradational and aggradational shelf systems, which are characterised by thick sediment successions supplied by rivers (Galloway and Hobday 1996), accommodation-dominated regimes, such as the Belgian transgressive shelf system, are characterised by a thin and fragmented Quaternary sediment cover, due to constant reworking of in situ available sediments, which made it very difficult, but challenging, to reconstruct the Quaternary evolution from.

Due to the constant reworking of older depositional environments to construct new ones, it was not possible to make a stratigraphic classification on the basis of core data alone, as lithological similar material could in fact belong to completely different depositional environments, across several seismic units. E.g. light-grey medium fine sands reoccur in seismic units U4, U5 and U7, representing sand flats or tidal channel infillings, storm-generated sand ridges or tidal sandbanks, respectively.
On the other hand, the Quaternary deposits, representing dynamic environments, can be lithologically strong heterogenic over short distances (vertical and horizontal) as well. To assess this, it is important to interpret seismic and core data in function of depositional environments, and not only in function of technical characterisation, which is the case e.g. in preliminary research for the construction of windmill parks. An interpretation in function of the depositional environment gives a good indication of what can be expected in the subsurface. E.g. a sand in a tidal sandbank deposit is expected to be rather homogenous in the vicinity, but a similar sand deposited in a tidal-flat environment suggests that in the nearby area also clayey deposits can be expected.

10.6 Outlook

The presented evolutionary model on the Quaternary of the BCS, mainly focused on the middle part of the Belgian shelf, where the densest seismic network and core data set are located. This confined study area should be pulled open to the most offshore area, where only very limited core data are available for the moment, and to the shallow most nearshore area, where almost no seismic data are available, because the present applied research vessel Belgica can not manoeuvre that close to the shore.
Although the shallow nearshore area is characterised by the presence of gas, and the multiple is expected shortly after the seafloor reflection, a nearshore seismic campaign offshore Nieuwpoort and De Panne with a small fishing vessel gave very promising results.
The offshore area would be interesting for investigating the oldest, Eemian, and presumably also Weichselian deposits north of the Offshore Scarp. While the nearshore area is recommended for reconstructions of historical coastlines, so the most recent Quaternary evolution.
Also additional research in the eastern Coastal Plain is recommended, in order to find out e.g. why the eastern shoreline retreated so much further landward than the western part since 2800 cal BP.

In addition, the story of the Quaternary evolution of the Belgian shelf should be integrated with the histories of the adjacent Dutch, French and British shelves. And in the near future a Quaternary geological map should be published to finally cover the blank spot in the southern North Sea. This will be an answer to many requests of dredgers and surveyors about the shallow subsurface of the Belgian Continental Shelf.

Nederlandse samenvatting

Inleiding

Wat betreft de Quartaire afzettingen is het Belgisch Continentaal Plat (BCP) één van de laatste ongekarteerde en onbekende gebieden van België. Door de afwezigheid van een uitgesproken shelfrand en het bijna volledig ontbreken van subsidentie (D'Olier 1981, Kiden et al. 2002, Vink et al. 2007), was er op het BCP zeer weinig accommodatieruimte om Quartaire sedimenten te laten accumuleren en bewaren. Bovendien is de sedimenttoevoer door grote rivieren (zoals Schelde, Rijn en Maas) steeds beperkt geweest tijdens het Holoceen (De Moor 1986, Beets en van der Spek 2000). Daardoor is het Quartaire dek op het BCP zeer onregelmatig en uiterst gefragmenteerd. Het is voornamelijk gemodelleerd in de vorm van geïsoleerde zandbanken door vroegere en hedendaagse getijdenstromingen. Het Quartaire dek is maximaal 45 m dik, maar gemiddeld minder dan 10 m. Dit dunne, onvolledige overblijfsel van een lange periode van complexe en dynamische veranderingen in afzettingsomstandigheden is de reden waarom er tot op heden nooit een coherente reconstructie gemaakt werd van de Quartaire evolutie van het BCP.

Nochtans is er een grote hoeveelheid aan gegevens over het BCP beschikbaar. Sinds het einde van de jaren '70 en het begin van de jaren '80 werd het BCP intensief opgevolgd in het kader van verscheidene nationale en internationale projecten. Dit resulteerde in één van de dichtste regionale seismische netwerken ter wereld. Meer dan 16.000 km aan hoge-resolutie reflectieseismische profielen zijn beschikbaar in de gegevensbestanden van het Renard Centre of Marine Geology (RCMG). Bovendien werd over de jaren heen een uitgebreide reeks van kernen genomen, o.a. met als doel de ondergrondse natuurlijke reserves te kwantificeren. Deze kernen en bijhorende boorbeschrijvingen zijn opgeslagen in de lithotheek van de Belgische Geologische Dienst (BGD). Maar, de voorgaande studies en analyses van deze datasets hebben zich doorgaans op één enkele zandbank of op een beperkt gebied van het BCP geconcentreerd. Tijdens deze studies werd dan ook voor elk van deze zandbanken en deelgebiedjes een nieuwe locale stratigrafie en interpretatie voorgesteld. Zelfs in het kader van twee uitvoerige projecten over de geologische structuur van het gehele BCP (Maréchal and Henriet 1983, 1986), kreeg elke zandbank zijn eigen stratigrafische interpretatie, onderverdeling en nomenclatuur, omdat het toen niet mogelijk was de complexe Quartaire structuur van de verschillende zandbanken met elkaar te correleren. Dus, ondanks de grote hoeveelheid aan beschikbare gegevens werden, buiten een aantal punctuele detailstudies, deze data nog nooit op een geïntegreerde, coherente wijze samengebracht, verwerkt en geïnterpreteerd. Eén van de redenen hiervoor was dat de seismische opnames enkel in papieren formaat beschikbaar waren.

Zodoende is de belangrijkste doelstelling van dit onderzoek -in het huidige digitale tijdperk- het archiveren, integreren en (her)interpreteren van alle bestaande datasets, seismische zowel als kernen, met als einddoel het uitwerken van een algemene stratigrafie van de Quartaire afzettingen op het BCP, en het ontwikkelen van een genetisch model voor de Quartaire geologische evolutie van het gebied.
Daar het BCP deze dagen steeds vaker terugkomt in de actualiteit, o.a. met thema's als de inplanting van 'offshore' windmolenparken en aanvragen tot uitbreiding van de zand- en grind-ontginningsgebieden, is een degelijke kennis van de aard en samenstelling van de ondiepe ondergrond van het BCP, die nauw samenhangt met zijn geologische evolutie, onontbeerlijk.

Digitale aanpak en ontwikkeling van een Quartair evolutiemodel

Nu, bijna 30 jaar na de aanvang van de acquisitie van de seismische data, werden meer dan 4000 km aan hoge-resolutie papieren seismische opnames gescand, geconverteerd in digitaal SEG-Y formaat, en geïntegreerd met 1300 km recent opgenomen data. Daarna werden deze seismische data sedimentologisch geverifieerd met meer dan 600 boorbeschrijvingen.
De twee immense datasets van seismische profielen en boorbeschrijvingen vormden de basis van deze studie, maar er werd ook rekening gehouden met gedetailleerde informatie van de westelijke Kustvlakte en de Vlaamse Vallei op land, literatuur over getijden- en golfprocessen op de shelf, informatie over de vorming en oorsprong van zandbanken in het algemeen, de studies over enkele specifieke zandbanken op het BCP, de gekende morfologie van het Basis-Quartair oppervlak en zelfs historische bewijzen van vroegere kustlijnen. Zoals bij een grote legpuzzel werden al deze aanwijzingen bijeengepast, om te komen tot een allesomvattend genetisch model voor de geologische evolutie van het BCP tijdens het Quartair.

De basis voor dit werk werd reeds gelegd door De Batist (1989) en Jacobs en De Batist (1996), die de Paleogene (vroegere Tertiaire) afzettingen onderzochten, en door Liu (1990) en Liu et al. (1992, 1993), die de morfologie van het Top-Paleogene oppervlak (tevens de basis van het Quartaire dek) zeer gedetailleerd beschreven. De seismisch-stratigrafische interpretatie van de Quartaire afzettingen startte vanuit de centraal gelegen Middelkerke Bank, waarvan de interne structuur reeds tijdens vorige studies grotendeels ontrafeld was (Lanckneus et al. 1991, De Moor et al. 1993, Stolk en Trentesaux 1993, Trentesaux 1993, Berné et al. 1994, Heyse et al. 1995, Stolk 1996, Trentesaux et al. 1999). Het werd snel duidelijk dat de omgevende zandbanken gekenmerkt werden door een gelijkaardige interne structuur, wat de mogelijkheid bood om de seismische type-stratigrafie van de Middelkerke Bank uit te breiden naar de rest van het BCP.

In totaal werden zeven seismische eenheden geïdentificeerd in de Quartaire afzettingen op het BCP, die elk begrensd zijn door discordanties. Na calibratie van de seismische karakteristieken met de kerndata, kregen deze seismische eenheden ook een lithologische betekenis. Een ingesneden vallei buiten de kust van Oostende, de Oostende Vallei (Maréchal en Henriet 1983), is opgevuld met drie seismische eenheden. Deze eenheden geven drie opeenvolgende fases weer in de transgressieve estuariene opvulling tijdens een relatieve zeespiegelstijging. De eerste eenheid (U1) vertegenwoordigt een midden-estuariene afzetting in een kronkelende getijdengeul aan de basis van de Oostende Vallei, de tweede eenheid (U2) weerspiegelt meer zeewaarts gelegen midden-estuariene afzettingen, en de derde eenheid (U3) stelt een buiten-estuariene afzetting voor. De opvullingen zijn afgesneden door een 'ravinement' oppervlak gevormd door vooroevererosie en mariene afvlakking tijdens mariene transgressie. Bovenop dit regionaal erosieoppervlak ligt een vierde seismische eenheid (U4), die de afzetting in een slikken-en-schorrenmilieu voorstelt dat zich ontwikkelde achter een kustbarrière in een getijden- of wadgebied. Bovenop deze eenheid, gescheiden door een tweede erosieoppervlak, bevindt zich een vijfde eenheid (U5) die de afzetting van door storm gegenereerde zandruggen weerspiegelt. Een zesde seismische eenheid (U6) werd geïnterpreteerd als een kustnabije afzetting bestaande uit herwerkt materiaal afkomstig van vroegere wadafzettingen. De zevende, en tevens bovenste eenheid (U7), vertegenwoordigt voornamelijk de recente getijdenzandbanken en geulafzettingen tussen de banken.

Omdat er geen onherwerkt, dateerbaar materiaal aanwezig is in de beschikbare kernen, was het niet mogelijk betrouwbare absolute dateringen te bekomen voor deze

seismische eenheden. Maar, benaderende ouderdommen konden worden afgeleid door hun afzettingshoogte (op hun beurt afgeleid op basis van het sedimentaire facies) te vergelijken met een gekende relatieve zeespiegelcurve van het gebied (Denys en Baeteman 1995, Siddall et al. 2006). Dus, de seismisch-stratigrafische eenheden vertegenwoordigen bepaalde afzettingsmilieus in een gegeven periode, gescheiden door erosieoppervlakken die belangrijke fases voorstellen in de Quartaire zeespiegelevolutie of veranderingen in de sedimentdynamiek daarmee gekoppeld.

Het Pleistoceen evolutiemodel

De Saale ijstijd

Tijdens de Saale ijstijd werden enkele van de meest prominente morfologische structuren van het Top-Paleogene oppervlak gevormd. Door de Oostende Vallei te vergelijken met de goed gekende Vlaamse Vallei, door het BCP te linken met het Nederlands Continentaal Plat, en door rekening te houden met de volgorde waarin de structuren elkaar doorsnijden kon volgend scenario worden uitgewerkt.
Tijdens de maximale ijskapuitbreiding van de Saale glaciatie ("Amersfoorter Stadium" tijdens de Drente glaciatie MIS6) vormde zich een proglaciaal ijsmeer tussen het Scandinavische en Britse ijs in het centrale Noordzee gebied, en een richel ten noorden van de Straat van Dover (Gibbard 2007). Het Rijn-Maas systeem mondde uit in dit proglaciaal meer, dat gelijkaardige hoogtes als het huidige gemiddeld zeeniveau bereikte, en vormde een delta dichtbij de huidige Nederlandse kustlijn. Tijdens de volgende deglaciatie, aan het einde van de Drente MIS6 ijstijd, steeg het meer tot boven de richel ten noorden van de Straat van Dover, veroorzaakte een doorbraak en liep vervolgens leeg. In respons op het zakkende meerniveau, sneed de Maas zich diep in in zijn vroegere vlechtende riviervlakte en zocht zijn weg naar het zuiden, naar de Straat van Dover toe, en vormde hierbij het 'Offshore Platform', de 'Offshore Scarp' en het 'Quaternary Basin' op zijn weg. Hoogstwaarschijnlijk vormden ook de rivieren van de Vlaamse Vallei een delta in het oorspronkelijke Saale proglaciaal meer. In reactie op het zakkende meerniveau sneden ook deze rivieren zich in, en vormden zo de oostelijke 'Kustvallei', de 'Oostende Vallei', en mogelijk kleinere aftakkingen in de huidige Nederlandse sector.
Toen de smeltwaterafvoer verminderde en enkel het dieper 'Axiale Kanaal' nog als drainageroute fungeerde, zochten de kleinere aftakkingen in de Nederlandse sector waarschijnlijk hun weg verder naar het noorden richting het Axiale Kanaal, sneden doorheen de vroegere Maas valleiwand, en vormden zo het 'Thornton Kanaal' en 'Noordelijke Vallei'. Waarschijnlijk sneed ook een kleine stroom in de Oostende Vallei zich verder in richting het Axiale Kanaal. Liu et al. (1992) suggereerden dat de Oostende Vallei de ontbrekende link vormde tussen de Vlaamse Vallei en de oostelijke Kustvallei op land, en het machtige Axiale Kanaal offshore, via de Noordelijke Vallei. De Oostende Vallei en de Noordelijke Vallei vormen echter twee gescheiden drainage systemen, die elk de Vlaamse Vallei met het Axiale Kanaal verbinden.

De Eem tussenijstijd

Op basis van de afzettingshoogte van de opvullingssedimenten van de Oostende Vallei en de bovenliggende discordantie, en de aanwezigheid van getijdenafzettingen bovenop deze discordantie, kon een Eem ouderdom afgeleid worden voor de invulling van de Oostende Vallei.

Tijdens de zeespiegelstijging van het Eem, overstroomde de zee de vroegere ingesneden valleien en deze evolueerden in estuaria. Ook de Oostende Vallei evolueerde snel in een typisch trechtervormig, getijdengedomineerd estuarium. Het bestond uit een buiten-estuarium, een midden-estuarium en een rivier-getijden overgangszone, ingedeeld volgens het model van Dalrymple and Choi (2007). De estuariene invulling van de Oostende Vallei wordt voorgesteld door drie seismische eenheden (U1-U2-U3). Deze geven telkens een meer zeewaarts deel van het estuarium weer, wat duidt op een landwaartse migratie van het estuariene milieu. Met stijgend zeeniveau migreerde het estuarium stroomopwaarts in de oostelijke Kustvallei, die de verbinding vormt tussen de Vlaamse en de Oostende Vallei. De estuariene afzettingen in de Oostende Vallei werden steeds grover en meer marien naar boven toe. Landwaarts- en lateraal-migrerende getijdengeulen, gepaard met golfwerking, erodeerden tijdens de transgressie gedeeltes van de meer landwaarts gelegen facies, en vormden de erosieoppervlakken tussen de seismische eenheden. Seismische eenheid U1 stelt een 'point-bar' opvulling voor van diep ingesneden getijdengeulen (tot 30 m onder de gemiddelde valleibodem). Deze werden gevormd door de initiële getijdenuitschuring in een midden-estuarien milieu. De bovenliggende seismische eenheid U2 vormt het zeewaarts gedeelte van een midden-estuariene omgeving. Het landwaarts gedeelte van het midden-estuarium en de kleiiger rivier-getijden overgangszone waren meer landwaarts gelegen, in de huidige oostelijke Kustvlakte. De bovenste eenheid U3 geeft een buiten-estuariene afzetting weer, terwijl het midden-estuarium en de rivier-getijden overgangszone opnieuw verder stroomopwaarts in de oostelijke Kustvallei migreerden. Het is mogelijk dat continentale, alluviale afzettingen, aanwezig in de Vlaamse Vallei (Formatie van Oostwinkel in de Leie vallei, De Moor en Van De Velde 1995, De Moor en Heyse 1974), de meanderende, kleiiger afzettingen vormen die volgen op de rivier-getijden overgangszone van het Oostende Vallei estuarium.

In de tussentijd migreerde ook de kustlijn landwaarts, en vooroevererosie en mariene planatie maakten de estuariene opvullingen gelijk met de zeebodem. In het offshore gebied was de vooroevererosie zo sterk, dat resten van de vroegere Eem afzettingen enkel nog in depressies in het Top-Paleogeen oppervlak teruggevonden worden. Het nivelleren van de Eem afzettingen die het Offshore Platform bedekken, met het Top-Paleogeen oppervlak ten zuiden van de Offshore Scarp, startte waarschijnlijk tijdens de mariene transgressie van het Eem, maar werd nog versterkt tijdens de Holocene mariene transgressie. Ook in de Oostende Vallei was de mariene planatie zo sterk, dat seismische eenheid U3 volledig gelijk gemaakt werd met het Top-Paleogeen oppervlak. Een 4 m hoge steilrand in dit vooroever-planatieoppervlak ('shoreface ravinement surface'), dwars over de Oostende Vallei in lijn met de Nearshore Slope Break, vertegenwoordigt waarschijnlijk een versnelling in de Eem zeespiegelstijging (van ca. -17 tot -13 m MLLWS).
Toen de Eem-zeespiegel zijn maximum niveau bereikte, vergelijkbaar met het huidige niveau, lag de kustlijn ongeveer 7 km landinwaarts van de huidige kustlijn (nabij Brugge). Net zoals de Oostende Vallei, werden ook de oostelijke Kustvallei en een gedeelte van de Vlaamse Vallei overschreden door de landwaarts terugschrijdende kustlijn en werden de valleien volledig overspoeld door de zee. De mariene invloed reikte in de Vlaamse Vallei tot 40 km landinwaarts, tot in de laaggelegen zijrivieren (De Moor et al. 1996). Een groot deel van de Vlaamse Vallei veranderde in een estuarium baai. Ondanks het feit dat de opvullingssedimenten van de Vlaamse Vallei sterk gelijken op de estuariene sedimenten in de Oostende Vallei, vormen ze toch niet de laatste fase van de voortdurende stroomopwaartse migratie van het "Oostende Vallei - oostelijke Kustvallei" estuarium. De verbinding tussen de Oostende en Vlaamse Vallei ligt namelijk parallel aan de kust, dus dat gebied overstroomde vrijwel onmiddellijk, zodat er geen tijd was voor het verder stroomopwaarts migreren van het estuarium. In plaats daarvan vormde zich een nieuw estuarium in de Vlaamse Vallei.

Het mariene transgressieoppervlak van het Eem (i.e. het vooroever-planatieoppervlak) wordt in het huidige offshore gebied gekenmerkt door een grindlaag. Deze laag kan afgezet zijn toen de terugschrijdende vooroever de grindrijke valleiopvullingen van de Maas en Oostende Vallei aansneed, waarna deze grinden verdeeld werden als een marien transgressie grind. Het is ook mogelijk dat het grind bestaat uit grofkorrelig materiaal dat locaal uitgesorteerd werd uit het direct onderliggende Paleogeen substraat (zoals schelpen, vroegere Paleogene rivieropvullingen, concreties, zandsteenbanken). Meestal wordt een marien transgressiegrind bedekt met enkele meter zand, i.e. de mariene transgressiezandlaag, maar in het offshore gebied, bovenop het Eem-planatieoppervlak en onder de initiële Holocene afzettingen, zijn geen open-mariene Eemiaan zanden aanwezig. In de oostelijke Kustvlakte en een deel van de Vlaamse vallei daarentegen, worden de getijden- en estuariene afzettingen wel bedekt door open-mariene sedimenten. Waarschijnlijk is dit omdat in de Kustvlakte en de Vlaamse Vallei, de mariene invasie gebeurde tijdens de Eem-zeespiegelhoogstand, toen de kustlijn veel trager terugschreed, en er meer tijd (en sediment) was voor de opbouw van een transgressiezandlaag.
Zowel in de oostelijke Kustvlakte als de Vlaamse Vallei wordt de finale fase van de Eem-opeenvolging gekenmerkt door de ontwikkeling van open-mariene getijdenafzettingen (open-kust schorren en slikken). Dit is een algemeen fenomeen in valleien tijdens de zeespiegelhoogstand, wanneer estuaria volledig opvullen en verdwijnen. Wanneer de rivier niet genoeg sediment aanlevert, maar het sediment aangevoerd wordt door golven of getijden, dan verandert het gebied niet in een delta, maar in een rechte, prograderende kustlijn in de vorm van respectievelijk een strandvlakte of open-kust getijdenafzetting (Dalrymple et al. 1992).

Tijdens het Eem, veranderde de hydrodynamische situatie op het BCP waarschijnlijk van gemengd golf-getijdengedomineerd langsheen de rechte kustlijnen en getijdengedomineerd in de Oostende Vallei tijdens de zeespiegelstijging, naar getijdengedomineerde langsheen de gehele kustlijn tijdens de zeespiegelhoogstand. Dit gebeurde vermoedelijk door een relatieve vermindering van de golfenergie (minder snelle toename) in vergelijking met de toenemende getijdenamplitude met de stijgende zeespiegel (en dus toenemende waterdiepte).

Mogelijk werd tijdens het Eem, minder of geen sediment afgezet op het mariene transgressieoppervlak en werd er geen transgressiezandlaag gevormd ten gevolge van de aanwezigheid van de Oostende Vallei, die een grote sedimenttoevoer eiste. De aanwezigheid van de Oostende Vallei is waarschijnlijk ook de reden voor de intense vooroevererosie die bijna alle eerdere Eemiaan afzettingen verwijderde. Simulatiemodellen van Roy et al. (1995) voorspellen namelijk dat variaties in het mariene zandbudget ervoor zorgen dat een transgressieve barrière de zeebodem erodeert als er een netto verlies is van zand, bvb. naar de Oostende Vallei, terwijl een zandlaag zal worden afgezet als er een netto aanwinst is van zand.
Waarschijnlijk speelde ook de initiële beschikbaarheid aan sediment een rol in de bewaring van vroegere afzettingen na vooroevererosie. Als de vroegere afzettingen slechts dun waren, zouden ze ook makkelijker volledig te verwijderen zijn.

De Weichsel ijstijd

In het begin van de Weichseliaanperiode (Vroeg Glaciaal, MIS 5d-5a) daalde het zeeniveau door ijsuitbreiding, en weldra lag de Noordzee droog. In onze regionen werd het klimaat redelijk koud, maar met een zeer hoge vochtigheidsgraad (Verbruggen et al. 1991). Dit veroorzaakte een intense en diepe rivierinsnijding omdat er nog geen permafrost was. De Vlaamse Vallei werd ingesneden tot ongeveer -17 m TAW, waarbij de Eem-sedimenten grotendeels verwijderd werden. In de Oostende Vallei sneed de

rivier zich in tot -21 m MLLWS. Het Vroeg Pleniglaciaal (MIS4) was gekenmerkt door een zeer koud en vochtig klimaat, en vlechtende riviersystemen. De aanwezigheid van permafrost beperkte de rivierinsnijding en de weinige vegetatie versterkte de smeltwaterafvoer, waardoor grote hoeveelheden sediment in de rivieren terechtkwamen. Dit was ook het geval tijdens het mildere Midden Pleniglaciaal (MIS3), toen de Vlaamse Vallei en haar zijrivieren opgevuld werden tot een niveau tussen 0 en +10 m TAW (De Moor en Van De Velde 1995, Fig. 2 in: Verbruggen et al. 1991). Dit resulteerde in een minstens 20 m dikke Weichsel-afzetting in de Vlaamse Vallei (De Moor en Van De Velde 1995, De Moor et al. 1996), terwijl in de Oostende Vallei helemaal geen riviersedimenten werden teruggevonden in de hernieuwde rivierinsnijding.
Tijdens het Laat Pleniglaciaal (MIS2) evolueerde het klimaat tot zeer koude en droge omstandigheden met sterk beperkte vegetatie. Eolische activiteit overheerste en vroegere rivierafzettingen werden opgewaaid tot dekzandruggen die langzaam de Vlaamse Vallei afdamden. Het hele noordwaarts gerichte afvoersysteem van de Vlaamse Vallei werd gedwongen oostwaarts af te buigen (De Moor en Van De Velde 1995). Sindsdien was de Oostende Vallei niet langer verbonden met de Vlaamse Vallei.
Mogelijke Weichsel-rivierafzettingen in de Oostende Vallei werden vermoedelijk verwijderd door windwerking, nadat de rivier was afgesneden van de Vlaamse Vallei door de dekzandrug. Ook tijdens de Holocene zeespiegelstijging kunnen mogelijke Weichsel-afzettingen in de Oostende Vallei verwijderd geweest zijn, dit door getijdengeulen vóór de afzetting van schorren en slikken (i.e. seismische eenheid U4).

Ook de vroegere Maas Vallei, die het BCP doorkruist, werd opnieuw ingesneden, wat blijkt uit de aanwezigheid van rivierafzettingen van Weichseliaan-ouderdom in het 'Quaternary Basin', in het verlengde van het Offshore Platform (Kirby en Oele 1975). Tijdens de Weichsel laagstand nam de Maas, tezamen met de Rijn, dezelfde positie in als tijdens de Saale laagstand, op de westelijke kust van Nederland (Busschers et al. 2007). Dus waarschijnlijk volgden ze ook offshore dezelfde zuidwaarts gerichte afwatering (Gibbard 2007).

Het Holoceen evolutiemodel

De initiële Holocene overstroming van de zuidelijke Noordzee

Rond ongeveer 12.500 cal BP drong het stijgende water het zuidelijk deel van de Noordzee opnieuw binnen, langs de Straat van Dover in het zuiden, en doorheen geulen langsheen de Dogger Bank in het noorden. Kustwaarts-gericht sedimenttransport kon het snel stijgende water niet bijhouden en het relicte landschap verdronk snel (van der Molen en van Dijck 2000). Volgens van der Molen en van Dijck (2000) overstroomde de landbrug tussen het noorden van Nederland en Groot-Brittannië reeds rond 9500 cal BP. Volgens Beets en van der Spek (2000) daarentegen was op dat moment de Zuidelijke Bocht nog steeds gescheiden van de noordelijke Noordzee. Wel bereikte de zee toen reeds de Belgische Kustvlakte via de Straat van Dover (Denys en Baeteman 1995, Beets en van der Spek 2000, Baeteman en Declercq 2002). Aanvankelijk plantte de getijdengolf zich voort als een voortschrijdende, gedempte golf langsheen de Belgische en Nederlandse kusten naar het noorden. Door het verbreden van het bekken naar het noorden toe en de dissipatie van de energie in de ondiepe zee, nam de getijdenamplitude zeer snel af weg van de Straat van Dover, wat resulteerde in microtidale omstandigheden in bijna de gehele Zuidelijke Bocht.
Omdat de getijden naar het noorden propageerden in het centrale 'Deep Water Channel' en naar het oosten in de ondiepe zee tussen het 'Deep Water Channel' en de kust, was de oriëntatie van de getijdenstromingen en het netto zandtransport kustwaarts gericht.

In deze Vroeg-Holocene periode, ontwikkelde zich waarschijnlijk een open getijdengebied in de Zuidelijke Bocht, vergelijkbaar met de huidige Duitse Bocht. Door het stijgen van het grondwater niveau met de zeespiegel mee, was het overstroomde getijdengebied afgezoomd met zoetwatermoerassen waarin veen accumuleerde, gekend als basisveen (Baeteman 2004).

Vorming en terugschrijding van een kustbarrière met achterliggend wadgebied

Met stijgend zeeniveau werd het Noordzeebekken dieper en werd de dissipatie van de getijdenenergie verminderd, waardoor het getij de Zuidelijke Bocht verder kon binnendringen. Alhoewel rond 9500 cal BP volgens Beets en van der Spek (2000) de Zuidelijke Bocht nog steeds gescheiden was van de noordelijke Noordzee, was het bekken toch groot genoeg voor de vorming van golven aan zijn oostelijke kust. Deze waren in staat tot het bouwen van een kustbarrière. Achter de kustbarrière ontwikkelde zich wadgebied, bestaande uit een geheel van getijdengeulen en zand- en kleiplaten (i.e. slikken en schorren), bewaard in seismische eenheid U4. Het zand nodig voor de opvulling van het wadgebied was afkomstig van de vooroever naast de zeegaten die de barrière-eilanden scheidden, en van ebdelta's gelegen in die zeegaten. Kustparallel en kustnormaal ('alongshore' en 'cross-shore') sedimenttransport leverde echter te weinig sediment naar de vooroever om dit sedimentverlies te compenseren, en de kustlijn werd gedwongen terug te schrijden (Beets en van der Spek 2000). Dit ging gepaard met erosie van de onderliggende afzettingen en vroegere wadafzettingen. Hiervan is bewijs gevonden aan de top van U4 in de vorm van een grindlaag bovenop het vooroever-planatieoppervlak of mariene transgressieoppervlak.

Zoals tijdens het Eem, kan de grindlaag afgezet zijn door de terugschrijdende vooroever die vroegere grindige valleiopvullingen aansneed (vb. Weichseliaan Maasafzettingen), of het grind kan bestaan uit grofkorrelig materiaal dat locaal herwerkt werd uit het direct onderliggende Paleogeen substraat. Op dit moment kan ook de onderliggende Eemiaan grindlaag als bron dienen. In tegenstelling tot de mariene transgressie van het Eem, was de Holocene mariene planatie niet zo extreem. De Eem afzettingen die het Offshore Platform bedekken, werden tijdens de Holocene mariene transgressie waarschijnlijk nog verder afgevlakt met het Top-Paleogeen oppervlak ten zuiden van de Offshore Scarp, tezamen met de eerdere Vroeg-Holocene open-getijdenafzettingen. Maar, dichter bij de kust liggen er wel nog resten van vroegere wadafzettingen onder het Holocene mariene transgressieoppervlak. Ook de afzetting van enkele meter zand, i.e. de Holocene transgressiezandlaag, bovenop het basisgrind is in tegenstelling tot de situatie tijdens het Eem. Uit deze zandlaag werden onder de invloed van stormen stormgegenereerde of kustverbonden ('shoreface-connected') zandruggen gevormd, die een diepe afdruk achterlieten in het oppervlak van U4. Onder andere in seismische eenheid U5 werden drie parallelle zandruggen herkend: een buitenste, middelste en kustnabije zandrug.

Vorming van stormgegenereerde zandruggen in de mariene transgressiezandlaag

Twee soorten kustverbonden zandruggen werden gevormd tijdens de barrière-terugschrijding: kustverbonden ruggen als producten van ebdelta's in zeegaten van een terugschrijdende barrière, i.e. Type 2B (ii) van Dyer en Huntley (1999); en zandruggen gemodelleerd in een transgressiezandlaag, achtergebleven na barrière-terugschrijding (Swift et al. 1973, Swift en Thorne 1991). De zandruggen hebben een verschillende oorsprong maar werden waarschijnlijk beiden gevormd als reactie op storm-geïnduceerde stromingen op de vooroever en aangrenzende shelf. Dit ging gepaard met uitschuring en insnijding in de geulen, de onderliggende U4 afzettingen eroderend, en tegelijk opbouw van de zandrugtoppen.

Op basis van morfologische aanwijzingen, behoren de Goote en Akkaertbank hoogst waarschijnlijk tot vroegere kustverbonden zandruggen. Het gaat hier enkel om de bovenste gedeelten van deze banken s.l., namelijk seismische eenheid U7. Hun positie ten opzichte van vroegere kustlijnen suggereert dat de Goote en Akkaertbank s.s. zich vormden respectievelijk rond 9500 en 8900 cal BP. Bij een iets hoger zeeniveau en op een meer landwaartse positie, vormde zich rond 8400 cal BP de 'buitenste zandrug' van seismische eenheid U5. Rond 8000 cal BP, wanneer de terugschrijdende kustlijn de huidige kustlijn bereikt in het meest westelijke punt van de Kustvlakte, begon ook de 'middelste rug' van U5 zich te vormen. Het centrale en oostelijke deel van de 'kustnabije rug' van U5 begon zich te ontwikkelen rond 7500 cal BP, toen de kustbarrière stabiliseerde. Met de steeds verder stijgende zeespiegel kwamen de zandruggen los van de kustlijn, maar ze bleven verder doorgroeien. Gebaseerd op de bewaarde afmetingen van de zandruggen wordt aangenomen dat de buitenste rug zich vormde tot ongeveer 7700 cal BP en de middelste tot ongeveer 7000 cal BP.

Stabilisatie van de kustbarrière rond 7500 cal BP

Sinds de overstroming van de zuidelijke Noordzee, plantte de getijdengolf zich voort parallel aan de kust in diep water, en van diep water naar de kust toe in de ondiepe zone tussenin. Substantiële volumes zand werden geërodeerd van de bodem en naar de kust getransporteerd door getijdenasymmetrie, geholpen door golfsuspensie (van der Molen en van Dijck 2000, van der Molen en de Swart 2001b). Dit zand voedde gedeeltelijk de vooroever van de barrière. Maar het meeste zand dat de barrière en achterliggende wadgebied voedde was afkomstig van het onderliggende substraat, geërodeerd door de barrière terugschrijding (Beets en van der Spek 2000). Alhoewel onvoldoende om de snelle relatieve zeespiegelstijging (0.7 cm/a van 10.000-7500 cal BP) te compenseren, moet deze grote zandtoevoer de kust terugschrijding hebben afgeremd (van der Molen en van Dijck 2000). Rond 7500 cal BP, vertraagde de relatieve zeespiegelstijging van 0.7 cm/a naar 0.4-0.25 cm/a, hetgeen resulteerde in een zandoverschot en dus in het opslibben van het wadgebied en de aanzet naar stabilisatie van de kustbarrière (Baeteman en Declercq 2002). Het opslibben van het wadgebied resulteerde in de evolutie van zoutwater (schorre) vegetatie naar rietvegetatie (kustveenmoeras of zoetwatermoeras), en derhalve in veenaccumulatie (Baeteman 1999, Baeteman 2004). Voordien konden wadplaten opslibben tot supratidaal niveau, maar door de snel stijgende zeespiegel vormden zich slechts enkele vegetatiehorizonten. Het is pas vanaf 7500 cal BP dat geïntercaleerde veenlaagjes zich vormden. In de westelijke Kustvlakte bereikte de kustlijn toen zijn maximale landwaartse positie. De kustbarrière stabiliseerde ongeveer 3 km landinwaarts van de huidige kustlijn (Baeteman 2005a). De barrière schreed terug parallel aan zijn vorige positie en hield een rechte kustlijn aan, maar met een hoek ten opzichte van de huidige kustlijn, waardoor het lijkt alsof de kustlijn verder terugschreed in de westelijke Kustvlakte. De oriëntatie van de initiële kustbarrière was in de eerste plaats hoogstwaarschijnlijk bepaald door de strekking van het pre-transgressieoppervlak, en de barrière schreed min of meer constant terug over zijn gehele lengte naar zijn positie van 7500 cal BP.

Veranderende hydrodynamica en vorming van getijdenbanken rond 7000 cal BP

Met steeds verder stijgende zeespiegel, kon een toenemende hoeveelheid getijdenenergie de Zuidelijke Bocht binnendringen vanuit het noorden. De getijden en stromingsamplitudes bleven toenemen tot ongeveer 7000 cal BP. Door de steeds grotere waterdieptes kon het getij de kust steeds dichter naderen, wat er voor zorgde dat het kustwaarts-gerichte netto zandtransportpatroon veranderde in een patroon van transport parallel aan de kust, i.e. littorale drift. Op hetzelfde moment vormde zich een

zand divergentiezone tussen Zeeland en Groot-Brittannië. De zandtransport richting keerde om langsheen de Belgische kust, wat zorgde voor een verminderde zandtoevoer naar de kust toe, wat nog meer versterkt werd door een verminderde zandsuspensie door windgolven toen het gebied dieper werd (van der Molen en van Dijck 2000).
De vertraging in de relatieve zeespiegelstijging na 7500 cal BP (Denys en Baeteman 2005) kon de verminderde sedimenttoevoer compenseren, hetgeen resulteerde in een zandoverschot en dus in het opslibben van het wadgebied zoals hierboven vermeld (Baeteman 1999, Baeteman 2004).

Tussen 7000 cal BP en het heden steeg de zeespiegel nog ongeveer 6 m, maar het getijdensysteem veranderde nog weinig en de invloed van golven op het getijdentransport verminderde geleidelijk (van der Molen en van Dijck 2000).
Hoogstwaarschijnlijk is het vanaf deze periode, toen het getijdensysteem gelijkaardig werd aan het huidige, en de buitenste en middelste zandrug van U5 hun maximaal bewaarde hoogte bereikte, dat de getijdenbanken van de Vlaamse en Hinder Banken regio zich konden beginnen vormen bovenop deze zandruggen. Deze getijdenbanken maken deel uit van seismische eenheid U7.
De verandering in sedimenttransportrichting zou ook gedeeltelijk het verschil in oriëntatie kunnen verklaren tussen de Zeeland Banken s.s., die min of meer parallel liggen aan de kust en gevormd werden toen de sedimenttransport richting loodrecht op de kust was, en de Vlaamse en Hinder Banken s.s. die een hoek maken met de huidige kustlijn, en een kleine hoek met de heersende belangrijkste getijdenrichting. Waarschijnlijk ontwikkelden zich vanaf 7000 cal BP ook zandduinen op de op dat moment niet meer actieve stormgegenereerde zandruggen van de Goote en Akkaertbank. De Thorntonbank s.s. is duidelijk een getijdenbank, maar ligt parallel met de Goote en Akkaertbank. Deze is mogelijk gevormd toen de sedimenttransport richting nog kustwaarts gericht was, maar toen ook de getijdenstromingen reeds sterk genoeg waren om getijdenbanken te vormen in de dieper gelegen offshore gebieden (kort voor 7000 cal BP?).

Hoogstwaarschijnlijk vormden de Vlaamse en Hinderbanken s.s. zich gelijktijdig rond 7000 cal BP, als antwoord van de zeebodem op een geschikt hydraulisch regime. En vormden zich niet diachroon, als antwoord op een gestage verandering in omstandigheden, zoals vooroever terugschrijding door zeespiegelstijging. Het is mogelijk dat 'zandbankvermenigvuldiging' (Caston 1972, Dyer en Huntley 1999) zich voordeed, maar enkel als een ondergeschikt proces.
Het materiaal waaruit de U7 zandbanken zijn opgebouwd, is afkomstig van locale erosie van onderliggende sedimenten. Dit kon afgeleid worden uit het dikwijls erosief karakter van de basis van de banken, en de aanwezigheid van diep ingesneden geulen er tussenin. Het is door de vorming van de U7 getijdenbanken dat de seismische eenheden zo fragmentarisch zijn en onregelmatig voorkomen. We veronderstellen dat deze eenheden oorspronkelijk werden afgezet over grote gebieden van het BCP, voordat ze geërodeerd werden door de vorming van de zandbanken.

Progradatie van de kustbarrière van 6800-5000 cal BP

Tussen 6800 en 6000 cal BP, verloor de relatieve zeespiegelstijging zijn stuwende kracht (Baeteman en Declercq 2002, Baeteman 2005a), en nam nog verder af tot een gemiddelde van 0.07 cm/a na 5500-5000 cal BP (Baeteman 1999). De relatieve zeespiegelstijging vertraagde zodanig dat zelfs de verminderde sedimenttoevoer de gecreëerde accommodatieruimte nog oversteeg, waardoor de kustbarrière progradeerde (behalve het centrale deel nabij Middelkerke dat min of meer stabiel bleef). Er vormde zich een barrière-complex met zeewaarts migrerende zeegaten en getijdengeulen, waarvan de resten nog steeds zichtbaar zijn in de huidige westelijke Kustvlakte (Baeteman 2007b).

Ondanks de tweede vertraging in de relatieve zeespiegelstijging, rond 5500 cal BP, bleef de barrière niet verder prograderen, maar stabiliseerde. Op dat moment lag de kustbarrière in het westen opnieuw zeewaarts van de huidige kustlijn. In het oosten was ze over de kustnabije stormgegenereerde zandrug geschoven, wat diens maximale ouderdom limiteert tussen 6800 en 5000 cal BP (i.e. de periode van barrière progradatie).
Ondertussen, sinds 6400 cal BP, duurden de periodes van veengroei steeds langer en de laterale uitbreiding van kustveenmoerassen werd steeds groter (Baeteman en Declercq 2002, Baeteman 2008). Tussen 5500 en 4500 cal BP was bijna de gehele kustvlakte veranderd in een kustveenmoeras met veenaccumulatie, het zogenaamde oppervlakteveen (Baeteman 1999, Beets en van der Spek 2000, Baeteman et al. 2002). Op dat moment waren de meeste getijdengeulen dus reeds opgevuld en buiten gebruik, want veen kan zich enkel beginnen ontwikkelen in gebieden buiten getijdeninvloed (Baeteman 2004). Door het toeslibben van de getijdengeulen werden ook de ebdelta's inactief en werden deze herwerkt. Het herwerkte materiaal vulde de zeegaten en vormde ook het westelijk deel van de kustnabije zandrug van U4. Deze zandrug is een Type 2B (i) kustverbonden zandrug volgens de indeling van Dyer en Huntley (1999), i.e. een (herwerkt) product van een ebdelta in een zeegat van een kustbarrière. Door de herwerking en herverdeling van de ebdelta's werd de kustlijn weer opgelijnd, wat o.a. gedeeltelijk de reden kan zijn waarom de barrière na 5000 cal BP stabiliseerde. De oplijning en verdwijning van de ebdelta's kon ervoor gezorgd hebben dat de littorale drift, werkzaam sinds 7000 cal BP, niet meer 'gevangen' kon worden voor de opbouw van de barrière.

Het sedimenttekort verantwoordelijk voor de stabilisatie van de barrière, is geen gevolg van een verhoogde sedimentbehoefte in het achterliggende getijdengebied, want het was reeds zo goed als volledig opgeslibd rond 5000 cal BP, maar het was veroorzaakt door een verminderde sedimenttoevoer van offshore naar de kust, ofwel doordat de littorale drift niet meer kon bijdragen tot de opbouw van de barrière door het verdwijnen van de ebdelta's, ofwel doordat de sedimenttoevoer gewoonweg uitgeput was door de eerdere progradatie (Baeteman 2008). Waarschijnlijk was de sedimenttoevoer niet volledig uitgeput maar continu verminderd sinds 7000 cal BP, wat uiteindelijk tot een relatief tekort leidde in vergelijking met de zeespiegelstijging. Dit is in tegenstelling tot de situatie voordien, toen de afname in sedimenttoevoer nog traag genoeg was om de zeespiegelstijging te compenseren, en zelfs voor een zand surplus te zorgen (en derhalve barrière-progradatie). Ook de vorming van de getijdenbanken sinds 7000 cal BP zal een verandering veroorzaakt hebben in het hydrodynamisch patroon en kustwaarts sedimenttransport. Hoogstwaarschijnlijk bleef de barrière-uitbreiding voortduren tot sedimenttoevoer van alle bovenvermelde bronnen tezamen (i.e. herwerking van ebdelta's, littorale drift en kustnormaal transport) niet langer de effecten van de zeespiegelstijging kon overtreffen.

<u>Hernieuwde intrede van een wadgebied en barrière terugschrijding van 2800 cal BP tot 1200 cal BP (750 AD)</u>

Na 2000-3000 jaar van onafgebroken veengroei, ontstond opnieuw een wadgebied achter de kustbarrière, en veengebieden werden getransformeerd in sub- en intertidale platen. De hernieuwde intrede van een getijdensysteem was geen gevolg van een hernieuwde zeespiegelstijging, want het zeeniveau steeg immers nog met dezelfde sterk afgezwakte trend als tijdens de veenvorming. Het werd waarschijnlijk veroorzaakt door het uitschuren van vroegere getijdengeulen door een verhoogde waterafvoer vanuit het binnenland, toegeschreven aan een klimatologische verandering rond 2800 cal BP in combinatie met menselijke activiteiten (Baeteman 2005b). Door inklinken van het veen en instorten van geulranden, kwam het oppervlak van de kustvlakte in een lager positie

te liggen. Dit resulteerde in een grotere komberging en bijgevolg diepe verticale insnijding van de getijdengeulen. Het sediment nodig voor de opvulling van deze diepe geulen kwam van de Vroeg- en Mid-Holocene getijdengeulen en de eroderende vooroever. Het gevolg hiervan was dat de kustbarrière opnieuw terugschreed, hierbij de eerdere wadafzettingen eroderend. Daar het meeste geërodeerde sediment nodig was voor de opvulling van de getijdengeulen, werd er waarschijnlijk geen uitgebreide transgressiezandlaag afgezet. Het is wel mogelijk dat een dun laagje van geërodeerde wadafzettingen afgezet werd beneden het niveau van de vooroever op het mariene transgressieoppervlak, als deel van seismische eenheid U6.

Het was pas rond 1400-1200 cal BP (550-750 AD) dat de sedimenttoevoer en komberging in evenwicht waren met de zeespiegelstijging, en dat de kustvlakte opnieuw evolueerde naar een supratidale omgeving (Baeteman 2004). Omdat er bijna geen sediment meer nodig was voor de opvulling van de overblijvende getijdengeulen, vertraagde waarschijnlijk de barrière-terugschrijding of stopte ze zelfs. Bij de stabilisatie van de kustbarrière bevond de kustlijn zich in het westen ter hoogte van de huidige positie. In het centrale deel vormde de kustlijn de zeewaartse limiet van een 'eiland', Testerep, omgeven door getijdengeulen. Op dit eiland bevonden zich de vroegere nederzettingen van Westende, Oostende en Middelkerke. In het oosten, bevond de kustlijn zich nog ongeveer 10 km zeewaarts van de huidige kustlijn, en vormde de zeewaartse limiet van het eiland 'Wulpen'. Sinds de opslibbing van het getijdengebied werd mogelijk de sedimenttoevoer gebruikt voor de uitbouw van een duinengordel. Volgens Augustyn (1995) was deze duinengordel verscheidene kilometers breed, overgroeid en zelfs bebost.

De paleo-reconstructies tonen aan dat de kustbarrière niet constant terugschreed over zijn gehele lengte. In het westelijke deel, schreed de barrière terug over een afstand van slechts 1 km, in het centrale gedeelte tussen Westende en Middelkerke schreed de barrière helemaal niet terug sinds zijn vorige positie van 5000-2800 cal BP, en in het oostelijk deel schreed de barrière tot 5.5 km terug. Verschillen in sedimenttoevoer naar de barrière en verschillen in sedimentbehoefte van het getijdengebied liggen waarschijnlijk aan de oorsprong hiervan, daar de snelheid van de zeespiegelstijging constant was langsheen de gehele kustlijn.

<u>Terugschrijding van de barrière in het begin van de 15de eeuw, beïnvloed door menselijke activiteiten</u>

Het tweede deel van de barrière terugschrijding na de stabilisatie rond 750 AD, tot aan de huidige kustlijn, was mede een gevolg van menselijke interventie. De bouw van havens en de omvorming van het natuurlijke landschap van de duinen naar een kunstmatig landschap, voornamelijk bedoeld voor het kweken van vee, leidde tot een langzame maar onomkeerbare degradatie van de duinen vanaf de 12de eeuw (Augustyn 1995).
Hevige noordwesten stormen kregen grip op het duinenlandschap en versnelden de achteruitgang, tot op het einde van de 14de/begin van de 15de eeuw nog enkel een smalle reep van onstabiele driftduinen overbleef, tot uiteindelijk in 1404 een noordwesten-stormvloed de duinenreep compleet vernietigde. Tijdens deze storm verdronk o.a. het gehele eiland Wulpen, hetgeen onomkeerbare hydrografische veranderingen teweegbracht in de Westerschelde.
Deze veranderingen resulteerden in sterkere getijdenstromingen in de monding van de Westerschelde, waardoor het originele vooroever-planatieoppervlak van de 2800-1200 cal BP terugschrijding en het door stormen verdronken oppervlak sterk verdiept werd, tot een evenwicht bereikt werd onder het nieuwe hydraulische regime. Dit gebeurde echter niet voor het midden van de 16de eeuw, want toen konden de contouren van het

verdronken eiland nog steeds waargenomen worden (Augustyn 1995), terwijl het evenwichtsoppervlak een diepte had van -12 m MLLWS vooraleer het bedekt werd met sedimenten. Dus ten minste na het midden van de 16de eeuw konden de sterk-organische, modderige sedimenten van de geërodeerde vroegere wadgebieden afgezet worden, afgewisseld met zandige stormlaagjes, in het beschutte gebied tussen Walcheren en een ondiepte nabij de huidige Wenduine Bank. Deze afzettingen zijn vertegenwoordigd in seismische eenheid U6.

Vorming van de Kustbanken s.s.

Na de afzetting van seismische eenheid U6, vormden de Kustbanken s.s. zich er bovenop (deze behoren tot seismische eenheid U7). Gebaseerd op morfologische aanwijzingen vertegenwoordigen deze banken kustverbonden zandruggen. Ze ontwikkelden zich waarschijnlijk simultaan als een reactie van de zeebodem op een geschikt hydraulisch regime van golven en getij, en niet als reactie op een terugschrijdende kustlijn, daar die reeds de huidige positie had bereikt voor de zandruggen zich konden vormen. De Wenduine Bank s.s. staat niet in verbinding met het strand, maar met een verhoging in eenheid U6. Dit lijkt sterk op de situatie in het noorden van Nederland en Duitsland, waar de zandruggen verdwijnen in de vooroever, vermoedelijk door het sterke getij- en golfregime dat daar heerst (Dyer en Huntley 1999). Alhoewel kustverbonden zandruggen werden beschouwd als een speciale klasse van stormgegenereerde zandruggen, is een stormgedomineerde setting niet noodzakelijk voor de vorming van kustverbonden zandruggen (van de Meene en van Rijn 2000).

De relatieve invloed van getij en golven tijdens het Holoceen

Gebaseerd op de afzettingsomstandigheden kan volgens het model van Boyd et al. (1992) de dominante invloed van golven of getij (of beiden) op een bepaald moment achterhaald worden.
Tijdens de Holocene relatieve zeespiegelstijging was de hydrodynamische situatie eerst getijdengedomineerd met de afzetting van een open getijdengebied in een nochtans microtidale omgeving. Dit werd gevolgd door een gemengde golf-getijdengedomineerde situatie met de ontwikkeling van een transgressieve barrière met achterliggend wadgebied (in vermoedelijk een mesotidale omgeving).
Deze barrière begon te prograderen, wat een typisch fenomeen is in een golfgedomineerde (of eventueel een gemengde golf-getijdengedomineerde) omgeving. Tenzij gemodelleerde golfhoogtes (van der Molen en de Swart 2001b) in werkelijkheid veel hoger waren, was op dat moment echter de omgeving getijdengedomineerd, want rond 6800 cal BP, toen de barrière zeewaarts begon te migreren, was het getij reeds macrotidaal. De golfhoogte is volgens modellen ook enkel maar toegenomen tot nu (van der Molen en de Swart 2001b). Toch is de huidige situatie getijdengedomineerd. Dit impliceert dat de barrière vermoedelijk onder getijdengedomineerde omstandigheden progradeerde en dat de kustparallelle getijdenstromingen (sinds 7000 cal BP) de door wind en golven teweeggebrachte littorale drift, die normaal gezien de barrière vormt, verving of versterkte.
Tenslotte evolueerde de kustbarrière tijdens de huidige zeespiegel-hoogstand niet tot open getijdenafzettingen, zoals verwacht zou worden op basis van het heersende getijdengedomineerd regime. In plaats daarvan evolueerde de barrière naar een gesloten kustlijn, mogelijks omdat de getijdenstroming kustparallel georiënteerd is, parallel aan de golfgeïnduceerde littorale drift, wat eerder een gesloten systeem bevordert dan de vorming van kustnormale getijdengeulen in een open getijdengebied.
Tijdens het Holoceen nam de getijdenamplitude langzaam toe door de stijgende zeespiegel, en daardoor verminderde de dissipatie van de getijdengolf in het dieper

wordende bekken. Ook de golfhoogte nam langzaam toe tot op heden, door een verminderde wrijving in ondiep water met toenemende waterdiepte (van der Molen en de Swart 2001b).

De belangrijkste vernieuwingen in het Quartaire evolutiemodel van het BCP

Naast het feit dat nu voor de allereerste keer een geïntegreerd model voor de Quartaire evolutie van het BCP is voorgesteld, zijn er nog enkele andere belangrijke vernieuwingen.

Hoofdstuk 6: de Pleistocene insnijding en opvulling van de Oostende Vallei

- De sterk uiteenlopende interpretaties en voorgestelde ouderdommen voor de opvullingssedimenten van de Oostende Vallei (Liu et al. 1993, Trentesaux 1993, Berné et al. 1994, Trentesaux et al. 1999) konden worden uitgeklaard.
- Het was reeds gesuggereerd dat de Oostende Vallei de zeewaartse extensie vormt van de afvoersystemen van de Vlaamse Vallei en Kustvallei op land en dit voornamelijk op basis van morfologische argumenten (Mostaert et al. 1989, Liu et al. 1992). Voor het eerst werd echter de Oostende Vallei gelinkt met de Vlaamse vallei in termen van opvullingssedimenten, afzettingsomstandigheden en timing.

Hoofdstuk 7: de Holocene transgressie, evolutie van een wadgebied en de vorming van stormgegenereerde zandruggen

- Getijdenafzettingen en kustbarrières werden reeds vroeger herkend in bepaalde zandbanken op het BCP (Maréchal en Henriet 1983, 1986), maar nu werd het gehele kustbarrière-systeem, bestaande uit resten van wadafzettingen en stormgegenereerde zandruggen gemodelleerd in de transgressiezandlaag na barrière terugschrijding, volledig uitgekarteerd. Bovendien werden vroegere kustlijnposities gereconstrueerd en voorgesteld in paleo-reconstructies.
- De Goote en Akkaertbank s.s., die tot de Zeeland Banken behoren, stellen waarschijnlijk resten voor van zulke stormgegenereerde zandruggen.
- Niet enkel de Quartaire evolutie van de continentale shelf werd besproken. De Holocene evolutie van de kustlijn werd sterk verweven met de evolutiegeschiedenis van de westelijke Kustvlakte (Baeteman 2004, 2005). Ook gegevens van geologische en archeologische reconstructies in Zeeland (Vos en van Heeringen 1997) en historische kustlijnreconstructies van het Westerscheldegebied (Coornaert 1989, Augustyn 1995, Termote 2006) werden in rekening gebracht. Deze integratie van gegevens van zowel offshore als onshore gebieden heeft ook bijgedragen tot een beter begrip van de evolutie op land.
- De kustlijnreconstructies van 8000 en 7500 cal BP tonen duidelijk aan dat de kustbarrière in het oosten niet eerder stopte met terugschrijden dan in het westen, bv. door de aanwezigheid van een verhevenheid of kaap in de Pleistocene ondergrond. Dit was in het verleden gesuggereerd op basis van de meer landwaartse positie van de kustlijn in het westen, ten opzichte van de huidige kustlijn, rond 7500 cal BP, en de hoge Pleistocene ondergrond in de huidige oostelijke Kustvlakte. Ook de volledige afwezigheid van een barrière-complex in de oostelijke Kustvlakte, in tegenstelling tot het westen, droeg bij tot dit idee (Baeteman 2007b, Denys 2007, Fettweis et al. 2007). In het huidige oostelijke offshore gebied echter, is geen enkel bewijs gevonden van een hooggelegen Pleistocene ondergrond. In feite schreed de kustlijn constant terug over zijn gehele lengte, en stabiliseerde langs de gehele lijn op hetzelfde tijdstip omdat de sedimenttoevoer de gecreëerde accommodatieruimte compenseerde,

als resultaat van een algemene zeespiegelvertraging. De accommodatieruimte in het westen was niet veel groter dan in het oosten, waardoor de barrière veel vlugger zou terugschrijden. De barrière schreed terug, als een rechte lijn, parallel aan zijn vorige positie, maar met een hoek ten opzicht van de huidige kustlijn, waardoor het leek alsof de kustlijn veel verder teruggeschreden was in de westelijke Kustvlakte. De oriëntatie van de kustlijn wordt in de eerste plaats bepaald door de strekking van het pre-transgressieoppervlak.

Hoofdstuk 8: Holocene getijdenbanken

- De Vlaamse Banken en Hinderbanken s.s. werden waarschijnlijk gelijktijdig gevormd, in reactie op een geschikt hydraulische regime, rond ongeveer 7000 cal BP, toen het getijdenregime macrotidaal werd en de onderliggende stormgegenereerde zandruggen inactief werden. De vorming van de getijdenbanken is niet gerelateerd met een terugschrijdende kustlijn, want op dat moment lag de kustlijn reeds ver van deze banken.
- Deze periode werd ook gekenmerkt door een verandering in het netto patroon van zandtransport, van kustwaarts naar kustparallel (van der Molen en van Dijck 2000). Deze omschakeling kan mogelijk het verschil in oriëntatie verklaren tussen de Zeeland Banken, die parallel aan de kust liggen en gevormd werden toen het sedimenttransport kustwaarts gericht werd, en de Vlaamse en Hinderbanken, die een hoek vormen met de huidige kustlijn.
- Met de afzetting van de getijdenbanken (seismische eenheid U7) werden de oorspronkelijk regionaal afgezette oudere afzettingen gefragmenteerd door erosie in de geulen tussen de banken, waarbij het geërodeerde materiaal gebruikt werd voor de opbouw van de naastliggende banken. Dus de getijdenbank s.s. vormt enkel het bovenste gedeelte van wat een 'zandbank' s.l. is. Het onderste gedeelte van de zandbank s.l. bestaat uit kustnabije, estuariene en wadafzettingen, die uitsteken boven de zeebodem, door de huidige erosie in de omringende geulen. Het is dus niet zo dat de getijdenbanken zich vormden bovenop bestaande kernen, implicerend dat de onderliggende afzettingen eerst werden geërodeerd, gemodelleerd in verhevenheden, vooraleer de getijdenbanken er zich bovenop vormden.
- Het grindig materiaal in de geulen tussen de banken is afkomstig van verschillende bronnen: i.e. vroegere grindige rivier- en meerafzettingen (Paleogene rivieren, Elster proglaciaal meer, Saale proglaciaal meer, Saale, Maas en Oostende Vallei, Weichsel Rijn/Maas, Thames), en *in* situ grofkorrelig materiaal van het Paleogeen substraat zelf (concreties, zandsteenbanken), dat aangesneden werd door de terugschrijdende kustlijn, en herverdeeld werd tijdens de Eem en Holocene transgressies.

Hoofdstuk 9: de Quartaire evolutie van het BCP, synthese en algemene opmerkingen

- De classificatie voor afzettingsmilieus langsheen een transgressieve of regressieve lineaire kustlijn, opgesteld door Boyd et al. (1992), voldoet niet om de huidige situatie langsheen de Belgische kust te verklaren. Onder getijdengedomineerde omstandigheden vormde zich hier een gesloten kustlijn, in plaats van de verwachte open getijdenafzettingen. Een mogelijke verklaring hiervoor is dat op de Belgische shelf, waar de maximale getijdenstromingen in het kustnabije gebied in NE richting lopen, parallel aan de kust, de getijdenstromingen de kustparallelle littorale drift versterken, waardoor de huidige kustlijn een golfgedomineerd uiterlijk heeft onder getijdengedomineerde omstandigheden.

De uitdaging van een shelf met een kleine accommodatieruimte

Het BCP is een typische transgressieve shelf, waar accommodatieruimte domineert boven sedimenttoevoer. Het BCP is een relatief stabiel gebied, dat niet beïnvloed wordt door tektonische of (glacio-) isostatische subsidentie of opheffing (D'Olier 1981, Kiden et al. 2002, Vink et al. 2007). Er is ook geen sediment 'bypassing' mogelijk door de afwezigheid van een uitgesproken shelf rand in de Zuidelijke Bocht. Toch is de relatief geringe accommodatieruimte, enkel gecreëerd door eustatische zeespiegelstijging tijdens het Eem en Holoceen, nog steeds groter dan de beschikbare hoeveelheid sediment, hetgeen een transgressieve stratigrafische architectuur tot gevolg had. In tegenstelling tot progradernde en aggraderende shelf-systemen, die gekenmerkt worden door dikke sedimentopeenvolgingen aangevoerd door rivieren (Galloway en Hobday 1996), worden accommodatiegedomineerde regimes, zoals het Belgisch transgressief shelf systeem, gekenmerkt door een dun en gefragmenteerd Quartair dek, door het constant herwerken van de in situ beschikbare sedimenten. Dit maakte het zeer moeilijk, maar vooral uitdagend, om op basis daarvan de Quartaire geologische evolutie te reconstrueren.

Door het constant herwerken van oude afzettingen voor het opbouwen van nieuwe, was het dan ook niet mogelijk een stratigrafische classificatie op te stellen op basis van de boorgegevens alleen, omdat lithologisch gelijkaardig materiaal in feite kan behoren tot totaal verschillende afzettingsmilieus, over verschillende seismische eenheden heen. Een bepaald type zand kan zowel voorkomen in seismische eenheden U4, U5 en U7, maar vertegenwoordigt respectievelijk, zandplaten of geulopvullingen, stormgegenereerde zandruggen en getijdenbanken. Seismisch onderzoek is dus onontbeerlijk voor de identificatie van belangrijke, regionale erosieoppervlakken, om zo de verschillende afzettingsomgevingen en -periodes te onderscheiden.
Anderzijds kunnen de seismische eenheden lithologisch ook sterk heterogeen zijn. Om dit te kunnen inschatten, is het belangrijk dat seismische data en boorgegevens steeds geïnterpreteerd worden naar afzettingsomstandigheden, en niet enkel in functie van technische karakterisering, zoals bv. bij een vooronderzoek voor de bouw van windmolenparken gebeurt. Een interpretatie naar afzettingsomstandigheden toe, geeft een goede indicatie van wat er in de ondergrond verwacht kan worden. Een zand in een getijdenbankafzetting is vermoedelijk redelijk homogeen in de omgeving, maar bij een gelijkaardig zand in aan wadafzettingsmilieu kan er ook klei verwacht worden in de buurt.

Blik op de toekomst

Het voorgestelde model voor het Quartaire evolutie op het BCP focust voornamelijk op het middelste gedeelte van de Belgische shelf, daar waar het dichtste seismische netwerk en de meeste boringen zich bevinden. Dit beperkte studiegebied zou nog verder opengetrokken moeten worden naar de meest offshore en meest kustnabije gebieden. Met bijkomende boringen in het offshore gebied zouden ten noorden van de Offshore Scarp de oudste afzettingen van het Eem, en mogelijk ook Weichsel, kunnen bestudeerd worden. Met bijkomende data in het ondiepe, kustnabije gebied, zouden de jongste Quartaire afzettingen meer in detail kunnen besproken worden, en zouden gedetailleerder reconstructies van historische kustlijnen kunnen worden opgemaakt. Ook bijkomend onderzoek in de oostelijke Kustvlakte is aangewezen, om bvb. te achterhalen waarom de oostelijke kustlijn zo veel verder terugschreed dan in het westen tussen 2800-1200 cal BP.
Daarbij zou de Quartaire geologische evolutie van het BCP moeten geïntegreerd worden met de geschiedenis van de aanliggende Nederlandse, Franse en Britse zones. In de

nabije toekomst dient ook een Quartairkaart gepubliceerd te worden, die eindelijk de witte vlek in de zuidelijke Noordzee bedekt. Het zou een welkom antwoord zijn op de vele vragen waarmee baggeraars en surveyors zitten omtrent de ondiepe ondergrond van het Belgisch Continentaal Plat.

References

Ameryckx, J.B., Verheye, W. and Vermeire, R., 1995. Bodemkunde.

Amos, C.L. and King, E.L., 1984. Bedforms of the Canadian Eastern seaboard: a comparison with global occurrences. Marine Geology, 57: 167-208.

Antoine, P., Coutard, J.P., Gibbard, P., Hallegouet, B., Lautridou, J.P. and Ozouf, J.C., 2003. The Pleistocene rivers of the English Channel region. Journal of Quaternary Science, 18(3-4): 227-243.

Ashley, G.M., 1990. Classification of large-scale subaqueous bedforms: a new look at an old problem. Journal of Sedimentary Petrology, 60(1): 160-172.

Augustyn, B., 1995. De evolutie van het duinecosysteem in Vlaanderen in de Middeleeuwen: antropogene factoren versus zeespiegelrijzingstheorie. [English version: http://www.armara.be/augustyn/dune-ecosystem.pdf 'Evolution of the dune ecosystem in Flanders during the Middle Ages: anthropogenic factors versus sea level change theory']. Historisch-Geografisch Tijdschrift, 13(1): 9-19.

Baak, J.A., 1936. Regional petrology of the southern North Sea. PhD thesis, Leyden University, Wageningen, 128 pp.

Baeteman, C., 1999. The Holocene depositional history of the IJzer palaeo-valley (Western Belgian coastal plain) with references to the factors controlling the formation of intercalated peat beds. Geologica Belgica, 2(3-4): 39-72.

Baeteman, C., 2004. The Holocene development of a tide-dominated coastal lowland. Western coastal plain of Belgium. Field Guide, The QRA Third International Postgraduate Symposium Fieldtrip. Belgian Geological Survey, Belgium.

Baeteman, C., 2005a. Geologische kaart van België 1/25.000. Profieltypenkaart van de Holocene kustafzettingen. De Panne-Oostduinkerke, Nieuwpoort-Leke, Middelkerke-Oostende. Belgische Geologische Dienst, Brussel.

Baeteman, C., 2005b. How subsoil morphology and erodibility influence the origin and pattern of late Holocene tidal channels: case studies from the Belgian coastal lowlands. Quaternary Science Reviews, 24(18-19): 2146-2162.

Baeteman, C., 2007a. De ontstaansgeschiedenis van onze kustvlakte, De Grote Rede (VLIZ), pp. 2-10.

Baeteman, C., 2007b. Roman peat-extraction pits as possible evidence for the timing of coastal changes: An example from the Belgian coastal plain. In: J. Beenakker, F. Horsten, A. De Kraker and H. Renes (Editors), Landschap in ruimte en tijd. Uitgeverij Aksant, Amsterdam, pp. 16-25.

Baeteman, C., 2008. De Holocene geologie van de Belgische Kustvlakte [The Holocene geology of the Belgian Coastal Plain]. Geological Survey of Belgium Professional Paper, 2008/2 (304). Koninklijk Belgisch Instituut voor Natuurwetenschappen. Belgische Geologische Dienst, Brussel, 36 pp.

Baeteman, C., Beets, D.J. and Van Strydonck, M., 1999. Tidal crevasse splays as the cause of rapid changes in the rate of aggradation in the Holocene tidal deposits of the Belgian Coastal Plain. Quaternary International, 56: 3-13.

Baeteman, C. and Declercq, P.-Y., 2002. A synthesis of early and middle Holocene coastal changes in the western Belgian lowlands. BELGEO, 2: 30.

Baeteman, C., Scott, D.B. and Van Strydonck, M., 2002. Changes in coastal zone processes at a high sea-level stand: a late Holocene example from Belgium. Journal of Quaternary Science, 17(5-6): 547-559.

Balson, P.S. and D'Olier, B., 1988. Thames Estuary, Sheet 51°N-00°E. Solid geology. 1:250 000 map series.

Beekman, A.A., 1921. Catalogus van kaarten, enz. betrekking hebbende op de oudere en tegenwoordige gesteldheid van Holland tusschen Maas en Y, aanwezig op de tentoonstelling in het Stedelijk Museum te Amsterdam, in september en october 1921. Koninklijk Nederlands Aardrijkskundig Genootschap, Leiden.

Beets, D.J. and van der Spek, A.J.F., 2000. The Holocene evolution of the barrier and the back-barrier basins of Belgium and The Netherlands as a function of late Weichselian morphology, relative sea-level rise and sediment supply. Geologie en Mijnbouw, Netherlands Journal of Geosciences, 79(1): 3-16.

Beets, D.J., De Groot, T.A.M. and Davies, H.A., 2003. Holocene tidal back-barrier development at decelerating sea-level rise: a 5 millennia record, exposed in the western Netherlands. Sedimentary Geology, 158(1-2): 117-144.

Belderson, R.H., 1986. Offshore tidal and non-tidal sand ridges and sheets: differences in morphology and hydrodynamic setting, Canadian Society of petroleum geologists, pp. 293-301.

Berné, S., 2002. Evolution of sand banks. C. R. Geoscience, 334: 731-732.

Berné, S., Trentesaux, A., Stolk, A., Missiaen, T. and De Batist, M., 1994. Architecture and long term evolution of a tidal sandbank: The Middelkerke Bank (southern North Sea). Marine Geology, 121(1-2): 57-72.

Berné, S., Lericolais, G., Marsset, T., Bourillet, J.F. and De Batist, M., 1998. Erosional offshore sand ridges and lowstand shorefaces: Examples from tide- and wave-dominated environments of France. Journal of Sedimentary Research, 68(4): 540-555.

Blaser, P.C., 2007. Tracermethoden in der Hydrologie: Kombination verschiedener Methoden und Anwendungen am Beispiel des Ledo-Paniselian-Aquifers in Belgien, PhD thesis, Ghent University, Gent, 235 pp.

Blum, M.D. and Törnqvist, T.E., 2000. Fluvial responses to climate and sea-level change: a review and look forward. Sedimentology, 47(s1): 2-48.

Bogemans, F. and Baeteman, C., 2003. Toelichting bij de Quartairgeologische kaart, kaartblad 19-20, Veurne-Roeselare. Vrije Universiteit Brussel, Belgische Geologische Dienst, Ministerie van de Vlaamse Gemeenschap, Afdeling Natuurlijke Rijkdommen en Energie.

Boggs, S., 1995. Principles of sedimentology and stratigraphy. Prentice-Hall, New Jersey.

Boyd, R., Dalrymple, R. and Zaitlin, B.A., 1992. Classification of Clastic Coastal Depositional-Environments. Sedimentary Geology, 80(3-4): 139-150.

Bridgeland, D.R., 2002. Fluvial deposition on periodically emergent shelves in the Quaternary: example records from the shelf around Britain. Quaternary International, 92: 25-34.

Bridgeland, D.R. and D'Olier, B., 1995. The Pleistocene evolution of the Thames and Rhine drainage systems in the southern North Sea Basin. In: R.C. Preece (Editor),

Island Britain: a Quaternary Perspective. Geological Society of London Special Publication, London, pp. 27-45.

Bronk Ramsey, C., 1995. Radiocarbon Calibration and Analysis of Stratigraphy: The OxCal Program Radiocarbon 37(5): 425-430.

Bronk Ramsey, C., 2001. Development of the Radiocarbon Program OxCal. Radiocarbon, 43(2A): 355-363.

Buisman, J., 1998-2000. Duizend jaar weer, wind en water in de Lage Landen, delen III en IV, 1450-1675. [http://www.knmi.nl/cms/content/21054/kleine_ijstijd]. Uitgeverij Van Wijnen, Franeker.

Buntinx, W., 1968. Waterdunen, een vergeten stad in Zeeuws Vlaanderen. Handelingen van de Maatschappij voor Geschiedenis en Oudheidkunde van Gent, XXII: 145-174.

Busschers, F.S., Kasse, C., van Balen, R.T., Vandenberghe, J., Cohen, K.M., Weerts, H.J.T., Wallinga, J., Johns, C., Cleveringa, P. and Bunnik, F.P.M., 2007. Late Pleistocene evolution of the Rhine-Meuse system in the Southern North Sea basin: imprints of climate change, sea-level oscillation and glacio-isostacy. Quaternary Science Reviews, 26(25-28): 3216-3248.

Busschers, F.S., Van Balen, R.T., Cohen, K.M., Kasse, C., Weerts, H.J.T., Wallinga, J. and Bunnik, F.P.M., 2008. Response of the Rhine-Meuse fluvial system to Saalian ice-sheet dynamics. Boreas, 37(3): 377-398.

Caston, V.N.D., 1972. Linear sand banks in the Southern North Sea. Sedimentology, 18: 63-78.

Caston, V.N.D., 1977. Quaternary deposits of the central North Sea 1: A new isopachyte map of the Quaternary deposits of the central North Sea. Report of the Institute of Geological Sciences 77(11): 1-8.

Caston, V.N.D., 1979. The Quaternary sediments of the North Sea. In: F.T. Banner, Collins, M.B., Massie, K.S. (Editor), The Northwest and European Shelf Seas: The Sea Bed and the Sea in Motion. Elsevier, Amsterdam, pp. 195-267.

Caston, G.F., 1981. Potential gain and loss of sand banks in the Southern Bight of the North Sea. Marine Geology, 41: 239-250.

Catuneanu, O., 2002. Sequence stratigraphy of clastic systems: concepts, merits, and pitfalls. Journal of African Earth Sciences, 35(1): 1-43.

Coornaert, M., 1989. Het tienderecht in de oorspronkelijke parochie Oostkerke en op het eiland Wulpen met de topografie en de geschiedenis van Wulpen. Rond de Poldertorens, XXXI (1: 5-35, 2: 3-32, 3: 3-43, 4: 3-36).

Cutler, K.B., Edwards, R.L., Taylor, F.W., Cheng, H., Adkins, J., Gallup, C.D., Cutler, P.M., Burr, G.S. and Bloom, A.L., 2003. Rapid sealevel fall and deepocean temperature change since the last interglacial period. Earth and Planetary Science Letters, 206: 253-271.

Dalrymple, R.W., 1992. Tidal depositional systems. In: R.G. Walker and N.P. James (Editors), Facies models; response to sea level change. Geological Association of Canada, pp. 195-218.

Dalrymple, R.W., Zaitlin, B.A. and Boyd, R., 1992. Estuarine Facies Models - Conceptual Basis and Stratigraphic Implications. Journal of Sedimentary Petrology, 62(6): 1130-1146.

Dalrymple, R.W., Boyd, R. and Zaitlin, B.A., 1994. History of research, types and internal organisation of incised-valley systems: introduction to the volume. In: R.W. Dalrymple, R. Boyd and B.A. Zaitlin (Editors), Incised-valley systems: origin and sedimentary

sequences. SEPM (Society for Sedimentary Geology), Special Publication 51, pp. 4-10.

Dalrymple, R.W. and Choi, K., 2007. Morphologic and facies trends through the fluvial-marine transition in tide-dominated depositional systems: A schematic framework for environmental and sequence-stratigraphic interpretation. Earth-Science Reviews, 81(3-4): 135-174.

Davis, R.A., 1988. Morphodynamics of the west-central Florida barrier system: the delicate balance between wave and tide domination, Coastal lowlands: geology and geotechnology. Kluwer, Dordrecht.

Davis, R.A., 1992. Depositional systems: an introduction to sedimentology and stratigraphy. Prentice Hall, New Jersey, 604 pp.

Davis, R.A., 1994. Geology of Holocene Barrier Island Systems. Springer-Verlag, Berlin Heidelberg.

Davis, R.A. and Hayes, M.O., 1984. What is a wave-dominated coast? Marine Geology, 60: 313-329.

De Batist, M., 1989. Seismo-stratigrafie en Struktuur van het Paleogeen in de Zuidelijke Noordzee. PhD Thesis, University of Ghent, Ghent, 107 pp.

De Batist, M., Trentesaux, A., Missiaen, T. and Berné, S., 1993. Chapter 15. Large scale internal structure of the bank. In: G. De Moor and J. Lanckneus (Editors), Sediment mobility and morphodynamics of the Middelkerke Bank. RESECUSED. Universiteit Gent , CEC, Brussel, pp. 168-187.

De Breuck, W., De Moor, G. and Maréchal, R., 1969. Lithostratigrafie van de kwartaire sedimenten in het Oostelijk Kustgebied (België). Natuurwetenschappelijk Tijdschrift, 51: 125-137.

de Kraker, A.M.J., 2002. De Westerschelde, een water zonder weerga: ontstaansgeschiedenis en kaartbeeld, havens, handel en scheepvaart, verkeer, verdronken dorpen, oorlog en verdedigingswerken, natuur en milieu en andere aspecten van de Westerschelde. Duerinck, Kloosterzande, The Netherlands, 228 pp.

De Maeyer, P., Wartel, S. and De Moor, G., 1985. Internal structures of the Nieuwpoort Bank, Southern North Sea. Netherlands Journal of Sea Research, 19(1): 15-18.

De Moor, G., 1963. Bijdrage tot de kennis van de fysische landschapsvorming in Binnen-Vlaanderen. Tijdschr. Belg. Ver. Aardr. Stud., 32: 329-443.

De Moor, G., 1985a. Present day morphodynamics on the Kwintebank and their meaning for the evolution of the Flemish Banks. In: G. Pichot (Editor), Proceedings "Progress in Belgian Oceanographic Research", Brussel.

De Moor, G., 1985b. Shelf bank morphology off the Belgian coast, recent methodological and scientific developments. In: M. Van Molle (Editor), Recent trends in Physical Geography in Belgium. Liber Amicorum, L. Peeters. V.U.B., Study series of the Vrije Universiteit Brussel, New series, Brussel, pp. 47-90.

De Moor, G., 1986. Het Continentaal Platform van de Noordzee gedurende het Kwartair. Water: Tijdschrift over Waterproblematiek, 31: 6-9.

De Moor, G., 1996. De zanden van de Vlaamse Vallei. In: F. Gullentops and L. Wouters (Editors), Delfstoffen in Vlaanderen. Ministerie van de Vlaamse Gemeenschap, Departement EWBL, Brussel, pp. 63-68.

De Moor, G. and Heyse, I., 1974. Litostratigrafie van de kwartaire afzettingen in de overgangszone tussen de kustvlakte en de Vlaamse Vallei in Noordwest-België. Natuurwet. Tijdschr., 56: 85-109.

De Moor, G. and Heyse, I., 1978. De morfologische evolutie van de Vlaamse Vallei. Aardrijkskunde, 4-1: 343-375.

De Moor, G. and Tavernier, R., 1978. Periglacial and paleogeography of the Quaternary: Periglacial deposits and sedimentary structures in the Upper-Pleistocene infilling of the Flemish Valley. Excursion guide.

De Moor, G., Lanckneus, J., Berné, S., Chamley, H., De Batist, M., Houthuys, R., Stolk, A., Terwindt, J., Trentesaux, A. and Vincent, C., 1993. Relationship between sea floor currents and sediment mobility in the southern North Sea, Symposium MAST Days, Brussel, pp. 193-207.

De Moor, G. and Van De Velde, D., 1995. Toelichting bij de Quartairgeologische kaart van België, Vlaams Gewest, kaartblad 14, Lokeren, schaal 1/50 000. Universiteit Gent, Lab Fysische Geografie, Ministerie van de Vlaams Gemeenschap, Afdeling Natuurlijke Rijkdommen en Energie.

De Moor, G., Lootens, M., Van De Velde, D. and Meert, L., 1996. Toelichting bij de Quartairgeologische kaart van Vlaanderen, kaartblad 21, Tielt, schaal 1/50 000. Ministerie van de Vlaamse Gemeenschap, Afdeling Natuurlijke Rijkdommen en Energie.

Deleu, S., 2001. Zeebodemmobiliteitsstudie van de Hinderbanken regio, Ghent University, Gent, 135 pp.

Deleu, S. and Van Lancker, V., 2007. Geological setting of gravel occurrences on the Belgian part of the North Sea. Annex in Van Lancker et al. (2007): Management, research and budgetting of aggregates in shelf seas related to end-users (Marebasse). Final Scientific Report, Belgian Science Policy, pp. 101-115.

Denys, L. and Baeteman, C., 1995. Holocene evolution of relative sea level and local mean high water spring tides in Belgium - a first assessment. Marine Geology, 124: 1-19.

Denys, S., 2007. De contrasterende Holocene sediment successie langsheen het westelijk en oostelijk deel van de Belgische kust: oorzaak en gevolgen, VUB, Brussels.

D'Olier, B., 1981. Sedimentary events during Flandrian sea-level rise in the south-west corner of the North Sea. In: S.-D. Nio, R.T.E. Schüttenhelm and T.C.E. van Weering (Editors), Holocene Marine Sedimentation in the North Sea Basin. Spec. Publs. int. Ass. Sediment., pp. 221-227.

Duane, D.B., Field, M.E., Meisburger, E.R., Swift, D.J.P. and Williams, J.S., 1972. Linear shoal on the Atlantic inner continental shelf, Florida to Long Island. In: D.J.P. Swift, D.B. Duane and O.H.J. Pilkey (Editors), Shelf sediment transport: process and pattern. Dowden, Hutchinson and Ross, Stroudsburg, pp. 477-498.

Dyer, K.R. and Huntley, D.A., 1999. The origin, classification and modelling of sand banks. Continental Shelf Research, 19: 1285-1330.

Ebbing, J.H.J., Laban, C., Frantsen, P.J. and Nederhof, H.P., 1992. Geologische kaart, kaartblad Rabsbank, Concessieblokken voor olie en gas S7, S8, S10 en S11 (51°20' N - 3°00' E). Rijks Geologische Dienst.

Ebbing, J.H.J. and Laban, C., 1996. Geological history of the area off Walcheren and Zeeuwsch-Vlaanderen (southwestern Netherlands), since the start of the Eemian. Mededelingen Rijks Geologische Dienst, 57: 251-267.

Eisma, D., Mook, W.G. and Laban, C., 1981. An early Holocene tidal flat in the Southern Bight. In: S.D. Nio, R.T.E. Schüttenhelm and T.C.E. Van Weering (Editors), Holocene

Marine Sedimentation in the North Sea Basin. Blackwell Scientific Publ., Oxford, pp. 229-237.

Fettweis, M., Du Four, I., Zeelmaekers, E., Baeteman, C., Francken, F., Houziaux, J.-S., Mathys, M., Nechad, B., Pison, V., Vandenberghe, N., Van den Eynde, D., Van Lancker, V. and Wartel, S., 2007. Mud Origin, Characterisation and Human Activities (MOCHA). Final Scientific Report.

Flemming, B.W., 1980. Sand transport and bedform patterns on the continental shelf between Durban and Port Elizabeth (southeast African continental margin). Sedimentary Geology, 26: 179-205.

Galloway, W.E. and Hobday, D.K., 1996. Terrigenous clastic depositional systems: applications to fossil fuel and groundwater resources. Springer, Berlin, 489 pp.

Gibbard, P.L., 2007. Europe cut adrift. Nature, 448: 259-260.

Gildersleeve, B., 1932. Some stages in the disintegration of glauconite American Mineralogist 17(3): 98-103.

Glaeser, J.D., 1978. Global distribution of barrier islands in terms of tectonic setting. Journal of Geology, 86: 283-297.

Gullentops, F. and Wouters, L., 1996. Ondergronds-Bovengronds-Delfstoffen in Vlaanderen, 22 transparanten. Ministerie van de Vlaamse Gemeenschap, Departement EWBL, Brussel.

Gupta, S., Collier, J.S., Palmer-Felgate, A. and Potter, G., 2007. Catastrophic flooding origin of shelf valley systems in the English Channel. Nature, 448(7151): 342-U5.

HAECON, 1986. Oppervlaktelaag van het Noordzee Continentaal Plat. Fase 2: uitgebreid geologisch onderzoek. Uitgevoerde trilboringen. Boorstaten, Belgisch Geologische Dienst, Afdeling KWAMGO.

Harris, P.T., 1988. Large-scale bedforms as indicators of mutually evasive sand transport and the sequential infilling of wide-mouthed estuaries. Sedimentary Geology, 57: 273-298.

Harris, P.T., Heap, A.D., Bryce, S.M., Porter-Smith, R., Ryan, D.A. and Heggie, D.T., 2002. Classification of Australian clastic coastal depositional environments based upon a quantitative analysis of wave, tidal, and river power. Journal of Sedimentary Research, 72(6): 858-870.

Hayes, M.O., 1979. Barrier island morphology as a function of tidal and wave regime. In: S.P. Leatherman (Editor), Barrier islands from the Gulf of Mexico to the Gulf of St. Lawrence. Academic Press, New York, pp. 1-29.

Heap, A.D., Bryce, S. and Ryan, D.A., 2004. Facies evolution of Holocene estuaries and deltas: a large-sample statistical study from Australia. Sedimentary Geology, 168(1-2): 1-17.

Heyse, I., 1979. Bijdrage tot de geomorfologische kennis van het noordwesten van Oost-Vlaanderen (België). Verhandelingen van de Koninklijke Academie voor Wetenschappen, Letteren en Schone Kunsten van België, Klasse der Wetenschappen, Jaargang XLI(155).

Heyse, I., Chamley, H., De Batist, M., De Moor, G., De Schaepmeester, G., De Winne, E., Houthuys, R., Lanckneus, J., Marsset, T., Pichot, G., Pollentier, A., Porter, C., Stolk, A., Terwindt, J., Tessier, B., Van Cauwenberghe, C. and Vanwesenbeeck, V., 1995. Sediment transport and bedform mobility in a sandy shelf environment, Second MAST Days and EUROMAR Market. EUROPEAN COMMISSION, Sorrento (IT).

Hoogendoorn, R. and Kluwer, L.F.J., 1990. Geological Survey of the Netherlands' high-energy hydraulically driven vibration corer for subsea sediments, Oceanology International Conference. U.K. proceedings, Brighton, U.K.

Houbolt, J.J.H.C., 1968. Recent sediments in the Southern Bight of the North Sea. Geologie & Mijnbouw, 47(4): 245-273.

Houthuys, R., 1989. Small-scale depositional structures of surface sediments of the Flemish Banks. In: G. Pichot (Editor), Progress in Belgian Oceanographic Research, Gent, pp. 165-177.

Huthnance, J.M., 1982a. On One Mechanism Forming Linear Sand Banks. Estuarine Coastal and Shelf Science, 14(1): 79-99.

Huthnance, J.M., 1982b. On the formation of sand banks of finite extent. Estuarine, Coastal and Shelf Science, 15: 277-299.

IMDC, 2007. Technisch-wetenschappelijke bijstand kustmorfologie: Onderzoek naar het modelleren van strandsuppleties met Litpack, i.o.v. Vlaamse Overheid, Maritieme Dienstverlening en Kust, Afdeling Kust.

Jacobs, P., 2000. Course notes 2000-2001: Littorale oceanografie. Universiteit Gent, Gent.

Jacobs, P. and De Batist, M., 1996. Sequence stratigraphy and architecture on a ramp-type continental shelf: the Belgian Palaeogene. Geological Society Special Publication, 117: 23-48.

Jelgersma, S., Oele, E. and Wiggers, A.J., 1979. Depositional History and coastal development in the Netherlands and the adjacent North Sea since the Eemian. In: E. Oele, Schüttenhelm, R.T.E., Wiggers, A.J. (Editor), The quaternary history of the North Sea. Acta Univ. Ups. Symp. Univ. Ups. Annum Quingentesimum Celebrantis 2, Uppsala, Sweden, pp. 115-142.

Kenyon, N.H., Belderson, R.H., Stride, A.H. and Johnson, M.A., 1981. Offshore tidal sand banks as indicators of net transport and as potential deposits. In: S.-D. Nio, R.T.E. Schüttenhelm and T.C.E. van Weering (Editors), Holocene Marine Sedimentation in the North Sea Basin, pp. 257-268.

Kiden, P., Denys, L. and Johnston, P., 2002. Late Quaternary sea-level change and isostatic and tectonic land movement along the Belgium-Dutch North Sea coast: geological data and model results. Journal of Quaternary Science, 17(5-6): 535-546.

King, C.A.M., 1963. Some Problems concerning Marine Planation and the Formation of Erosion Surfaces. Transactions and Papers (Institute of British Geographers)(33): 29-43.

King, C.A.M., 1972. Beaches and coasts. Edward Arnold, London.

Kirby, R. and Oele, E., 1975. The geological history of the Sandettie-Fairy Bank area. Phil. Trans. R. Soc. Lond. A., 279: 257-267.

Kroon, A., Larson, M., Möller, I., Yokoki, H., Rozynski, G., Cox, J. and Larroude, P., 2008. Statistical analysis of coastal morphological data sets over seasonal to decadal time scales. Coastal Engineering, 55(7-8): 581-600.

Laban, C. and Schüttenhelm, R.T.E., 1981. Some new evidence on the origin of the Zeeland Ridges. In: S.-D. Nio, R.T.E. Schüttenhelm and T.C.E. van Weering (Editors), Holocene Marine Sedimentation in the North Sea Basin. Blackwell Scientific Publ., Oxford, pp. 239-245.

Labeyrie, L.D., Duplessy, J.C. and Blanc, P.L., 1987. Variations in mode of formation and temperature of oceanic deep waters over the past 125,000 years. Nature, 327: 477-482.

Lambeck, K., Esat, T.M. and Potter, E.K., 2002. Links between climate and sea levels for the past three million years. Nature, 419(6903): 199-206.

Lanckneus, J., De Moor, G., Berné, S., Chamley, H., De Batist, M., Henriet, J.P. and Trentesaux, A., 1991. Cartographie du Middelkerke Bank: dynamique sedimentaire, structure geologique, facies sedimentaires, International Symposium Ocean Space Advanced Technologies European Show, Brest, pp. 11.

Lanckneus, J., Van Lancker, V., Moerkerke, G., Van den Eynde, D., Fettweis, M., De Batist, M. and Jacobs, P., 2001. Investigation of the natural sand transport on the Belgian Continental Shelf (BUDGET). Final report. Federal Office for Scientific, Technical and Cultural Affairs (OSTC).

Le Bot, S., Van Lancker, V., Deleu, S., De Batist, M. and Henriet, J.P., 2003. Tertiary and Quaternary geology of the Belgian Continental Shelf. Scientific Support Plan for a Sustainable Development Policy, SPSD II. PPS Science Policy, Brussel, 75 pp.

Lea, D.W., Martin, P.A., Pak, D.K. and Spero, H.J., 2002. Reconstructing a 350 ky history of sealevel using planktonic Mg/Ca and oxygen isotope records from a Cocos Ridge core. Quaternary Science Reviews 21: 283-293.

Leatherman, S.P., 1983. Barrier dynamics and landward migration with Holocene sea-level rise. Nature, 301: 415-418.

Liu, A.C., 1990. A seismic and geomorphological study of the erosion surface at the top of the Tertiary in the Southern North Sea (Belgian and Northern French sectors.). Unpublished Ph.D. Thesis, Gent University, Gent, Vol1: 119 pp. + Vol2: 97 fig.

Liu, A.C., Missiaen, T. and Henriet, J.P., 1992. The morphology of the top-Tertiary erosion surface in the Belgian sector of the North Sea. Marine Geology, 105: 275-284.

Liu, A.C., De Batist, M., Henriet, J.P. and Missiaen, T., 1993. Plio-Pleistocene scour hollows in the Southern Bight of the North Sea. Geologie & Mijnbouw, 71: 195-204.

Maréchal, R. and Henriet, J.P., 1983. Seismisch onderzoek op het Belgisch Continentaal Plat. Eerste faze. Ontginningszone 2. Rapport. Vol. 1-2, Ministerie van Economische Zaken. Administratie van het Mijnwezen, Brussel.

Maréchal, R. and Henriet, J.P., 1986. Studie oppervlaktelaag van het Belgisch continentaal plat. Seismische prospectie. Eindverslag Sector B. Volume 1; Volume 2; Volume 3, Universiteit Gent, Laboratorium voor Aardkunde, Ministerie van Economische Zaken, Administratie van het Mijnwezen, Belgische Geologische Dienst.

Masselink, G., Kroon, A. and Davidson-Arnott, R.G.D., 2006. Morphodynamics of intertidal bars in wave-dominated coastal settings -- A review. Geomorphology, 73(1-2): 33-49.

McMillan, A.A., 2005. A provisional Quaternary and Neogene lithostratigraphical framework for Great Britain. Netherlands Journal of Geosciences-Geologie En Mijnbouw, 84(2): 87-107.

Meyus, Y., De Smedt, F., Walraevens, K. and Batelaan, O., 2000. Hydrogeologische codering van de ondergrond van Vlaanderen (HCOV). Water, @wel 8: 1-13.

Meyus, Y., Cools, J., Adyns, D., Zeleke, S.Y., Woldeamlak, S.T., Batelaan, O. and De Smedt, F., 2005. Vlaams Grondwater Model. Hydrogeologische detailstudie van de ondergrond in Vlaanderen. Eindrapport en bijlagen, Ministerie van de Vlaamse Gemeenschap, Departement Leefmilieu en Infrastructuur, Administratie Milieu-, Natuur-, Land- en Waterbeheer, AMINAL, afdeling Water, Brussels.

Miles, P., Schaming, M. and Lovera, R., 2007. Resurrecting vintage paper seismic records. Marine Geophysical Researches, 28(4): 319-329.

Mitchum, R.M.J. and Vail, P.R., 1977. Seismic stratigraphic interpretation procedure. In: C.E. Payton (Editor), Seismic stratigraphy: applications to hydrocarbon exploration. AAPG Memoir 26, pp. 135-144.

Mitchum, R.M.J., Vail, P.R. and Thomson, S., 1977a. The depositional sequence as a basic unit for stratigraphic analysis. In: C.E. Payton (Editor), Seismic stratigraphy: applications to hydrocarbon exploration. AAPG Memoir 26, pp. 53-62.

Mitchum, R.M.J., Vail, P.R. and Sangree, J.B., 1977b. Stratigraphic interpretation of seismic reflection patters in depositional sequences. In: C.E. Payton (Editor), Seismic stratigraphy: applications to hydrocarbon exploration. AAPG Memoir 26, pp. 117-133.

Mostaert, F. and De Moor, G., 1989. Eemian and Holocene sedimentary sequences on the Belgian coast and their meaning for sea level reconstruction. In: J.P. Henriet and G.D. Moor (Editors), The Quaternary and Tertiary Geology of the Southern Bight, North Sea. Ministry of Economic Affairs, Belgian Geological Survey, Gent, pp. 137-148.

Mostaert, F., Auffret, J.P., De Batist, M., Henriet, J.P., Moons, A., Sevens, E., Van den Broeke, I. and Verschuren, M., 1989. Quaternary shelf deposits and drainage patterns off the French and Belgian Coasts. In: J.P. Henriet and G.D. Moor (Editors), The Quaternary and Tertiary Geology of the Southern Bight, North Sea. Ministry of Economic Affairs, Belgian Geological Survey, Gent, pp. 111-118.

Nichols, G., 1999. Sedimentology and stratigraphy. Blackwell Science Ltd., Oxford.

Off, T., 1963. Rhythmic linear sand bodies cuased by tidal currents. Bulletin of the American Association of Petroleum Geology, 47: 324-341.

OSPAR, 2000. Quality Status Report 2000, Region II – Greater North Sea, OSPAR Commission, London.

Paepe, R. and Baeteman, C., 1979. The Belgian coastal plain during the Quaternary. In: E. Oele, R.T.E. Schuettenhelm and A.J. Wiggers (Editors), The Quaternary History of the North Sea. Acta Universitatis Upsaliensis, Symposium Universitatis Upsaliensis Annum Quingentesiumum Celebrantis. University of Uppsala, Uppsala, pp. 143-146.

Pattiaratchi, C. and Collins, M., 1987. Mechanisms for Linear Sandbank Formation and Maintenance in relation to Dynamical Oceanographic Observations. Prog. Oceanog., 19: 117-176.

Peters, J.J., 2006. Belang van de Vlakte van de Raan voor de morfologische evoluties van het Schelde-estuarium. In: J. Coosen, J. Mees, J. Seys and N. Fockedey (Editors), Studiedag: De Vlakte van de Raan van onder het stof gehaald. Oostende, 13 oktober 2006. Vlaams Instituut van de Zee (VLIZ). VLIZ Special Publication 35, Oostende, Belgium, pp. 30-42.

Pritchard, D.W., 1967. What is an estuary? Physical viewpoint. In: G.H. Lauff (Editor), Estuaries. American Association for the Advancement of Science, Publication 83, pp. 3-5.

Reimer, P.J., Baillie, M.G.L., Bard, E., Bayliss, A., Beck, J.W., Bertrand, C.J.H., Blackwell, P.G., Buck, C.E., Burr, G.S., Cutler, K.B., Damon, P.E., Edwards, R.L., Fairbanks, R.G., Friedrich, M., Guilderson, T.P., Hogg, A.G., Hughen, K.A., Kromer, B., McCormac, G., Manning, S., Ramsey, C.B., Reimer, R.W., Remmele, S., Southon, J.R., Stuiver, M., Talamo, S., Taylor, F.W., van der Plicht, J. and Weyhenmeyer, C.E., 2004. IntCal04 terrestrial radiocarbon age calibration, 0-26 cal kyr BP. Radiocarbon, 46(3): 1029-1058.

Reinson, G.E., 1992. Transgressive barrier island and estuarine systems. In: R.G. Walker and N.P. James (Editors), Facies models; response to sea level change. Geological Association of Canada, pp. 179-194.

Reynaud, J.Y., Tessier, B., Proust, J.N., Dalrymple, R., Bourillet, J.F., De Batist, M., Lericolais, G., Berné, S. and Marsset, T., 1999. Architecture and sequence stratigraphy of a late Neocene incised valley at the shelf margin, southern Celtic Sea. Journal of Sedimentary Research, 69(2): 351-364.

Rieu, R., van Heteren, S., van der Spek, A.J.F. and De Boer, P.L., 2005. Development and preservation of a mid-holocene tidal-channel network offshore the western Netherlands. Journal of Sedimentary Research, 75(3): 409-419.

Roy, P.S., 1984. New South Wales estuaries: their origin and evolution. In: B.G. Thom (Editor), Coastal Geomorphology in Australia. Academic Press, Sydney, pp. 99-121.

Roy, P.S., Cowell, P.J., Ferland, M.A. and Thom, B.G., 1995. Wave-dominated coasts. In: R.W.G. Carter and C.D. Woodroffe (Editors), Coastal evolution: Late Quaternary shoreline morphodynamics. University Press, Cambridge.

Roy, P.S., Williams, R.J., Jones, A.R., Yassini, R., Gibbs, P.J., Coates, B., West, R.J., Scanes, P.R., Hudson, J.P. and Nichol, S., 2001. Structure and function of south-east Australian estuaries. Estuarine, Coastal and Shelf Science, 53: 351-384.

Salomon, J.C. and Allen, G.P., 1983. Role sedimentologique de la mare dans les estuaires a fort marnage. Compagnie Francais des Petroles. Notes and Memoires, 18: 35-44.

Schaming, M., Muller, G., Miles, P.R. and Munschy, M., 2000. SeisTrans - Creation of SEG-Y files from images of paper seismic records (poster S71A-02), AGU Fall Meeting AGU, San Francisco.

Schüttenhelm, R.T.E. and Laban, C., 2005. Heavy minerals, provenance and large scale dynamics of seabed sands in the Southern North Sea: Baak's (1936) heavy mineral study revisited. Quaternary International, 133-134: 179-193.

Shackleton, N., 2000. The 100,000 year ice-age cycle identified and found to lag temperature, carbon dioxide and orbital eccentricity. Science, 289: 1897–1902.

Siddall, M., Rohling, E.J., Almogi-Labin, A., Hemleben, C., Meischner, D., Schmelzer, I. and Smeed, D.A., 2003. Sea-level fluctuations during the last glacial cycle. Nature, 423(6942): 853-858.

Siddall, M., Chappell, J. and Potter, E.K., 2006. Eustatic Sea Level During Past Interglacials. In: F. Sirocko, T. Litt, M. Claussen and M.-F. Sanchez-Goni (Editors), The climate of past interglacials. Elsevier, Amsterdam, pp. 75-92.

Smith, A.J., 1985. A catastrophic origin for the palaeovalley system of the eastern English Channel. Marine Geology, 64(1-2): 65-75.

Snedden, J.W., Tillman, R.W., Kreisa, R.D., Schweller, W.J., Culver, S.J. and Winn JR., R.D., 1994. Stratigraphy and genesis of a modern shoreface-attached sand ridge, Peahala ridge, New Jersey. Journal of sedimentary research, B64(4): 560-581.

Snedden, J.W. and Dalrymple, B., 1999. Modern shelf sand ridges: from historical perspective to a unified hydrodynamic and evolutionary model, Isolated Shallow Marine Sand Bodies: Sequence Stratigraphic Analysis and Sedimentologic Interpretation. SEPM Special Publication No. 64. SEPM, pp. 13-28.

Sommé, J., 1979. Quaternary coastlines in northern France. In: E. Oele, R.T.E. Schuettenhelm and A.J. Wiggers (Editors), The Quaternary History of the North Sea. Acta Universitatis Upsaliensis, Symposium Universitatis Upsaliensis Annum Quingentesiumum Celebrantis. University of Uppsala, Uppsala, pp. 147-158.

Spaink, 1973. De 'Fauna van Angulus pygmaeus' en de 'Fauna van Spisula subtruncata' in de Zuidelijke Noordzeekom. Internal Report 578, Rijks Geologische Dienst, Afdeling Macropalaeontologie.

Stolk, A., 1996. Chapter 16. Task 6: Analysis and control of internal structures by coring. Subtasks 6.1-6.2-6.3-6.4: Middelkerke Bank area: Sedimentological investigations. In: I. Heyse and G. De Moor (Editors), STARFISH final report. University of Gent (B), Department of Geography, Gent, pp. 16.1-16.33.

Stolk, A. and Trentesaux, A., 1993. Chapter 12. Small scale sedimentary structure analysis by vibrocoring. In: G. De Moor and J. Lanckneus (Editors), Sediment mobility and morphodynamics of the Middelkerke Bank. Universiteit Gent - CEC, Gent - Brussels, pp. 133-143.

Streif, H., 1990. Quaternary sea-level changes in the North Sea, an analysis of amplitudes and velocities. In: P. Brosche and Südermann (Editors), Earth's rotation from eons to days. Springer-Verlag, Berlin, pp. 201-214.

Stride, A.H., 1989. Modern deposits, quasi-deposits and some Holocene sequences in the Southern Bight, North Sea. In: J.P. Henriet and G. De Moor (Editors), The Quaternary and Tertiary Geology of the Southern Bight, North Sea. Ministry of Economic Affairs, Belgian Geological Survey, Gent, pp. 149-159.

Swift, D.J.P., 1975. Tidal sand ridges and shoal-retreat massifs. Marine Geology, 18: 105-134.

Swift, D.J.P., 1976. Continental shelf sedimentation. In: D.J. Stanley and D.J.P. Swift (Editors), Marine sediment transport and environmental management. John Wiley, New York, pp. 311-350.

Swift, D.J.P., 1985. Response of the shelf floor to flow. In: R.W. Tillman, D.J.P. Swift and R.G. Walker (Editors), Shelf sands and sandstone reservoirs. SEPM short course notes, Tulsa, pp. 135-241.

Swift, D.J.P., Duane, D.B. and McKinney, T.F., 1973. Ridge and swale topography of the middle Atlantic Bight, North America: secular response to the Holocene hydraulic regime. Marine Geology, 15: 227-247.

Swift, D.J.P., Phillips, S. and Thorne, J.A., 1991. Sedimentation on continental margins, IV: lithofacies and depositional systems. In: D.J.P. Swift, G.F. Oertel, R.W. Tillman and J.A. Thorne (Editors), Shelf sand and sandstone bodies: geometry, facies and sequence stratigraphy. Blackwell, Berlin, pp. 89-152.

Swift, D.J.P. and Thorne, J.A., 1991. Sedimentation on continental margins, I: a general model for shelf sedimentation. In: D.J.P. Swift, G.F. Oertel, R.W. Tillman and J.A. Thorne (Editors), Shelf sand and sandstone bodies: geometry, facies and sequence stratigraphy. Blackwell, Berlin, pp. 3-32.

Tavernier, R. and De Moor, G., 1974. L'Évolution du Bassin de l'Escaut. In: P. Macar and F. Gullentops (Editors), L'Évolution Quaternaire des bassins fluviaux de la Mer du Nord Méridionale. Cent. Soc. géol. Belg., Liège, pp. 159-233.

Termote, J., 2006. De Vlakte van de Raan in historisch-geografisch perspectief. In: J. Coosen, J. Mees, J. Seys and N. Fockedey (Editors), Studiedag: De Vlakte van de Raan van onder het stof gehaald. Oostende, 13 oktober 2006. Vlaams Instituut van de Zee (VLIZ). VLIZ Special Publication 35, Oostende, Belgium, pp. 43-51.

Tesch, P. and Reinhold, T., 1946. De bodem van het zuidelijk uiteinde der Noordzee. Tijdschr. Kon. Ned. Aard. Gen., 63: 72-84.

Thieler, E.R., Schwab, W.C., Gayes, P.T., Pilkey, O.H.J., Cleary, W.J. and Scanlon, K.M., 1999. Paleoshorelines on the U.S. Atlantic and Gulf Continental Shelf: Evidence

for sea-level stillstands and rapid rises during deglaciation. In: C.H. Fletcher and J.V. Matthews (Editors), The Non-steady State of the Inner Shelf and Shoreline: Coastal Change on the Time Scale of Decades to Millennia in the late Quaternary. Inaugural Meeting of IGCP Project #437 "Coastal Environmental Change During Sea Level Highstands", University of Hawaii, Honolulu, USA, pp. 230.

Thomas, R.G., Smith, D.G., Wood, J.M., Visser, J., Calverleyrange, E.A. and Koster, E.H., 1987. Inclined Heterolithic Stratification - Terminology, Description, Interpretation and Significance. Sedimentary Geology, 53(1-2): 123-179.

Tornqvist, T.E., Wallinga, J., Murray, A.S., de Wolf, H., Cleveringa, P. and de Gans, W., 2000. Response of the Rhine-Meuse system (west-central Netherlands) to the last Quaternary glacio-eustatic cycles: a first assessment. Global and Planetary Change, 27(1-4): 89-111.

Toro, F., Mayerle, R., Poerbandono and Wilkens, J., 2005. Patterns of Hydrodynamics in a Tidally-Dominated Coastal of the German North Sea. Die Küste, 69(PROMORPH).

Trentesaux, A., 1993. Structure et dynamique sédimentaire du Middelkerke Bank, Mer du Nord méridionale. Unpublished Ph.D. Thesis, Université des Sciences et Technologies de Lille, Lille, 229 pp.

Trentesaux, A., Berné, S., De Batist, M. and Chamley, H., 1993a. Architecture interne d'un banc sableux tidal de la Mer du Nord Méridionale. Comptes rendus de l'academie des sciences, 316(II): 99-106.

Trentesaux, A., Stolk, A., Berné, S., De Batist, M. and Chamley, H., 1993b. Le Middelkerke Bank - Mer du Nord méridionale; première datations indirectes des dépôts a partir d'informations sismiques et lithologiques, 4ième Congrès Français de Sédimentologie - Résumés. ASF, Paris, pp. 345-346.

Trentesaux, A., Stolk, A. and Berné, S., 1999. Sedimentology and stratigraphy of a tidal sand bank in the southern North Sea. Marine Geology, 159: 253-272.

van de Meene, J.W.H. and van Rijn, L.C., 2000. The shoreface-connected ridges along the central Dutch coast - part 1: field observations. Continental Shelf Research, 20(17): 2295-2323.

Van den Broeke, I., 1984. Een seismisch-stratigrafische studie van het Kwartair van de zandbanken van de Hindergroep in het westelijk deel van het Belgisch continentaal plat., University of Gent, Gent, 43 pp.

Van den Eynde, D., 2001. 2D sediment transport model (total load). MU-SEDIM. MUMM.

van der Molen, J., 2002. The influence of tides, wind and waves on the net sand transport in the North Sea. Continental Shelf Research, 22(18-19): 2739-2762.

van der Molen, J. and van Dijck, B., 2000. The evolution of the Dutch and Belgian coasts and the role of sand supply from the North Sea. Global and Planetary Change, 27: 223-244.

van der Molen, J. and de Swart, H.E., 2001a. Holocene tidal conditions and tide-induced sand transport in the southern North Sea. Journal of Geophysical Research, 106(c5): 9339-9362.

van der Molen, J. and de Swart, H.E., 2001b. Holocene wave conditions and wave-induced sand transport in the southern North Sea. Continental Shelf Research, 21(16-17): 1723-1749.

Van Lancker, V., 1999. Sediment and morphodynamics of a siliciclastic near coastal area, in relation to hydrodynamical and meteorological conditions: Belgian Continental Shelf. Unpublished Ph.D. Thesis, Ghent University, Ghent, 194 pp.

Van Lancker, V., Du Four, I., Verfaillie, E., Deleu, S., Schelfaut, K., Fettweis, M., Van den Eynde, D., Francken, F., Monbaliu, J., Giardino, A., Portilla, J., Lanckneus, J., Moerkerke, G. and Degraer, S., 2007. Management, research and budgetting of aggregates in shelf seas related to end-users (Marebasse). Final Scientific Report, Belgian Science Policy.

van Veen, J., van der Spek, A.J.F., Stive, M.J.F. and Zitman, T., 2005. Ebb and flood channel systems in the Netherlands tidal waters. Journal of Coastal Research, 21(6): 1107-1120.

Vandenberghe, J., 1995. Timescales, Climate and River Development. Quaternary Science Reviews, 14(6): 631-638.

Veenstra, H.J., 1964. Geology of the Hinder Banks, southern North Sea. Hydrograph. Newsl., 1: 72-80.

Veenstra, H.J., 1969. Gravels of the Southern North Sea. Marine Geology, 7(5): 449-464.

Verbruggen, C., Denys, L. and Kiden, P., 1991. Paleo-ecologische en geomorfologische evolutie van Laag- en Midden-België tijdens het Laat-Kwartair. De Aardrijkskunde 1991(3): 357-376.

Verwaest, T., 2008. De impact van aggregaatextractie op de kustveiligheid bij storm, Studiedag: Duurzaam beheer van de zand- en grindwinning op het Belgisch Continentaal Plat. FOD Economie, Brugge.

Vink, A., Steffen, H., Reinhardt, L. and Kaufmann, G., 2007. Holocene relative sea-level change, isostatic subsidence and the radial viscosity structure of the mantle of northwest Europe (Belgium, the Netherlands, Germany, southern North Sea). Quaternary Science Reviews, 26(25-28): 3249-3275.

Vos, P.C. and de Wolf, H., 1993. Reconstruction of sedimentary environments in Holocene coastal deposits of the southwest Netherlands; the Poortvliet boring, a case study of palaeoenvironmental diatom research. In: H. van Dam (Editor), Hydrobiologia. Twelfth international diatom symposium. Kluwer Academic Publishers, Belgium, pp. 297-306.

Vos, P. and van Heeringen, R.M., 1997. Holocene geology and occupation history of the province of Zeeland (SW Netherlands). In: M.M. Fischer (Editor), Mededelingen Nederlands Instituut voor Toegepaste Geowetenschappen: Holocene evolution of Zeeland (SW Netherlands). TNO, pp. 5-109.

Waelbroeck, C., Labeyrie, L., Michel, E., Duplessy, J.C., McManus, J.F., Lambeck, K., Balbon, E. and Labracherie, M., 2002. Sea-level and deep water temperature changes derived from benthic foraminifera isotopic records. Quaternary Science Reviews, 21(1-3): 295-305.

Walker, R.G. and Plint, A.G., 1992. Wave and storm dominated shallow marine systems. In: R.G. Walker and N.P. James (Editors), Facies Models: Response to Sea Level Change. Geological Association of Canada, pp. 219–238.

Wartel, S. and Vansieleghem, L., 1985. Kartering Kustvlakte en Kontinentaal Plat. Sedimentologie van de Holoceneafzettingen. Rapport 1 &2, Koninklijk Instituut voor Natuurwetenschappen, Afdeling Mineralogie en Petrografie.

Weise, B.R. and White, W.A., 1980. Padre Island national seashore: a guide to the geology, natural environments, and history of a Texas barrier island, Guidebook 17. Texas Bureau of Economic Ecology.

Wintein, W., 2004. Ontstaan en evolutie van het landschap in de Zwinstreek. Museum of local history "SINCFALA" [Online: http://www.sincfala.be/beeldenbank/geschiedenis/geschiedeniswintein.pdf] pp. 1-34.

Yang, C.S., 1989. Active, moribund and buried tidal sand ridges in the East China Sea and the Southern Yellow Sea. Marine Geology, 88: 97-116.

Zaitlin, B.A., Dalrymple, R.W. and Boyd, R., 1994. the stratigraphic organization of incised-valley systems associated with relative sea-level change. In: R.W. Dalrymple, R. Boyd and B.A. Zaitlin (Editors), Incised-valley systems: origin and sedimentary sequences. SEPM (Society for Sedimentary Geology), Special Publication 51, pp. 45-60.

Appendix A
Available core data

ID	Date	X ED50	Y ED50	Type	Core length (m)	Extras
RGD-R15-19/boring 56	25/08/1936	495682.152	5684355.937	?	9.40	Macrofauna report
RGD-R15-20/boring 57	29/08/1936	485200.682	5682182.123	?	10.50	Macrofauna report
RGD-RWS-pulsboring 71	25/08/1937	470807.350	5709090.920	?	7.70	Macrofauna report
RGD-R15-18/boring 72	1/09/1937	492673.493	5679138.503	?	3.50	Macrofauna report
RGD-R15-17/boring 74	6/09/1937	486639.042	5684062.630	?	11.60	Macrofauna report
RGD-R15-16/boring 84	1/08/1938	481969.452	5672214.143	?	9.85	Macrofauna report
RGD-R9-68/pulsboring 85	1/09/1964	499807.426	5712096.377	?	10.00	Macrofauna report
RGD-S10-83/pulsboring 87	1/09/1964	520742.452	5697402.300	?	8.30	Macrofauna report
RGD-S10-81/boring 55	1/09/1965	514784.421	5694014.141	?	11.00	Macrofauna report
RGD-S10-82-02/boring 58	1/09/1965	518507.222	5690658.905	?	11.60	Macrofauna report
RGD-69/HT5	1/05/1969	472416.491	5696662.390	Vibrocore (Zenkovitz)	0.90	
RGD-69/HT35 (R6-8)	?	494028.483	5726929.219	?	2.30	
RGD-69/T68	1/05/1969	519876.971	5696472.040	Vibrocore (Zenkovitz)	2.32	
RGD-69/T70	1/05/1969	515067.646	5696270.192	Vibrocore (Zenkovitz)	2.60	
RGD-69/T72	1/05/1969	510141.626	5696288.904	Vibrocore (Zenkovitz)	2.75	
RGD-69/T73	1/05/1969	507842.906	5696253.956	Vibrocore (Zenkovitz)	2.00	
RGD-69/T75	1/05/1969	505039.637	5698505.629	Vibrocore (Zenkovitz)	2.35	
RGD-69/T76	1/05/1969	503765.064	5698751.675	Vibrocore (Zenkovitz)	2.00	
RGD-69/T79	1/05/1969	497337.810	5703168.750	Vibrocore (Zenkovitz)	0.42	
RGD-69/T81	1/05/1969	509487.365	5694928.337	Vibrocore (Zenkovitz)	2.80	
RGD-69/T87	1/06/1969	522577.038	5693084.976	Vibrocore (Zenkovitz)	2.40	
RGD-69/T88	1/06/1969	519145.054	5690753.937	Vibrocore (Zenkovitz)	2.00	
RGD-69/T90	1/06/1969	513567.950	5693609.147	Vibrocore (Zenkovitz)	2.00	
RGD-69/T110	1/06/1969	501738.059	5697761.991	Vibrocore (Zenkovitz)	2.00	
RGD-69/T137	?	503458.130	5724084.560	?	2.26	
RGD-69/HT91	1/10/1969	474702.855	5725104.467	Vibrocore (Zenkovitz)	2.90	
RGD-69/HT95	1/10/1969	474501.627	5734683.095	Vibrocore (Zenkovitz)	2.92	
RGD-70/H27	1/08/1970	521800.289	5693915.726	Vibrocore (Zenkovitz)	3.70	
RGD-70/H30	1/08/1970	495070.130	5692203.290	Vibrocore (Zenkovitz)	0.35	
RGD-70/H31	1/08/1970	517340.809	5692446.626	Vibrocore (Zenkovitz)	3.20	
RGD-73/GS12	1/02/1973	494337.750	5728751.660	Flushcore (Geod[illegible]	5.00	
RGD-73/GS13	?	546579.293	5731528.000	?	2.90	
RGD-73/GS9	1/02/1973	502356.940	5737152.480	Flushcore (Ge[illegible]	8.60	Ostracods analysis
RGD-73/GD12	1/03/1973	472454.770	5742510.580	Straight drilling (Geodoff)	2.90	
RGD-73/GS56	1/08/1973	468822.617	5734035.347	Flushcore (Geodoff)	2.50	
RGD-74/GS04	1/03/1974	522731.675	5693085.663	Flushcore (Geodoff)	9.00	Macrofauna report
RGD-74/GS05	1/03/1974	514329.268	5690923.511	Flushcore (Geodoff)	8.40	Macrofauna report
RGD-74/GS49	?	511367.666	5709514.009	?	10.00	
RGD-75/MK13	3/07/1975	509828.495	5698389.044	Flushcore (Geodoff)	10.00	
RGD-76/H14	1/06/1976	519159.812	5697118.060	Vibrocore (Zenkovitz)	2.50	
RGD-76/H16	1/06/1976	516485.738	5699796.456	Vibrocore (Zenkovitz)	3.74	
RGD-76/H36	22/06/1976	501580.100	5708914.540	Vibrocore (Zenkovitz)	0.70	
RGD-77/MK37	1/04/1977	505913.420	5710894.950	Flushcore (Geodoff)	10.00	
RGD-77/MK38	1/04/1977	502923.960	5717565.490	Flushcore (Geodoff)	10.00	
RGD-77/MK39	?	505419.560	5722387.080	?	8.30	
RGD-77/MK42	1/06/1977	504062.869	5688464.475	Flushcore (Geodoff)	8.00	Macrofauna report
RGD-77/MK43	1/06/1977	497873.040	5691367.244	Flushcore (Ge[illegible]	5.30	Macrofauna report
RGD-77/MK44	1/06/1977	501255.478	5696896.836	Flushcore (Geodoff)	9.00	Macrofauna report
RGD-77/MK45	1/06/1977	504385.658	5695570.156	Flushcore (Ge[illegible]	9.60	Macrofauna report
RGD-77/MK46	1/06/1977	502919.912	5691058.705	Flushcore (Geodoff)	10.00	Macrofauna report
RGD-77/MK47	1/06/1977	517309.207	5696061.056	Flushcore (Geod[illegible]	10.00	
RGD-77/MK48	1/06/1977	510822.782	5693911.517	Flushcore (Geodoff)	10.00	
RGD-77/MK49	1/06/1977	506879.490	5694429.860	Flushcore (Ge[illegible]	10.00	Macrofauna report
RGD-77/MK61	?	500595.550	5724237.880	?	10.00	
RGD-77/MK62	?	503090.100	5728996.580	?	10.00	
RGD-78/H10	1/06/1978	486784.760	5672971.810	Vibrocore (Zenkovitz)	1.29	
RGD-78/H11	1/06/1978	486784.760	5672971.810	Vibrocore (Zenkovitz)	0.96	
RGD-78/H12	1/06/1978	480397.010	5672127.230	Vibrocore (Zenkovitz)	1.00	
RGD-78/H13	1/06/1978	480397.010	5672127.230	Vibrocore (Zenkovitz)	1.00	
RGD-78/H14	1/06/1978	477561.150	5671644.550	Vibrocore (Zenkovitz)	1.81	Pollen analysis
RGD-78/H15	1/06/1978	470037.910	5673073.100	Vibrocore (Zenkovitz)	1.63	
RGD-78/H16	1/06/1978	469979.880	5673104.330	Vibrocore (Zenkovitz)	3.20	
RGD-78/H17	1/06/1978	488255.390	5696446.810	Vibrocore (Zenkovitz)	0.10	
RGD-78/H5	1/06/1978	476757.970	5687125.510	Vibrocore (Zenkovitz)	0.15	Pollen analysis
RGD-78/H6	1/06/1978	484974.290	5677641.550	Vibrocore (Zenkovitz)	3.90	Pollen analysis
RGD-78/H7	1/06/1978	486773.550	5676153.750	Vibrocore (Zenkovitz)	3.82	Pollen analysis
RGD-78/H8	1/06/1978	481318.750	5680063.200	Vibrocore (Zenkovitz)	3.56	Pollen analysis
RGD-78/H9	1/06/1978	488088.450	5674482.340	Vibrocore (Zenkovitz)	2.35	Pollen analysis
RGD-78/GD15	1/11/1978	484726.977	5724230.042	Straight drilling (Geodoff)	3.00	
RGD-79/H29	1/04/1979	504496.094	5701779.831	Vibrocore (Zenkovitz)	4.00	
RGD-79/H32	1/04/1979	499267.470	5706875.350	Vibrocore (Zenkovitz)	0.65	
RGD-N1262/B1	28/06/1980	486088.430	5723299.270	?	59.60	
RGD-80/MK123	?	488479.290	5751964.180	?	8.00	
RGD-80/MK124	?	464413.940	5750470.740	?	6.30	
RGD-80/MK125	18/08/1980	465445.000	5733624.840	?	10.00	
RGD-80/MK126	18/08/1980	453835.620	5724448.790	Flushcore (Geodoff)	7.80	Macrofauna report
RGD-80/MK127	?	442183.360	5715237.620	?	8.00	
RGD-80/MK128	?	442106.590	5696638.500	?	5.00	
RGD-80/MK130	20/08/1980	453532.570	5706037.370	Flushcore (Ge[illegible]	10.00	Macrofauna report
RGD-80/MK131	20/08/1980	465500.080	5696519.150	Flushcore (Geodoff)	8.00	
RGD-80/MK132	25/08/1980	499903.240	5687165.360	Flushcore (Geod[illegible]	7.00	
RGD-80/MK133	26/08/1980	487960.840	5677973.490	Flushcore (Geodoff)	10.00	
RGD-80/MK136	26/08/1980	465084.590	5678078.240	Flushcore (Geod[illegible]	6.00	
RGD-80/GD138	28/08/1980	487985.460	5696663.700	Flushcore (Geodoff)	4.20	
RGD-80/GD139	28/08/1980	499460.070	5705330.640	Flushcore (Geod[illegible]	6.00	
RGD-80/GD140	28/08/1980	488490.474	5714920.810	Flushcore (Geodoff)	8.00	
RGD-80/GD141	28/08/1980	476533.683	5705631.941	Flushcore (Geod[illegible]	6.00	
RGD-80/GD142	29/08/1980	477062.085	5724351.716	Flushcore (Geodoff)	7.00	
RGD-81/MK60	4/08/1981	471454.768	5724781.932	Flushcore (Geod[illegible]	10.00	
RGD-81/MK71	?	447008.960	5694329.760	?	10.00	
RGD-81/MK72	6/08/1981	454320.043	5701395.882	Flushcore (Geodoff)	10.00	
RGD-81/MK73	6/08/1981	469548.884	5717718.018	Flushcore (Geodoff)	10.00	
RGD-82/MK180	24/08/1982	470172.022	5709187.293	Flushcore (Geodoff)	10.00	
RGD-47/E19-1	8/10/1986	518803.600	5704654.834	Straight drilling	20.60	

ID	Date	X ED50	Y ED50	Type	Core length (m)	Extras
RGD-87/MK136	17/06/1987	495395.835	5714520.563	Flushcore (Geodoff)	7.00	
RGD-87/MK137	17/06/1987	502087.547	5711982.495	Flushcore (Geodoff)	10.00	
RGD-87/MK139	18/06/1987	501694.829	5705788.123	Flushcore (Geodoff)	10.00	
RGD-87/MK140	18/06/1987	508392.595	5706137.692	Flushcore (Geodoff)	6.00	
RGD-87/MK266	16/09/1987	471264.037	5739149.564	Flushcore (Geodoff)	8.00	
TB01	21/09/1976	500000.000	5696285.000	Vibrocore	4.80	
TB02	21/09/1976	500000.000	5694436.000	Vibrocore	3.85	
TB03	21/09/1976	500000.000	5692565.000	Vibrocore	3.93	
TB04	21/09/1976	500000.000	5690709.000	Vibrocore	4.45	
TB05	21/09/1976	500000.000	5688868.000	Vibrocore	4.74	
TB06	21/09/1976	500000.000	5687020.000	Vibrocore	3.75	
TB08	21/09/1976	500000.000	5683328.000	Vibrocore	4.50	
TB09	21/09/1976	500000.000	5681457.000	Vibrocore	3.20	
TB10	28/09/1976	501163.000	5696285.000	Vibrocore	5.00	
TB11	28/09/1976	501163.000	5694436.000	Vibrocore	5.00	
TB12	28/09/1976	501163.000	5692565.000	Vibrocore	4.62	
TB13	28/09/1976	501163.000	5690709.000	Vibrocore	5.10	
TB14	28/09/1976	501163.000	5688868.000	Vibrocore	4.43	
TB15	28/09/1976	501163.000	5687020.000	Vibrocore	2.25	
TB19	20/09/1976	502327.000	5696285.000	Vibrocore	4.87	
TB20	20/09/1976	502327.000	5694436.000	Vibrocore	4.45	
TB21	20/09/1976	502327.000	5692565.000	Vibrocore	4.68	
TB22	21/09/1976	502327.000	5690709.000	Vibrocore	4.66	
TB23	21/09/1976	502327.000	5688868.000	Vibrocore	4.30	
TB24	21/09/1976	502327.000	5687020.000	Vibrocore	4.00	
TB25	21/09/1976	502327.000	5685162.000	Vibrocore	3.05	
TB27	21/09/1976	503490.000	5696285.000	Vibrocore	4.00	
TB28	27/09/1976	503490.000	5694436.000	Vibrocore	4.10	
TB29	27/09/1976	503490.000	5692565.000	Vibrocore	5.05	
TB30	27/09/1976	503490.000	5690709.000	Vibrocore	5.10	
TB31	27/09/1976	503490.000	5688868.000	Vibrocore	4.55	
TB32	27/09/1976	503490.000	5687020.000	Vibrocore	4.95	
TB33	27/09/1976	503490.000	5685162.000	Vibrocore	4.68	
TB34	27/09/1976	503490.000	5683328.000	Vibrocore	3.00	
TB35	20/09/1976	504653.000	5696285.000	Vibrocore	3.80	
TB36	20/09/1976	504653.000	5694436.000	Vibrocore	3.03	
TB37	20/09/1976	504653.000	5692565.000	Vibrocore	3.44	
TB38	20/09/1976	504653.000	5690709.000	Vibrocore	3.20	
TB39	20/09/1976	504653.000	5688868.000	Vibrocore	3.37	
TB40	20/09/1976	504653.000	5687020.000	Vibrocore	4.18	
TB41	17/09/1976	504653.000	5685162.000	Vibrocore	4.70	
TB42	17/09/1976	504653.000	5683328.000	Vibrocore	?	
TB43	24/09/1976	505816.000	5696285.000	Vibrocore	3.97	
TB44	27/09/1976	505816.000	5694436.000	Vibrocore	4.60	
TB45	27/09/1976	505816.000	5692565.000	Vibrocore	5.00	
TB46	27/09/1976	505816.000	5690709.000	Vibrocore	4.75	
TB47	27/09/1976	505816.000	5688868.000	Vibrocore	4.52	
TB48	27/09/1976	505816.000	5687020.000	Vibrocore	4.70	
TB49	27/09/1976	505816.000	5685162.000	Vibrocore	4.65	
TB50	17/09/1976	506980.000	5696285.000	Vibrocore	4.80	
TB51	17/09/1976	506980.000	5694436.000	Vibrocore	4.22	
TB52	17/09/1976	506980.000	5692565.000	Vibrocore	3.50	
TB53	17/09/1976	506980.000	5690709.000	Vibrocore	3.12	
TB54	17/09/1976	506980.000	5688868.000	Vibrocore	4.60	
TB55	17/09/1976	506980.000	5687020.000	Vibrocore	4.60	
TB56	15/09/1976	506980.000	5685162.000	Vibrocore	5.00	
TB57	24/09/1976	508143.000	5696285.000	Vibrocore	4.55	
TB58	24/09/1976	508143.000	5694436.000	Vibrocore	4.41	
TB59	24/09/1976	508143.000	5692565.000	Vibrocore	4.00	
TB60	24/09/1976	508143.000	5690709.000	Vibrocore	3.74	
TB61	24/09/1976	508143.000	5688868.000	Vibrocore	4.54	
TB62	24/09/1976	508143.000	5687020.000	Vibrocore	4.59	
TB64	6/09/1976	509306.000	5696285.000	Vibrocore	4.70	
TB65	6/09/1976	509306.000	5694436.000	Vibrocore	4.62	
TB66	6/09/1976	509306.000	5692565.000	Vibrocore	5.18	
TB67	6/09/1976	509306.000	5690709.000	Vibrocore	3.73	
TB68	6/09/1976	509306.000	5688868.000	Vibrocore	3.34	
TB69	15/09/1976	509306.000	5687020.000	Vibrocore	4.45	
TB70	6/09/1976	510469.000	5696285.000	Vibrocore	3.48	
TB71	6/09/1976	510469.000	5694436.000	Vibrocore	3.53	
TB72	6/09/1976	510469.000	5692565.000	Vibrocore	3.23	
TB73	31/08/1976	510469.000	5690709.000	Vibrocore	2.74	
TB74	1/09/1976	510469.000	5688868.000	Vibrocore	2.80	
TB75	15/09/1976	510469.000	5687020.000	Vibrocore	4.15	
TB76	8/09/1976	511633.000	5696285.000	Vibrocore	4.29	
TB77	8/09/1976	511633.000	5694436.000	Vibrocore	4.58	
TB78	7/09/1976	511633.000	5692565.000	Vibrocore	4.15	
TB79	1/09/1976	511633.000	5690709.000	Vibrocore	4.45	
TB80	1/09/1976	511633.000	5688868.000	Vibrocore	3.72	
TB81	15/09/1976	511633.000	5687020.000	Vibrocore	4.75	
TB82	8/09/1976	512796.000	5696285.000	Vibrocore	4.73	
TB83	8/09/1976	512796.000	5694436.000	Vibrocore	4.57	
TB84	8/09/1976	512796.000	5692565.000	Vibrocore	3.25	
TB85	8/09/1976	512796.000	5690709.000	Vibrocore	2.46	
TB86	8/09/1976	512796.000	5688868.000	Vibrocore	3.48	
TB87	15/09/1976	513959.000	5696285.000	Vibrocore	4.55	
TB88	13/09/1976	513959.000	5694436.000	Vibrocore	4.30	
TB89	13/09/1976	513959.000	5692565.000	Vibrocore	4.30	
TB90	13/09/1976	513959.000	5690709.000	Vibrocore	3.49	
TB91	7/09/1976	513959.000	5688868.000	Vibrocore	4.30	
TB92	13/09/1976	515122.000	5696285.000	Vibrocore	3.60	
TB93	13/09/1976	515122.000	5694436.000	Vibrocore	4.65	
TB94	14/09/1976	515122.000	5692565.000	Vibrocore	2.44	
TB95	13/09/1976	515122.000	5690709.000	Vibrocore	4.45	

ID	Date	X ED50	Y ED50	Type	Core length (m)	Extras
TB96	7/09/1976	515122.000	5688868.000	Vibrocore	4.45	
TB97	14/09/1976	516286.000	5696285.000	Vibrocore	4.45	
TB98	14/09/1976	516286.000	5694436.000	Vibrocore	4.87	
TB99	13/09/1976	516286.000	5692565.000	Vibrocore	3.10	
TB100	13/09/1976	516286.000	5690709.000	Vibrocore	5.00	
TB101	13/09/1976	516286.000	5688868.000	Vibrocore	4.00	
TB102	14/09/1976	517449.000	5696285.000	Vibrocore	4.00	
TB103	14/09/1976	517449.000	5694436.000	Vibrocore	4.60	
TB104	14/09/1976	517449.000	5692565.000	Vibrocore	4.03	
TB105	14/09/1976	517449.000	5690709.000	Vibrocore	3.39	
TB106	14/09/1976	517449.000	5688868.000	Vibrocore	5.00	
TB107	14/09/1976	518612.000	5696285.000	Vibrocore	4.50	
TB108	14/09/1976	518612.000	5694436.000	Vibrocore	3.88	
TB109	14/09/1976	518612.000	5692565.000	Vibrocore	4.54	
TB110	14/09/1976	518612.000	5690709.000	Vibrocore	3.32	
TB112	22/09/1976	519775.000	5696285.000	Vibrocore	5.08	
TB113	22/09/1976	519775.000	5694436.000	Vibrocore	2.40	
TB114	23/09/1976	519775.000	5692565.000	Vibrocore	3.65	
TB115	23/09/1976	519775.000	5690709.000	Vibrocore	4.70	
TB116	22/09/1976	520939.000	5696285.000	Vibrocore	4.64	
TB117	22/09/1976	520939.000	5694436.000	Vibrocore	4.81	
TB118	23/09/1976	520939.000	5692565.000	Vibrocore	4.85	
TB119	23/09/1976	520939.000	5690709.000	Vibrocore	5.15	
TB120	22/09/1976	522102.000	5696285.000	Vibrocore	4.14	
TB121	23/09/1976	522102.000	5694436.000	Vibrocore	4.00	
TB122	23/09/1976	522102.000	5692565.000	Vibrocore	5.10	
TB123	23/09/1976	522102.000	5690709.000	Vibrocore	3.40	
TB124	22/09/1976	523265.000	5696285.000	Vibrocore	4.84	
TB125	23/09/1976	523265.000	5694436.000	Vibrocore	5.15	
TB126	23/09/1976	523265.000	5692565.000	Vibrocore	3.85	
TB128	22/09/1976	524428.000	5696285.000	Vibrocore	4.70	
TB129	23/09/1976	524428.000	5694436.000	Vibrocore	5.20	
TB130	23/09/1976	524428.000	5692565.000	Vibrocore	4.00	
TB131	22/09/1976	525592.000	5696285.000	Vibrocore	5.01	
TB132	23/09/1976	525592.000	5694436.000	Vibrocore	5.00	
TB133	24/09/1976	525592.000	5692565.000	Vibrocore	3.15	
TB134	6/09/1976	510186.000	5693509.000	Vibrocore	4.70	
TB135	7/09/1976	511077.000	5692584.000	Vibrocore	3.54	
TB136	7/09/1976	511968.000	5691659.000	Vibrocore	4.01	
TB137	15/09/1976	513927.000	5689656.000	Vibrocore	4.50	
TB138	6/09/1976	510437.000	5693664.000	Vibrocore	3.90	
TB139	15/09/1976	511794.000	5691658.000	Vibrocore	3.92	
TB140	20/09/1976	513286.000	5690735.000	Vibrocore	3.12	
TB141	15/09/1976	514139.000	5689842.000	Vibrocore	5.13	
TB142	15/09/1976	514720.000	5689473.000	Vibrocore	4.12	
TB250	4/10/1984	498856.003	5696283.019	Vibrocore (Zenkovitz)	4.94	Photos
TB251	4/10/1984	498823.968	5694421.110	Vibrocore (Zenkovitz)	4.69	Photos
TB252	4/10/1984	498824.971	5692579.105	Vibrocore (Zenkovitz)	3.73	Photos
TB253	9/10/1984	498849.022	5690751.113	Vibrocore (Zenkovitz)	4.69	Photos
TB254	10/10/1984	498850.029	5688880.092	Vibrocore (Zenkovitz)	4.64	Photos
TB255	10/10/1984	498844.001	5687011.081	Vibrocore (Zenkovitz)	4.95	Photos
TB256	3/10/1984	498836.027	5685184.113	Vibrocore (Zenkovitz)	3.50	Photos
TB257	3/10/1984	498841.011	5683335.016	Vibrocore (Zenkovitz)	4.70	Photos
TB258	3/10/1984	498825.975	5681455.013	Vibrocore (Zenkovitz)	3.00	Photos
TB259	10/10/1984	498831.029	5679606.038	Vibrocore (Zenkovitz)	2.47	Photos
TB260	4/10/1984	497701.982	5696305.116	Vibrocore (Zenkovitz)	3.96	Photos
TB261	4/10/1984	497672.996	5694426.086	Vibrocore (Zenkovitz)	4.35	Photos
TB262	10/10/1984	497685.972	5692588.079	Vibrocore (Zenkovitz)	2.12	Photos
TB263	9/10/1984	497691.014	5690731.063	Vibrocore (Zenkovitz)	4.83	Photos
TB264	10/10/1984	497670.981	5688859.052	Vibrocore (Zenkovitz)	5.05	Photos
TB265	10/10/1984	497673.031	5687011.056	Vibrocore (Zenkovitz)	4.58	Photos
TB266	3/10/1984	497664.981	5685168.076	Vibrocore (Zenkovitz)	4.00	Photos
TB267	3/10/1984	497671.980	5683317.086	Vibrocore (Zenkovitz)	4.80	Photos
TB268	3/10/1984	497680.028	5681458.094	Vibrocore (Zenkovitz)	3.60	Photos
TB269	3/10/1984	497688.024	5679623.017	Vibrocore (Zenkovitz)	3.00	Photos
TB270	4/10/1984	496526.036	5696286.119	Vibrocore (Zenkovitz)	3.00	Photos
TB271	4/10/1984	496539.978	5694439.094	Vibrocore (Zenkovitz)	4.41	Photos
TB272	10/10/1984	496515.014	5692568.080	Vibrocore (Zenkovitz)	2.00	Photos
TB273	9/10/1984	496524.986	5690706.055	Vibrocore (Zenkovitz)	0.64	Photos
TB274	10/10/1984	496523.004	5688866.064	Vibrocore (Zenkovitz)	3.73	Photos
TB275	13/08/1986	512429.019	5698558.093	Vibrocore (Zenkovitz)	4.75	Photos
TB276	13/08/1986	512292.971	5699087.031	Vibrocore (Zenkovitz)	3.28	Photos
TB277	13/08/1986	512700.991	5701850.018	Vibrocore (Zenkovitz)	4.62	Photos
TB278	13/08/1986	510665.005	5703465.100	Vibrocore (Zenkovitz)	4.03	Photos
TB279	13/08/1986	508833.998	5701321.092	Vibrocore (Zenkovitz)	4.00	Photos
TB280	12/08/1986	508119.993	5698127.093	Vibrocore (Zenkovitz)	4.20	Photos
TB281	12/08/1986	506778.975	5698592.028	Vibrocore (Zenkovitz)	4.27	Photos
TB282	12/08/1986	505276.033	5699623.113	Vibrocore (Zenkovitz)	3.00	Photos
TB283	13/08/1986	505588.996	5703138.120	Vibrocore (Zenkovitz)	4.00	Photos
TB284	12/08/1986	503784.977	5701008.086	Vibrocore (Zenkovitz)	3.54	Photos
TB285	22/08/1986	502321.015	5701855.126	Vibrocore (Zenkovitz)	1.37	Photos
TB286	21/08/1986	499977.015	5702883.031	Vibrocore (Zenkovitz)	3.52	Photos
TB287	21/08/1986	497776.031	5698572.042	Vibrocore (Zenkovitz)	4.52	Photos
TB288	21/08/1986	498557.023	5702883.039	Vibrocore (Zenkovitz)	3.83	Photos
TB289	9/08/1986	496519.973	5687021.074	Vibrocore (Zenkovitz)	2.77	Photos
TB290	15/08/1986	496530.993	5683335.101	Vibrocore (Zenkovitz)	3.70	Photos
TB291	14/08/1986	496515.036	5681452.102	Vibrocore (Zenkovitz)	4.28	Photos
TB292	14/08/1986	496520.029	5679611.020	Vibrocore (Zenkovitz)	2.60	Photos
TB293	26/09/1986	495364.972	5705551.025	Vibrocore (Zenkovitz)	3.40	Photos
TB294	21/08/1986	495382.989	5701844.029	Vibrocore (Zenkovitz)	4.46	Photos
TB295	21/08/1986	495747.990	5699683.052	Vibrocore (Zenkovitz)	1.28	Photos
TB296	24/08/1986	495392.013	5696266.020	Vibrocore (Zenkovitz)	0.98	Photos
TB297	24/08/1986	495403.999	5694402.089	Vibrocore (Zenkovitz)	4.18	Photos
TB298	11/08/1986	495355.016	5688845.105	Vibrocore (Zenkovitz)	3.51	Photos

ID	Date	X ED50	Y ED50	Type	Core length (m)	Extras
TB299	10/08/1986	495312.992	5687026.064	Vibrocore (Zenkovitz)	3.18	Photos
TB300	15/08/1986	495328.028	5683347.090	Vibrocore (Zenkovitz)	4.12	Photos
TB301	14/08/1986	495324.967	5681482.098	Vibrocore (Zenkovitz)	4.50	Photos
TB302	14/08/1986	495386.024	5679619.054	Vibrocore (Zenkovitz)	4.94	Photos
TB303	14/08/1986	495345.022	5677759.112	Vibrocore (Zenkovitz)	3.73	Photos
TB304	21/08/1986	494927.001	5700457.084	Vibrocore (Zenkovitz)	2.10	Photos
TB305	21/08/1986	494553.004	5698126.117	Vibrocore (Zenkovitz)	4.18	Photos
TB306	26/09/1986	494238.999	5692612.111	Vibrocore (Zenkovitz)	0.69	Photos
TB307	10/08/1986	494162.021	5687027.047	Vibrocore (Zenkovitz)	2.87	Photos
TB308	25/08/1986	494182.994	5685161.016	Vibrocore (Zenkovitz)	4.80	Photos
TB309	15/08/1986	494207.984	5683317.116	Vibrocore (Zenkovitz)	3.50	Photos
TB310	14/08/1986	494147.972	5681468.093	Vibrocore (Zenkovitz)	1.25	Photos
TB311	16/08/1986	494164.033	5679617.097	Vibrocore (Zenkovitz)	3.28	Photos
TB312	25/08/1986	494183.026	5677755.093	Vibrocore (Zenkovitz)	1.94	Photos
TB313	27/09/1986	493051.023	5705590.072	Vibrocore (Zenkovitz)	0.69	Photos
TB314	22/08/1986	493042.029	5698143.110	Vibrocore (Zenkovitz)	3.54	Photos
TB315	26/09/1986	493025.015	5692586.067	Vibrocore (Zenkovitz)	4.00	Photos
TB316	10/08/1986	493028.022	5688823.104	Vibrocore (Zenkovitz)	2.72	Photos
TB317	15/08/1986	493157.003	5683328.108	Vibrocore (Zenkovitz)	3.89	Photos
TB318	14/08/1986	493033.031	5681447.044	Vibrocore (Zenkovitz)	5.00	Photos
TB319	19/09/1986	493032.986	5677718.069	Vibrocore (Zenkovitz)	3.96	Photos
TB320	19/09/1986	492977.972	5675844.046	Vibrocore (Zenkovitz)	3.95	Photos
TB321	26/09/1986	491915.036	5692547.022	Vibrocore (Zenkovitz)	1.96	Photos
TB322	10/08/1986	492288.976	5687321.048	Vibrocore (Zenkovitz)	3.16	Photos
TB323	15/08/1986	491882.973	5683280.060	Vibrocore (Zenkovitz)	3.00	Photos
TB324	14/08/1986	491354.031	5681857.109	Vibrocore (Zenkovitz)	4.92	Photos
TB325	17/08/1986	491438.002	5678599.069	Vibrocore (Zenkovitz)	4.49	Photos
TB326	5/09/1986	491822.992	5675873.024	Vibrocore (Zenkovitz)	3.44	Photos
TB327	27/09/1986	490724.994	5705573.030	Vibrocore (Zenkovitz)	3.90	Photos
TB328	22/08/1986	490764.988	5698153.110	Vibrocore (Zenkovitz)	1.30	Photos
TB329	24/08/1986	490721.004	5694419.110	Vibrocore (Zenkovitz)	3.42	Photos
TB330	26/09/1986	490719.982	5690680.048	Vibrocore (Zenkovitz)	1.10	Photos
TB331	10/08/1986	490674.002	5688812.110	Vibrocore (Zenkovitz)	3.20	Photos
TB332	21/09/1986	489573.026	5681431.075	Vibrocore (Zenkovitz)	3.63	Photos
TB333	12/09/1986	490710.002	5675873.048	Vibrocore (Zenkovitz)	5.00	Photos
TB334	19/09/1986	490699.978	5674401.102	Vibrocore (Zenkovitz)	3.74	Photos
TB335	11/08/1986	489536.975	5687043.068	Vibrocore (Zenkovitz)	3.74	Photos
TB336	18/08/1986	490066.986	5685399.080	Vibrocore (Zenkovitz)	4.08	Photos
TB337	14/08/1986	489999.009	5682451.017	Vibrocore (Zenkovitz)	4.30	Photos
TB338	14/08/1986	489527.020	5678195.068	Vibrocore (Zenkovitz)	4.66	Photos
TB339	16/09/1986	489520.026	5675919.068	Vibrocore (Zenkovitz)	3.76	Photos
TB340	5/09/1986	489543.007	5674022.014	Vibrocore (Zenkovitz)	2.14	Photos
TB341	24/09/1986	489049.029	5704253.056	Vibrocore (Zenkovitz)	0.86	Photos
TB342	24/09/1986	488087.010	5703593.067	Vibrocore (Zenkovitz)	0.32	Photos
TB343	24/09/1986	487795.977	5702443.030	Vibrocore (Zenkovitz)	0.38	Photos
TB344	22/08/1986	487613.969	5701723.029	Vibrocore (Zenkovitz)	1.32	Photos
TB345	24/08/1986	488400.980	5694431.018	Vibrocore (Zenkovitz)	0.87	Photos
TB346	11/08/1986	488392.014	5687022.095	Vibrocore (Zenkovitz)	3.50	Photos
TB347	15/08/1986	489053.004	5684044.061	Vibrocore (Zenkovitz)	3.75	Photos
TB348	17/08/1986	488910.025	5679474.068	Vibrocore (Zenkovitz)	4.12	Photos
TB349	4/09/1986	488389.021	5675915.073	Vibrocore (Zenkovitz)	3.72	Photos
TB350	5/09/1986	488388.975	5674027.073	Vibrocore (Zenkovitz)	2.55	Photos
TB351	18/08/1986	487234.970	5685192.112	Vibrocore (Zenkovitz)	4.21	Photos
TB352	18/08/1986	487425.015	5682796.043	Vibrocore (Zenkovitz)	4.00	Photos
TB353	18/08/1986	487045.967	5682049.103	Vibrocore (Zenkovitz)	4.35	Photos
TB354	18/08/1986	487599.011	5681637.023	Vibrocore (Zenkovitz)	4.45	Photos
TB355	17/08/1986	487801.995	5679501.072	Vibrocore (Zenkovitz)	4.50	Photos
TB356	4/09/1986	487205.023	5675912.017	Vibrocore (Zenkovitz)	3.48	Photos
TB357	5/09/1986	487202.020	5674049.044	Vibrocore (Zenkovitz)	3.87	Photos
TB358	19/09/1986	487431.016	5672368.105	Vibrocore (Zenkovitz)	2.68	Photos
TB359	24/09/1986	486492.000	5701020.029	Vibrocore (Zenkovitz)	0.88	Photos
TB360	22/09/1986	486108.040	5698150.087	Vibrocore (Zenkovitz)	0.62	Photos
TB361	22/09/1986	486099.003	5694452.052	Vibrocore (Zenkovitz)	3.82	Photos
TB362	24/09/1986	486071.023	5690673.015	Vibrocore (Zenkovitz)	1.08	Photos
TB363	20/08/1986	486560.986	5687041.072	Vibrocore (Zenkovitz)	3.21	Photos
TB364	18/08/1986	486028.023	5685240.107	Vibrocore (Zenkovitz)	3.53	Photos
TB365	25/08/1986	486034.039	5683371.076	Vibrocore (Zenkovitz)	4.66	Photos
TB366	25/08/1986	486014.978	5681459.081	Vibrocore (Zenkovitz)	3.94	Photos
TB367	28/08/1986	486033.029	5677742.050	Vibrocore (Zenkovitz)	4.88	Photos
TB368	5/09/1986	486019.985	5674054.039	Vibrocore (Zenkovitz)	3.59	Photos
TB369	15/09/1986	485507.028	5672178.036	Vibrocore (Zenkovitz)	3.28	Photos
TB370	24/09/1986	484933.965	5700106.026	Vibrocore (Zenkovitz)	0.84	Photos
TB371	22/09/1986	484306.995	5695001.116	Vibrocore (Zenkovitz)	0.66	Photos
TB372	20/08/1986	484920.002	5687054.020	Vibrocore (Zenkovitz)	3.31	Photos
TB373	25/08/1986	484897.007	5683369.099	Vibrocore (Zenkovitz)	2.00	Photos
TB374	25/08/1986	484887.008	5681481.101	Vibrocore (Zenkovitz)	3.43	Photos
TB375	29/08/1986	485183.002	5678605.106	Vibrocore (Zenkovitz)	4.06	Photos
TB376	4/09/1986	484876.008	5675893.040	Vibrocore (Zenkovitz)	3.30	Photos
TB377	5/09/1986	484857.010	5674056.024	Vibrocore (Zenkovitz)	3.35	Photos
TB378	6/09/1986	484853.001	5672187.053	Vibrocore (Zenkovitz)	3.62	Photos
TB379	6/09/1986	484880.032	5670768.057	Vibrocore (Zenkovitz)	4.00	Photos
TB380	20/08/1986	483733.970	5687029.096	Vibrocore (Zenkovitz)	2.48	Photos
TB381	22/09/1986	483716.007	5684421.019	Vibrocore (Zenkovitz)	4.07	Photos
TB382	31/08/1986	483709.016	5681452.038	Vibrocore (Zenkovitz)	3.54	Photos
TB383	31/08/1986	483733.972	5679657.017	Vibrocore (Zenkovitz)	3.67	Photos
TB384	29/08/1986	483739.018	5677783.106	Vibrocore (Zenkovitz)	3.84	Photos
TB385	5/09/1986	483699.009	5674085.059	Vibrocore (Zenkovitz)	3.50	Photos
TB386	6/09/1986	483672.022	5672198.032	Vibrocore (Zenkovitz)	3.57	Photos
TB387	6/09/1986	483697.993	5670330.081	Vibrocore (Zenkovitz)	4.46	Photos
TB388	23/09/1986	482590.979	5701863.055	Vibrocore (Zenkovitz)	1.56	Photos
TB389	23/09/1986	482649.008	5700046.058	Vibrocore (Zenkovitz)	0.64	Photos
TB390	23/09/1986	482621.007	5696318.043	Vibrocore (Zenkovitz)	2.20	Photos
TB391	22/09/1986	482624.973	5692622.080	Vibrocore (Zenkovitz)	0.77	Photos
TB392	20/08/1986	482545.986	5688935.097	Vibrocore (Zenkovitz)	1.72	Photos

ID	Date	X_ED50	Y_ED50	Type	Core length (m)	Extras
TB393	22/09/1986	482591.994	5685183.092	Vibrocore (Zenkovitz)	3.23	Photos
TB394	20/09/1986	482751.006	5683509.040	Vibrocore (Zenkovitz)	2.65	Photos
TB395	16/09/1986	482553.992	5681495.121	Vibrocore (Zenkovitz)	2.66	Photos
TB396	11/09/1986	482575.016	5679607.022	Vibrocore (Zenkovitz)	3.28	Photos
TB397	11/09/1986	482545.988	5677751.018	Vibrocore (Zenkovitz)	4.15	Photos
TB398	20/09/1986	482540.973	5673161.066	Vibrocore (Zenkovitz)	3.50	Photos
TB399	7/09/1986	482518.968	5670342.095	Vibrocore (Zenkovitz)	2.17	Photos
TB400	15/09/1986	482089.979	5668973.040	Vibrocore (Zenkovitz)	3.66	Photos
TB401	22/09/1986	481389.026	5685186.015	Vibrocore (Zenkovitz)	4.00	Photos
TB402	16/09/1986	481137.009	5681947.016	Vibrocore (Zenkovitz)	3.68	Photos
TB403	11/09/1986	481375.999	5679637.062	Vibrocore (Zenkovitz)	3.80	Photos
TB404	11/09/1986	481360.981	5677780.010	Vibrocore (Zenkovitz)	3.43	Photos
TB405	4/09/1986	481566.032	5675904.036	Vibrocore (Zenkovitz)	3.62	Photos
TB406	5/09/1986	481378.027	5674071.087	Vibrocore (Zenkovitz)	3.82	Photos
TB407	7/09/1986	481381.973	5672221.099	Vibrocore (Zenkovitz)	3.08	Photos
TB408	7/09/1986	481382.995	5670333.094	Vibrocore (Zenkovitz)	2.82	Photos
TB409	8/09/1986	481353.003	5668490.023	Vibrocore (Zenkovitz)	1.78	Photos
TB410	23/09/1986	480310.973	5700024.022	Vibrocore (Zenkovitz)	1.45	Photos
TB411	23/09/1986	480286.995	5696304.113	Vibrocore (Zenkovitz)	3.50	Photos
TB412	22/09/1986	480319.970	5692611.028	Vibrocore (Zenkovitz)	1.06	Photos
TB413	12/09/1986	480246.012	5688926.053	Vibrocore (Zenkovitz)	3.59	Photos
TB414	22/09/1986	479896.026	5685621.081	Vibrocore (Zenkovitz)	3.36	Photos
TB415	20/09/1986	479859.983	5682973.047	Vibrocore (Zenkovitz)	3.23	Photos
TB416	11/09/1986	480219.995	5679619.062	Vibrocore (Zenkovitz)	3.65	Photos
TB417	11/09/1986	480212.011	5677812.028	Vibrocore (Zenkovitz)	3.94	Photos
TB418	7/09/1986	480201.019	5670341.091	Vibrocore (Zenkovitz)	4.80	Photos
TB419	8/09/1986	479900.022	5668590.051	Vibrocore (Zenkovitz)	2.86	Photos
TB420	16/09/1986	478600.970	5683851.081	Vibrocore (Zenkovitz)	3.36	Photos
TB421	11/09/1986	479050.005	5674952.102	Vibrocore (Zenkovitz)	3.23	Photos
TB422	7/09/1986	479036.015	5673022.107	Vibrocore (Zenkovitz)	3.68	Photos
TB423	7/09/1986	479686.971	5670297.065	Vibrocore (Zenkovitz)	3.06	Photos
TB424	8/09/1986	479200.025	5669322.047	Vibrocore (Zenkovitz)	3.32	Photos
TB425	20/09/1986	478997.967	5667698.105	Vibrocore (Zenkovitz)	4.34	Photos
TB426	23/09/1986	477965.016	5700041.019	Vibrocore (Zenkovitz)	0.66	Photos
TB427	23/09/1986	477959.030	5696327.036	Vibrocore (Zenkovitz)	3.20	Photos
TB428	10/09/1986	477878.032	5673379.077	Vibrocore (Zenkovitz)	3.26	Photos
TB429	9/09/1986	477986.994	5673701.006	Vibrocore (Zenkovitz)	2.72	Photos
TB430	19/09/1986	477868.009	5671676.049	Vibrocore (Zenkovitz)	2.95	Photos
TB431	19/09/1986	476676.033	5668531.101	Vibrocore (Zenkovitz)	3.61	Photos
TB432	7/09/1986	478074.024	5669265.025	Vibrocore (Zenkovitz)	3.52	Photos
TB433	8/09/1986	477872.988	5666649.023	Vibrocore (Zenkovitz)	3.66	Photos
TB434	10/09/1986	476713.037	5677817.113	Vibrocore (Zenkovitz)	4.21	Photos
TB435	10/09/1986	476712.970	5674938.084	Vibrocore (Zenkovitz)	4.18	Photos
TB436	9/09/1986	476312.975	5672407.102	Vibrocore (Zenkovitz)	4.25	Photos
TB437	8/09/1986	476701.973	5666670.116	Vibrocore (Zenkovitz)	4.72	Photos
TB438	10/09/1986	475938.988	5678152.111	Vibrocore (Zenkovitz)	4.84	Photos
TB439	10/09/1986	475812.016	5677528.037	Vibrocore (Zenkovitz)	4.32	Photos
TB440	10/09/1986	475595.021	5675922.067	Vibrocore (Zenkovitz)	4.69	Photos
TB441	10/09/1986	475625.978	5674800.023	Vibrocore (Zenkovitz)	3.84	Photos
TB442	8/09/1986	475522.982	5669178.051	Vibrocore (Zenkovitz)	4.15	Photos
TB443	8/09/1986	475517.020	5666715.118	Vibrocore (Zenkovitz)	3.00	Photos
TB444	21/09/1986	475532.970	5665807.017	Vibrocore (Zenkovitz)	1.87	Photos
TB445	10/09/1986	474380.989	5676857.067	Vibrocore (Zenkovitz)	3.34	Photos
TB446	20/09/1986	474323.009	5674917.055	Vibrocore (Zenkovitz)	3.68	Photos
TB447	10/09/1986	474362.006	5674073.101	Vibrocore (Zenkovitz)	3.55	Photos
TB448	9/09/1986	474797.028	5673085.055	Vibrocore (Zenkovitz)	3.65	Photos
TB449	9/09/1986	474367.020	5670401.012	Vibrocore (Zenkovitz)	3.50	Photos
TB450	8/09/1986	474360.013	5668526.043	Vibrocore (Zenkovitz)	4.23	Photos
TB451	8/09/1986	474371.996	5666685.016	Vibrocore (Zenkovitz)	3.46	Photos
TB452	21/09/1986	474369.976	5665833.049	Vibrocore (Zenkovitz)	3.54	Photos
TB453	10/09/1986	473229.035	5675994.075	Vibrocore (Zenkovitz)	3.30	Photos
TB454	9/09/1986	473195.969	5672267.117	Vibrocore (Zenkovitz)	3.38	Photos
TB455	9/09/1986	473209.972	5670376.017	Vibrocore (Zenkovitz)	4.00	Photos
TB456	20/09/1986	472021.972	5666705.084	Vibrocore (Zenkovitz)	3.09	Photos
TB457	21/09/1986	472990.984	5665757.051	Vibrocore (Zenkovitz)	3.74	Photos
TB458	9/09/1986	471576.985	5668461.095	Vibrocore (Zenkovitz)	1.50	Photos
TB459	21/09/1986	472051.997	5665861.058	Vibrocore (Zenkovitz)	4.40	Photos
TB460	27/09/1986	472054.022	5663020.083	Vibrocore (Zenkovitz)	3.95	Photos
TB461	8/09/1986	471196.032	5670374.045	Vibrocore (Zenkovitz)	3.38	Photos
TB462	9/09/1986	470947.035	5667940.047	Vibrocore (Zenkovitz)	1.07	Photos
TB463	21/09/1986	470363.994	5665452.047	Vibrocore (Zenkovitz)	4.40	Photos
TB464	27/09/1986	470770.004	5662553.034	Vibrocore (Zenkovitz)	3.56	Photos
TB465	28/09/1986	500821.000	5698727.000	Vibrocore (Zenkovitz)	4.35	
TB466	28/09/1986	505302.000	5698199.000	Vibrocore (Zenkovitz)	3.42	
TB467	28/09/1986	518203.000	5693380.000	Vibrocore (Zenkovitz)	4.78	
TB468	28/09/1986	517587.000	5691201.000	Vibrocore (Zenkovitz)	2.23	
GII192	10/06/1977	502448.000	5699867.000	Vibrocore (Zenkovitz)	3.40	
GII193	10/06/1977	501653.000	5699655.000	Vibrocore (Zenkovitz)	1.40	
B158	30/06/1977	492408.000	5689924.000	Vibrocore (Zenkovitz)	4.75	
B160a	?	?	?	Vibrocore (Zenkovitz)	2.30	
B65a	30/06/1977	509144.000	5694543.000	Vibrocore (Zenkovitz)	3.20	
B65ab	30/06/1977	509144.000	5694543.000	Vibrocore (Zenkovitz)	3.60	
B85a	30/06/1977	512709.000	5690967.000	Vibrocore (Zenkovitz)	2.20	
G212	22/07/1977	489985.000	5701050.000	Vibrocore (Zenkovitz)	3.55	
G214	22/07/1977	489378.000	5700748.000	Vibrocore (Zenkovitz)	4.15	
G215	22/07/1977	489675.000	5700341.000	Vibrocore (Zenkovitz)	4.70	
G216	22/07/1977	488969.000	5700542.000	Vibrocore (Zenkovitz)	5.30	
G218	22/07/1977	488402.000	5700190.000	Vibrocore (Zenkovitz)	1.30	
G220	22/07/1977	487889.000	5699937.000	Vibrocore (Zenkovitz)	3.20	
G221	22/07/1977	488154.000	5699540.000	Vibrocore (Zenkovitz)	2.00	
G222a	22/07/1977	487215.000	5699771.000	Vibrocore (Zenkovitz)	0.80	
G223	22/07/1977	487538.000	5699390.000	Vibrocore (Zenkovitz)	2.75	

ID	Date	X ED50	Y ED50	Type	Core length (m)	Extras
83A04	5/06/1905	476119.998	5670385.085	?	2.60	Macrofauna report
83A05	1983	474380.024	5672245.039	?	3.50	Macrofauna report
85A01	1985	479903.790	5666841.280	gestoken boring op strand	19.93	Gamma-log, RX-photos
85A02	1985	476764.796	5669416.928	Vibrocore (GEOMAREX test)	0.80	Gamma-log, RX-photos
BGD-RIG-Kwinte999A	25/02/1980	474224.692	5679815.942	Straight drilling	25.00	
DBGD-86/3/SWB	1/08/1986	503763.774	5684769.462	Straight drilling	10.00	Photos
DBGD-86/4SEWB	1/08/1986	508418.668	5686813.933	Straight drilling	11.00	Photos
DBGD-86/GR1	1/08/1986	494185.960	5679711.170	Straight drilling	80.00	Photos
DBGD-86/SB1	1/08/1986	489666.021	5675621.941	Straight drilling	20.00	Photos
BGD- 88/3/NWB	1/05/1988	475402.425	5670789.436	Straight drilling	19.00	Photos
DBGD-88/SB2	1/05/1988	491390.030	5676619.670	Straight drilling	25.50	Photos
Uitdiep-MiddelkerkeBank (=UiT	1/05/1988	481498.290	5681483.625	Straight drilling	19.00	Photos
BGD-Goote II 88/6	1/06/1988	490194.860	5700489.760	Straight drilling	80.00	
BGD-OSB 88/7	1/06/1988	486411.020	5681319.950	Straight drilling	45.00	Photos
BGD-THB 87/5	1/06/1988	497433.510	5709310.390	Straight drilling	50.00	Photos
Tr1ab	24/04/1991	483567.586	5684573.876	Vibrocore (Trilflip)	2.80	
Tr2	24/04/1991	483069.432	5684909.980	Vibrocore (Trilflip)	4.44	
Tr3	24/04/1991	482913.383	5684837.957	Vibrocore (Trilflip)	?	
Tr4	24/04/1991	482787.344	5685156.056	Vibrocore (Trilflip)	?	
Tr5	25/04/1991	482265.183	5685336.112	Vibrocore (Trilflip)	?	
Tr6	25/04/1991	482157.149	5685480.156	Vibrocore (Trilflip)	4.30	
Tr7	25/04/1991	482163.151	5685708.227	Vibrocore (Trilflip)	3.10	
Tr8	25/04/1991	481809.042	5686002.318	Vibrocore (Trilflip)	3.49	
Tr9	3/09/1991	484701.937	5687400.751	Vibrocore (Trilflip)	4.49	
Tr10	3/09/1991	484857.985	5687304.721	Vibrocore (Trilflip)	4.11	
Tr11	3/09/1991	485056.047	5687154.674	Vibrocore (Trilflip)	3.42	
Tr12	3/09/1991	485290.119	5687004.628	Vibrocore (Trilflip)	2.65	
Tr13	3/09/1991	485578.208	5686776.557	Vibrocore (Trilflip)	4.24	
Tr14	3/09/1991	484455.861	5687604.814	Vibrocore (Trilflip)	4.24	
Tr15	3/09/1991	484245.796	5687718.849	Vibrocore (Trilflip)	4.72	
Tr16	3/09/1991	483969.710	5687946.920	Vibrocore (Trilflip)	5.00	
Tr17	3/09/1991	483801.658	5688084.962	Vibrocore (Trilflip)	4.76	
Tr18	3/09/1991	481580.971	5680522.622	Vibrocore (Trilflip)	5.35	
Tr19	3/09/1991	481250.869	5680804.709	Vibrocore (Trilflip)	3.34	
Tr20	3/09/1991	480932.770	5681056.787	Vibrocore (Trilflip)	2.86	
Tr21	5/09/1991	480710.702	5681266.852	Vibrocore (Trilflip)	4.54	
Tr22	5/09/1991	480398.605	5681482.919	Vibrocore (Trilflip)	5.00	
Tr23	5/09/1991	480170.535	5681680.980	Vibrocore (Trilflip)	3.57	
Tr24	5/09/1991	479954.468	5681861.036	Vibrocore (Trilflip)	2.92	
Tr25	5/09/1991	479828.429	5681951.064	Vibrocore (Trilflip)	3.23	
Tr26	5/09/1991	479684.384	5682089.107	Vibrocore (Trilflip)	5.42	
Tr27	5/09/1991	479600.358	5682131.120	Vibrocore (Trilflip)	5.41	
Tr28	5/09/1991	483561.584	5684579.878	Vibrocore (Trilflip)	5.00	
Tr29	5/09/1991	483357.521	5684741.928	Vibrocore (Trilflip)	4.71	
Tr30	5/09/1991	483153.458	5684903.978	Vibrocore (Trilflip)	5.26	
Tr31	5/09/1991	483003.411	5685012.011	Vibrocore (Trilflip)	?	
Tr32	5/09/1991	482841.361	5685144.052	Vibrocore (Trilflip)	?	
Tr33	5/09/1991	482637.298	5685282.095	Vibrocore (Trilflip)	?	
Tr34	5/09/1991	482523.263	5685390.128	Vibrocore (Trilflip)	?	
Tr35	5/09/1991	482427.233	5685462.151	Vibrocore (Trilflip)	?	
Tr36	5/09/1991	482307.196	5685552.178	Vibrocore (Trilflip)	5.13	
Tr37	5/09/1991	482157.149	5685642.206	Vibrocore (Trilflip)	3.29	
Tr38	10/09/1991	480038.494	5678001.842	Vibrocore (Trilflip)	4.93	
Tr39	10/09/1991	479672.380	5678319.940	Vibrocore (Trilflip)	2.62	
Tr40	10/09/1991	479318.271	5678602.027	Vibrocore (Trilflip)	3.24	
Tr41	10/09/1991	479036.183	5678842.102	Vibrocore (Trilflip)	2.59	
Tr42	10/09/1991	478622.055	5679124.189	Vibrocore (Trilflip)	3.46	
Tr43	10/09/1991	478255.942	5679472.297	Vibrocore (Trilflip)	4.83	
Tr44	10/09/1991	477811.804	5679826.406	Vibrocore (Trilflip)	5.01	
Tr45b	10/09/1991	477361.665	5680204.523	Vibrocore (Trilflip)	3.56	
Tr46	11/09/1991	486478.487	5687922.912	Vibrocore (Trilflip)	2.73	
Tr47	11/09/1991	486220.407	5688114.972	Vibrocore (Trilflip)	3.98	
Tr48	11/09/1991	485998.338	5688241.011	Vibrocore (Trilflip)	3.32	
Tr49	11/09/1991	485794.275	5688379.053	Vibrocore (Trilflip)	4.41	
Tr50	11/09/1991	485650.230	5688499.091	Vibrocore (Trilflip)	5.57	
Tr51	11/09/1991	485404.154	5688691.150	Vibrocore (Trilflip)	5.32	
Tr52	11/09/1991	485308.125	5688793.182	Vibrocore (Trilflip)	5.20	
Tr53	11/09/1991	485050.045	5688967.235	Vibrocore (Trilflip)	5.44	
Tr54	12/09/1991	484335.824	5685810.258	Vibrocore (Trilflip)	5.56	
Tr55	12/09/1991	484035.731	5686014.322	Vibrocore (Trilflip)	5.63	
Tr56	12/09/1991	483759.645	5686236.390	Vibrocore (Trilflip)	2.05	
Tr57	12/09/1991	483567.586	5686398.440	Vibrocore (Trilflip)	2.59	
Tr58	12/09/1991	483423.541	5686530.481	Vibrocore (Trilflip)	2.72	
Tr59	12/09/1991	483321.510	5686644.517	Vibrocore (Trilflip)	3.12	
Tr60	12/09/1991	483135.452	5686770.556	Vibrocore (Trilflip)	4.65	
Tr61	12/09/1991	482865.369	5686956.613	Vibrocore (Trilflip)	3.87	
Tr90	1/10/1993	484785.963	5688907.217	Vibrocore	?	
Tr91	1/10/1993	484347.827	5683985.694	Vibrocore	3.37	
Tr92	1/10/1993	483783.653	5684435.833	Vibrocore	4.40	
Tr93	1/10/1993	482673.309	5685270.091	Vibrocore	?	
Tr94	1/10/1993	482721.324	5685234.080	Vibrocore	?	
Tr95	1/10/1993	481677.001	5686044.331	Vibrocore	3.78	
Tr96	1/10/1993	481430.925	5686248.394	Vibrocore	3.82	
Tr97	1/10/1993	481376.908	5680396.583	Vibrocore	4.31	
Tr98	1/10/1993	481130.832	5680576.639	Vibrocore	4.15	
Tr99	1/10/1993	480824.737	5680780.702	Vibrocore	3.52	
Tr100	1/10/1993	480476.629	5681014.774	Vibrocore	4.02	
Tr101	1/10/1993	479432.306	5681692.984	Vibrocore	4.23	
Tr102	1/10/1993	479060.191	5681927.056	Vibrocore	3.77	
Tr103	1/10/1993	476155.292	5678265.923	Vibrocore	4.23	
Tr104	1/10/1993	476671.452	5677905.812	Vibrocore	4.00	
Tr105	1/10/1993	477079.578	5677617.723	Vibrocore	4.15	
Tr106	1/10/1993	477307.648	5677467.676	Vibrocore	4.29	

ID	Date	X ED50	Y ED50	Type	Core length (m)	Extras
Tr107	1/10/1993	477877,825	5677059,550	Vibrocore	2,65	
Tr108	1/10/1993	478387,983	5676711,442	Vibrocore	3,07	
Tr109	1/10/1993	478826,118	5676405,348	Vibrocore	4,10	
Tr110	1/10/1993	479096,202	5676231,294	Vibrocore	4,05	
Tr111	1/10/1993	482631,296	5683439,525	Vibrocore	4,50	
Tr112	1/10/1993	482217,168	5683763,625	Vibrocore	4,40	
Tr113	1/10/1993	481953,086	5683973,690	Vibrocore	2,80	
Tr114	1/10/1993	481785,034	5684093,727	Vibrocore	3,58	
Tr115	1/10/1993	481628,986	5684231,770	Vibrocore	2,52	
Tr116	1/10/1993	481478,939	5684339,803	Vibrocore	3,88	
Tr117	1/10/1993	481388,912	5684411,826	Vibrocore	4,00	
Tr118	1/10/1993	481328,893	5684471,844	Vibrocore	4,28	
Tr119	1/10/1993	480986,787	5684747,930	Vibrocore	2,70	
Tr120	1/10/1993	480836,741	5684873,969	Vibrocore	3,58	
Tr121	1/10/1993	482721,324	5685228,078	Vibrocore	?	
Tr122	1/10/1993	482661,305	5685264,089	Vibrocore	?	
Tr123	1/10/1993	483663,616	5687676,836	Vibrocore	4,39	
Tr124	1/10/1993	483777,651	5687604,814	Vibrocore	?	
Tr125	1/10/1993	483903,690	5687520,788	Vibrocore	4,11	
Tr126	1/10/1993	484017,725	5687442,764	Vibrocore	?	
Tr127	1/10/1993	484173,774	5687334,730	Vibrocore	?	
Tr128	1/10/1993	484323,820	5687232,699	Vibrocore	?	
Tr129	1/10/1993	484479,868	5687124,665	Vibrocore	?	
Tr130	1/10/1993	484617,911	5687040,639	Vibrocore	4,29	
Tr131ab	1/10/1993	484893,996	5686860,583	Vibrocore	3,97	
Tr132	1/10/1993	475267,017	5676195,282	Vibrocore	3,00	
Tr133	1/10/1993	475681,145	5675919,197	Vibrocore	3,90	
Tr134	1/10/1993	475969,234	5675715,134	Vibrocore	2,64	
Tr135ab	1/10/1993	476521,405	5675337,017	Vibrocore	3,90	
Tr136	1/10/1993	477109,587	5674916,887	Vibrocore	3,82	
A	1/10/1993	485074,052	5689771,484	Vibrocore	1,75	
B	1/10/1993	486400,463	5688745,167	Vibrocore	3,41	
C	1/10/1993	484587,902	5689291,336	Vibrocore	3,69	
D	1/10/1993	485182,086	5688721,159	Vibrocore	3,45	
E	1/10/1993	483237,484	5683043,402	Vibrocore	3,90	
F	1/10/1993	485104,061	5689555,417	Vibrocore	1,79	
G	1/10/1993	481887,066	5686356,427	Vibrocore	3,91	
H	1/10/1993	483261,491	5684279,785	Vibrocore	3,24	
I	1/10/1993	482751,333	5687850,890	Vibrocore	3,80	
J	1/10/1993	482889,376	5687952,922	Vibrocore	?	
K	1/10/1993	483693,625	5687478,775	Vibrocore	?	
L	1/10/1993	484383,839	5686476,465	Vibrocore	4,35	
M	1/10/1993	484787,000	5686236,000	Vibrocore	4,30	
ODB-B1	12/08/1998	461574,760	5680746,070	Flushcore	25,00	
ODB-B2	1/09/1998	461464,260	5680739,490	Flushcore	10,00	
BKR-2/A B32	?	519921,000	5690139,037	Straight drilling	40,40	
79/06 (site 22)	?	482073,740	5776804,880	?	200,25	
BH 89/1	?	467836,000	5732651,000	?	36,14	
RIG-B1bis (DB1bis)	?	515712,310	5687652,900	?	70,00	
RIG-B2 (DB2)	?	513974,490	5687504,200	?	100,00	
RIG-B3 (DB3)	?	514936,310	5689561,500	?	65,00	
RIG-B4 (DB4)	?	513202,210	5690079,330	?	65,00	

Appendix B
Lithologs of some specific cores

LEGEND

- rootlet
- G glauconite
- oyster fragment
- shell
- shell fragment
- bioturbation
- plant remnant
- h humic debris
- v peat fragment
- sea-urchin debris
- gastropod
- gravel
- clay ball/lens
- sharp boundary
- gradual boundary
- erosional boundary
- clayey
- silty
- sandy

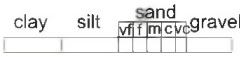

vf = very fine, f = fine, m = medium, c = coarse, vc = very coarse

clay

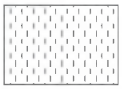

silt

alternation of peat, clay and sand layers

alternation of clay and sand layers

alternation of clay and silt layers

shell gravel

grain size of the main inclusion

clay lamina

coarsening downwards

coarsening upwards

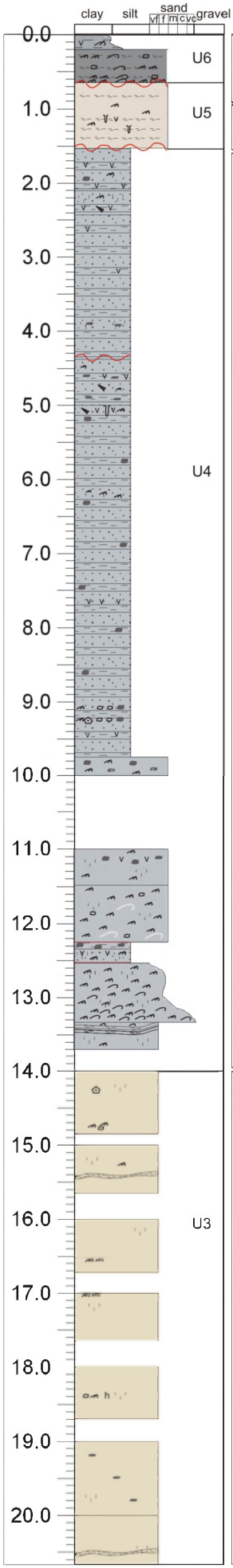

0.00-0.20: black-grey clay with a sporadic peat fragment, a thin sand layer with shell fragments; very fine shell grit spread over the clay.
0.20-0.65: dark grey to black fine sand with clayey zones (0.5 cm parallel even clay laminae). The clayey zones contain lots of shell fragments, small gravel and whole shells.

0.65-1.53: brown-grey fine sand with clayey beds with black clay lenses (more frequent from 1.10 downwards). Some shell fragments, peat detritus and sporadic bioturbation occur in the clay layers.

1.53-9.75: alternation of grey, very fine, silty sand layers and grey, thin clay layers. They contain lots of peat detritus between 1.52-2.08. The clay and peat detritus layers are mm thick and parallel even. A sporadic shell and clay chunk occurs. The sand layers contain shell fragments (a.o. hydrobia) from 2.08 downwards.

3.80-4.00: very fine, silty sand with thin clay lenses.

4.35-5.00: fine to medium sand with many laminae consisting of flat-rolled clay chunks. Little shell grit, shell fragments (a.o. hydrobia), and peat detritus.

5.00-9.75: fine sand with many clay laminae, containing some peat fragments and sand lenses. At the top bioturbation, some shells (a.o. hydrobia), and peat fragments.

7.65: lots of peat detritus

9.10 and 9.17: level with gravel and coarse grains, clay balls, shell and sea-urchin fragments.

9.75-10.00: grey, fine sand with some clay lenses, flat peaty clay chunks and shell fragments

11.00-12.25: grey, fine silty sand containing many shell fragments, and many irregular clay chunks and rolled peat fragments between 11.13-11.23. From 11.48 towards the base, more shell fragments (a.o. oyster) and some gravel occur.

12.25-12.53: grey, fine, silty sand with many clay layers consisting of clay chunks. Some shell fragments and many peat fragments occur as well.

12.53-13.33: grey, fine silty sand with lots of shell fragments and whole shells increasing downwards.

13.33-13.70: grey, very fine silty sand, with some silty clay lenses (layers) and whole shells at the top. Dispersed very fine shell grit.

14.00-35.10: grey-brown (beige) silty very fine sand with a sporadic (rust-brown oxidised) clay flaser. Some fine shell grit occurs, as well as occasional sea-urchin needles.
14.77: some shell fragments and gravel

16.55: lots of shell grit

17.00: lens with shell grit

18.40: black humic lens, few shell fragments, silex

19.00-20.00: very few shell fragments, some clay lenses

20.50: clay flasers

Core: GR1 (1/3)

Date: 08/1986
Location: Grote Rede
UTM position (ED50): E 494185.96 m
N 5679711.17 m
Core length: 80 m
Description: 46 m
Water depth: -7 m MLLWS

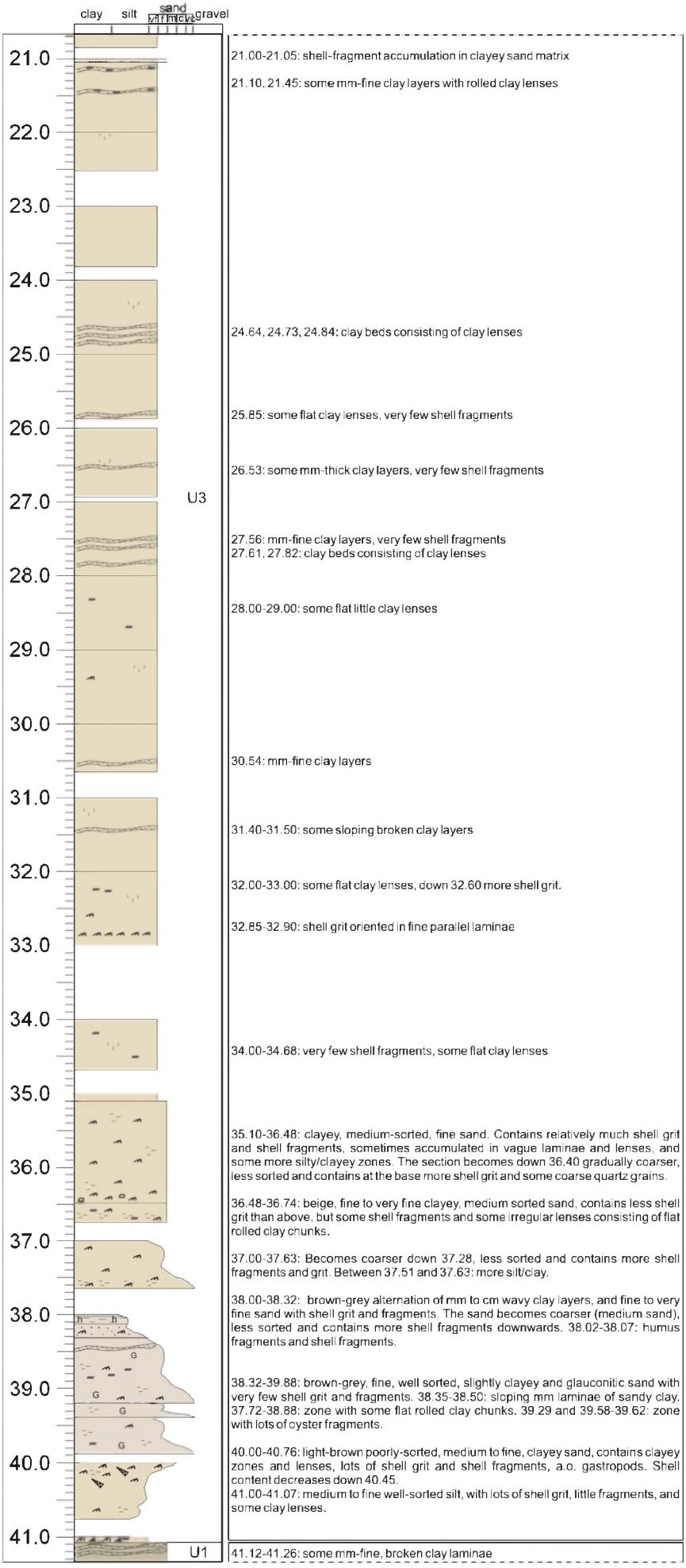

Core: GR1 (2/3)
Date: 08/1986
Location: Grote Rede
UTM position (ED50): E 494185.96 m
N 5679711.17 m
Core length: 80 m
Description: 46 m
Water depth: -7 m MLLWS

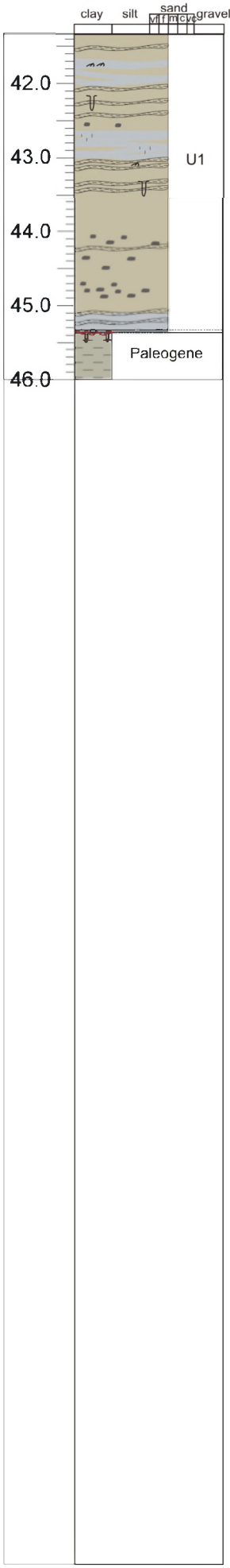

41.07-45.33: light-brown, sometimes grey, medium to fine relatively well-sorted, slightly clayey sand, with a rare shell fragment. The section is characterised by the occurrence of sometimes strongly broken (bioturbated?), rust-coloured (oxidised) clay laminae, lenses, chunks and flasers.
42.07-42.44: some mm clay laminae and lenses, broken and wavy.

42.70-42.97: slightly silty
43.05-43.15: wavy, not parallel clay lenses and layers, with a layer containing fine shell grit.
43.33-43.48: layered, broken (bioturbated?) clay lenses.

44.00-44.15: fine clay lenses
44.18-44.20: irregular clay lenses and chunks
44.22-44.25: fine, wavy clay layers
44.68-44.90: flat-rolled clay lenses and chunks
45.00-45.33: better sorted sand, some horizontal clayey sand laminae
45.33-45.36: heterogeneous mixture of fine, medium sorted sand, gravel, clay lenses (of underlying clay)

45.36-46.00: green-brown clay with bioturbations at the top

Core: GR1 (3/3)

Date: 08/1986
Location: Grote Rede
UTM position (ED50): E 494185.96 m
N 5679711.17 m
Core length: 80 m
Description: 46 m
Water depth: -7 m MLLWS

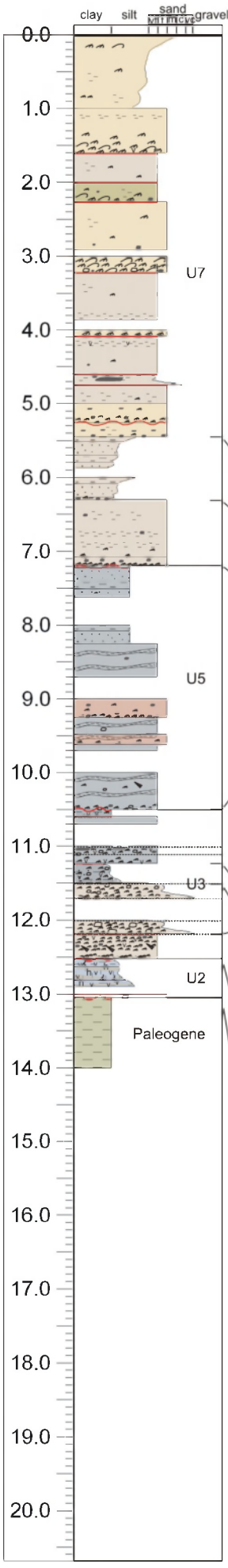

0.00-1.00: yellow-brown, fine sand, from 0.52 down slightly more clayey.
0.11-0.15: laminae with many shell fragments and whole shells. Elsewhere sporadic shell fragments and little shell grit.

0.82: level with little shell fragments.
1.00-1.60: yellow-brown, fine sand with at 1.10: some clayey (brown) flasers. Down 1.30 m, shell fragments increase.
1.50-1.60: sand with many shells, shell fragments and a peat fragment.
1.60-2.00: grey-brown, fine to very fine, slightly clayey sand, sporadic fine shell grit.
2.00-2.26: green-brown, fine to very fine, slightly clayey sand, containing shell fragments and clay chunks. Down 2.16 much more shell fragments, shells and larger clay chunks.
2.26-2.92: yellow-brown, fine sand, with little shell grit, an occasional shell and some more clayey zones. At the base some more clay chunks.
3.00-3.22: yellow-brown, fine sand. At the base: some gravel, brown clay chunks, cemented shell fragments and whole shells.
3.22-3.87: grey-brown, slightly clayey very fine sand, little shell grit. 3.77-3.84: black (reduction), clayey, very fine sand laminae.
4.00-4.08: yellow-brown, fine sand with horizontal-layered shell fragments.
4.08-4.60: grey-brown, very fine, slightly clayey sand, with few shell fragments and few clay lenses. 4.12-4.20: irregular clayey zone with thin small clay lenses and peat remnants.
4.60-4.75: grey-brown, clayey, fine to very fine sand, clay content reduces downwards. 4.62-4.66: black, more clayey/silty chunk with sandy lenses.
4.75-5.00: grey-brown, fine sand, more clayey down 4.83. Between 4.87-4.93: more clayey and siltier laminae (grey reduced), little shell fragments and shell grit.
5.00-5.26: yellow-brown, fine sand with at the top some horizontal and sloping clay lenses with few shell fragments. Downwards an increase of shell fragments and brown clay chunks.
5.26-5.45: yellow-brown, slightly clayey brown sand with sporadic shell fragment.
5.35-5.45: irregular more clayey zone with thin clay lenses and chunks.
5.45-6.30: alternation of grey-brown fine sand and brown mm clay layers or flasers. Number and thickness of clay layers increases downward. At the base, chaotic irregular clay chunks. Few shell fragments.
6.30-7.08: grey-brown, slightly clayey fine sand. Around 6.50 irregular more clayey zones. Sporadic clay lenses. 6.70-6.80, 6.84-6.95: black, more clayey zones. More shell grit down 6.90.
7.08-7.19: brown-grey, heterogeneous mixture of mostly brown, soft clay chunks at the top, at the base mixed with the underlying sand and many shell fragments.

7.19-8.25: alternation of grey, fine to very fine sand and many mm and cm clay laminae, little fine shell grit.
8.25-8.70: grey, fine to very fine sand, no clay laminae but zones with very irregular clay strings, occasionally clay chunks.
9.00-9.25: brown sand, slightly clayey with clay chunks, clay layer and shell fragments, bottom 5 cm lots of shell fragments and clay chunks.
9.25-9.48: grey, fine to very fine sand, with irregular clay strings, gravel fragment at 9.40.
9.48-9.62: brown, coarser sand, black irregular clayey zone at the top, and shell fragments.
10.00-10.50: grey, fine to very fine sand, with irregular clay strings; more shell fragments than above, sometimes concentrated in horizontal laminae; sporadic gravel and a gastropod. 10.43-10.50: shell fragments mixed with gravel and underlying clay.

10.50-10.60: grey to dark grey clay with irregular sandier zones with many shell fragments, many little black amorphous peat fragments.
10.60-11.24 (10.70-11.00 lacks): grey, very fine sand. 11.00-11.10: heterogeneous mixture of clay and sand mixed with shells, rolled and angular silex, elongated-rolled clay chunks, and black amorphous peat remnants. 11.10-11.24: shell grit, strongly diluted in clayey sand, at the base many flat amorphous peat fragments, colonies of bryozoa on thick-walled shells.
11.24-11.50: dark-grey, sandy clay with lots of shell grit, fragments, rolled silex and peat fragments, some very large shells. Shell fragments increase downwards.
11.50-12.18 (11.70-12.00 lacks): grey-brown, compact package of shell fragments with many rolled silex, in a clayey matrix. 12.00-12.18: larger and more gravel
12.18-12.44: brown-grey, horizontally-layered shell fragments and gravel in a fine sand matrix with brown clay chunks and peat fragments. Gastropods mainly at 12.35.
12.44-12.52: light-grey, sloping-layered, fine sand with fine shell grit. Some loping thin lamination formed by shell concentrations.

12.52-12.90: irregular alternation of blue-grey, clay laminae and brown-grey, clayey silt with irregular clayey zones, clay lenses, fine sand lenses, and many rootlet penetrations with oxidation spots around. The section is peaty to strongly humic.
13.00-13.05: rust-brown, medium-fine sand with coarser grains and broken silex.

13.05-14.00: green-grey heavy compact clay

Core: NWB

Date: 05/1988
Location: Nieuwpoort Bank
UTM position (ED50): E 475402.425 m
N 5670789.436 m
Core length: 19 m
Description: 14 m
Water depth: -4.3 m MLLWS

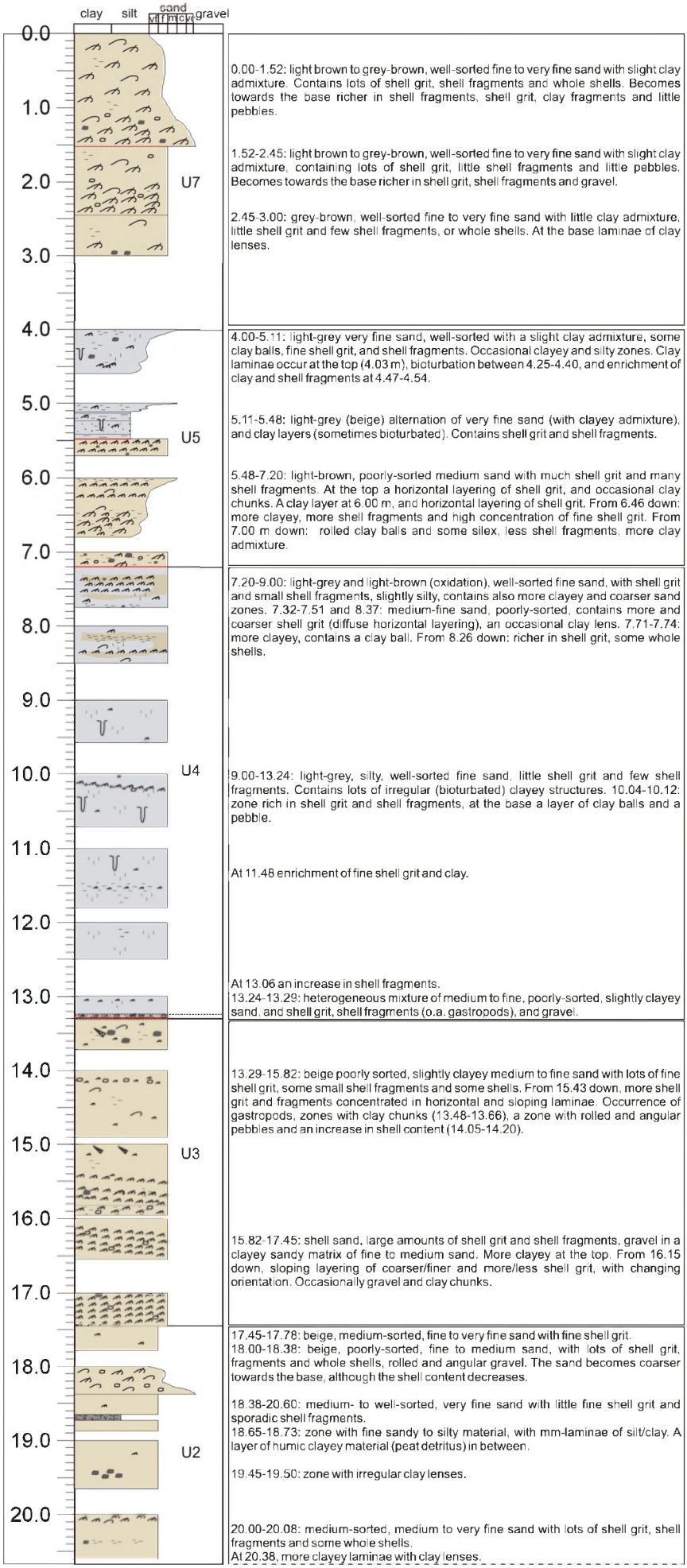

0.00-1.52: light brown to grey-brown, well-sorted fine to very fine sand with slight clay admixture. Contains lots of shell grit, shell fragments and whole shells. Becomes towards the base richer in shell fragments, shell grit, clay fragments and little pebbles.

1.52-2.45: light brown to grey-brown, well-sorted fine to very fine sand with slight clay admixture, containing lots of shell grit, little shell fragments and little pebbles. Becomes towards the base richer in shell grit, shell fragments and gravel.

2.45-3.00: grey-brown, well-sorted fine to very fine sand with little clay admixture, little shell grit and few shell fragments, or whole shells. At the base laminae of clay lenses.

4.00-5.11: light-grey very fine sand, well-sorted with a slight clay admixture, some clay balls, fine shell grit, and shell fragments. Occasional clayey and silty zones. Clay laminae occur at the top (4.03 m), bioturbation between 4.25-4.40, and enrichment of clay and shell fragments at 4.47-4.54.

5.11-5.48: light-grey (beige) alternation of very fine sand (with clayey admixture), and clay layers (sometimes bioturbated). Contains shell grit and shell fragments.

5.48-7.20: light-brown, poorly-sorted medium sand with much shell grit and many shell fragments. At the top a horizontal layering of shell grit, and occasional clay chunks. A clay layer at 6.00 m, and horizontal layering of shell grit. From 6.46 down: more clayey, more shell fragments and high concentration of fine shell grit. From 7.00 m down: rolled clay balls and some silex, less shell fragments, more clay admixture.

7.20-9.00: light-grey and light-brown (oxidation), well-sorted fine sand, with shell grit and small shell fragments, slightly silty, contains also more clayey and coarser sand zones. 7.32-7.51 and 8.37: medium-fine sand, poorly-sorted, contains more and coarser shell grit (diffuse horizontal layering), an occasional clay lens. 7.71-7.74: more clayey, contains a clay ball. From 8.26 down: richer in shell grit, some whole shells.

9.00-13.24: light-grey, silty, well-sorted fine sand, little shell grit and few shell fragments. Contains lots of irregular (bioturbated) clayey structures. 10.04-10.12: zone rich in shell grit and shell fragments, at the base a layer of clay balls and a pebble.

At 11.48 enrichment of fine shell grit and clay.

At 13.06 an increase in shell fragments.
13.24-13.29: heterogeneous mixture of medium to fine, poorly-sorted, slightly clayey sand, and shell grit, shell fragments (o.a. gastropods), and gravel.

13.29-15.82: beige poorly sorted, slightly clayey medium to fine sand with lots of fine shell grit, some small shell fragments and some shells. From 15.43 down, more shell grit and fragments concentrated in horizontal and sloping laminae. Occurrence of gastropods, zones with clay chunks (13.48-13.66), a zone with rolled and angular pebbles and an increase in shell content (14.05-14.20).

15.82-17.45: shell sand, large amounts of shell grit and shell fragments, gravel in a clayey sandy matrix of fine to medium sand. More clayey at the top. From 16.15 down, sloping layering of coarser/finer and more/less shell grit, with changing orientation. Occasionally gravel and clay chunks.

17.45-17.78: beige, medium-sorted, fine to very fine sand with fine shell grit.
18.00-18.38: beige, poorly-sorted, fine to medium sand, with lots of shell grit, fragments and whole shells, rolled and angular gravel. The sand becomes coarser towards the base, although the shell content decreases.

18.38-20.60: medium- to well-sorted, very fine sand with little fine shell grit and sporadic shell fragments.
18.65-18.73: zone with fine sandy to silty material, with mm-laminae of silt/clay. A layer of humic clayey material (peat detritus) in between.

19.45-19.50: zone with irregular clay lenses.

20.00-20.08: medium-sorted, medium to very fine sand with lots of shell grit, shell fragments and some whole shells.
At 20.38, more clayey laminae with clay lenses.

Core: OSB (1/2)

Date: 06/1988
Location: Oostende Bank
UTM position (ED50): E 486411.02 m
N 5681319.95 m
Core length: 45 m
Description: 40 m
Water depth: -5.7 m MLLWS

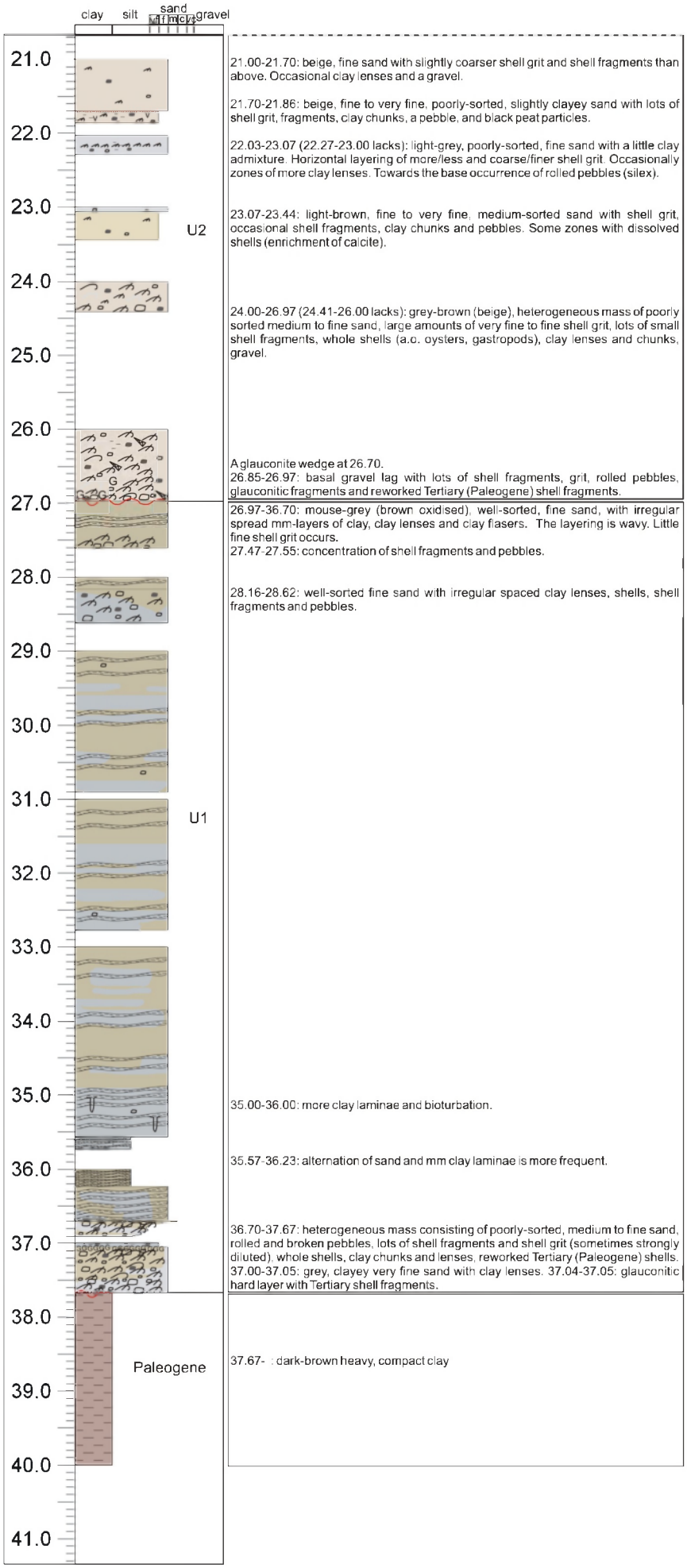

Core: OSB (2/2)
Date: 06/1988
Location: Oostende Bank
UTM position (ED50): E 486411.02 m
N 5681319.95 m
Core length: 45 m
Description: 40 m
Water depth: -5.7 m MLLWS

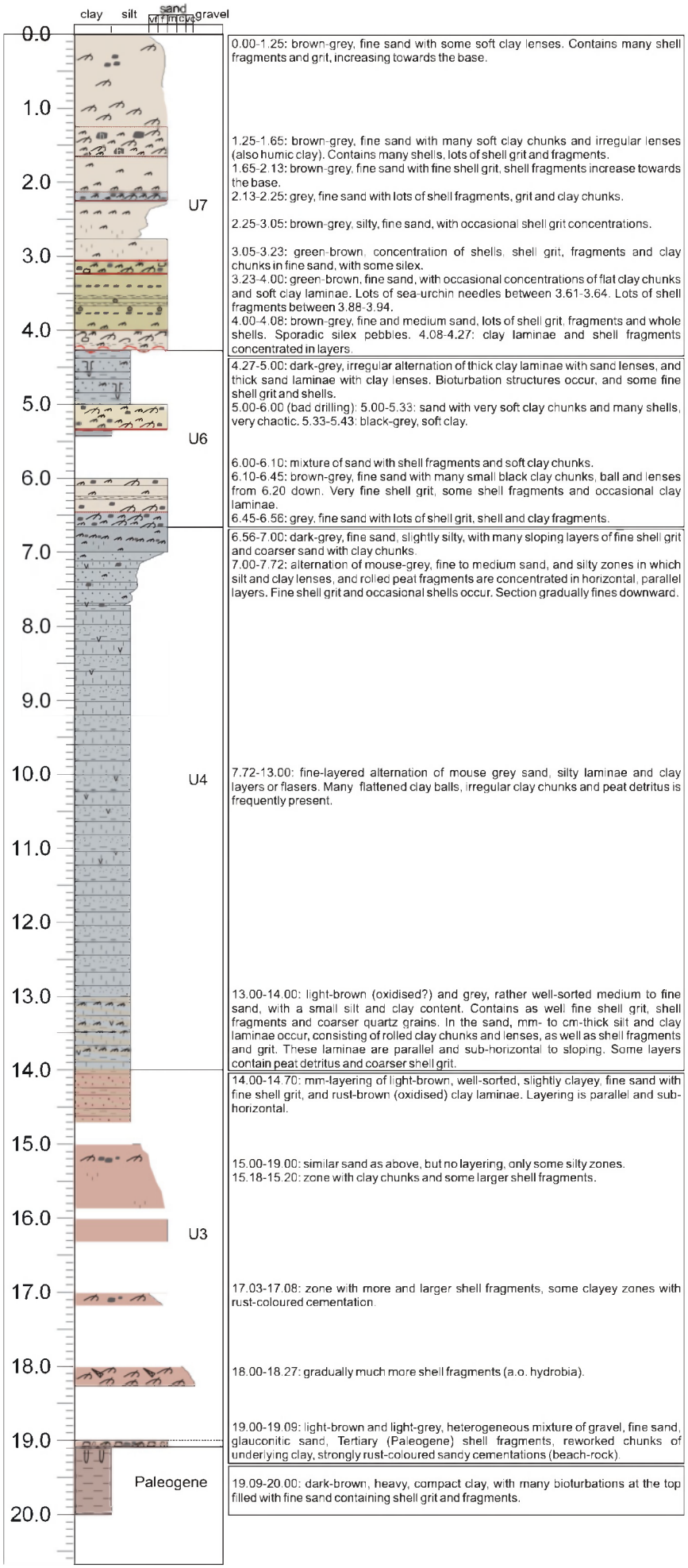

0.00-1.25: brown-grey, fine sand with some soft clay lenses. Contains many shell fragments and grit, increasing towards the base.

1.25-1.65: brown-grey, fine sand with many soft clay chunks and irregular lenses (also humic clay). Contains many shells, lots of shell grit and fragments.
1.65-2.13: brown-grey, fine sand with fine shell grit, shell fragments increase towards the base.
2.13-2.25: grey, fine sand with lots of shell fragments, grit and clay chunks.

2.25-3.05: brown-grey, silty, fine sand, with occasional shell grit concentrations.

3.05-3.23: green-brown, concentration of shells, shell grit, fragments and clay chunks in fine sand, with some silex.
3.23-4.00: green-brown, fine sand, with occasional concentrations of flat clay chunks and soft clay laminae. Lots of sea-urchin needles between 3.61-3.64. Lots of shell fragments between 3.88-3.94.
4.00-4.08: brown-grey, fine and medium sand, lots of shell grit, fragments and whole shells. Sporadic silex pebbles. 4.08-4.27: clay laminae and shell fragments concentrated in layers.

4.27-5.00: dark-grey, irregular alternation of thick clay laminae with sand lenses, and thick sand laminae with clay lenses. Bioturbation structures occur, and some fine shell grit and shells.
5.00-6.00 (bad drilling): 5.00-5.33: sand with very soft clay chunks and many shells, very chaotic. 5.33-5.43: black-grey, soft clay.

6.00-6.10: mixture of sand with shell fragments and soft clay chunks.
6.10-6.45: brown-grey, fine sand with many small black clay chunks, ball and lenses from 6.20 down. Very fine shell grit, some shell fragments and occasional clay laminae.
6.45-6.56: grey, fine sand with lots of shell grit, shell and clay fragments.

6.56-7.00: dark-grey, fine sand, slightly silty, with many sloping layers of fine shell grit and coarser sand with clay chunks.
7.00-7.72: alternation of mouse-grey, fine to medium sand, and silty zones in which silt and clay lenses, and rolled peat fragments are concentrated in horizontal, parallel layers. Fine shell grit and occasional shells occur. Section gradually fines downward.

7.72-13.00: fine-layered alternation of mouse grey sand, silty laminae and clay layers or flasers. Many flattened clay balls, irregular clay chunks and peat detritus is frequently present.

13.00-14.00: light-brown (oxidised?) and grey, rather well-sorted medium to fine sand, with a small silt and clay content. Contains as well fine shell grit, shell fragments and coarser quartz grains. In the sand, mm- to cm-thick silt and clay laminae occur, consisting of rolled clay chunks and lenses, as well as shell fragments and grit. These laminae are parallel and sub-horizontal to sloping. Some layers contain peat detritus and coarser shell grit.

14.00-14.70: mm-layering of light-brown, well-sorted, slightly clayey, fine sand with fine shell grit, and rust-brown (oxidised) clay laminae. Layering is parallel and sub-horizontal.

15.00-19.00: similar sand as above, but no layering, only some silty zones.
15.18-15.20: zone with clay chunks and some larger shell fragments.

17.03-17.08: zone with more and larger shell fragments, some clayey zones with rust-coloured cementation.

18.00-18.27: gradually much more shell fragments (a.o. hydrobia).

19.00-19.09: light-brown and light-grey, heterogeneous mixture of gravel, fine sand, glauconitic sand, Tertiary (Paleogene) shell fragments, reworked chunks of underlying clay, strongly rust-coloured sandy cementations (beach-rock).

19.09-20.00: dark-brown, heavy, compact clay, with many bioturbations at the top filled with fine sand containing shell grit and fragments.

Core: SB1

Date: 08/1986
Location: Stroombank
UTM position (ED50): E 489666.021 m
N 5675621.941 m
Core length: 20 m
Description: 19.80 m
Water depth: -4 m MLLWS

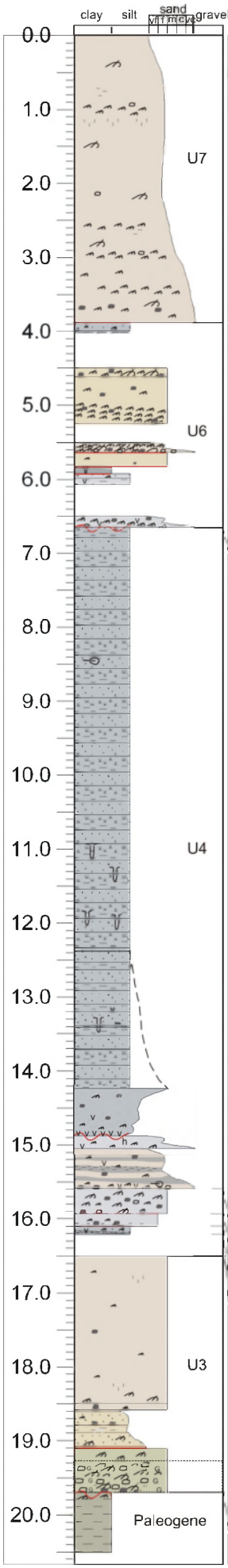

0.00-3.88: brown to grey-brown, well-sorted, very fine to fine sand with an occasional shell fragment and a rare pebble. Contains little clay admixture and occasionally silty zones.

Local higher concentration of shell fragments at 0.95-1.02. Higher silt content at 1.16-1.17.

From 2.55 down, higher concentration of shell fragments, clay balls, shells and silex.

From 3.73 down, sub-horizontal layering of shell grit, shells and clay lenses.

3.88-4.02: alternation of black clay laminae, with grey, fine sand laminae, containing fine shell grit.
4.50-4.62: light-brown, fine sand with lots of shells, fragments and large grey, clay chunks.
4.62-5.25: light-brown, fine sand with few shell fragments, fine shell grit and clay lenses. 4.97-5.25: sub-horizontal to sloping layering of shell grit.
5.50-5.63: concentration of shell fragments, mixed with sand at the top and clay chunks at the base, whole shells and little gravel occur at the base as well.
5.63-5.83: grey-brown, fine sand with little fine shell grit, sporadic clay lens.
5.83-5.92: black, soft clay, bioturbation filled with sand.
5.92-6.07: alternation of cm horizontal layers of clayey medium sand, medium sand plus shell grit, and clay. Shell fragments occur, as well as a sporadic peat fragment in the sandy clay.
6.50-6.65: light-grey, fine sand with shell grit and clay chunks. Shell content increases down 6.58, and is diffusely layered with shell fragments, gravel, peat and clay chunks.

6.65-12.38: regular, horizontal-layered alternation (mm-0.5 cm) of silty fine sand, peat detritus and clay. Sporadic traces of bioturbation.

8.45: wood piece

10.97, 11.38, 11.80, 11.91: bioturbation structures

12.38-13.41: alternation of clay-sand, with increasing thickness and number of sand layers. Peat fragments occasionally occur (again peat detritic layering down 12.70), bioturbation at 13.29.

13.41-14.25: at the top, diffuse, horizontal-layered fine sand with sporadic shell fragments, down 13.73 again alternation of clay, sand and peat detritus, but sand layers dominate.
14.25-14.88: fine sand with irregular clayey and peaty lenses, occasional shell fragments and shell grit. The base is a peat detritus layer.
14.88-15.05: beige, medium sand, poorly-sorted, rich in shell fragments and little shell grit, but which increases towards the base. Humic clay chunks and peat fragments occur.
15.05-15.59: light-brown and grey alternation of well-sorted fine sand with fine shell grit, fine laminated clay, peat lenses, and sand with peat chunks and clay lenses. Towards the base it becomes sandier and at the base occurs a heterogeneous mixture of fine shell grit, fragments, gravel, peat detritus, wood fragments and humic clay chunks.
15.59-15.93: light-grey, heterogeneous mixture of medium sand, lots of shell grit, fragments, clay chunks, coarse quartz grains and gravel.
15.93-16.10: light-grey, very fine sand with little shell grit. Towards the base more clay admixture in a diffuse layering. 16.02-16.03: rolled clay balls and shell grit.
16.10-16.21: grey alternation of sloping clay and sand laminae with lots of shell grit, and peat chunks.

16.50-18.50: beige, well-sorted, fine sand with little shell grit and a sporadic clay chunk. Frequently siltier and more clayey zones. Towards the base more shell fragments.

18.50-18.58: diffuse layering of well-sorted, fine sand, containing shell fragments, grit, and clay chunks.
18.58-19.11: light-brown to light brown-grey alternation of clay laminae, clayey fine sand and well-sorted fine sand with clay lenses. At the top few shell fragments which increase towards the base, where some larger fragments occur. Oyster at 18.86, flat-rolled clay chunks at 18.73-18.76.
19.11-19.70: grey-green, heterogeneous mixture of medium, poorly-sorted sand, shell grit, fragments, whole shells, rolled and angular gravel. Shells are strongly weathered/diluted. Coarser shell fragments towards the base. Glauconitic sand from 19.30 downwards. 19.50-19.70: gravel in matrix of poorly-sorted clay and glauconitic sand, containing reworked clay fragments from below.

19.70-20.50: dark-green, heavy, compact clay, shell fragments at the top

Core: SB2

Date: 05/1988
Location: Stroombank
UTM position (ED50): E 491390.03 m
N 5676619.67 m
Core length: 25.5 m
Description: 20.5 m
Water depth: -4.1 m MLLWS

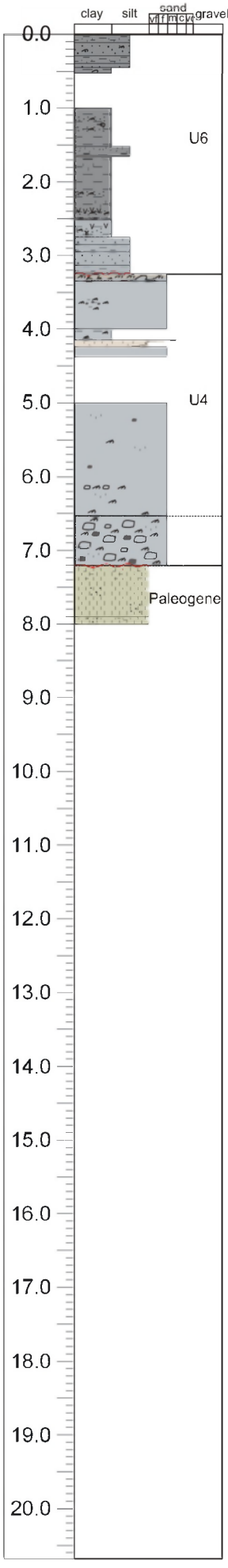

0.00-0.45: originally black (brown-grey after drying) alternation of silty, soft clay and fine sand, containing little very fine shell grit, and some little whole shells.

0.45-1.65 (0.52-1.00 lacks): black, soft clay with irregular sand lenses. 0.49: concentration of shells.
1.27-1.29: laminae of silty, fine sand with shell grit and fragments; on top sea-grass remnants and other organic material
1.52-1.65: alternation of strongly silty, fine sand with shell fragments, fine sandy silt, and silt and clay in a diffuse horizontal layering.
1.65-2.52: black, slightly silty, soft clay, with regularly cm-thick sand layers with shell grit. Between 2.41-2.44: rather much peat detritus in the clay.

2.52-2.75: dark-grey, soft clay, slightly silty, with lots of fine peat detritus. 2.60-2.66: zone with fine silty sand. Bioturbation structures at 2.66-2.70. 2.74: cm horizontal layering of concentrated peat detritus
2.75-3.25: same clay as above, with some thin (mm to cm) horizontal sand layers.

3.25-3.35: grey and brown-grey, heterogeneous mixture of shells, shell grit, sand and clay chunks, gravel.
3.35-4.00: grey, medium sand with fine shell grit. At 3.65: irregular zone with clayey sand and clay with shell fragments around.
4.00-4.38: poor drilling; 4.00-4.15: soft clay chunk with some shell fragments. 4.15-4.24: grey-brown, silty sand. 4.24-4.38: grey, fine to medium fine sand.

5.00-6.53: grey, slightly silty, fine sand, sporadic shell fragments, flat-rolled clay balls.

6.15: level with some gravel and reworked Tertiary (Paleogene) shell. From 6.35 down, more shell fragments.

6.53-7.20: grey, slightly silty, fine sand with much gravel (all sizes, very angular), clay chunks, silex fragments, Tertiary shell fragments, and lots of fine shell grit.

7.20-7.90: grey-green, fine sandy silt, clayey zone at the top.

7.90-8.00: grey-green, clayey, fine sand silt.

Core: SWB
Date: 08/1986
Location: between shore and Wenduinebank
UTM position (ED50): E 503763.774 m
N 5684769.462 m
Core length: 10 m
Description: 8 m
Water depth: -5.85 m MLLWS

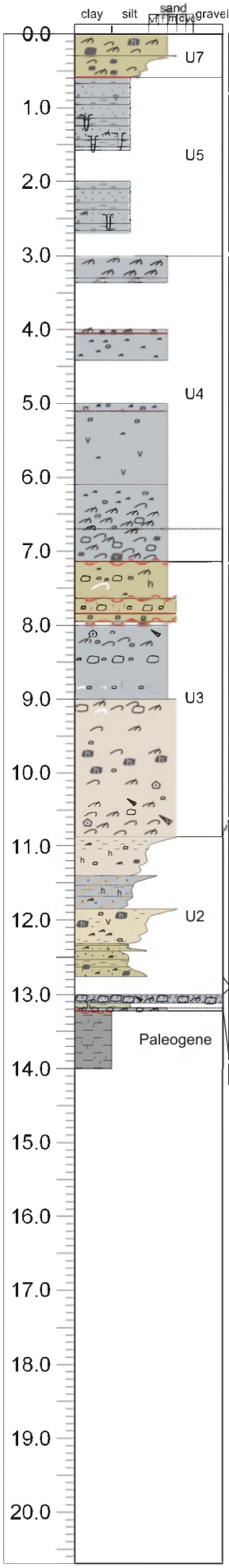

0.00-0.58: green-brown fine sand, clayey zones with rolled, strongly silty and humic clay fragments, lots of shell grit, shell fragments and whole shells. Towards the base, the number of silty, rolled clay fragments increases, less shell grit, many large shells and shell fragments.

0.58-3.00: grey alternation of fine to very fine clayey sand with irregular (mm-) clay laminae, bioturbations, few shell fragments, irregular peat fragment.

3.00-3.30: grey fine sand with lots of coarse shell grit

3.30-4.05 (3.36-4.00 lacks): grey fine sand with lots of shell grit, few coarse quartz grains and many gravels and large shell fragments at the base (a.o. silex).

4.05-5.10 (4.42-5.00 lacks): grey fine sand with very much fine shell grit, sporadic shell and silex fragments. Many pebbles and shell fragments at the base.

5.10-6.10: grey fine sand with angular small pebbles at the top, little very fine shell grit, sporadic small lenses of peat. Section becomes gradually coarser.

6.10-7.14: grey shell sand, with at the top small shell fragments and pebbles, becoming coarser towards the base, with whole shells, and larger and bigger pebbles. Becomes a strongly heterogeneous mixture of shell fragments, grit, gravel and fine sand. Rolled (soft) clay fragments containing peat remnants occur.

7.14-7.64: brown-green fine sand, little fine shell grit, sporadic shell fragments. Between 7.30-7.38 many pebbles, angular and rolled clay fragments. Humus fragment and strongly weathered oyster fragments at the base.
7.64-7.84: green-brown heterogeneous mixture of medium-fine sand, small and large rolled and angular silex pebbles, and silty, cemented sand.
7.84-7.95: brown-green heterogeneous mixture of medium fine sand, few shell fragments, sporadic small pebbles.
8.00-9.00: grey fine sand with shell fragments and small pebbles, sea-urchin. 8.18-8.28: more shell fragments and whole shells. 8.42-8.55: lots of silex, rolled and broken. 8.80-8.88: heterogeneous zone with shells (oysters) and gravel.

9.00-10.87: light-brown (beige) medium sand with lots of fine shell grit, shell fragments and occasionally whole shells, occasionally little pebbles. Becomes more heterogeneous towards the base: gravel becomes coarser, more shells (a.o. gastropods), shell fragments and shell grit, sea-urchin fragments. 9.00-9.10: angular and rounded silex (4 cm), oyster fragments and reworked Tertiary (Paleogene) shells. 9.66-10.00: clay balls with humus.

10.87-11.40: grey-brown, slightly clayey, fine sand with very few shell fragments, occasionally a gravel fragment. At the top, some clay layers, black humic lenses. Towards the base, the sand becomes finer and shell fragments decrease. A clay chunk at 11.22.
11.40-11.85: sloping mm-layering of grey, clayey sand laminae, alternated with brown sand layers. Occasional shell fragment. Towards the base humic clay laminae.
11.85-12.32: grey-brown, slightly clayey, medium fine sand, irregular humic clay lenses and laminae, some gravel, concentrated shell fragments, peat remnants. Towards the base the clay laminae increase and cementation occurs.
12.32-12.76: green-brown fining-upward sequences of fine sand with clay layers and lenses. Little shell grit, sporadic small peat fragment, from 12.60 clay balls.

13.00-13.12: grey, very heterogeneous mixture of gravel (a.o. silex), and shells (gastropods as well) in a clayey matrix.
13.12-13.18: dark-green fine sand (with calcite cement) and humic clay
13.18-13.22: grey heterogeneous mixture of fine sand, large and small gravel, and shell fragments.

13.22- : dark grey compact silty clay

Core: UIT (UITDIEP)

Date: 05/1988
Location: Uitdiep swale
UTM position (ED50): E 481,498.290 m
N 5,681,483.625 m
Core length: 19 m
Described: 14 m
Water depth: -14.3 m MLLWS

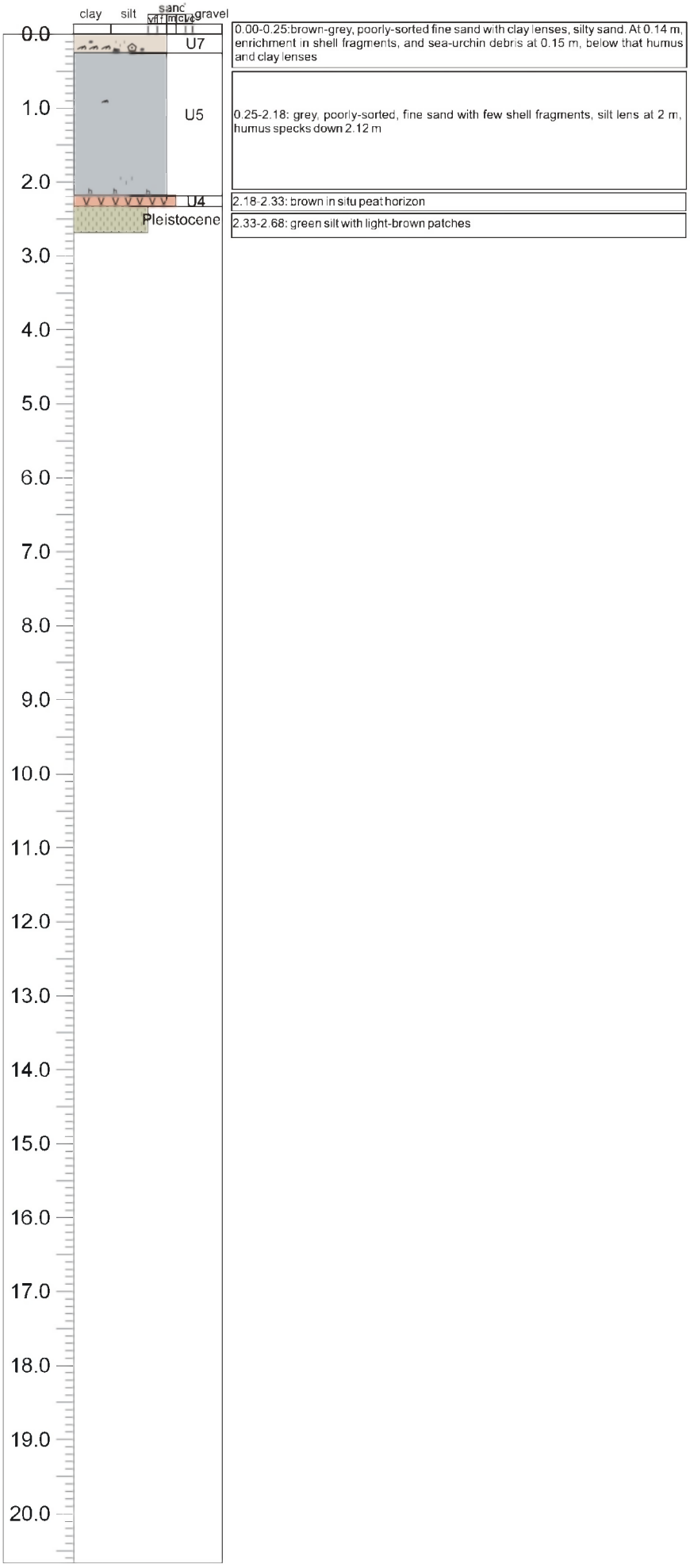

Core: TB358
Date: 19/09/1986
Location: offshore Middelkerke
UTM position (ED50): E 487,431.016 m
N 5,672,368.105 m
Core length: 2.68 m
Water depth: -10 m MLLWS

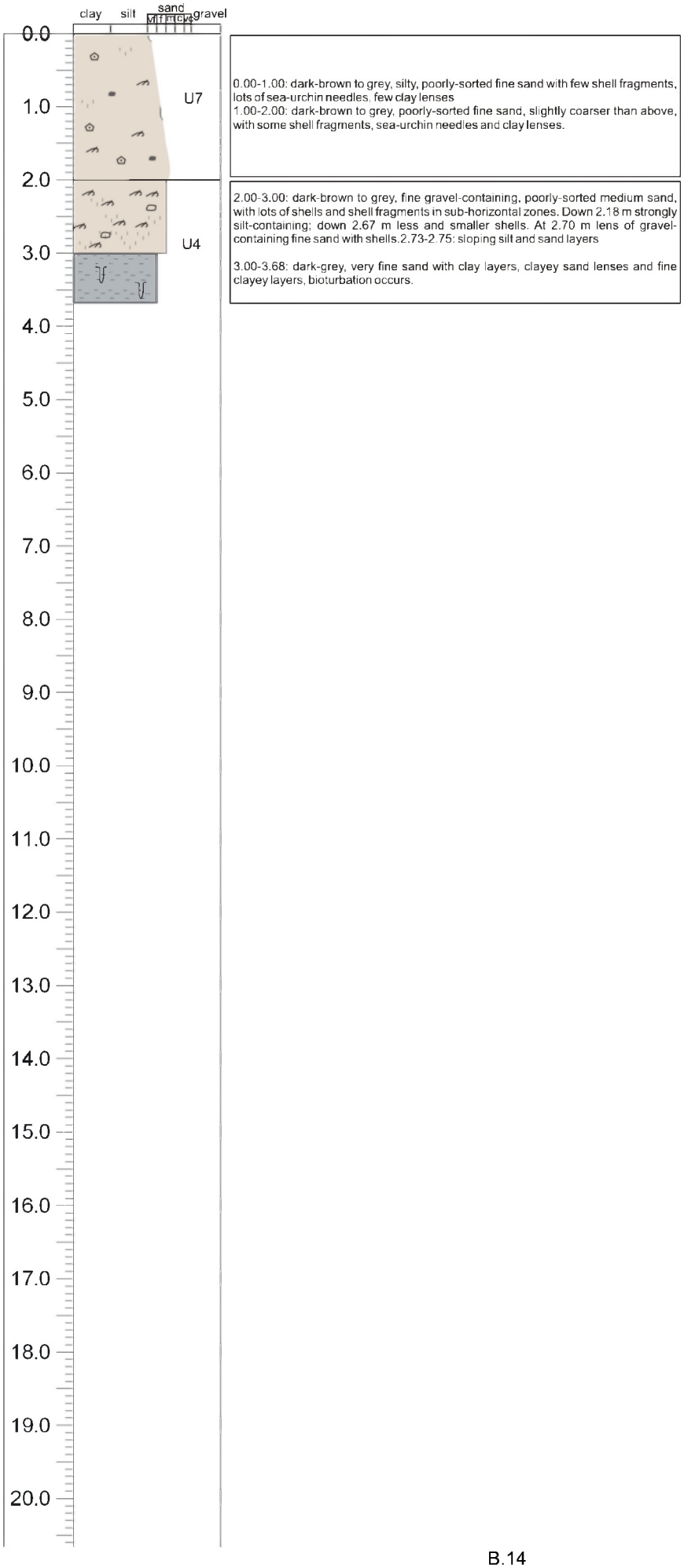

0.00-1.00: dark-brown to grey, silty, poorly-sorted fine sand with few shell fragments, lots of sea-urchin needles, few clay lenses
1.00-2.00: dark-brown to grey, poorly-sorted fine sand, slightly coarser than above, with some shell fragments, sea-urchin needles and clay lenses.

2.00-3.00: dark-brown to grey, fine gravel-containing, poorly-sorted medium sand, with lots of shells and shell fragments in sub-horizontal zones. Down 2.18 m strongly silt-containing; down 2.67 m less and smaller shells. At 2.70 m lens of gravel-containing fine sand with shells.2.73-2.75: sloping silt and sand layers

3.00-3.68: dark-grey, very fine sand with clay layers, clayey sand lenses and fine clayey layers, bioturbation occurs.

Core: TB402
Date: 16/09/1986
Location: Uitdiep swale
UTM position (ED50): E 481,137.009 m
N 5,681,947.016 m
Core length: 3.68 m
Water depth: -15 m MLLWS

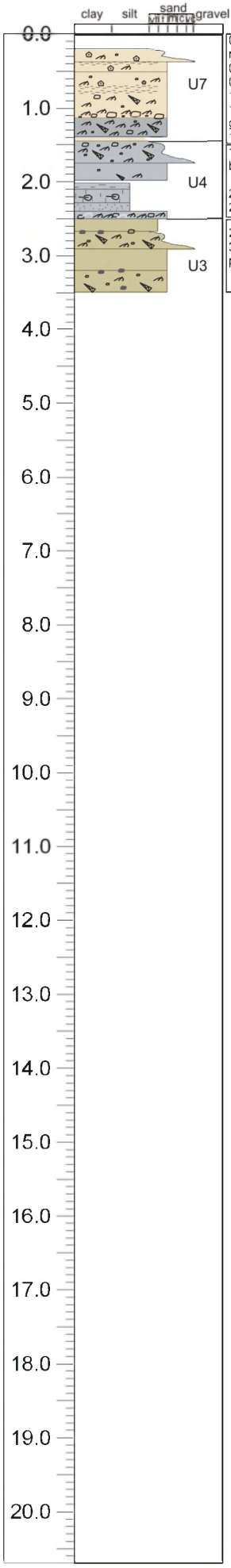

0.20-0.37: yellow-brown, fine sand, coarsening downwards, containing sea-urchin needles, few shell fragments and a small pebble.
0.37-1.14: yellow-brown, fine sand with occasional clay layers (0.37-0.39, 0.70, 0.75), some pebbles, sea-urchin debris, and shell fragments (a.o. gastropods). From 1.00-1.14: heterogeneous mixture of fine to coarse sand, gravel and shell fragments.
1.14-1.39: dark grey fine to medium sand, containing lots of shell fragments (a.o. gastropods), and some gravel.
1.39-1.45: yellow-brown, very fine sand.

1.45-1.98: grey, fine sand, with many shell fragments (a.o. gastropods) and pebbles between 1.45 and 1.75 (number and size decreases downwards).

2.02-2.50: grey alternation of silt, clay and sand layers, plant remnants at 2.20.
2.40-2.50: accumulation of shell fragments (a.o. oysters), and pebbles.

2.50-3.49: yellow to green-grey fine sand, no shells between 2.50-2.67 and 2.91-3.20. Many shells (a.o. many gastropods), some clay balls, and some small silex pebbles between 2.67-2.91 and 3.20-3.49..

Core: Tr08
Date: 24/05/1991
Location: Middelkerke Bank
UTM position (ED50): E 481809.0416 m
N 5686002.317 m
Core length: 3.49 m
Description: 3.49 m
Water depth: -22.0 m MLLWS

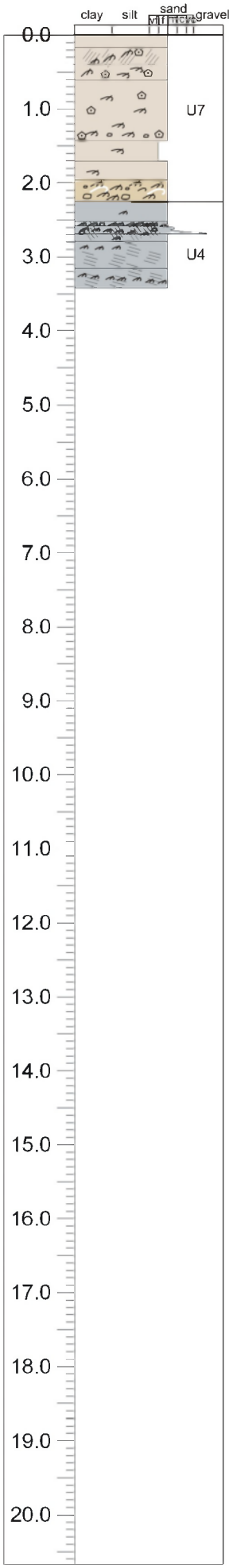

0.00-0.61: grey-brown, fine sand with cross stratification, shell and sea-urchin fragments along the layering. Increasing shell content towards the base.

0.51-1.42: brown-grey, fine sand with shell fragments, sea-urchin needles and gravel; increase of shell content towards the base.

1.42-1.71: brown-grey, very fine sand with few shell fragments.
1.71-1.95: brown-grey, fine sand with few shell fragments.
1.95-2.25: yellow-grey, coarse-grained, heterogenic mixture of gravel, shell fragments and whole shells (a.o. oysters).

2.25-2.52: grey, fine sand with few shell fragments.
2.52-2.80: grey, fine to medium sand with sub-horizontal layering, many shell fragments and some gravel along the layering.
2.80-3.42: grey, fine sand with sub-horizontal thin lamination, some shell fragments along the layering around 2.85 and 3.25.

Core: Tr11
Date: 03/09/1991
Location: Uitdiep swale
UTM position (ED50): E 485,056.047 m
N 5,687,154.674 m
Core length: 3.42 m

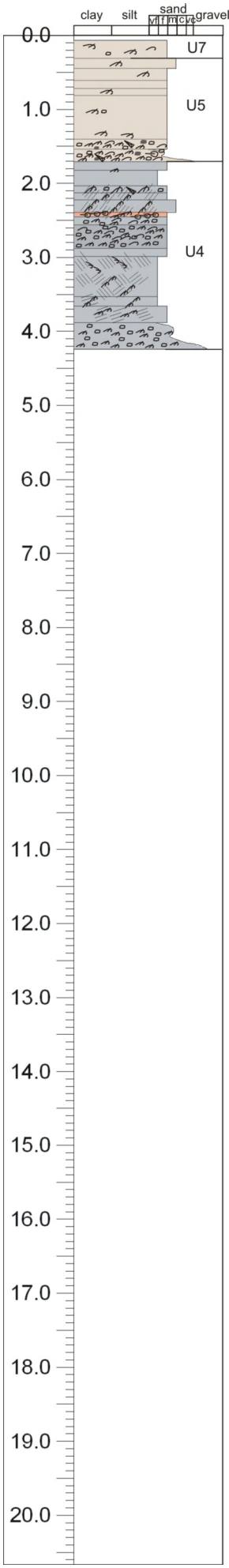

0.00-0.31: grey-brown, fine sand with shell fragments, whole shells and occasional gravel.

0.31-1.40: grey-brown and brown-grey fine sand with some shell fragments and occasional gravel.

1.40-1.71: brown-grey, fine sand with many shell fragments (a.o. gastropods), whole shells, gravel, clay balls and plant fragments.

1.71-2.02: grey, fine to very fine sand with few shell fragments.
2.02-2.39: grey, fine to medium sand with cross stratification, shell fragments along the laying. Many shell fragments (a.o. gastropods) and some gravel at the top.
2.39-2.45: brown, fine sand with cross stratification, shell and plant fragments along the layering.
2.45-2.88: grey, coarse-grained heterogenic mixture of shell fragments, whole shells and gravel.

2.88-3.88: grey, very fine to fine sand with cross stratification, shell fragments along the layering.

3.88-4.24: grey, fine to medium sand with many shell fragments and gravel.

Core: Tr13

Date: 03/09/1991
Location: Uitdiep swale
UTM position (ED50): E 485,578.208 m
N 5,686,776.557 m
Core length: 4.24 m

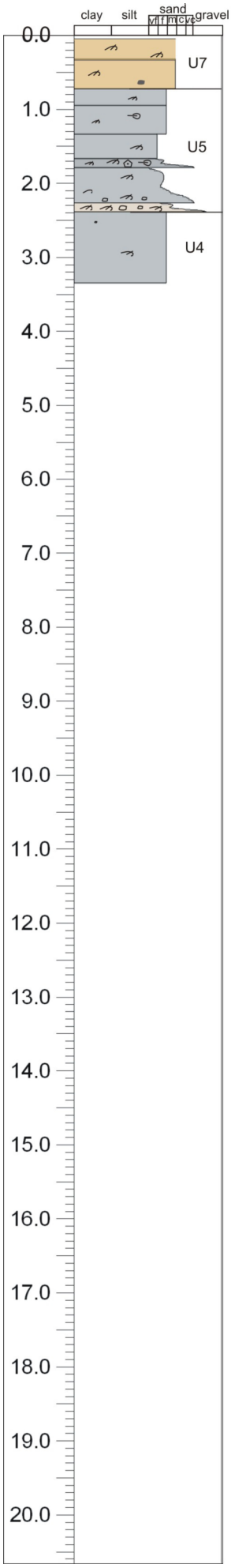

0.05-0.72: yellow-brown, medium sand with an occasional clay lens, many shell fragments between 0.05 and 0.32 m

0.72-1.65: grey, fine to medium sand with few shell fragments and an occasional plant fragment.
1.65-1.79: dark-grey, very fine sand with abundant shell and sea-urchin fragments and an occasional plant fragment.
1.79-2.25: grey, fine sand, coarsening downward, with some shell fragments. Towards the base, more shell fragments, occasional whole shells and gravel.
2.25-2.38: brown-grey, medium to coarse sand, with many shell fragments and gravel.

2.38-3.34: grey, fine sand with very few shell fragments and occasional gravel.

Core: Tr19
Date: 03/09/1991
Location: Uitdiep swale
UTM position (ED50): E 481,250.869 m
N 5,680,804.709 m
Core length: 3.34 m

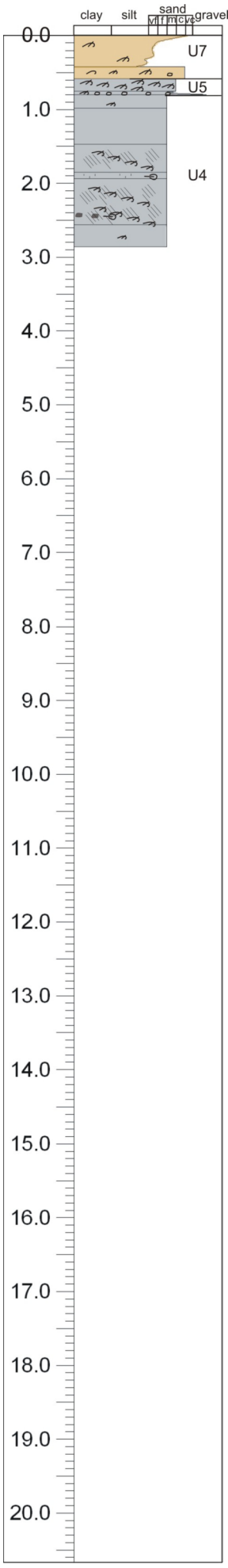

0.00-0.58: yellow-brown, coarse to medium sand with shell fragments. More shell fragments and gravel towards the base.

0.58-0.80: grey, fine sand with shell fragments in sloping layers. The base is coarse-grained, consisting of gravel and shell fragments.

0.80-2.86: grey, fine sand with some shell fragments.

1.48-1.85: cross stratification with shell fragments along the layers. 1.85-1.95: grey, fine sand with silt admixture, and plant fragment.

1.95-2.55: cross stratification with shell fragments along the layers; brown clay lenses and plant fragments around 2.40.

Core: Tr20
Date: 03/09/1991
Location: Uitdiep swale
UTM position (ED50): E 480,932.770 m
N 5,681,056.787 m
Core length: 2.86 m

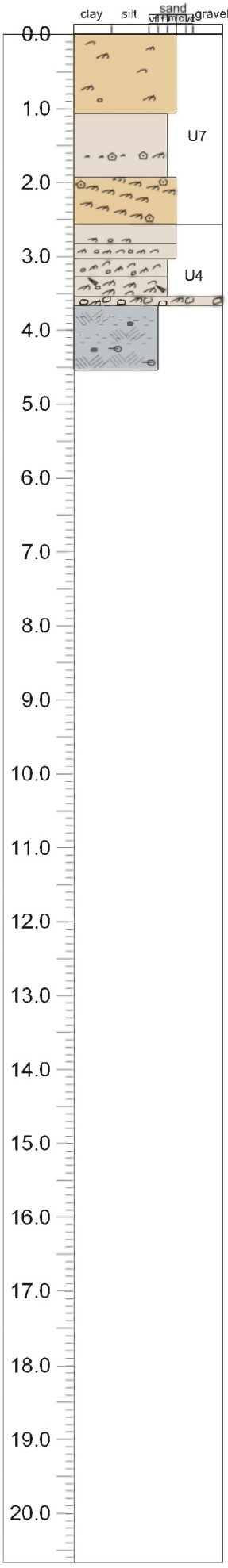

0.00-1.05: yellow-brown, medium sand with many shell fragments, whole shells and some occasional gravel.

1.05-1.92: grey-brown, fine sand with only shell and sea-urchin fragments in a layer at 1.65.

1.92-2.55: yellow-brown, fine to medium sand, with cross stratification. shell fragments and sea-urchin debris along the layering.

2.55-3.03: grey-brown medium sand with shell fragments and gravel in some horizontal layers.
3.03-3.27: grey-brown fine sand with cross stratification, shell fragments and an occasional gravel along the layering.
3.27-3.54: grey-brown fine sand with shell fragments (a.o. gastropods) and pebbles (flint, granite).
3.54-3.67: grey-brown coarse-grained layer, with large pebbles and many shell fragments.
3.67-4.54: grey fine sand with mud layers in cross stratification, plant fragments and clay balls occur.

Core: Tr21
Date: 05/09/1991
Location: Uitdiep swale
UTM position (ED50): E 480,710.702 m
N 5,681,266.852 m
Core length: 4.54 m

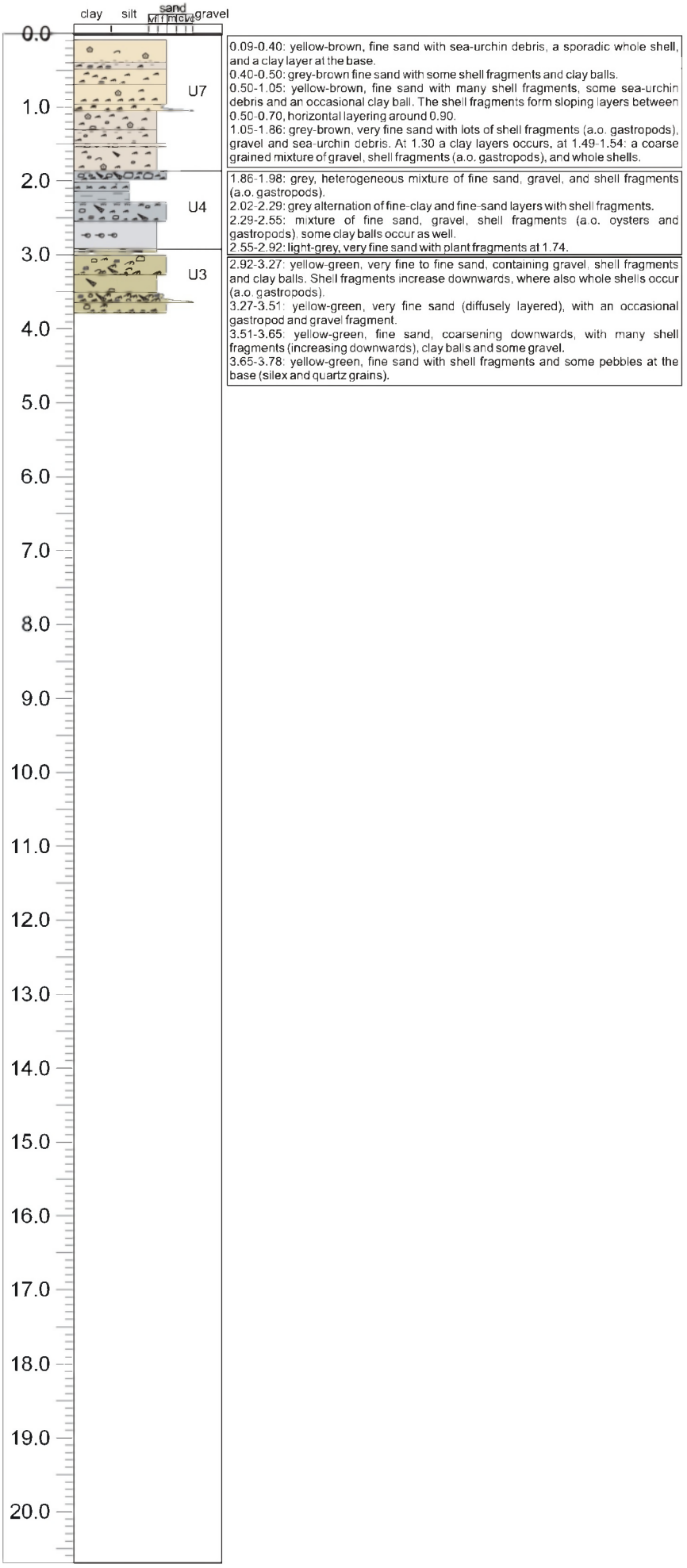

0.09-0.40: yellow-brown, fine sand with sea-urchin debris, a sporadic whole shell, and a clay layer at the base.
0.40-0.50: grey-brown fine sand with some shell fragments and clay balls.
0.50-1.05: yellow-brown, fine sand with many shell fragments, some sea-urchin debris and an occasional clay ball. The shell fragments form sloping layers between 0.50-0.70, horizontal layering around 0.90.
1.05-1.86: grey-brown, very fine sand with lots of shell fragments (a.o. gastropods), gravel and sea-urchin debris. At 1.30 a clay layers occurs, at 1.49-1.54: a coarse grained mixture of gravel, shell fragments (a.o. gastropods), and whole shells.

1.86-1.98: grey, heterogeneous mixture of fine sand, gravel, and shell fragments (a.o. gastropods).
2.02-2.29: grey alternation of fine-clay and fine-sand layers with shell fragments.
2.29-2.55: mixture of fine sand, gravel, shell fragments (a.o. oysters and gastropods), some clay balls occur as well.
2.55-2.92: light-grey, very fine sand with plant fragments at 1.74.

2.92-3.27: yellow-green, very fine to fine sand, containing gravel, shell fragments and clay balls. Shell fragments increase downwards, where also whole shells occur (a.o. gastropods).
3.27-3.51: yellow-green, very fine sand (diffusely layered), with an occasional gastropod and gravel fragment.
3.51-3.65: yellow-green, fine sand, coarsening downwards, with many shell fragments (increasing downwards), clay balls and some gravel.
3.65-3.78: yellow-green, fine sand with shell fragments and some pebbles at the base (silex and quartz grains).

Core: Tr95

Date: 01/10/1993
Location: Middelkerke Bank
UTM position (ED50): E 481677.0007 m
N 5686044.330 m
Core length: 3.78 m
Description: 3.78 m
Water depth: -22.0 m MLLWS

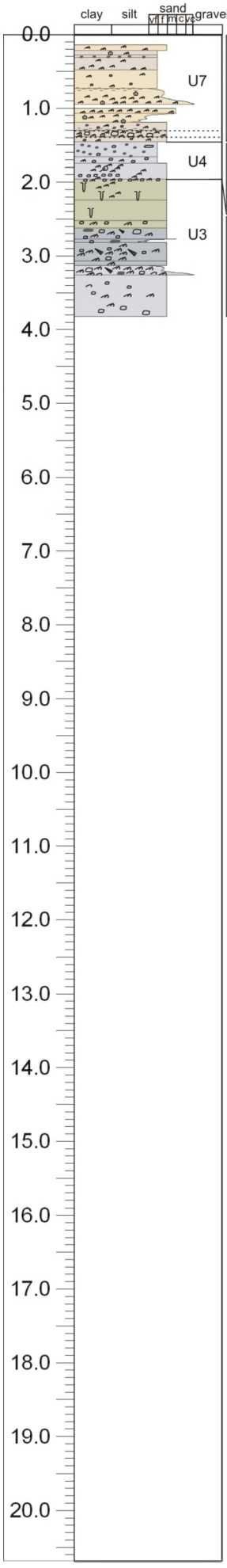

0.14-1.46: yellow-brown and grey-brown, very fine to fine sand, with lots of shell fragments, generally increasing in number downwards (from 0.81). Also clay balls (0.28-0.31, 1.19-1.30), sea-urchin debris, and an occasional gravel occur, as well as a clay layer at 1.73 and 1.30.

Between 1.30 and 1.39 a heterogeneous gravel layer is present.

1.46-1.96: light-grey, very fine to fine sand, containing lots of clay balls forming sloping layers between 1.46 and 1.66. Some pebbles occur and has the highest concentration between 1.66 and 1.75. Between 1.66 and 1.96 shell fragments are present, between 1.75 and 1.96 forming sloping layers. A sporadic plant fragment occurs as well.

1.96-2.62: green-grey, fine sand with some shell fragments, bioturbations and some pebbles at the base.
2.62-3.26: grey, fine sand with many shell fragments (a.o. gastropods), and gravel, sporadically clay balls occur.
3.26-3.82: light-grey, fine sand with some shell fragments and small pebbles.

Core: Tr96
Date: 01/10/1993
Location: Middelkerke Bank
UTM position (ED50): E 481430.9245 m
N 5686248.393 m
Core length: 3.82 m
Description: 3.82 m
Water depth: -23.0 m MLLWS

Appendix C
Corresponding photos of the specific cores

GEOLOGICAL SURVEY OF BELGIUM - BELGISCHE GEOLOGISCHE DIENST

Core: GR1 (0-5 m)

Date: 08/1986
Location: Grote Rede
UTM position (ED50): E 494185.96 m
N 5679711.17 m

Core length: 80 m
Water depth: -7 m MLLWS

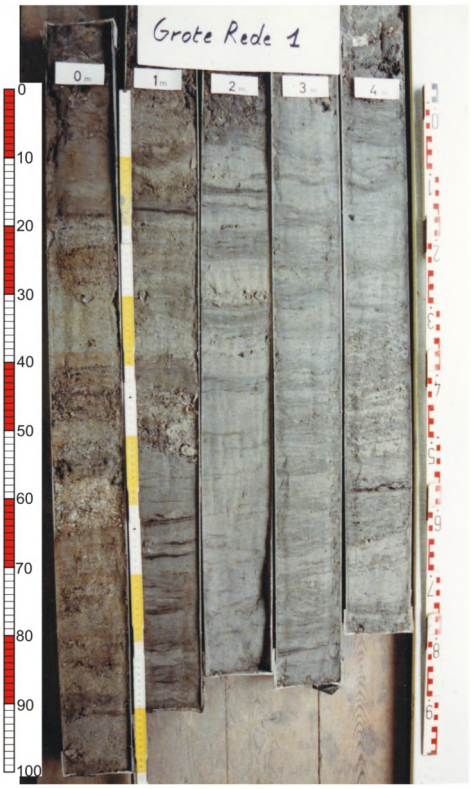

GEOLOGICAL SURVEY OF BELGIUM - BELGISCHE GEOLOGISCHE DIENST

Core: GR1 (5-25 m)

Date: 08/1986
Location: Grote Rede
UTM position (ED50): E 494185.96 m
N 5679711.17 m

Core length: 80 m
Water depth: -7 m MLLWS

GEOLOGICAL SURVEY OF BELGIUM - BELGISCHE GEOLOGISCHE DIENST

Core: GR1 (25-46 m)

Date: 08/1986
Location: Grote Rede
UTM position (ED50): E 494185.96 m
N 5679711.17 m

Core length: 80 m
Water depth: -7 m MLLWS

GEOLOGICAL SURVEY OF BELGIUM - BELGISCHE GEOLOGISCHE DIENST

Core: NWB

Date: 05/1988
Location: Nieuwpoort Bank
UTM position (ED50): E 475402.425 m
N 5670789.436 m

Core length: 19 m
Water depth: -4.3 m MLLWS

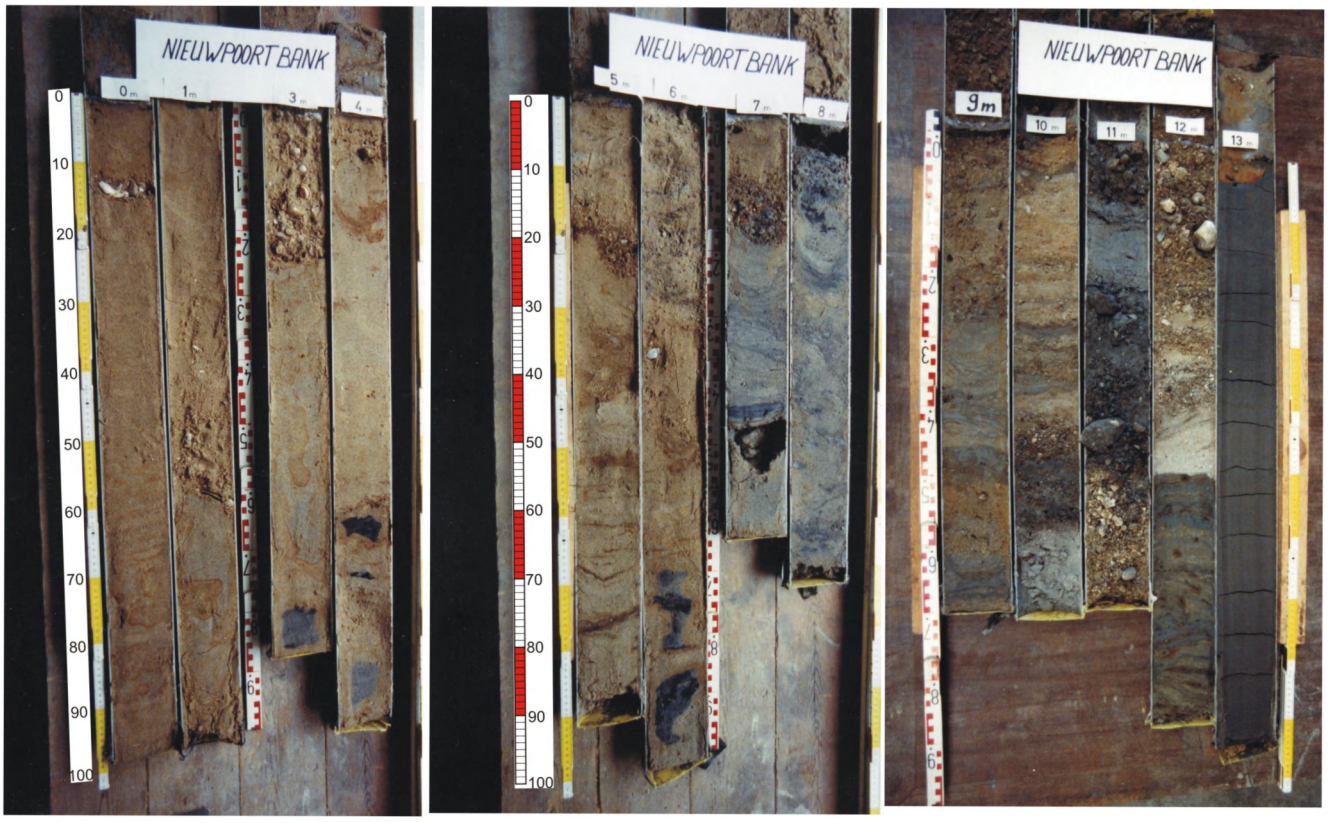

GEOLOGICAL SURVEY OF BELGIUM - BELGISCHE GEOLOGISCHE DIENST

Core: OSB (0-20 m)

Date: 06/1988
Location: Oostende Bank
UTM position (ED50): E 486411.02 m
N 5681319.95 m

Core length: 45 m
Water depth: -5.7 m MLLWS

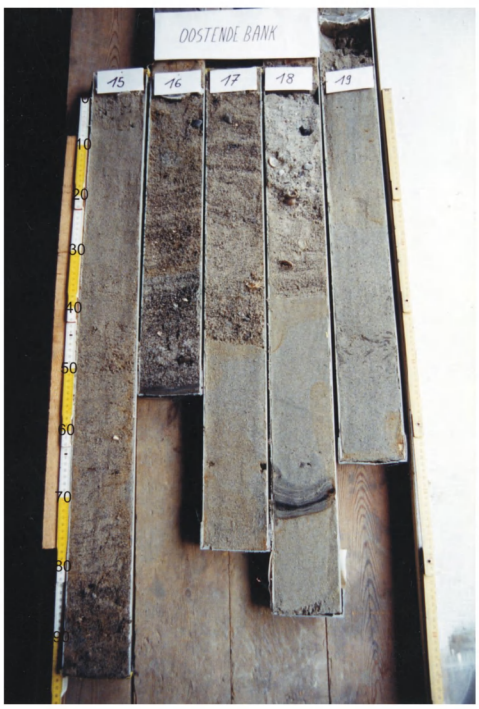

GEOLOGICAL SURVEY OF BELGIUM - BELGISCHE GEOLOGISCHE DIENST

Core: OSB (20-40 m)

Date: 06/1988
Location: Oostende Bank
UTM position (ED50): E 486411.02 m
N 5681319.95 m

Core length: 45 m
Water depth: -5.7 m MLLWS

GEOLOGICAL SURVEY OF BELGIUM - BELGISCHE GEOLOGISCHE DIENST

Core: SB1

Date: 08/1986
Location: Stroombank
UTM position (ED50): E 489666.021 m
N 5675621.941 m

Core length: 20 m
Water depth: -4 m MLLWS

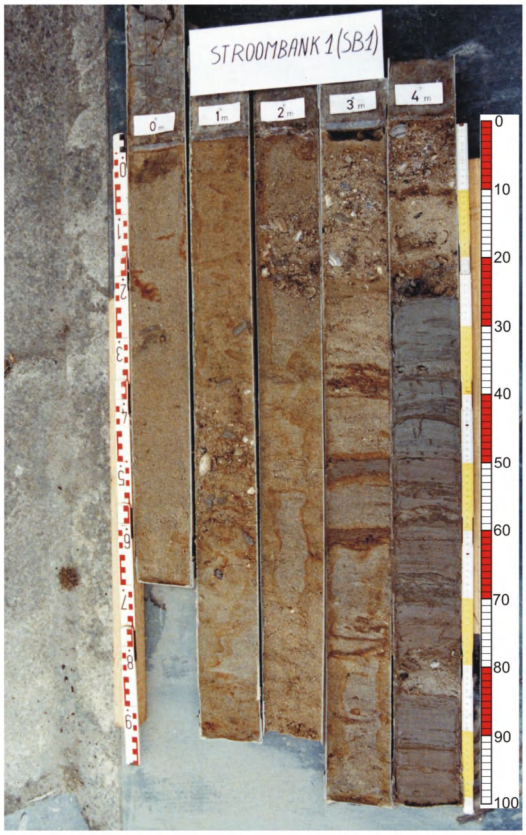

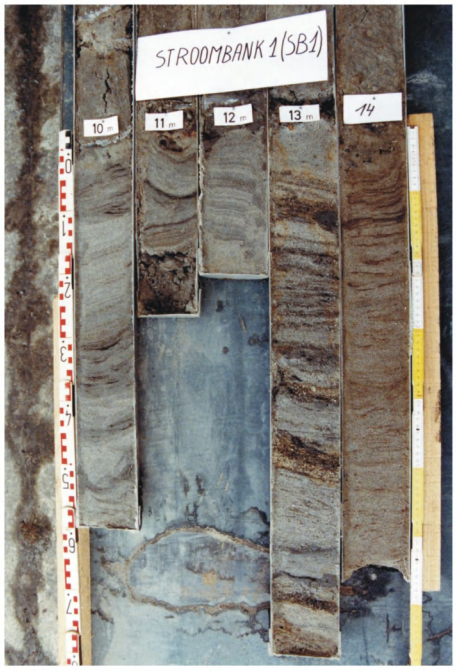

GEOLOGICAL SURVEY OF BELGIUM - BELGISCHE GEOLOGISCHE DIENST

Core: SB2

Date: 05/1988
Location: Stroombank
UTM position (ED50): E 491390.03 m
N 5676619.67 m

Core length: 25.5 m
Water depth: -4.1 m MLLWS

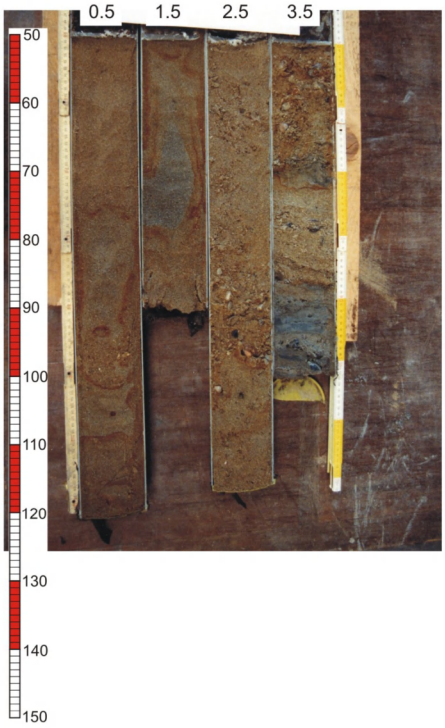

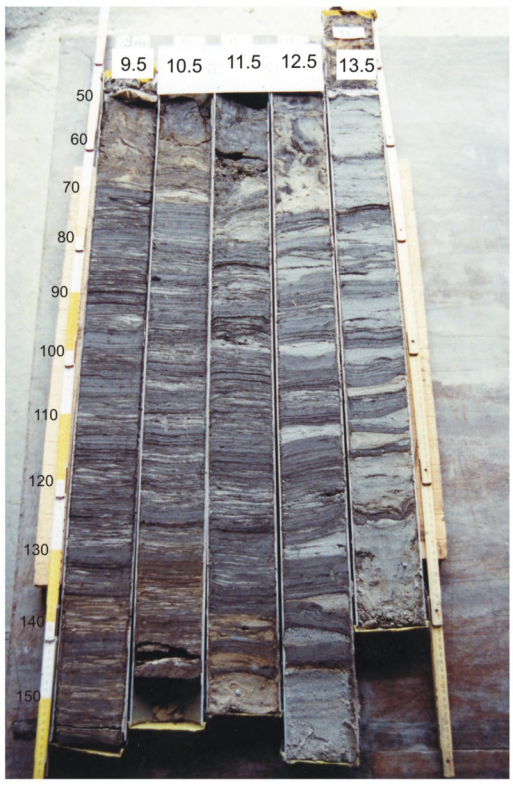

GEOLOGICAL SURVEY OF BELGIUM - BELGISCHE GEOLOGISCHE DIENST

Core: SWB

Date: 08/1986
Location: between shore and Wenduinebank
UTM position (ED50): E 503763.774 m
N 5684769.462 m

Core length: 8 m
Water depth: -5.85 m MLLWS

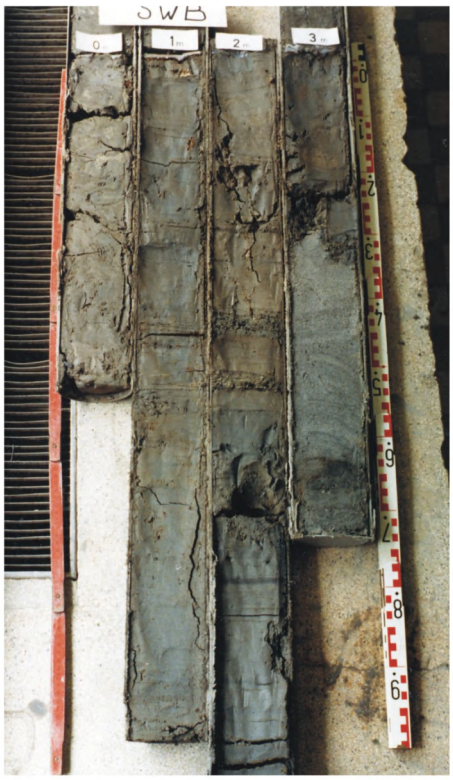

GEOLOGICAL SURVEY OF BELGIUM - BELGISCHE GEOLOGISCHE DIENST

Core: UIT (UITDIEP)

Date: 05/1988
Location: Uitdiep swale
UTM position (ED50): E 481,498.290 m
N 5,681,483.625 m

Core length: 19 m
Water depth: -14.3 m MLLWS

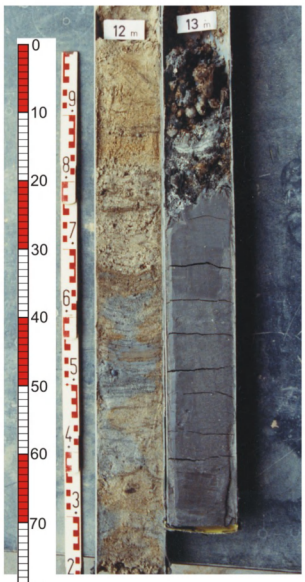

GEOLOGICAL SURVEY OF BELGIUM - BELGISCHE GEOLOGISCHE DIENST

Core: TB358

Date: 19/09/1986
Location: offshore Middelkerke
UTM position (ED50): E 487,431.016 m
N 5,672,368.105 m

Core length: 2.68 m
Water depth: -10 m MLLWS

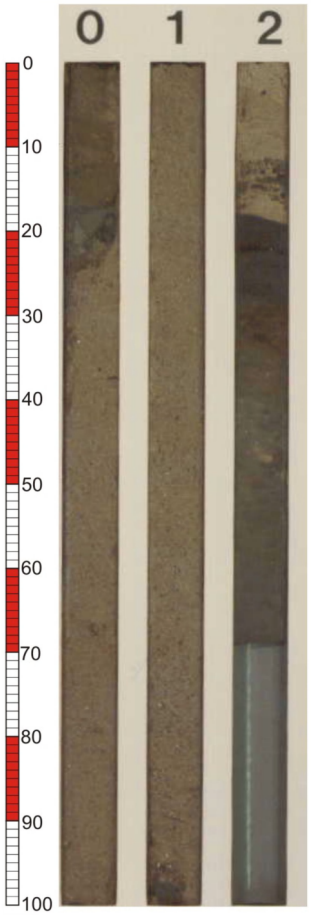

GEOLOGICAL SURVEY OF BELGIUM - BELGISCHE GEOLOGISCHE DIENST

Core: TB402

Date: 16/09/1986
Location: Uitdiep swale
UTM position (ED50): E 481,137.009 m
N 5,681,947.016 m

Core length: 3.68 m
Water depth: -15 m MLLWS

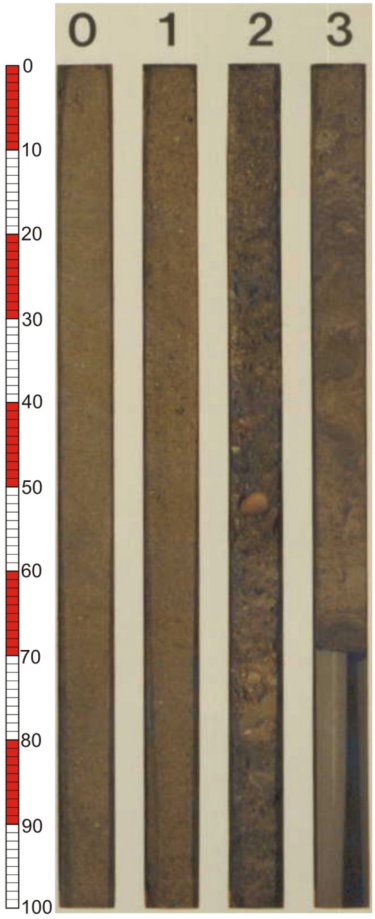

Since the late ‘70’s, in the framework of several national and international projects, such as the extension of the harbour of Zeebrugge, and the search for potentially exploitable near-surface sediments, the Quaternary cover of the Belgian Continental Shelf (BCS) has been intensively investigated. However, apart from some detail studies on certain sandbanks and distinct research areas, where for each sandbank a new stratigraphic classification and interpretation was proposed, the available seismic and core data were never processed or interpreted in an integrated coherent way. In a time when only analogue data were available, it was not possible to correlate the complex Quaternary structure of the diverse sandbanks and research areas with one another.

Now, in this digital era, almost 30 years after their acquisition, more than 4000 km of high-resolution paper seismic recordings have been scanned, converted into digital ‘SEG-Y’ format, integrated with 1300 km of modern acquired data, and ground-truthed with more than 600 core descriptions. This digital approach made it possible to develop –for the very first time– a model for the geological evolution of the BCS during the Quaternary, which was the main goal of this thesis.

Not only the two immense data sets of seismic profiles and core descriptions formed the foundation of this study. Also the detailed knowledge of the western Coastal Plain and Flemish Valley on land, literature on tidal and wave processes on the BCS, formation and origin of sandbanks, the morphology of the Base-Quaternary surface, the knowledge from studies on particular sandbanks on the BCS, and even historical evidence of former coastlines, have been considered. All these clues have been put together as in a giant jigsaw puzzle, to come to a comprehensive model for the Quaternary history of the BCS.

UNIVERSITEIT GENT
Faculteit Wetenschappen
RCMG
Geological Survey of Belgium
FWO VLAANDEREN
Fonds Wetenschappelijk Onderzoek
Research Foundation – Flanders